Rare-Metal Metallogeny in Newfoundland and Labrador

by

Randy R. Miller

Geological Survey Branch
Newfoundland Department of Mines and Energy

Final Report
Geoscience Contract
Project NC.1.2.1

Canada-Newfoundland Cooperation Agreement
on Mineral Development
(1990 - 1994)

February 1994

RARE-METAL METALLOGENY IN NEWFOUNDLAND AND LABRADOR

A Preliminary Report

Canada - Newfoundland
Mineral Development Agreement 1989 - 1994

By Randy R. Miller
Geological Survey Branch
Newfoundland Department of Mines and Energy

February 22, 1994

TABLE OF CONTENTS

1.0 Introduction

Rare-Metal Mineralization

Recent work on the rare-metal mineralization in the Strange Lake Zr-Y-Nb-Be-REE deposit (Miller, 1986, 1990) and in the Letitia Lake Nb-Be±Y showings (Miller, 1987) has led to the development of an exploration model for rare-metal mineralization associated with felsic rocks (Miller, 1988). This model can be successfully applied to other similar rare-metal deposits (eg. Thor Lake, N.W.T. - Trueman et al. 1985; Jabal S'aid, Saudi Arabia - Drysdale et al., 1984; Hackett, 1986) and thus has application to the exploration for undiscovered rare-metal mineralization. The aim of this project is to apply the model to felsic-rock settings, to evaluate the rare-metal potential and to encourage exploration activity for rare metals in the Province of Newfoundland and Labrador. This preliminary report outlines the results of this project.

The rare-metal elements, which include Y, Be, Nb, REE, Ta, Zr, have rapidly become indispensable in the "high tech" industries, and, as a result, the demand for these elements has been steadily increasing. This increasing demand has encouraged the exploration for economic deposits of rare metals throughout the world. The "high tech" uses of the rare metals as a group include the use of these elements in the manufacturing of: laser garnets, high temperature / high strength ceramics, super conducting materials / super magnets, speciality steels, oil products, lamp / television phosphors & nuclear reactor components. Many of these materials are used in aerospace, defense, electronics and computer industries (Table 1-1). Generally speaking, these industries are continuously growing and thus are fuelling the growing demand for new sources / supplies of the rare metals. Estimates of the increase in demand for these elements, after considering new uses and the introduction of substitute materials, ranges from 3 to 10% (U.S. Bureau of Mines, 1985) up to the year 2000.

To date, the two significant rare-metal deposits discovered in Labrador are a result of exploration programs for U, in the Strange Lake region (Miller, 1986), and Cu-Zn, in the Mann #1 case (Brummer, 1960). The fact that these exploration programs were not aimed at rare-metal mineralization is due to: 1) the very small number of companies focussing on rare-metal exploration versus the traditional commodities such as Fe, U, Au, Cu or Zn, 2) the relatively small markets, and, 3) the high costs of any exploration program in Labrador. Thus, the rare metal discoveries in Labrador were "fortuitous" rather than "by design". The development of an empirical model should help lower the costs, by assisting companies to

Table 1-1 Some uses of the rare-metal elements

ELEMENT	MATERIAL PRODUCED	PRODUCTS MANUFACTURED
BERYLLIUM	Be metal	Aircraft components
	BeO ceramics	Electronic components
		Microchips and circuit boards
	Be-Cu alloys	Automobile parts
		Electronics
		Missile components
NIOBIUM	High strength, low alloy steels	Pipe for oil / gas pipelines
		Automobile components
		Drilling pipe
	Nb metal	Electronic components
		Carbide tools
		Superconductors
		Supermagnets
		Jet-Engine components
RARE EARTHS	High strength, low alloy steels	Pipe for oil / gas pipelines
	Ceramic raw material	Colouring agent
		Light-absorbing agent
		High-temperature ceramics
	Phosphors	Televison / Monitor colour tubes
	Permanent magnets	Headphones, speakers, generators, alternators, Electric motors
	Garnets	Microwave garnets
		Laser garnets
	Chemicals	Petroleum catalysts
	Electronics	Capacitors
		Cathodes and electrodes
		Thermisters
		Semiconductors
YTTRIUM	Phosphors	Television / Monitor colour tubes
		Fluorescent lamp tubes
	Garnets	Laser crystals
		Microwave crystals
	Stabillized zirconia ceramics	Cutting edges
		Automobile parts
		Tool dies
ZIRCONIUM	Refractories	Zirconium bricks
		Zirconium sand
	Ceramics	Oxygen sensors in furnaces
		Oxygen sensors in gas engines
		Colouring agent
		Electronic components
		Circuit boards
		Cutting edges
		Automobile parts
	Abrasives	Glass polishing compounds

focus on smaller areas for evaluation, which will better identify the potential that will attract rare-metal exploration companies to Labrador and insular Newfoundland.

When compared to Labrador, insular Newfoundland provides a more favourable environment for exploration and development. Exploration costs are much lower due to the more extensively developed infrastructure, the larger workforce and the larger number of services available. These factors also mean that, unlike Labrador, significant discoveries of rare-metal mineralization are more likely to be developed. Thus, insular Newfoundland is a better place to find rare-metal deposits and to bring them into production.

Geological Settings of Rare-Metal Mineralization

The metallogenic model developed for high level peralkaline rock-hosted rare-metal mineralization is based on the metallogenic studies of the Strange Lake Zr-Y-Nb-Be-REE deposit (Miller, 1986), the Mann-Type Nb-Be±Y showings in the Letitia Lake area (Miller, 1987; Batterson and Miller, 1987), the mineralization observed in the undersaturated phases of the Red Wine Instrusive Suite (Miller, 1988) and the mineralization described in the Flowers River Igneous Suite (Hill, 1981; Miller, 1988). The general geological settings and the geochemistry of the mineralization in these Labrador-based examples are certainly not representative of all of the many different kinds of rare metal deposits found world-wide. Literature research indicates that the major settings have been described in the model. These settings are illustrated in Figure 1-1.

This model indicates that rare-metal mineralization (ie. complex mineralization including one or more of Zr, Y, REE, Nb, Ta, Be) generally occurs in dominantly felsic peralkaline and near peralkaline anorogenic intrusions and their near-vent extrusive equivalents (Miller, 1987). Four geolgical settings - mineralization modes have been identified in Labrador (Miller, 1989):

1) pegmatite - aplite dykes and late-stage, roof-zone phases in high-level peralkaline granite plutons or associated satellite bodies that did not vent to the surface (eg. Strange Lake peralkaline granite - Miller, 1989),
2) pegmatite and pegmatite - aplite dykes in the roof zone of vented peralkaline granites and as disseminated mineralization in the near-vent extrusive equivalents or associated subvolcanic satellite bodies (eg. Flowers River Igneous Suite, Shallow Lake peralkaline granite - Hill, 1981; Miller, 1989),
3) subvolcanic veins associated with peralkaline quartz syenites and as disseminated mineralization in the associated peralkaline trachytes within the

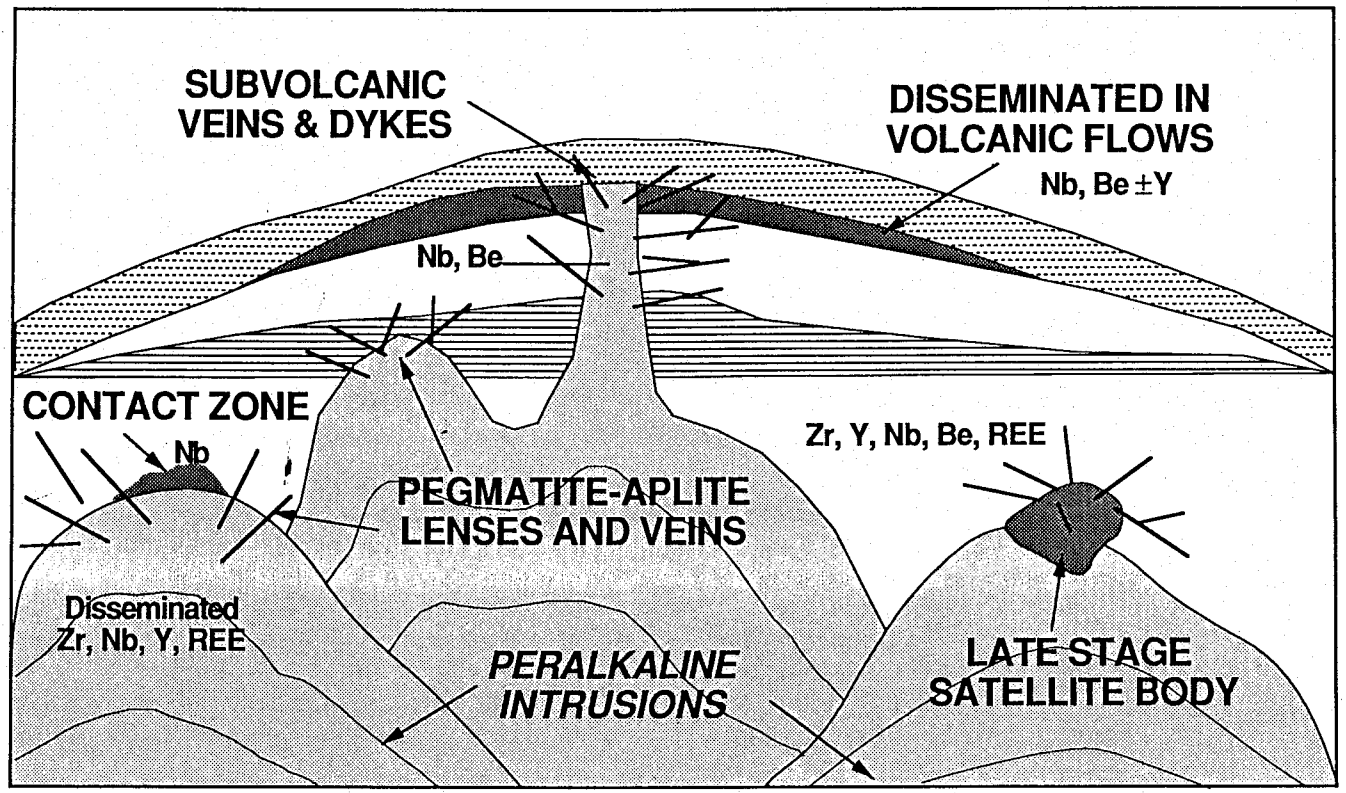

Figure 1-1 *Rare-metal mineralization model: Setting 1—late-stage satellite bodies and associated pegmatite—aplite veins associated with unvented plutons (granite); settings 2 and 3—veins and disseminated mineralization in near vent volcanic rocks and subvolcanic equivalents (granite or syenite); setting 4—disseminated mineralization and contact zones in unvented plutons (granite and undersaturated syenites).*

near-vent environment (eg. Mann#1 and Two Tom Lake deposits - Miller, 1987), and,

4) disseminated mineralization within high-level, unvented(?), undersaturated peralkaline complexes (eg. Red Wine Alkaline Intrusive complex - Curtis and Currie, 1981).

Some of these generalized geological settings or environments have been identified in insular Newfoundland (Miller, 1989). Table 1-2 lists the areas and geological units chosen for this study and the rare-metal setting expected in these areas and Figures 1-2 and 1-3 give this location. Each of these areas was evaluated initially by reconnaissance mapping and sampling programs. All outcrops visited are assessed for rare-metal mineralization; selected outcrops are measured for radioactivity (total counts; EDA GRS-500 Spectrometer) and sampled for geochemical and/or thin-section analysis. Samples collected were petrographically and chemically studied to help determine the rock type and degree of peralkalinity (a key factor in rare-metal environments) and to determine the representative rare-metal values of the outcrop.

Settings number 1 and 3 (above) have been found to contain significant tonnages of high grade mineralization (Miller, 1988). High values of rare metals have been found in settings 2 and 4, although significant tonnages have not been outlined.

These same settings have also been shown to contain significant rare-metal mineralization in other parts of the world such as the Northwest Territories (Thor Lake, Trueman et al, 1984), Greenland (Industrial Minerals,1988a, 1988b), Australia (Ramsden et al, 1993) and Saudi Arabia (Drysdale et al., 1984; Jackson, 1986).

The Thor Lake deposit exhibits many of the characteristics of Setting #1 above, although there are many uncertainties and complications with regard to the genesis of this Be-Nb-Ta-Y-REE-Ga deposit (Trueman et al, 1984; Birkett, 1988). The mineralization occurs in several zones, some associated with metasomatized granite pegmatite and some associated with highly altered peralkaline granite (Grace Lake Granite) and amphibole ± olivine ± pyroxene syenite (Thor Lake Syenite). There has been no evidence to suggest that either the syenite or granite was vented to the surface, although the high level nature of these rocks is evident. The high degree of metasomatizm reported in the Thor Lake deposits suggests there was late stage development of rare-metal mineralization. In this case the late stage nature is not manifested dominantly by pegmatite-aplite or vein formation but by intense hydrothermal-metasomatic activity, possibly associated with pegmatite formation.

Several rare-metal deposits and showings associated with high level peralkaline felsic rocks have been described from Saudi Arabia (Drysdale et al., 1984). All of these examples

Table 1-2 **Rare-Metal Targets in Newfoundland and Labrador**

Target	Setting	Plutonic Phase	Volcanic Phase
Topsail Igneous Suite			
Little Pond Brook volcanic suite	2	Topsails peralkaline granite	Little Pond Brook volcanic suite (per±)
Gaff Topsail peralkaline granite	1,2	Gaff Topsail peralkaline granite	?
Sheffield Lake area	2	?	Sheffield Lake peralkaline volcanic rocks
Baie Verte Peninsula			
Cape St. John area	2	Seal Is. Bight peralkaline granite	Cape St. John Group (per?)
Micmac Lake Group	2	?	Micmac Lake Group (per±)
Kings Point Complex	1,2	Feldspar porphyritic syenite (per?)	KPC peralkaline ash-flow tuffs
Le Grande Pierre Area			
Mooring Cove Formation	2	Cross Hills peralkaline granite?	Mooring Cove Formation (per±)
Cross Hills peralkaline granite	1,2	Cross Hills peralkaline granite?	Mooring Cove Formation (per±)
Burin Peninsula			
Grand Beach complex	2	St. Lawrence peralkaline granite ?	Grand Beach ash-flow tuffs (per?)
St. Lawrence peralkaline granite	1,2	St. Lawrence peralkaline granite	Rocky Ridge complex peralkaline ash-flows
Terranceville Area	2	?	Southern Hills facies - Love Cove Group (per?)
Bull Arm Formation			
Traytown Area	1,2	Louil Hills peralkaline granite	Musgravetown Group (per?)
Port Blandford Area	2	?	Musgravetown Group (per?)
Musgravetown Area	2	?	Musgravetown Group (per±)
Plate Cove Area	2	?	Musgravetown Group (per?)
Clarenville Area	2	?	Musgravetown Group (per?)
Hodges Cove Area	2	?	Musgravetown Group (per?)
Sunnyside Area	2	?	Musgravetown Group (per?)
Masters Head Area	2	?	Musgravetown Group (per?)
Does Hills Area	2	?	Musgravetown Group (per?)
Flowers River Igneous Suite	1,2	Flowers River peralkaline granite	Nuiklavik peralkaline ash-flow tuffs

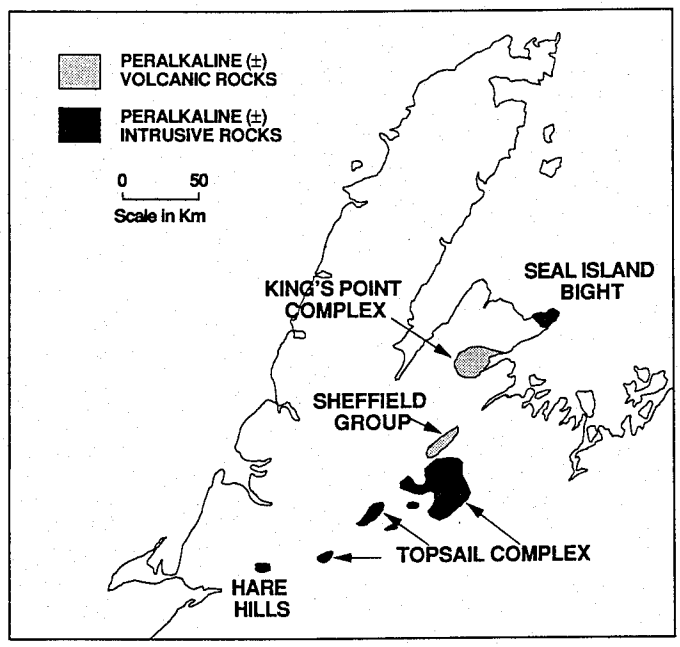

Figure 1-2 *Rare-metal targets in north–western Newfoundland; peralkaline and peralkaline-related volcanic and high-level plutonic rocks.*

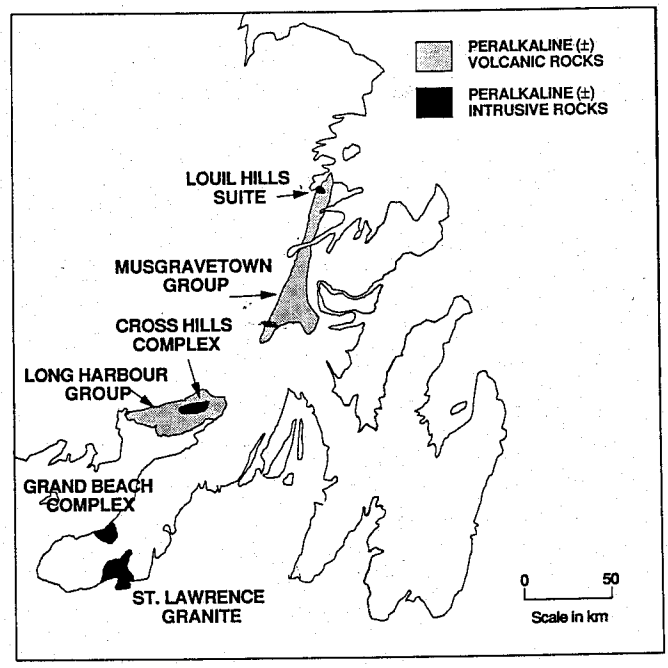

Figure 1-3 *Rare-metal targets in south–eastern Newfoundland; peralkaline and peralkaline-related volcanic and high-level plutonic rocks.*

are associated with granites or syenites which have not been vented to the surface (Jackson, 1986). One particularly well studied example is the Jabal Sa'id pegmatite-aplite hosted Nb-Zr-Y-REE-Sn-Ta deposit (Hackett, 1986). The mineralization occurs within a composite pegmatite-aplite body which occurs at the contact of a peralkaline granite. This mineralization corresponds to Setting # 1 and is very similar to the Strange Lake deposit.

Two separate exploration programs in Greenland (Industrial Minerals, 1988a, 1988b) valuated eudialyte-bearing peralkaline undersaturated phases of the Illimassuaq felsic complex. Both properties are being evaluated for Zr-Y-REE deposits similar to the mineralization observed in the Red Wine undersatured rocks and Setting #4.

The Brockman Nb-Ta-Y-Zr-REE deposit in Australia occurs as disseminated mineralization in trachytic flows and tuffs of the Brockman volcanics. Mineralogical and other studies of the volcanic host rocks (Ramsden et al. 1993) indicate that many are incompatible-element-enriched but alkali-poor (ie. not peralkaline in the strict sense but peralkaline in affinity). Thus, the host rocks are similar to some host rocks in the Letitia Lake Group and the Flowers River Igneous Suite and are similar in geological setting to Setting #3.

Table 1-3 lists the minimum and maximum values of some rare-metal elements in the various host rocks of rare metal deposits and showings in Labrador. These values have been divided into volcanic and intrusive rocks for comparative purposes. Note that a significant rare-metal deposit has been outlined in the Strange Lake peralkaline granite (Dawe, 1984) and a sizeable resource is suggested at the Mann #1 syenite (Dujardin, 1960) and within the Letitia Lake Group volcanic rocks. This compilation of geochemical data should be useful to exploration geologists wishing to evaluate the potential of a particular rare-metal exploration target (ie. potential of a high-level peralkaline suite or complex). Thus, targets with rare-metal values within or near the ranges indicated in Table 1-3 should be given further evaluation, particularly if the potential settings are the same.

The ranges of rare-metal values in the showings and deposits in Labrador are listed in Table 1-4. Not all showings have uniformly high values of all rare-metal elements; for example the Letitia Lake showings have abnormally low Zr values but significant Be and Nb values. This table can also be used as a guide in exploration programs.

Table 1-3 Minimum and maximum values of rare-metal concentrations in rare-metal host rocks in Labrador.

Setting	Host	Zr	Y	Nb	Be	U	C.P.S.
Setting 1	Strange Lake granite	2000	600	250	30	7	500-1000
		5000	1500	500	80	30	
Setting 2	Flowers River granite	600	100	50	-	2	300-600
		1100	150	150	-	6	
Setting 2	Flowers River volcanics	1000	100	40	-	2	300-2000
		8000	600	300	-	6	
Setting 3	Letitia Lake syenites	700	50	50	7	1	300-700
		3600	300	400	50	12	
Setting 3	Letitia Lake Group	200	60	20	5	3	350-600
		2000	200	800	100	6	
Setting 4	Red Wine nepheline syenite	500	50	90	-	1	—
		5000	200	300	-	14	

Sources of data: Strange Lake granite–Miller, 1986; Flower River volcanics–Hill, 1981; Letitia Lake Group–Miller, 1987; Flowers River granite–Hill, 1981; Letitia Lake syenites–Miller, 1987; Red Wine nepheline syenite–Curtis and Currie, 1981; rare-metal values in p.p.m.

Table 1-4 Rare-metal concentrations in deposits and showings in Labrador.

Setting	Deposit or Showing	Zr	Y	Nb	Be	U	C.P.S.
Setting 1	Strange Lake granite	5,000	2,000	1,000	200	50	1000
		27,000	16,000	15,000	5,000	300	10,000
Setting 2	Flowers River granite	20,000	2,200	1,000	-	-	1500
Setting 3	Letitia Lake showings	40	150	100	30	5	1000
		180	2,400	10,000	2,500	180	10,000
Setting 4	Red Wine nepheline syenite	20,000	2,200	1,000	-	-	—

Sources of data: Strange Lake granite–Miller, 1986; Letitia Lake showings–Miller, 1987; Flowers River granite–Hill, 1981; Red Wine nepheline syenite–Curtis and Currie, 1981; rare-metal values in p.p.m.

Evaluation of Targets

The modes of occurrence of rare-metal mineralization make it difficult to visually identify it in the field. Rare metal-bearing pegmatitic lenses, veins and dykes, as found in Settings 1, 2 and 3, are usually the easiest to identify if the rare-metal minerals are coarse grained. On the other hand, aplitic, fine grained and disseminated mineralization, particularly in the volcanic environments of Settings 2 and 3, is very difficult to verify due to the fine grainsize. Thus, rare-metal potential cannot be very accurately evaluated in many areas before chemical analyses are available.

A rough positive correlation between rare-metal contents and radioactivity (total counts) in samples studied from both the Letitia Lake showings and the Strange Lake deposit indicates that radioactivity can be used to help determine rare-metal potential.

2.0 Topsails Intrusive Suite

Introduction

The Topsails igneous suite (TIS; Whalen and Currie, 1983) is located in western Newfoundland south and east of Grand Lake and north and west of the community of Buchans (Figure 1-2).

Three parts of the TIS were chosen as reconnaisance targets to evaluate the rare metal potential of the peralkaline rocks in the suite. One target, here called the Gaff Topsail peralkaline granite, consists of medium grained peralkaline granite. The other two targets, here called the Little Pond Brook volcanic suite and the Sheffield Lake area, consist of, in part, peralkaline volcanic and hypabyssal rocks. The peralkaline rocks in these three areas fit the criteria as potential sourses of rare metals.

The Gaff Topsail peralkaline granite, which occurs in the northern part of the Topsails igneous suite, outcrops over an area of approximately 650 km^2. A total of 39 geochemistry and thin section samples were collected from this target. Access was by truck on the old railway bed and by helicopter to more remote areas. The aim was to obtain widespread samples covering a large part of the outcrop area.

The Little Pond Brook volcanic suite forms a subcircular structure approximately 12 km in diameter. It occurs in the central part of the TIS just south of Grand Lake. This target was accessed by a helicopter-supplied camp. A total of 79 thin section and 73 geochemistry samples were collected to help determine the volcanic stratigraphy and to evaluate the rare metal potential.

The Sheffield Lake area occurs on the far northern edge of the TIS. There are two small targets in this area, here called Mt. Seemore and North Hill. Both consist of elongate bodies, Mt. Seemore being 10 km long and North Hill being 4 km long. Access is by road in both cases. The rare metal potential at Mt. Seemore is evaluated with 28 thin section and 20 geochemical samples, whereas at North Hill it is evaluated with 4 thin section and 4 geochemical samples.

General Geology

The Topsails igneous suite consists of a suite of Late Ordovician to Early Silurian plutons and related bimodal volcanic rocks (Whalen 1989, Whalen and Currie 1990, Whalen et al. 1987) that occur in the Notre Dame subzone of the Dunnage lithotectonic

zone (Williams et al. 1988). The outcrop area of the suite is 2200 km^2 and it occurs in a belt 125 km long by 40 km wide.

Host rocks of the TIS, which are Ordovician or older in age, include ophiolitic rocks, portions of the Buchans Group and Glover Formation, and a suite of deformed granodioritic and granitic rocks. The oldest host rocks, the ophiolitic suite (undated), are intruded by the suite of deformed granodioritic and granitic rocks (467 - 460 Ma; Whalen et al. 1987). The Buchans Group is approximately 473 Ma (Dunning et al. 1987).

Members of the TIS, which range in age from 438 to 427 Ma (Whalen et al 1987), include the Rainy Lake Complex, comprising gabbroic to granodioritic rocks, the Springdale Group, consisting of bimodal volcanic rocks, a number of felsic hypabyssal to volcanic bodies and a series of monzonitic to granitic intrusions (Whalen and Currie 1990). Felsic intrusive members (monzonitic to granitic rocks) of the TIS include (Figure 2-3): a syenite to granite suite, coarse grained peralkaline granite and marginal phases of the coarse grained peralkaline granite (Whalen et al. 1987). All members of theTIS are described in detail in Whalen and Currie (1983, 1986, 1987, 1990), Whalen (1990) and Taylor et al. 1980.

2.1 Little Pond Brook Volcanic Suite

Introduction

The Litttle Pond Brook Volcanic Suite (LPB) occurs as a subcircular sequence of porphyries (12 km in diameter) that is located on the southern shore of Grand Lake approximately 30 km southeast of the community of Deer Lake (insular Newfoundland; Figure 1-2). Recent mapping by Whalen and Currie (1986) indicate that the rocks of this suite have some peralkaline characteristics which suggests that there is some potential for volcanic-hosted rare-metal deposits. This potential was evaluated with a 7 day geological mapping and lithogeochemcial sampling program.

The entire work area is essentially only accessible by helicopter, although some portions are accessible by boat access with a 500 m climb from Grand Lake. A total of 4 traverses were run from a helicopter-supplied camp on a small pond on a tributary of Little Pond Brook, approximately located in the centre of the outcrop area. Most of the area was accessible by foot traverse from this camp and the remainder was sampled by helicopter.

Samples were collected from a total of 79 sample sites (TS91044 to TS91122); thin section samples were collected from all 79 sites and geochemical samples were collected from 73 of these sites. Each geochemical sample has been analysed for major elements and a suite of trace elements, including rare metals, and several samples have also been analysed for rare earth elements. The sample locations (NTS coordinates), rock type and other data (e.g scintillometer readings) are given in Appendix A-1.

Geology

The quartz-feldspar porphyry unit, to which the LPB suite belongs, is the youngest member of the Topsail igneous suite (U-Pb zircon - 427±3 Ma; Whalen et al. 1987). It is thought to represent high-level subvolcanic plutons which are slightly younger than the nearby coarser grained intrusive rocks of similar composition (Whalen et al. 1987). The LPB suite is the largest of eight such plutons identified by Whalen et al. (1987).

Porphyritic rocks of the LPB volcanic suite can be divided into the following four units in order of decreasing age: feldspar-quartz-amphibole porphyry (FQA porphyry), feldspar-quartz porphyry (FQ porphyry), feldspar+quartz-poor porphyry ([F+Q]-poor porphyry) and feldspar porphyry (F porphyry). Present exposures indicate that the LPB volcanic rocks reached a thickness of at least 450 m.

The geology of the suite displays an asymmetrical ring-like pattern. Feldspar porphyry forms a elongate central zone in the northwest-central area and is surrounded by successive partial rings of each of the older units with the oldest unit (FQA porphyry) forming the outside ring. The occurrence of [F+Q]-poor porphyry is only found to the north of the central unit. Field evidence suggests that the F porphyry (really F-poor porphyry) and the [F+Q]-poor porphyry may be closely related as they appear to be gradational. Older crystal-rich porphyries form the outer rings which are most prominent to the east and south of the central zone.

The lowermost unit of the LPB volcanic suite is the 200 m thick FQA porphyry which is thought to conformably lie on volcanics of the Springdale Group based on the similar ages of these rocks (Springdale Group - 429±4 Ma; Little Pond Brook volcanic suite - 427±3 Ma; Whalen et al 1987), although this relationship was not observed in this study nor has it been reported previously (Whalen and Currie 1984, Whalen et al. 1987). The FQ porphyry (50 to 120 m thick) overlies the FQA porphyry, however the contact relationship between these two units in unknown. The next youngest unit (0 - 100 m thick) is the[F+Q]-poor porphyry, which rarely contains fragments of the lower units and in some locations contains a FQ porphyritic matrix. The F porphyry, which is at least 80 m thick, overlies [F+Q] porphyry and has a gradational relationship with this unit.

The feldspar-quartz-amphibole porphyry is characterized by 20 to 40% microperthitic feldspar (1 to 4 mm wide), 10 to 15% quartz (1 to 3 mm wide) and < 3% mafic mineral (mainly amphibole; < 1 mm wide) phenocrysts in an aphanitic to very fine grained matrix. The colour is characteristically grey-green or red-brown and phenocrysts are commonly embayed and broken. In thin section amphibole phenocrysts, amphibole oikocrystic aggregates, poikolitic amphibole in the matrix, clinopyroxene, hematized opaque minerals and zircon are commonly found. In many samples the matrix is recrystallized, contains granophyric- or spherulitic-textured lenticular zones and layers, collapsed fiamme, fine layering and sparse volcanic rock fragments. The abundance of phenocrysts precludes a lava flow origin for this unit, whereas many of the features observed in the FQA porphyry are characteristic of ash-flow tuffs. Thus most occurrences of FQA porphyry in the LPB volcanic suite are thought to be deposited as ash-flow tuffs with the possibility that some outcrops may also be hypabyssal or sub-volcanic intrusions.

Feldspar-quartz porphyry of the LPB suite has many characteristics similar to those of the underlying FQA porphyry, including similar sizes, textural features and amounts of feldspar and quartz phenocrysts. This porphyry also exhibits many ash-flow tuff textures including layering, lenticular zones and fiamme, and broken crystals. In contrast to the underlying unit, hematized mafic minerals are found instead of amphibole, plagioclase as

well as microperthite (most abundant) occurs and sparse but widespread coarse granophyric-textured fragments (i.e. hypabyssal rock fragments) are found. There is some textural evidence to suggest that some of the hematized mafic minerals may be amphibole. Most FQA porphyry outcrops are distinguished from hematized FQ outcrops by the pink-brown to medium red-brown colour of the FQ porphyry.

The [F+Q]-poor porphyry is characterized by total quartz plus feldspar phenocryst content of 10% and phenocryst grainsize < 2 mm. Some occurrences are aphyric to sparsely porphyritic. It is distinguished from the phenocryst-poor upper F porphyry by having quartz phenocrysts although aphyric varieties of each unit are essentially the same illustrating the gradational relationship between these two units. The [F+Q]-poor porphyry commonly exhibits the characteristic textures of ash-flow tuffs in outcrop and thin section including: abundant flattened fiamme and lenticular zones, layering, lithophysia and other gas structures, flattened pumice fragments, sphericular textures and fragment-rich facies. Fragment types observed include layered aphyric, aphyric aphanitic and quartz-feldspar porphyry fragments. The colour ranges from light pink-brown to dark red-brown. Feldspar phenocrysts are most commonly microperthitic but plagioclase phenocrysts are no uncommon. This unit is also interpreted to have been deposited as ash-flow tuff.

The LPB feldspar porphyry is characterized by < 5 to 15 % feldspar phenocrysts, <1 to 2 mm wide; in some localities feldspar may be as high as 20%. The matrix of this unit is commonly aphanitic, is banded and contains streaks, blebs, hematite patches and vuggy zones. Its colour ranges from light straw-brown to dark red-brown. Most feldspar phenocrysts are microperthitic in composition but minor plagioclase feldspar is common. Small (< 3 mm wide) very fine grained quartz-feldspar rock fragments are sparsely found in this unit. Chlorite, opaque minerals and hematized dark-coloured minerals are also accessory mineral phases. This unit is also interpreted to have been deposited as ash-flow tuff.

A diabase dyke and a composite rhyolite-basaltic dyke (Whalen and Currie 1984) were also observed in the LPB area. Both dykes cross-cut LPB volcanic rocks but the relationship between these rocks is unknown.

Results

As mentioned previously, spectrometer data was used in the field to make a preliminary evaluation of rare-metal concentrations in outcrops. Radioactivity measurements for the LPB volcanic suite are listed in Appendix A-1 and summary data for these measurements are listed in Table 2-1. These data indicate that the two crystal-rich units have relatively low and very similar minimum, maximum and average total count values. The [F+Q]-poor porphyry has the highest average and maximum values of the four main units and the F porphyry has values intermediate to those of the other units. The values observed are low to intermediate when compared to known rare-metal showings (see Introduction); these values would suggest low potential for rare metals. The highest value obtained from the LPB volcanic suite was 670 cps from an aphyric flow (TS91097) that occurs in the upper part of the stratigraphy.

Table 2-1 Summary Spectrometer Data

Rock Type	Min.	Max.	Average	Number
F Porphy	390	450	415.4	13
FQ poor	380	550	455.0	9
FQ Porph	300	450	362.8	16
FQA Porph	310	430	370.3	17

The geochemical data from the LPB samples are found in Appendix B-1 and averages and unique samples from this data set are tabulated in Appendix C-1. The geochemical data indicate that most example of FQA porphyry and the QF porphyry have essentially the same chemistry; a major difference being the higher Fe_2O_3/FeO ratio in the hematite-bearing QF porphyry vs the amphibole-bearing FQA porphyry. The F porphyry is characterized by lower SiO_2 and incompatible elements (e.g. Zr, Y) and higher Al_2O_3 and compatible elements (e.g. Ba, Sr).

Two groups of rocks exhibit high Zr and other incompatible element values: 1) some samples of FQA porphyry (FQA (1) - Appendix C-1) and, 2) most samples of [F+Q]-poor porphyry ([F+Q]-poor (2) - Appendix C-1). High values of incompatible elements are generally characteristic rare-metal mineralization-producing magmatic systems.

DISCUSSION

The geochemical data from the LPB volcanic suite, when plotted in the discrimination plots of Whalen et al., (Figure indicates that this suite can be classified as A-type; this isn't a surprise as Whalen et al. used analyses from the Topsail Igneous Suite to help define the A-type field. These data also indicate that some phases of the LPB volcanic suite are peralkaline, as indicated in some cases by A.I. > 1.00 or Zr > 500 p.p.m.

Studies of chemical alteration of peralkaline volcanic rocks (e.g. Houghton et al, 1991; Baker and Henage, 1977) indicate that Na, K, F and Cl, amongst other elements, are susceptible to transport during crystallization or by normal hydrothermal activity in a volcanic field. The Agpaitic Index (A.I.) can be altered downwards from magmatic values by geochemical transport of Na_2O or K_2O if Al_2O_3 remains inert. This may have happened for many of the FQA, QF and [F+Q]-poor porphyritic ash-flows in the LPB volcanic suite. The high values of Zr and other incompatible elements in these rocks are characteristic of mildly peralkaline volcanic rocks (i.e. A.I. 1.00 - 1.08), however the A.I. usually ranges from 0.70 - 1.00 in these rocks.

CONCLUSIONS

Both the spectrometer data and the geochemical data of the samples collected indicate that the LPB volcanic suite has low-medium potential for rare-metal mineralization. The geochemcial data does indicate that part of the magma produced in the LPB volcanic event is peralkaline in nature and the remainder is A-type in nature but not peralkaline. These features indicate that the LPB volcanic suite is in the right environment for rare-metal mineralization however rare-metal concentrating processes appear to have been non-operative or inefficient in this case.

The available data indicates that the LPB volcanic suite is not a good target for rare-metal exploration.

2.2 Gaff Topsail Granite

Introduction

The Gaff Topsail granite (GTG) is an irregular-shaped peralkaline granite body that has maximum dimensions of 45 km long and 30 km wide. It is located in the northern part of the Topsails igneous suite outcrop area between Buchans and Sheffield Lake (Figure 1-2). This body represents the largest extent of peralkaline rocks, approximately 650 km^2, in the TIS and thus has some potential for rare-metal mineralization. This potential was evaluated with a four day geological mapping and lithogeochemical sampling program.

The northeastern half of the Gaff Topsail granite is mostly accessible by off-road truck from the abandoned Newfoundland Railway bed. The southern and western parts of the GTG are mostly accessible by helicopter. A total of three foot traverses were run from the railway bed and one helicopter traverse was used to sample the more remote areas.

Both thin section and geochemical samples were collected from a total of 39 sites (TS91030 to TS91043 and TS91123 to TS91147). Each geochemical sample has been analysed for major elements and a suite of trace elements, including rare metals. The sample locations (NTS coordinates), rock type and other data (e.g scintillometer readings) are given in Appendix A.

Geology

The Gaff Topsail granite is the largest pluton of coarse amphibole peralkaline granite in the Topsail igneous suite. It is rimmed by peralkaline to subalkaline marginal phases, that are generally finer grained rocks, most of which are thought to be high-level marginal or roof zone phases of this granite (Whalen and Currie 1990). The marginal phases, as mapped by Whalen and Currie (1983), were not a sampling target of this program although some fine grained and porphyritic rocks were sampled from minor outcrops within the coarse grained body.

The geology of the Topsails igneous suite in the vicinity of the the Gaff Topsail granite is illustrated in Whalen and Currie (1983). The lack of outcrop in some portions of the GTG and the small size of outcrops in others make it difficult to subdivide the granite on the basis of petrographical or mapping data. Most samples collected are coarse grained amphibole granite.

The coarse grained amphibole granite mainly consists of microperthitic feldspar, alkali amphibole and quartz. Trace minerals include aegirine, zircon and astrophyllite. Quartz grains are normally anhedral, 2 - 4 mm in size and range from 15 to 35% of the rock. Feldspar occurs as anhedral grains, 2 - 6 mm in size, that range from 60 to 80% of the rock. Amphibole, the main mafic mineral, occurs as grains that range from 1 to 3 mm in size, are subhedral to euhedral and constitute 3 to 8 % of the granite. This granite ranges in colour from cream, to greenish-white to yellow to beige and pink; many other pastel colours are also locally present.

Marginal phases include feldspar-quartz-amphibole porphyry and fine grained granite. The feldspar-quartz-amphibole porphyry consists of 1 - 6 mm feldspar, quartz and amphibole phenocrysts in a very fine grained (less than 0.25 mm) matrix of the same minerals. Phenocryst concentrations range from 10 to 60%. Fine grained granite consists of quartz, feldspar and amphibole grains less than 2 mm in size.

Results

Geochemical data from the GTG samples are tabulated in Appendix B-2 and averages and unique values are displayed in Appendix C-2. Most of the samples (medium grained amphibole granite) that exhibit very similar chemical analyses, are characterized by Zr contents of 536 - 765 p.p.m. Several anomalous samples, including two medium grained amphibole granite, a very fine grained dark-coloured inclusion and an amphibole granite porphyry, are characterized by Zr values between 800 and 1020 p.p.m. Other samples, thought to be marginal phases of the granite, exhibit much lower Zr values (165 - 500 p.p.m.).

Discussion

The medium grained amphibole granite, the group of anomalously high Zr granite samples and the analyses from the marginal phases all plot in the A-type granite field of Whalen et al. (1987; analyses from the same suite were used by Whalen et al. to define this field). Most of these samples are mildly peralkaline (A.I. 0.96 - 1.06); only the amphibole porphyritic granite is non-peralkaline.

Figure 6 also illustrates the similarities between the LPB volcanic suite and the GTG. Neglecting minor differences caused by alteration in volcanic rocks, it is evident that: 1) the medium grained amphibole granite is the plutonic equivant of the the FQA (2) and QF porphyries (LPB), 2) the amphibole granite porphyry (Appendix C-2) is very

similar to the F porphyries, and 3) the high Zr intrusive rocks are similar to the high-Zr FQA (1) porphyries (LPB).

Conclusions

The most abundant rocks in the GTG are relatively poor in rare-metals compared to the nearby LPB volcanic suite and are extremely low compared to the rocks associated with rare-metal deposits. The data does indicate that the GTG is the plutonic precurser of the LPB volcanic suite and it is generally peralkaline in nature. However, high concentrations of rare-metals were not discovered.

The GTG has low potential for rare-metal mineralization and is thus not a good target for rare-metal exploration.

2.3 Sheffield Lake Area

Introduction

Two small targets, the Mt. Seemore and North Hill targets, are located in the vicinity of Sheffield Lake. Both targets have been mapped as quartz-feldspar porphyry, similar to the Little Pond Brook volcanic suite, and thus represent high-level felsic rocks that are thought to be peralkaline in part (Taylor et al. 1980; Whalen and Currie 1983; Coyle et al. 1986). The Mt. Seemore target also contains comenditic volcanic rocks (Taylor et al. 1980) and thus these rocks have some potential for rare-metal mineralization. Both targets were jointly sampled and mapped over a two day period to evaluate the rare-metal potential.

The Sheffield Lake area is readily accessible by road from the Trans Canada Highway. Mt. Seemore was foot traversed for 1 1/2 days and North Hill was foot traversed for one half of a day in 1991. Minor field checking and sampling was carried out on Mt. Seemore in 1992.

A total of four sites, with both thin section and geochemical samples (TS91021 to TS91024), were sampled in the North Hill area. Twenty-eight thin section and 20 geochemical samples (TS91001 to TS91020, TS91025 to TS91029, and TS92001 to TS92003) were collected from the Mt. Seemore area. Each geochemical sample has been analysed for major elements and a suite of trace elements, including rare metals. The sample locations (NTS coordinates), rock type and other data are given in Appendix A-3.

Geology

Mapping indicates that the quartz-feldspar porphyry of these two targets belongs to the last phase of the TIS (Whalen and Currie 1983); North Hill and Mt. Seemore are two of the eight such bodies mapped in the TIS. These two bodies differ from the Little Pond Brook volcanic suite as oikocrystic amphibole-bearing peralkaline flows have been reported in them (Taylor et al. 1980; Coyle et al 1986). All are thought to represent peralkaline-subalkaline hypabyssal-volcanic bodies that are not necessarily related to the peralkaline granite of the TIS (Whalen et al 1987).

The TIS rocks of North Hill and Mt. Seemore can be divided into oikocrystic amphibole porphyry, feldspar-quartz-amphibole ash-flow tuff, feldspar-quartz ash-flow tuff and phenocryst-poor ash-flow tuff and tuff-breccia. The feldspar-quartz-amphibole ash-flow tuff can be further subdivided into phenocryst-rich and normal phases based on

the amount of feldspar phenocrysts. North Hill and the northern portion of Mt. Seemore are dominantly feldspar-quartz ash-flow tuff, whereas feldspar-quartz-amphibole ash-flow tuff and oikocrystic amphibole porphyry are abundant in the southern part of Mt. Seemore.

Oikocrystic amphibole porphyry is characterized by 5 - 15% amphibole grains that poikolitically enclose minute quartz and feldspar from the matrix. Aegirine, opaque minerals and aenigmatite are also found as oikocrysts. Oikocrysts commonly range from 1 to 5 mm across and consist of several rectangular-shaped grains of amphibole in a flower-like aggregate. The matrix is commonly very fine grained to aphanitic and consists of recrystallized grains, but is also coarser grained in some localities. Similar amphibole oikocrysts are locally found in some feldspar-quartz-amphibole porphyries. The oikocrystic amphibole porphyry, in some places, contains lenticular bands and other features common in ash-flow tuffs, indicating that some occurrences are probably highly welded and compacted ash-flow tuff.

Phenocryst-poor ash-flow tuff and tuff-breccia is chacteristically either devoid of phenocrysts or contains less than 10% small (< 2 mm across) phenocrysts of quartz and feldspar. The tuff-breccia at the southern end of Mt. Seemore is aphyric and consists of layered ignimbritic fragments in a recystallized matrix of similar composition and colour. The ash-flow tuff from the northern end of Mt. Seemore is characterized by quartz and plagioclase feldspar phenocrysts and abundant coarser lenticular bands in a very fine grained recrystallized matrix; rare very fine grained granophyric rock fragments are also present. These phenocryst-poor ash-flow units are fairly similar to those found in the Little Pond Brook volcanic suite.

Feldspar-quartz ash-flow tuff is characteristically a red-brown colour, aphanitic to very fine grained and contains 20 to 40% phenocrysts. Feldspar phenocrysts, commonly both plagioclase and microperthite, range in size from 1 to 5 mm in size and from 20 to 40% of the rock. Quartz phenocrysts are normally less than 2 mm across and range from 3 to 8% of the rock. Broken phenocrysts and embayed quartz grains are rare to common. The matrix is normally very fine grained and recrystallized. Rock fragments are sparsely found.

Feldspar-quartz-amphibole ash-flow tuff is characterized by the presence of amphibole, in oikocrysts or as single grains, a very fine grained to fine grained matrix, broken phenocrysts and a beige to orange-brown colour. The feldspar phenocryst-rich (> 60% phenocrysts) variety commonly contains a granophyric or relatively coarse grained feldspar-quartz recrystallized matrix; in some samples matrix material has recrystallized onto feldspar and quartz phenocrysts. The normal subvariety, in contrast, commonly

contains less than 45% phenocrysts and has a finer grained matrix. Granophyric fragments are rarely found in both subvarieties.

Results

The geochemical data from the Sheffield Lake area targets are tabulated in Appendix B-3 and the averaged data for several petrographic groups are displayed in Appendix C-3. Four geochemical units can be defined with the Zr data: 1) amphibole Porphyritic ash-flow tuff (1250 - 1650 p.p.m), 2) Feldspar-quartz-amphibole (FQA-1) porphyritic and Aphyric ash-flow tuff (1000 - 1150 p.p.m.), 3) Feldspar-quartz-amphibole (FQA-2) porphyritic ash-flow tuff (660 - 750 p.p.m.), and, 4) Feldspar-quartz ± amphibole porphyritic ash-flow (380 - 560 p.p.m.).

Discussion

All samples plot in the A-type field of Whalen et al (1987) in the same region as samples from the LPB volcanic suite and the GTG. Similarly, many samples from the Sheffield Lake targets are mildly peralkaline or nearly peralkaline; alkali loss from ash-flow tuffs may be the cause of A.I. being < 1 for some of these samples.

Further comparison of the Sheffield Lake samples with the LPB and GTG samples indicates: 1) the FQA (1) porphyritic ash-flow tuff at Sheffield Lake and LPB are very similar, 2) the FQA (2) porphyritic ash-flow tuff at Sheffield Lake and LPB and the QF porphyritic ash-flow tuff from LPB are very similar, 3) the trace element signatures of the F porphyritic ash-flow tuff from LPB and the FQ±A porphyritic ash-flow tuff from the Sheffield Lake area are similar - the major elements are somewhat different, and, 4) amphibole porphyritic ash-flow (Mt. Seemore) was not observed in the other two areas.

The occurrence of mildly peralkaline porphyritic ash-flow tuffs and related rocks in the Sheffield Lake area indicates that this area has the right environment for rare-metal mineralization. However, the lack of extremely high rare-metal values in the samples studied suggests that the wasn't a viable concentration mechanism operative to form rare-metal mineralization.

The A porphyritic ash-flow tuff on the southern portion of the Mt. Seemore target has the highest values of rare-metals observed in the TIS area. Values of rare-metals, in particular Zr and Y, are much higher than average for A-type rocks (Whalen et al. 1987)

but comparison with rocks associated with the Strange Lake and Letitia Lake area rare-metal deposits suggests that the values are not high enough.

Conclusions

Ash-flow tuffs in the Mt. Seemore and North Hill areas have rare-metal values similar to or higher than those from the LPB volcanic suite and the GTG. Amphibole porphyritic ash-flow tuffs are anomalously high in Zr and Y but mineralized samples were not observed. The further differentiation of the magma responsible for the amphibole porphyritic ash-flow tuff could produce such mineralization. Thus the area around the occurrence of amphibole porphyritic ash-flow tuffs has medium potential for rare-metals but surrounding areas in the Sheffield Lake targets have low potential. However, the small occurrence of amphibole porphyritic ash-flow tuffs severely limits the size of the target.

3.0 Eastern Baie Verte Peninsula

Introduction

The Baie Verte Peninsula (BVP) is located in west-central Newfoundland between White Bay on the west and Notre Dame Bay on the east (Figure 1-2). The suites studied from the BVP are all located east of the Baie Verte-Brompton Line.

Three suites were chosen as reconnaissance targets to evaluate the rare-metal potential of the peralkaline and related rocks on the BVP. The Cape St. John Group target occurs in the northern part of the BVP and consists of mafic-felsic volcanic rocks, the Cape Brule porphyry and the Seal Island Bight granite. The Micmac Lake Group consists of mafic and felsic volcanic rocks and is found in the south-central part of the peninsula. The final target, the Kings Point Complex, is a composite volcano-plutonic complex located in the south-eastern part of the BVP. The peralkaline and related rocks in these three areas fit the criteria as potential sources of rare metals.

The Cape St. John Group (CSJ) and related rocks outcrop over an area of approximately 400 km^2. A total of 74 samples were collected with seven road and foot traverses - 38 of these were analysed. The aim was to obtain widespread representative samples covering a large part of the outcrop area.

The Micmac Lake Group (MLG) forms a belt approximately 65 km long and < 1 - 5 km wide; sampling was carried out on the north-central part of the belt where the width ranges from 1 - 3 km. A total of 10 samples were collected, five of which were analysed, from roadside outcrops during a one day period. The aim of the sampling strategy was to determine the overall geochemical character of the felsic volcanic rocks of the MLG and to evaluate their potential as rare-metal sources.

The Kings Point Complex (KPC) covers approximately 210 km^2 and consists of a large number of subvolcanic-hypabyssal and volcanic phases. This complexity and the potential for rare-metal mineralization singled out the KPC for a more extensive mapping and sampling program. A total of 34 mapping-sampling traverses were carried out by woods road and foot traverse to give a complete geographical coverage of the KPC during parts of the 1990, 1991, and 1992 field seasons. Areas of enhanced peralkalinity were mapped and sampled in more detail during 1991 and 1992. This sampling program collected 304 samples for thin sectioning and 224 samples which were analysed. The most peralkaline volcanic rocks of this complex were the main target of this sampling program once they had been identified and mapped.

General Geology

The Cape St. John Group and related rocks, Micmac Lake Group and Kings Point Complex all belong to a group of Silurian plutons and related bimodal volcanic rocks (Hibbard 1983, Coyle and Strong 1987, Whalen et al. 1987) that occur in the Notre Dame subzone of the Dunnage lithotectonic zone (Williams et al. 1988). The Baie Verte Peninsula rocks occupy an area, approximately 90 km long, in the northern portion of the Notre Dame subzone. The Springdale Group and the Topsails Igneous Suite, to the south, are roughly correlative with these rocks (Coyle and Strong 1987, Whalen et al. 1987).

The host rock of the MLG, the Cape Brule Porphyry (CSJ) and the KPC is the Burlington Granodiorite (Hibbard 1983) which is approximately 440 - 460 Ma (Hibbard 1983, Dallmeyer and Hibbard 1984). Radiometric ages of the target rocks indicate that they are Silurian or younger: Cape St. John Group - 427 Ma (U/Pb zircon; Coyle 1990), Kings Point Complex - 427 Ma (U/Pb zircon; Coyle 1990), Micmac Lake Group 362±15 (Rb/Sr whole rock; Pringle 1978), Seal Island Bight Granite - 414 to 435 Ma (U/Pb zircon; Hibbard 1983). Field relationships indicate that the Seal Island Bight Granite is younger than the Cape St. John Group and the Cape Brule Porphyry is contemporaneous with the Cape St. John Group. The Micmac Lake Group unconformably sits on the Burlington Granodiorite and is considered younger than the KPC (KPC pebbles in MLG conglomerate - Coyle and Strong 1987).

Parts of the Kings Point Complex (427 Ma - Coyle 1990) are interpreted to be contemporaneous with the upper portion of the nearby Springdale Group (Coyle and Strong 1987), which is 429 - 432 Ma (Chandler et al. 1987, Whalen et al. 1987, Coyle 1990). A correlation has also been made between the KPC and the Topsails Igneous Suite (Coyle and Strong 1987) based on a structural reconstruction (Coyle and Strong 1987), the age of some members of the Topsails Igneous Suite (427 Ma and 429 Ma - U/Pb zircon; Whalen et al. 1987) and the KPC (427 - Coyle 1990), and the relationship between the Topsails Igneous Suite (TIS) and the Springdale Group (TIS intrudes Springdale Group - Whalen et al 1987), and relationship between the Springdale Group and the KPC (see above). The nearly contemporaneous ages of these suites suggest a tectonic and petrological connection and may have some bearing on the potential for rare-metal mineralization.

3.1 Cape St. John and related rocks

Introduction

The Cape St. John Group and related rocks (CSJ) consists of the Cape Brule Porphyry, the Seal Island Bight Granite and the Cape St. John Group volcanic rocks. These rocks are located on the north-eastern tip of the BVP near the communities of La Scie, Woodstock and Nippers Harbour (insular Newfoundland; Figure 1-2). The age correlation with the KPC and the TIS to the south (Coyle and Strong 1987), the occurrence of peralkaline granite (DeGrace et al. 1976; Hibbard 1983) and the presence of felsic volcanic rocks with peralkaline trace element affinities (DeGrace et al. 1976) indicate that there is some potential for rare-metal mineralization in the CSJ. This potential was evaluated during a seven day geological mapping and lithogeochemical sampling program.

The entire work area was accessible by road. The Cape Brule Porphyry was sampled on two road transects, the Seal Island Bight by one foot traverse, and the Cape St. John Group by three road transects and three short foot traverses.

Samples were collected from a total of 74 sample sites (CJ90001 to CJ90074); thin section samples were collected from all 74 sites and geochemical samples were collected from 73 of these sites. A suite of 38 geochemical samples were analysed for major elements and a group of trace elements, including rare metals. The sample locations (NTS coordinates), rock type and other data (e.g. scintillometer readings) are given in Appendix A-4.

Geology

The Cape St. John Group (DeGrace et al. 1976; Hibbard 1983) consists of a sequence of subaerial volcanic flows and pyroclastic rocks up to 3500 m thick. Five units have been described (DeGrace et al. 1976): 1) sandstone and conglomerate (basal unit), 2) mafic flows and pyroclastics, 3) quartz-feldspar crystal tuff, 4) andesitic to dacitic pyroclastic rocks and flows, and, 5) rhyolitic and trachytic ash-flow tuffs (upper unit). Samples were collected mainly from the uppermost unit due to its widespread occurrence and the abundance of felsic ash-flow tuffs. The majority of the rocks in the upper unit consist of aphyric to [feldspar + quartz]-poor ash-flows. These rocks contain 0 - 10% quartz + feldspar (plagioclase or microperthite) phenocrysts, commonly up to 3 mm across, in an aphanitic to very fine grained recrystallized matrix. Layering, rare broken

feldspar grains, lenticular zones and ghost fiammé are observed and suggest an ash-flow origin for many of these rocks. Quartz and carbonate veins and pods are common.

The Cape Brule Porphyry consists of anhedral, resorbed and recrystallized quartz phenocrysts (< 5 - 30%), which are commonly 1 to 3 mm across, and subhedral and broken feldspar phenocrysts (< 5 - 40%), which range from 1 to 6 mm across. The matrix is commonly fine to very fine grained and consists of chlorite, magnetite, amphibole, carbonate, quartz and feldspar grains < 0.5 mm across; one sample has a granophyric matrix. The feldspar phenocrysts are dominantly microperthite but plagioclase phenocrysts, which are usually smaller, are commonly observed. The common occurrence of resorbed quartz and broken quartz and feldspar grains indicate that the Cape Brule Porphyry may be, in part, an extrusive crystal-rich ash-flow tuff; this is in agreement with Hibbard (1983) who observed ash-flow textures, including columnar joints and layering in portions of the Cape Brule Porphyry.

The Seal Island Bight Granite (formerly called a syenite by DeGrace et al. 1976 and Hibbard 1983) is a fine to medium grained (1 - 3 mm grainsize) peralkaline granite. It contains 45 - 80 % subhedral perthitic feldspar, with minor plagioclase, 15 - 30 % anhedral quartz and < 5 % mafic minerals. The mafic minerals include riebeckite, aegirine and magnetite. This intrusion forms a circular outcrop area of approximately 4 km^2 at the far eastern end of the study area.

Results

Spectrometer data for the samples collected are listed in Appendix A and summary statistics for the main rocks types are listed in Table 3-1. The range of total count readings for the felsic rocks is 210 to 480 cps. Comparison of these values with those from mineralized peralkaline rocks in Labrador (Introduction Table ??) indicates that based on radioactivity these rocks have low potential for rare-metal mineralization.

Table 3-1 Summary Spectrometer Data

Rock Type	Average	Range	Number
Aphyric (2)	335	250 - 460	4
Per Gran	269	240 - 295	4
QF Porph	318	210 - 480	29
Mafic flow	200	120 - 260	4

The geochemical data for the CSJ rocks are listed in Appendix B-4 and the averages and unique sample values are tabulated in Appendix C-4. Zr and other trace elements can be used to divide the aphyric ash-flows into two groups: 1) low-Zr group with 112 - 460 ppm, and, 2) high-Zr group with 529 - 648 ppm. A good correspondence is observed in geochemical values between the high-Zr aphyric ash-flows and the Seal Island Bight granite, and between the Cape Brule Porphyry and the low-Zr aphyric ash-flows.

The highest rare-metal values observed in the CSJ data set are observed in the high-Zr aphyric ash-flows and the Seal Island Bight Peralkaline granite in which Zr is up to 692 ppm and Y up to 79 ppm; these are relatively low values.

Discussion

The rocks from all three portions of the CSJ area, in particular the intrusive rocks, can be classified as A-type (Whalen et al. 1987); the Seal Island Bight granite was used by Whalen et al. (1987) to define their A-type field. The Seal Island Bight granite is mildly peralkaline, whereas the correlated high-Zr aphyric ash-flows are slightly non-peralkaline - this may be due to alkali loss in the volcanic rocks.

The high-Zr aphyric ash-flows, which are geochemically correlated with the Seal Island Bight granite, are also spatially associated with the granite suggesting that they may be extrusive products of the Seal Island Bight magmatic system. The correspondence, both geochemically and spatially, of the Cape Brule porphyry and many of the low-Zr ash-flow tuffs also suggests a close magmatic relationship between these rocks. These correlations suggest that there was a peralkaline source (Seal Island Bight) in the eastern part of the belt and a non-peralkaline source (Cape Brule) in the western part of the belt that was producing contemporaneous ash-flow tuffs.

Comparison of the CSJ averaged data with that from the Topsails Igneous Suite indicates some correspondence between the Seal Island Bight granite, the Gaff Topsails granite and some QF porphyries in the Topsails Igneous Suite. These similarities further confirm the tentative temporal correlation and further suggest similar tectonic settings.

Conclusions

All data collected indicate that these rocks have a low potential for rare-metal mineralization. These rocks are in the right environment for rare-metal mineralization but the concentrating processes were not operative at the erosion level sampled. Thus, the Cape St. John Group and related rocks are not good targets for rare metals.

3.2 Micmac Lake Group

Introduction

The Micmac Lake Group (MLG) occurs as a thin belt, < 1 - 6 km wide, which extends from just north of Flatwater Pond to Birchy Lake in the south-central part of the BVP (insular Newfoundland; Figure 1-2). The presence of trachytic and rhyolitic ash-flow tuffs in this group in association with mafic flows (Hibbard, 1983) indicate that there is some potential for rare-metal mineralization in the MLG. This potential was evaluated with a one day geological mapping and lithogeochemical sampling reconnaissance program.

The entire work area was accessible by woods access roads from the Baie Verte Highway. Rocks along three roads running perpendicular to the MLG strike were sampled in this program.

Samples were collected from a total of 10 sample sites (ML90001 to ML90007; KP90104 to KP90106); thin section and geochemical samples were collected from all 10 sites. A suite of four geochemical samples were analysed for major elements and a group of trace elements, including rare metals. The sample locations (NTS coordinates), rock type and other data (e.g. scintillometer readings) are given in Appendix A-5.

Geology

The Micmac Lake Group has been divided into a Lower Sequence and an Upper Sequence (Hibbard, 1983), which are separated by a prominent erosional surface. The Lower Sequence is characterized by aphyric ash-flows and rhyolite flows, whereas the Upper Sequence is characterized by quartz-feldspar porphyritic ash-flows, mafic flows and red conglomerate. The Lower Sequence occurs in the eastern part of the outcrop area, is up to 750 m thick and unconformably overlies the Burlington Granodiorite (Hibbard, 1983). The Upper Sequence is up to 1150 m thick and occurs in the western portion of the outcrop area (Hibbard, 1983).

Samples collected from the Lower Sequence are aphyric or phenocryst-poor ash-flow tuffs (< 8 % quartz + feldspar) characterized by oikocrystic amphibole (altered to opaques in some samples) in the groundmass and ash-flow textures. The Upper Sequence samples range from phenocryst-rich (10 - 30% feldspar + quartz) to aphyric ash-flow tuffs; two samples of red conglomerate where also collected.

Results

Spectrometer data for the samples collected are listed in Appendix A-5. The total count readings range from 95 (mafic flow) to 410 (aphyric ash-flow) cps. Comparison of these values with those from rare-metal showings, indicates that the Micmac Lake rocks have low potential for rare-metals.

The geochemical data for the MLG are listed in Appendix B-5. The first two samples (ML90003, ML90004) have been tentatively assigned to the Upper Sequence and the last two samples belong to the Lower Sequence (ML90005, ML90006).

The highest rare-metal values observed in the MLG data set are observed in the Lower Sequence ash-flow tuffs where Zr is near 1500 ppm and Y values are from 117 - 158 ppm. One of the Upper Sequence samples is extremely low in rare metals (e.g. Zr 91 ppm) and the other has moderate values (e.g. Zr 610 ppm).

Discussion

All analysed members of the Lower Sequence and one of those from the Upper Sequence plot in the anorogenic or A-type granite field of Whalen et al. (1987) suggesting a similar environment between these rocks and those from the Topsails Igneous Suite and the Cape St. John area.

The oikocrystic amphibole-bearing comenditic ash-flows from the Lower Sequence are very similar in chemistry and mineralogy to the amphibole porphyritic ash-flows found at Mt. Seemore (30 km to the SW) in the Sheffield Lake area. This suggests that the MLG has a similar tectonic environment and, perhaps, a similar age as the Sheffield Lake rocks (Topsails Igneous Suite).

Coyle et al. (1985) correlated the Sheffield Lake volcanic rocks (informally called the Sheffield Lake Group - Coyle et al. 1985) with the Springdale Group. Whalen and Currie (1988) also correlated these rocks and the Micmac Lake Group with the Springdale Group; all called the Springdale Group in their map. This implies a similar age for these rocks as well as a similar tectonic setting and agrees with the geochemical similarities outlined above.

Conclusions

All data collected indicate that the Upper Sequence of the MLG has a low potential for rare-metal mineralization, similar to that of the Cape St. John Group. The Lower

Sequence of the MLG exhibits higher than average rare-metal values and its comenditic chemistry indicates that there are large amounts of rare-metals in the magmatic system. Evidence of a magma chamber in which rare-metals could have been concentrated is lacking and thus the rare-metal concentrations of the observed ash-flows are not extremely high.

The Lower Sequence of the Micmac Lake Group has a moderate potential for rare-metals, however the small extent and absence of a caldera structure makes the discovery of rare-metal mineralization difficult.

3.3 Kings Point Complex

Introduction

The Kings Point Complex (KPC - Mercer et al. 1985) consists of a series of peralkaline to metaluminous volcanic, hypabyssal and plutonic rocks. These rocks are located on the southeastern portion of BVP near the communities of Kings Point, Middle Arm and Burlington (insular Newfoundland; Figure 1-2). The age correlation with the MLG to the west, the TIS to the south and the CSJ to the north (Coyle and Strong 1987, Hibbard 1983) and the occurrence of peralkaline intrusions and volcanic rocks (Mercer et al. 1985, Kontak and Strong 1986) indicate that there is potential for rare-metal mineralization in the KPC. This potential was evaluated during a 34 day geological mapping and lithogeochemical sampling program carried out over three years.

Much of the work area is accessible by woods access roads in variable conditions. Samples were collected along the woods access roads and from foot traverses into the interior of the complex. This program was designed to initially (in 1990) collect samples from all areas and all units of the KPC. Follow-up and more detailed studies were carried out in 1991 and 1992 to sample and map the areas of peralkaline ignimbrites - these ignimbrites having the best potential for rare metals.

Samples were collected from a total of 304 sample sites (KP90001 to KP90176; KP91001 to KP91073; KP92001 to KP92055); thin section samples were collected from all 304 sites and geochemical samples were collected from 269 of these sites. A suite of 224 geochemical samples were analysed for major elements and a group of trace elements, including rare metals; a representative suite of samples were also analysed for REE. The sample locations (NTS coordinates), rock type and other data (e.g. scintillometer readings) are given in Appendix A-6.

Geology

The Kings Point Complex (Mercer et al. 1985) consists of a sequence of felsic subaerial ash-flows, which are at least 900 m thick, and a suite of felsic hypabyssal to subvolcanic intrusive rocks (Mercer et al. 1985, Kontak and Strong 1986, this study). The host rocks mainly consist of the Burlington Granodiorite, with minor mafic flows that have been correlated with the Betts Cove Ophiolite (Hibbard 1983, Mercer et al 1985). The east-central and south-eastern border of the KPC is bounded by the Green Bay Fault (Hibbard 1983). Figure 3-1 illustrates the generalized geology of the KPC as compiled

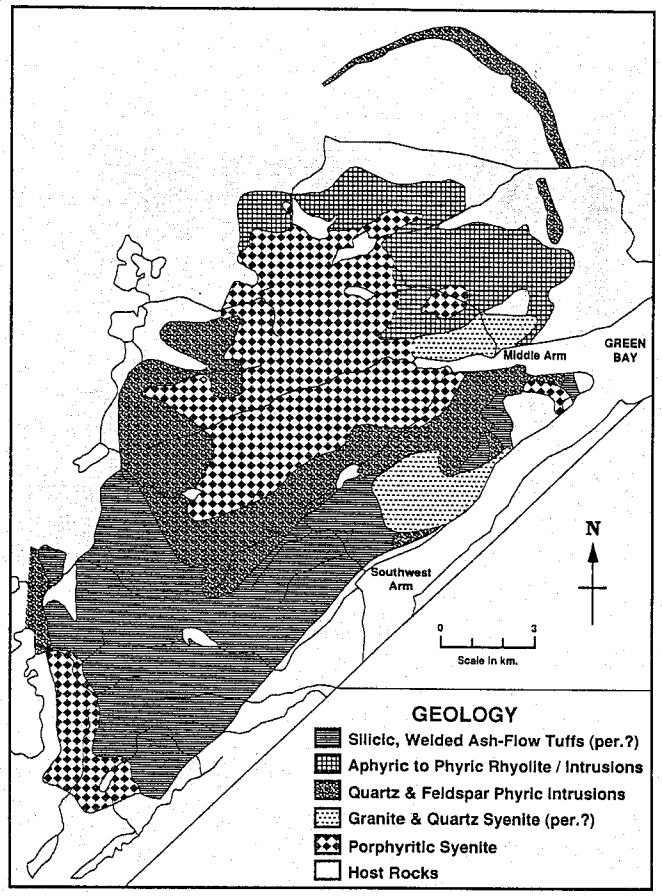

Figure 3-1 *General geology of the Kings Point complex (after Mercer* et al., *1985; Kontak and Strong, 1986).*

from Mercer et al. (1985), Kontak and Strong (1986), Coyle and Strong (1988), Prior (1988) and the mapping in this study.

The intrusive rocks of the KPC are quite variable in texture and composition but two main phases can be recognized: F±Q Porphyritic Syenite (Unit 3), and Medium grained to Fine grained Granite (Unit 4). The intrusive relationships between these two units were not directly observed and are thus uncertain although some geochemical evidence suggests that Unit 4 may be the oldest. Based on the field evidence, the relationship between the intrusive rocks and the volcanic rocks is also uncertain.

The volcanic rocks have been divided into three units and several subunits based on field and geochemical criteria (oldest to youngest): Lower Unit (5), Middle Unit (6) and Upper Unit (7). The Lower Unit (Unit 5) consists of over 50 m of aphyric to QF-porphyritic ash-flow tuff, -lapilli tuff and -breccia. The Middle Unit (Unit 6) consists of at least 370 m of aphyric to sparsely porphyritic ash-flow tuffs (6A), QF±A porphyritic ash-flow tuffs (6P), and amphibole-bearing ash-flow tuffs (6AAf). The Upper Unit (Unit 7) consists of aphyric (7A) to QF porphyritic (7P) ash-flow tuffs and breccias, and coarser grained, possibly intrusive, equivalents (7PG).

Each unit of the KPC will be discussed in more detail in the following sections.

Unit 3 - F±Q Porphyritic Syenite. This intrusive unit occupies approximately 25 % of the present outcrop of the KPC and occurs as one large, irregularly shaped, body with a series of satellite bodies (≈ 60 km^2), located in the north-central part of the complex, and a smaller body in the southern part. It ranges from feldspar-porphyritic syenite to feldspar±quartz porphyritic quartz syenite and granite (also see Kontak and Strong 1986); less commonly non-porphyritic equivalents are observed. It usually contains < 5% rounded to subrounded fine grained mafic inclusions (< 5 cm across; rarely up to several m in size).

This unit is characterized by 10 - 30 % subhedral feldspar phenocrysts, more rarely up to 45 %, which range in size from 3 - 10 mm. Microperthite is commonly the dominant feldspar but minor plagioclase is not uncommon. Up to 5 % quartz phenocrysts, less than 4 mm across, are sparsely found in some outcrops. The matrix is commonly granophyric and graphic granite-textured quartz and feldspar with accessory magnetite, pale clinopyroxene (augite to titanaugite) and amphibole are the observed minerals. Inclusions are usually very fine grained, but rare coarser grained inclusions contain plagioclase feldspar and clinopyroxene.

Unit 4 - Medium grained to Fine grained Granite. This unit occurs as a series of four small bodies, ranging in size from 1 - 3 km^2, which are located along the eastern contact of the complex. The two southerly bodies and the most northerly are dominated by massive fine grained granite with subordinate medium grained granite. The other body is mainly medium grained granite. The fine grained granite rarely contains mafic very fine grained inclusions similar to those found in Unit 3. In one locality, Unit 3 contains inclusions of quartz-feldspar porphyry (Unit 6?), thus Unit 3 is in part younger than Unit 6.

The fine grained granite consists of 75 to 95 % feldspar, commonly less than 2 mm, less than 5 to 25 % quartz up to 3 mm in size, and 3 - 8 % amphibole less than 1 mm in size. Feldspar occurs as single grains of microperthite and plagioclase or in massive granophyric / graphic granite-textured quartz-feldspar intergrowths. In some cases, microperthite and / or plagioclase phenocrysts are found in a granophyric matrix; spherulitic textures are rarely found.

Unit 5 - Lower Unit. The aphyric to QF-porphyritic ash-flows of this unit are stratigraphically the lowest of the volcanic units and occur in the smallest outcrop area, however the distribution is widespread throughout the complex. They occur in a well defined unit in the northeastern part of the complex and in scattered occurrences in the south-central and southern part of the complex. The distribution of this unit is difficult to establish because its tuffaceous members are not easily distinguished by field criteria from some members of Unit 6 and 7. The stratigraphic location and chemical data have been used to identify outcrops of Unit 5; the stratigraphy of the south-central occurrences is not well established due to probable fault complications.

In the northeastern occurrence, the Lower Unit is dominantly a feldspar-quartz porphyritic ash-flow tuff to breccia consisting of up to 40% fragments which range in size from < 1 to 30 cm. Fragments consist of subangular to subrounded aphyric flows, quartz-feldspar porphyry or granite (Burlington Granodiorite ?). The south-central occurrence is a plagioclase, k-feldspar and quartz porphyritic ash-flow tuff.

Unit 6 - Middle Unit. The members of this unit outcrop in over 25% of the area of the complex. They are quite varied in texture, ranging from aphyric to sparsely porphyritic (6A), to porphyritic (6AAf, 6P). All outcrops display an aphyric groundmass (6A, 6P, 6AAf) and are interpreted to be mostly ash-flow units or related to ring dykes and ring dyke vents.

The quartz-feldspar porphyritic ash-flows (Unit 6P) are found in two main areas, a subcircular area in the northeastern part of the complex (White Hills area) and an elongate area in the southern portion of the complex (Bartlett Creek area). These rocks range from phenocryst-poor (5 - 10%) to phenocryst-rich (30 - 45%) units with an aphyric groundmass. Microperthitic feldspar is the most common phenocryst (up to 40 %) and quartz (3 - 15 %) and amphibole (0 - 15 %) are less abundant. Phenocrysts are commonly broken and range from 1 to 4 mm in size. The matrix is usually recrystallized and exhibits ash-flow textures such as fiammé and layering.

The amphibole-bearing ash-flows (6AAf) are characterized by the occurrence of oikocrystic phenocrysts or aggregates of black amphibole and the absence or presence of subordinate amounts of quartz and feldspar phenocrysts. Overall, the texture ranges from highly welded and compacted, layered, ash-flows to oikocrystic amphibole and red-spotted, more massive, flows to massive or layered aphyric flows with fine grained amphibole and aegirine microphenocrysts in the groundmass. The amphibole commonly occurs as grains up to 1 mm in size, which occur in aggregates or as oikocrystic grains and aggregates of grains up to 2 mm across. Aegirine is commonly subhedral and occurs as single grains up to 0.2 mm across. Quartz and feldspar phenocrysts are sparsely found. Ash-flow textures are commonly found in most occurrences. The red spots observed in outcrop appear to be zones of very fine grained secondary hematite in the matrix, which may be pseudomorphing an unknown mineral.

Amphibole-bearing ash-flows have been the focus of the detailed follow-up work in the KPC due to their medium-high potential for rare-metal mineralization. Five areas, identified here as the Bartlett Creek, Upper Rattling Brook, Water Supply Lake, Middle Arm Point and White Hills areas were mapped and sampled in detail. These ash-flows form at least two partial ring structures, one in the White Hills area and one in the Bartlett Creek area; small ring segments are found in the Middle Arm Point and Water Supply Lake areas and a larger straight line segment is found on the southern flank of Middle Arm Bay. All of these areas generally contain the same textural varieties of Unit 6AAf, although the arrangement of these varieties, the attitude of the bedding and the relationships with the nearby units are commonly difficult to generalize. Contact relationships in the Middle Arm Point and the Upper Rattling Brook area indicate that 6AAf is intrusive into the overlying FQA porphyritic ash-flows (Unit 6P). In many localities 6AAf units dip very steeply (50 - 90%). These contact, stratigraphic and other relationships suggest that many of the amphibole ignimbrites are formed within a ring dyke or near the vent site of the ring dyke system. These locations should contain the products of low volume eruptions with higher potential for rare-metal mineralization.

Large thicknesses, up to 350 m, of aphyric to sparsely porphyritic members of Unit 6 (6A) are closely associated with the amphibole-bearing ash-flows (6AAf) in the White Hills and the Bartlett Creek areas; smaller thicknesses (commonly < 10 m) are associated with the Upper Rattling Brook and Water Supply Lake occurrences. These members commonly display fiammé and compaction features characteristic of ash-flow tuffs; sparse, very fine amphibole grains are also observed in some outcrops. Stratigraphic relationships indicate that these ash-flows are generally higher in the stratigraphy than the occurrences of Unit 6P.

Unit 7 - Upper Unit. The Upper Unit generally consists of aphyric (7A) to QF porphyritic (7P) ash-flow tuffs and breccias and possible intrusive equivalents (7PG). Many of these rocks are difficult to distinguish from rocks of similar texture in Unit 6, however radiometric readings and geochemistry readily distinguishes between samples and outcrops of both units. Unit 7 forms an almost complete concentric ring surrounding the main feldspar-porphyritic syenite body and the associated satellite bodies (Unit 3). It also occurs as two elongate bodies, one in the southern part of the complex and the other on the southeastern boundary. The total estimated thickness of this unit is at least 600 m.

Most of Unit 7 outcrops in the concentric ring contain porphyritic ash-flow tuffs with an aphanitic to fine grained groundmass. Many localities in this concentric ring (e.g. Cross Country Pond and Upper Rattling Brook areas) may be intrusive equivalents of Unit 7P (Unit 7GP) or were formed in the interiors of thick, hot, ash-flows or in the core of ring dykes; these may be best termed hypabyssal rocks. Kontak and Strong (1986) favour an intrusive relationship with a gradational contact between Unit 7 and Unit 3. This unit is characterized by 20 - 35 % microperthitic feldspar and 5 - 15 % quartz phenocrysts from 1 to 4 mm across. Oikocrystic amphibole, anhedral amphibole and rarely clinopyroxene occur as grains up to 1 mm across and in quantities up to 5 %. Broken crystals, resorbed quartz, fiammé and compaction features indicate that most occurrences are ash-flow tuffs.

Aphyric ash-flow tuffs and breccias (7A) are most common in the southeastern body. They are characterized by the general absence of phenocrysts and a very fine grained, recrystallized, matrix. Aphyric fragments, spherulitic textures in the matrix and some ash-flow textures such as fiammé are also found.

Structure. The overall structure of the complex is fairly complicated, but the suggestion that it is probably a ring complex associated with caldera collapse (Hibbard 1983 and references therein, Coyle and Strong 1987, Mercer et al 1985) has been confirmed in this

study. The newly defined volcanic stratigraphy suggests that the KPC is most likely composed of several nested calderas with a large central resurgent intrusion.

Individual calderas are inferred from ring dykes which are defined, in part, by the occurrence of amphibole-bearing ash-flows and dykes of Unit 6AAf. These rocks define at least one partial caldera in the White Hills area (5 x 4 km), one in the Bartlett Creek area (4 x 4 km) and the segments of one or two others in the Middle Arm Point and Water Supply Lake areas. The large ring dyke on the northern end of the complex may also outline another caldera, this being at least 10 x 10 km in dimension; other calderas are likely but poorly defined. The position of the Unit 3 Porphyritic Syenite in a central part of the complex suggests that this intrusion may represent a resurgent intrusion into the previously formed and down faulted volcanic sequence. Unit 4 syenite and granite occurs as small intrusions located on, or near the Green Bay fault and may be younger rocks associated with the fault-forming tectonic activity.

The timing between the volcanic rocks of Unit 6 and Unit 7 is very uncertain. Ring dyke amphibole-bearing ash-flow tuffs (Unit 6AAf) are intrusive into Unit 7 porphyries (7P) in some localities (e.g. Middle Arm Point) suggesting that some of Unit 6 is younger than Unit 7. However, Unit 7 porphyries (7P) are topographically and in some cases stratigraphically (?) above Unit 6 rocks. The paucity of outcrop in some areas makes it very difficult to determine the stratigraphy and to recognize faults or other structural elements which may complicate the map pattern. Some of the conflicting evidence may be indicative of contemporaneous deposition of Unit 6 and Unit 7.

Results

Spectrometer data for the samples collected are listed in Appendix A-6 and summary statistics for the main rocks types are listed in Table 3-2. The range of total count readings for the felsic rocks is 210 to 660 cps; one anomalous sample gave a reading of 2500 cps. Comparison of these values with those from mineralized peralkaline rocks in Labrador (Table 1-3, 1-4) indicates that, based on radioactivity, these rocks, with the exception of the anomalous value from the pegmatite vein, have low to medium potential for rare metals. The pegmatite vein spectrometer data indicate very high potential for rare-metal mineralization. Note that the radiometric average data for the rock types clearly subdivide volcanic rocks of Unit 6 (400 - 476 cps) from those of the plutonic rocks (245 - 369 cps) and those of the other volcanic units (Unit 5 and 7; 264 - 353 cps).

Table 3-2 Summary Spectrometer Data

Unit	Average	Range	Number
3	245	210 - 280	12
4	369	325 - 420	5
5	353	310 - 400	4
6A	476	370 - 660	10
6AAf	470	360 - 630	36
6P	413	400 - 440	7
6P(3)	401	260 - 580	18
7A	309	230 - 420	7
7P(1)	264	220 - 500	19
7P poor	315	220 - 570	13
P(2)	323	220 - 570	6
P±A	288	250 - 350	6
Peg vein	2500	-	1

The geochemical data for the KPC rocks are listed in Appendix B-6 and the averages and unique sample values are tabulated in Appendix C-6. Zr and other trace elements can be used to divide the volcanic rocks into Units 5, 6 or 7 and to subdivide each unit: 1) Unit 6AAf is defined by Zr averages of 1400 - 1600 ppm, 2) Unit 6A is defined by a Zr average of 1344 ppm, 3) Unit 6P is defined by Zr averages of 821 - 1324 ppm, 4) Unit 7A is defined by Zr averages of 317 - 350 ppm, 5) Unit 7P is defined by Zr averages of 522 - 640 ppm, and, 6) Unit 5 is defined by a Zr average of 121 ppm. Unit 3 plutonic rocks have Zr values of 489 - 524 ppm and Unit 4 granites have an average value of 189 ppm Zr.

The highest rare-metal values observed in the KPC data set are observed in Unit 6 amphibole-bearing ash-flow tuffs, in which individual values range from 1188 to 1611 ppm Zr and 96 to 212 ppm Y. These values, particularly the Zr values, are very anomalous for rare metals but are not indicative of rare-metal mineralization.

Discussion

Most of the rocks from the Kings Point Complex, in particular the intrusive and porphyritic rocks (Unit 3, 6, and 7), can be classified as A-type (Whalen et al. 1987). The volcanic rocks of Unit 5 and the fine grained plutonic rocks of Unit 3 are metaluminous rocks and not considered related to A-type rocks.

The occurrence of fine grained mafic inclusions in Unit 3, the presence of mafic dykes throughout the complex and other evidence lead Kontak and Strong (1986) to suggest that there may have been felsic and mafic magma mixing in the KPC magma chamber. This conclusion may also be applied to parts of Unit 4 which also contains similar mafic inclusions.

Both Kontak and Strong (1986) and Mercer et al. (1985) have suggested that the peralkalinity of Unit 6 and 7 is due to metasomatic processes connected to the mildly peralkaline feldspar-porphyritic syenite (Unit 3) and possible intrusive equivalents of QF porphyries, particularly in Unit 7). The data collected from this study indicate that metasomatism was not responsible for the peralkalinity of the volcanic rocks. Some lines of evidence that are used to indicate a magmatic origin for these rocks are: 1) the great thickness of Unit 6 ash-flows, 2) the presence of single magmatic amphibole grains in many ash-flows in Unit 6, 3) the consistent chemistry of amphibole-bearing ash-flows (Unit 6AAf), aphyric rocks (Unit 7A) and porphyries (Unit 7P) in widespread areas and within single outcrops, 4) the consistent stratigraphy of amphibole-bearing ash-flows (Unit 6AAf), aphyric rocks (Unit 7A) and porphyries (Unit 7P) in widespread areas and within single outcrops, 5) evidence for the intrusion of peralkaline ring dykes into the volcanic pile, 6) the lack of cross-cutting alkali-rich hydrothermal veins and associated rare-metal mineralization, 7) the unlikely mobility of Zr, Y, REE, and other incompatible elements, and poorly mobile elements (e.g. Al) with the alkalis, 8) the relatively low concentrations of F, CO_2 and H_2O that are needed to facilitate hydrothermal processes, 9) the lack of a continuum of chemical analyses between peralkaline (Unit 6 and most of Unit 7) and non-peralkaline rocks (Unit 5), and, 10) the lack of metasomatic peralkaline rocks, as metasomatic veins and fenites, in the host rocks.

Comparison of the KPC averaged data (Appendix C-6) with that from the Topsails Igneous Suite (Appendix C-1, C-2 and C-3), the Micmac Lake Group (Appendix C-5) and the Cape St. John rocks (Appendix C-4) suggests several similarities: 1) the FQA porphyries from the LPB volcanic suite (FQA [1] and FQA[2]) have similar chemistry to porphyries in the KPC (6P and 7P), 2) the Q-poor (1) rocks of the LPB volcanic suite are geochemically similar to aphyric flows in Unit 6A, 3) some minor quartz syenitic and granitic phases in the KPC have very similar chemistry as the Gaff Topsail granite, 4) the amphibole-bearing porphyry and aphyric units in the MLG have comparable chemistry to rocks of similar texture in the KPC, 5) in the CSJ, the low-Zr aphyric rocks have some similarities with Unit 5, the Seal Island Bight granite is chemically similar to some QFA porphyries (Unit 7P) and the high-Zr aphyric rocks are similar to phenocryst-poor

porphyries in Unit 7P of the KPC, and, 6) the Sheffield Lake targets contain rocks whose textures and geochemistry are almost exactly the same as some units in KPC (6A, 6AAf).

These similarities further confirm the tentative temporal correlation of the KPC and nearby A-type and peralkaline rocks and further suggest similar tectonic settings for these complexes.

The suggestion of Coyle and Strong (1987) that the Sheffield Lake rocks and the Kings Point Complex belong to the same complex is strongly confirmed by the near identical textural and geochemical characteristics of these rocks. Movement along the Green Bay strike-slip fault has separated the two portions of the original complex (Coyle and Strong 1987).

Conclusions

All data collected indicate that Kings Point Complex has a medium potential for rare-metal mineralization. These rocks are representative of a high-level volcanic-plutonic environment in which rare-metals and other incompatible elements are anomalously high. The present study detected no occurrences of high concentrations of rare-metals as found in rare-metal showings and deposits (Table 1-3, 1-4). The present data suggest that a rare-metal concentrating process was operative but not very efficient. More detailed work, including sampling, in Unit 6 may uncover pegmatite-aplite bodies or ash-flows from the upper part of the magma chamber where rare-metals commonly concentrate.

4.0 Grand Le Pierre Area

Introduction

The Grand Le Pierre area (GLP) is located in south-eastern Newfoundland just north of Fortune Bay (Figure 1-3). Two suites of rocks, the peralkaline granites of the Cross Hills Plutonic Suite and a part of the Mooring Cove Formation of the Long Harbour Group, were chosen as targets for the evaluation of rare-metal mineralization.

The focus of the study in the Mooring Cove Formation was a 16 km^2 area at the northeast end of the Femme Syncline, north of English Harbour East. A total of 36 samples were collected, during a three day sampling and mapping program. The aim of this program was to obtain reconnaissance mapping and geochemical data from the Mooring Cove Formation to evaluate its rare-metal potential.

The peralkaline granite associated with the Cross Hill Plutonic Complex (O'Brien et al. 1984, Tuach 1991), here called the Cross Hills granite, mainly occurs as two bodies north of Grand Le Pierre. The western body is elongate and occupies an area of 8 km^2 and the eastern body is more equant-shaped and occupies an area of 6 km^2. Five samples were collected from the eastern body during one foot traverse - all of these were analysed. The western body was sample during a three day program in which 28 samples, 24 of which were analysed, were collected.

General Geology

The Mooring Cove Formation is the second youngest of the four formations of the Long Harbour Group (O'Brien et al, 1984). The lower part of the group consists of felsic volcanic rocks of the Belle Bay Formation and possible facies equivalent sandstone and greywacke of the Anderson's Cove Formation. The Mooring Cove Formation unconformably overlies the Belle Bay and Anderson's Cove formations and consists of peralkaline ash-flow tuffs and mafic flows and sills. The upper part of the Long Harbour Group is called the Rencontre Formation, which unconformably overlies the Mooring Cove Formation and consists of conglomerates and sandstones. Unpublished data (O'Brien and others, 1993) suggest that the Long Harbour Group is Late Proterozoic in age and the Mooring Cove Group is approximately 552 Ma. The main area evaluated consists of the basal portion of the Mooring Cove Formation where it overlies Belle Bay Formation.

The Cross Hills peralkaline granite is one phase of the Cross Hills Plutonic Suite, which consists of gabbro, granodiorite, biotite granite and peralkaline granite phases (O'Brien et al. 1984, Tuach 1991). It intrudes the Belle Bay and Anderson's Cove Formations of the Long Harbour Group. Unpublished U-Pb zircon data (Dunning in Tuach 1991) indicates that the peralkaline granite is $547^{+3}/_{-6}$ Ma or slightly younger than the Long Harbour Group. The peralkaline granite is the only phase of the Cross Hills Plutonic Suite evaluated in this program.

The similar ages of the felsic peralkaline rocks of the Mooring Cove Formation and the peralkaline granite of the Cross Hills granite suggest a cogenetic relationship. Both of these rocks are good targets for rare-metal mineralization.

4.1 Mooring Cove Formation

Introduction

The Mooring Cove Formation consists of peralkaline felsic ash-flows and mafic sills and dykes (O'Brien et al. 1984) which have anomalous values of rare metals indicative of some potential for rare-metal mineralization. The rocks evaluated are located 6 km northeast of Grand Le Pierre (insular Newfoundland; Figure 1-3). This potential was evaluated during a three day geological mapping and lithogeochemical sampling program.

The entire work area is accessible from the Grand Le Pierre to English Harbour East road and was sampled by three foot traverses. The target area was evaluated with a reconnaissance sampling program of one foot traverse in 1990. Two follow-up traverses to the base of the formation were required to further evaluate the highly anomalous rare-metal values obtained from this part of the formation.

Samples were collected from a total of 36 sample sites (MC90001 to MC90018; MC92005 to MC92022); thin section samples were collected from all 36 sites and geochemical samples were collected from 35 of these sites. A suite of 27 geochemical samples were analysed for major elements and a group of trace elements, including rare metals. The sample locations (NTS coordinates), rock type and other data (e.g. scintillometer readings) are given in Appendix A-7.

Geology

The Mooring Cove Formation in the northeast end of the Femme Syncline consists of two main units of mafic sills/flows and a sequence of felsic aphyric ash-flow tuffs. The subaerial ash-flow tuffs and subordinate ash-flow breccias display many ash-flow features such as fiammé, columnar joints, lithophysia and compaction features. A fine grained felsic dyke, which cross-cuts the basal part of the Mooring Cove Formation, has also been mapped in the study area.

The lowermost unit observed is the upper member of the Belle Bay Formation, which is a knobby weathering, light green, lithophysea-rich aphyric ash-flow.

The basal unit of the Mooring Cove formation consists of red, aphyric, columnar-jointed, ash-flow tuffs, which locally contain red lithophysia-rich massive ash-flows. Many occurrences of this unit contain very fine grained amphibole microphenocrysts in

an aphanitic matrix. Light green lithophysia-rich aphyric ash-flow tuff and, locally, ash-flow breccia occurs next in the stratigraphy.

A mafic flow unit occurs at the top of the stratigraphy of the detailed study area. In this area it is very fined grained and massive.

The youngest unit in the area is a felsic dyke which crosscuts the basal ash-flow tuffs of the Mooring Cove Formation. It is very fine grained to aphanitic, is aphyric and contains flow banding in some localities. Contacts are intrusive and host rocks fragments are found near the contacts. The width ranges from < 0.5 to 3 m and bifurcates into three smaller veins in the lowest part of the Mooring Cove Formation; it was not observed in the Belle Bay Formation in the study area. This dyke rock is generally featureless in thin section.

Outside of the detailed study area, samples were collected from the upper portion of the Mooring Cove Formation exposed in the Femme Syncline. These samples were mainly from massive to layered aphyric ash-flow tuff and ash-flow tuff-breccia. These rocks exhibited similar hand sample and thin section features as those in the detailed study area.

Some of the massive (i.e. non-columnar jointed) aphyric rocks at the base of the MCF are very similar to two trachytic dykes (?) observed in the Belle Bay Formation less than 0.5 km from the study area (Tuach 1991). The southernmost of these dykes could represent the northward extension of rocks observed in the study area. The descriptions of these rocks are very similar. In thin section, these rocks exhibit a very fine grained trachytic texture.

Results

Spectrometer data for the samples collected are listed in Appendix A-7 and summary statistics for the main rocks types are listed in Table 4-1. The range of total count readings for the felsic volcanic rocks is 240 to 600 cps. The felsic dyke ranges from 650 to 720 cps and the mafic flows have a value of 155 cps. Comparison of these values with those from mineralized peralkaline rocks in Labrador (Table 1-3, 1-4) indicates that, based on radioactivity, these rocks have low potential for rare-metals. The possible exception to this conclusion is the felsic dyke which, although not exceeding high, has values much higher than normal for peralkaline rocks.

Table 4-1 Summary Spectrometer Data

Unit	Average	Range	Number
Aphyric Ash Flow	431	172 - 690	19
Trachyte	533	500 - 600	3
Felsic dyke	690	650 - 720	3
Mafic Flow	172	120 - 240	3

The geochemical data for the MCF rocks are listed in Appendix B-7 and the averages and unique sample values are tabulated in Appendix C-7. The rare-metal values of most of the aphyric ash-flows are restricted to normal values for these rocks (e.g. 958 ppm Zr). However, several examples of trachytic (lower SiO_2) aphyric flows, located at the base of the Mooring Cove Formation, are characterized by much higher rare-metal values (e.g. 273 ppm Nb, 1601 ppm Zr, 143 ppm Y) and high Al_2O_3 values (16.54 %). The highest rare-metal values observed in the MCF data set are observed in the felsic dyke which has values of 2800 ppm Zr, 476 ppm Nb and 265 ppm Y. These are very encouraging rare-metal values.

Discussion

The high values of incompatible elements indicate that the volcanic rocks in the Mooring Cove Formation can be classified as A-type (Whalen et al. 1987). None of the samples studied have Na or K values indicative of peralkaline rocks but the high rare-metal values and low Al_2O_3 observed are characteristic of peralkaline rocks. The presence of widespread pyritic alteration throughout the formation indicates that hydrothermal activity may have leached alkalis from these rocks.

The limited geochemical data from the upper part of the Belle Bay Formation indicate that it is not closely related to the MCF, as it is metaluminous and impoverished in incompatible elements. The high incompatible element concentrations, the subaerial nature of the ash-flows and the presence of significant mafic flows within the MCF indicate that it belongs to a bimodal volcanic suite.

The trachytic rocks to the north of the study area are geochemically identical (Tuach 1991) to the trachytic rocks observed in the study area. In both cases they are found to be younger than the Belle Bay Formation and roughly equivalent to the base of the MCF (i.e. they do not cut MCF rocks higher up in the stratigraphy). These rocks have been correlated with the Cross Hills granite (Tuach 1991). The close association with the MCF

and Tuach's correlation establishes a tentative link between the Cross Hills granite and the MCF. It is suggested that the trachytic rocks represent the initial magmatism from the Mooring Cove magmatic event.

It is commonly observed that the first volcanic products of a magma chamber are the most differentiated due to concentration of incompatible elements towards the top of a magma chamber (e.g. Hildreth 1981 and many other authors). The highest values of rare-metals in the Mooring Cove Formation have been found at the base of the sequence. The indications that the underlying Belle Bay Formation is unconformably overlain and that it is not geochemically related to the Mooring Cove magmatic system suggests that the basal part of the MCF represents the most differentiated magma. This indicates that the basal zone of the MCF in the Femme Syncline is one area in the MCF that has the best potential for rare-metals.

Conclusions

All data collected indicate that most of the Mooring Cove Formation has a low potential for rare-metal mineralization. However, the anomalous rare-metal values in trachytic rocks and an aphyric felsic dyke at the very base of the formation indicate that there is medium potential for rare-metal mineralization in this part of the stratigraphy. It is recommended that the basal portion of the Mooring Cove Formation in other parts of its outcrop area be evaluated for rare-metal mineralization.

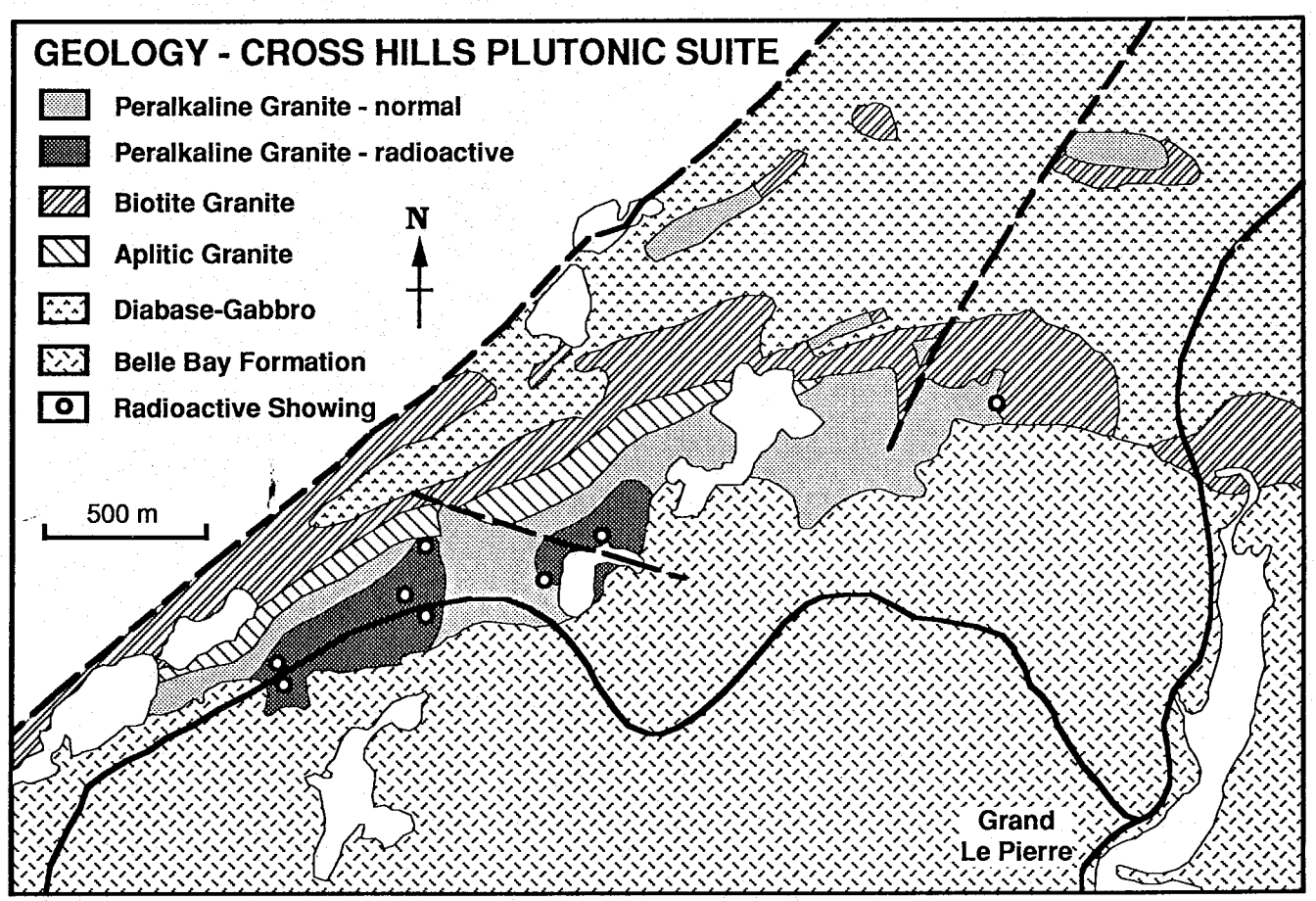

Figure 4-1 *Geology of the Cross Hills Plutonic Suite; location of radioactive showings and the radioactive peralkaline granite (after Saunders and Tuach, 1989).*

4.2 Cross Hills Granite

Introduction

The Cross Hills peralkaline granite (CHG) consists of aplite, pegmatite-aplite veins, fine to medium grained granite and coarser medium grained granite. The rocks evaluated are located in two areas, one is 6 km northeast of Grand Le Pierre and the other is 3 km northwest of Grand Le Pierre (insular Newfoundland; Figure 1-3). High rare-metal values have been reported from this area by Hopfengaertner (1982) and Tuach (1991). The rare-metal potential for these rocks was evaluated during a three day geological mapping and lithogeochemical sampling program.

The entire work area is accessible from the Grand Le Pierre - English Harbour East road and was sampled by four foot traverses; the northwest area is cut by this road. The northeast area was evaluated during a foot traverse (1990). The northwest area was evaluated in 1990 and was mapped and sampled in more detail in 1992.

Samples were collected from a total of 33 sample sites (MC90019 to MC90039; MC92001 to MC92004; MC92023 to MC92030); thin section samples were collected from all 33 sites and geochemical samples were collected from 31 of these sites. A suite of 29 geochemical samples were analysed for major elements and a group of trace elements, including rare metals. The sample locations (NTS coordinates), rock type and other data (e.g. scintillometer readings) are given in Appendix A-8.

Geology

The geology of the Cross Hills Plutonic Suite is discussed in detail by O'Brien et al (1984) and Tuach (1991). The peralkaline granite has been divided into six phases based on grain size and radiometric reading: peralkaline aplite, peralkaline pegmatite-aplite veins, fine grained to medium grained and medium grained normal peralkaline granite (low radiometric readings: 345 - 470 cps) and fine grained to medium grained and medium grained radioactive peralkaline granite (high radiometric readings: 500 - 1020 cps).

Figure 4-1 illustrates the geology of the northwest body of the CHG. This body is dominated by normal peralkaline granite which is intruded, mostly in its western portion, by veins, pods and dykes of pegmatite-aplite and radioactive peralkaline granite. Peralkaline aplite is in contact with biotite aplite in the western part of this body (Tuach

1991). The northeastern body is mainly homogeneous fine to medium grained and medium grained normal peralkaline granite.

The medium grained granite (radioactive and normal) is characterized by 50 - 70 % microperthite feldspar, 30 - 40 % quartz and 3 - 8 % mafic minerals. Grainsize is 2 - 4 mm and texture is dominated by subhedral feldspar surrounded by granophyric feldspar-quartz. The mafic minerals are commonly amphibole, opaques and less commonly, aegirine.

The fine to medium grained granite (radioactive and normal) is characterized by grainsizes less than 2 mm and the predominance of granophyric texture. Opaque minerals are the most common accessory phase and their abundance is normally less than 3 %.

The aplite is characterized by grainsizes less than 0.5 mm. Granophyric and spherulitic textures are normally found and opaque minerals and chlorite are the most common accessory minerals.

Pegmatite-aplite veins have quite varied grainsizes and mineral proportions. Microperthite, quartz and granophyric quartz+feldspar are the most common grains observed. See Tuach (1991) and Saunders and Tuach (1989) for a more detailed description of the mineralogy of the mineralized pegmatites.

Results

Spectrometer data for the samples collected is listed in Appendix A-8 and summary statistics for the main rocks types are listed in Table 4-2. The range of total count readings for the normal peralkaline granite is 345 to 470 cps, for the radioactive peralkaline granite it is 500 to 1020 cps and for the pegmatite-aplite bodies it is 500 to 1400 cps. The radioactive peralkaline granite and the pegmatite-aplite bodies compare favourably with those from mineralized peralkaline rocks in Labrador (Table 1-3, 1-4). This indicates that these rocks have medium to high potential for rare-metals.

Table 4.2 Summary Spectrometer Data

Rock Type	Average	Range	Number
Aplite	383	370 - 400	4
Normal Per. Granite	399	345 - 485	9
F-Mg Normal Per Granite	416	350 - 470	5
F-Mg Radioactive Per. Granite	690	500 - 1020	4
Radioactive Per. Granite	604	520 - 660	7
Peg-aplite	970	500 - 1400	4

The geochemical data for the CHG phases are listed in Appendix B-8 and the averages and unique sample values are tabulated in Appendix C-8. The rare-metal values for the normal granite and the associated peralkaline aplite ranges from 245 - 1056 ppm Zr, with averages of 301 - 729 ppm Zr. The radioactive peralkaline granite, including the pegmatite - aplite bodies, range from 799 - 8490 ppm Zr, with averages of 1168 - 1388 ppm Zr and high values of 4430 and 8490 ppm Zr. Values for the radioactive granites and particularly, the pegmatite-aplite veins, compare very favourably with those of rare-metal mineralization in Labrador.

Discussion

The late stage veins, dykes and pods of radioactive peralkaline granite and its pegmatite-aplite phase are the source of high values of rare-metals. The small size of the highly mineralized pegmatite aplite veins (< 5 to 15 cm wide and traceable for several metres) shows only small amounts of this high grade mineralization. However, the high values indicate that the concentration mechanisms were operating in the CHG and larger tonnages of rare-metal mineralization may have gathered in another portion of the magma chamber. Tuach (1991) indicates that the top of the magma chamber is orientated towards the southern, peralkaline-bearing, part of the composite biotite granite - peralkaline granite body and that the two granites represent two different liquids in a magma chamber. Liquid-liquid and crystal liquid processes operating in this magma chamber (Tuach 1991) may have been responsible for the mineralized veins. The occurrence of these veins and the associated late stage radioactive granite intrusive into the southwestern end of the northwestern body suggest that the locus of the concentrating mechanism may have been below the present day erosion level, perhaps in a cupola in the upper part of the now tilted magma chamber.

A comparison of geochemistry data from the peralkaline granites of the CHG and the peralkaline ash-flows of the Mooring Cove Formation suggest many similarities between these suites. These include: 1) similar geochemistry between the aphyric ash-flows and peralkaline granite, and, 2) the occurrence of rocks of trachytic-syenitic composition in both suites. These compositional similarities and the similarities in age indicate that the Mooring Cove Formation may have vented from the Cross Hill magma chamber or another similar magma chamber in the region (Tuach 1991).

Conclusions

The Cross Hills peralkaline granite has a medium to high potential for rare-metal mineralization. This mineralization occurs at the present day erosional level as < 15 cm veins of limited extent. However, some evidence indicates larger tonnages of high grade rare-metal mineralization may be at depth. The CHG magma chamber has concentrated incompatible elements, including rare-metals, in the top of chamber to form a peralkaline magma and associated rare-metal mineralization.

The northwestern body of the CHG is highly recommended as an exploration target for rare-metals.

5.0 Burin Peninsula

Introduction

The Burin Peninsula (BP) is located in south-eastern Newfoundland between Fortune Bay and Placentia Bay (Figure 1-3). Three groups of rocks, the St. Lawrence peralkaline granite, the Grand Beach complex and the Love Cove Group in the Terranceville area, were chosen as targets for the evaluation of rare-metal mineralization in this area.

The St. Lawrence peralkaline granite is an irregular-shaped body approximately 300 km^2 (Figure 5-1) in area. A total of 72 sites were sampled, during a six day sampling and mapping program. The aim of this program was to obtain representative samples, mapping and geochemical data from the St. Lawrence Granite and related rocks (Rocky Ridge complex and Winterland porphyry) and the related fluorite veins to evaluate their rare-metal potential.

The Grand Beach Complex is a porphyritic ash-flow complex which is approximately 50 km^2 in area. A total of 52 sites were sampled from this target during three days of traversing. This program was designed to obtain geological data and samples from all phases and all parts of the complex to evaluate the rare-metal potential.

A total of seven samples were collected from two parts of the Southern Hills Facies of the Love Cove Group near Terranceville and Bay L'Argent to evaluate the geochemistry of these felsic volcanic rocks. These data were required to evaluate whether the Love Cove Group was a good target for rare-metal mineralization.

General Geology

The Burin Peninsula is part of the Avalon Terrane tectonostratigraphic zone (Williams et al 1989). Most of the Burin Peninsula is underlain by Proterozoic felsic volcanic rocks and related sediments of the Love Cove - Marystown Groups (Strong et al. 1977). Smaller areas are underlain by the volcanic rocks of the Burin and sediments of the Inlet Group. The volcanic and sediments of these groups are intruded by the St. Lawrence granite, which is 374±2 Ma (U/Pb zircon - Kerr et al. 1993), and are overlain / crosscut by the Grand Beach caldera complex, which is $396^{+6}/_{-4}$ Ma (U/Pb zircon - Krogh et al. 1988).

The differences in ages suggest that the three targets in the BP are tectonically and metallogenically unrelated. Their only similarities are their occurrence in the Avalon Terrane, their felsic nature and the potential for rare-metal mineralization.

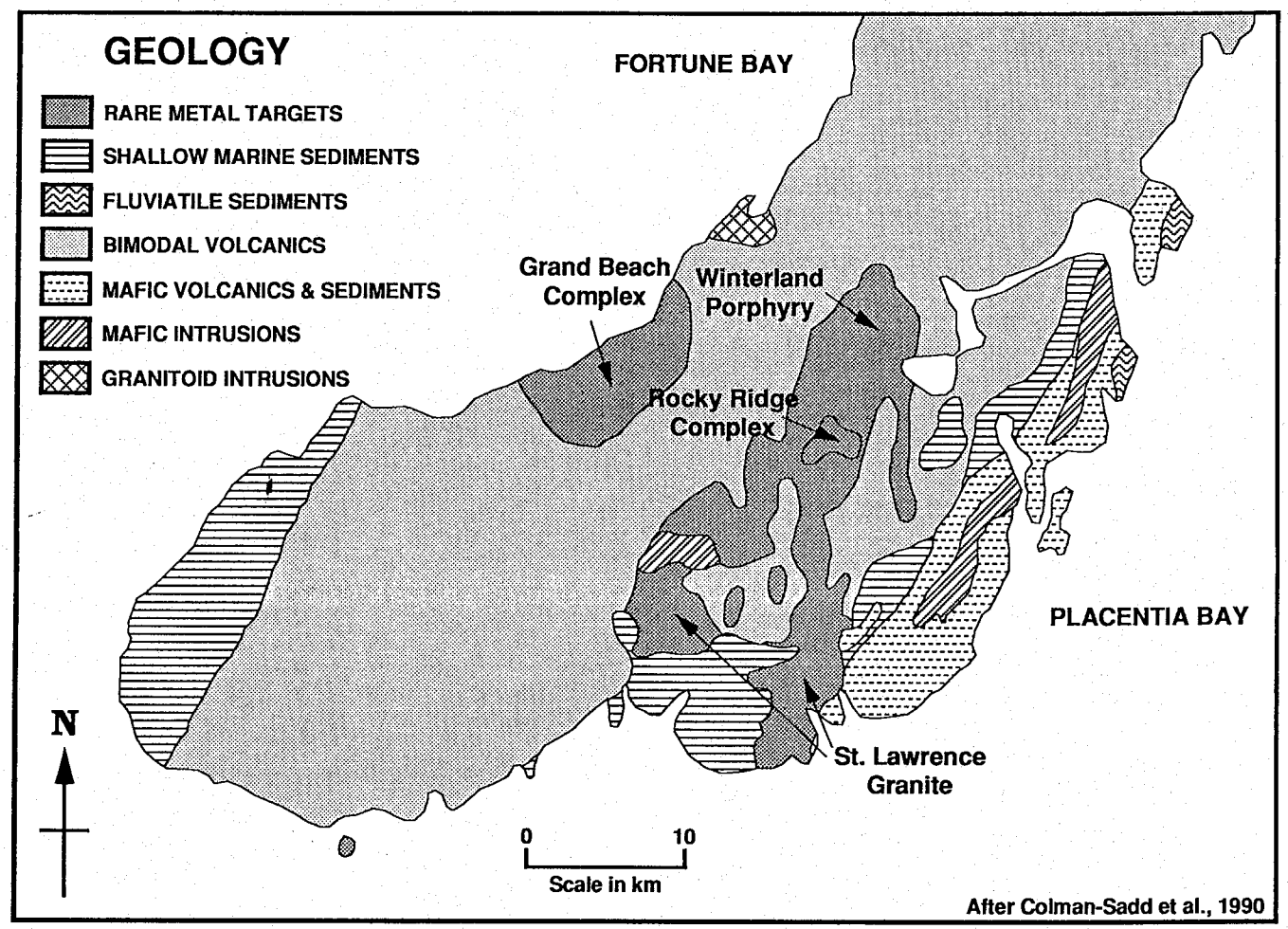

Figure 5-1 *General geology of the southern portion of the Burin Peninsula; location of the Grand Beach complex, Winterland porphyry, Rocky Ridge complex and St. Lawrence Granite (after Colman-Sadd* et al., *1990).*

5.1 Grand Beach Caldera Complex

Introduction

The Grand Beach Complex ($396^{+6}/_{-4}$ Ma; Krogh et al. 1988) consists of a series of quartz-feldspar porphyries and porphyritic ash-flow tuffs and lithic-breccias which are in fault contact and overly the Late Proterozoic Marystown Group. This complex is located at the community of Grand Beach, on Fortune Bay, 25 km west of Marystown, on the Burin Peninsula (insular Newfoundland; Figure 1-3). The rare-metal potential was evaluated during a three day geological mapping and lithogeochemical sampling program.

The entire work area is accessible from the Marystown to Grand Bank highway (Highway 11). The target area was adequately sampled by four inland foot traverses, one beach traverse of almost continuous outcrop and one roadside traverse. Outcrop is sparse and often highly fractured and weathered in the inland portions.

Samples were collected from a total of 52 sample sites (GB90001 to GB90052); thin section samples were collected from all 52 sites and geochemical samples were collected from 49 of these sites. A suite of 39 geochemical samples were analysed for major elements and a group of trace elements, including rare metals. The sample locations (NTS coordinates), rock type and other data (e.g. scintillometer readings) are given in Appendix A-9.

Geology

The Grand Beach complex is dominantly composed of QF porphyry and porphyritic ash-flow tuffs. Although the exposure is poor along most contacts, it is thought to overly mafic volcanic rocks of the much older Marystown Group (O'Brien et al 1977). The porphyritic rocks of the complex have been divided into the following mappable units: 1) QF porphyry, 2) QF porphyry (mafic inclusions), and, 3) porphyritic ash-flow tuffs and lithic breccias. Minor unmappable phases, also found in the complex include: aphyric ash-flow, volcanogenic sandstone and conglomerate, feldspar porphyritic ash-flow, quartz porphyritic ash-flow and mafic flows (inclusions in ash-flow tuffs). Most outcrops in the complex exhibit hand sample or thin section textures indicative of ash-flow deposits, thus samples labeled QF porphyry or QF porphyry (mafic inclusions) are also probably ash-flow units.

The poor outcrop exposure and massive nature of most rocks within the complex prevented determination of stratigraphic and structural relationships between most units. However, a general map pattern between the major units was established from the mapping program (Figure 5-1-1). Quartz-feldspar porphyritic ash-flow tuff and lithic breccia, and minor amounts of volcanogenic sediments, aphyric ignimbrite and feldspar porphyritic ignimbrite occur in a 1 - 2 km wide zone on the outer portion of the complex. The central part of the complex contains quartz-feldspar porphyry and quartz-feldspar porphyry with mafic inclusions.

The quartz-feldspar porphyritic ash-flow tuff and lithic ash-flow breccia is characterized by 15 - 25 % feldspar and 5 - 15 % quartz phenocrysts in an aphanitic to very fine grained matrix. Feldspar grains are commonly broken, range in size from < 1 to 3 mm and are microperthitic with minor plagioclase grains in many outcrops. Quartz grains are commonly resorbed and broken and range in size from 1 to 3 mm. The lithic-breccias generally contain 5 to 50% subrounded to subangular quartz-feldspar porphyry, feldspar porphyry and mafic very fine grained fragments which range from < 1 to 10 cm in size. Ash-flow textural features such as layering, fiammé and lenticular features are commonly found.

The quartz-feldspar porphyry contains 10 - 20 % feldspar and 10 - 15 % quartz phenocrysts in an aphanitic to very fine grained matrix. The texture is massive, fragments are rare to sparse and ash-flow textures are not common. Feldspar grains are commonly broken, as observed in thin section, and are microperthitic with rare to sparse plagioclase. Quartz grains are commonly resorbed and broken.

Fine grained, mafic-rich, dark-coloured inclusions range from < 1 to 5 cm in the inclusion-bearing quartz-feldspar porphyry. These inclusions are subrounded and commonly occupy < 3% of the outcrop. The quartz-feldspar porphyry matrix to the inclusions is similar to the quartz-feldspar porphyry unit and probably is a variety of that unit.

Results

Spectrometer data for the samples collected are listed in Appendix A-9 and summary statistics for the main rocks types are listed in Table 5-1. The range of total count readings for all of the felsic volcanic rocks in the complex is 280 - 680 cps; the highest value is for a quartz-feldspar porphyritic ash-flow. The averages are very similar for all rock types in the complex.

Table 5-1 Summary Spectrometer Data

Rock Type	Average	Range	Number
QF Ash-flow (M)	419	340 - 525	10
QF Ash-flow	413	320 - 680	18
QF Porph	380	280 - 545	12

The geochemical data for the GBC rocks are listed in Appendix B-9 and the averages and unique sample values are tabulated in Appendix C-9. The rare-metal values of all samples analysed from the complex are exceedingly low (e.g. 89 - 348 ppm Zr).

Most of the quartz-feldspar porphyritic rocks of the complex have a very similar chemistry which is characterized by high silica values (averages from 76.07 - 77.06), low rare-metal values and relatively low alumina values (averages from 11.97 - 12.28). These similarities indicate that all of these phases are cogenetic.

A suite of low-silica rocks (SiO_2 69.90 - 71.85) is also found within the complex. These rocks are not widespread but appear to be younger than the high-silica rocks and are recognized by the predominance of feldspar over quartz phenocrysts. Many are found in the outer, ash-flow tuff and lithic-breccia zone.

Discussion

The rocks of the Grand Beach complex are very low in incompatible elements, however they plot in the field of A-type granites (Whalen et al. 1987) and have many of the characteristics of A-type granites such as high Nb, low Sr, low Ca and low Al_2O_3.

The presence of mafic inclusions in some of the phases of the complex suggest that the magma chamber may have contained mafic and felsic magmas which mixed during some ash-flow eruptions.

The roughly circular-shape of the complex, the occurrence of a crude concentric zoning and dominantly ash-flow nature of the rocks suggest that this may be an ash-flow caldera (Smith and Bailey 1968). The lack of structural and stratigraphic information makes this a very tentative conclusion.

Conclusions

All data collected indicate that the Grand Beach has no potential for rare-metal mineralization. Anomalously high Th values are responsible for some of the higher scintillometer values and the high radiometric signature of the complex (Pittman 1978).

5.2 St. Lawrence Granite and related hypabyssal to volcanic rocks.

Introduction

The St Lawrence pluton is a high-level, irregularly-shaped, mildly peralkaline to non-peralkaline granite. It extends from the community of St. Lawrence, on Placentia Bay (insular Newfoundland; Figure 1-3), 25 km northwards and is about 10 km wide. It has an age, as indicated by U-Pb zircon geochronology, of 374 ±2 Ma. (Kerr et al. 1993). The Rocky Ridge complex and Winterland porphyry, consisting of felsic extrusive rocks and porphyries, are thought to be associated with the St. Lawrence pluton (Strong et al. 1978). The rare-metal potential of this pluton, the associated fluorite veins and the possible extrusive equivalents were evaluated during a six day geological mapping and lithogeochemical sampling program.

Most of the pluton is accessible from the St. Lawrence to Lawn highway and a number of trails and roads branching off of it. The northern part of the pluton, the Rocky Ridge complex and the Winterland porphyry, are accessable from dirt roads leaving the Marystown-Grand Bank highway from the community of Wintertown and the Marystown airport. The target area was adequately sampled by a combination of foot traverses and roadside traverses. Outcrop is sparse in many parts of the study area, with the most abundant outcroppings being in stream beds or on the top of hills..

Samples were collected from a total of 72 sample sites (SG90001 to SG90072); thin section samples were collected from all 72 sites and geochemical samples were collected from 71 of these sites. A suite of 60 geochemical samples were analysed for major elements and a group of trace elements, including rare metals. The sample locations (NTS coordinates), rock type and other data (e.g. scintillometer readings) are given in Appendix A-10.

Geology

The St. Lawrence pluton ranges from quartz-feldspar porphyry, to quartz-feldspar porphyritic granite to medium grained granite. The porphyries are reported to be more abundant in the western portion of the pluton particularly at the contacts (Teng and Strong 1976). Fluorite veins and rare aplitic veins cut the pluton, particularly in its southeastern portion. The three main phases of the pluton and the fluorite veins are characterized below.

Quartz-feldspar porphyry. This unit commonly contains 25 to 30 % feldspar phenocrysts, 1 to 4 mm across, and 15 to 25 % quartz phenocrysts, 1 to 4 mm across. The matrix of this unit is commonly aphanitic to very fine grained. Quartz-feldspar porphyry is not widespread - most porphyritic rocks in the pluton have a fine grained granitic matrix. Phenocrysts are sub to euhedral and the matrix exhibits no pyroclastic textures suggesting that this unit is intrusive.

Quartz-feldspar porphyritic granite. The porphyritic granite unit can be characterized as a fine grained granite with feldspar and quartz phenocrysts. Feldspar (microperthite) phenocrysts range from 5 to 15 % and 3 to 10 mm across. Quartz phenocrysts are commonly from 5 to 10 % and 2 to 6 mm across. The matrix is less than 1 mm in grainsize and consists of 60 to 75 % feldspar and 5 to 20 % quartz. Dark minerals, commonly hematite or chlorite and less commonly riebeckite or aegirine, are less than 5 % and less than 2 mm in size. In many cases, the matrix contains granophyric textured quartz and feldspar.

Medium grained granite. This unit consistently contains 60 to 75 % microperthitic and minor plagioclase feldspar, 1 to 5 mm across, 15 to 30 % quartz, 2 to 5 mm across, and 5 to 10 % riebeckite, chlorite or aegirine, less than 2 mm across. The texture is massive with grains being generally subhedral. Zircon and fluorite are accessory minerals. Peralkaline minerals, such as riebeckite and aegirine are only locally found.

Fluorite veins. These veins, where sampled, cross-cut the host granite, ranging in size from < 1 to 3 m thick. Microcrystalline massive to banded, mainly purple fluorite dominates. In many localities the fluorite veins are filled with angular granite breccia fragments. The veins are described in detail by Howse et al. 1983.

The Wintertown porphyry occurs in the far northern portion of the felsic complex associated with the St. Lawrence pluton. It consists of poorly exposed and highly weathered feldspar-quartz porphyry. Feldspar phenocrysts range from 5 to 10 %, are 1 to 3 mm in size, quartz phenocrysts are 2 to 5 %, 1 to 2 mm in size, and oikocrystic amphibole aggregates are 5 to 10 % and less than 0.5 mm in size. The matrix is very fine grained and recrystallized. Quartz is commonly broken and resorbed suggesting an ash-flow origin for this unit.

The Rocky Ridge complex is composed of amphibole-bearing granite and a series of feldspar and feldspar-quartz porphyries and porphyritic ash-flows. The granitic rocks include quartz-feldspar porphyry with a granophyric matrix and porphyritic granite with large microperthitic phenocrysts, riebeckite, aegirine and magnetite. A feldspar porphyritic intrusion, also found in the area, consists of microperthite phenocrysts with quartz, feldspar, granophyre, magnetite and chlorite in the matrix. Feldspar and quartz-

feldspar ash-flows in the Rocky Ridge complex consist of broken feldspar and quartz grains, aphyric and feldspar porphyritic fragments, and, abundant ash-flow textures such as fiammé and layering. One such unit also has oikocrystic amphibole in the matrix indicating its peralkaline nature.

Results

Spectrometer data for the samples collected are listed in Appendix A-10. The range of total count readings for all of the felsic rocks studied is 230 - 860 cps; the highest value is for a medium grained granite. The average values indicate that the medium grained granite, porphyritic granite and quartz-feldspar porphyry of the St. Lawrence pluton are the most radioactive.

The geochemical data for the SLG rocks are listed in Appendix B-10 and the averages and unique sample values are tabulated in Appendix C-10. The rare-metal values of the samples analysed range from quite low values (e.g. < 150 ppm Zr) to very high (1317 ppm Zr.). The fluorite veins contain almost no Zr (i.e. 2 - 11 ppm) but abundant Y (i.e. 582 - 747).

The zirconium values of the phases of the St. Lawrence pluton can be used to subdivide the pluton in two zones: a low Zr (154 - 356 ppm Zr) and a high Zr (447 - 1317 ppm Zr) zone. The high Zr zone is located in the main eastern lobe of the pluton, whereas the low Zr zone is located in the southwestern lobe of the granite. The three textural phases of the high-Zr zone have identical geochemical signatures. Very few samples from the St. Lawrence pluton are peralkaline (agpaitic index greater than 1.00; Appendix B-10; also see Kerr et al. 1993b).

The Rocky Ridge complex contains rocks of syenitic-trachytic composition and felsic peralkaline ash-flows.

The Wintertown porphyry is a also a peralkaline body.

Discussion

The low-Zr zone of the St. Lawrence pluton contains all of the textural phases of the high Zr zone. However, it appears to be characterized by the absence of large fluorite veins and the occurrence of a large number of base-metal showings (Strong et al. 1978). Some phases of this zone are geochemically very similar to the low Zr quartz-feldspar ash-flow tuffs of the Grand Beach suite suggesting that they may be genetically related. Although this zone of the St. Lawrence pluton was not dated, the difference in ages

between these two complexes is small enough (396 Ma vs 374 Ma) to suggest that they may be part of the same tectonic event or formed in similar tectonic settings of slightly different age; Kerr et 1993a. Alternatively, the low-Zr zone, which is not peralkaline in nature, may be the same age as the Grand Beach suite and thus older than the St. Lawrence pluton.

Conclusions

All data collected indicate that the St. Lawrence pluton and related rocks have low to medium potential for rare-metal mineralization. The peralkaline granite contains anomalous rare-metal values but exhibits no instances of high concentrations observed in rare-metal showings (e.g. Strange Lake). However, the high values of Y in the fluorite veins, some of which have been mined in the recent past for fluorite, suggest that Y may be sought as a valuable by-product of fluorite production.

5.3 Terranceville Area.

Introduction

The Southern Hills Facies of the Love Cove Group, near Terranceville and Bay L'Argent (insular Newfoundland; Figure 1-3), consist of rhyolitic flows, felsic welded ash-flow tuff and related pyroclastic rocks (O'Brien et al, 1984). The rare-metal potential of these volcanic rocks was evaluated during a one day geological mapping and lithogeochemical sampling program.

These rocks are accessible from the Terranceville highway and the Bay L'Argent - Little Harbour East road. Reconnaissance sampling was carried out at roadcuts in the Love Cove Group.

Samples were collected from a total of seven sample sites (TV92001 to TV92007); thin section and geochemical samples were collected from all seven sites. All geochemical samples were analysed for major elements and a group of trace elements, including rare metals. The sample locations (NTS coordinates), rock type and other data (e.g. scintillometer readings) are given in Appendix A-11.

Geology

The geology of the Love Cove Group in this part of the Burin Peninsula is discussed in detail by O'Brien et al. (1984). The Southern Hills facies is the uppermost of three facies in the Love Cove Group - the Grandy's Pond and Deer Park Pond facies are the others. All samples collected, excepting one, were aphyric felsic ash-flows with layering and fiammé.

Results

Spectrometer data for the samples collected are listed in Appendix A-11. The range of total count readings for all of the rocks studied is 280 - 400 cps.

The geochemical data for the SLG rocks are listed in Appendix B-11. The rare-metal values of the samples analysed range from quite low values (i.e. 175 ppm Zr) to fairly high (i.e. 1168 ppm Zr.).

Discussion

Samples collected in the Bay L'Argent region consist of low silica and high silica ash-flow tuffs with high rare-metal values reflecting their peralkaline nature: carbonate alteration of feldspars removed some Na_2O from these rocks resulting in agpaitic indices less than 1.00 in most cases.

Conclusions

All data collected indicate that the Southern Hills facies has low to medium potential for rare-metal mineralization. The peralkaline ash-flow tuffs contain anomalous rare-metal values but exhibit no instances of high concentrations observed in rare-metal showings (e.g. Strange Lake). More detailed geochemical studies may locate the source caldera for these ash-flows and thus improve the potential for rare-metals, as low volume highly differentiated rare-metal enriched fractions of magma chambers are more likely to occur within the caldera.

6.0 Bull Arm Formation

Introduction

The Bull Arm Formation, part of the Musgravetown Group, is found in eastern Newfoundland from Bonavista Bay to Bull Arm (Figure 1-3). Nine outcrop areas of the Bull Arm Formation and the Louil Hills peralkaline granite were chosen as targets for the evaluation of rare-metal mineralization in this part of insular Newfoundland. These areas, which occur in a band from Traytown in the north to Bellevue in the south are designated (Figure 6-1): 1) Traytown and Louil Hills, 2) Port Blandford, 3) Musgravetown, 4) Plate Cove, 5) Clarenville, 6) Hodges Cove, 7) Sunnyside, 8) Masters Head, and, 9) Doe Hills.

The Traytown-Louil Hills target consists of the peralkaline granite portion of the Louil Hills Intrusive Suite, which is approximately 1 km^2, and three rhyolitic units, less than 500 m thick, of felsic volcanic rocks in the western Musgravetown basin (Bull Arm Formation?). A total of 14 sites were sampled, five in the felsic volcanic rocks and nine in the Louil Hills peralkaline granite, during a one day sampling and mapping program. The aim of this program was to obtain representative samples, mapping and geochemical data from these rocks to evaluate their rare-metal potential.

The Port Blandford area was sampled in a one day program, which provided a section through the Musgravetown and Love Cove Groups on the southwest and south side of Clode Sound. A total of 19 samples were collected to help evaluate the rare-metal potential of these two groups in this area.

Sampling in the Musgravetown area, consisted of 2½ days of work in a 25 km^2 area of the Bull Arm Formation. A total of 35 samples were collected to evaluate the rare-metal potential in mafic and felsic volcanic rocks.

The Plate Cove target consists of a 10 km x 1.5 km zone of Bull Arm Formation felsic volcanic rocks. This zone was sampled and mapped in a northern and a southern cross section; a total of ten samples were collected.

Three separate bands of Bull Arm Formation were sampled in the Clarenville area: Clarenville (15 km long x 1 km wide), North West Brook (10 km long x 2 km wide) and Random Island (10 km long x 3 km wide). A total of 19 samples were collected in this one day reconnaissance program, six in the Clarenville band, eight in the North West Brook band and five in the Random Island band.

A total of three samples were collected from the Hodges Cove band of Bull Arm Formation which is 3 km x 2 km.

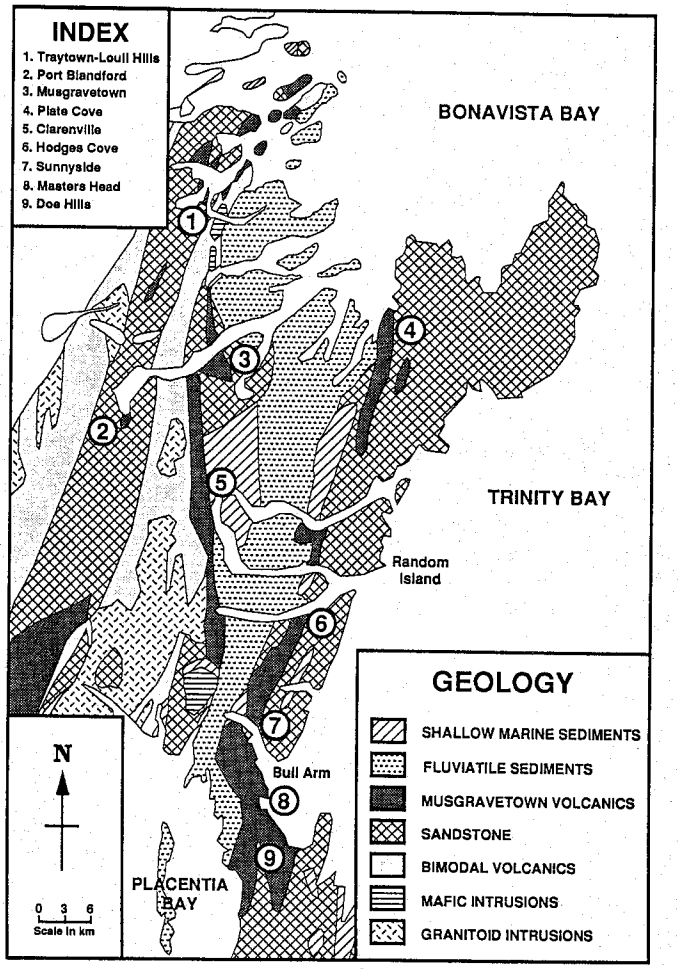

Figure 6-1

After Colman-Sadd et al., 1990

The Sunnyside target of the Bull Arm Formation is 3 km x 7 km. A total of 31 felsic volcanic rock samples were collected during a two day sampling and mapping program to evaluate this target.

Bull Arm Formation in the Masters Head area occupies an area 3 km x 4 km and consists of felsic volcanic rocks. A total of 12 samples were collected during a one day traverse,to evaluate the rare-metal potential.

The Doe Hills area consists of a zone of Bull Arm Formation 12 km x 8 km. A three day sampling program collected a total of 82 samples to evaluate the rare-metal potential of the Bull Arm Formation felsic volcanic rocks.

General Geology

The Musgravetown Group occurs in the western part of the Avalon Terrane tectonostratigraphic zone of eastern Newfoundland (Williams et al, 1989). The Precambrian stratigraphy in this region consists of (O'Brien, 1993, 1994): at its base, intermediate pyroclastic volcanic rocks and arenaceous rocks of the Love Cove Group (620±2 Ma; O'Brien et al. 1992), overlying marine siliciclastic sediments of the Connecting Point Group (620 - 610 Ma; O'Brien et al. 1992) and overlying fluviatile clastic sediments and bimodal volcanic rocks of the Musgravetown Group (580 - 560 Ma O'Brien et al. 1992; $570\ ^{+5}/_{-3}$ Ma, Coyle 1990).

The Musgravetown Group has traditionally been subdivided into the Cannings Cove, Bull Arm, Deer Harbour / Rocky Harbour and Crown Hill Formations (Greene et al. 1984). Recent work by O'Brien and coworkers (e.g. O'Brien 1993, 1994) has defined several complications and stratigraphic inconsistencies with this stratigraphic nomenclature. In the northern part of the study area, the Musgravetown Group is split into a western belt and an eastern belt (O'Brien 1993) by the older Love Cove Group. Connecting Point Group to the east of the eastern belt separates a third belt, here called the far eastern belt. The far eastern belt has been subdivided into areas "east of the Indian Arm Fault" and "west of the Indian Arm Fault" (O'Brien 1994).

The western belt or basin is composed of subaerial felsic volcanic rocks, red sandstone and shale and grey to yellow-green sandstone (O'Brien 1993); none of these units have been correlated with the traditional stratigraphic section and are unnamed. In the eastern belt the stratigraphy passes upwards from red boulder and cobble conglomerates (Cannings Cove Formation), to bimodal volcanic rocks to red clastic sediments (O'Brien 1993, 1994). West of the Indian Arm Fault, in the far eastern belt, the Musgravetown Group stratigraphy passes from red siltstone and sandstone to red pebble

conglomerate of the Crown Hill Formation (O'Brien 1994). East of the Indian Arm Fault the Bull Arm Formation is observed to pass upwards into a grey-green conglomerate and sandstone (O'Brien 1994). Felsic to mafic volcanic rocks occur in all three belts or basins described above, however only those volcanic rocks in the far eastern belt have been assigned to this formation.

The three belts of Musgravetown Group defined by the work of O'Brien (1993, 1994) split the target areas, some of which may not contain actual Bull Arm Formation, into three groups. The western group consists of the Traytown and Port Blandford areas, the eastern group consists of the Musgravetown and the Clarenville and North West Brook portions of the Clarenville target, and the far eastern group consists of the Plate Cove, Hodges Cove, Random Island portion of the Clarenville area, Sunnyside, Masters Head and Doe Hills areas. There is some speculation, requiring precise age dates to substantiate, that one or more of these belts may not be Musgravetown Group (O'Brien 1993, 1994, personal communication 1994).

The overall similarities of the target areas, whether they are Bull Arm Formation or not, such as the presence of felsic volcanic rocks belonging to a bimodal suite, were the basis of choosing them for this evaluation.

6.1 Traytown and Louil Hills

Introduction

The Traytown - Louil Hills target consists of felsic volcanic rocks of the western basin of the Musgravetown Group and the peralkaline granite portion of the Louil Hills Intrusive Suite. The Louil peralkaline granite is located just east of the community of Traytown, on the northeast arm of Alexander Bay, which is on Bonavista Bay (Figure 6-1). The three bands of felsic volcanic rocks are located just north of the community of Traytown, on Alexander Bay. The rare-metal potential was evaluated during a one day geological mapping and lithogeochemical sampling program.

The four targets in this area are all accessible from the network of roads and highways in the Traytown region. Outcrop of volcanic rocks is excellent along the shoreline and the outcrop of the Louil Hills peralkaline granite is everywhere very good.

Samples were collected from a total of 14 sample sites (BA90001 to BA90014); thin section samples were collected from all 14 sites and geochemical samples were collected from 13 of these sites. A suite of two geochemical samples from the volcanic rocks and seven from the granite were analysed for major elements and a group of trace elements, including rare metals. The sample locations (NTS coordinates), rock type and other data (e.g. scintillometer readings) are given in Appendix A-12.

Geology

The Traytown occurrences of felsic volcanic rocks consist of aphyric to sparsely plagioclase-porphyritic ash-flow tuffs (?) in the two eastern units and quartz and quartz-feldspar sparsely (less than 10 %) porphyritic ash-flow tuffs and lithic breccias in the western unit. These rocks, particularly in the east, are interbedded with grey-green volcaniclastic sediments (?).

The Louil Hills granite is a medium to fine grained rock consisting of 30 - 40 % quartz, commonly 2 to 5 mm across, 50 - 60 % feldspar, commonly 2 to 6 mm across, and up to 5 % accessory minerals, less than 2 mm across, which include riebeckite, magnetite, biotite and zircon. Fine grained varieties have a grainsize commonly less than 1 mm across.

Results

Spectrometer data for the samples collected are listed in Appendix A-12. The range of total count readings for all of the felsic volcanic rocks in the complex is 140 - 260 cps and for the granite they range from 380 to 750 cps. The granites on the north side of Northeast Arm have higher radiometric readings (480 - 750 cps) than those on the south side of Northeast Arm (380 - 400 cps).

The geochemical data for the Traytown - Louil Hills rocks are listed in Appendix B-12 and the averages and unique sample values are tabulated in Appendix C-12-1. The rare-metal values of all samples analysed from the area are characteristically low (e.g. 252 to 565 ppm Zr).

Discussion

The geochemical analyses from volcanic rocks have quite different rare-metal values, however the high values of CaO and the low Agpaitic Index (no evidence for Na depletion) suggest that these rocks are not peralkaline or anorogenic in nature. The high rare-metal values for one sample (e.g. 565 ppm Zr) indicate that there are complications with this interpretation.

The difference, as defined by radiometric values, between rocks on either side of Northeast Arm is also observed in rare-metal values (e.g. 420 to 499 ppm Zr vs 252 to 388 ppm Zr) and the occurrence of alkali amphibole, which is present in most rocks to the north and absent, with magnetite or biotite instead, to the south. These differences suggest that the rocks to the north are truly peralkaline in nature and those to the south may be coeval, non-peralkaline varieties formed in the same magma chamber.

The Louil Hills peralkaline granite is, in general, very similar to the Gaff Topsail (Section 2.2) and Seal Island Bight (Section 3.1) peralkaline granites and it plots in the A-type granite field of Whalen et al. (1987).

Conclusions

The volcanic rocks of the Musgravetown Group in this area and the granites of the Louil Hills Intrusive Suite appear to have low potential for rare-metal mineralization. The report of high rare-metal values (e.g. 1500 ppm Zr) in felsite dykes indicates that the potential for the peralkaline granite may be somewhat higher but the scarcity of these dykes suggests low quantities of high rare-metal-bearing rocks.

6.2 Port Blandford

Introduction

The Port Blandford sampling and mapping program consisted of sampling a section through the western basin of the Musgravetown Group and the Love Cove Group to the east. The sampled section at first follows the Trans Canada Highway from Salmon Brook to Port Blandford and then follows the Port Blandford to Musgravetown road to the community of Bunyans Cove (Figure 6-1). This geological mapping and lithogeochemical sampling program was carried out in one day.

Samples were collected from a total of 19 sample sites (BA90015 to BA90028 and BA90054 to BA90058); thin section and geochemical samples were collected from all 14 sites. A suite of six geochemical samples from the Musgravetown Group and two from the Love Cove Group were analysed for major elements and a group of trace elements, including rare metals. The sample locations (NTS coordinates), rock type and other data (e.g. scintillometer readings) are given in Appendix A-12.

Geology

The Musgravetown Group consists of red and grey, layered, sandstone and tuffaceous sandstone containing quartz and feldspar grains, commonly less than 1 mm across. A zone of mafic flows and felsic rocks occurs between Port Blandford and the Love Cove Group. The mafic flows are quartz amygdular and feldspar-phyric. The felsic rocks consist of aphyric to sparsely feldspar-phyric tuffs or ash-flow tuffs and red sandstone and pebble conglomerate near the Love Cove Group contact. See O'Brien (1992) for the detailed geology of this area.

The Love Cove Group consists of light grey to green, massive to layered, sheared intermediate to felsic (?) tuffs and flows. Feldspar porphyritic fragments, in a similar matrix, were observed at one locality.

Results

Spectrometer data for the samples collected in the Musgravetown Group (BA90015 to BA90023 and BA90054 to BA90058) and the Love Cove Group (BA90024 to BA90028) are listed in Appendix A-12. The range of total count readings for

Musgravetown Group rocks is 65 (mafics) to 270 (sandstone) cps and for the Love Cove Group they range from 170 to 380 cps.

The geochemical data for the Musgravetown rocks (BA90016, BA90019, BA90022, BA90054, BA90056 and BA90057) and the Love Cove Group (BA90025 and BA90028) are listed in Appendix B-12 and the unique sample values are tabulated in Appendix C-12-2. The rare-metal values of all samples analysed from the area are characteristically low (e.g. 62 to 472 ppm Zr).

Discussion

The Musgravetown Group geochemical data indicates that it consists of basaltic flows, variable composition tuffaceous sandstone and felsic volcanic rocks. The felsic volcanic rocks have several geochemical affinities with similar rock types in the Traytown - Louil Hills area. Both suites of rocks are characterized by low agpaitic ratios, high Na_2O/K_2O, low rare-metals and very low Rb/Sr. These similarities suggest a tectonic and perhaps stratigraphic equivalence.

The Love Cove Group samples analysed consist of intermediate to low SiO_2 felsic rocks. They have some similar characteristics to the Musgravetown Group such as low agpaitic ratios, higher CaO, low rare-metals and low Rb/Sr. They differ by having much higher Na_2O/K_2O.

Conclusions

The volcanic rocks of the western basin of the Musgravetown Group and the Love Cove Group have very low potential for rare-metal mineralization.

6.3 Musgravetown Area

Introduction

The eastern basin of the Musgravetown Group, in the Musgravetown area, consists of red pebble conglomerate - sandstone, mafic volcanic rocks and felsic volcanic rocks. The sampled area lies between Bunyans Cove and Musgravetown and is bound in the north by Clode Sound (Figure 6-1). The initial geological mapping and lithogeochemical sampling program was carried out in 1½ days and a follow-up program lasted one day.

Samples were collected from a total of 25 sample sites in 1990 (BA90029 to BA90053) and ten sites in 1992 (BA92001 to BA92010); thin section samples were collected from 35 sites and geochemical samples were collected from 34 sites. A suite of 25 geochemical samples were analysed for major elements and a group of trace elements, including rare metals. The sample locations (NTS coordinates), rock type and other data (e.g. scintillometer readings) are given in Appendix A-12.

Geology

The Musgravetown Group, in this eastern basin, consists of a lowermost unit of red conglomerate and sandstone with minor mafic rocks (Cannings Cove Formation), an overlying unit of vesicular basalt and related tuff and an uppermost unit of aphyric and feldspar-phyric ash-flow tuffs. O'Brien (1993) has produced a map outlining the detailed stratigraphic and structural features of this region (Figure 6-2).

The Cannings Cove Formation consists of a minor lower mafic flow unit and the main red conglomerate and sandstone unit. The sandstone is interbedded with the conglomerates and consists of feldspar, quartz and lithic fragments, commonly less than 1 mm across, and is massive. The conglomerates range from pebble to boulder polymictic conglomerates.

The dominantly mafic volcanic unit above the Cannings Cove Formation consists of mafic vesicular flows, grey, layered, intermediate tuff, and thin, interbedded, massive felsic flows (?). The mafic flows are vesicular to amygduloidal with a diabasic-textured matrix; amygdules commonly consist of calcite or chlorite. Intermediate tuff is very fine grained and contains layers less than 5 mm. Three thin bands of felsic aphyric to sparsely feldspar-phyric flows and/or ash-flows were sampled in the mafic unit.

The felsic unit consists of aphyric to feldspar-phyric ash-flow tuffs and lithic-breccias with minor mafic flows. The bottom of the unit consists of interbedded mafic

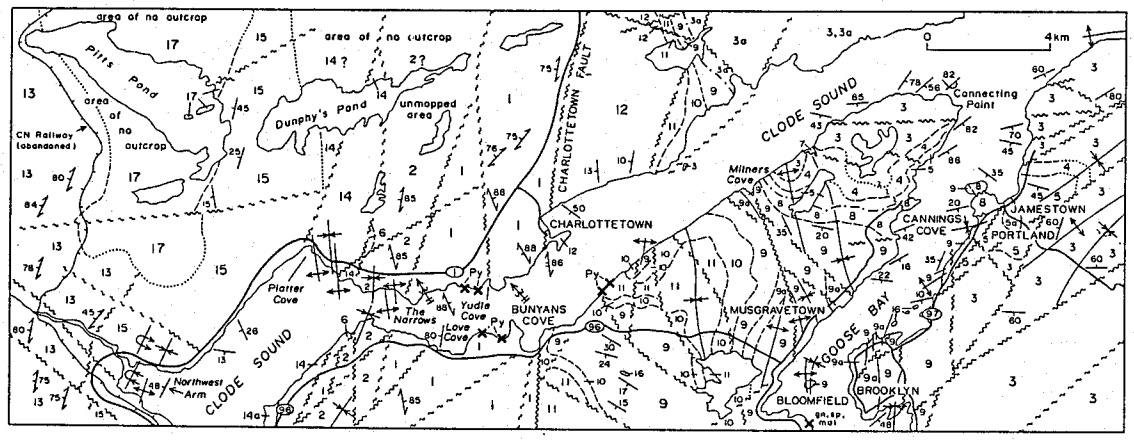

LEGEND (for Figure 3)

DEVONIAN ?

TERRA NOVA GRANITE

17 *Mainly massive, pink to buff, coarse-grained, K-feldspar porphyritic biotite granite; minor pink, fine- and medium-grained, K-feldspar porphyritic granite; rare equigranular granite and aplite*

LATE PRECAMBRIAN

16 *Dark-grey, fine-grained diorite; medium- to coarse-grained gabbro*

MUSGRAVETOWN GROUP (Units 8 to 15)

Western belt (Units 13 to 15)

15 *Red, purple and maroon, locally micaceous sandstone and lesser siltstone; minor coarse-grained red sandstone and pebble to cobble conglomerate; minor red shale and grey sandstone*

14 *Green, yellow, buff and grey, crossbedded sandstone; minor pebble conglomerate;* **14a,** *basalt*

13 *Red, yellow, buff, and purple, massive to strongly foliated tuffs and flows of felsic and intermediate composition; unseparated red felsic ash-flow tuff and banded rhyolite; minor mafic tuffs*

Eastern belt (Units 8 to 12: numbering reflects stratigraphic order within the belt but does bear on the relative ages of eastern and western belts of the Musgravetown Group)

12 *Unseparated red sandstone, red and maroon pebble to cobble conglomerate, and grey and green sandstone*

11 *Red, pink and pale-purple rhyolitic and rhyodacitic flows, ash-flow tuff and related pyroclastic rocks, including rheo-ignimbrite and related autobrecciated tuffs and flows; parataxitic and eutaxitic banded pumice-rich and pumice-poor tuff, flow-banded and massive rhyolite; unseparated purple and red, fine-grained, feldspar porphyry and felsite*

10 *Mainly dark-grey and green, locally maroon, vesicular basalt; minor basaltic breccia, mafic tuff and agglomerate; minor red sandstone and conglomerate; mafic lahar, conglomerate and mafic tuff*

9 *Red and maroon, polymict, pebble, cobble and boulder conglomerate; minor red and lesser grey and green sandstone and siltstone; locally contains thin, unseparated mafic flows;* **9a,** *basalt and mafic breccia*

8 *Pale-green cobble and pebble conglomerate; minor green and grey sandstone; rare red sandstone*

7 *Dark-green and grey, medium-grained hornblende gabbro*

6 *Equigranular, quartz-rich, hornblende - biotite granite*

CONNECTING POINT GROUP (Units 3 to 5)

5 *Green sandstone and minor granule conglomerate, grey and green siltstone;* **5a,** *minor red sandstone and siltstone*

4 *Pale-grey and green, interbedded, granule, pebble and cobble conglomerate and sandstone*

3 *Grey, black and grey-green, thin- to medium-bedded, fine-grained sandstone, siltstone and shale; minor medium- to thick-bedded green sandstone and siliceous siltstone; minor chert, tuff and tuffaceous sandstone;* **3a,** *grey and black phyllite, shale, siltstone and sandstone*

LOVE COVE GROUP (Units 1 and 2)

2 *Grey meta-arenite, phyllite, tuffaceous sandstone and conglomerate, siltstone and chert; minor unseparated metavolcanic rocks*

1 *Strongly foliated, chlorite- to biotite-grade, felsic to intermediate metavolcanic rocks of mainly pyroclastic origin; sericite schist and phyllite; minor quartz-phyric rhyolite flows, mafic flows and tuffs, and epiclastic metasedimentary rocks; unseparated pretectonic and posttectonic diabase dykes*

KEY

Geological contact (defined, approximate, assumed)
Unconformable contact
Bedding, tops known (horizontal, inclined, vertical, overturned)
Bedding, tops unknown (inclined, vertical)
Axial trace of syncline
Axial trace of anticline
Axial trace of overturned anticline
Axial trace of overturned syncline
Fault (defined, approximate, assumed)
Cleavage or foliation: first generation (inclined, vertical)
Cleavage or foliation: second generation (inclined, vertical)
Second-generation folds (arrow in direction of plunge)
Mineral occurrence × py

ABBREVIATIONS

py.....pyrite
gn.....galena
sp.....sphalerite
mal.....malachite

Figure 6-2 *Preliminary map of the (NTS) 2D/8NE–2C/5NW area.*

After O'Brien 1993

amygduloidal flows and aphyric ash-flow tuffs with layering and abundant ash-flow textures. The remainder of the unit consists of aphyric to feldspar-phyric ash-flow tuffs and lithic-breccias. Feldspar ranges from < 1 to 15%, 1 to 3 mm across and is commonly broken. Aphyric and sparsely feldspar-phyric, subangular to subrounded fragments are found in the lithic-breccias.

Results

Spectrometer data for the samples collected are listed in Appendix A-12. The range of total count readings for these Musgravetown Group rocks is 100 (mafic rocks) to 720 (felsic volcanic rocks) cps. The majority of the radiometric readings indicate little or no potential for rare metals, however the few highly anomalous values indicate some potential.

The geochemical data for the Musgravetown rocks are listed in Appendix B-12 and the averages and unique sample analyses are tabulated in Appendix C-12-3. The rare-metal values are quite variable, but high values (e.g. Zr > 1000 ppm) in several samples are encouraging.

Discussion

Geochemically the rocks in the Musgravetown sample area can be subdivided into three units: one is characterized by higher Al_2O_3, high Na_2O/K_2O and low Rb/Sr; rare-metal values are highly variable, another is characterized by the opposite features, and the last is characterized by low Al_2O_3 low alkalis and very high rare-metal values (e.g. 1577 - 3892 ppm Zr). The high Na_2O/K_2O group includes all of the mafic to intermediate rocks and the felsic ash-flows interbedded with mafic flows at the bottom of the uppermost unit. The low Na_2O/K_2O rocks are found in the upper part of the uppermost unit. The third group occurs as felsic flows or ash-flows in the main mafic flow (middle) unit of Musgravetown Group in the area.

The high Na_2O/K_2O geochemical group is similar to Musgravetown Group rocks observed in the western belt or basin. The upper, low Na_2O/K_2O group has no counterpart in the western basin.

Conclusions

The highest rare-metal values are found in the uppermost portion of the felsic unit (i.e. the low Na_2O/K_2O geochemical group) and the small felsic flows (?) found in the mafic unit. These highly anomalous felsic units clearly demonstrate the existence of anomalously high rare-metal values in the volcanic-feeding magma systems in this region. This area has medium to high potential for rare-metal mineralization and should be the subject of further follow-up.

6.4 Plate Cove Area

Introduction

The Plate Cove area of the Musgravetown Group occurs in the far eastern belt or basin of the Musgravetown Group (O'Brien, 1994). The sampled area lies between Plate Cove, in the north, and the highway between Southern Bay and Port Rexton (Figure 6-1). This geological mapping and lithogeochemical sampling program was carried out in one day.

Samples were collected from a total of ten sample sites (BA90064 to BA90073); thin section samples were collected from ten sites and geochemical samples were collected from nine sites. A suite of eight geochemical samples were analysed for major elements and a group of trace elements, including rare metals. The sample locations (NTS coordinates), rock type and other data (e.g. scintillometer readings) are given in Appendix A-12.

Geology

The Musgravetown Group rocks in the Plate Cove sample area, located in the far eastern basin (east of Indian Arm Fault), consist of mafic flows and aphyric, feldspar-phyric and quartz-feldspar-phyric ash-flow tuffs. These rocks have been correlated by O'Brien (1994) to the Bull Arm Formation.

All ash-flow tuffs in this unit contain broken feldspar, fiammé and other structures characteristic of ash-flow tuffs. The feldspar-phyric variety consists of <1 - 5 % feldspar grains, less than 2 mm across. The quartz-feldspar porphyritic variety consists of 2 - 15 % quartz grains, < 2 mm across and 2 - 8 % feldspar grains, < 2 mm across; one sample of this variety also contains aphyric and quartz-feldspar porphyritic fragments.

Results

Spectrometer data for the samples collected are listed in Appendix A-12. The range of total count readings for these Musgravetown Group rocks is 120 (mafic flows) to 410 (felsic volcanic rocks) cps. These radiometric readings indicate little or no potential for rare-metal mineralization.

The geochemical data for the Musgravetown rocks are listed in Appendix B-12 and the averages and unique sample analyses are tabulated in Appendix C-12-4. The rare-metal values, using Zr as an example, range from 136 to 792 ppm.

Discussion

Two of the geochemical groups observed in the Musgravetown area are also observed in the Plate Cove area: high Na_2O/K_2O and low Na_2O/K_2O. In this area the high Na_2O/K_2O rocks have very low rare-metal values and the other group has the characteristically high rare-metal values (e.g. Zr 539 - 792 ppm) and low Al_2O_3 values of peralkaline volcanic rocks. However, the low total alkalis, which may be due to Na-leaching, result in agpaitic ratios below 1.00. There appears to be continuity of the high Na_2O/K_2O felsic suite in the Musgravetown Group throughout all three belts or basins defined by O'Brien (1993, 1994). The low Na_2O/K_2O group has not been observed in the western belt.

Conclusions

The relatively high rare-metal values indicate that these rocks have peralkaline affinities. However, there is no indication of extreme enrichment of rare-metals. The Plate Cove area has a low potential for rare-metal mineralization.

6.5 Clarenville Area

Introduction

The Clarenville area targets have been split into three zones to facilitate the discussion: Clarenville belt, Random Island belt and the North West Brook belt. The Clarenville belt is located between the community of Clarenville and George's Brook, the Random Island belt is located east of the community of Britannia on Random Island and the North West Brook belt is located near the community of the same name (Figure 6-1). This geological mapping and lithogeochemical sampling program was carried out in one day.

Samples were collected from a total of 19 sample sites (BA90059 to BA90063 and BA90077 to BA90090); thin section samples were collected from 19 sites and geochemical samples were collected from 18 sites. A suite of seven geochemical samples were analysed for major elements and a group of trace elements, including rare metals. The sample locations (NTS coordinates), rock type and other data (e.g. scintillometer readings) are given in Appendix A-12.

Geology

The Clarenville belt and the North West Brook belt are located in the eastern basin of the Musgravetown Group between the Love Cove and Connecting Point Groups. The Random Island belt is located in the far eastern basin of the Musgravetown Group to the east of the Connecting Point Group.

The Random Island belt contains red to grey arkosic sandstones with pebbly zones and very fine grained tuffaceous sandstones with coarser grained lenses. These rocks were not studied in detail due to the obvious sedimentary environment of most of the rocks observed.

The North West Brook belt consists of massive, maroon, feldspar porphyries of unknown origin. They are characterized by an aphanitic matrix and < 5 to 15% plagioclase feldspar phenocrysts up to 3 mm across.

Rocks in the Clarenville belt consist of maroon, massive to layered aphyric flows and ash-flows.

Results

Spectrometer data for the samples collected are listed in Appendix A-12. The range of total count readings for these Musgravetown Group rocks is 150 to 205 cps in the Random Island belt, 180 to 420 in the North West Brook belt and 180 to 320 in the Clarenville belt. These radiometric readings indicate little or no potential for rare metals.

The geochemical data for these rocks are listed in Appendix B-12 and the averages and unique sample analyses are tabulated in Appendix C-12-5. The rare-metal values, using Zr as an example, range from 111 to 438 ppm.

Discussion

The geochemistry of the rocks in the North West Brook and Clarenville belts is dominated by Al_2O_3-rich intermediate to felsic rocks which appear to fit neither of the grouping identified in the areas to the north. The low rare-metal values and the low agpaitic ratios suggest that these rocks are not connected to those rocks of peralkaline nature or affinity in the northern areas.

Conclusions

The relatively low rare-metal values indicate that these rocks have a very low potential for rare-metal mineralization.

6.6 Hodges Cove

Introduction

This area was sampled to obtain a few reconnaissance samples. This belt of Musgravetown Group rocks is located around the community of Hodges Cove in the Southwest Arm of Random Sound (Figure 6-1). This geological mapping and lithogeochemical sampling program was carried out in a partial day.

Samples were collected from a total of three sample sites (BA90074 to BA90076); thin section and geochemical samples were collected from all three sites. One geochemical sample was analysed for major elements and a group of trace elements, including rare metals. The sample locations (NTS coordinates), rock type and other data (e.g. scintillometer readings) are given in Appendix A-12.

Geology

The Hodges Cove belt occurs in the far western belt of Musgravetown rocks. The rocks consist of a sequence of maroon, very fine grained tuffs and tuffaceous sediments with interbedded mafic flows. The groundmass of these rocks consists of quartz and feldspar grains.

Results

Spectrometer data for the samples collected are listed in Appendix A-12. The range of total count readings for these Musgravetown Group rocks is 170 - 270 cps. These radiometric readings indicate little or no potential for rare-metal mineralization.

The geochemical data for one sample are listed in Appendix B-12 and Appendix C-12-6. The rare-metal values, using Zr as an example, are low (325 ppm Zr).

Discussion

The Hodges Cove sample is very similar to aphyric and feldspar-phyric rocks in the North West Brook and Clarenville belts. The low rare-metal values and the low agpaitic ratios suggest that the rocks of this belt are not connected to rocks of peralkaline nature or affinity in the northern areas.

Conclusions

The relatively low rare-metal values indicate that these rocks have a very low potential for rare-metals.

6.7 Sunnyside Area

Introduction

The Sunnyside belt of the Musgravetown Group consists of aphyric, feldspar and quartz porphyritic ash-flow tuffs. It is located just northeast of the community of Sunnyside on the north shore of Bull Arm (Figure 6-1). This geological mapping and lithogeochemical sampling program was carried out in two days.

Samples were collected from a total of 31 sample sites (BA90091 to BA90121); thin section samples were collected from 31 sites and geochemical samples were collected from 27 sites. A suite of 19 geochemical samples were analysed for major elements and a group of trace elements, including rare metals. The sample locations (NTS coordinates), rock type and other data (e.g. scintillometer readings) are given in Appendix A-12.

Geology

The Sunnyside occurrence of the Musgravetown Group occurs east of the Connecting Point Group and thus belongs to the far eastern basin or belt. These rocks are almost consistently felsic and consist of a group of aphyric ash-flows, quartz, feldspar and quartz-feldspar porphyritic ash-flow tuffs and associated lithic breccias, with minor mafic flows.

The lithic breccias commonly range from 5 to 40 % subrounded to subangular fragments from < 0.5 to 15 cm across. Fragment types range from aphyric to sparsely feldspar-phyric to quartz-feldspar-phyric. The groundmass is commonly aphanitic to very fine grained.

The feldspar, quartz and feldspar-quartz porphyries with low quantities of phenocrysts commonly have from 0 - 3 % quartz grains and 0 - 3 % feldspar grains, ranging from 1 - 2 mm across. The feldspar is commonly microperthite and the groundmass is usually aphanitic.

The sparsely porphyritic and aphyric ash-flows commonly exhibit abundant lithophysia, radial-textured structures, fiammé and banding. Almost all units sampled are ash-flows.

Results

Spectrometer data for the samples collected are listed in Appendix A-12. The range of total count readings for these Musgravetown Group rocks is 70 (mafic flow) to 460 (felsic volcanic rocks) cps. The majority of the radiometric readings indicate little or no potential for rare metals.

The geochemical data for the Sunnyside samples are listed in Appendix B-12 and the averages and unique sample values are tabulated in Appendix C-12-7. The rare-metal values are generally low but quite variable (e.g. Zr 212 to 785 ppm).

Discussion

Most of the aphyric and quartz-bearing porphyries in the Sunnyside area are characterized by very low Na_2O/K_2O, low Al_2O_3 high Rb/Sr, low rare-metal values (e.g. 212 - 462) and agpaitic ratios between 0.93 to 0.96. These features are unique amongst the felsic rocks observed in the Musgravetown Group in this study. The presence of low SiO_2 (near 66 %) lithic breccias with feldspar-phyric clasts or feldspar-phyric ash-flows establishes a link between the Clarenville, North West Brook and Hodges Cove rocks.

Conclusions

All samples studied in the Sunnyside area have low to intermediate values of rare-metals (e.g. 212 - 785 ppm Zr) and low radiometric values indicating low potential for rare-metal mineralization.

6.8 Masters Head Area

Introduction

The Masters Head area of the Musgravetown Group consists of feldspar porphyritic ash-flow tuffs and lithic breccias. It is located on the south side of Bull Arm, 7 km west of the community of Southern Harbour (Figure 6-1). This geological mapping and lithogeochemical sampling program was carried out in one day.

Samples were collected from a total of 12 sample sites (BA90136 to BA90147); thin section samples were collected from 12 sites and geochemical samples were collected from 11 sites. A suite of five geochemical samples were analysed for major elements and a group of trace elements, including rare metals. The sample locations (NTS coordinates), rock type and other data (e.g. scintillometer readings) are given in Appendix A-12.

Geology

The Masters Head occurrence of the Musgravetown Group occurs east of the Connecting Point Group and thus belongs to the far eastern basin or belt. These rocks form a sequence of plagioclase feldspar-phyric ash-flow tuffs and lithic breccias with associated mafic flows.

The ash-flows contain < 5 - 10 % sparsely broken feldspar phenocrysts which range from 1 - 5 mm in size. The matrix is aphanitic to fine grained and contains fiammé, lenticular structures and layering.

Lithic breccias contain 20 - 40 % subrounded to subangular fragments from 0.5 to 20 cm across. The matrix is aphyric to feldspar-phyric ash-flow tuff. Fragments are commonly aphyric or feldspar-phyric.

Results

Spectrometer data for the samples collected are listed in Appendix A-12 The range of total count readings for these Musgravetown Group rocks is 85 (mafic flow) to 370 (felsic volcanic rocks) cps. The majority of the radiometric readings indicate little or no potential for rare-metal mineralization.

The geochemical data for the Masters Head samples are listed in Appendix B-12 and the averages and unique sample values are tabulated in Appendix C-12-8. The rare-metal values are very low (e.g. Zr 199 to 267 ppm).

Discussion

The Masters Head felsic volcanic rocks are characterized by very low rare-metal values, fairly equivalent Na_2O and K_2O values and low Rb and fairly high Sr. This set of characteristics is relatively unique amongst the other felsic rocks studied in the Musgravetown Group.

Conclusions

All samples studied in the Masters Head area have low values of rare-metals (e.g. 199 to 267 ppm Zr) and low radiometric values indicating very low potential for rare-metal mineralization.

6.9 Doe Hills Area

Introduction

The Doe Hills area of the Musgravetown Group consists feldspar porphyritic, aphyric and quartz-feldspar porphyritic ash-flow tuffs and lithic breccias. It is located on the south side of Bull Arm, near the communities of Little Harbour East (Placentia Bay), Chance Cove and Bellvue (Figure 6-1). This geological mapping and lithogeochemical sampling program was carried out in three days.

Samples were collected from a total of 82 sample sites (BA90122 to BA90135 and BA90148 to BA90215); thin section samples were collected from 82 sites and geochemical samples were collected from 81 sites. A suite of 29 geochemical samples were analysed for major elements and a group of trace elements, including rare metals. The sample locations (NTS coordinates), rock type and other data (e.g. scintillometer readings) are given in Appendix A-12.

Geology

The Doe Hills occurrence of the Musgravetown Group occurs east of the Connecting Point Group and thus belongs to the far eastern basin or belt. These rocks form two separate sequences of volcanic rocks: 1) a sequence of plagioclase feldspar-phyric ash-flow tuffs and lithic breccias with associated mafic flows, and 2) a unit of quartz-feldspar porphyritic ash-flow tuffs and lithic breccias.

The quartz-feldspar porphyritic ash-flow tuffs and lithic breccias occur in the central part of the Doe Hills area and are flanked on both sides by feldspar-phyric ash-flow tuffs and lithic breccias. Green, layered to massive, siltstones and red sandstones, siltstones and conglomerates flank the feldspar-phyric units to the east on the outer borders of the Musgravetown Group. Connecting Point Group are in contact with these sedimentary rocks to the west.

The feldspar-bearing ash-flow tuffs occur as a feldspar-poor, 2 to 10 % phenocrysts, and a feldspar-rich, 25 to 35 % phenocrysts, variety. Feldspar grains are plagioclase and range from < 1 to 3 mm in size. Textures indicate an ash-flow origin and sparse aphyric fragments are common. Secondary sericite and epidote are found in many of the plagioclase-bearing ash-flows.

Lithic breccias and lapilli tuffs, that have a feldspar-phyric matrix, contain 10 to 70 % angular to subangular fragments which range in size from < 1 to 30 mm. Fragments

commonly consist of: several colours of aphyric flows (?), feldspar-porphyritic ash-flows, and dark green, mafic to intermediate, flows (?). The matrix usually has textures indicative of ash-flows and contains 5 to 10 % plagioclase feldspar grains.

Quartz-feldspar ash-flow tuffs contain < 2 to 15 % feldspar grains, from 1 to 3 mm across, and < 2 to 15 % quartz grains, from < 1 to 3 mm across. Minor concentrations of aphyric or quartz-feldspar porphyritic fragments may also been observed in some outcrops.

Lithic breccias and lapilli-tuffs with quartz and feldspar in the matrix have from 5 to 80 % fragments in a matrix of quartz-feldspar ash-flow tuffs similar in character to those described above. Fragments are dominantly quartz-feldspar porphyric with minor amounts of aphyric fragments. They are subangular to angular and range from <1 to 15 cm in size.

Results

Spectrometer data for the samples collected are listed in Appendix A-12. The range of total count readings for these Musgravetown Group rocks is 140 (mafic flow) to 600 (quartz-feldspar lithic ash-flow breccia) cps. The majority of the radiometric readings indicate low or no potential for rare-mineralization.

The geochemical data for the Doe Hills samples are listed in Appendix B-12 and the averages and unique sample values are tabulated in Appendix C-12-9. The rare-metal values are very low (e.g. Zr 133 to 540 ppm).

The Doe Hills geochemical data can also be roughly divided into two groups based on phenocrysts: 1) a feldspar-phyric group, and, 2) a quartz-feldspar-phyric group. The feldspar porphyries are quite variable in composition due, in part, to the fact that some analyses are from lithic breccias with a variety of fragment types, but they can be characterized by: 1) high alumina (> 13.5 to 16.5 %), 2) low silica (< 71 %), 3) high CaO (0.8 to 5.0 %), 4) low Zr (< 300 ppm), and, 5) low Rb/Sr. The quartz-feldspar porphyries can be further subdivided into two subgroups but they are generally characterized by: 1) high silica (70 - 76 %), 2) low MgO (< 0.20 %), and, 3) low TiO_2 (< 0.15 %). The two subgroups of quartz-feldspar porphyry can be divided on the basis of alumina (> 14.5 % vs. < 13.0 %).

Discussion

The majority of the rocks in the Doe Hills area contain high alumina, high CaO and low concentrations of incompatible elements indicating that they are neither peralkaline in composition nor related to peralkaline rocks.

The feldspar porphyries show some similarities with similar rock types in the Masters Head, Sunnyside and Clarenville areas. The volcanic rocks in these areas may be linked through formation from similar sources or in similar tectonic settings. The low alumina quartz-feldspar porphyries in the Doe Hills also have some similarities with the similar rocks in the Sunnyside area providing further evidence to suggest a similar environment and tectonic setting. It appears that the high alumina rocks are more abundant and the low alumina rocks are less abundant in the Doe Hills area than in the Sunnyside area.

Conclusions

All samples studied in the Doe Hills area have low values of rare-metals (e.g. 133 to 405 ppm Zr) and low radiometric values indicating very low potential for rare-metal mineralization. One anomalous sample, containing 801 ppm Y but low values of Zr and Nb, has not been followed-up to date. However, the unfavourable environment for rare metals and lack of significant quantities in this area suggest that further work in this area is not justified.

7.0 Flowers River Igneous Suite

Introduction

The Flowers River Igneous Suite (FRIS) consists of a series of peralkaline to metaluminous volcanic, hypabyssal and plutonic rocks (Hill 1982). These rocks are located near the coast of Labrador in the vicinity of Flowers River and Hunt Lake southwest of the coastal community of Davis Inlet and northwest of the coastal community of Hopedale (Labrador; Figure 7-1). The reports of peralkaline rocks in the region (Hill 1981, Collerson 1982) and the indications of high values of Y and Zr in the volcanic rocks (Hill 1982, Miller 1988) indicate that there is high potential for rare-metal mineralization FRIS. This potential was evaluated during a three day geological mapping and lithogeochemical sampling program carried out over two years.

The Flowers River area is accessible by helicopter or float plane; several small lakes in the map area allow float plane access. The area was initially mapped in and sampled in 1991 during a four week program which consisted of 21 foot traverses and two days of helicopter supported sampling and mapping. Follow-up in the parts of the map area indicating the best potential for rare-metal mineralization and in those areas where more geological mapping was needed was carried out the 1992 program. This program consisted of 13 days of traversing and one day of helicopter supported sampling and mapping.

Samples were collected from a total of 404 sample sites, 273 collected in 1991 (FR91001 to FR91273) and 131 collected in 1992 (FR92001 to FR92131); thin section samples were collected from all 404 sites and geochemical samples were collected from 346 of these sites. A suite of 343 geochemical samples were analysed for major elements and a group of trace elements, including rare metals; a representative suite of samples were also analysed for REE. The sample locations (NTS coordinates), rock type and other data (e.g. scintillometer readings) are given in Appendix A-13.

Geology

The geology of the Flowers River volcanic rocks has been the focus of a detailed study to determine the structure and stratigraphy of the Nuiklavik. This detailed study was needed to help determine the source and control of the rare-metal mineralization. This work is described in Section 7.1.

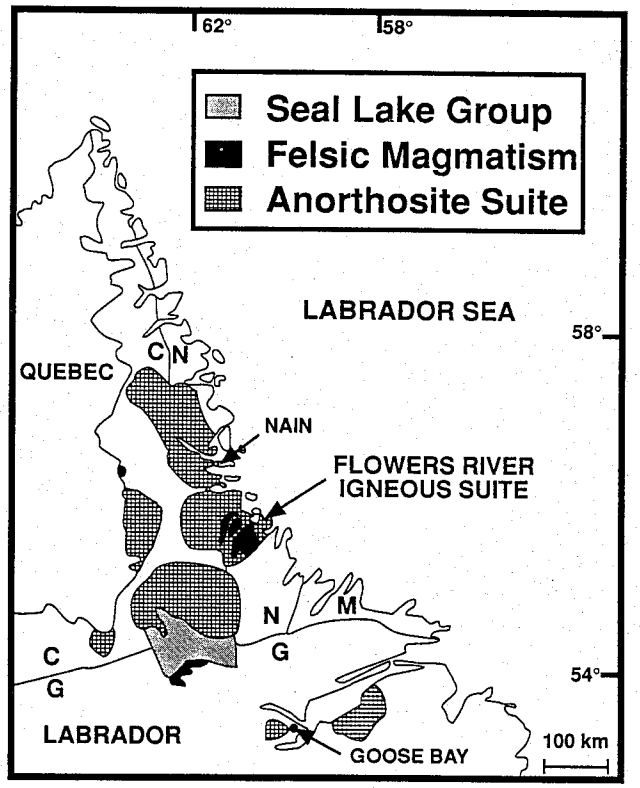

Figure 7-1 *Location map of the Flowers River Igneous Suite and the Nuiklavik felsic volcanic rocks, Labrador. Structural provinces: C = Churchill, N = Nain, G = Grenville, M = Makkovik.*

Results

Spectrometer data for the samples collected are listed in Appendix A-13. The range of total count readings for the felsic rocks is 190 to 3000 cps. A total of 27 samples, collected in this program, have radiometric readings greater than or equal to 1000 cps. Comparison of these values with those from mineralized peralkaline rocks at Strange Lake (Table 1-3, 1-4) indicate that, based on radioactivity, these rocks have a high potential for rare-metal mineralization. Note that most of the highly radioactive rocks are found in Unit 4 aphyric ash-flow tuff (average 938 cps), aphyric ash-flow breccia (1189 cps) and quartz-poor ash-flow tuff (average 895 cps).

The geochemical data for the KPC rocks are listed in Appendix B-13 and the averages and unique sample values are tabulated in Appendix C-13. The geochemical data have been grouped into geochemically similar groups within each unit and rock type. They have also been grouped by the absence or presence of widespread alteration of the groundmass and phenocrysts of feldspar.

The highest rare-metal values observed in the Nuiklavik data set are observed in Unit 4 aphyric ash-flow tuff (average 4663 ppm Zr and 419 ppm Y), aphyric ash-flow breccia (average 6099 ppm Zr and 582 ppm Y) and quartz-poor ash-flow tuff (average 5505 ppm Zr and 563 ppm Y). Grab sample values are up to 21104 ppm Zr and 1888 ppm Y. These values are extremely anomalous for rare metals and are indicative of high potential for rare-metal mineralization.

Discussion

The study of the Flowers River Igneous Suite, the Nuiklavik volcanic rocks and the associated mineralization is still on-going. However, several aspects of the petrology and the metallogeny of these rocks are presently well-enough understood to warrant discussion: 1) the nature of the metasomatic event observed throughout much of the suite, and, 2) some aspects of the mineralization. Some aspects of the rare-metal mineralization are discussed in Section 7.2 and the Na-depletion metasomatic event and its relationship to mineralization is discussed in Section 7.3.

Conclusions

All data collected indicate that the Nuiklavik volcanic rocks, in particular Unit 4 aphyric and quartz-poor ash-flow tuffs and lithic breccias, have a high potential for rare-metal mineralization. These rocks represent the upper, highly differentiated, fluid of one or several peralkaline magma chambers associated with at least two calderas of the Nuiklavik nested cauldron complex. This fluid occupied a relatively small proportion of the magma chamber and erupted as very low volume ash-flow tuffs and ash-flow lithic breccias. The mineralization was concentrated within the host calderas very close to the source vent(s).

The Nuiklavik volcanic rocks represent a third major resource, Strange Lake and Letitia Lake being the others, of rare-metal mineralization in Labrador. It is thus very difficult to explain why this area has not been staked and prospected for rare-metal mineralization by a mineral exploration company.

7.1 Geology and Stratigraphy of the Nuiklavik volcanic suite

I Introduction

The Flowers River Cauldron Complex (FRCC) is a Middle Proterozoic (1271 Ma; Brooks in Hill 1991) felsic peralkaline cauldron complex consisting of a number of partially eroded nested calderas. This complex occupies an area of approximately 100 km^2, intrudes the Nain structural province, and is located near the coast of Labrador, 70 km south of Nain (Figure 1).

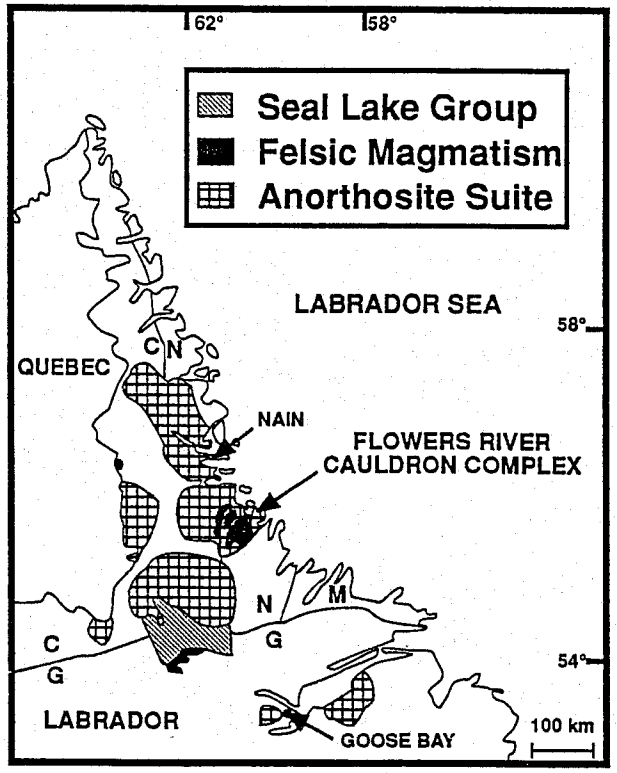

Figure 1

Volcanic rocks of the FRCC were first mapped in 1953 (Beavan, 1954) by BRINEX during a reconnaissance exploration program; they were named the 'Nuiklavik volcanic rocks' in that report. The granites and volcanic rocks in the vicinity were further mapped in 1971, at a scale of 1:250,000, by the Geological Survey of Canada (Taylor, 1979). Hill (1981, 1982) studied the regional geology (1:100,000 scale) of the Flowers River and Notokwanon River areas, which included the Flowers River Igneous Suite, FRCC and related rocks. The geochemistry and Rb-Sr geochronology of some of the granitic rocks of the region, including the Flowers River peralkaline granites, is given in Collerson (1982). White (1980), Hill (1981, 1982), Hill and Thomas (1983), Hill and

Miller (1990) and Hill (1991) report on various other aspects of the geology, geochemistry and tectonic setting of the Flowers River Igneous Suite. More recent geological investigations have been reported in Miller (1992, 1993), Miller and Abdel-Rahman (1992) and Abdel-Rahman and Miller (1993).

Geological investigations by Hill (1981, 1982) and the follow-up geochemical work of McConnell (1984) concluded that the Nuiklavik volcanic rocks contain numerous small showings of pyrite, sphalerite, galena, molybdenite and fluorite, with high radioactivity associated with some of the pyrite-bearing rocks. White (1980), Hill (1982) and our on-going geochemical investigations show that the volcanic rocks are enriched in rare metals (Y, Zr, REE), reaching values of economic interest (Miller 1988, 1993).

The Flowers River Igneous Suite is one of several peralkaline anorogenic complexes which were formed in Labrador during the Middle Proterozoic (Hill and Miller 1990). The other complexes are the Strange Lake peralkaline complex (Miller 1986), the Letitia Lake Group and the Red Wine Intrusive Suite (Hill and Thomas 1983; Miller 1987). These peralkaline rocks, along with the Flowers River Igneous Suite, occur within a large belt of anorogenic magmatic activity that extends from the southwestern United States to Scandinavia (e.g., Herz 1969, Emslie 1978a, Winchester and Max 1987, Windley 1989). Igneous complexes of this anorogenic belt were emplaced ca. 1200 - 1500 Ma.

In this paper we use the terms 'cauldron' and 'cauldron complex' to denote the overall volcanic-subvolcanic structure, including the nested collapse zones, the floor zone, ring dykes and other products of the associated magma chambers. The term 'caldera' is used to designate the individual collapse structures which became part of the cauldron complex.

Numerous examples of Phanerozoic cauldron-caldera complexes have been studied in some detail (cf. Lipman 1984; Mahood 1984; Elston 1984). But, even among these Phanerozoic complexes, there is a major lack of detailed studies of the structure, stratigraphy and eruptive style of peralkaline volcanos (Houghton et al. 1992). Many fewer investigations have been carried out on Proterozoic peralkaline cauldron-caldera complexes (e.g. Kellogg 1985), as most known peralkaline Proterozoic complexes are deeply eroded with little or no volcanic material preserved. This paper, which is part of an on-going project to study the volcanic rocks and rare-metal mineralization of the FRCC, provides information on a small, well-preserved, relatively unmetamorphosed, Proterozoic peralkaline cauldron complex. We present here a detailed geological map of the cauldron complex, report on the details of the stratigraphy, petrography and structure of the volcanic units, and interpret the cauldron complex evolution.

II Regional Geology

The Flowers River Igneous Suite intrudes Archean gneisses of the Nain Province (Hopedale block), Lower Proterozoic gneisses (reworked Archean?; Ryan 1990; Ermanovics and Ryan 1990) of the Churchill (Rae) Province (Hoffman 1990), and the Proterozoic Nain Plutonic Suite (Figure 2).

Archean gneisses of the Nain Province are sporadically exposed within the Flowers River Igneous Suite and Nain Plutonic Suite as roof pendants or inliers and they form an extensive unit to the east (Hill 1982, Ermanovics 1990). These rocks form part of the Hopedale block of the Nain or North Atlantic Craton and have an age range of 3.1 to 3.2 Ga. (Ermanovics 1990).

Churchill Province gneisses occur on the western edge of the Flowers River Igneous Suite and Nain Plutonic Suite plutonic rocks in the study area. These gneisses consist of Tasiuyak-type metasedimentary gneiss (Thomas and Morrison 1991), mylonite and metavolcanic-metasedimentary rocks of the Ingrid Group (Ermanovics and Ryan 1990); the Ingrid Group is in fault contact with the Hopedale block to the east. Available age data suggest that the Churchill gneisses are Archean rocks which were reworked during the Lower Proterozoic (Ermanovics and Ryan 1990; Ryan et al. 1992). Magmas of the Flowers River Igneous Suite and the Nain Plutonic Suite appear to have intruded the crust at or near the contact between the rocks of the Churchill Province (Torngat orogen) and rocks of the Nain Craton.

Members of the Nain Plutonic Suite, found in contact with the Flowers River Igneous Suite or as roof pendants and xenoliths within it, include, in order of decreasing age, gabbro-anorthosite, ferrodiorite and related rocks, and subsolvus granitic plutons. Reconstruction of the previously disaggregated plutons (Figure 3), based on geological maps (Hill 1982; Thomas and Morrison 1991) and a computer-enhanced regional aeromagnetic data (provided by J. Kilfoil, 1992), reveals that the present site of the investigated cauldron complex was the locus of the following intrusions: a 45 km diameter gabbro-anorthosite, a 37 km diameter ferrodiorite and the intrusions of the Flowers River Igneous Suite, which range from < 1 to 12 km wide and <1 to 45 km long. Age data for these plutons range from 1411 ± 18 Ma (Rb-Sr; Brooks in Hill 1982) for the Flowers Bay Anorthosite, to 1292 Ga for the Notokwanon quartz monzonite (U-Pb zircon; Ryan et al. 1992) and 1291 the Char Lake quartz monzonite (U-Pb zircon; Brooks 1983).

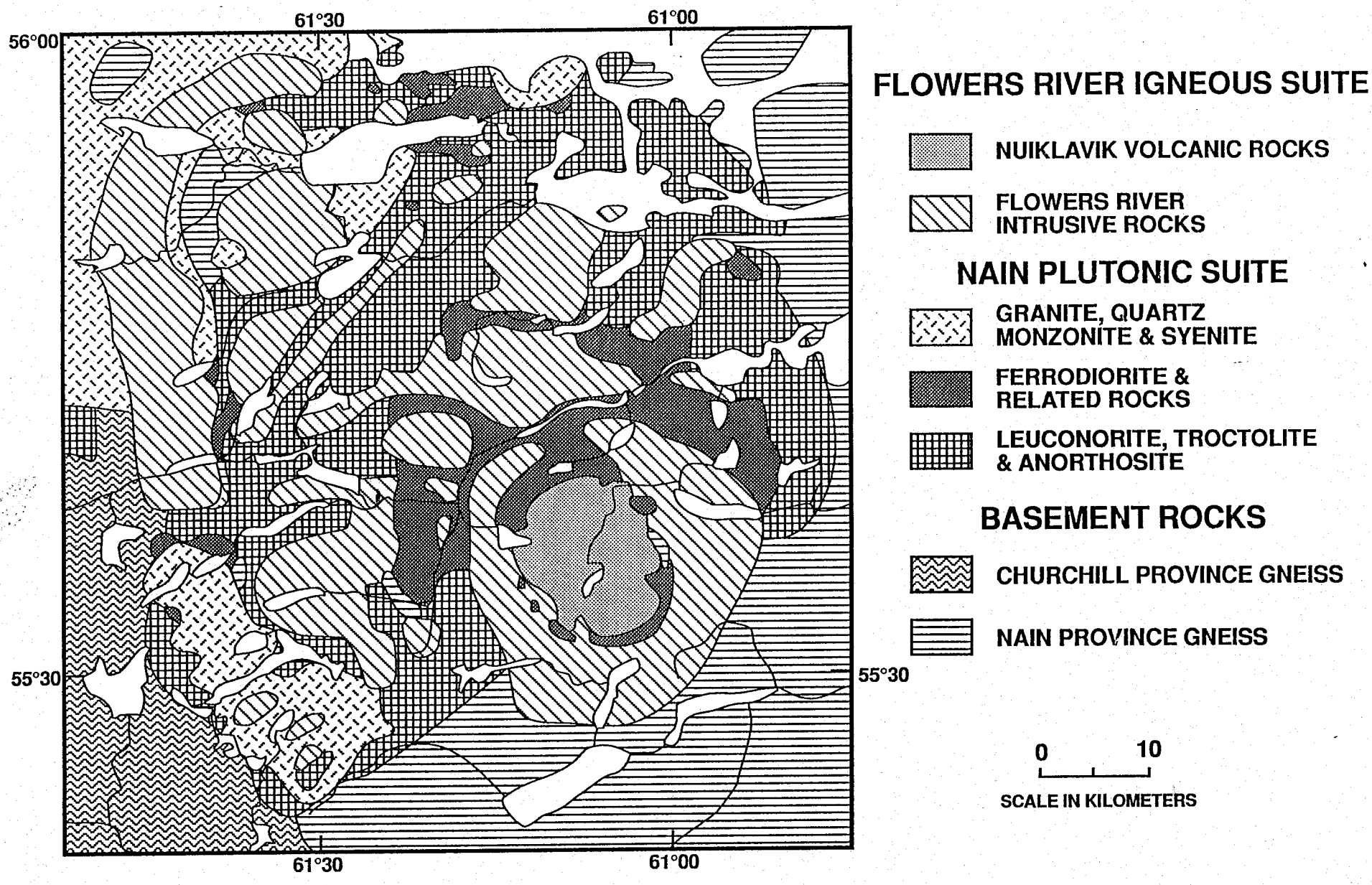

Figure 2. Regional geology in the vicinity of the Flowers River cauldron complex; modified from Thomas and Morrison (1991) and Hill (1981, 1982 and 1991).

Figure 3. Regional sequence-timing map illustrating the various pre-cauldron complex regional intrusions and their relationship to the basement rocks and the Flowers River cauldron complex.

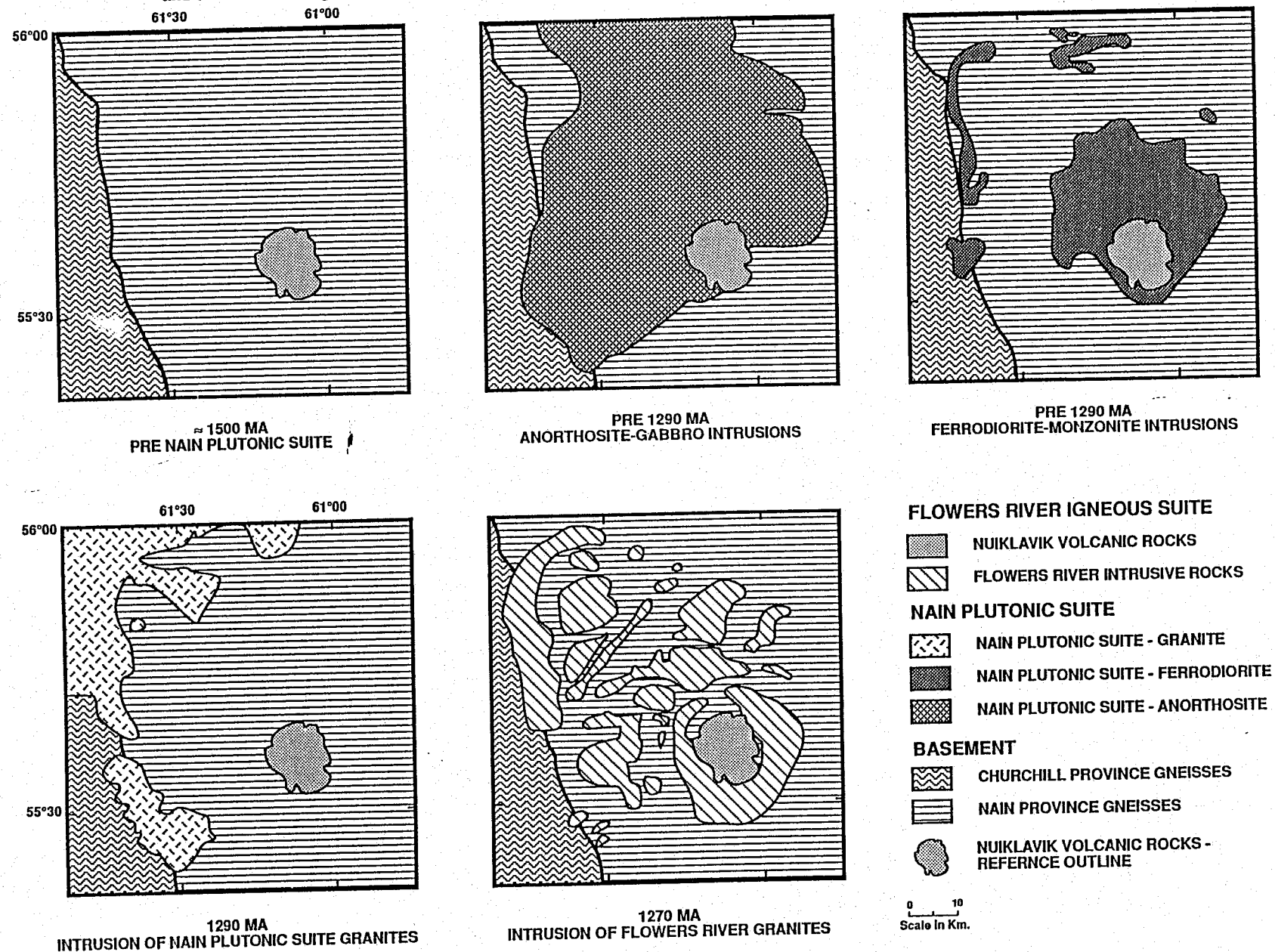

III Geology and stratigraphy of the cauldron complex

The Flowers River Igneous Suite was defined by Hill (1981, 1982) to include the peralkaline granite and related volcanic rocks in the vicinity of Flowers River. The suite is divided into volcanic and plutonic units: Flowers River intrusive rocks and Nuiklavik volcanic rocks (Miller 1992).

Peralkaline granites of the Flowers River Igneous Suite have been subdivided (Hill 1982) into normal, marginal and chilled phases, based on textural and mineralogical criteria: normal granite is medium to coarse grained and contains essential peralkaline amphibole or pyroxene, marginal granite is medium to coarse grained and contains Na-poor mafic minerals, and the chilled granite is fine grained or porphyritic in nature. The marginal granite most commonly contains olivine and occurs on the margins of plutons (Hill 1982), whereas the chilled granite occurs around the Nuiklavik volcanics and in the upper portions of some plutons in the Flowers River Igneous Suite. Collerson (1982) also observed chemical and mineralogical differences between the 'marginal' and 'normal' granites and thus subdivided them into aegirine-amphibole peralkaline granite and pyroxene-olivine granite.

In this study the Flowers River intrusive rocks have been subdivided into coarse to medium grained and fine grained-porphyritic (microgranite) varieties. Chemical and petrographic analysis of individual samples and outcrops allow a further subdivision into peralkaline and clinopyroxene-amphibole-fayalite subalkaline granite. The proposed subdivision recognizes that:

1) peralkaline and subalkaline (olivine-bearing) granites do occur and the implied chemical differences may be genetically significant in the FRCC;
2) porphyritic, fine grained and granophyric varieties of both peralkaline and olivine granites are present; these textural varieties have petrogenetic significance; and
3) peralkaline and olivine-bearing granites are difficult to distinguish in the field, particularly for fine grained varieties and where olivine is altered, which is a common occurrence.

Olivine gabbro and gabbro sills, associated with the lower portion of the Nuiklavik volcanic rocks, have also been included in the Flowers River Igneous Suite due to the close spatial and temporal association between these rocks.

The geological map of the FRCC is given in Figure 4 and the general stratigraphy of the Nuiklavik volcanic rocks is outlined in Figure 5. A number of nested calderas have been identified on the basis of stratigraphic and structural data (see below) and some unique stratigraphic features are found in some of the individual calderas; these are illustrated in the correlated stratigraphic sections of Figure 6.

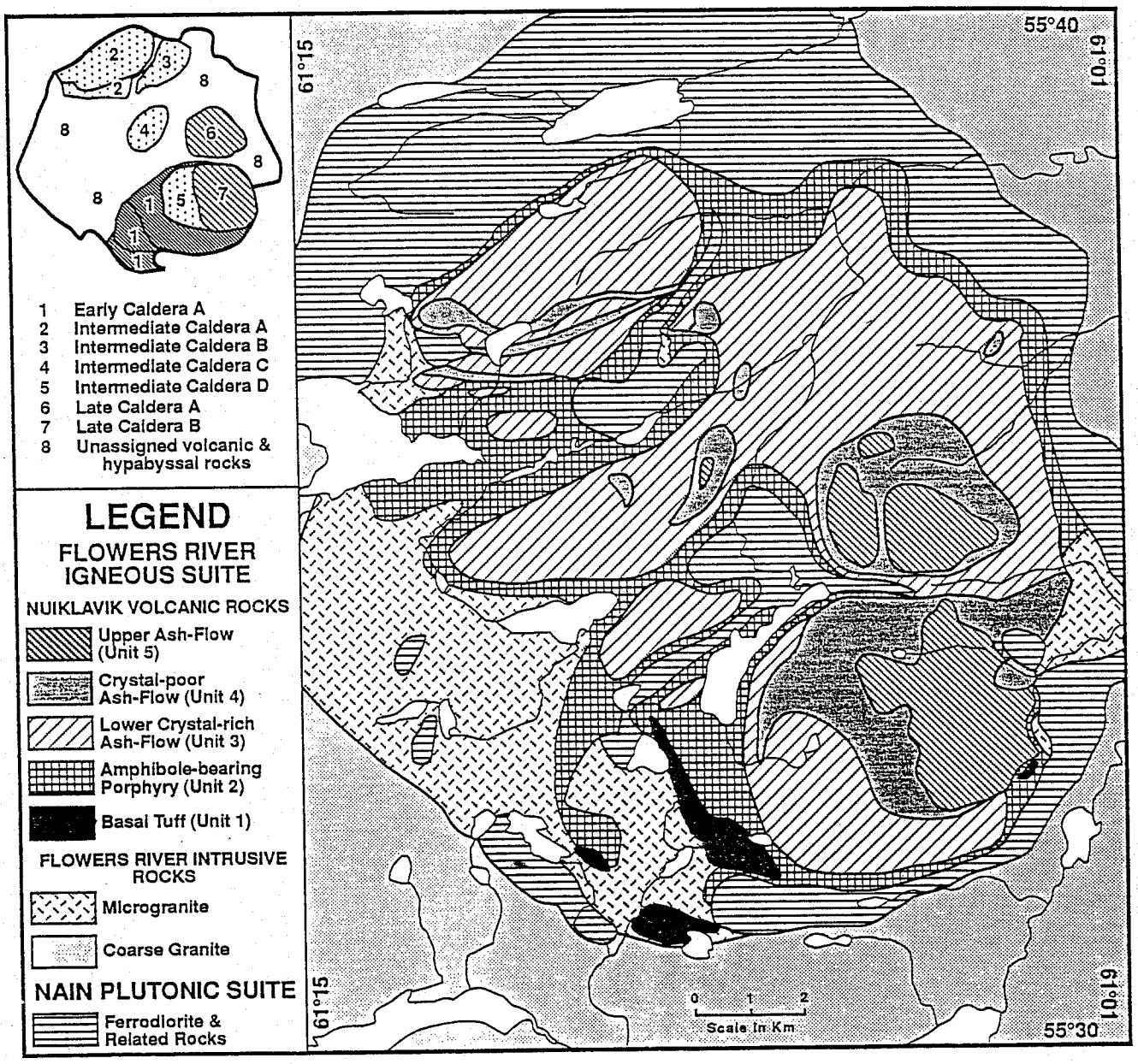

Figure 4. General geology of the Flowers River cauldron complex with an insert outlining the identified nested calderas; modified from Miller 1992 and 1993.

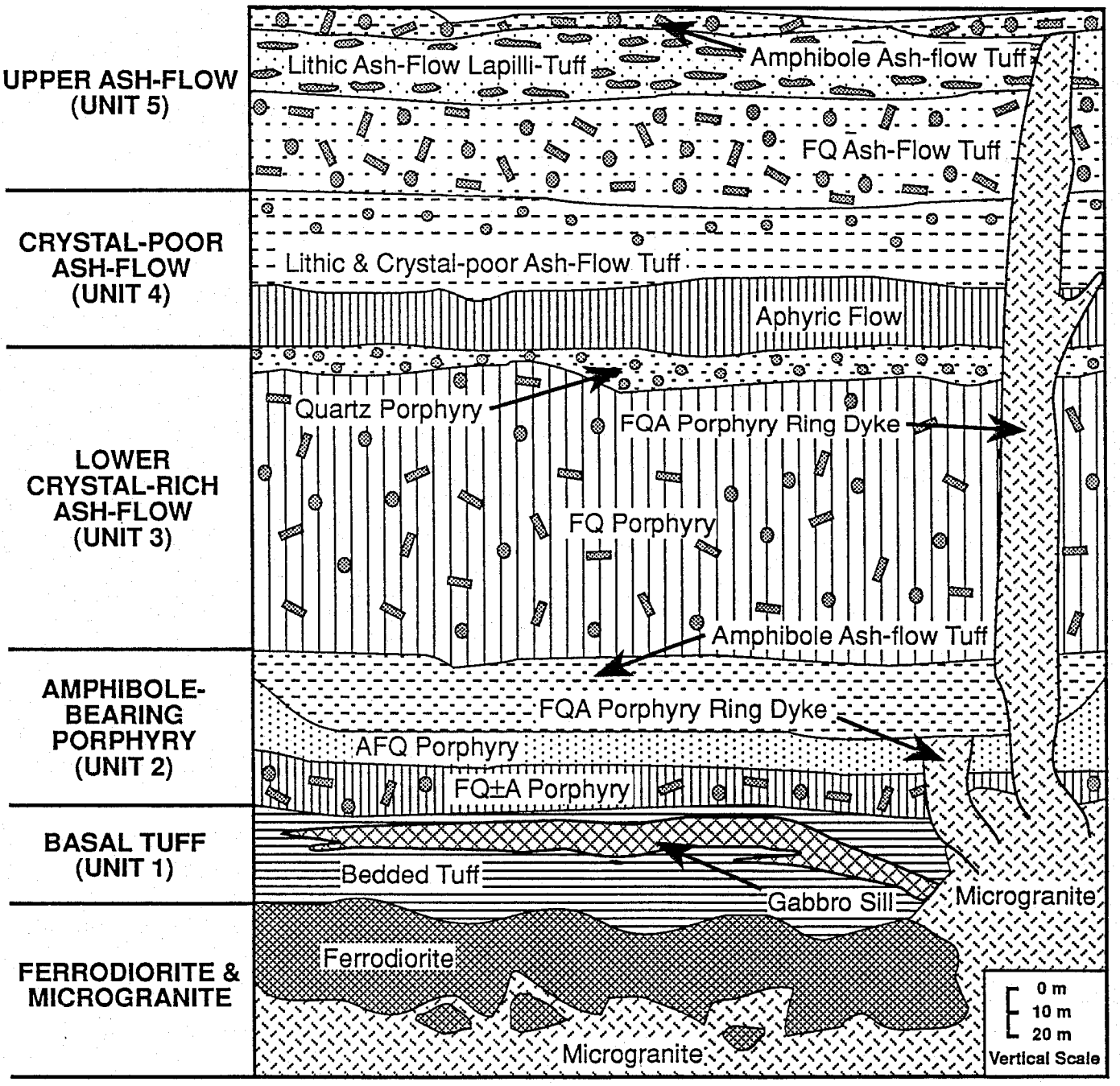

Figure 5. Generalized stratigraphic section of the Nuiklavik volcanic rocks. F = feldspar, Q = quartz and A = amphibole.

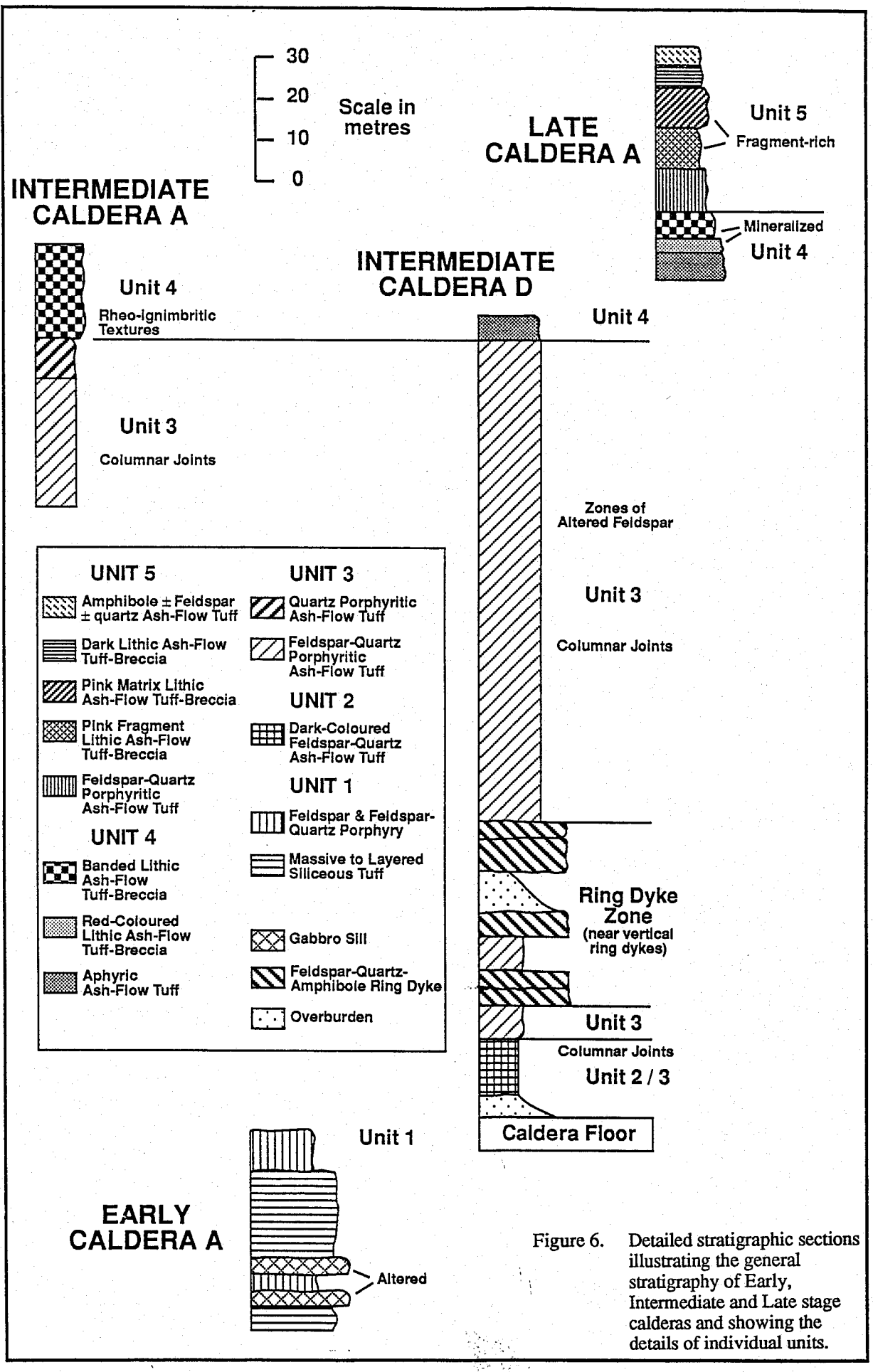

Figure 6. Detailed stratigraphic sections illustrating the general stratigraphy of Early, Intermediate and Late stage calderas and showing the details of individual units.

A description of the various lithologic plutonic and volcanic units of the exposed stratigraphic section and a correlation between sections mapped in various parts of the complex are given below.

A. Flowers River intrusive rocks

1. Coarse to medium grained granite (Coarse granite)

Coarse peralkaline granite is observed as a 1 to 3 km wide three-sided partial ring around the FRCC and as 5 to 30 m dykes which cross-cut the floor rocks of the FRCC (ferrodiorite and related rocks or gabbro-anorthosite of the Nain Plutonic Suite) In general terms, the coarse to medium grained granite is older than microgranite. The occurrence of a feldspar-quartz porphyry dyke cutting coarse granite and the absence of coarse granite dykes throughout the volcanic sequence, except in Unit 1, indicate that this granite is older than most of the Nuiklavik volcanic rocks (Figure 5).

Peralkaline and subalkaline coarse to medium granite can best be distinguished in thin section by the presence of olivine or its alteration products, pale clinopyroxene and/or biotite in subalkaline granite and the presence of aegirine-augite and/or arfvedsonite in peralkaline granite. Field and petrographic data indicate that most of the three-sided ring consists of subalkaline granite. Minor peralkaline granite is observed on the outer edges of the ring and also occurs in most of the coarse to medium grained dykes cross-cutting the floor of the FRCC. This granite variety is medium to coarse grained (3 - 10 mm), grades locally to pegmatite and generally has a hypidiomorphic texture. It is white to pink to red in colour, and consists of perthite, quartz and either black alkali-amphibole and clinopyroxene or olivine, biotite, pale to light green clinopyroxene and calcic amphibole.

2 Microgranite

The finer grained microgranite occurs as a large mappable unit on the western and southwestern edge of the FRCC (Figure 4), as a smaller unit on the eastern edge of the complex, and as thin, 1 to 30 m thick, sills or dykes within the complex. Field relationships indicate that the microgranite is structurally above the coarse to medium granite and that it is, in part, younger than Unit 1 and Unit 2 of the Nuiklavik volcanic rocks (Figure 5).

Textural varieties identified in this unit are: granophyric, aplitic and porphyritic microgranite. Some samples of the porphyritic microgranite resemble the feldspar-quartz-amphibole porphyry of the lower crystal-rich tuff (Unit 2), as both contain similar

phenocryst minerals embedded in a fine to very fine grained granophyric matrix; a gradational relationship between these rocks is fairly obvious.

The microgranites generally have the same mineral assemblage as that found in the coarse to medium grained granite. Mafic minerals are commonly less abundant in granophyric and aplitic varieties. Thus, it is commonly difficult to determine whether a microgranite sample belongs to the peralkaline or subalkaline subvariety.

The majority of the microgranitic dykes within the FRCC are subalkaline granite dykes as pale clinopyroxene, olivine and biotite are common mafic minerals in these dykes. Cross-cutting relationships indicate that subalkaline microgranite dykes are younger than coarse peralkaline granite dykes, the olivine gabbro and Unit 1 of the volcanic rocks and they are older than Unit 3 of the volcanic rocks. Field relationships between the granophyric microgranite, peralkaline and subalkaline dykes within the FRCC indicate that these rock types are structurally and possibly genetically related.

3. Olivine gabbro

Olivine gabbro sills, which range in size from 5 to at least 40 m thick, are intimately associated with the bedded to massive, very fine grained to aphanitic, tuffs of Unit 1. Most minerals within the gabbro range in grain size from less than 0.5 to 3 mm across and exhibit diabasic texture. Field relationships indicate that it is younger than Unit 1 volcanic rocks but the absence of olivine gabbro sills in rocks of the younger units suggest that the sills are only slightly younger to contemporaneous with Unit 1 (Figure 5) and were confined to early stages of the cauldron complex formation. Conflicting contact and other relationships between these sills, Unit 1 bedded tuff, previously interpreted to be chilled peralkaline granite (Hill 1982), and 'peralkaline granite' (i.e. subalkaline and peralkaline microgranite and coarse grained granite) have been reported by others (Taylor 1979, p. 68; Hill 1981, p. 13). Detailed mapping indicates that the olivine gabbro is younger than Unit 1 and older than subalkaline and peralkaline microgranite (Figure 5); this accounts for evidence indicating that the gabbro was both younger and older than 'peralkaline granite'.

These sills consist of variably altered olivine, plagioclase laths and clinopyroxene commonly replaced by amphibole; amphibole, biotite, opaque minerals and apatite are common accessories. Preliminary interpretation suggests that these sills may be related to the Nain or Harp dykes as described by Wiebe (1985) and Gower et al. (1990).

B. Nuiklavik volcanic rocks

The Nuiklavik volcanic rocks are presently exposed from their base, on the floor of the FRCC, to an apparent thickness of approximately 340 m. The preserved stratigraphy, which mainly consists of a variety of porphyritic and aphyric ash-flow tuffs and lithic tuff-breccias, a minor air-fall (?) unit and rare aphyric lava flow, is mostly subaerial and dominantly pyroclastic in origin. Erosional breaks and volcanoclastic sediments have not been observed between individual pyroclastic sheets or units.

Unit 1. Basal tuffs, porphyries and related rocks (Basal unit)

This unit is characterized by well-bedded waterlain or air-fall aphanitic to very fine grained tuffs (beds <2 to 100 mm) and massive to faintly bedded aphanitic to very fine grained siliceous rocks. In one occurrence, limestone, up to 6 m thick, is interbedded with the volcanic rocks. Intermediate feldspar porphyry and aphyric flows (?) and minor felsic quartz - feldspar porphyry are also found. Vertical exposures indicate that these bedded tuffs are stratigraphically higher than the massive siliceous and quartz-feldspar porphyritic rocks and the feldspar porphyry occurs above the bedded tuffs (Figure 6, section B). Observed thicknesses, including the associated olivine gabbro sills, are up to 60 m.

Outcrops of Unit 1 are most abundant in the southwestern portion of the FRCC but small outcrops are also found along the eastern and southeastern contacts (Figure 4). These rocks are interpreted to rest on the floor of the FRCC as they are the oldest volcanic units observed (Figure 5). Olivine gabbro sills, which are also characteristic of this unit, veins of subalkaline granite and fluorite-bearing peralkaline microgranite cross-cut members of Unit 1.

Unit 2. Amphibole-bearing porphyry

Lithologies of this crystal-rich ash-flow tuff unit include a basal dark-coloured feldspar-quartz ± amphibole porphyry and an upper oikocrystic amphibole porphyry and amphibole ash-flow tuff. Unit 2 is widespread throughout the FRCC but is most commonly found in the western half of the complex (Figure 4 and 6). This unit ranges in thickness from 10 to 40 m thick.

Dark feldspar-quartz porphyry is found at the base of the amphibole-bearing crystal-rich unit, and forms a layer reaching up to 30 m in thickness. It directly overlies Unit 1 or monzonitic and granitic rocks of the floor of the FRCC (Figure 4). It is generally dark grey in colour, containing phenocrysts of feldspar (25%) and quartz (15%) that are embedded in a greyish-black, aphanitic to very fine grained matrix. Feldspar

phenocrysts form subhedral, large grains (3-7 mm across), mostly buff, pink or red in colour. The matrix contains microphenocrysts, mostly amphibole and chlorite. Well-developed columnar joints are locally present. Data indicate that this rock is a strongly welded ash-flow tuff.

Oikocrystic amphibole porphyry and amphibole ash-flow tuff are spatially associated and commonly grade into one another. Amphibole constitutes up to 30% of the rock and occurs either as single grains or linear and oikocrystic aggregates; feldspar and quartz phenocrysts are commonly sparse. In amphibole porphyry, oikocrysts of bluish-black alkali amphibole and rare euhedral to subrounded greenish aegirine grains (1-5 mm across) are embedded in a fine grained flinty, pinkish-white groundmass, and grade locally into amphibole ash-flow tuff. The latter contains highly flattened white fiammé with fine grained alkali-amphibole grains formed along (or decorating) fiammé outlines. This rock forms a widespread but locally occurring thin layer (< 10 m thick) overlying either the floor rocks along the edges of the FRCC or dark feldspar-quartz porphyry (Unit 2), and rarely occurs as blocks (2-3 m across) within peralkaline microgranite or subalkaline dykes. Amphibole ash-flow tuff is also intimately associated with peralkaline microgranite dykes in the northwest part of the complex. In one locality, it contains inclusions of dark feldspar-quartz-amphibole porphyry and exhibits abundant rheo-ignimbritic textures (Figure 7) and, in another locality, it is found as inclusions in a lithic ash-flow tuff-breccia.

Unit 3. Lower crystal-rich ash-flow tuff

This rock type is most widespread and ranges in thickness from 50 to 120 m (Figure 4). It is a buff, brownish to reddish-grey crystal-rich rock, containing 20-30% euhedral to subhedral large feldspar phenocrysts (3-6 mm long), and 5-15% subhedral to embayed quartz phenocrysts; minor small amphibole phenocrysts are also locally present. The groundmass is fine grained to aphanitic. A quartz-mafic clot porphyritic variety, which contains either feldspar phenocrysts altered to a dark mineral assemblage or subangular dark-coloured aphanitic fragments, is abundant in the middle portion of Unit 3. Feldspar-quartz porphyry is commonly found at the base of the unit. Spectacular, well-developed five- or six-sided columnar joints are common in large, well-exposed outcrops; the columns found vary from 45 to 70 cm wide and reach up to 10 m long (Figure 8).

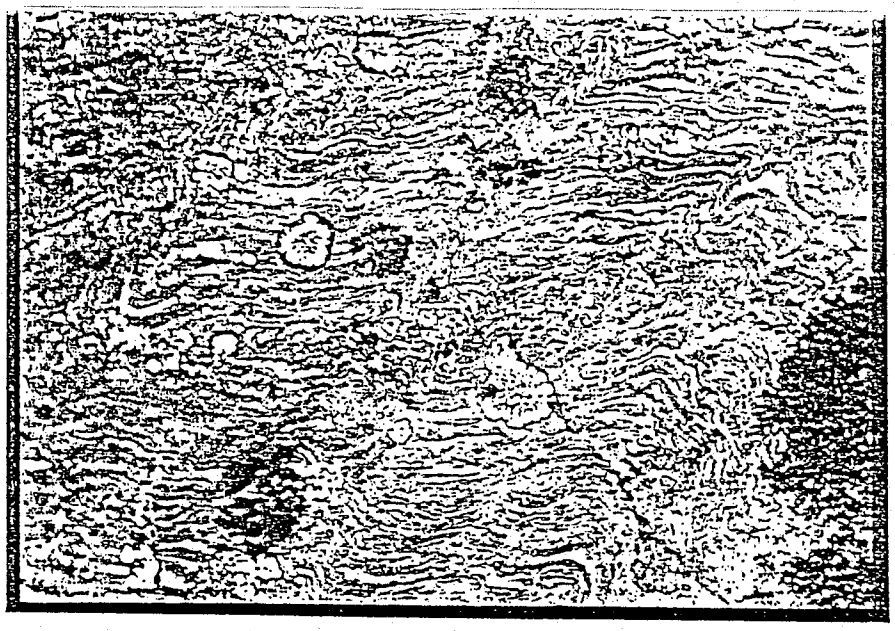

Figure 7

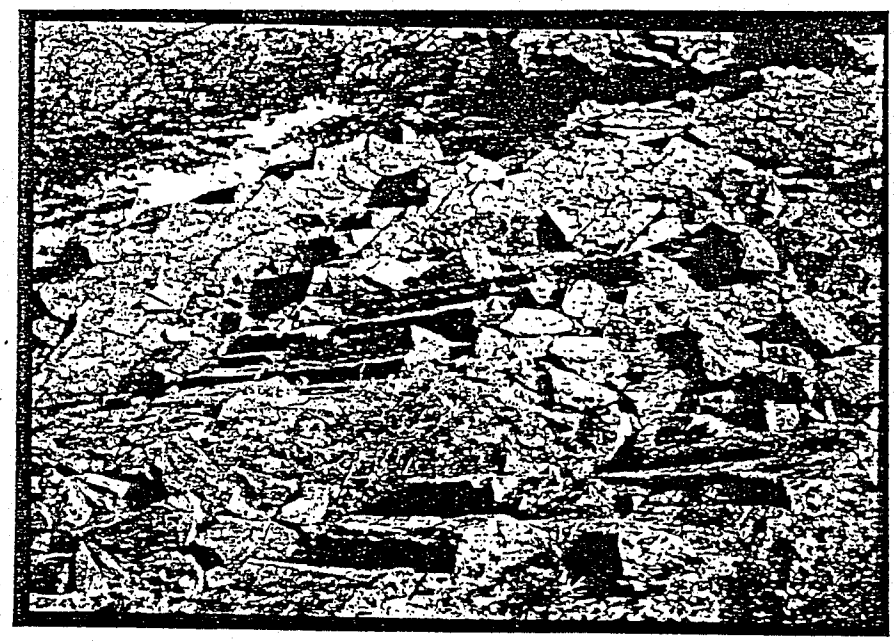

Figure 8

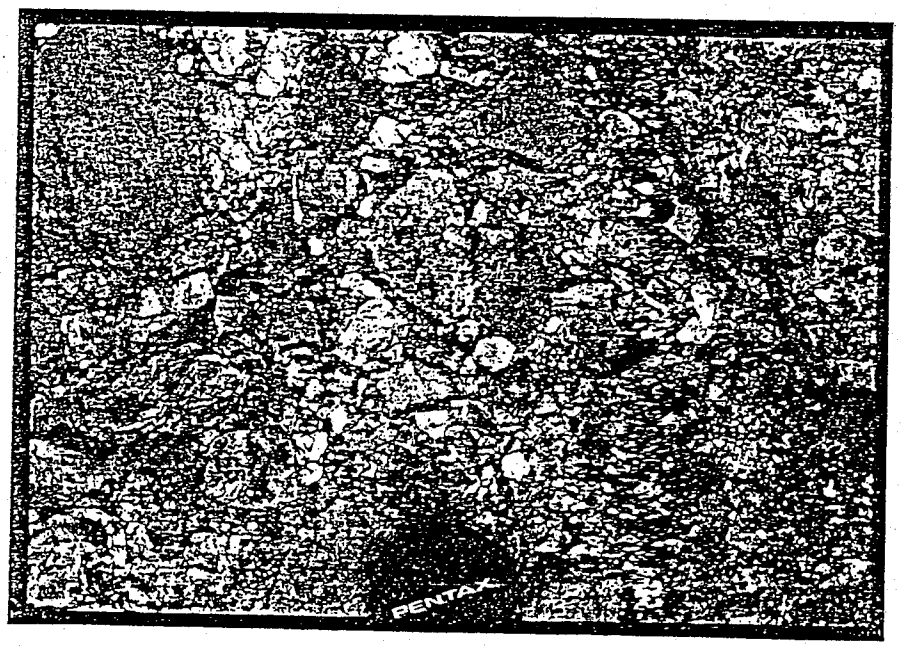

Figure 9

Figure 7. Outcrop illustrating well-developed rheomorphic textures in amphibole ash-flow tuff (Unit 2); these flow-like structures form after the hot ash-flow tuff has deposited (Intermediate Caldera A).

Figure 8. Outcrop of large, well-developed columnar joints in feldspar-quartz porphyry (Unit 3); these are 40 - 80 cm in diameter and commonly 10 m in length. Columns are commonly six-sided (Intermediate Caldera A).

Figure 9. Angular to subrounded, matrix-poor volcanic breccia within the crystal-poor tuffs (Unit 4). Fragments are mostly aphyric massive ash-flow tuff (Unit 4) with minor amounts of layered ash-flow tuff (Unit 4) and feldspar-quartz crystal-rich ash-flow tuff (Unit 3); the matrix is commonly phenocryst-poor. This occurrence marks the location of the probable vent for Intermediate Caldera B.

Unit 4. Crystal-poor ash-flow tuff

The crystal-poor ash-flow tuff unit consists of a basal aphyric to phenocryst-poor subunit and a series of aphyric, phenocryst-poor and quartz-bearing ash-flow tuffs and lithic ash-flow tuff-breccias. This unit ranges from 25 to 100 m thick and is widespread throughout the FRCC, but the most extensive outcrops are found in the southeast and eastern portions of the complex.

The aphyric to phenocryst-poor subunit varies in colour from black to red; greyish, buff and pinkish varieties are less common. Aphyric varieties generally contain no phenocrysts, but some localities contain < 5-10% mostly anhedral quartz and rare feldspar phenocrysts, commonly of small size (1-2 mm across), which occur in a very fine grained to aphanitic matrix. In other outcrops, the rock contains up to 8% phenocryst-like black spots; these may either represent altered mafic minerals, or devitrified glass shards. Pyrite, up to 1%, is also present in some samples. This subunit is characterized by columnar joints (10-40 cm in cross section) and massive texture although rare auto-breccia and local gradational variation into the ignimbritic textures of the upper subunits can be found. Its thickness ranges from 10 - 40 m. This subunit is thought to represent lava flows or vent plugging lavas in some cases and / or a highly compacted and welded ash-flow tuff in others.

Ash-flow tuff varieties vary in texture from: 1) intensely welded, containing highly flattened fiammé with gentle foliations of alternating black and pinkish-red discontinuous fine bands, occasionally showing convolute secondary flow structures, to 2) coarse, slightly-welded ash-flow tuff with lenticular collapsed pumice fragments, typically 0.5-1 cm across. Quartz-phyric (10 - 20% quartz) ash-flow tuffs, which occur in the upper portions of the unit, are less abundant than aphyric ash-flows. Small lithic fragments, up to 2 cm in size, sparsely occur in the ash-flow tuffs.

Lithic ash-flow tuff-breccias are common in the BVN caldera, which occurs in the eastern portion of the FRCC (Figure 4 and 6, section D). These tuff-breccias contain 10 to 60 % angular to sub-angular lithic fragments (clasts) which commonly range in size from 2 to 40 cm across (Figure 9). The fragments commonly include massive aphyric (most abundant), quartz-poor ash-flow tuff and aphyric ash-flow tuff from the underlying subunits of Unit 4; rare feldspar-quartz porphyry clasts from Unit 3 are also found. Individual lithic ash-flow tuff-breccia sheets vary from 4 to 10 m thick whereas the entire package of sheets is up to 50 m thick. Columnar joints are absent in this subunit.

Unit 5. Upper ash-flow tuff

The upper ash-flow tuff is stratigraphically the highest unit preserved in the FRCC (Figure 5). It is found in the calderas of the southeastern portion of the complex (Figure 5) where it reaches a minimum thickness of 100 m. This unit can be divided into basal feldspar-quartz ash-flow tuff, aphyric to phenocryst-poor lithic ash-flow lapilli-tuff and the upper amphibole ash-flow tuff.

The basal feldspar-quartz ash-flow tuff is locally columnar-jointed and always contains abundant broken phenocrysts and shards. It consists of 20 - 30% subhedral to euhedral, reddish-brown feldspar phenocrysts and 10 -15 % quartz phenocrysts, embedded in a dark reddish aphanitic matrix; magnetite and amphibole grains are sparse but widespread in the matrix. The minimum thickness, in different areas, ranges from 10 to 60 m.

Aphyric to phenocryst-poor lithic ash-flow lapilli-tuff is only found in the main northest caldera (caldera IIIa; Figure 6). It consists of 40 - 60% flattened ash-flow fragments that originate in Unit 4 and lower part of Unit 5, commonly range in size from 1 -10 cm and are pink to beige in colour. This subunit ranges in thickness from 20 - 25 m.

The uppermost preserved subunit in Unit 5 consists of amphibole-feldspar and amphibole ash-flow tuff which are similar to those described in Unit 2. Amphibole phenocrysts (10 - 30%) are the characteristic feature of this rock. The amphibole is < 2 mm across and occurs as oikocrystic aggregates and linear strings, which parallel ash-flow textures, and individual phenocrysts. Overall texture ranges from ash-flow with fiammé and other welding and compaction features to massive amphibole porphyry. This subunit has a mininum thickness of 10 m and occupies the uppermost part of the preserved volcanic section of the FRCC.

IV Petrography of the FRCC

A. Flowers River intrusive rocks

1. Peralkaline Granite

The peralkaline granites, both coarse to medium grained and microgranite varieties are hypersolvus in nature, and commonly contain perthite (60%), quartz (30%), alkali amphibole, aegirine, astrophyllite and ilmenite, with accessory annite, aenigmatite, zircon, apatite, allanite, monazite and fluorite. Unmixing of the original single feldspar phase (presumably sanidine) at a high subsolidus temperature (above 600°C) produced perthite. A micrographic perthite-quartz intergrowth, which rims large feldspar grains, is not uncommon. Interstitial, large anhedral quartz grains contain inclusions of perthite, zircon and ilmenite. Large, poikilitic, inclusion-filled, anhedral alkali-amphibole (mostly arfvedsonite) occurs as interstitial grains between perthite and quartz, and rarely as radial fibrous aggregates. Less commonly it alters to astrophyllite and ilmenite, and rarely to aegirine.

Golden yellow astrophyllite commonly occupies the exterior and interior of arfvedsonite grains; it is produced mostly by metasomatic alteration of arfvedsonite (Abdel-Rahman 1992). Aegirine is occasionally observed replacing the amphibole. Rare aenigmatite occurs as small globular deep-red grains. Minute apatite needles and globular aenigmatite constitute rare inclusions in amphibole. Ilmenite is the main opaque phase, commonly forming anhedral grains associated with mafic silicates.

Peralkaline microgranitic rocks contain higher contents of highly turbid perthite which reflects the reddish colour of microgranite in hand samples. Phenocrysts in porphyritic microgranite are characterized by a thick serrated rim formed by overgrowth of matrix material. Graphic texture obviously characterizes granophyric microgranite varieties; the latter is occasionally aegirine-rich.

2. Subalkaline granite

The texture of the subalkaline granite is commonly similar to that described for the peralkaline granite, however they differ in mafic and accessory minerals.

Coarse to medium grained subalkaline mostly consists of hypersolvus feldspar and variable quartz contents (< 5 - 30 %). Rare to sparse fayalitic olivine, commonly altered to reddish or yellow-coloured phases (i.e. iddingsite and bowlingite), is present as small anhedral grains poikilitically enclosed in aggregates of amphibole ± biotite ± clinopyroxene ± magnetite. Ubiquitous, zoned zircon, locally in hopper-shaped crystals, fluorite and allanite are closely associated with the amphibole. Clinopyroxene, which

commonly occurs as anhedral grains enclosed by later amphibole, ranges from pale, non-pleochroic augite to light green, moderately pleochroic, hedenburgite; this is in contrast with the highly pleochroic green aegirine-augite found in peralkaline granite. Amphibole is commonly green to brown in colour indicative of calcic to sodic-calcic varieties. Quartz occurs as anhedral to interstitial grains, in granophyric intergrowths with feldspar and, less commonly, as anhedral porphyritic blebs surrounded by subhedral, small, amphibole grains.

In some samples, olivine or its alteration products are absent but the occurrence of pale clinopyroxene, biotite or calcic amphibole are common characteristic features.

Porphyritic subalkaline microgranite dykes, which cut the FRCC, contain a large content of phenocrysts (40-60%), mostly of feldspar (30-50%) and quartz (10-20%), with some mafic mineral microphenocrysts, embedded in a devitrified micro- to cryptocrystalline groundmass of similar mineralogy. The groundmass rarely exhibits a micrographic texture, and may contain randomly oriented, tiny acicular feldspar laths. Feldspar forms euhedral, commonly twinned grains, mostly of highly turbid perthitic alkali feldspar. Occasionally it contains inclusions of quartz and chloritized amphibole. Quartz (2-4 mm across) is typically embayed and exhibits perlitic fractures. Phenocrysts are surrounded by thin rims of fine cryptocrystalline matrix material developed by incipient devitrification. Mafic minerals (less than 10% of the mode) occur either as poikilitic microphenocrysts of pleochroic alkali amphibole with some aegirine, or as aggregates of chloritized amphibole + chlorite + green biotite + opaque phases. Euhedral phenocrysts of poikilitic alkali amphibole, occasionally altered to astrophyllite and ilmenite are also present. Accessory zircon is common, occasionally forming microphenocrysts.

3. Olivine gabbro

Olivine gabbro is commonly highly altered. Olivine is not generally observed but alteration products of it and other minerals such as clinopyroxene and plagioclase are common. Clinopyroxene commonly alters to amphibole or chlorite, but when present it is light pink colour (titanaugite) or it is colourless (augite).

B. Nuiklavik volcanic rocks

Unit 1. Basal tuffs, porphyries and related rocks (Basal Unit)

The bedded tuff is composed of well sorted, thinly bedded devitrified volcanic dust and shards and cryptocrystalline felsic material. The latter is a mosaic of anhedral, serrated minute perthitic alkali feldspar intergrown with quartz as well as minute aggregates of weakly chloritized biotite of unusual greenish-yellow colour. The layering is commonly defined by grainsize differences and variable amounts of minute mafic minerals.

Siliceous massive to weakly banded units commonly contain cryptocrystalline to microcrystalline mosaics of quartz, potassium feldspar and albite. Mafic minerals are rare and the feldspar is commonly sericitized.

Feldspar and quartz-feldspar porphyry are characterized by subhedral microperthitic feldspar phenocrysts (2 - 5 mm), embayed quartz phenocrysts and a recrystallized quartz-feldspar matrix. Very fine grained chlorite grains and opaque minerals are common.

Unit 2. Amphibole-bearing porphyry.

Dark feldspar-quartz porphyry - This porphyritic rock contains 30-50% phenocrysts of feldspar (20-30%), quartz (10-20%) and minor amphibole. Feldspar forms large, euhedral to subhedral grains, typically 2-5 mm across of highly turbid perthitic alkali feldspar, which rarely show both carlsbad- and baveno twinning. Quartz phenocrysts are commonly embayed, smaller in size (1-3 mm across) and less abundant than feldspars. It exhibits the outline of ß-quartz, and is occasionally surrounded by a thin rim of a much finer, cryptocrystalline groundmass material. Mafic minerals are now aggregates of chlorite + opaque phases. Phenocrysts occasionally show glomeroporphyritic texture. The groundmass is a microcrystalline assemblage, mostly of anhedral quartz and feldspars which exhibit serrated boundaries. Recrystallization textures commonly developed in the groundmass are interpreted to result by devitrification or dense welding of hot pyroclastic material. Zircon is a common accessory.

Oikocrystic amphibole porphyry and ignimbrite - This rock is composed of alkali amphibole oikocrysts (15-25% of the mode) with minor aegirine, feldspar and quartz microphenocrysts (5%), embedded in a microcrystalline groundmass. The latter is a mosaic of anhedral quartz, feldspars and opaque phases and is attributed to devitrification. Oikocrystic alkali amphibole (2-5 mm across), either a product of vapour

phase crystallization or liquid phase agglomeration, poikilitically encloses groundmass materials. Zircon and a high-relief colourless mineral are common accessories.

In the amphibole-bearing ash-flow tuff, alkali amphibole and aegirine oikocrysts are molded around rare feldspar + quartz phenocrysts, lithic clasts and recrystallized bands and shard-like materials. In some samples, these mafic minerals commonly occur parallel to quartz-feldspar bands. The rock occasionally exhibits micrographic intergrowth of quartz and feldspars, with poorly developed spherulites in alternating feldspathic bands. The groundmass is a cryptocrystalline mosaic of anhedral quartz, feldspars and minute aegirine laths which can be attributed to devitrification.

Unit 3. Lower crystal-rich ash-flow tuff

Feldspar-quartz crystal-rich ash-flow tuff is characterized by abundant subhedral feldspar phenocrysts (20 - 35%) and subordinate embayed to subhedral quartz phenocrysts (10 - 20%) in a recrystallized quartz-feldspar mosaic matrix. Broken grains and shards of quartz and less commonly feldspar are found in the matrix. Layering and other compaction features are less common. Feldspar grains are commonly altered to sericite or chlorite.

Rock fragments are rare or occur sparsely in columnar-jointed examples of feldspar-quartz ash-flow tuff. Although not ubiquitous in this rock, small fragments (<2 mm), consisting of fine grained feldspar-quartz aggregates, or granophyric aggregates are found in a number of localities. A few samples also contain plagioclase xenocrysts (albite-oligioclase). The granophyric (microgranite) fragments in Unit 3 indicate that Unit 3 magmas either passed through older microgranite underlying the floor of the FRCC or contemporaneous microgranite forming in the source magma chamber during the ash-flow eruptions.

Quartz-mafic ash-flow tuff, which is commonly columnar-jointed, contains similar abundances of phenocrysts as the more common feldspar-quartz ash-flow tuff. In most cases the mafic aggregates consist of chloritized feldspar grains or rarely chloritized aphyric rock fragments or shards; the intermediate steps of the feldspar alteration process can also be observed in thin section. The quartz-mafic ash-flow tuff is thus only a hydrothermally altered version of the feldspar-quartz ash-flow tuff.

Unit 4. Crystal-poor ash-flow tuff.

Crystal-poor to aphyric rocks - These rocks contain either rare or minor phenocrysts of quartz (3-8%), feldspar (2-5%) and opaque phases, embedded in a cryptocrystalline to microcrystalline feldspathic groundmass; the latter is a mosaic of anhedral quartz and feldspars. Quartz phenocrysts are small (1-2 mm across), commonly embayed, and exhibit perlitic fractures; they are paramorphs after ß-quartz. Feldspar grains are also small (1-2 mm across), strongly turbid and/or sericitized, and are mostly perthitic alkali feldspar.

Groundmass minerals are commonly filled with opaque Fe-Ti oxide dust which may have produced the various (black, grey and reddish) colours of the rock. Interstitial very fine chlorite and biotite in the groundmass (giving a greyish colour) are present. Occasionally, quartz-feldspar intergrowth gives rare spherulitic and micrographic textures which can be attributed to devitrification. Variable degrees of coarsening of groundmass materials produced heterogeneous grain size in a few samples. Aphyric and pyrite-rich varieties are present.

Most commonly, this crystal-poor tuff grades into welded tuff with well represented devitrified fiammé, lithic fragments, layering and shards, and may represent densely welded equivalents of this unit. Some other examples of this unit are massive.

Ash-flow tuff and lithic ash-flow tuff-breccia - This rock is mostly a quartz-bearing to phenocryst-poor tuff that also contains rare, commonly altered feldspar phenocrysts, mafic clots, and lithic or pumice clasts. Quartz (0-30%) occurs either as relatively large unbroken grains (2-5 mm across), or as fragmental angular grains of variable size (Figure 9). It exhibits perlitic fractures and it is commonly surrounded by a serrated thin rim of fine cryptocrystalline feldspathic groundmass material formed by incipient devitrification. Rare feldspar phenocrysts (0-8%) are commonly altered to minute sericite, epidote, zoisite, chlorite or clay minerals. Mafic blebs are now replaced mostly by fine chlorite aggregates and opaque phases; scarce chloritized amphibole clots are rare. The groundmass includes fine devitrified shard materials and occasionally exhibits perlitic fractures. Accessory zircon is ubiquitous and occasionally form microphenocrysts.

Lithic clasts of devitrified and/or welded felsic materials of variable shape and size are present; these are very common (reaching up to 40%) in some ash-flow sheets forming lithic ash-flow tuff-breccias. These lithic ash-flow tuff-breccias are dominantly composed of aphyric fragments with lesser amounts of quartz porphyry, quartz-poor porphyry and feldspar-quartz porphyry fragments. All observed clasts originate from the basal rocks of Unit 4 and the ash-flow tuffs of Unit 3.

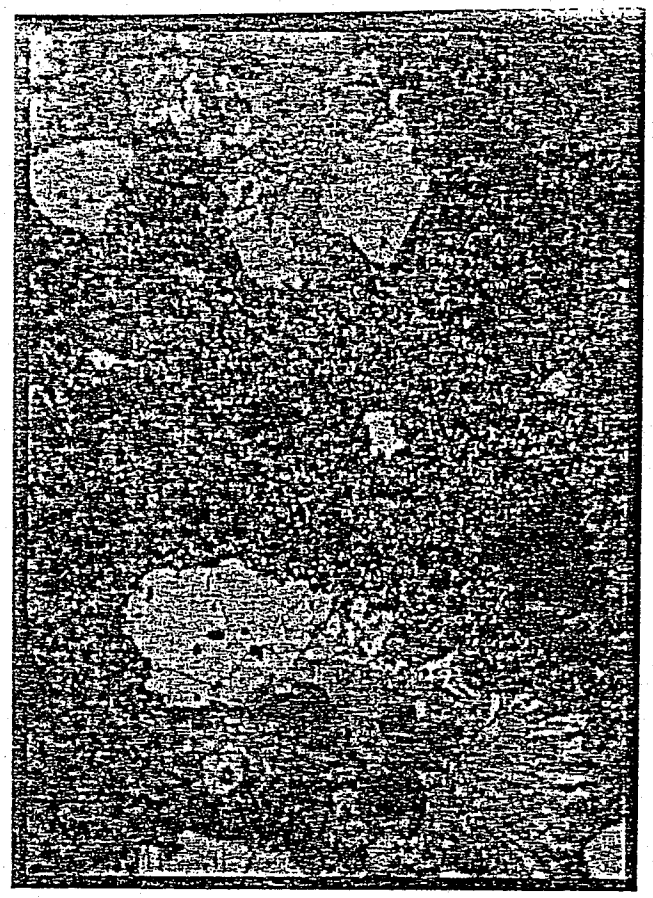

Figure 10b

Figure 10d

Figure 10a

Figure 10c

Figure 10a. Granophyric texture in peralkaline microgranite; note the arrangement of granophyric quartz and feldspar around the feldspar phenocryst in the centre of the photomicrograph.

Figure 10b. Photomicrograph of a small feldspar-quartz granophyric rock fragment (< 2 mm wide) found in many occurrences of feldspar-quartz crystal-rich ash-flow tuff of Unit 3 and Unit 5. This texture occurs in granophyric and porphyritic microgranite on the western margin of the complex (Figure 10a).

Figure 10c. Photomicrograph of a partially chloritized feldspar phenocryst in a mafic-quartz ash-flow tuff of Unit 3. Mafic-quartz ash-flow tuff (field term) is formed by hydrothermally alteration of feldspar-quartz ash-flow tuff; incipient, partially and complete alteration is observed in the cauldron complex. This alteration is mainly confined to Unit 3 feldspar-quartz ash-flow tuffs but is found sparsely in Unit 5 feldspar-quartz ash-flow tuffs as well.

Figure 10d. Photomicrograph of upper ash-flow tuff (Unit 5), showing fragmented quartz phenocrysts (broken along former perlitic fractures) in a devitrified tuffaceous quartzo-feldspathic matrix.

A thin sheet of this unit is made up of a non-welded to poorly-welded pumice-rich tuff. Devitrified lenticular pumice clasts (black lenses in hand-samples) showing typical eutaxitic textures are present. Uncollapsed pumice exhibits original fibrous structure. Occasionally, fine-aggregates of chlorite, green biotite and secondary quartz fill vesicles and micro-cavities that occupy centers of some devitrified pumice lenticles. Due to the non-collapsed nature of the pumice, there are few or no glass shards present.

This unit also contains sheets of intensely welded and devitrified ash-flow tuff. Devitrification products (quartz and feldspars) cut across shard- and some fiammé structures; rare, perfect axiolitic textures with parallel intergrowth of quartz and feldspars are well represented, and the original forms of shards are partly retained. Lenticular pumice fragments, with their characteristic tails, have undergone compaction and welding, resulting in complete collapse and elimination of internal pumice structure, and are moderately to highly flattened. Eutaxitic textures are common. In crystal-rich ignimbrite, welding and extreme compaction produced highly flattened and contorted shards molded against embayed quartz phenocrysts (Figure 10 or 11 - photos).

The groundmass is a cryptocrystalline to microcrystalline mosaic of anhedral quartz and feldspar intergrowth, occasionally forming recrystallized or coarser feldspathic irregular patches. Coarsening may have accompanied a later silicification event. All pumice, shards and groundmass materials are completely devitrified. The textures indicate that welding was complete before devitrification. In some samples, groups of spherulites (some containing acicular amphibole; Figure 11 - photos), as well as spherulites with concentric bands are well represented. In general, the variable shape and size of the commonly broken phenocrysts, clasts and shards, development of secondary minerals filling micro-cavities, and late silicification, may all have reduced the porosity, thus giving such relatively dense, hard rock.

Unit 5. Upper ash-flow tuff.

Feldspar-quartz ash-flow tuff - The basal feldspar-quartz ash-flow tuff of Unit 5 commonly consists of embayed perlitic fractured quartz grains, from <1 to 3 mm across, and anhedral to subhedral embayed grains, from <1 to 4 mm across, of microperthitic feldspar; broken fragments of these minerals, particularly quartz are also abundant. Accessory minerals include magnetite grains, amphibole and chloritized amphibole, and zircon. The matrix varies from aphanitic to fine recrystallized to coarse recrystallized and is red to brown to beige in colour; layering in the matrix is common. Rare aphyric, quartz-feldspar and granophyric fragments, similar to those observed in the Lower ash-

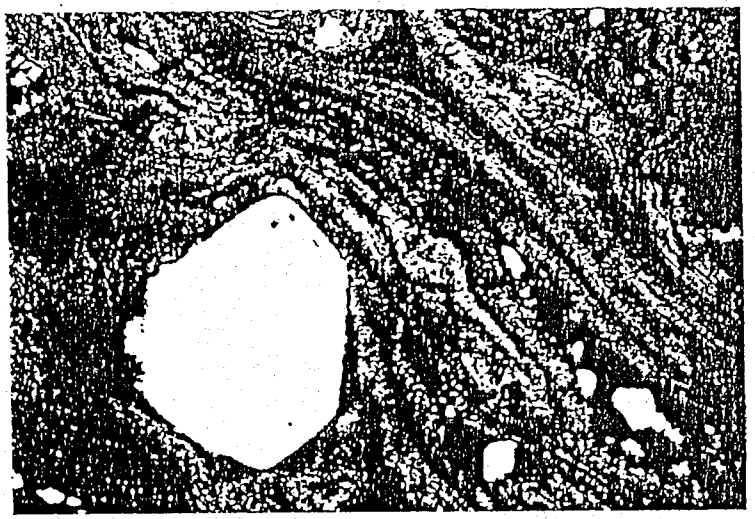

Figure IIa

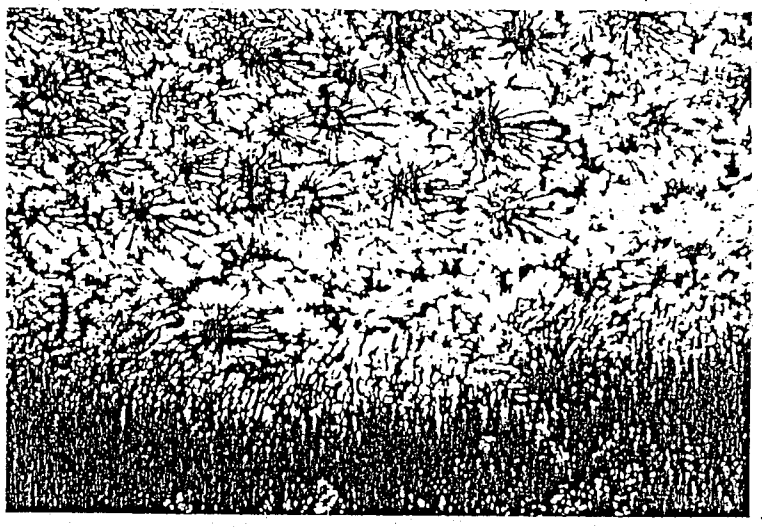

Figure IIb

Figure IIc

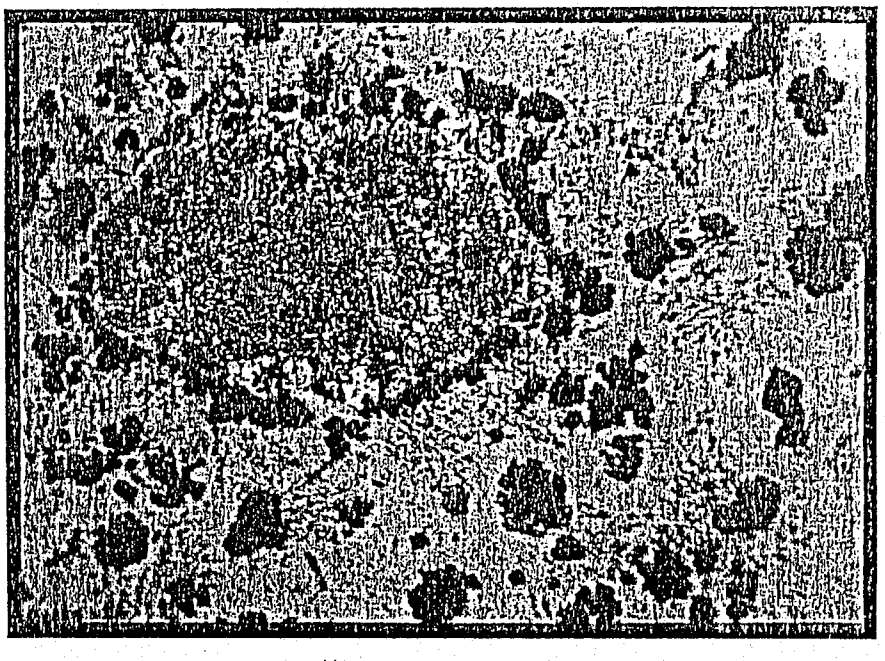

Figure IId

Figure 11a. Photomicrograph of highly welded tuff showing highly flattened and distorted shards molded against quartz phenocrysts. Note that some shards (upper centre) retain original Y-shaped form.

Figure 11b. Photomicrograph illustrating devitrification and coarsening of the groundmass in a previously welded ash-flow. Groups of spherulites contain radial alkali amphibole needles.

Figure 11c. Broken quartz and feldspar phenocrysts in photomicrograph of feldspar-quartz ash-flow tuff (Unit 5; Late Caldera A). Feldspars are sericitized and exhibit a smaller degree of breakage than the angular fragments of quartz. Note the compaction textures in the matrix.

Figure 11d. Oikocrystic amphibole aggregates in amphibole ash-flow tuff (Unit 5; Late Caldera B). This photomicrograph displays a rim of aggregates around a feldspar-amphibole fragment probably derived from the nearby ring dyke (feeder dyke?).

flow unit (Unit 3), have also been recognized in widely scattered outcrops of the Upper ash-flow tuff.

Aphyric to phenocryst-poor lithic ash-flow lapilli-tuff - This subunit is characterized by recrystallized aphyric fragments and rare feldspar-quartz porphyry fragments in a very fine grained hematized matrix. The matrix is commonly aphyric to sparsely porphyritic (< 1% broken and unbroken quartz and feldspar phenocrysts) and is layered. Aphyric fragments are commonly flattened and exhibit a rim of recrystallized matrix material up to 1 mm thick.

Upper amphibole-feldspar and amphibole ash-flow tuff - Petrographically the amphibole and amphibole-feldspar ash-flow tuffs are gradational with feldspar contents increasing and layering decreasing from amphibole to amphibole-feldspar ash-flow tuff. Quartz phenocrysts are rare in these rocks but quartz is common as small grains or in the recrystallized aggregates of the matrix. Amphibole and pyroxene commonly occur as oikocrystic aggregates of minerals, < 1 mm in size, or as poikilitic grains which contain small matrix quartz grains. Mafic grains and aggregates commonly form strings to define the layering in the ash-flow tuff.

V Structure

Constituent Calderas of the FRCC

The initial mapping of the FRCC and vicinity (1:100,000 scale) and the aeromagnetic pattern of the region (GSC Map 6242G) lead Hill (1981, 1982, 1991; Hill and Miller 1990) to postulate that the Flowers River Igneous Suite rocks are part of a caldera - ring structure. Rings of peralkaline granite (Figure 3) were thought to have been progressively truncated to the south culminating with the occurrence of the volcanic rocks in a caldera on the southeastern edge of the Flowers River Igneous Suite. This hypothesis, which was the basis of the present study of the structure and geology of the FRCC, requires the size of the structures to be from 13 to 30 km in diameter, with the larger structures to the northwest and the smaller, younger, structure (FRCC) to the southeast.

We suggest that the complex has evolved as a series of small overlapping or nested calderas rather than one large caldera. This interpretation is based on:

1) presence of several ring dyke-ring fault systems (Figure 12), which outline several of the postulated calderas,
2) structural data, including attitude of volcanic strata (Figure 12), which can best be explained by this proposal,
3) stratigraphic discontinuities (Figure 4),
4) presence of slivers of cauldron complex floor between these calderas (Figure 4), and
5) the presence of aeromagnetic anomalies (Figure 13 and Table 1) which outline several small arcuate, elliptical and circular areas (calderas and groups of calderas).

The structural data and the observed stratigraphy have been interpreted to derive the location of a number of ring dyke or ring fault systems outlining at least seven complete or nearly complete calderas, many caldera segments and some inferred, poorly defined, calderas (Figure 14). Cross-sections through the northern (Figure 15) and the southern (Figure 16) portions of the FRCC better illustrate the relationship between the observed stratigraphy and the structural interpretation. The seven well-defined calderas and related caldera segments (Table 2) have been grouped, on the basis of inferred age, into Early Calderas, Intermediate Calderas and Late Calderas. These calderas are described below:

Early Caldera A (Bear Valley South nested structure):

Early Caldera A, found at the southeastern portion of the FRCC (Figure 16), is defined by inward dipping beds (30 - 65 °) and subalkaline granite ring dykes (near

Table 1 Summary of Magnetic Susceptibility Data for Rocks in the FRCC

Rock Type	Range (low values)	No.	Range (high values)	No.	Comments
Unit 5	< 0.01 - 0.10	15	0.23 - 2.3	22	amphibole is common throughout this unit Unit 5 is not thick or widespread enough to significantly influence the aeromagnetic data the most magnetic members of Unit 5 are the feldspar-quartz ash-flow tuffs
Unit 4	< 0.01 - 0.10	91	0.15 - 3.4	9	Unit 4 is generally non-magnetic anomalous samples are in the upper portion of this unit and may be mis-identified
Unit 3	< 0.01 - 0.03	63	0.25, 0.90	2	non-magnetic
Unit 2	< 0.01 - 0.05	27	0.29 - 3.0	6	generally non-magnetic
Unit 1	< 0.01 - 0.03	23			non-magnetic
Gabbro	< 0.01 - 0.02	2	0.09 - 0.93	17	generally magnetic two low magnetic samples are highly altered
Coarse to Medium Granite					
CAF granite	0.03	2	0.15 - 0.57	6	generally moderately magnetic
Peralkaline Granite	0.01 - 0.12	9	0.44 - 1.2	3	generally non-magnetic more magnetic rocks occur at or within 1 km of contact with volcanic rocks
Microgranite					
FQA porphyry	< 0.01 - 0.06	17	0.15 - 1.9	18	quartz-rich (younger) dykes are generally non-magnetic olivine-bearing and quartz-poor (older) dykes are more magnetic
Feldspar porphyry	0.02 - 0.15	5	0.31 - 0.82	3	more magnetic rocks occur at or within 1 km of contact with volcanic rocks
Fine grained (granophyric)	0.01 - 0.12	8	0.82 - 3.1	6	more magnetic rocks occur at or within 1 km of contact with volcanic rocks
Nain Plutonic Suite	0.01 - 0.09	4	0.15 - 4.3	10	generally very magnetic; some small dykes have low magnetic values

measurements in 10 x 10(-6) CGS units
measurements obtained with a EDA K2 Portable Magnetic Susceptibility Meter on 3 - 7 mm thick rock slabs

Table 2 Structural and Descriptive Summary Data for the Constituent Calderas of the FRCC.

Caldera	Size	Caldera Fill	Fill Volume (km3)	Subsidence Depth (m)	Subsidence Mechanism*	Caldera Defined By	Caldera Cuts	Comments
Early Caldera A	5 x 7 km	Unit 2	1 - 5 ?	> 60	Piston	ring dykes	NPS or Unit 1	encloses two younger calderas; part of Bear Valley nested structure; step-like southwest margin.
Intermediate Caldera A (Camp Creek Caldera)	3.5 x 6 km	mainly Unit 3 minor Unit 2 & 4	> 5	> 250	Trapdoor	ring dykes	NPS or Unit 2	complete caldera; step-like southern margin; minor lithic ash-flow tuff-breccias.
Intermediate Caldera B (Fragment Hill Caldera)	1 - 3 km (?)	Unit 3 & 4	> 0.4	> 120	Piston	ring dykes	NPS or Unit 2	eastern margin undefined; lithic ash-flow tuff-breccias (clasts 0.1 - 1.0 m) define vent.
Intermediate Caldera C (Three Creek Hill Caldera)	2 x 3 km	mainly Unit 3 & 4 minor Unit 5	> 3	> 210	Piston	ring dykes & faults	NPS & Unit 2	very minor Unit 5 (?) feldspar-quartz ash-flow tuff.
Intermediate Caldera D (Columnar-Joint Hill Caldera)	5 x 5.5 km	mainly Unit 3 & 4	> 6	> 200	Piston	ring dykes & faults	Unit 2 & NPS?	1/3 of caldera is covered by Late Caldera B; part of Bear Valley nested structure.
Late Caldera A (Bear Valley North Caldera)	3 x 3.5 km	Unit 4 & 5	> 2	> 220	Asymmetric Piston or Trapdoor	faults ?	Unit 3	abundant lithic ash-flow tuff-breccias; hosts significant rare-metal mineralization; largest preserved section of Unit 5 stratigraphy.
Late Caldera B (Bear Valley South Caldera)	3 x 5.5 km	Unit 4 & 5	> 4	> 240	Trapdoor	faults ?	Unit 1, 2 & Unit 3	minor lithic ash-flow tuff-breccia; abundant feldspar-quartz ash-flow tuff; part of Bear Valley nested structure; hosts significant rare-metal mineralization.

NPS = Nain Plutonic Suite.

* Trapdoor Subsidence - down drop of fault block occurs along a hinge line; relatively no down drop on the hinge line and progressively more further from the hinge line.

* Piston Subsidence - amount of subsidence is approximately the same for all parts of the down faulted block.

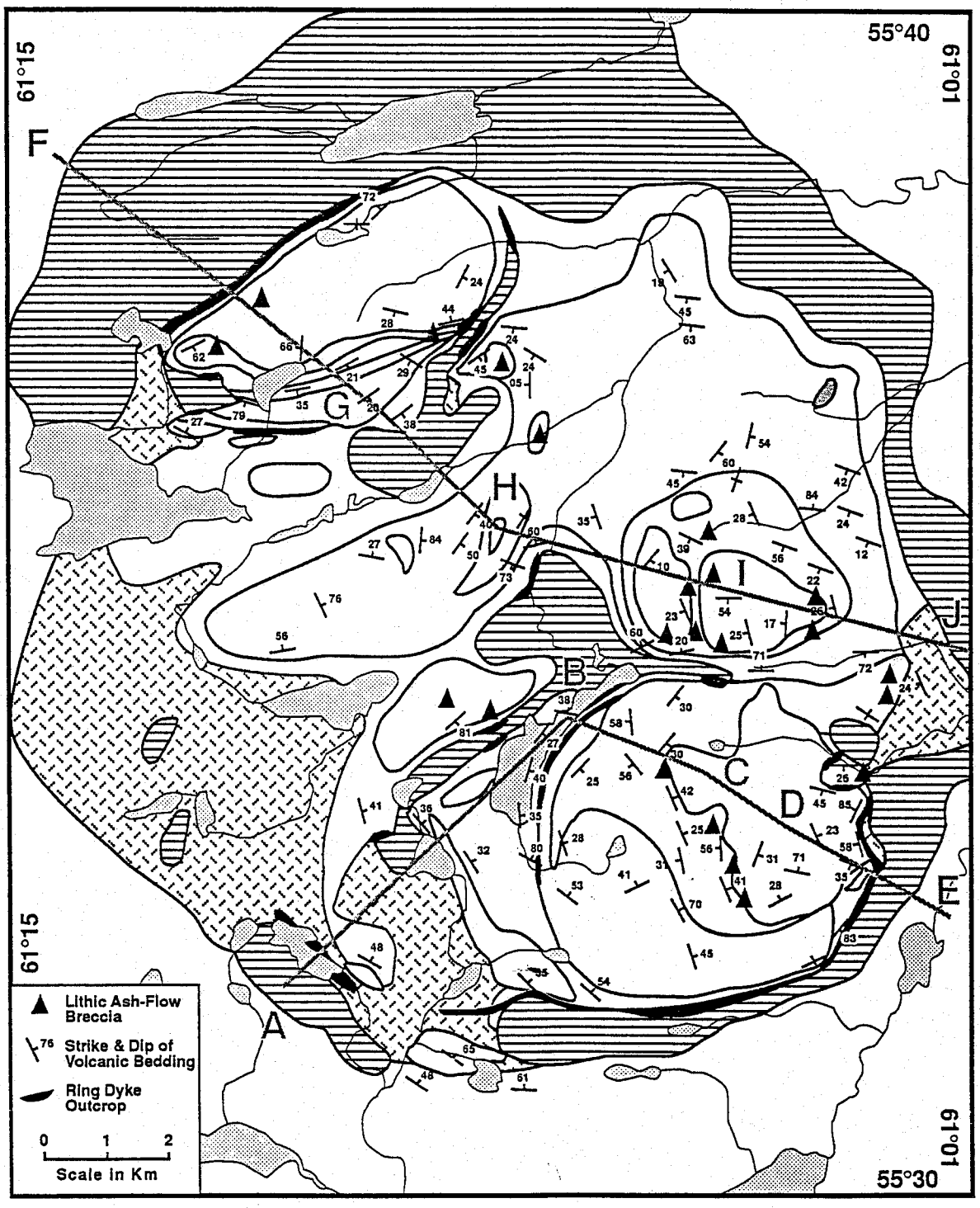

Figure 12. Attitudes of bedding and contacts, location of ring dykes, orientation of section lines A-E (Figure 15) and F-J (Figure 16), and sites of lithic ash-flow breccias in the Flowers River cauldron complex. See Figure 4 for geology of the Nuiklavik volcanic rocks (no pattern).

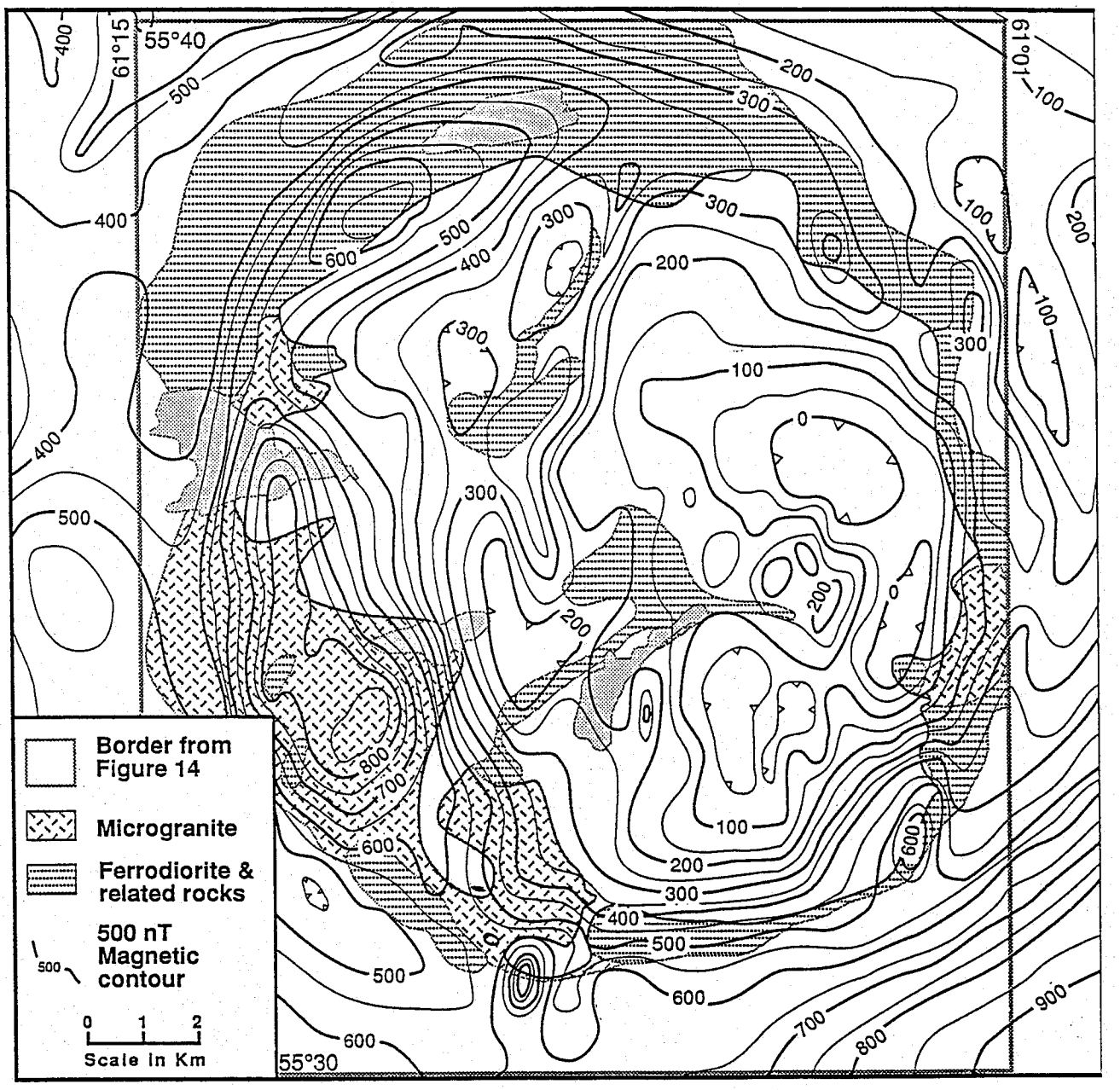

Figure 13. Computer-manipulated aeromagnetic map of the Flowers River cauldron complex. Aeromagnetic digital data for the mapped area has been corrected to the Definitive Geomagnetic Reference Field by G.J. Kilfoil using techniques described in Kilfoil, 1991. A reference border and the geology of the non-volcanic rocks of the complex have been taken from Figure 14 to aid in the interpretation of the magnetic data. Refer to Table 1 for magnetic susceptibility data for rocks of the cauldron complex.

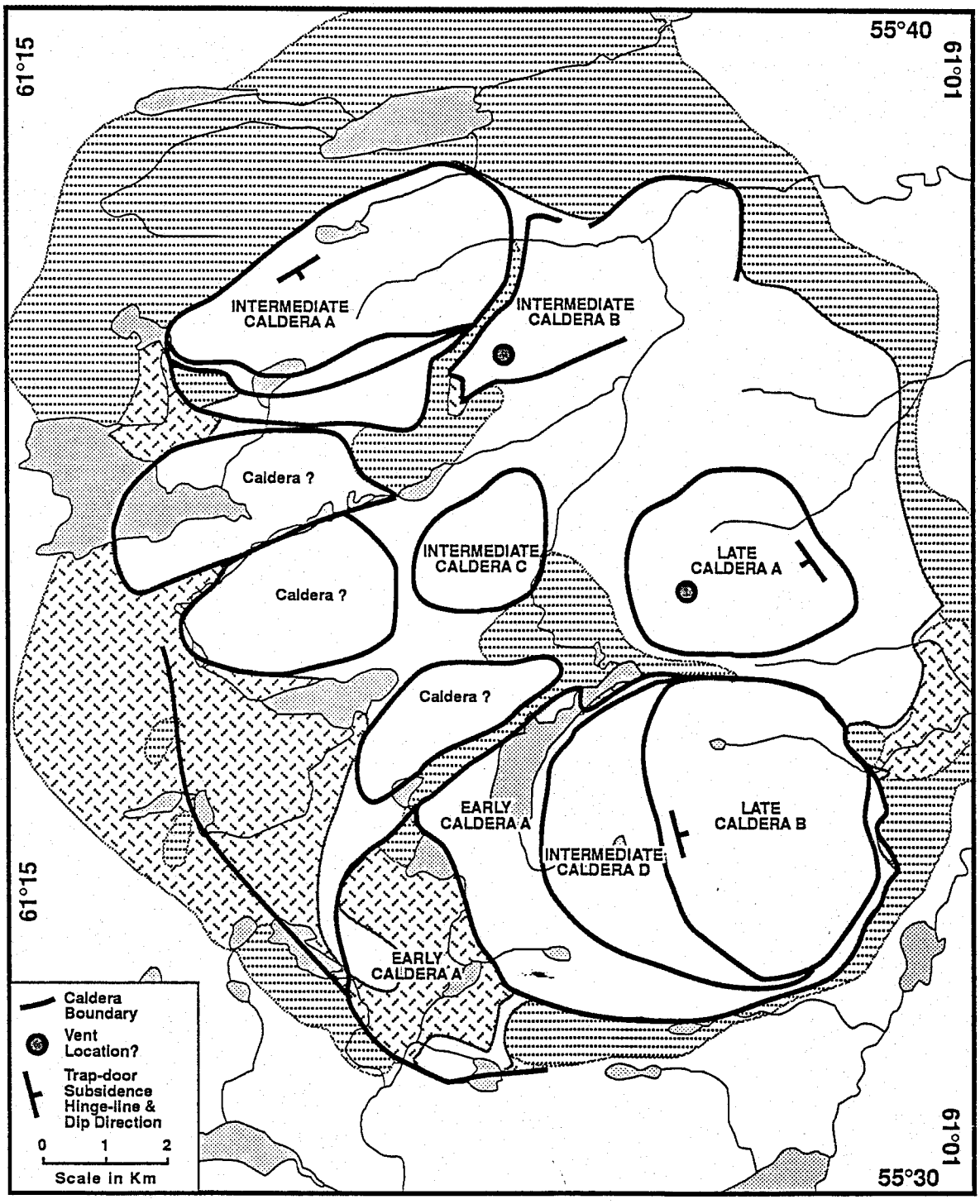

Figure 14 Location of individual calderas identified using stratigraphic, structural and aeromagnetic data. Calderas assigned to Early, Intermediate or Late stages of evolution are discussed in the text. Other calderas outlined are poorly defined; caldera structures have not been observed in the blank areas due to lack of data.

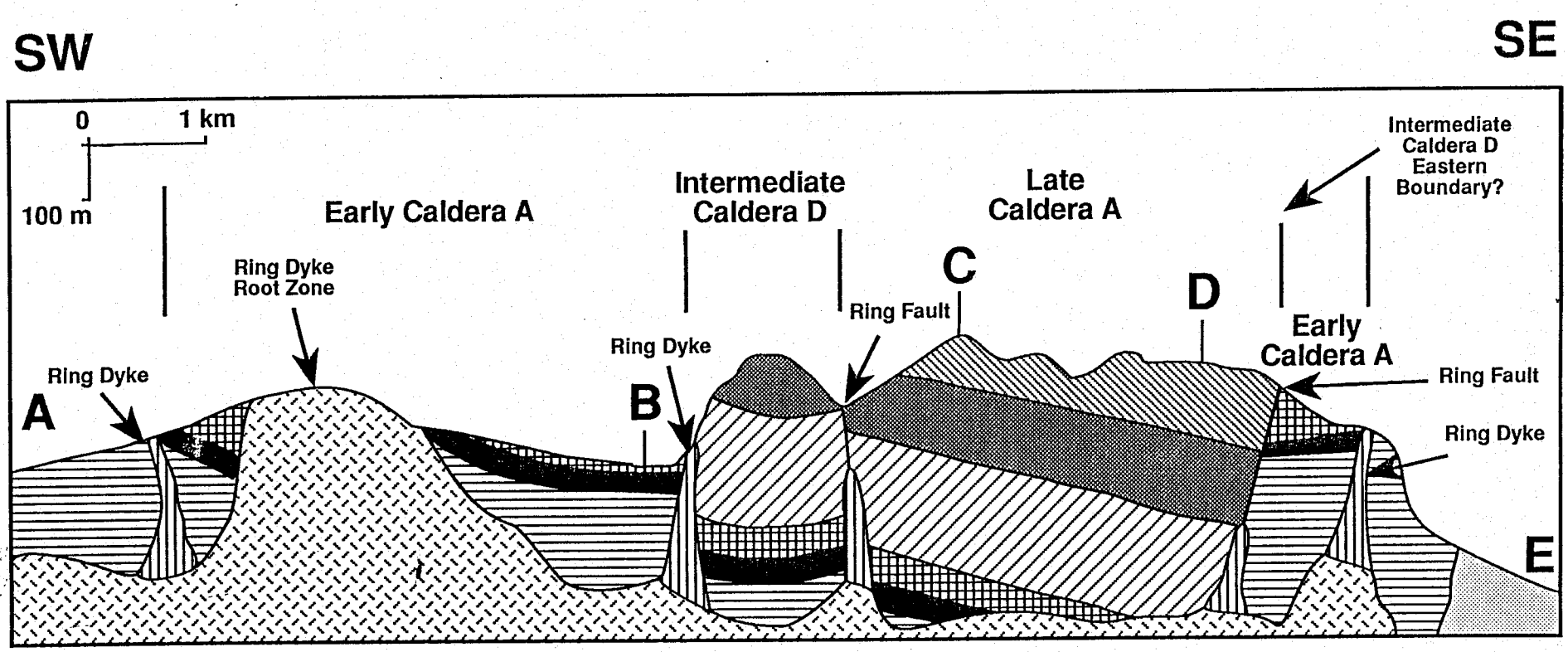

Figure 15 Interpretive cross-section A-E of the southern portion of the FRCC. Early Caldera A, Intermediate Caldera D and Late Caldera A collectively form the Bear Valley nested caldera structure. Note the vertical exaggeration. Section line is located in Figure 12.

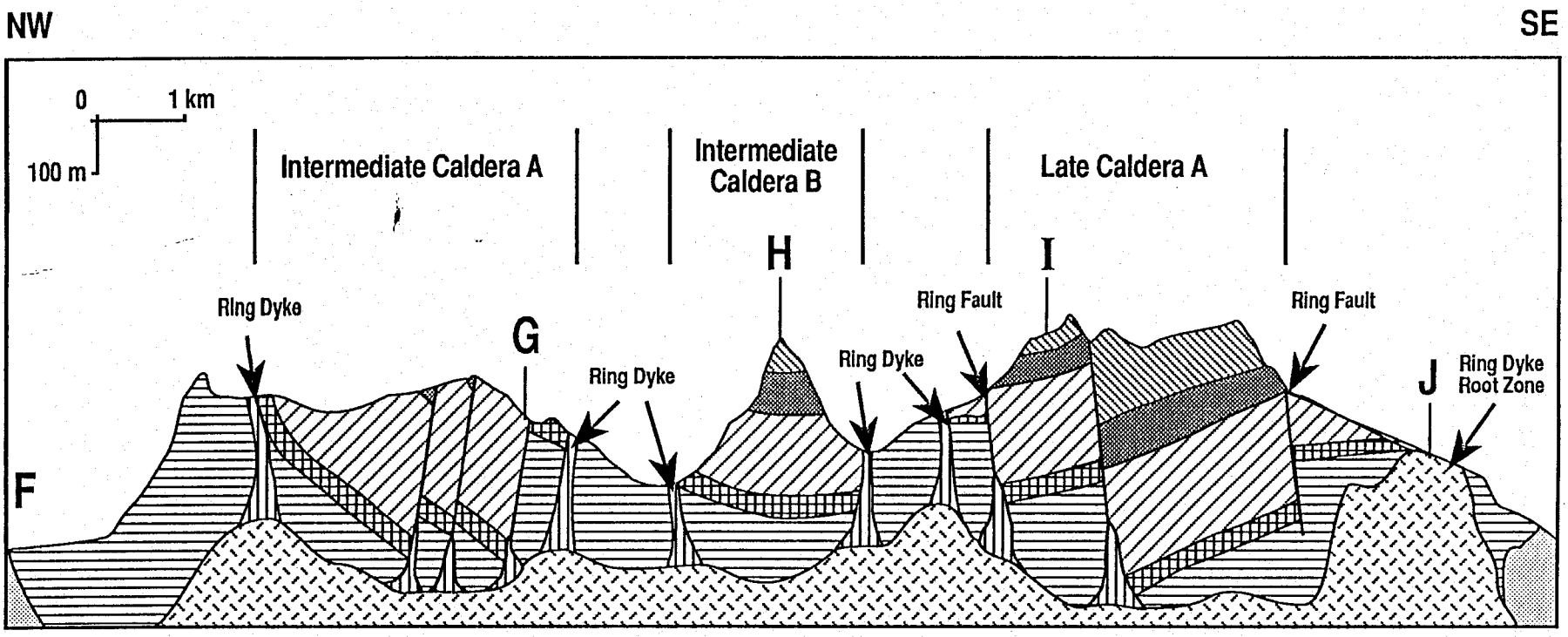

Figure 16 Interpretive cross-section F-J of the northern portion of the FRCC. Note the vertical exaggeration. Section line is located in Figure 12.

vertical dips) on its outer margin which outline an area of 5 by 7 km (Table 2). It contains Unit 1 bedded tuffs and gabbro sills and Unit 2 ash-flow tuffs that form a composite section up to ??? m thick, however Unit 1 probably represents the floor of this caldera and Unit 2 ash-flow tuffs the caldera fill (> ??? m). This caldera corresponds with a zone of relatively high magnetic anomalies (Figure 13), which suggests that caldera fill is relatively thin and contains a relatively small proportion of low magnetic susceptibility Unit 1 and Unit 2 (Table 1) volcanic rocks. Relatively higher magnetic susceptibility gabbro sills, subalkaline granite and microgranite intrusions (Table 1) must account for the positive anomaly. Early Caldera A encompasses two later, smaller, calderas which together form the Bear Valley South nested structure.

Intermediate Caldera A (Camp Creek caldera):

The Camp Creek caldera occurs on the northwestern margin of the complex and has dimensions of 3.5 and 6 km (Table 2). Caldera fill, which is at least 250 m thick, includes ash-flow tuffs of Units 2, 3 and 4. Ring faults and dyke systems cut basement rocks (i.e. FRCC floor rocks) on the outer margins and FRCC floor rocks and Unit 2 on the inner margins (Figure 12). Bedding attitudes, most of which dip 20 - 40° towards the southeast, indicate that this caldera was formed by a trapdoor-like mechanism (Figure 15); the most subsidence occurred at the southeastern margin and the least at the northwestern margin. The aeromagnetic data clearly defines this caldera (Figure 13) because the relatively low magnetic susceptibility of caldera fill rocks are clearly distinguished from the relatively high magnetic susceptibility of FRCC floor rocks (Table 1).

Intermediate Caldera B (Fragment Hill caldera):

The margins of the Fragment Hill caldera are only well-defined to the northwest and southwest were they cut FRCC floor rocks (Figure 13 and 14). The available data suggests that this is either a caldera segment or a poorly defined caldera. The unique feature of this segment is the occurrence of the central vent of the caldera in the surviving segment. Bedding attitudes, which dip from 5 to 45° towards the postulated vent (Figure 12), and the occurrence of a tuff-breccia unit, containing upper Unit 3 and Unit 4 fragments, from 1 - 100 cm across, support this conclusion. The caldera fill in Unit 3 and Unit 4 and available dips suggest a piston-like caldera subsidence of at least 110 m. The Intermediate A and B calderas have similar fill and similar contact rocks, thus they may be relatively contemporaneous in age.

Intermediate Caldera C (Three Creek Hill caldera):

This caldera is not well-defined (Figure 13 and 14). It is filled with Unit 3 and Unit 4 ash-flow tuff including an unusual feldspar-poor-quartz-poor ash-flow tuff and a small amount of Unit 5 (?) feldspar-quartz ash-flow tuff (Figure 15). Vertical bedding dips at two localities and a ring dyke system on one margin suggest that this caldera is approximately 2 km by 3 km. Bedding orientations within the caldera dip from 28 to 73° towards the centre of the caldera indicating that the caldera was formed by a piston-like subsidence. Caldera fill is at least 210 m thick.

Intermediate Caldera D (Bear Valley South nested structure):

Assuming a symmetrical structure, this caldera is approximately 5.5 km by 5 km in dimension (Figure 14). It is filled by Unit 3, Unit 4 and minor amounts of Unit 5 (?) and it abuts against Unit 2 rocks (Early Caldera A). The observed outer contacts contain ring dykes and the style of subsidence appears to have been piston-like as bedding dips 22 - 70° inwards (Figure 12). The minimum amount of caldera fill measured on the exposed cliff section is 200 m (Figure 6, section C); the presence of a low magnetic anomaly under this caldera may be interpreted to indicate a much larger thickness of low magnetic susceptibility felsic volcanic rock (Table 1). Intermediate Caldera D forms a part of the Bear Valley South nested structure. The caldera fill of both the Intermediate C and Intermediate D calderas is very similar (Table 2).

Late Caldera A (Bear Valley North caldera):

Late Caldera A is 3 by 3.5 km and cuts Unit 3 columnar-jointed ash-flow tuffs; ring dykes are not observed (Figure 12). It is filled with 220 m (composite section) of Unit 4 and Unit 5 ash-flow tuff and lithic ash-flow tuff-breccia (Figure 6, section D; Figure 15). Both lithic ash-flow tuff-breccia and rare-metal mineralization are abundant in this caldera. It also contains the thickest and most varied preserved section of Unit 5. Bedding measurements, which generally dip 20 - 56° towards the west-southwest (Figure 12), indicate that the subsidence mechanism was either a trapdoor or asymmetric piston-like mechanism with the most subsidence occurring to the west. The caldera is outlined by vertical dipping beds, FRCC floor rocks or stratigraphic breaks (Figure 12 and 14). The aeromagnetic map indicates that there is a faint relatively magnetic high over the outcrop of Unit 5 rocks. Table 1 indicates that many Unit 5 rocks have much higher magnetic values than the other Nuiklavik volcanic rocks.

Late Caldera B (Bear Valley South nested structure):

This caldera, which is 5.5 by 3 km, overlaps the eastern margin of Intermediate caldera D and is enclosed by Early Caldera A. It is filled by at least 240 m

(composite sections) of Unit 4 aphyric and phenocryst-bearing ash-flow tuff and minor lithic tuff-breccia and abundant Unit 5 crystal-rich ash-flow tuff. It cuts lower members of Unit 4 and it is defined by breaks in the stratigraphy and bedding rather than by ring dykes (Figure 4 and 12). Bedding measurements, which generally dip 12 - 71° to the east (Figure 12), indicate that a trapdoor or asymmetrical piston-like mechanism was responsible for the subsidence with the most subsidence occurring on the eastern margin and the least on the western margin. The aeromagnetic map (Figure 13) indicates that a great thickness of low magnetic susceptibility rocks (Table 1) must underlie this caldera. The structural interpretation (Figure 14) indicates that approximately one-third of the Intermediate Caldera D is under the younger caldera. Rare-metal mineralization is very abundant in the Unit 4 ash-flow tuffs and lithic ash-flow tuff-breccias of this caldera.

The magnetic susceptibility data (Table 1) indicates that the Nuiklavik volcanic rocks are relatively non-magnetic and thus they could be recognized by negative magnetic anomalies (Figure 13). The exception to this observation is a large portion of Unit 5, which has magnetic susceptibility values that are amongst the highest measured. Yet Unit 5 is relatively thin compared to the other units thus it would not substantially raise or modify the negative magnetic anomaly expected for the volcanic rocks. In contrast, substantial proportions of the granitic rocks, olivine gabbro and Nain Plutonic Suite rocks (FRCC floor rocks) are one to two orders of magnitude higher. Moderate quantities of these rocks in an area would result in positive magnetic anomalies relative to the volcanic rocks. The high magnetic values of FRCC floor rocks (0.51 - 4.3) and many ring dykes (0.41 - 1.9), in contrast to the Nuiklavik volcanic rocks (< 0.1 - 0.10), make the aeromagnetic data map (Figure 13) useful for structural interpretation:

a) The outline of Intermediate Caldera A (Figure 12) is supported by the magnetic data;
b) The overall outline of the zone of nested volcanic-filled calderas is indicated by the negative magnetic anomaly; positive anomalies on the borders reflect the relatively magnetic Nain Plutonic Suite outcrop and the outcrop of subalkaline granite and peralkaline microgranite;
c) The exposure of Nain Plutonic Suite rocks (i.e. the floor of the FRCC) and the many ring dykes within the outcrop area of the volcanic rocks is generally outlined; these confirm portions of the boundaries of the constituent calderas;

d) These data can be used to postulate the location of other calderas on the western margin of the FRCC; one negative anomaly in this area probably represents a thick sequence of Nuiklavik volcanic rocks.

Ring Faults

The outer ring fault - ring dyke system, because it is a composite of many smaller nested systems, may be young or old in any particular locality depending on the age of the bounding caldera. The oldest ring fault - ring dyke system, which bounds Unit 1 and Unit 2, is well-exposed in a creek bed on the southeastern margin of the FRCC (Figure 17 - upper). In this locality the ring dyke system is composed of five microgranite feldspar-quartz-amphibole porphyry ring dykes which range in size from 1 to 10 m wide, and three coarse peralkaline granite dykes that range in size from 1 - 20 m thick. The total thickness of ring dykes in this zone is 47 m and all measured contacts or bedding attitudes are near vertical. Dykes cut floor rocks (e.g. ferrodiorite and related rocks of the Nain Plutonic Suite), other dykes, as indicated by abundant intrusive breccia, and the observed volcanic rocks (feldspar porphyry of Unit 2? and feldspar-quartz porphyry of Unit 3?). These relationships suggest that this particular zone (≈ 150 m wide) was the locus for either a number of ring fault systems, each related to a different caldera, or repeated ring dyke intrusion over the life of one caldera.

Another ring dyke - ring fault system is well-exposed in a creek bed which crosses the contact of Intermediate Caldera A (Figure 17 - lower). This ring dyke system consists of four feldspar-quartz-amphibole porphyry — ignimbrite composite dykes which range in size from 2 to 8 m wide. The composite porphyry—ignimbrite dykes exhibit dips which range from 17 to 90°, although the majority of the dips are 80 to 90°; lower dips occur in the amphibole ignimbrite part of the composite dykes. These dykes, which are similar to but smaller than the ash-flow tuff dykes (10 - 100 m) found in the Grizzly Peak caldera (Fridrich et al. 1991; Fridrich and Mahood 1984), appear to represent near surface gas-charged magma which produced both lava-like and pyroclastic textures. Unit 3 or lower Unit 4 rocks occur on the southern side of the ring dykes and Unit 4 rocks occur on the northern side. The caldera bounding fault system, defined by the ring dykes, placed different units next to each other; many stratigraphic inconsistencies can be solved when these bounding faults are fully recognized.

The younger, generally more deeply filled calderas (Late Calderas) are not outlined by ring dyke systems. This indicates that either magma was not intruded along the ring fault zone or, more likely, the extra thickness of the fill prevented magma from penetrating to the higher levels exposed, except possibly in a few ring fault vent

Figure 17 Cross-sections through a ring fault-ring dyke zone on the outer boundary of the FRCC (upper section) and on the inner margin of Intermediate Caldera A (lower section).

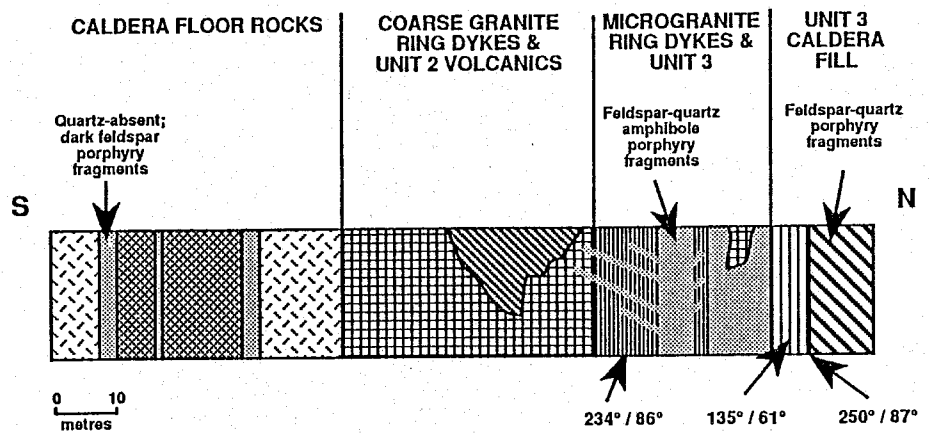

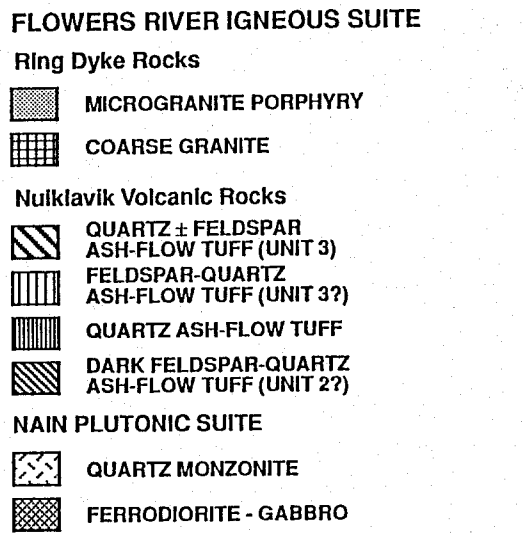

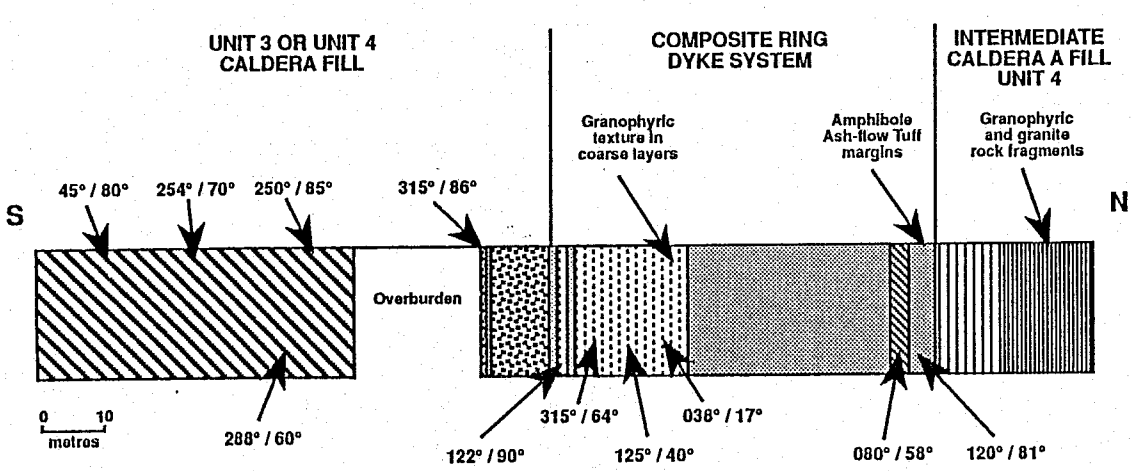

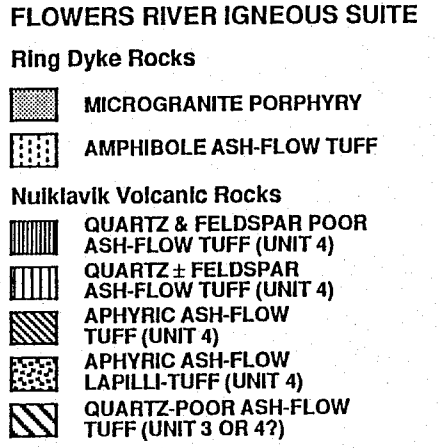

locations. A spectrum of ring dyke occurrence can thus be postulated for the FRCC: a) medium grained large (> 5 m) ring dykes in the root zone of the ring dyke; b) porphyritic smaller ring dykes (2 - 10 m) in the low to intermediate zones; c) porphyritic - ignimbritic composite ring dykes in the upper zone and d) ignimbritic dykes or the absence of ring dykes near the surface and / or ignimbritic deposits from a small ring fault vent.

VI Discussion

Age of the FRCC

At the present time an absolute age of the Nuiklavik volcanic rocks and the FRCC is not available but a relative age estimate can be made based on the field relationships observed. Zircon U-Pb ages for the vicinity (see Miller et al. 1993 for a compilation of these data) indicate that the coarse peralkaline granite is 1271 ± 15 Ma (Char Lake - Brooks in Hill, 1991), the older granites of the Nain Plutonic Suite are 1291 ± 1 Ma (Char Lake - Brooks 1983) and 1292 ± 4 Ma (Notakwanon pluton - Ryan et al. 1992), and the Nain dykes are approximately 1273 Ma (1276 ± 23 Ma - Wiebe in Gower et al. 1990; Nutak dykes ca. 1268 Ma - Roddick in Cadman et al. 1993; Harp dykes 1273 ± 1 Ma - Cadman et al. 1993).

The olivine gabbro sills that crosscut Unit 1 have been tentatively correlated with the Nain dykes based on location, petrography and their relative age (see Gower et al. 1990 and Cadman et al. 1993). The relative age is placed between 1271 and 1290 Ma as peralkaline granite veins cut these sills in the FRCC and olivine gabbro sills crosscut Unit 1 which unconformably sits on Nain Plutonic Suite rocks. The absolute age for the Nain dykes suggests that the olivine gabbro sills are ca 1273 Ma. These relationships also fix the relative age of Unit 1 as being slightly older than the olivine gabbro sills in the range 1273 - 1290 Ma.

The absence of peralkaline granite (coarse and microgranite), subalkaline granite and olivine gabbro sills or dykes in Unit 3 or higher also suggests that the FRCC (at least Units 3 to 5 and perhaps Unit 2) is contemporaneous or slightly younger than the granites (i.e. ca 1271 Ma.) and younger than the olivine gabbro. The common presence of microgranite and the less common occurrence of coarse granite fragments in Unit 3 and 5 also indicates that some volcanic units are younger than the granitic rocks. Feldspar-quartz and quartz porphyry dykes, with aphanitic to very fine grained matrices, and ring dykes, which also cut peralkaline granite, further indicate that the volcanic rocks are younger than the peralkaline granite.

Nature of the volcanic assemblage; its eruptive character:

Silicic volcanism produces a wide variety of deposits from blocky lava flows to ash-flow tuffs that exhibit varying degrees of compaction and welding, with complete welding and rheomorphism of ash-flows resulting in rocks which can be easily confused with large silicic lava flows (e.g. Milner et al. 1992).

In view of the data presented above, volcanic units of the FRCC exhibit features characteristic of both ash-flow tuff and lava flows. For example, most porphyries show features common in lavas as they contain unbroken phenocrysts, rare lithic fragments, generally massive but with occasional flow banding, and locally show rare auto-brecciation, with the absence of basal breccia; the later is also considered to be diagnostic of a lava-flow origin (Henry and Wolff 1992).

On the other hand, ignimbritic features are well preserved in various sheets within each of the identified ash-flow tuff units; these include planar flow contacts, typical pyroclastic features, such as non-welded to welded devitrified fiammé and glass shards with eutaxitic texture, and perlitic fractures. Also, preservation of fragmental texture as lithic clasts and broken phenocrysts, which vary widely in size within crystal-rich tuff (Figure 10 or 11 - photo), suggests ash-flow tuff. Various units occur as sheets with relatively consistent stratigraphic position, unlike lava flows which generally occur as domes or tongues with blunt margins.

As rheomorphism of ignimbritic sheets results in lava-like flowage, many of the features within a rheomorphic ignimbrite (or rheo-ignimbrite) will be similar to those characteristic of lava flows. Thus the presence of features characteristic of both volcanic types within the FRCC suggests that at least part of its volcanic assemblage is rheo-ignimbritic. High eruption temperature suggested by the abundance of well-developed columnar joints is consistent with our interpretation of the rheomorphism of some tuff. Generally, columnar joints are very scarce, or do not occur in the non-crystalline, non-welded parts of the ash-flow units; thus the abundance of such well-developed columnar joints in several volcanic (lava-like) porphyry units in the FRCC (Figure 8), suggests that the porphyries are of rheomorphic origin.

Nature of the Magma Chamber

It is clear that the spatially associated subalkaline and / or peralkaline granites are the best candidates for the source of magma which produced the Nuiklavik volcanic rocks. The occurrence of ring dykes within the FRCC, the presence of microgranite inclusions in ash-flow tuff that are petrographically similar to nearby granite intrusions (O'Brient 1986), and the close temporal relationships between all of these rocks further support this conclusion. The occurrence of a few granophyric inclusions in numerous widespread outcrops of feldspar-quartz ash-flow tuffs of Unit 3 and Unit 5 strongly indicates that the granophyric microgranite was formed as a consequence of rapid crystallization by pressure release, through ash-flow tuff eruptions, in a parental magma chamber. This rules out the possibility that the granophyric microgranite intrusions are

post-volcanism resurgent intrusions similar to those found in the Salma Caldera (Kellogg 1985). It also indicates that the parental magma chamber(s) had a relatively small volume as pressure quench textures do not usually occur in large batholith-size intrusions.

Caldera collapse could not have occurred as the result of the small volume eruptions of the FRCC calderas unless the parent magma chambers were at a shallow depth (Mahood 1984). The absence of floor rock inclusions (e.g. ferrodiorite or related rocks of the Nain Plutonic Suite) in the volcanic ash-flow units indicate a short conduit that also requires a shallow parent magma chamber (Mahood 1984).

The occurrence of such a large number of nested or clustered calderas in a small area argues for: 1) a shallow magma chamber that was periodically replenished with magma or 2) for a series of small shallow intrusions in the same area (Lipman 1984). The former hypothesis requires a shallow magma chamber at least 13 km in diameter (i.e. the size of the FRCC) that produced a number of small calderas during each of at least three episodes of magma replenishment. The latter hypothesis requires caldera development over many small magma chambers, 1-7 km in diameter, which were intruded in at least three episodes. The Christmas Mountains caldera complex (Henry and Price 1989) is an example of a single magma chamber (8 x 5 km in size) which produced four small calderas (1 - 1.5 km). However, the instrusive style of nearby contemporaneous granitic intrusions, which occur as numerous small stocks and dykes (< 10 km in diameter), provides the potential multiple sources required to for the individual caldera. It is difficult to favour one hypothesis over the other and without the results of the ongoing geochemical studies to help in drawing a conclusion.

The shape of these magma chamber(s) is uncertain but the postulated relatively small size (1 - 13 km in diameter) and the small amount of subsidence in the related calderas suggest that they were laccolith or sheet-like bodies, as opposed to batholiths or stocks, in the order of 1 - 4 km in thickness. There is evidence for the occurrence of at least one relatively large peralkaline granite sill (at least 200 m thick) in the region (i.e. not related to FRCC ring dykes; Collerson 1982). Ryan (1991) also indicates that many of the Nain Plutonic Suite intrusions, particularly the rapakivi and related granites, occur as horizontal sill-like bodies.

Reviews of calderas and cauldrons (Elston 1984, Henry and Price 1984, Mahood 1984) indicate that small caldera size, small parent magma chambers and small volumes of erupted materials are common for peralkaline felsic magmas. The FRCC contains a large number of calderas that formed over one or possibly several large, shallow, laccoliths or sills on the order of 1 - 13 km in diameter.

Evolution of the Flowers River cauldron complex

The regional geology and the structure and stratigraphy of the FRCC provides sufficient data to determine the stages and some detail of the evolution of this cauldron complex. An outline of the proposed model is illustrated in Figure 18 and a more detailed discussion of the various stages is given below:

Regional uplift and erosion

As Hill (1991) and others have pointed out, the vicinity of the FRCC was the focus of the intrusion of large volumes of anorogenic magma (Nain Plutonic Suite) circa 1290 - 1411 Ma. Studies of contact metamorphic relationships around the youngest of these intrusions (Berg 1977) indicate that they intruded to depths of 6 to 14 km. In the Flowers River area there are at least two major intrusions (Figure 3) on the order of 40 km in diameter that intruded the crust during this period.

Regional block faulting or ring fracturing (Stage I - Smith and Bailey 1968) was coincident with uplift and intrusion of the Nain Plutonic Suite. Many of the Nain Plutonic Suite intrusions are thought to have been emplaced as sheets along the edge and in the voids on top of subsidence blocks formed during this period of uplift (Emslie 1978b; Ryan 1991). The faults, formed during this period, may have acted as the localizing structures for the intrusion of the slightly younger peralkaline and related granites and magmas that eventually formed the Nuiklavik volcanic rocks and the Flowers River intrusive rocks (Figure 18A).

Approximately 4 to 12 km of erosion must have occurred in the period 1290 to 1271 Ma (0.21 - 0.63 mm / year) to expose the depositional surface for the Nuiklavik volcanic rocks; sediments of the correct age are unknown in the region.

Precaldera regional volcanism

Unit 1 of the FRCC is quite anomalous when compared to the other units due to: 1) the occurrence of olivine gabbro sills thought to correlate with Nain dykes, 2) the presence of a limestone member interbedded with thinly bedded tuffs and siliceous-cherty beds; all likely shallow water deposits, 3) the dominance of waterlain or air-fall tuff (plinian pyroclastic activity rather than ash-flow activity), and, 4) the abundance of intermediate rocks (e.g. feldspar porphyries rather than feldspar-quartz porphyries). These anomalies indicate that Unit 1 was likely deposited in shallow water and is the product of plinian volcanic activity which was intermediate to felsic in composition. These features argue against Unit 1 being formed as caldera fill. These volcanics were more likely produced by regional strata volcanos ca. 1290 Ma (Figure 18B). Olivine gabbro sills and

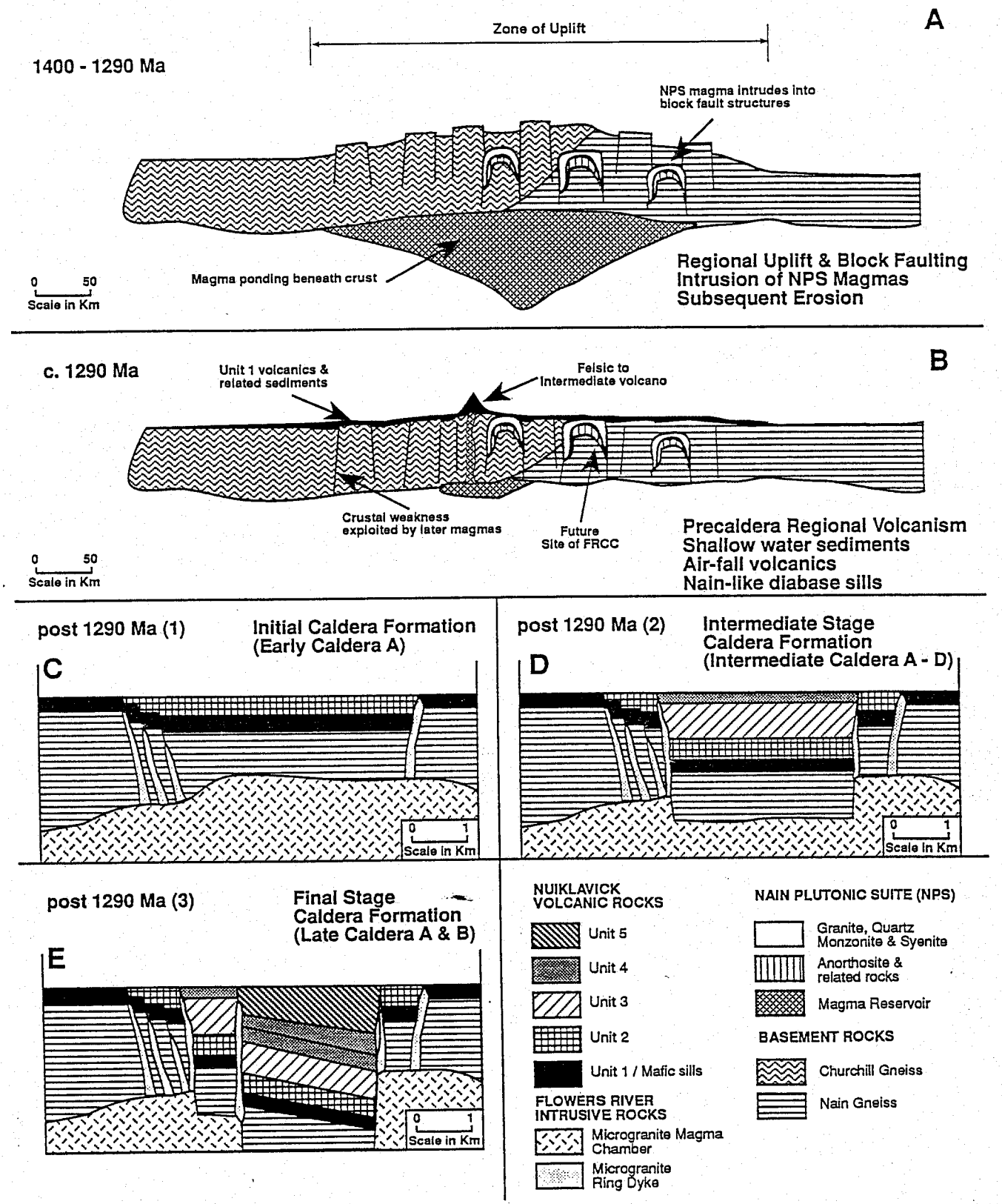

Figure 18 Model illustrating the stages of development of the FRCC. Note scale large differences of scale between diagrams A and B and diagrams C, D and E. See the text for a discussion of this figure.

dykes, related to the Nain dykes, intruded these volcanic rocks ca 1273 Ma. Although the top of Unit 1 is not well-exposed in the FRCC there does not appear to be any evidence for either a major depositional or erosional event after the deposition of Unit 1. The presence of intermediate to felsic plinian activity previous to ash-flow activity has been observed in many regions of caldera formation (e.g. Lipman 1984, Self et al. 1986).

Initiation of the FRCC

The length of the break between Unit 1 volcanism and the initiation of caldera-related volcanism (Unit 2) is unknown; perhaps only differences in magma source and eruptive-style and not a significant time break are reflected in the volcanic products. The FRCC calderas were initiated by the intrusion of small, 5 - 13 km in diameter and perhaps 1 - 4 km thick, peralkaline or subalkaline granite bodies (Figure 18C).

The initial calderas, perhaps related to one intrusion or a series of intrusions, produced Early Caldera A and possibly other poorly defined early calderas now filled with Unit 2 (Figure 18C). The segments on the southwest side of Early Caldera A probably represent incremental step-like collapse (e.g. Walker 1984, Rytuba and McKee 1984, Fridrich et al. 1991) of the caldera (i.e. piston-like central collapse with marginal step-like faults). The regional volcanics of Unit 1 are preserved as the floor of this early caldera and Unit 2 ash-flows are the caldera fill. Megabreccias (e.g. Lipman 1976) or debris flows that are commonly found in calderas with high relief between the floor and the rim of the caldera are absent. This suggests that either the rate of subsidence of this caldera was relatively slow, the rate of filling was relatively fast or the amount of subsidence was very small (or a combination of all three). Other calderas, with Unit 2 fill, must have been located in the central and northwestern portions of the FRCC to account for the Unit 2 deposits in these areas. Estimates of the volume of Unit 2 ash-flow tuffs produced in Early Caldera A are in the order of 1 - 5 km^3; the minimum amount of subsidence was approximately 50 m in this caldera. There is no evidence of a major amount of erosion between Unit 2 and subsequent volcanism from other calderas.

Unit 2 caldera fill is mainly densely welded, columnar-jointed, feldspar-quartz amphibole-bearing ash-flow tuffs and rheo-ignimbritic flows. These rocks are indicative of hot volcanic eruptions (Mahood 1984, Milner et al. 1992), commonly peralkaline in nature. Lithic tuff-breccias are absent and there are no other indications of the location of a vent.

Ring fault zones are outlined by feldspar-quartz-amphibole porphyritic microgranite dykes (fine to very fine grained matrix). Intrusion breccias in the outer or border ring dyke systems indicate prolonged intrusion of several different textural and

compositional (felsic to intermediate) varieties of ring dyke. Inner ring dyke systems contain only one textural-compositional type of ring dyke. The volcanic expression of these dykes appears to be the amphibole ± feldspar layered ash-flow tuffs (Unit 2) locally found on the margin (ring dyke vent sites?) of the caldera.

Most of the larger intrusions and some of the ring dykes were intruded during this stage of the evolution of the FRCC. Peralkaline and subalkaline granite intrusions, both coarse and microgranite varieties, occur around the edges of the FRCC, particularly in the western, southwestern and southeastern margins, and as dykes cutting the Nain Plutonic Suite rocks in the floor zone of the FRCC. The widespread presence of microgranite inclusions, particularly granophyric microgranite inclusions, in ash-flow tuffs probably indicates that these intrusive rocks represent subvolcanic magma in the source magma chamber(s). Intrusive rocks do not cross-cut volcanic rocks higher than Unit 2 in the stratigraphy.

Intermediate Calderas

Intermediate stage volcanism (Figure 18D) produced four recognizable calderas in the FRCC (Intermediate Calderas A, B, C and D). These calderas are characterized by ash-flow tuff fill consisting of relatively thick deposits of Unit 3 and minor amounts of Unit 4 and Unit 5.

Unit 3 volcanic fill in these calderas consists of highly welded, columnar-jointed feldspar-quartz ash-flow tuff and minor lithic ash-flow tuff-breccia, which commonly display rheomorphic textures. These features indicate that this caldera fill was deposited as hot ash-flow tuffs. Subsequent alteration of the feldspars in some of this unit indicates a significant amount of syn- and post-depositional hydrothermal activity.

Unit 4 volcanics range from aphyric aphanitic lava flows or ash-flow tuffs and aphyric to phenocryst-poor layered ash-flow tuffs and lithic ash-flow tuff-breccias; the degree of welding ranges from dense to minor. Lithic ash-flow tuff-breccia contains aphyric flow and minor feldspar-quartz porphyritic ash-flow tuff fragments which are less than 1 m wide.

Ring dykes intrude the ring fault systems of the intermediate stage calderas. These ring dykes occur as feldspar-quartz-amphibole porphyry (fine to very fine grained matrix) and feldspar-quartz-amphibole porphyry—amphibole ignimbrite composite dykes. Extrusive equivalents of these dykes have not been identified.

Megabreccias or debris flow deposits have not been found in any of the intermediate stage calderas. We conclude that the rate of subsidence was equal to the rate of volcanic deposition. Inward dipping beds (commonly 20 - 70°) in all four intermediate

stage calderas indicate that a significant amount of subsidence occurred during and late in the ash-flow tuff deposition process (Mahood 1984, Walker 1984, Henry and Price 1989). These conclusions suggest that the timing and amount of ash-flow tuff deposition is directly related to subsidence in such a way that the ash-flow tuff volcanism triggered subsidence and the volume of ash-flow tuff deposited approximately equals or exceeds the volume of the depression created by subsidence.

Estimates indicate (Table 2) that these four calderas each produced a minimum of 0.4 - 6 km^3 (total > 14 km^3) of ash-flow fill and the amount of subsidence ranged from > 120 - 250 m. The estimated amount of collapse, the estimated volume of erupted materials and the size of the calderas (Table 2; 1 - 6 km in diameter) all fall within the range observed by Mahood (1984) for strongly peralkaline calderas.

The lack of chaotic collapse breccias in the exposed floor of these calderas (Gudmundsson 1988; Scandone 1990) and abundant structural data indicate that block subsidence was the dominant collapse mechanism in these calderas. Bedding measurements in Intermediate Caldera A indicate that it subsided by a trapdoor or hinge mechanism similar to that described for the Bonanza caldera (Varga and Smith 1984) and other calderas (see Lipman 1984). The other three calderas formed by a piston-like mechanism of subsidence.

Final Stage Calderas

Two late stage calderas, between 3 and 5.5 km (Late Caldera A and B), have been recognized as forming in a final stage of caldera development (Figure 18e). These calderas are characterized by relatively thick deposits of Unit 4 and Unit 5 caldera fill. Quartz porphyritic ash-flow tuff and lithic ash-flow tuff-breccia and aphyric lithic ash-flow tuff-breccia are also common.

The Unit 4 volcanics comprise columnar-jointed aphyric flows and ash-flow tuffs and aphyric to phenocryst-bearing layered ash-flow tuffs and lithic ash-flow tuff-breccias. These rocks are commonly densely welded and rheomorphic.

Unit 5 is best observed in Late Caldera A where it is characterized by thick deposits (> 40 m) of amphibole-bearing phenocryst-rich ash-flow tuff (commonly columnar-jointed) lithic ash-flow tuff-breccias, amphibole porphyry and aphyric layered ash-flow tuff. The upper portions of this unit contain the first appearance of ubiquitous amphibole found above the amphibole ignimbrites of Unit 2.

The final stage of caldera development is generally characterized by the absence of ring dykes and the presence of amphibole±feldspar porphyritic ash-flow tuff, which may be the extrusive equivalent of the deeper level ring dykes. This suggests that the

caldera fill is sufficiently thick to retard the intrusion of ring dykes along the ring fault zone but to perhaps allow the formation of ring fault zone vents in a few localities.

Late Caldera A produced a minimum of 2 km^3 of caldera fill and has a minimum subsidence of 220 m. Late Caldera B, which has the largest amount of preserved caldera fill, has a minimum volume of 4 km^3 of fill and a minimum of 240 m of subsidence. The total amount of final stage caldera fill is at least 7 km^3. Even though these calderas exhibit the most subsidence of any calderas in the FRCC, there is no evidence of debris flows from the caldera rim. The implication for low relief and relatively equal rates of subsidence and deposition are similar to that of the older calderas.

Bedding orientations for Late Caldera A and B suggest trapdoor subsidence. The trapdoor or differential subsidence mechanism appears to be more prominent in this stage than the earlier stages. Trapdoor collapse is also thought to produce low scarps and thus few or no debris flow deposits (Walker 1984). It is also related to small volume eruptions (< 100 km^3) with < 1 km of collapse (Varga and Smith 1984, Lipman 1984). This type of subsidence mechanism is also observed to be common for peralkaline magmas (Henry and Price 1984). Elston (1984) observed that trapdoor structures commonly occurred in the early stages of development or on the fringes of a cluster of calderas and that they were formed by repeated small eruptions (also see Lipman 1984). The asymmetrical or trapdoor calderas in the FRCC mainly occur in the final stage of cauldron complex development but they all occur around the fringes of the FRCC and there is abundant evidence for small and, in some cases, repeated small eruptions.

Rare-metal mineralization is most abundant in the Unit 4 lithic and crystal-poor ash-flow tuff-breccias of Late Caldera A and B. These are among the last calderas to form and the only ones with extensive deposits of Unit 5. Late Caldera A, in particular, has thick (36 m) mineralized Unit 4 lithic-rich ash-flow tuffs (Miller 1993). The mineralization is stratabound and does not appear to be related to late stage veining or hydrothermal activity, rather it appears to be a function of the evolving magma chamber.

Post Caldera

There is no evidence for the existence of a resurgent intrusion as outlined in the caldera development model of Smith and Bailey (1968). The bedding orientations do not form an outward dipping dome and there are no late cross-cutting intrusive rocks in the FRCC. As discussed previously the scale of the individual calderas and the small volume of volcanic material produced indicates that the parent magma chamber(s) was very small and did not become resurgent after collapse due to solidification of the magma depleted

chamber (Smith and Bailey 1968, Marsh 1984). Furthermore, Mahood (1984) has observed that resurgent intrusions are not common in strongly peralkaline calderas.

The occurrence of the FRCC at the surface today and the relatively unmetamorphosed nature of the volcanic rocks indicates that the region has experienced very little erosion and/or no uplift since ca. 1270 Ma (Hill 1991).

Mineralization

The rare-metal (Y and Zr) mineralization in the FRCC is stratabound disseminated mineralization which occurs in Unit 4 ash-flow tuff and lithic ash-flow tuff-breccia (Miller, 1993). It is most widespread in the two Final Stage calderas that contain relatively thick deposits of Unit 5 ash-flow tuff and lithic ash-flow tuff-breccia (BVN and BVS calderas). Unlike the hydrothermal vein-type mineralization commonly associated with calderas (Smith and Bailey 1968, Lipman 1984), this rare-metal mineralization appears to be related to the evolving magma in the parent magma chamber. Our studies of this mineralization are ongoing.

7.2 Rare-metal Mineralization

Introduction

A large number of radioactive showings were identified in the 1991 field season in the Flowers River cauldron complex (Figure 7-2; Miller, 1992b). These showings were considered to be rare-metal showings based on the correlation between radioactivity and rare-metal contents observed at the Strange Lake deposit and the Letitia Lake rare-metal showings (Table 1-3, 1-4). Subsequent rare-metal analyses (see Table B-13 for analyses and Table 7-1 for the most anomalous values from 1991 samples) confirm that the highest rare-metal values correlate very well with the highest radioactivity measurements.

Mineralization

Interest was initially focused on the Nuiklavik volcanic rocks by the anomalous values for Y observed in some of these rocks. Statistical analysis of Y values in just over 200 chemical analyses (from samples collected in 1991) yield the results found in Table 7-2. These averages, tabulated by subunit, indicate, with only a few exceptions, that the Flowers River granites (microgranite = 96 ppm and coarse granite = 50 ppm), the Basal Unit (31 ppm; Unit 1)), the Amphibole-bearing Porphyritic Unit (78 and 136 ppm; Unit 2) and the Lower Crystal-rich Ash-Flow Unit (72 - 103 ppm; Unit 3), which collectively make up approximately two thirds of the volcanic stratigraphy, contain low, economically uninteresting, concentrations of Y and other rare-metals. The exceptions, a granite aplite (432 ppm) and the amphibole ignimbrite subunit (318 ppm) of the Amphibole-bearing Porphyritic Unit (Unit 2), contain anomalous Y values but they are minor in extent.

The highest values of Y were obtained from the Crystal-poor and Quartz-phyric Ash-flow Unit (Unit 4) which has average values, for all but one of its subunits, from 300 to 600 ppm and contains all samples, but one, which have values over 490 ppm Y (Table 7-1). The aphyric or basal subunit has an average of 130 ppm Y, which is similar to that of the units which occur below it.

The Upper Ash-Flow Unit (Unit 5) exhibits Y values which increase upwards from 189 ppm for the feldspar-quartz ash-flow tuff, through 373 for the ash-flow lapilli tuff and to 506 for the amphibole ignimbrite. Note that the amphibole ignimbrite subunit in the Amphibole-bearing Porphyritic Unit (Unit 2) has average Y values which are 200 ppm less than that of the Upper Ash-Flow Unit (Unit 5). Also note that one of the

Table 7-1 Highly anomalous rare-metal analyses from the Nuiklavik felsic volcanic rocks

Field No.	Rock Type	Nb	Zr	Th	Y	La	Ce	Be	Coordinates N	Coordinates E	Spectr.
FR-91-075	Aphyric Ash-Flow Tuff (Unit 4)	338	4912	79	492	392	1081	19.7	6164775	614305	1000
FR-91-076	Aphyric Ash-Flow Tuff (Unit 4)	350	5185	82	499	359	1006	18.9	6164710	614315	760
FR-91-149	Quartz-poor Ash-Flow Tuff (Unit 4)	328	6622	86	499	551	1416	13.9	6156605	622605	940
FR-91-257	Aphyric Flow (Unit 4)	382	4999	104	501	340	1130	10.4	6159180	622750	980
FR-91-277	Quartz-poor Ash-Flow Tuff (Unit 4)	205	4578	91	502	363	922	14.2	6164010	613730	800
FR-91-248	Aphyric Ash-Flow Tuff (Unit 4)	365	4937	92	525	364	689	8.8	6158845	623005	970
FR-91-266	Quartz-poor Ash-Flow Tuff (Unit 4)	153	3905	57	529	923	1867	26.5	6163630	614070	560
FR-91-207	Aphyric Ash-Flow Breccia (Unit 4)	324	4151	86	533	338	929	30.9	6160785	620955	810
FR-91-249	Quartz Ash-Flow Breccia (Unit 4)	361	5118	94	537	480	1067	9.1	6158840	623025	880
FR-91-209	Amphibole Ignimbrite (Unit 5)	327	4286	82	546	107	558	16.8	6161050	621020	750
FR-91-111	Quartz Ash-Flow Tuff (Unit 4)	357	6195	113	552	437	1180	50.5	6158390	620255	1050
FR-91-213	Aphyric Ash-Flow Tuff (Unit 4; fragment)	375	6277	118	553	399	1178	25.3	6161030	622495	2220
FR-91-097	Quartz-poor Ash-Flow Tuff (Unit 4)	365	4702	94	584	45	452	14.6	6161905	620610	850
FR-91-098	Aphyric Ash-Flow Tuff (Unit 4)	405	5300	107	587	289	1062	28.9	6161840	620590	900
FR-91-016	Quartz-poor Ash-Flow Tuff (Unit 4)	429	5838	116	640	410	1237	28.3	6162585	616090	1000
FR-91-017	Aphyric Ash-Flow Breccia (Unit 4)	473	7085	116	692	59	593	12.7	6162615	616075	1120
FR-91-211	Quartz Ash-Flow Tuff (Unit 4)	521	8094	164	792	534	1542	40.9	6161080	622435	1150
FR-91-10	Aphyric Ash-Flow Breccia (Unit 4)	616	10519	271	910	845	2278	19.5	6159700	620200	2050
FR-91-214	Aphyric Ash-Flow Breccia (Unit 4)	646	11162	222	1024	596	1876	33.6	6161010	622570	2000
FR-91-114	Quartz-poor Ash-Flow Tuff (Unit 4)	647	9382	202	1039	809	2151	16.9	6157690	620985	1500
FR-91-134	Quartz-poor Ash-Flow Tuff (Unit 4)	766	11569	247	1161	766	2237	13.1	6156950	621205	1750
FR-91-141	Quartz Ash-Flow Tuff (Unit 4)	1414	21104	403	1888	604	2518	54.5	6157160	621125	3000

Chemical analyses by I.C.P. analysis; values in p.p.m.
Spectr. = cps reading from an EDA GRS-500 spectrometer set for total counts (TC1)

Table 7.2 Rare-metal values and averages for stratigraphic units in the Nuiklavik felsic volcanic rocks

	Nb	Zr	Th	Y	La	Ce	Be	Spectr.
Upper Ash-Flow Unit (#5)								
Amphibole Ignimbrite	329	4502	94	462	310	808	13	840
Amphibole Ignimbrite	327	4286	82	546	107	558	17	750
Ash-Flow Lapilli Tuff	325	2100	44	373	140	410	17	520
Feldspar-Quartz Ash-Flow Tuff−Average (7)	134	2115	28	189	234	513	11	464
Crystal-poor and Quartz-phyric Ash-Flow Unit (#4)								
Quartz Ash-Flow Tuff−Average (6)	307	5586	90	480	302	878	27	816
Quartz Ash-Flow Breccia−Average (4)	218	3548	57	308	331	662	11	690
Quartz Ash-Flow Tuff (non-compacted)	1414	21104	403	1888	604	2518	55	3000
Aphyric Ash-Flow Tuff−Average (6)	283	4663	79	419	249	803	14	938
Aphyric Ash-Flow Tuff (non-compacted)	338	4912	79	492	392	1081	20	1000
Aphyric Ash-Flow Tuff (non-compacted)	350	5185	82	499	359	1006	19	760
Aphyric Ash-Flow Breccia−Average (7)	383	6099	115	582	348	2059	17	1189
Quartz-poor Ash-Flow Tuff−Average (12)	321	5505	100	563	509	1200	17	895
Quartz-poor Ash-Flow Breccia	184	3736	35	228	75	403	4	520
Quartz-poor Ash-Flow Breccia	137	2030	36	197	33	154	7	420
Feldspar + Quartz-poor Ignimbrite−Average (17)	214	3657	58	326	276	805	19	669
Aphyric Flow−Average (22)	87	1729	15	130	191	438	7	334
Lower Crystal-rich Ash-Flow Unit (#3)								
Quartz Porphyry−Average (5)	46	803	14	72	147	303	5	320
Quartz Porphyry Breccia	42	974	18	90	114	284	6	400
Quartz Porphyry Breccia	72	1378	21	94	118	317	5	250
Quartz-Mafic Porphyry−Average (11)	44	759	7	75	112	252	5	314
Feldspar-Quartz Porphyry−Average (10)	74	1156	12	103	162	360	7	327
Amphibole-bearing Porphyritic Unit (#2)								
Amphibole-bearing Ignimbrite−Average (13)	291	3568	47	318	225	642	29	545
Amphibole-Feldspar-Quartz Porphyry−Average (22)	117	1604	12	136	262	572	11	358
Feldspar-Quartz ± Amphibole Porphyry−Average (28)	47	850	8	78	159	321	7	315
Basal Tuff Unit (#1)								
Bedded & Massive Tuffs−Average (6)	13	232	8	31	27	71	5	298
Carbonate Unit	1	3	0	3	6	9	0	150
Gabbro Sill	3	182	0	31	23	53	1	200
Gabbro Sill	4	157	0	31	25	54	3	185
Flowers River Granites								
Granite Aplite	289	5599	92	432	315	838	33	940
Microgranite−Average (13)	80	1210	17	96	184	407	10	341
Coarse Granite−Average (7)	55	692	6	50	135	300	5	254

Average (6) = 6 samples used to calculate average
Rare-metal analyses by I.C.P. analysis

amphibole ignimbrite samples has a highly anomalous Y value (546 ppm) and is thus the only highly anomalous sample outside of Unit 4.

The relative relationships observed for Y between the various subunits and units of the Nuiklavik volcanic rocks are also observed for the other rare-metals listed in Table 7-1. Zirconium values, in particular, mirror the relationships outlined above and they also reflect the highly anomalous, economically very interesting, absolute values of Y.

For the purposes of this study, highly anomalous Y analyses are any analyses above 490 ppm Y. A total of 21 samples occur in the highly anomalous range of values (see Figure 7-2 for sample locations). Most of these samples occur in the Crystal-poor and Quartz-phyric Ash-Flow Unit (Unit 4), particularly the quartz-poor ash-flow, the aphyric ash-flow and the quartz ash-flow subunits. Almost all of the aphyric ash-flow samples are highly anomalous (11 out of 15), whereas the quartz-poor ash-flow and quartz ash-flow subunit have an anomalous population which is approximately one-third of the total (6 out of 17 and 3 out of 10 respectively); samples with Y values over 900 ppm are evenly distributed between these three subunits.

Figure 7-3 is a complete detailed section of an exposure of the rare metal-enriched Crystal-poor and Quartz Ash-Flow Unit (Unit 4; see Figure 7-2 for location). The mineralized samples are found in quartz-poor ash-flow tuff and breccia, and quartz ash-flow tuff and breccia. Fragment types are dominantly aphyric flows and quartz-poor ash-flow tuff; many if not all fragments are also mineralized. This section contains 32 m of mineralized ash-flow units which have Y values in the range 550 - 1020 ppm. Other mineralized partial sections of this unit range from 4 to 10 m thick with comparable or higher Y values. Figure 7-2 illustrates the distribution of the Crystal-poor and Quartz-phyric Ash-flow Unit (Unit 4) and the location of the highly mineralized samples in it.

Petrographic studies of the mineralization are ongoing. The aphanitic to very fine grained nature of the mineralized units have made it very difficult to identify rare-metal minerals. Preliminary results suggest that the rare-metal mineralization occurs as sub-microscopic grains in the groundmass of the ash-flow tuff and in the groundmass of breccia fragments.

Conclusions

Highly anomalous Y and other rare-metal mineralization occurs in felsic ash-flow tuffs and breccias of the Crystal-poor and Quartz-phyric Ash-Flow Unit (Unit 4) of the Nuiklavik volcanic rocks. This mineralization has been observed to be 32 m thick in one

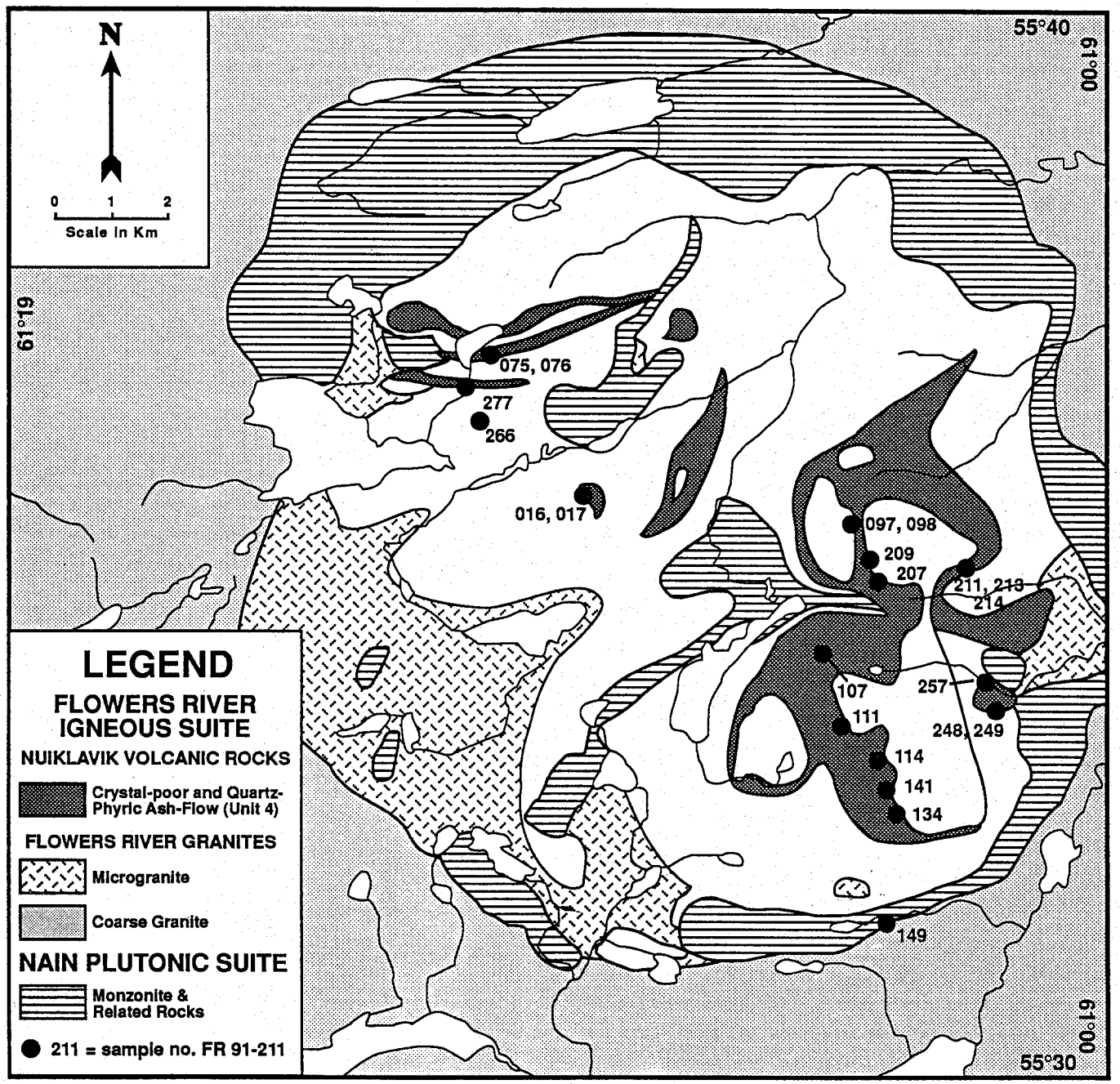

Figure 7-2 *Location of samples with highly anomalous Y values in the Nuiklavik felsic volcanic rocks and location of the Crystal-poor and quartz-phyric ash-flow Unit (Unit 4), which has a high potential for rare-metal mineralization; 214 = location of detailed section used in Figure 5.*

Nb	Zr	Th	Y
122	1885	27	175
521	8094	164	792
375	6277	118	553
646	11162	222	1024
112	1941	20	240
118	211	22	176

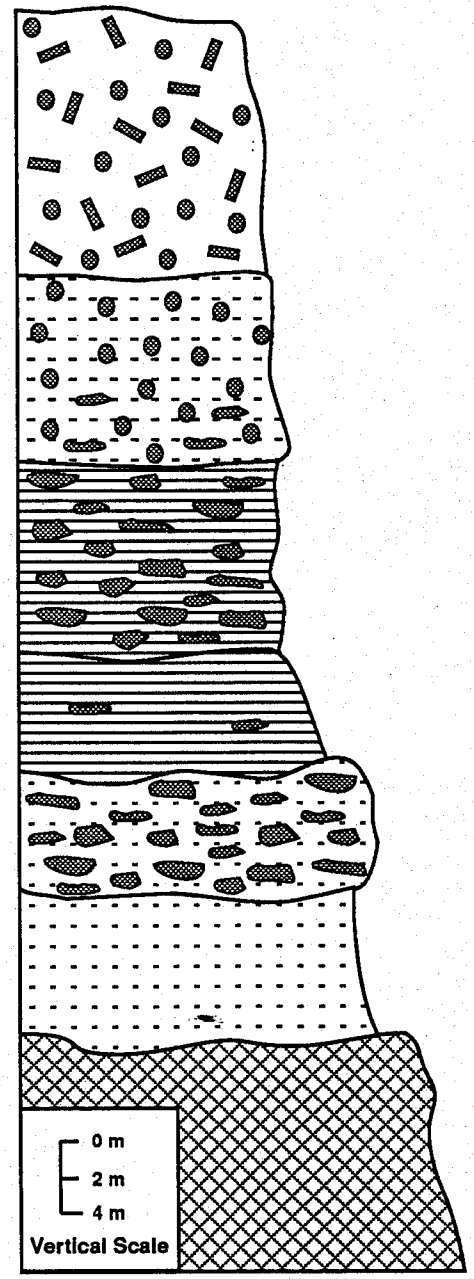

Upper Ash-Flow Tuff (Unit 5)

Quartz Ash-Flow Tuff (Unit 4)

Aphyric Lithic Ash-Flow Breccia (Unit 4)

Quartz-poor Ash-Flow Tuff (Unit 4)

Ash-Flow Breccia (Unit 4)

Aphyric Ash-Flow Tuff (Unit 4)

Quartz-poor Flow (Unit 4)

Figure 7-3 *A complete detailed section through the Crystal-poor and quartz-phyric ash-flow Unit of the Nuiklavik felsic volcanic rocks; this unit contains the most anomalous Y and other rare-metal values.*

occurrence and at least 4 m thick over an area of 14 square kilometers; Y values range from 300 to 1900 ppm in this unit and Zr values are commonly greater than 4000 ppm.

The Nuiklavik volcanic suite is an excellent target for rare-metal mineralization. This preliminary work has established the stratigraphy of the volcanic suite and has outlined the location of the stratigraphically controlled rare-metal mineralization. More detailed exploration work, including drilling and metallurgical work, is needed to further evaluate this mineralization. These rare-metal showings, located in the Flowers River area, are presently open for claim staking.

7.3 Extreme Na-Depletion in the Nuiklaik Peralkaline Volcanic Rocks

Introduction

Metasomatism in the Nuiklavik volcanic rocks has been previously discussed by White (1980), Hill (1881, 1982) and Hill and Thomas (1983). These studies documented Na loss in volcanic rocks of the FRCC. The mechanism was thought to involve alteration of feldspar phenocrysts and removal of Na from the devitrified-recrystallized groundmass. The following further documents the process of Na-depletion and evaluates this metasomatic event in terms of the formation of significant concentrations of rare-metal mineralization.

Volcanic rocks that exhibit Na-depletion are common throughout Units 2, 3 and 4 of the complex and within all recognized calderas (Figures 7-4 and 7-5). Feldspars in Unit 5, particularly in the upper members, are generally unaltered. Depletion is best displayed in feldspar-quartz ash-flow tuffs where feldspar is usually partially to completely replaced by a light green to black mafic (chlorite-like) mineral; this is commonly characteristic of extreme Na-depletion. These rocks were field-mapped as quartz-mafic porphyries (Miller, 1992) and are most commonly found in the upper portion of the columnar-jointed porphyritic ash-flow tuffs of Unit 3. Alteration is not easily recognized in either outcrop or hand samples of aphyric and other phenocryst-poor members of the suite. The locations of samples discussed in this study can be found in Figure 7-6.

Petrography

The feldspar-quartz crystal-rich ash-flow tuff of Unit 3 displays the most obvious signs of the Na-depletion process and thus is the best unit to study with regard to textural and mineralogical changes. This unit is characterized by abundant (20 to 35%) subhedral feldspar phenocrysts, from 3 to 6 mm long and subordinate (10 to 20%) embayed to subhedral quartz phenocrysts in a recrystallized quartz-feldspar mosaic groundmass. Broken grains and shards of quartz and less commonly feldspar are found in the groundmass. Feldspar phenocrysts, broken grains and groundmass feldspar are most susceptible to the alteration process.

Feldspar grains commonly exhibit alteration ranging from a dusting of sericitic alteration, to complete sericitization and from incipient alteration along cleavages to almost complete replacement by a chlorite-like mineral (Table 7-3); Plate 1 illustrates the

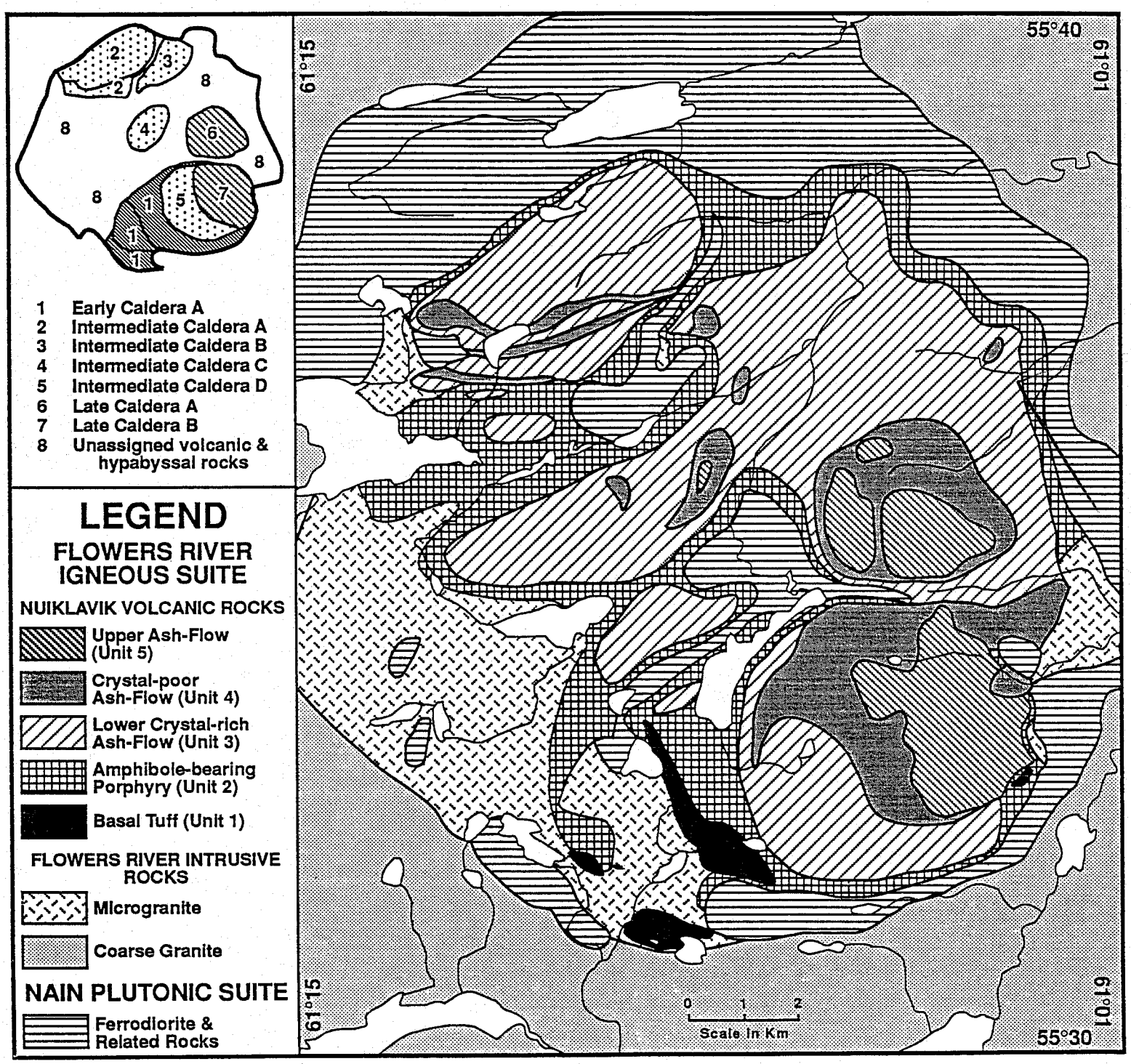

Figure 7-4 - Geology of Flowers River Cauldron Complex (Miller and Abdel-Rahman, in prep.). Insert outline recognized caldera structures in the cauldron complex.

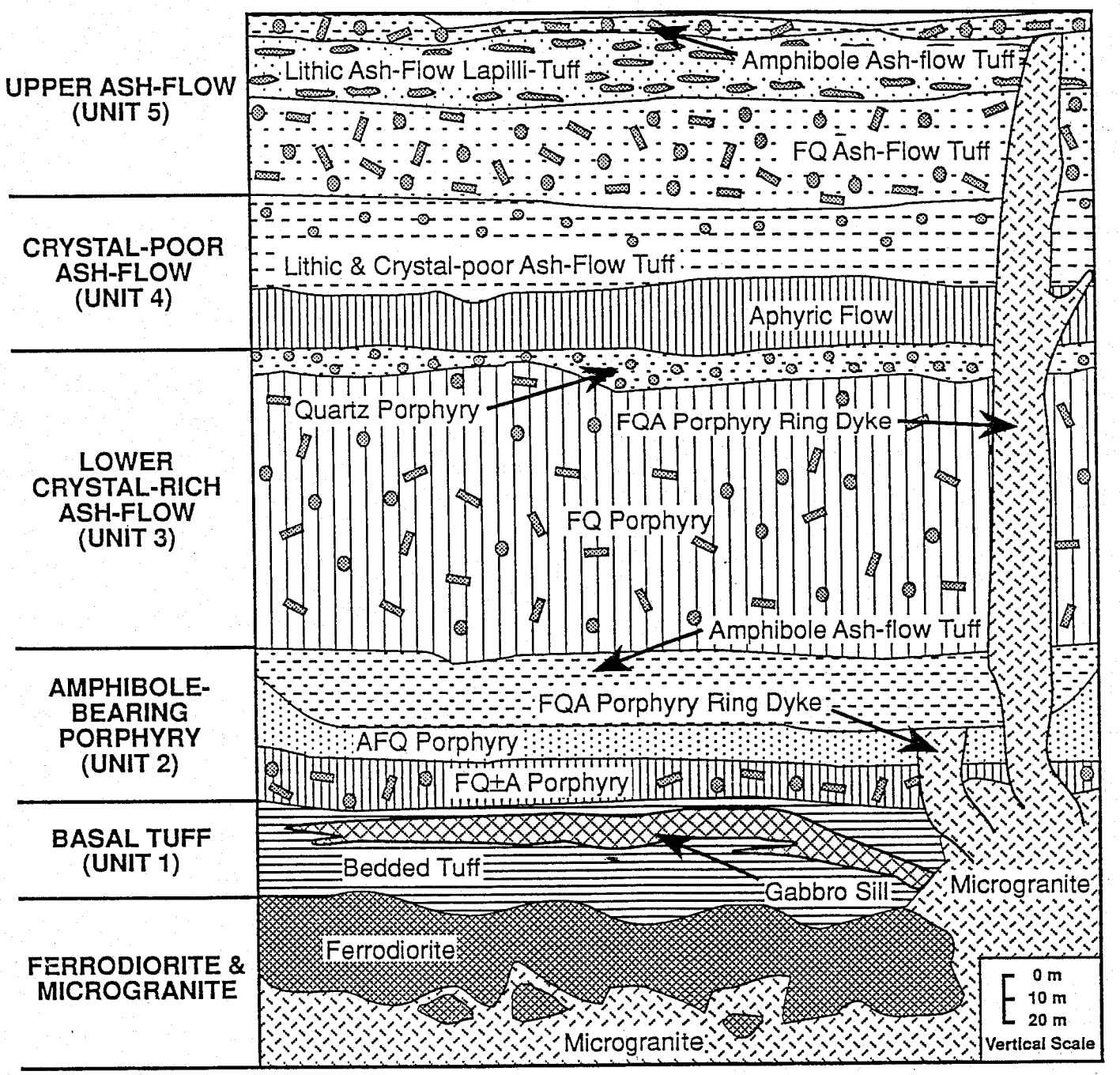

Figure 7-5 - Generalized stratigraphic section of the Flowers River Cauldron Complex (Miller and Abdel-Rahman, in prep.).

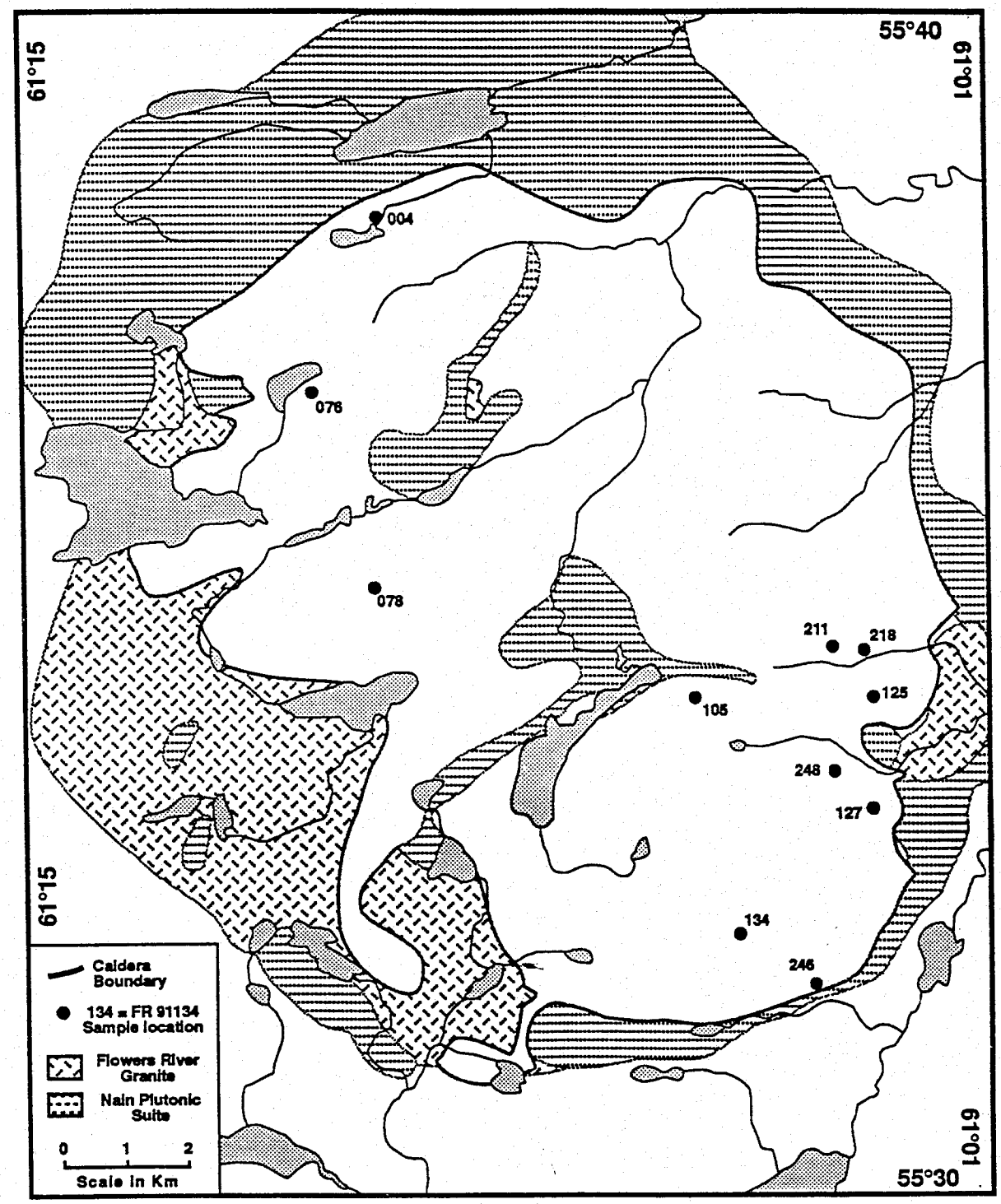

Figure 7-6 - Sample locations in the Flowers River Cauldron Complex.

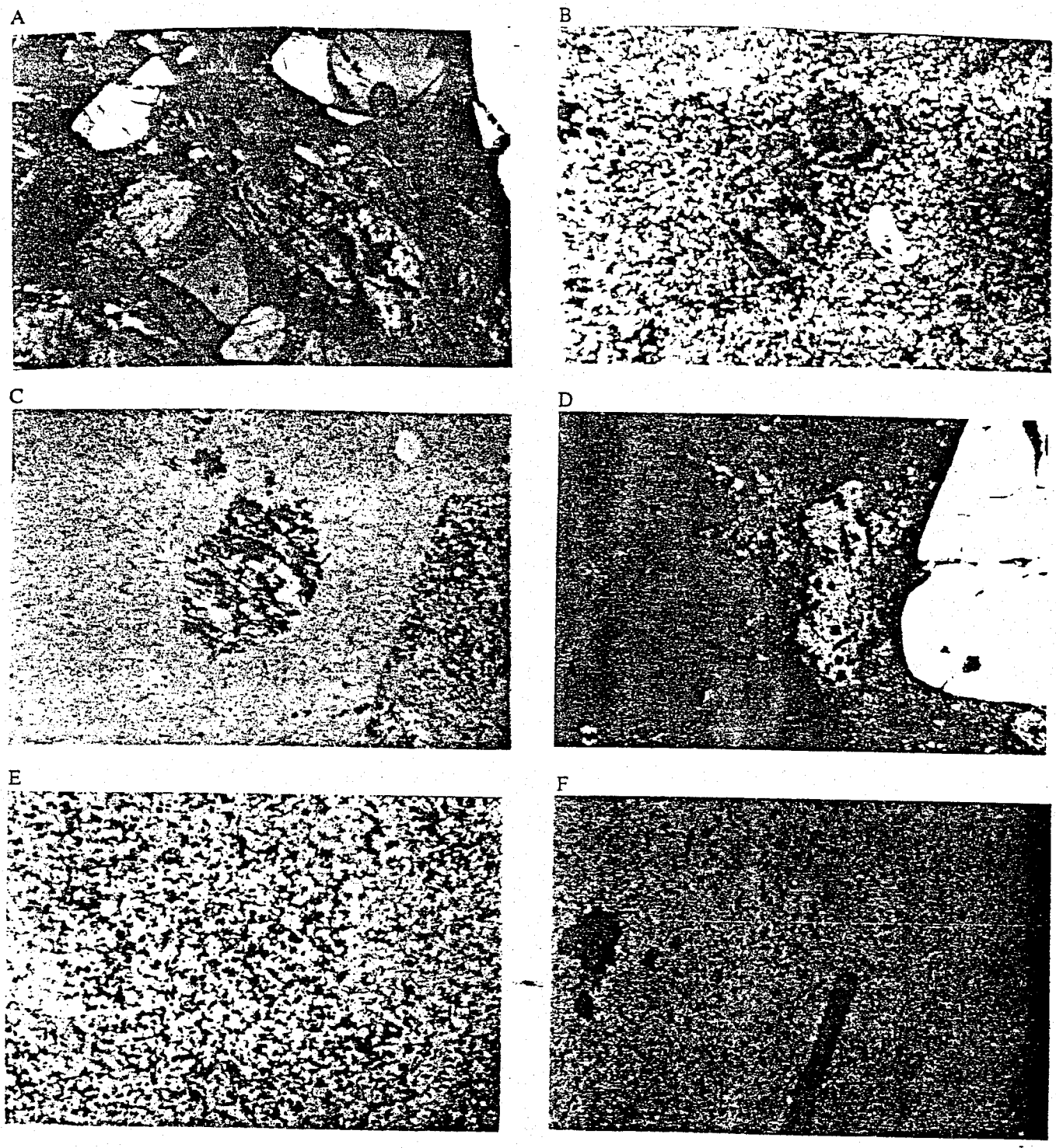

Plate 1. *Photomicrographs of feldspar and mafic mineral alteration in peralkaline ash-flow tuffs. 1a, photomicrograph: unaltered feldspar in a feldspar-quartz porphyritic ash-flow tuff; resorbed quartz and sub-euhedral feldspar; x-nicols, 2.5 x power (FR92091). 1b, photomicrograph: incipient chloritic alteration of feldspar in a feldspar-quartz ash-flow tuff; chlorite in matrix and chlorite patches in feldspar; 2.5 x power (FR91291). 1c, photomicrograph: extreme chloritic alteration of feldspar in a feldspar-quartz ash-flow tuff; 2.5 x power (FR91034). 1d, photomicrograph: extreme sericitic alteration of feldspar in a feldspar-quartz ash-flow tuff; subhedral to resorbed quartz surrounding feldspar phenocryst replaced by light-coloured sericite; x-nicols, 2.5 x power (FR91125). 1e. photomicrograph: chloritic alteration of feldspar in the groundmass of an aphyric ash-flow tuff; groundmass consists of chlorite and quartz; 2.5 x power (FR91105). 1f, photomicrograph: alteration of alkali-amphibole to chlorite; elongate and equant amphibole phenocrysts completely replaced by chlorite; 2.5 x power (FR91033).*

Table 1 Characteristics of Alteration in Study Samples*

Sample	Unit No.	Rock Type	Feldspar	Matrix	Mafic Minerals
FR91004	3	Feldspar-quartz ash-flow	minor sericite & chlorite	chlorite	chlorite
FR91076	4	Aphyric ash-flow	—	?	chlorite
FR91078	3	Quartz ash-flow	30% replaced by chlorite	chlorite	—
FR91105	4	Aphyric ash-flow	—	chlorite	chlorite
FR91125	4	Altered feldspar-quartz ash-flow	chloritized	chlorite	chlorite?
FR91127	5	Feldspar-quartz porphyry (ring dyke ?)	relatively unaltered	unaltered	amphibole
FR91134	4	Quartz-poor ash-flow	—	chlorite	—
FR91211	4	Quartz-feldspar ash-flow breccia	sericite & hematized chlorite	chlorite	—
FR91218	3	Quartz ash-flow (zeolites)	—	—	—
FR91246	3	Quartz-feldspar ash-flow	sericite & hematized chlorite	chlorite	—
FR91248	4	Aphyric ash-flow	—	minor chlorite	—

* Thin section observations

progression from samples that appear relatively unaltered (Plate 1a) to samples that exhibit extreme alteration of feldspar grains (Plate 1c, d, e).

Alteration in the groundmass of the porphyritic units and in the aphyric units (e.g. the lower member of Unit 4) is not as easy to identify. Plate 1e illustrates alteration of groundmass feldspar (?) in a highly altered sample. The green mineral found in the groundmass is thought to be the same as that found replacing feldspar phenocrysts.

White (1980) reports the presence of a microcrystalline green mineral replacing albite in microperthitic feldspar and provides a partial microprobe analysis indicating enrichment of Fe and Al and depletion in Na and Si relative to unaltered albite; identification of the green mineral was not possible from the available data. Microprobe analyses indicated that Na-depletion also occurred in the groundmass. Hill (1982) reports that electron back-scatter photomicrographs of feldspar phenocrysts in volcanic porphyry indicate that Na can be almost completely absent in the groundmass even though feldspar phenocrysts appear to be relatively unaffected; similar back-scatter observations for K indicate that it is abundant in the groundmass and the feldspar phenocrysts of altered rocks.

Microscopically, the main alteration products of the microperthitic feldspars are either sericite or the chlorite-like mineral. Sericite alteration occurs on the K-feldspar phase of some microperthites and the chlorite-like mineral on the albite phase. The chlorite-like mineral ranges from weakly to moderately pleochroic pale brown or green to medium-dark brown or green. It commonly occurs as a microcrystalline mosaic but is also sparsely found as large grains up to 0.1 mm in some feldspars. Anomalous interference colours, the habit and pleochroism suggest that this mineral is a member of the chlorite family.

Rare-metal minerals are very small, with the exception of sparse zircon grains, and have not been identified. The observed zircon grains appear to be unaltered, however it is not possible to petrographically evaluate other rare-metal minerals.

Similar extreme alteration has not be observed or reported in the associated hypabyssal ring dykes or the nearby subvolcanic granites of the Flowers River intrusive suite.

Chemistry

A representative suite of 30 samples of extremely altered to unaltered volcanic rocks from the Nuiklavik volcanic suite was chosen to study the chemistry of the alteration process; the major and trace element chemistry of 11 of these samples is listed in Table 7-

Table 2 Geochemical data for poorly to extremely altered Nuiklavik volcanic rocks ^

Sample	1004•	1076	1078	1105	1125	1127	1134	1211	1218	1246	1248
Unit #	3	4	3	4	4	5	4	4	3	3	4
SiO2	75.05	75.65	80.80	79.40	76.65	73.60	75.10	77.55	86.30	75.85	72.85
TiO2	0.31	0.23	0.26	0.38	0.30	0.29	0.40	0.25	0.26	0.26	0.25
Al2O3	11.61	9.85	10.45	10.46	10.85	10.63	8.70	8.91	10.14	10.88	10.66
Fe2O3	1.21	1.15	0.89	0.96	0.97	2.55	1.63	6.62	0.70	2.63	3.31
FeO	1.77	5.05	1.35	2.04	5.06	2.71	5.57			1.71	3.15
FeOtot°	2.86	6.09	2.15	2.90	5.93	5.01	7.04	5.96	0.63	4.08	6.13
MnO	0.06	0.08	0.01	0.03	0.07	0.06	0.10	0.04	0.01	0.04	0.06
MgO	0.26	0.02	0.10	0.03	0.04	0.02	0.03	0.10	0.01	0.15	0.06
CaO	0.47	0.16	0.01	0.01	0.01	0.14	0.01	0.04	0.06	0.03	0.15
Na2O	3.60	0.05	0.01	0.05	0.05	3.70	0.01	0.08	0.11	1.21	3.06
K2O	4.51	4.43	3.11	2.88	3.10	4.56	2.06	3.46	0.63	4.86	4.29
P2O5	0.03	0.01	0.04	0.03	0.01	0.01	0.02	0.01	0.02	0.01	0.01
H2O+	0.48	1.65	1.97	1.86	2.08	0.50	2.47	1.60	1.56	1.96	0.95
H2O-	0.21	0.22	0.27	0.28	0.20	0.13	0.24	0.17	0.32	0.35	0.17
S	0.02	0.07	0.00	0.03	0.01	0.04	0.02	0.02	0.05	0.02	0.14
CO2	0.19	0.09	0.11	0.07	0.06	0.12	0.27	0.06	0.04	0.10	0.13
Total*	99.89	99.41	99.48	98.73	99.86	99.41	98.19	100.00	100.31	100.25	99.91
A. I.	0.93	0.50	0.32	0.31	0.32	1.04	0.26	0.44	0.09	0.67	0.91
Rb	161	542	181	145	257	277	295	721	33	218	389
Ba	252	23	61	91	21	37	29	31	45	84	20
Sr	28	9	3	3	3	7	4	11	8	9	12
Pb	233	169	39	25	43	65	134	228	<1	18	68
Zn	285	516	34	54	165	312	606	506	15	106	454
La	174	359	119	245	250	278	766	534	58	158	364
Ce	367	1006	273	473	647	688	2237	1542	139	329	689
Y	92	499	71	137	264	249	1161	792	50	131	525
Th	13	82	9	9	46	35	247	164	18	18	92
Sc	1.7	<0.1	1.2	0.7	0.1	0.2	<0.1	<0.1	1.4	0.3	<0.1
U	3.3	14.2	2.5	2.9	8.8	6.2	42.4	23.7	7.5	3.1	12.4
Zr	808	5185	743	1595	2935	2585	11569	8094	747	1443	4937
Nb	57	350	48	74	180	164	766	521	45	95	365
F	338	1200	214	250	380	747	447	622	221	98	397

^ Extremely altered samples have Na2O < 0.10%

• Add FR9 to this number to obtain sample number

° FeOtot = total Fe calculated as FeO

* Total includes ZrO2

Trace elements in ppm; ICP and AA analysis Newfoundland Geological Survey Branch Laboratory; U by neutron activation; F by specific ion electrode;

Major elements in wt. %; ICP analysis Newfoundland Geological Survey Branch Laboratory; CO2, S and H2O+ by IR analysis.

A.I. = Agpaitic Index = molar ((Na2O + K2O)/Al2O3)

3. The most striking observation from the data in Table 7-4 is the almost complete absence of Na_2O is some samples of the volcanic suite (i.e. less than 0.1 %). Samples with very little or no Na_2O are most often characterized by replacement of feldspar phenocrysts and groundmass feldspar by the green chlorite-like mineral (compare Table 7-3 and Table 7-4).

The extent of the Na-depletion is best observed in a Na_2O-Harker diagram (Figure 7-7) of the data set, where Na_2O falls from almost 4 wt. % to virtually 0 wt. %; this diagram also indicates that Na-depletion is generally, but not always, accompanied by SiO_2 enrichment. Figure 7-8 illustrates other geochemical trends that correlate with Na-depletion. These include a decrease in Al_2O_3 and K_2O and increases in H_2O and ZrO_2; H_2O+ provides the best correlation with Na_2O. Generally speaking, if a rock has any one of the following geochemical features then it will also have little or no Na_2O (Figures 7-7 and 7-8): $H_2O > 1.0\%$, $Al_2O_3 < 10.5\%$, $K_2O < 3.8\%$, $SiO_2 > 77.5\%$ and $Zr > 5000$ ppm; the opposite does not hold (i.e. rocks with $> 3.8\%$ K_2O may also have little or no Na_2O).

Some of the observations made of the behaviour of various elements in low Na_2O rocks can be further tested by plotting some of these elements against each other (Figures 7-7 and 7-9). In these diagrams, the following is observed: 1) Al_2O_3, SiO_2, H_2O+ and K_2O provide internally consistent plots, with regard to Na_2O depletion, 2) overlap between the fields of Na-depleted and Na-enriched fields is observed in all plots with perhaps H_2O vs. Al_2O_3 providing the best separation between fields, 3) K_2O vs. SiO_2 gives the best approximation of a linear plot, and, 4) ZrO_2 and SiO_2 are not internally consistent (see Discussion). The scatter in these plots and the overlap between fields of Na-poor and Na-rich rocks are characteristic of an alteration process affecting various precursor rocks to varying degrees.

The rare-metal mineralization in the cauldron complex can best be characterized by plotting rare-metals against each other (Figure 10; Zr vs. Y, Zr vs. Nb). These plots, in contrast to the plots of most major elements, illustrate highly correlated straight-line relationships between most pairs of rare-metals and other incompatible elements (e.g. REE, Y, Nb, Zr, U, Th). The plot of ZrO_2 vs. SiO_2 (Figure 7-7) illustrates the chaotic relationship observed between incompatible elements and major elements in the cauldron complex; Fe as FeO (Figure 7-10) is the only major element that exhibits a relatively good correlation with incompatible elements. Some compatible trace elements (Sc and Ba) also exhibit good correlation (i.e. negative correlation) with the incompatible elements (Figure 7-10; Zr vs. Ba).

Some of the relationships between trace elements, rare-metal mineralization and the Na_2O depletion process can be illustrated in normalized diagrams (Figure 7-11). Hill and

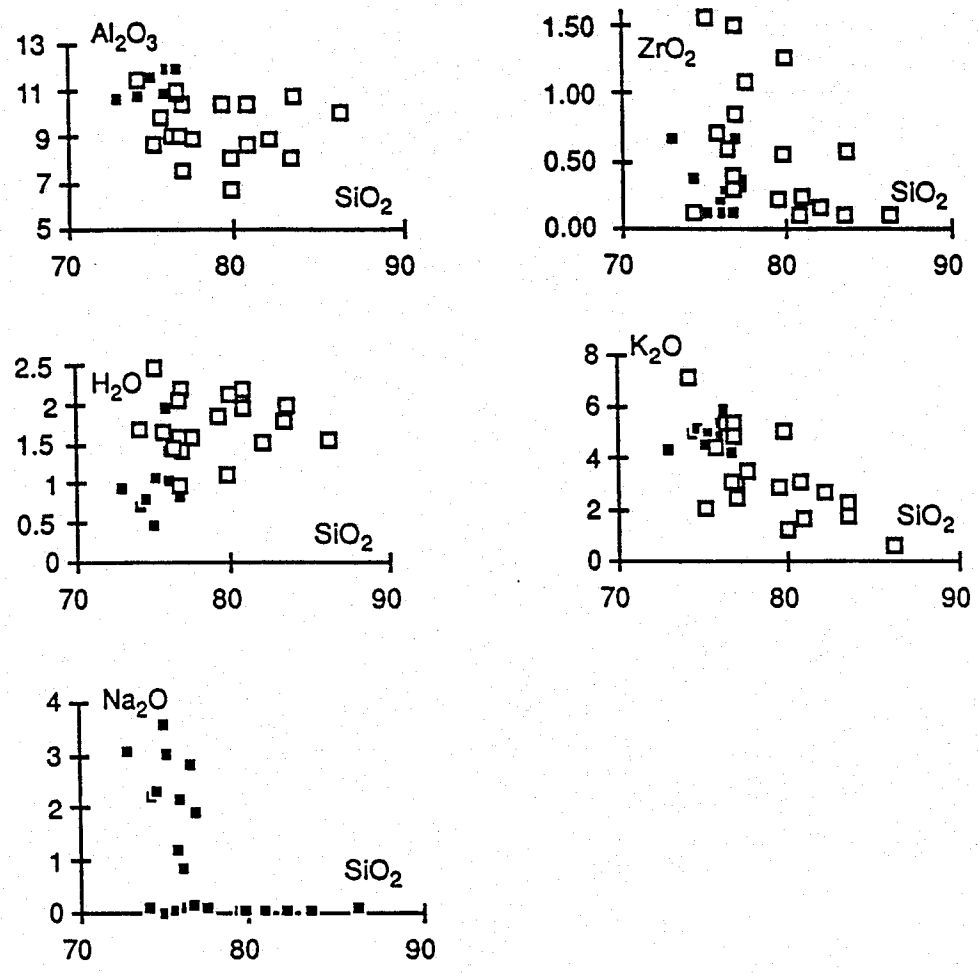

Figure 7-7 - Harker diagrams of altered and relatively unaltered rocks (Na_2O, ZrO_2, K_2O, H_2O, Al_2O_3); filled squares are relatively unaltered samples (all samples in Na_2O vs. SiO_2 plot); unfilled squares are altered samples ($Na_2O < 0.2$ wt. %).

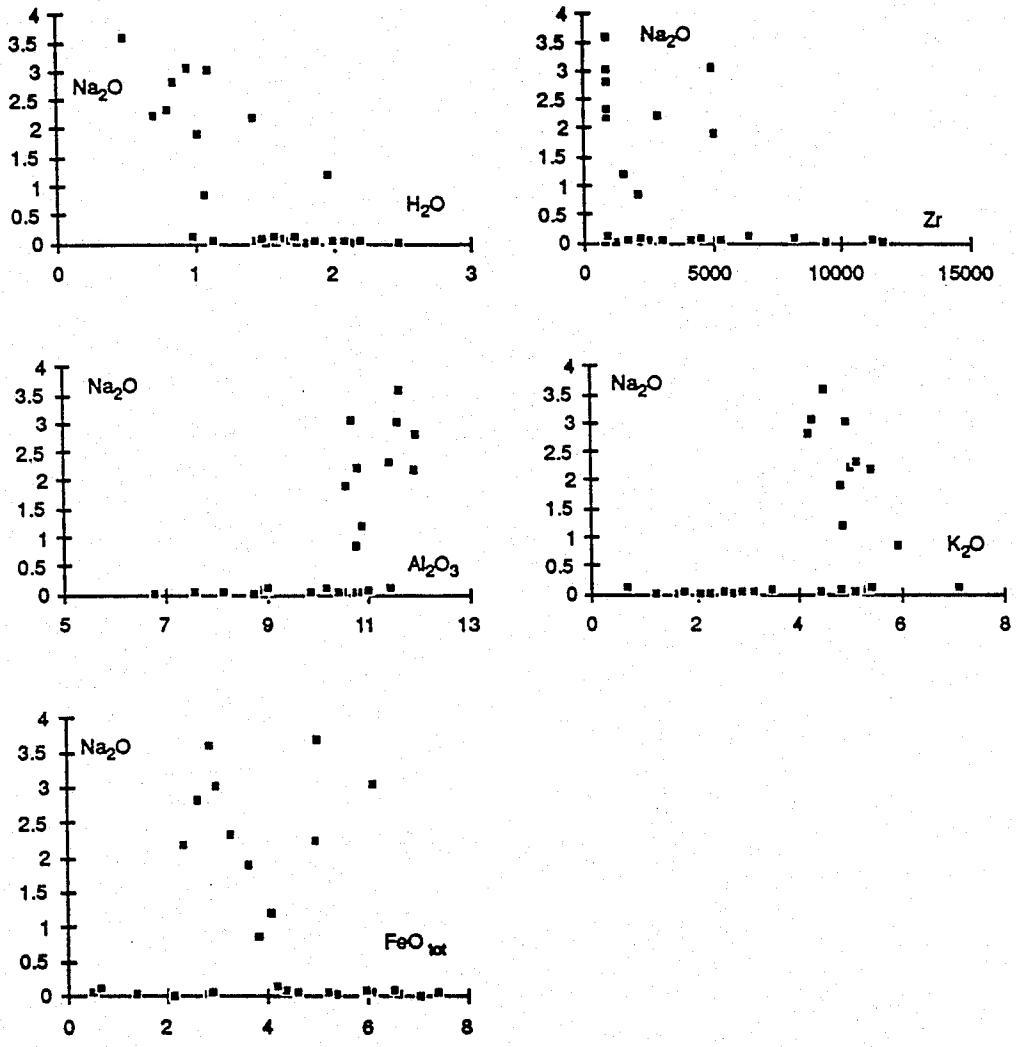

Figure 7-8 - The relationship between the Na-depletion process and other elements; Na_2O vs. Al_2O_3, K_2O Zr, H_2O.

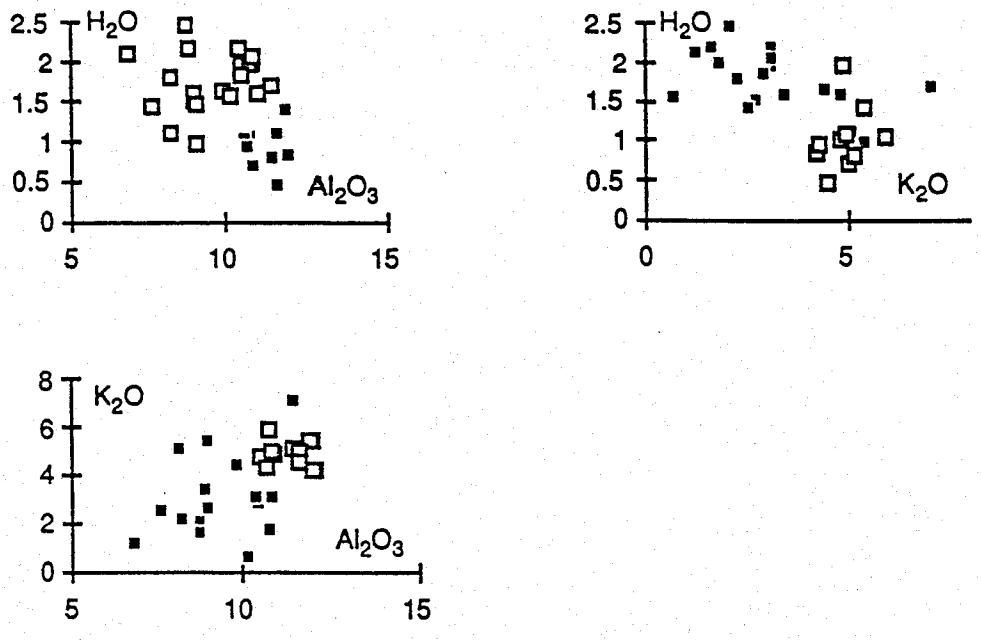

Figure 7-9 - The relationship between elements potentially involved in the Na-depletion process (H_2O vs. Al_2O_3, H_2O vs. K_2O, K_2O vs. Al_2O_3; filled squares are relatively unaltered samples ($Na_2O > 1.2$ wt. %); unfilled squares are altered samples ($Na_2O < 0.2$ wt. %).

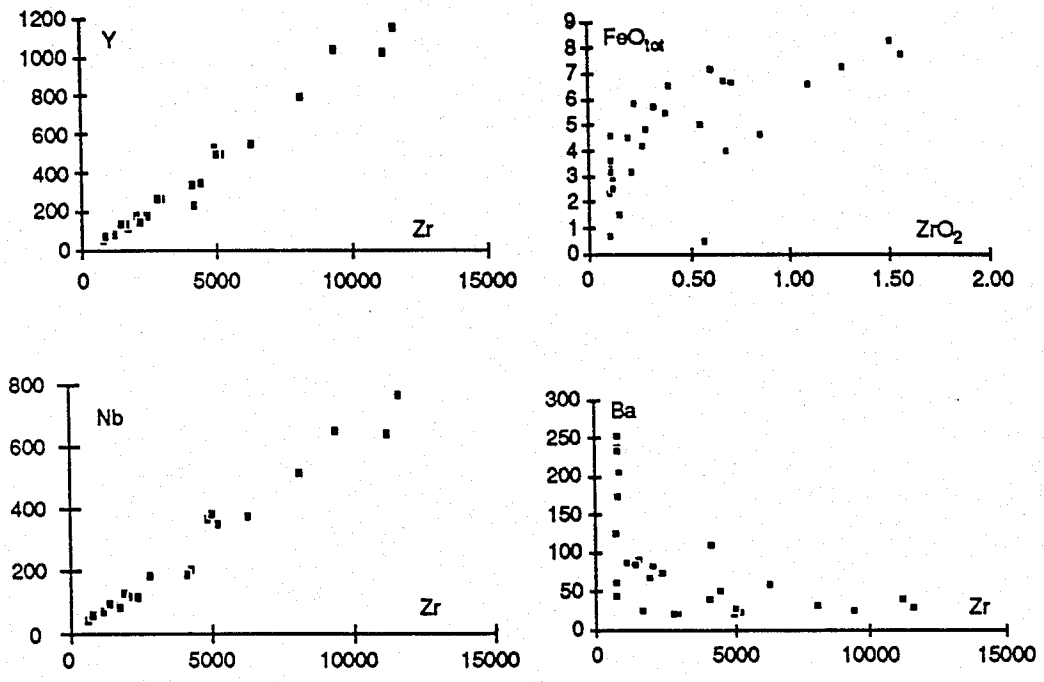

Figure 7-10 - The relationship between incompatible elements (Zr vs. Y, Zr vs. Nb), compatible and incompatible elements (Zr vs. Ba) and FeOtotal vs. ZrO_2.

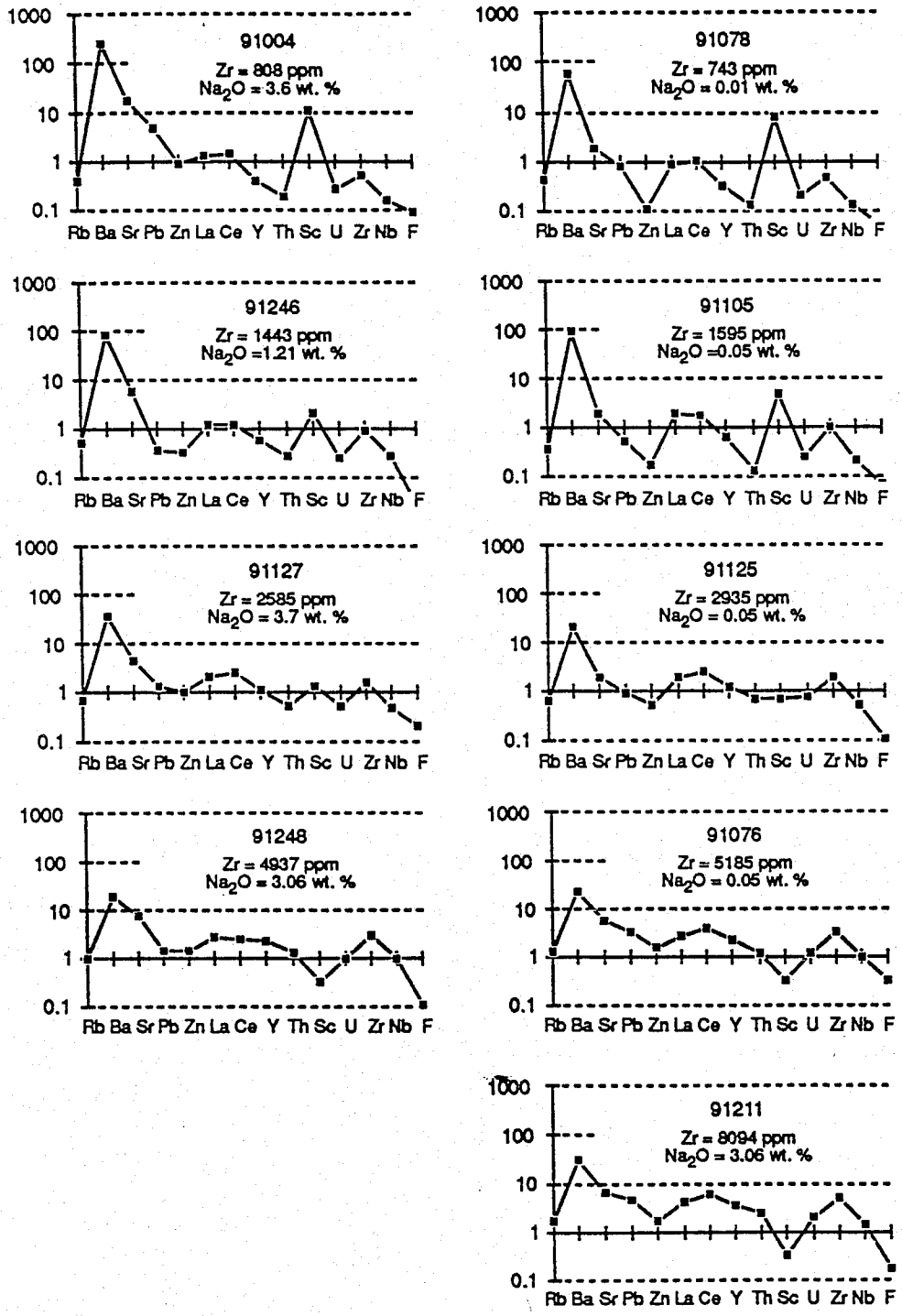

Figure 7-11 - Comendite normalized trace element data for a suite of Na-poor and relatively Na-rich rocks of various Zr concentrations. The normalizing data is from sample 301a (MacDonald et al. 1987), a comenditic obsidian from the Naivasha complex, Kenya Rift Valley. High Na samples are found in the left hand column and low Na samples in the right hand column. Rows contain samples of nearly equivalent Zr concentrations. Compare samples in any row to determine the effect of the Na-depletion event on trace elements on rocks of similar Zr concentrations. Elements are in order of relative ionic radii / ionic charge.

Thomas (1983) demonstrated that rocks in the Flowers River Cauldron Complex have trace element affinities with comendites and pantellerites in unaltered volcanic suites. A relatively unaltered comendite obsidian, from Naivasha complex, Kenya Rift Valley, was used as a normalizing factor for this study (MacDonald et al 1987; Table 4, sample no. 301a). Thus values near one on the normalized diagrams indicate chemical compositions near those of this comendite and values much higher or much lower than one indicate higher or lower chemical compositions. Figure 7-11 is arranged in a matrix with the left hand column for high Na (> 1.2% Na_2O) rocks and right hand column for low Na (< 0.2% Na_2O) rocks; the rows represent rows of equal Zr, with Zr increasing downwards. The similar patterns for high Na and low Na rocks at equal Zr values (i.e. compare two diagrams in any row) readily illustrate that most trace elements are relatively unaffected by the Na-depletion event. The columns of the matrix also illustrate the pattern of increasing U, Th, REE, Nb, Y, Be, Zn and Rb with increasing Zr and decreasing Ba and Sc with increasing Zr.

Discussion

1. Nature of the alteration process

Certain features of the alteration process are readily apparent and clearly distinguished from magma differentiation and other processes. The mineralogical features of the alteration process indicate that: 1) Na was lost from albitic feldspar upon replacement by chlorite, 2) H_2O was added to both phases in microperthite to form chlorite and sericite, and, 3) Fe was added to albite to make chlorite. It is less clear whether K, Al, Fe or Si are mobile or immobile during the alteration event. These mineralogical-petrographical features can only indicate what is happening to a particular mineral and do not tell us whether chemical components are mobile or conserved on the outcrop or handsample scale.

The geochemical data confirm that Na is lost from the system during the alteration process. Correlation of low Na from obviously highly altered rocks with other elements gives an indication that high H_2O and Si and low K and Al may also result from the alteration process. Data from other studies suggest that K is unaffected by the process (Hill, 1982) and that depletion of Si and Na and enrichment of Al and Fe accompany the chloritization process (White, 1980). Some of these conclusions are contradictory if mineral scale processes are compared to handsample scale processes but may be resolvable on the hand sample scale (i.e. other minerals may be forming or may be replaced elsewhere in the system to conserve one or more of the elements giving the contradictory conclusions). Handsample scale data (i.e. whole rock chemical data)

indicate that rocks containing high H_2O and Si and low K and Al are more likely to be altered. The FeO_{total} vs. Na_2O data plot clearly indicates that FeO_{total} does not correlate with Na_2O, thus FeO_{total} is conserved on an outcrop scale and Fe used by chlorite to replace albite is obtained from within the host rock.

Studies of more recent peralkaline volcanic rocks (e.g. Mayor Island - Weaver et al. 1990; Kenya Rift Valley - Baker and Henage, 1977) indicate that crystallization and devitrification of obsidians and other glassy rocks can lead to quantifiable loss of Na and other elements but the amount of Na-depletion is commonly less than 20% of the original Na. The addition of H_2O to feldspar to form sericite and chlorite and the correlation of high H_2O with low Na_2O indicates that the replacement process is due mainly to hydrothermal activity; devitrification or crystallization may be responsible for a small component of the Na-depletion.

2. Relationship between the alteration and differentiation processes

The volcanic rocks in the FRCC are the products of one large magma chamber or a series of small magma chambers fed from a common source (Miller and Abdel-Rahman, in prep.). As such, individual volcanic units are samples of the magma chamber(s) as it evolved and should thus exhibit some kind of chemical differentiation trend. The Na-depletion process, a post-deposition process, imprints its chemical signature on top of that produced by magma differentiation. Trends observed on data plots used to characterize the Na-depletion process must be evaluated to determine what effect the underlying differentiation trend has.

It is commonly observed that differentiation of peralkaline magmas leads to declining Al_2O_3, as observed in Figure 7-7, and increasing SiO_2, although not to the extremes in Figure 7-7. Thus, the correlation of low Al_2O_3 with low Na_2O may be completely or partially due to the differentiation process. Felsic volcanic rocks with over 76% SiO_2 are commonly considered to be non-representative of magma compositions (i.e. silicified rocks or rocks with cumulate quartz). In the FRCC, high SiO_2 rocks (> 78% SiO_2) contain low values of Na_2O suggesting that the high SiO_2 may be due to the Na-depletion event or perhaps a separate silicification event.

The decline of K_2O in Figure 7-7 is contrary to normal peralkaline differentiation trends, suggesting that the occurrence of low K_2O in low Na_2O rocks is probably connected to the Na-depletion process.

3. Relationship between the alteration and mineralization processes

Rare-metal mineralization in peralkaline granites and volcanic rocks is thought to be due to either a metasomatic (i.e. hydrothermal) event (e.g. Salvi and Williams-Jones, 1990a,b; Ramsden et al. 1993) or the formation of incompatible enriched residual liquids in a magma chamber (e.g. Birkett and Miller, 1990). If the rare-metal mineralization (Zr, Y, Nb, REE) in the FRCC is due to a metasomatic event then it is mostly likely related to the Na-depletion hydrothermal event.

The ZrO_2 vs. SiO_2, the SiO_2 vs. Na_2O and the ZrO_2 vs. Na_2O plots (Figurse7- 7 and 7-8) clearly indicate that either ZrO_2 or SiO_2 are not involved in the Na-depletion event. High SiO_2 values (> 80% SiO_2) correlate with low ZrO2 (< 0.6% ZrO_2), whereas it has been established that high SiO_2 and high ZrO_2 correlate with low Na_2O. Several lines of evidence suggest that Zr and the other incompatible elements are relatively immobile during the Na-depletion process: 1) the excellent correlation of Zr vs. the other incompatible elements (Figure 7-10) contrasts significantly with the scatter plots of SiO_2 vs. other major elements (Figure 7-7) and SiO_2 vs. the incompatible elements (Figure 7-7), 2) Ba and Sc exhibit excellent correlation with incompatible elements (Figure 7-10), whereas SiO_2 vs. Ba or Sc plots are scatter plots, 3) comparison of selected trace element normalized plots for Na_2O-rich (> 1.2%) vs. Na_2O-poor (< 0.2%) at comparable Zr values (Figure 7-11) gives identical plots for rare-metals, Zn, Ba and Sc, 4) the lack of petrographic evidence of the growth of rare-metal-bearing minerals in conjunction with chloritization of feldspar, and, 5) the lack of correlation of rare-metals with Na_2O (Figure 7-8).

The high positive correlation of Zr, Y, Nb, U, Th, and REE and the high negative correlation of rare-metals with Ba and Sc (Figure 7-10) strongly argue for a magmatic process for the concentration of rare-metals in the Nuiklavik volcanic suite.

This conclusion does not account for the fact that all high Zr samples (>5000 ppm) contain little or no Na_2O (<0.1%), contrary to all known peralkaline differentiation trends. However, all known occurrences of volcanic rocks with >5000 ppm Zr occur in Unit 4 which, generally speaking, appears to be the upper limit of Na-depleted rocks. This observation indicates that at least some and perhaps all of the hydrothermal activity responsible for Na-depletion and feldspar replacement is related to Unit 4 volcanism.

8.0 Conclusions

At present, field observations, radioactivity measurements and some geochemical data are available for the samples collected. These data, in particular the geochemical data, can be used to make an evaluation of rare-metal potential in the targets studied. Table 8-1 outlines the rock types discovered, the potential setting of rare-metal mineralization, the range of Zr and Y values and an evaluation of the rare-metal potential.

The Topsails Igneous Suite, in particular the peralkaline volcanic phases, exhibit anomalous values of Zr and Y. However, these values are not high enough when compared to the mineral deposits in Labrador. There is some potential for rare-metals in the volcanic rocks if better indications of a rare-metal concentrating process could be discovered in the area. At the present time, this area would be given a low priority for exploration.

The Baie Verte Peninsula targets have metaluminous and peralkaline phases which give similar results as the Topsails Igneous Suite. The Micmac Lake Group and Kings Point Complex show some potential for rare metals. More work should be planned for the Micmac Lake Group for a more thorough evaluation. The Kings Point Complex should have some more follow-up as the potential should be there for concentration of rare-metals but it has not been realized to date.

The Le Grande Pierre area contains the peralkaline granite of the Cross Hills complex and the peralkaline ash-flow tuffs of the Mooring Cove Formation. Both of these rock types have shown potential for very anomalous concentrations of rare metals and thus are very good targets. The best approach for further exploration in the Cross Hills peralkaline granite is to drill to several hundred metres depth, into the zone of radioactive granite. The Mooring Cove Formation has only been evaluated in one small area. The base of this formation should be evaluated in all other occurrences.

The Burin Peninsula targets range from metaluminous to peralkaline ash-flows to peralkaline granite and associated fluorite veins. The Grand Beach complex has no potential for rare metals. The St. Lawrence granite and Terrenceville area have some potential but should not be a high priority. Of special interest are the high values of Y in the fluorite veins. These high values may be recoverable from a fluorite mining operation if an economical metallurgical process were available.

The Bull Arm Formation, or at least the felsic ash-flow tuffs in the Musgravetown Group, has very low to no potential for rare metals except for in the Musgravetown area. Peralkaline ash-flow tuffs and dykes(?) contain very high values of rare metals. This indicates the potential for concentration of rare metals but does not establish the existence of

Table 8-1 **Evaluation of Rare-Metal Targets in Newfoundland and Labrador**

Target	Rock Type	Setting	Zr Values (ppm)	Y Values (ppm)	Rare-Metal Potential
Topsail Igneous Suite					
Little Pond Brook volcanic suite	Peralkaline & metaluminous ash-flows	2	800 - 1100	80 - 140	Low - Medium
Gaff Topsail peralkaline granite	Peralkaline Granite	1, 2	700 - 1000	60 - 100	Low
Sheffield Lake area	Peralkaline & metaluminous ash-flows	2	900 - 1500	140 - 180	Medium
Baie Verte Peninsula					
Cape St. John area	Peralkaline granite & metaluminous ash-flows	2	500 - 700	60 - 80	Low
Micmac Lake Group	Peralkaline ash-flow tuffs	2	600 - 1600	100 - 160	Medium
Kings Point Complex	Peralkaline & metaluminous ash-flows / intrusions	1, 2	1000 - 1600	100 - 220	Medium
Le Grande Pierre Area					
Mooring Cove Formation	Peralkaline ash-flows and hypabyssal dykes	2	200 - 2800	100 - 270	Medium - High
Cross Hills peralkaline granite	Peralkaline granite	1, 2	1000 - 8500	100 - 1000	High
Burin Peninsula					
Grand Beach complex	Metaluminous ash-flows	2	100 - 400	80 - 120	None
St. Lawrence peralkaline granite	Peralkaline granite	1, 2	700 - 1000	80 - 160	Low
	Fluorite veins	1, 2	–	500 - 800	Bi-product?
Terranceville Area	Peralkaline ash-flow tuffs	2	500 - 1200	100 - 150	Low - Medium
Bull Arm Formation					
Traytown Area	Peralkaline granite & metaluminous ash-flows	1, 2	400 - 600	80 - 120	Low
Port Blandford Area	Metaluminous ash-flows	2	< 500	< 80	None
Musgravetown Area	Peralkaline & metaluminous ash-flows	2	600 - 4000	70 - 250	Medium - High
Plate Cove Area	Metaluminous ash-flows	2	400 - 700	50 - 100	Low
Clarenville Area	Metaluminous ash-flows	2	200 - 400	30 - 50	None
Hodges Cove Area	Metaluminous ash-flows	2	300	50	None
Sunnyside Area	Metaluminous ash-flows	2	300 - 800	90 - 160	Low
Masters Head Area	Metaluminous ash-flows	2	200 - 300	< 40	None
Does Hills Area	Metaluminous ash-flows	2	100 - 400	40 - 100	Low
Flowers River Igneous Suite	Peralkaline ash-flow tuffs, hypabyssal dykes & peralkaline granites	1,2	800 - 6000 9000 - 14000	100 - 600 600 - 1800	Very High

high quantities. This area should be further evaluated with a follow-up sampling program looking more closely at the peralkaline dykes.

The Flowers River Igneous Suite, in particular the Nuiklavik volcanic rocks, should be the target of a well-financed exploration program. Its potential for substantial quantities of low to medium grade Zr - Y- REE mineralization is very high. The observation of high concentrations of rare metals in a stratigraphic unit up to 32 m thick and found over a wide area, makes this area an exciting new prospect. The present lack of exploration interest in this area is disappointing. Perhaps further promotion of this excellent prospect will attract more interest.

9.0 References

Abdel-Rahman, A.M. 1992. Mineral chemistry and paragenesis of astrophyllite from Egypt. Mineralogical Magazine, 56.

Abdel-Rahman, A.M. and Miller, R.R. 1993. The Flowers River anorogenic caldera complex, Labrador: Stratigraphy and evolution. Geological Association of Canada - Mineralogical Association of Canada, Joint Annual Meeting, Abstracts, 18: A1.

Baker, B.H. and Henage, L.F. 1977. Compositional changes during crystallization of some peralkaline silicic lavas of the Kenya Rift Valley. Journal of Volcanology and Geothermal Research, 2: 17-28.

Barua, M.C. 1980: Geology of uranium-molybdenum-bearing rocks of the Aillik-Makkovic Bay area, Labrador. Unpublished M.Sc. thesis, Queen's University, Kingston, Ontario, 76 pages.

Batterson, M. and Miller, R. 1987: a new Y-Nb-Be showing in the western part of the Central Mineral Belt, Labrador. Newfoundland Department of Mines, Mineral Development Division, Open File 13L/1 (66), 5 pages.

Beavan, A.P. 1954. Report on exploration in Labrador and Newfoundland, 1953. Unpublished report for BRINEX, Newfoundland Department of Mines and Energy, Mineral Development Division, Open File NFLD (0119).

Berg, J.H. 1977. Regional geobarometry in the contact aureoles of the anorthositic Nain complex, Labrador. Journal of Petrology, 14: 399-430.

Birkett, T.C., Miller, R.R. 1990. The role of hydrothermal processes in the granite-hosted Zr, Y, REE deposit at Strange Lake, Quebec / Labrador: Evidence from fluid inclusions: Discussion. Geochimica et Cosmochimica Acta, 55: 3443-3445.

Blaxland, A.B. and Curtis, L.W. 1977: Chronology of the Red Wine alkaline province, central Labrador. Canadian Journal of Earth Sciences, Volume 14, pages 1940-1946.

Brooks, C. 1983. U/Pb zircon geochronological ages - a report to Energy Mines and Resources concerning contract No 1 EMR-MMD-82-0052 and amendment No. 1, March 30, 1983. Taurpio Incorporated, R.R. 1, Vankleek Hill, Ontario, 32 pages. Open File No. Lab (519).

Cadman, A.C., Heaman, L., Tarney, J., Wardle, R.J. and Krogh, T.E. 1993. U-Pb geochronology and geochemical variation within two Proterozoic mafic dyke swarms, Labrador. Canadian Journal of Earth Sciences, in press.

Chandler, F.C., Sullivan, R.W., and Currie, K.L., 1987: The age of the Springdale Group, western Newfoundland, and correlative rocks — evidence of a Llandovery overlap assemblage in the Canadian Appalachians. Trans. R. Soc. Edinburgh Earth Sciences. 78: 41-49.

Collerson, K.D. 1982. Geochemistry and Rb-Sr geochronology of associated Proterozoic peralkaline and subalkaline anorogenic granites from Labrador. Contributions to Mineralogy and Petrology, 81: 126-147.

Colman-Sadd, S.P., Hayes, J.P. and Knight, I. 1990: Geology of the island of Newfoundland. Newfoundland Department of Mines and Energy, Geological Survey Branch, Map 90-01

Coyle, M., 1990: Geology, geochemistry and geochronology of the Springdale Group, an early Silurian caldera in central Newfoundland. Unpublished Ph.D. thesis, Memorial University of Newfoundland, St. John's, NF. 310 pages.

Coyle, M., Strong, D.F. and Dingwell, D.B. 1986: Geology of the Sheffield Lake group, west-central Newfoundland. *In* Current Research, Part A, Geological Survey of Canada, Paper 86-1A, pages 455-459. Canadian Journal of Earth Sciences, 24: 1135-1148.

Coyle, M. and Strong, D.F., 1987: Geology of the Springdale Group: a newly recognized Silurian epicontinental-type caldera in Newfoundland.

Coyle, M. and Strong, D.F., 1988: Middle Paleozoic Calderas and Plutons of west-central New Field Trip Guidebook A10. OAC-MAC.

Curtis, L.W. and Currie, K.L. 1981: Geology and petrology of the Red Wine Alkaline Complex, Central Labrador. Geological Survey of Canada, Bulletin 294.

Dallmeyer, R.D. and Hibbard, J., 1984: Geochronology of the Baie Verte Peninsula, Newfoundland: implications for the tectonic evolution of the Humber and Dunnage Zones of the Appalachian orogen. J. Geol. 92: 489-512.

Dawe, R. 1984: Mineral-based opportunities in Newfoundland and Labrador. A presentation to Japanese business representatives in Tokyo, Japan. Newfoundland Department of Mines, unpublished document.

DeGrace, J.R., Kean, B.F., Hsu, E. and Green, T. 1976: Geology of the Nippers Harbour map area (2E/13), Newfoundland. Newfoundland Department of Mines and Energy, Mineral Development Division, Report 76-3.

Dujardin, R.A. 1961: Ten Mile Lake drilling report. Unpublished report for Rio Tinto Exploration Limited. [13L/1 (12)].

Dunning, G.R., Kean, B.F., Thurlow, J.G. and Swinden, H.S., 1987: Geochronology of the Buchans, Roberts Arm and Victoria Lake Groups and Mansfield Cove Complex, Newfoundland, Canadian Journal of Earth Sciences, 24: 1175-1184.

Duthou, J.L., Pillet, D. and Chenevoy, M. 1986: Rb-Sr geochronology of the Lac Brisson peralkaline granite (Labrador, N.E. Canada). Abstract, International Geochemica Cosmochemica Congress, Cambridge meeting.

Emslie, R.F., 1978a. Elsonian magmatism in Labrador: age, characteristics and tectonic setting. Canadian Journal of Earth Sciences, 15: 438-453.

Emslie, R.F., 1978b. Anorthosite massifs, rapakivi granites, and Late Proterozoic rifting of North America. Precambrian Research, 7: 61 - 98.

Elston, W.E. 1984. Mid-Tertiary ash flow tuff cauldrons, southwestern New Mexico. Journal of Geophysical Research, 89: 8733-8750.

Ermanovics, I. in press. Geology of the Hopedale block, southern Nain Province, and the adjacent Proterozoic terranes, Labrador, Newfoundland. Geological Survey of Canada, Memoire 431.

Ermanovics, I. and Ryan, A.B. 1990. Early Proterozoic orogenic activity adjacent to the Hopedale block of the southern Nain Province. Geoscience Canada, 17: 293-297

Fridrich, C.J., Smith, R.P., DeWitt, E, and McKee, E.H. 1991. Structural, eruptive, and intrusive evolution of the Grizzly Peak caldera, Sawatch Range, Colorado. Geological Society of America Bulletin, 103: 1160-1177.

Fridrich, C.J. and Mahood, G.A. 1984. Reverse zoning in the resurgent intrusions of the Grizzly Peak cauldron, Sawatch Range, Colorado. Geological Society of America Bulletin, 95: 779-787.

Ghandi, S.S. 1978: Geological setting and genetic aspects of uranium occurrences in the Kaipokok Bay - Big River area, Labrador. Economic Geology, Volume 73, pages 1492-1522.

Gower, C.F., Flanagan, M.J., Kerr, A. and Bailey, D.G. 1982: Geology of the Kaipokok - Big River area, Central Mineral Belt, Labrador. Newfoundland Department of Mines and Energy, Mineral Development Division, Report 82-7, 77 pages.

Gower, C.F., Rivers, T., and Brewer, T.S. 1990. Middle Proterozoic mafic magmatism in Labrador, eastern Canada. *in* Gower, C.F. Rivers, T., and Ryan, B, eds., Mid-Proterozoic Laurentia-Baltica: Geological Association of Canada, Special Paper, 38: 485-506.

Greene, B., Blackwood, R.F., Hibbard, J., Hill, J. and Kirby, R., 1984: Mineral Occurrence Map, Bonavista, Newfoundland, Department of Mines and Energy, Mineral Development Division. Map 84-21.

Gudmundsson, A. 1988. Formation of collapse calderas. Geology, 16: 808-810.

Henry, C.D. and Price, J.G. 1984. Variations in caldera development in the Tertiary volcanic field of Trans-Pecos, Texas. Journal of Geophysical Research, 89: 8765-8786.

Henry, C.D. and Price, J.G. 1989. The Christmas Mountains caldera complex, Trans-Pecos, Texas, Geology and development of a laccocaldera. Bulletin Volcanology 52: 97-112.

Henry, C.D. and Wolff, J.A. 1992. Distinguishing strongly rheomorphic tuffs from extensive silicic lavas. Bulletin Volcanology 54: 171-186.

Herz, N. 1969. Anorthosite belts, continental drift, and the anorthosite event. Science, 164: 944-947.

Hibbard, J. 1983: Geology of the Baie Verte Peninsula, Newfoundland. Newfoundland Department of Mines and Energy, Mineral Development Division, Memoir 2.

Hildreth, E.W., 1981: Gradients in silicic magma chambers: Implications for lithospheric magnatism. Journal of Geophysicial Research, Volume 86, pages 10153-10192.

Hill, J.D., 1981. Geology of the Flowers River area, Labrador. Newfoundland Department of Mines and Energy, Mineral Development Division, Report 81-6, 40 p.

Hill, J.D., 1982. Geology of the Flowers River-Notakwanon River area, Labrador. Newfoundland Department of Mines and Energy, Mineral Development Division, Report 82-6, 140 p.

Hill, J.D., 1991. Emplacement and tectonic implications of the mid-Proterozoic peralkaline Flowers River igneous suite, north-central Labrador. Precambrian Research, 49: 217-227.

Hill, J.D. and Miller, R.R. 1991. A review of Middle Proterozoic epigenic felsic magmatism in Labrador. *In* Gower, C.F. Rivers, T., and Ryan, B, eds., Mid-Proterozoic Laurentia-Baltica: Geological Association of Canada, Special Paper, **38:** 417-431.

Hill, J.D. and Thomas, A. 1983. Correlation of two Helikian peralkaline granite - volcanic centres in central Labrador. Canadian Journal of Earth Sciences, **20:** 753-763.

Hoffman, P.F. 1990. Subdivision of the Churchill Province and extent of the Trans-Hudson Orogen. *in* Lewry, J.F. and Stauffer, M.R., eds., The Early Proterozoic Trans-Hudson Orogen of North America: Geological Association of Canada, Special Paper, **37:** 15 - 38.

Hopfengartner, D.F. 1982: Assessment report: geology, geophysics, and geochemistry on License 1989, Claim Block 2455, Grand Le Pierre area, NTS 1M/10, Newfoundland. Unpublished report by Saarberg Interplan. [1M/10 (205)]

Houghton, B.F., Weaver, S.D., Wilson, C.J.N. and Lanphere, M.A., 1992: Evolution of a Quaternary peralkaline volcano: Mayor Island, New Zealand. Journal Volcanology Geothermal Research, 51: 217-236.

Kerr, A., Dickson., W.L., Hayes, J.P., and Fryer, B.J. 1993a: Devonian postorogenic granites on the southeastern margin of the Newfoundland Appalachians: A review of geology, geochemistry, petrogenesis and mineral potential. *In* Current Research. *Edited* by C.P. Periera, D.G. Walsh and R.F. Blackwood, Newfoundland Department of Mines and Energy. Geological Survey Branch. Report 93-1. pp. 239-277.

Kerr, A., Dunning, G.R., and Tucker, R.D., 1993b: The youngest Paleozoic plutonism of the Newfoundland Appalachians: U-Pb ages from the St. Lawrence and François granites. Newfoundland Department of Mines and Energy, St. John's, Newfoundland

King, A.F. 1963: Geology of Cape Makkovik peninsula, Aillik, Labrador. unpublished M.Sc. thesis, Memorial University of Newfoundland, St. John's, Newfoundland, 114 pages.

King, A.F. 1988: Geology of the Avalon Peninsula, Newfoundland (parts of 1K, 1L, 1M, 1N, and 2C). Newfoundland Department of Mines, Mineral Development Division, Map 88-01.

Kontak, D.J. and Strong, D.F. 1986: The volcano-plutonic King's Point complex, Newfoundland. In Current Research, Part A, Geological Survey of Canada, Paper 86-1A, pages 465-470.

Krogh, T.E., Strong, D.F., O'Brien, S.J., and Papezik, V.S. 1988. Precise U-Pb zircon dates from the Avalon Terrane in Newfoundland. Canadian Journal of Earth Sciences, 25: 442-453.

Lipman, P.W. 1976. Caldera-collapse breccias in the western San Juan Mountains, Colorado. Geological Society of America Bulletin, 87: 1397-1410.

Lipman, P.W., 1984. The roots of ash-flow calderas in western North America: windows into the tops of granitic batholiths. Journal of Geophysical Research, 89: 8801-8841.

Mahood, G.A. 1984. Pyroclastic rocks and calderas associated with strongly peralkaline magmatism. Journal of Geophysical Research, 89: 8540-8552.

Marsh, B.D. 1984. On the mechanics of caldera resurgence. Journal of Geophysical Research, 89: 8245-8251.

MacDonald, R., Davies, G.R., Bliss, C.M., Leat, P.T., Bailey, D.K. and Smith, R.L. 1987. Geochemistry of high silica peralkaline rhyolites, Naivasha, Kenya Rift Valley. Journal of Petrology, 28: 979-1008.

McConnell, J. 1984. Reconnaissance and detailed geochemical surveys for base metals in Labrador. Newfoundland Department of Mines and energy, Mineral Development Division, Report 84-2, 114 p.

Mercer, B., Strong, D.F., Wilton, D.H.C. and Gibbons, D. 1985: The King's Point Complex, western Newfoundland. In Current Research, Part A, Geological Survey of Canada, Paper 85-1A, pages 737-741.

Miller, R. R., 1986. Geology of the Strange Lake alkalic complex and the associated Zr-Y-Nb-Be-REE mineralization. Current Research. Newfoundland Department of Mines and Energy, Mineral Development Division. Report 86-1: 11-19.

Miller, R.R. 1986a: Geology of the Strange Lake Alkalic Complex and the associated Zr-Y-Nb-Be-REE mineralization. In Current Research. Newfoundland Department of Mines and Energy, Mineral Development Division, Report 86-1, pages 11-19.

Miller, R.R. 1986b: Preliminary data from rock samples of the Letitia Lake area, Labrador. Newfoundland Department of Mines and Energy, Mineral Development Division, Open File 13L/63, 8 pages.

Miller, R.R. 1987: The relationship between Mann-type Nb-Be mineralization and felsic peralkaline intrusives, Letitia Lake Project, Labrador. In Current Research. Newfoundland Department of Mines and Energy, Mineral Development Division, Report 87-1, pages 83-91.

Miller, R.R. 1988. Yttrium (Y) and other rare metals (Be, Nb, Ta, Zr) in Labrador. Current Research, Newfoundland Department of Mines, Mineral Development Division. Report 88-1: 229-245.

Miller, R. R. 1989: Rare-metal targets in insular Newfoundland. In Current Research. Newfoundland Department of Mines and Energy, Geological Survey Branch, Report 89-1, pages 171-179.

Miller, R. R. 1990: The Strange Lake pegmatite—aplite-hosted rare-metal deposit, Labrador. In Current Research. Newfoundland Department of Mines and Energy, Geological Survey Branch, Report 90-1, pages 171-182.

Miller, R. R., 1992. Preliminary Report of the Stratigraphy and Mineralization of the Nuiklavik Volcanic Rocks of the Flowers River Igneous Suite. Newfoundland Department of Mines and Energy, Geological Survey Branch. Current Research 92-1: 251-258.

Miller, R. R. 1992a: Preliminary report of the stratigraphy and mineralization of the Nuiklavik volcanic rocks of the Flowers River Igneous Suite. In Current Research. Newfoundland Department of Mines and Energy, Geological Survey Branch, Report 92-1, pages 251-258.

Miller, R. R. 1992b: Y and Other Rare Metal Lithogeochemical Results from the Flowers River Igneous Suite, Labrador. Newfoundland Department of Mines and Energy, Geological Survey Branch, OPEN FILE 13N/11/43.

Miller, R.R. 1993. Geology and rare-metal mineralization of the Nuiklavik volcanic rocks of the Flowers River Igneous Suite, Labrador. Newfoundland Department of Mines and Energy, Geological Survey Branch. Report 93-1: in press.

Miller, R. R., and Abdel-Rahman, A.R., 1992. Geology and rare metal mineralization of the Nuiklavik volcanics of the Flower River Igneous Suite, Labrador. Geological Association of Canada - Mineralogical Association of Canada, Joint Annual Meeting, Wolfville, Abstracts, 17: A79.

Milner, S.C., Duncan, A.R. and Ewart, A. 1992. Quartz latite rheo-ignimbrite flows of the Etendeka Formation, north-western Namibia. Bulletin Volcanology, 54: 200-219.

Minatidis, D.S. 1975: A comparative study of trace element geochemistry and mineralogy of some uranium deposits of Labrador, and evaluation of some uranium exploration techniques in glacial terrain. unpublished M.Sc. thesis, Memorial University of Newfoundland, St. John's, Newfoundland, 216 pages.

Morse, S.A.1961: Petrographic notes on Aillik molybdenum showings, Labrador (N.T.S. 13O/3). British Newfoundland Exploration Ltd. Unpublished document G-61003, 4 pages. [13O/3 (47)].

O'Brien, S.J., Nunn, G.A.G., Dickson, W.L. and Tuach, J. 1984: Geology of the Terrenceville (1M/10) and Gisborne Lake (1M/15) map areas, southeast Newfoundland. Newfoundland Department of Mines and Energy, Mineral Development Division, Report 84-4.

O'Brien, S.J., Strong, P.G. and Evans, J.L. 1977: The geology of the Grand Bank (1M/4) and Lamaline (1L/13) map areas, Burin Peninsula, Newfoundland. Newfoundland Department of Mines and Energy, Mineral Development Division, Report 77-7.

O'Brien, S.J. 1987: Geology of the Eastport (west half) map area, Bonavista Bay, Newfoundland. Newfoundland Department of Mines and Energy, Mineral Development Division, Report 87-1, pages 257-270.

O'Brien, S.J., 1993: A preliminary account of geological investigations in the Clode Sound-Goose Bay region, Bonavista Bay, Newfoundland (NTS 2C5/NW and 2D8/NE). *In* Current Research. Newfoundland Department of Mines and Energy, Geological Survey Branch, Report 93-1, pages 293-309.

O'Brien, S.J., 1994: On the geological development of the Avalon Zone in the area between Ocean Pond and Long Islands, Bonavista Bay (Parts of NTS 2C/5 and NTS 2C/12). Current Research. Newfoundland Department of Mines and Energy, Geological Survey Branch, Report 94-1, pages 1-13.

O'Brien S.J., and Holdsworth, R.E., 1992: Geological development of the Avalon Zone, the easternmost Gander Zone, and the ductile Dover Fault in the Glovertown (2D/9, east half) map area, eastern Newfoundland. *In* Current Research, Newfoundland Department of Mines and Energy, Geological Survey Branch, Report 92-1, pages 171-184.

O'Brien, S.J., O'Neil, P.P., King, A.F. and Blackwood, R.F. 1988: Eastern margins of the Newfoundland Appalachians — A cross-section of the Avalon and Gander Zones. GAC-MAC Field Trip Guidebook B4, pages 80-81.

O'Brient, J.D. 1986. Preservation of primary magmatic features in subvolcanic pegmatites, aplites and granite from Rabb Park, New Mexico. American Mineralogist, 71: 608-624.

Pitman, P. 1978: Diamond drilling logs and location map of the diamond drilling done by B.P. Minerals in Newfoundland during 1978. Unpublished report for B.P. Minerals Ltd. [1M/4(176)].

Pringle, J., 1978: Rb-Sr ages of silicic igneous rocks and deformation, Burlington Peninsula, Newfoundland. Canadian Journal of Earth Sciences, 15: 293-300.

Prior, G.J., 1988: Geology and lithogeochemistry of the Kings Point Property, Baie Verte Peninsula, Newfoundland NTS 12H/9. Unpublished report for Teck Explorations Limited submitted to the Newfoundland Department of Mines. 12H/9 (1076).

Ramsden, A.R., French, D.H. and Chalmers, D.I. 1993. Volcanic-hosted rare-metal deposit at Brockman, Western Australia. Mineralogy and geochemistry of the Niobium Tuff. Mineralium Deposita, 28: 1-12.

Ryan, A.B. 1990. Does the Labrador-Québec border area of the Rae (Churchill) Province preserve vestiges of an Archean history? Geoscience Canada, 17: 255-259.

Ryan, A.B. 1990. Makhavinekh Lake pluton, Labrador, Canada: geological setting, subdivisions, mode of emplacement, and a comparison with Finnish rapakivi granites. Precambrian Research, 51: 193-225.

Ryan, B., Krogh, T.E., Heaman, L., Scharer, U., Philippe, S., and Oliver, G. 1991. On recent geochronological studies in the Nain Province, Churchill Province and Nain Plutonic Suite, north-central Labrador. Current Research, Newfoundland Department of Mines and Energy, Geological Survey Branch. Report 91-1: 257-261.

Rytuba, J.J. and McKee, E.H. 1984. Peralkaline ash flow tuffs and calderas of the McDermitt volcanic field, southeast Oregon and north central Nevada. Journal of Geophysical Research, 89: 8616-8628.

Salvi, S. and Williams-Jones, E. 1990a. The role of hydrothermal processes in the granite-hosted Zr, Y, REE deposit at Strange Lake, Quebec / Labrador: Evidence from fluid inclusions. Geochimica et Cosmochimica Acta, **54:** 2403-2418.

Salvi, S. and Williams-Jones, E. 1990b. The role of hydrothermal processes in the granite-hosted Zr, Y, REE deposit at Strange Lake, Quebec / Labrador: Evidence from fluid inclusions: Reply. Geochimica et Cosmochimica Acta, **55:** 3447-3449.

Saunders, C.M. and Tuach, J. 1989: Zr-Nb-Y-REE mineralization in the Cross Hills Plutonic Suite. In Current Research. Newfoundland Department of Mines, Mineral Development Division, Report 89-1, pages 181-192.

Scandone, R. 1990. Chaotic collapse of calderas. Journal of Volcanology and Geothermal Research, 42: 285-302.

Self, S., Goff, F., Gardner, J.N., Wright, J.V., and Kite, W.M. 1986. Explosive rhyolitic volcanism in the Jemez Mountains: Vent locations, caldera development and relation to regional structure. Journal of Geophysical Research, 91: 1779-1798.

Smith, R.L. & Bailey, R.A. 1968. Resurgent cauldrons. Geological Society of America Bulletin, 113: 613-662.

Strong, D.F., Fryer, B.J. and Kerrich, R. 1984: Genesis of the St. Lawrence fluorspar deposits as indicated by fluid inclusion, rare earth element, and isotopic data.

Strong, D.F., O'Brien, S.J., Taylor, S.W., Strong, P.G. and Wilton, D.H. 1978: Geology of the Marystown (1M/3) and St. Lawrence (1L/14) map areas, Newfoundland. Newfoundland Department of Mines and Energy, Mineral Development Division, Report 77-8.

Taylor, F.C., 1979. Reconnaissance geology of a part of the Canadian Shield, northeastern Quebec, northern Labrador and Northwest Territories. Geological Survey of Canada, Memoir 393, 99 p.

Taylor, R.P., Strong, D.F. and Kean, B.F. 1980: The Topsails igneous complex: Silurian-Devonian peralkaline magmatism in western Newfoundland. Canadian Journal of Earth Sciences, Volume 17, pages 425-439.

Teng, H.C. and Strong, D.F. 1976: Geology and geochemistry of the St. Lawrence peralkaline granite and associated fluorite deposits, southeast Newfoundland.

Thomas, A. 1980: A summary of geology and data collected during 1978 in the Red Wine Lake-Letitia Lake area, central Labrador. Newfoundland Department of Mines and Energy, Mineral Development Division, Open File 13L (56), 44 pages.

Thomas, A. 1981: Geology along the southwestern margin of the Central Mineral Belt, Labrador. Newfoundland Department of Mines and Energy, Mineral Development Division, Report 81-4, 40 pages.

Thomas, A. and Morrison, R.S. 1991. Geological map of the central part of the Ugjoktok River (NTS 13N/5 and parts of 13M/8, and 13N/6), Labrador (with accompanying notes). Newfoundland Department of Mines and Energy, Geological Survey Branch. Map 91-160.

Tuach, J., 1991: The geology and geochemistry of the Cross Hills Plutonic Suite, Fortune Bay, Newfoundland (1M/10). Newfoundland Department of Mines and Energy, Geological Survey Branch, Report 91-2, 73 pages.

U.S. Bureau of Mines 1985: Mineral Commodity Summaries.

U.S. Bureau of Mines 1985: Mineral Facts and Problems, 1985 Edition. U.S. Bureau of Mines, Bulletin 675.

U.S. Bureau of Mines 1987: Mineral Commodity Summaries.

Venkatswaren, G.P. 1983: A report on the geological, geophysical and geochemical assessment work, Strange Lake area, Newfoundland-Labrador, N.T.S. Sheet 24A/8. Unpublished report, Iron Ore Company of Canada. [24A/8 (6)]

Varga, R.J. and Smith, B.M. 1984. Evolution of the Early Oligocene Bonanza caldera, northeast San Juan volcanic field, Colorado. Journal of Geophysical Research, 89: 8679-8694.

Walker, G.P.L. 1984. Downsag calderas, ring faults, caldera sizes, and incremental caldera growth. Journal of Geophysical Research, 89: 8407-8416.

Watson-White, M.V. 1974: A petrological study of acid volcanic rocks in part of the Aillik Series, Labrador. unpublished M.Sc. thesis, McGill University, Montreal Quebec, 92 pages.

Weaver, S.D., Gibson, I.L., Houghton, B.F. and Wilson, C.J.N. 1990: Mobility of rare earth and other elements during crystallization of peralkaline silicic lavas. Journal of Volcanology and Geothermal Research, 43: 57-70.

Whalen, J.B., 1989: The Topsails igneous suite, western Newfoundland: an Early Silurian subduction-related magmatic suite? Canadian Journal of Earth Science. 26, pages 2421-2434.

Whalen, J.B. and Currie, K.L. 1983: The Topsails igneous terrane of western Newfoundland. In Current Research, Part A, Geological Survey of Canada, Paper 83-1A, pages 15-23.

Whalen, J.B. and Currie, K.L. 1984: Peralkaline granite near Hare Hill, south of Grand Lake, Newfoundland. In Current Research, Part A, Geological Survey of Canada, Paper 84-1A, pages 181-184.

Whalen, J.B. and Currie, K.L., 1984: The Topsails igneous terrane, Western Newfoundland: evidence for magma mixing. Contrib. Mineral . Petrol. 87 : 319-327.

Whalen, J.B. and Currie, K.L., 1990: The Topsails igneous suite, western Newfoundland; Fractionation and magma mixing in an "orogenic" A-type granite suite. Geological Survey of Canada, Special Paper 246, pages 287-297.

Whalen, J.B., Currie, K.L. and Chappell, B.W. 1987a: A-Type Granites: Descriptive and geochemical data. Geological Survey of Canada, Open File 1411.

Whalen, J.B., Currie, K.L., and van Breemen, O. 1987b: Episodic Ordovician-Silurian plutonism in the Topsails igneous terrane, western Newfoundland. Transactions of the Royal Society of Edinburgh: Earth Sciences, 78: 17-28.

White, C.A., 1980. The petrology and geochemistry of peralkaline granite and volcanics near Davis Inlet, Labrador. Unpublished M.Sc. Thesis, Memorial University of Newfoundland, ST. John's, 210 p.

Wiebe, R.A. 1985. Proterozoic basalt dikes in the Nain anorthosite complex, Labrador. Canadian Journal of Earth Sciences, 22: 1149-1157.

Williams, H., Colman-Sadd, S.P. and Swinden, H.S., 1988: Tectonic-stratigraphic subdivisions of central Newfoundland. *In* Current Research, Part B. Geological Survey of Canada, Paper 88-1B, pages 91-98.

Williams, H., Piasecki, M.A.J. and Colman-Sadd, S.P., 1989: Tectonic relationships along the proposed central Newfoundland Lithoprobe transect and regional correlations. *In* Current Research, Part B, Geological Survey of Canada, Paper 89-1B, p. 55-66.

Windley, B.F. 1989. Anorogenic magmatism and the Grenvillian orogeny. Canadian Journal of Earth Sciences, 26: 479-489.

Table A-1 Little Pond Brook Field Sample Data

Field Sample Number	Rock Type	U.T.M. Coordinate N	U.T.M. Coordinate E	U.T.M. Zone	Thin Section	Geochem.	Total Counts
TS91045	F porph.	5425580	484680	21U	Y	Y	400
TS91046	QF frag	5426355	484805	21U	Y	Y	400
TS91047	QF porph.	5426355	484805	21U	Y	Y	380
TS91048	QF porph.	5427095	485220	21U	Y	Y	360
TS91049	QF porph.	5427495	484925	21U	Y	Y	360
TS91050	FQA porph.	5427325	484280	21U	Y	Y	395
TS91051	QF porph.	5427100	483605	21U	Y	Y	380
TS91052	QF-poor	5426910	483410	21U	Y	Y	550
TS91053	QF-poor	5427525	481115	21U	Y	Y	380
TS91054	QF-poor	5427760	480665	21U	Y	Y	480
TS91055	QF-poor	5427850	480495	21U	Y	Y	490
TS91056	QF-poor	5427775	480495	21U	Y	N	470
TS91057	QF-poor	5427695	480490	21U	Y	Y	490
TS91058	QF-poor	5426410	480250	21U	Y	Y	460
TS91059	F porph.	5426215	480270	21U	Y	Y	450
TS91060	F porph.	5425765	480830	21U	Y	Y	415
TS91061	F porph.	5425815	482570	21U	Y	Y	395
TS91062	QF porph.	5424800	484795	21U	Y	Y	345
TS91063	FQA porph.	5425295	485675	21U	Y	Y	350
TS91064	FQA porph.	5425390	486695	21U	Y	Y	340
TS91065	FQA porph.	5424995	488235	21U	Y	Y	310
TS91066	FQA porph.	5424435	488360	21U	Y	Y	410
TS91067	FQA porph.	5423995	488545	21U	Y	Y	360
TS91068	FQA porph.	5423490	488160	21U	Y	Y	335
TS91069	FQA porph.	5422995	487495	21U	Y	Y	375
TS91070	FQA porph.	5422590	486890	21U	Y	Y	370
TS91071	FQA porph.	5423395	486115	21U	Y	Y	350
TS91072	FQA porph.	5423940	485665	21U	Y	Y	350
TS91073	FQA porph.	5424395	485090	21U	Y	Y	350
TS91074	QF porph.	5424740	484255	21U	Y	Y	325
TS91075	QF porph.	5425085	484695	21U	Y	Y	360
TS91076	QF porph.	5425470	485000	21U	Y	Y	340
TS91077	QF porph.	5426710	484495	21U	Y	Y	300
TS91078	QF-poor	5426710	484495	21U	Y	Y	470
TS91079	QF-poor	5426850	483660	21U	Y	Y	525
TS91080	F porph.	5426695	483300	21U	Y	Y	390
TS91081	F porph.	5426510	483395	21U	Y	Y	430
TS91082	F porph.	5426395	483600	21U	Y	Y	430
TS91083	F porph.	5426100	483710	21U	Y	Y	450
TS91084	F porph.	5425800	483895	21U	Y	Y	430
TS91085	F porph.	5425445	483935	21U	Y	Y	400
TS91086	F porph.	5424910	483200	21U	Y	Y	400
TS91087	F porph.	5424575	483230	21U	Y	Y	410
TS91088	QF porph.	5424045	483290	21U	Y	Y	325

Table A-1 Little Pond Brook Field Sample Data

Field Sample Number	Rock Type	U.T.M. Coordinate N	U.T.M. Coordinate E	U.T.M. Zone	Thin Section	Geochem.	Total Counts
TS91089	QF porph.	5424410	483860	21U	Y	Y	340
TS91090	Diabase	5423950	483810	21U	Y	N	180
TS91091	QF porph.	5423585	483630	21U	Y	Y	380
TS91092	QF porph.	5423175	483295	21U	Y	Y	350
TS91093	QF porph.	5422685	482910	21U	Y	Y	450
TS91094	QF porph.	5422575	482165	21U	Y	Y	410
TS91095	QF porph.	5422555	482000	21U	Y	N	n/a
TS91096	FQA porph.	5422255	481710	21U	Y	Y	410
TS91097	Aphyric	5422300	481555	21U	Y	Y	670
TS91098	FQA porph.	5422010	481045	21U	Y	Y	400
TS91099	FQA porph.	5421670	481695	21U	Y	Y	350
TS91100	Comp. Dyke	5421510	482510	21U	Y	Y	400
TS91101	FQA porph.	5421490	483530	21U	Y	Y	410
TS91102	FQA porph.	5421600	484655	21U	Y	Y	430
TS91103	FQA porph.	5422095	485395	21U	Y	Y	n/a
TS91104	FQA porph.	5422520	486180	21U	Y	Y	n/a
TS91105	FQA porph.	5423560	484620	21U	Y	Y	n/a
TS91106	FQA porph.	5427995	486595	21U	Y	Y	n/a
TS91107	FQA porph.	5427195	488470	21U	Y	Y	n/a
TS91108	FQA porph.	5425700	489300	21U	Y	Y	n/a
TS91109	FQA porph.	5424810	489605	21U	Y	Y	n/a
TS91110	FQA porph.	5421500	488500	21U	Y	Y	n/a
TS91111	FQA porph.	5420060	487355	21U	Y	Y	n/a
TS91112	FQA porph.	5420535	484660	21U	Y	Y	n/a
TS91113	FQA porph.	5421060	480440	21U	Y	Y	n/a
TS91114	FQA porph.	5418900	479600	21U	Y	Y	n/a
TS91115	FQ porph.	5422950	479650	21U	Y	Y	n/a
TS91116	F porph.	5424450	479800	21U	Y	Y	n/a
TS91117	QF-poor	5424150	478500	21U	Y	Y	n/a
TS91118	QF porph.	5426850	479100	21U	Y	Y	n/a
TS91119	QF-poor	5426850	479100	21U	Y	Y	n/a
TS91120	QF-poor	5427780	479450	21U	Y	Y	n/a
TS91121	QF-poor	5427220	479770	21U	Y	Y	n/a
TS91122	QF-poor	5427550	479900	21U	Y	Y	n/a

Table A-2 Gaff Topsail Field Sample Data

Field Sample Number	Rock Type	U.T.M. Coordinate N	U.T.M. Coordinate E	U.T.M. ZONE	Thin Section	Geochem.	Total Counts
TS91030	F Porph.	5451290	510310	21U	Y	Y	n/a
TS91031	A Gran.	5450400	510135	21U	Y	Y	n/a
TS91032	A Gran.	5446880	513960	21U	Y	Y	265
TS91033	A Gran.	5444860	506910	21U	Y	Y	n/a
TS91034	A Gran.	5441605	505315	21U	Y	Y	n/a
TS91035	A Gran.	5435990	506590	21U	Y	Y	340
TS91036	A Gran.	5434980	503500	21U	Y	Y	n/a
TS91037	A Gran.	5431390	504240	21U	Y	Y	n/a
TS91038	Fg. A Gran.	5432610	507440	21U	Y	Y	340
TS91039	A Gran. Porph.	5432615	507440	21U	Y	Y	320
TS91040	Fg. A Gran.	5428095	505450	21U	Y	Y	n/a
TS91041	A Gran. Porph.	5428830	512460	21U	Y	Y	n/a
TS91042	A Gran.	5430450	516790	21U	Y	Y	240
TS91043	A Gran.	5428090	505450	21U	Y	Y	n/a
TS91123	A Gran.	5445130	525690	21U	Y	Y	n/a
TS91124	A Gran.	5446160	526000	21U	Y	Y	n/a
TS91125	A Gran.	5446720	526655	21U	Y	Y	n/a
TS91126	A Gran.	5447190	527480	21U	Y	Y	n/a
TS91127	A Gran.	5447045	528635	21U	Y	Y	n/a
TS91128	A Gran. Porph.	5445540	529405	21U	Y	Y	n/a
TS91129	A Gran.	5432920	528010	21U	Y	Y	n/a
TS91130	A Gran.	5433005	528855	21U	Y	Y	n/a
TS91131	A Gran.	5433030	529530	21U	Y	Y	n/a
TS91132	A Gran.	5434490	529790	21U	Y	Y	n/a
TS91133	A Gran. Porph.	5435360	529905	21U	Y	Y	n/a
TS91134	A Gran.	5436180	529900	21U	Y	Y	n/a
TS91135	A Gran.	5437205	530060	21U	Y	Y	n/a
TS91136	A Gran.	5437710	527550	21U	Y	Y	n/a
TS91137	A Gran.	5437795	528250	21U	Y	Y	n/a
TS91138	A Gran.	5440530	527995	21U	Y	Y	n/a
TS91139	Mafic Incl.	5441735	526610	21U	Y	Y	n/a
TS91140	A Gran.	5441738	526610	21U	Y	Y	n/a
TS91141	A Gran.	5442585	526635	21U	Y	Y	n/a
TS91142	A Gran.	5441960	528225	21U	Y	Y	n/a
TS91143	A Gran.	5442240	529385	21U	Y	Y	n/a
TS91144	A Gran.	5442270	532410	21U	Y	Y	n/a
TS91145	A Gran.	5441290	532200	21U	Y	Y	n/a
TS91146	A Gran.	5441110	531110	21U	Y	Y	n/a
TS91147	A Gran.	5440580	529300	21U	Y	Y	n/a

Table A-3 Sheffield Lake Field Sample Data

Field Sample Number	Rock Type	U.T.M. Coordinate N	U.T.M. Coordinate E	U.T.M. ZONE	Thin Section	Geochem.	Total Counts
TS91001	Aphyric	5459910	517255	21U	Y	Y	n/a
TS91002	FQA Porph	5459640	517030	21U	Y	Y	n/a
TS91003	FQA Porph	5459135	517090	21U	Y	Y	n/a
TS91004	A Porph	5459290	516995	21U	Y	Y	n/a
TS91005	FQA Porph	5459290	516995	21U	Y	Y	n/a
TS91006	FQA Porph	5459290	516995	21U	Y	Y	n/a
TS91007	A Porph	5459300	516795	21U	Y	Y	n/a
TS91008	FQA Porph	5459295	516645	21U	Y	Y	n/a
TS91009	FQA Porph	5459200	516355	21U	Y	Y	n/a
TS91010	FQA Porph	5458830	516450	21U	Y	Y	n/a
TS91011	A Porph	5458660	516450	21U	Y	N	n/a
TS91012	FQA Porph	5458775	518745	21U	Y	N	n/a
TS91013	A Porph	5458870	517060	21U	Y	Y	n/a
TS91014	FQA Porph frag	5459430	517755	21U	Y	Y	n/a
TS91015	FQA Porph frag	5460105	518085	21U	Y	Y	n/a
TS91016	FQA Porph	5461055	518905	21U	Y	Y	n/a
TS91017	FQA Porph	5461145	519265	21U	Y	Y	n/a
TS91018	FQA Porph	5461510	519590	21U	Y	Y	n/a
TS91019	FQA Porph	5461795	520135	21U	Y	Y	n/a
TS91020	A Porph	5459140	517260	21U	Y	Y	n/a
TS91021	FQ Porph.	5471100	533995	21U	Y	Y	n/a
TS91022	FQ Porph.	5470390	533325	21U	Y	Y	n/a
TS91023	FQ Porph.	5470110	532625	21U	Y	Y	n/a
TS91024	FQ Porph.	5469750	531930	21U	Y	Y	n/a
TS91025	FQ Porph.	5464040	523470	21U	Y	Y	n/a
TS91026	FQ Porph.	5463860	524200	21U	Y	Y	n/a
TS91027	FQA Porph	5464790	524200	21U	Y	Y	n/a
TS91028	A Porph	5464910	523845	21U	Y	Y	n/a
TS91029	FQA Porph	5464770	523590	21U	Y	Y	n/a
TS92001	A Porph	5459070	517080	21U	Y	N	n/a
TS92002	A Porph	5458920	517260	21U	Y	N	n/a
TS92003	A Porph	5458920	517260	21U	Y	N	n/a

Table A-4 Cape St. John Volcanic Suite Field Sample Data

Field Sample Number	Rock Type	U.T.M. Coordinate N	U.T.M. Coordinate E	U.T.M. ZONE	Thin Section	Geochem	Total Counts
CJ90001	Per Granite	5537555	605400	21U	Y	Y	280
CJ90002	Per Granite	5537995	605310	21U	Y	Y	240
CJ90003	Per Granite	5537000	605775	21U	Y	Y	295
CJ90004	Per Granite	5537795	606395	21U	Y	Y	260
CJ90005	QF Porph	5534780	604400	21U	Y	Y	270
CJ90006	Mafic Flow	5534780	604400	21U	Y	Y	120
CJ90007	Aphyric A-F	5533720	604005	21U	Y	Y	260
CJ90008	Fg Granite	5535375	600140	21U	Y	Y	270
CJ90009	Quartz vein	5535300	601245	21U	Y	Y	100
CJ90010	Aphyric A-F	5533490	601225	21U	Y	Y	310
CJ90011	Aphyric flow	5532995	601455	21U	Y	Y	310
CJ90012	QF Porph	5532420	601245	21U	Y	Y	360
CJ90013	Mafic Flow	5530460	602955	21U	Y	Y	n/a
CJ90014	Aphyric flow	5530460	602955	21U	Y	Y	n/a
CJ90015	F flow	5531275	602115	21U	Y	Y	360
CJ90016	F A-F breccia	5531350	601645	21U	Y	Y	320
CJ90017	Aphyric flow	5531950	601280	21U	Y	Y	460
CJ90018	Aphyric flow	5531005	599415	21U	Y	Y	330
CJ90019	Aphyric flow	5530095	598290	21U	Y	Y	410
CJ90020	Aphyric flow	5531680	592330	21U	Y	Y	400
CJ90021	Aphyric flow	5530915	592325	21U	Y	Y	380
CJ90022	QF Porph A-F	5530590	592420	21U	Y	Y	380
CJ90023	QF Porph A-F	5530225	592975	21U	Y	Y	380
CJ90024	QF Porph A-F	5529585	593430	21U	Y	Y	280
CJ90025	Mafic Flow	5529090	593710	21U	Y	Y	210
CJ90026	Q Porph	5527100	586595	21U	Y	Y	280
CJ90027	QF Porph	5527895	587340	21U	Y	Y	290
CJ90028	Mafic Flow	5530750	583775	21U	Y	Y	260
CJ90029	Aphyric flow	5530145	583725	21U	Y	Y	n/a
CJ90030	QF Porph	5529560	583495	21U	Y	Y	n/a
CJ90031	QF Porph	5534500	605810	21U	Y	Y	270
CJ90032	Aphyric A-F	5534080	606245	21U	Y	Y	290
CJ90033	Mafic tuff?	5533580	606125	21U	Y	Y	210
CJ90034	Aphyric A-F	5532940	605990	21U	Y	Y	210
CJ90035	QF Porph	5532940	605990	21U	Y	Y	250
CJ90036	Aphyric flow	5532400	606060	21U	Y	Y	270
CJ90037	Aphyric flow	5532000	606095	21U	Y	Y	250
CJ90038	Aphyric flow	5531695	605210	21U	Y	Y	320
CJ90039	Q porph flow	5532130	604930	21U	Y	Y	235
CJ90040	F porph A-F	5532865	604425	21U	Y	Y	250
CJ90041	QF Porph	5528045	586525	21U	Y	Y	210
CJ90042	QF Porph	5528450	585580	21U	Y	Y	320
CJ90043	QF Porph	5529195	584775	21U	Y	Y	370
CJ90044	QF Porph	5529395	582500	21U	Y	Y	390
CJ90045	QF Porph	5529710	581400	21U	Y	Y	320
CJ90046	QF Porph	5529920	580595	21U	Y	Y	300

Table A-4 Cape St. John Volcanic Suite Field Sample Data

Field Sample Number	Rock Type	U.T.M. Coordinate N	U.T.M. Coordinate E	U.T.M. ZONE	Thin Section	Geochem	Total Counts
CJ90047	QF Porph	5529995	579840	21U	Y	Y	290
CJ90048	QF Porph	5530265	578765	21U	Y	Y	280
CJ90049	QF Porph	5519705	580695	21U	Y	Y	430
CJ90050	QF Porph	5520295	581005	21U	Y	Y	480
CJ90051	QF Porph	5521495	581050	21U	Y	Y	380
CJ90052	QF Porph	5522015	581295	21U	Y	Y	400
CJ90053	QF Porph	5522595	581795	21U	Y	Y	320
CJ90054	QF Porph	5523110	582000	21U	Y	Y	320
CJ90055	QF Porph	5524600	582190	21U	Y	Y	220
CJ90056	QF Porph	5524940	582910	21U	Y	Y	320
CJ90057	QF Porph	5525200	583660	21U	Y	Y	260
CJ90058	QF Porph	5525820	584310	21U	Y	Y	280
CJ90059	QF Porph	5526000	585195	21U	Y	Y	320
CJ90060	QF Porph	5526585	585980	21U	Y	Y	290
CJ90061	QF Porph	5530790	577680	21U	Y	Y	220
CJ90062	Aphyric A-F	5527920	591495	21U	Y	Y	300
CJ90063	Aphyric flow	5527495	591690	21U	Y	Y	310
CJ90064	Aphyric flow	5526990	591855	21U	Y	Y	330
CJ90065	Aphyric flow	5526700	592215	21U	Y	Y	345
CJ90066	Aphyric flow	5527910	589000	21U	Y	Y	285
CJ90067	Aphyric flow	5528270	588975	21U	Y	Y	370
CJ90068	Aphyric flow	5528890	589000	21U	Y	Y	355
CJ90069	Aphyric flow	5529275	588985	21U	Y	Y	320
CJ90070	Aphyric flow	5529545	588885	21U	Y	Y	350
CJ90071	Aphyric flow	5529440	587330	21U	Y	Y	320
CJ90072	Aphyric flow	5529110	587190	21U	Y	Y	315
CJ90073	Aphyric flow	5528980	586920	21U	Y	Y	330
CJ90074	QF porph	5528500	586495	21U	Y	Y	240

Table A-5 Mic Mac Lake Field Sample Data

Field Sample No.	Rock Type	U.T.M. Coordinate N	U.T.M. Coordinate E	U.T.M. ZONE	Thin Section	Geochem.	Total Counts
ML90001	Conglomerate	5484320	538310	21U	Y	Y	210
ML90002	QF Porph.	5484530	537790	21U	Y	Y	370
ML90003	Aphy. Ash-flow	5484760	537395	21U	Y	Y	410
ML90004	QF Ash-Flow	5485455	537995	21U	Y	Y	270
ML90005	QF Ash-Flow	5490000	539735	21U	Y	Y	340
ML90006	Aphy. Flow	5506220	548510	21U	Y	Y	320
ML90007	QF Ash-Flow	5506610	547895	21U	Y	Y	350
KP90104	Breccia	5499345	545175	21U	Y	Y	280
KP90105	Felsic flow?	5499345	545175	21U	Y	Y	115
KP90106	Mafic flow	5499345	545175	21U	Y	Y	95

Table A-6 Kings Point Field Sample Data

Field Samp No.	Rock Type	U.T.M. Coordinate N	U.T.M. Coordinate E	U.T.M. ZONE	Thin Section	Geo Chem	Total Counts
KP90001	Fg Granite	5498795	561720	21U	Y	Y	n/a
KP90002	Q-F Porphyry	5498475	561450	21U	Y	Y	n/a
KP90003	Q-F Porphyry	5498250	560999	21U	Y	Y	n/a
KP90004	Q Syenite - Granite	5486550	548680	21U	Y	Y	n/a
KP90005	Mg Granite	5486550	548680	21U	Y	N	n/a
KP90006	Fg Granite	5487700	550120	21U	Y	Y	n/a
KP90007	Fg Granite	5488795	551740	21U	Y	Y	n/a
KP90008	F porphyry	5490050	550795	21U	Y	Y	n/a
KP90009	Q-F porphyry	5488890	547900	21U	Y	Y	n/a
KP90010	Mg Granite	5488760	547295	21U	Y	N	n/a
KP90011	F-Mg Granite	5499310	562495	21U	Y	Y	n/a
KP90012	F-Mg Granite	5499810	563500	21U	Y	Y	n/a
KP90013	F-Mg Granite	5500910	564060	21U	Y	Y	n/a
KP90014	Aphyric Flow	5500740	563485	21U	Y	Y	n/a
KP90015	Mg Granite	5500600	562670	21U	Y	Y	n/a
KP90016	F-Mg Granite	5500370	562195	21U	Y	Y	n/a
KP90017	F-Mg Granite	5499940	561860	21U	Y	Y	n/a
KP90018	F-Mg Granite	5499470	562090	21U	Y	Y	n/a
KP90019	F porphyry	5486200	550590	21U	Y	N	n/a
KP90020	Aphyric Flow Breccia	5485995	550300	21U	Y	Y	n/a
KP90021	Mg Granite	5485100	548260	21U	Y	N	n/a
KP90022	Fg Granite	5485300	548040	21U	Y	Y	n/a
KP90023	F-Mg Granite	5486595	546300	21U	Y	Y	n/a
KP90024	Q-F Porphyry	5491070	547070	21U	Y	Y	n/a
KP90025	Q-F Porphyry	5491490	547040	21U	Y	Y	n/a
KP90026	Q-F Porphyry	5492035	546820	21U	Y	N	n/a
KP90027	Q-F Porphyritic Flow	5493310	546730	21U	Y	Y	n/a
KP90028	Q-F porphyritic Granite	5495995	546650	21U	Y	Y	n/a
KP90029	Aphyric Flow Breccia	5497130	546410	21U	Y	N	n/a
KP90030	Q-F poor Porphyry	5497540	546500	21U	Y	Y	n/a
KP90031	Mg Granite	5498810	545920	21U	Y	N	n/a
KP90032	F Porphyritic syenite	5499120	554530	21U	Y	Y	n/a
KP90033	F Porphyritic syenite	5499400	553540	21U	Y	Y	n/a
KP90034	F Porphyritic syenite	5504100	560690	21U	Y	Y	n/a
KP90035	Aphyric flow -spotted	5503950	559999	21U	Y	Y	n/a
KP90036	F porphyritic syenite	5503670	559420	21U	Y	Y	n/a
KP90037	F porphyritic syenite	5502750	558310	21U	Y	Y	n/a
KP90038	Fg Syenite	5502750	558310	21U	Y	N	n/a
KP90039	Q-F Porphyry	5502300	557920	21U	Y	Y	n/a
KP90040	F porphyritic Syenite	5501875	557295	21U	Y	Y	n/a
KP90041	Q syenite - syenite	5501470	556490	21U	Y	Y	n/a
KP90042	F-poor porphyry	5500960	555450	21U	Y	Y	n/a
KP90043	Q syenite - syenite	5500960	555450	21U	Y	Y	n/a
KP90044	F porphyritic Q syenite	5501100	554250	21U	Y	Y	n/a
KP90045	Aphyric flow spotted	5501180	553920	21U	Y	Y	n/a
KP90046	Q-F Porphyry	5501320	553000	21U	Y	Y	n/a

Table A-6 Kings Point Field Sample Data

Field Samp No.	Rock Type	U.T.M. Coordinate N	U.T.M. Coordinate E	U.T.M. ZONE	Thin Section	Geo Chem	Total Counts
KP90047	F porphyritic Syenite	5501330	551630	21U	Y	Y	n/a
KP90048	Q-F Porphyry	5501300	551010	21U	Y	Y	n/a
KP90049	Q-F Porphyry	5491320	554260	21U	Y	Y	n/a
KP90050	Q-F Porphyry	5491280	552495	21U	Y	Y	n/a
KP90051	Q-F Porphyry	5492390	552660	21U	Y	Y	n/a
KP90052	Aphyric flow	5492910	553320	21U	Y	Y	n/a
KP90053	Q-F Porphyry	5493600	553810	21U	Y	Y	n/a
KP90054	Q-F Porphyry	5493740	554740	21U	Y	Y	n/a
KP90055	Q-F Porphyry	5493330	555490	21U	Y	Y	n/a
KP90056	Q-F Porphyry	5492295	555190	21U	Y	Y	n/a
KP90057	Q porphyry	5496440	547920	21U	Y	Y	n/a
KP90058	Q porphyry	5496195	549320	21U	Y	Y	n/a
KP90059	Q-F Porphyry	5494790	550120	21U	Y	Y	n/a
KP90060	Q-F Porphyry	5492470	548895	21U	Y	Y	n/a
KP90061	Q-F Porphyry	5492910	547290	21U	Y	Y	n/a
KP90062	F Porphyritic Q Syenite	5503595	561965	21U	Y	Y	275
KP90063	F Porphyritic Q Syenite	5503760	562920	21U	Y	Y	280
KP90064	Q-F Porphyry	5503420	563425	21U	Y	Y	270
KP90065	Q-F Porphyry	5503750	564245	21U	Y	Y	260
KP90066	Q-F Porphyry	5503945	565110	21U	Y	Y	260
KP90067	Diorite	5503685	565655	21U	Y	Y	160
KP90068	Q-F-A Porphyry	5503160	565065	21U	Y	Y	380
KP90069	Q-F Porphyry	5502110	565040	21U	Y	Y	325
KP90070	Q-F porphyritic syenite	5501810	564130	21U	Y	Y	570
KP90071	Q-F porphyry	5502055	563425	21U	Y	Y	300
KP90072	Q-F porphyry	5502695	563045	21U	Y	Y	270
KP90073	F porphyritic Q syenite	5507080	562695	21U	Y	Y	250
KP90074	Q-F porphyry	5507100	561495	21U	Y	Y	370
KP90075	Mafic dyke	5507320	560800	21U	Y	Y	100
KP90076	Aphanitic flow	5507260	560520	21U	Y	Y	450
KP90077	Syenite	5507070	559925	21U	Y	Y	250
KP90078	F porphyritic syenite	5506395	559000	21U	Y	Y	240
KP90079	F porphyritic syenite	5505970	558120	21U	Y	Y	260
KP90080	F porphyritic syenite	5505520	556780	21U	Y	Y	225
KP90081	F porphyritic syenite	5505090	555560	21U	Y	Y	255
KP90082	Q-F porphyry	5504380	554360	21U	Y	Y	270
KP90083	F porphyritic syenite	5504500	552695	21U	Y	Y	270
KP90084	Q-F porphyritic granite	5502000	560770	21U	Y	Y	350
KP90085	Q-F porphyry	5501540	561225	21U	Y	Y	280
KP90086	F porphyritic Q syenite	5500985	561505	21U	Y	Y	340
KP90087	Mg Granite	5500090	560895	21U	Y	Y	400
KP90088	Q syenite	5499700	560280	21U	Y	Y	380
KP90089	Ash-flow breccia	5499665	559940	21U	Y	Y	230
KP90090	Q-F porphyry	5499665	559940	21U	Y	N	n/a
KP90091	Q-F porphyry	5499345	559040	21U	Y	Y	235
KP90092	Q-F porphyry	5499970	558150	21U	Y	Y	270

Table A-6 Kings Point Field Sample Data

Field Samp No.	Rock Type	U.T.M. Coordinate N	U.T.M. Coordinate E	U.T.M. ZONE	Thin Section	Geo Chem	Total Counts
KP90093	Q-F porphyry	5500995	559195	21U	Y	Y	n/a
KP90094	F porphyritic syenite	5502895	559775	21U	Y	Y	270
KP90095	Q-F porphyry	5501560	549945	21U	Y	Y	225
KP90096	Q-F porphyry	5502295	549975	21U	Y	Y	270
KP90097	Q-F porphyry	5503640	550740	21U	Y	Y	225
KP90098	F porphyritic syenite	5507030	557395	21U	Y	Y	240
KP90099	F porphyry	5507030	557395	21U	Y	N	n/a
KP90100	F porphyritic syenite	5506795	556010	21U	Y	Y	290
KP90101	F porphyritic Q syenite	5506665	554995	21U	Y	Y	230
KP90102	F porphyritic Q syenite	5506800	554455	21U	Y	Y	n/a
KP90103	Granodiorite	5507065	553250	21U	Y	N	n/a
KP90107	Q-F porphyry	5456980	555910	21U	Y	Y	500
KP90108	Aphyric flow breccia	5497400	556865	21U	Y	Y	300
KP90109	Vein	5497170	556925	21U	Y	Y	2500
KP90110	Aphyric flow breccia	5496210	557540	21U	Y	Y	295
KP90111	Aphyric flow	5495790	557395	21U	Y	Y	275
KP90112	Aphyric flow breccia	5494995	556675	21U	Y	Y	330
KP90113	Aphyric flow breccia	5495075	556010	21U	Y	Y	270
KP90114	Q-F porphyry	5495490	555540	21U	Y	Y	330
KP90115	Q-F porphyry	5496300	554995	21U	Y	Y	310
KP90116	Q-F porphyritic syenite	5497195	554390	21U	Y	Y	240
KP90117	Q-F porphyritic	5499090	552210	21U	Y	Y	340
KP90118	Q syenite - granite	5498100	552295	21U	Y	Y	270
KP90119	Q-F porphyritic granite	5497510	552040	21U	Y	Y	320
KP90120	A porph Flow Red spot	5497495	551825	21U	Y	Y	410
KP90121	Q-F porphyry	5497215	550225	21U	Y	Y	400
KP90122	Q-F porphyry	5497890	549360	21U	Y	Y	480
KP90123	Q-F porphyry	5498400	548865	21U	Y	Y	410
KP90124	Mafic flow	5499785	549990	21U	Y	Y	450
KP90125	A porph Flow Red spot	5499945	550160	21U	Y	Y	540
KP90126	Q-F porphyritic granite	5500050	551885	21U	Y	Y	260
KP90127	Q-F porphyritic granite	5511800	556410	21U	Y	Y	250
KP90128	Q-F porphyritic granite	5510525	556335	21U	Y	Y	220
KP90129	Q-F porphyritic granite	5509810	556200	21U	Y	Y	250
KP90130	F porphyritic syenite	5509510	555945	21U	Y	Y	210
KP90131	F porphyritic syenite	5509085	554995	21U	Y	Y	220
KP90132	Mafic dyke	5510495	555090	21U	Y	Y	110
KP90133	F-Q porphyritic Q syenite	5510495	555090	21U	Y	Y	220
KP90134	Hematite vein	5510495	555090	21U	Y	N	210
KP90135	Q-F porphyry	5511000	554795	21U	Y	Y	240
KP90136	Q-F porphyry	5513295	567690	21U	Y	Y	250
KP90137	Q-F porphyry	5513995	567510	21U	Y	Y	240
KP90138	Q-F porphyry	5514475	567275	21U	Y	Y	230
KP90139	Ash-flow breccia	5515095	567000	21U	Y	Y	350
KP90140	Q poor ash-flow	5515730	566920	21U	Y	Y	400
KP90141	Q-F porphyry	5516095	566080	21U	Y	Y	285

Table A-6 Kings Point Field Sample Data

Field Samp No.	Rock Type	U.T.M. Coordinate N	U.T.M. Coordinate E	U.T.M. ZONE	Thin Section	Geo Chem	Total Counts
KP90142	Q-F porphyry	5516595	565665	21U	Y	Y	270
KP90143	Q-F porphyry	5517020	564990	21U	Y	Y	230
KP90144	Q-F porphyry	5512855	559495	21U	Y	Y	230
KP90145	Q-F porphyry	5512400	559130	21U	Y	Y	280
KP90146	Q-F porphyry	5512000	559880	21U	Y	Y	270
KP90147	F porphyritic syenite	5511330	560210	21U	Y	Y	230
KP90148	Q-F porphyry	5511600	561585	21U	Y	Y	260
KP90149	Q-F porphyry	5511670	562675	21U	Y	Y	220
KP90150	Q-F porphyry	5512295	563370	21U	Y	Y	240
KP90151	Syenite	5506395	564960	21U	Y	Y	360
KP90152	Q-F porphyry	5506995	564735	21U	Y	Y	250
KP90153	Q-F porphyry	5508440	564465	21U	Y	Y	285
KP90154	Q-F porph. / porphyritic gran.	5508820	565195	21U	Y	Y	270
KP90155	Q-F porph. / porphyritic gran.	5508850	565790	21U	Y	Y	290
KP90156	Aphyric flow	5509070	566500	21U	Y	Y	520
KP90157	Q-F-A porphyry	5509050	566950	21U	Y	Y	430
KP90158	Q-F porphyry breccia	5508695	566895	21U	Y	N	n/a
KP90159	Q-F porphyry	5508695	566895	21U	Y	Y	480
KP90160	Q-F porphyry	5507845	566920	21U	Y	Y	310
KP90161	Syenite	5506155	565895	21U	Y	Y	420
KP90162	Aphyric flow	5511500	567080	21U	Y	Y	320
KP90163	Q porphyry	5511040	567190	21U	Y	Y	420
KP90164	Q-F Porphyry	5510295	567365	21U	Y	Y	220
KP90165	Q-F Porphyry	5509640	566695	21U	Y	Y	420
KP90166	Q-F Porphyry	5509895	566245	21U	Y	Y	375
KP90167	Q-F Porphyry	5510195	565800	21U	Y	Y	425
KP90168	Q Porphyry	5510590	564800	21U	Y	Y	n/a
KP90169	A porph Flow Red spot	5510400	564795	21U	Y	Y	n/a
KP90170	Q-F-A Porphyry	5509890	564810	21U	Y	Y	n/a
KP90171	Q-F-A Porphyry	5509625	564295	21U	Y	Y	n/a
KP90172	Q-F porphyritic granite	5509700	563710	21U	Y	Y	n/a
KP90173	Q-F porphyry	5509845	562495	21U	Y	Y	n/a
KP90174	Q-F porphyry	5509390	560930	21U	Y	Y	n/a
KP90175	Granodiorite	5511435	565195	21U	Y	N	n/a
KP90176	Q-F porphyry	5517690	559985	21U	Y	Y	n/a
KP91001	Q Porphyritic Syenite	5500810	549875	21U	Y	Y	510
KP91002	Q-F Porphyry	5500520	549825	21U	Y	Y	280
KP91003	A porph Flow red spot	5500350	549720	21U	Y	Y	400
KP91004	A porph Flow red spot	5500125	549870	21U	Y	Y	585
KP91005	A porph Ash-flow Red spot	5499950	549990	21U	Y	Y	525
KP91006	Aphyric Ash-flow	5499130	549855	21U	Y	N	565
KP91007	A porph Ash-flow red spot	5499090	550545	21U	Y	Y	550
KP91008	Aphyric flow Fg A red spot	5498900	550775	21U	Y	Y	400
KP91009	Aphyric flow (red)	5498880	550710	21U	Y	Y	525
KP91010	Q-F-A Porphyry	5498955	550860	21U	Y	Y	340
KP91011	A porph Ash-flow red spot	5498190	551080	21U	Y	Y	420

Table A-6 Kings Point Field Sample Data

Field Samp No.	Rock Type	U.T.M. Coordinate N	U.T.M. Coordinate E	U.T.M. ZONE	Thin Section	Geo Chem	Total Counts
KP91012	A porph Flow red spot	5498110	551290	21U	Y	Y	n/a
KP91013	Q-F-A Porphyry	5498300	551410	21U	Y	N	310
KP91014	Q Syenite - Granite	5499895	551575	21U	Y	N	285
KP91015	Q-F-A Porphyry	5500200	550020	21U	Y	N	310
KP91016	Q-F Porphyry	5500395	550140	21U	Y	Y	340
KP91017	A-Q Porphyry	5500640	550210	21U	Y	Y	480
KP91018	A-Q Porphyry	5500895	550290	21U	Y	N	420
KP91019	QF Porphyritic Granite	5498340	551965	21U	Y	N	280
KP91020	Q-F-A Porphyritic Granite	5497640	551680	21U	Y	Y	340
KP91021	A porph Ash-flow	5497170	551935	21U	Y	Y	460
KP91022	A porph Flow red spot	5496680	552115	21U	Y	Y	420
KP91023	A porph Flow red spot	5496700	552430	21U	Y	Y	450
KP91024	A porph Ash-flow red spot	5495870	552830	21U	Y	Y	460
KP91025	A porph Ash-flow red spot	5495945	553900	21U	Y	Y	380
KP91026	Aphyric Ash-flow (red)	5495980	554830	21U	Y	Y	545
KP91027	Aphyric Ash-flow Fg A	5496065	554740	21U	Y	Y	360
KP91028	Aphyric Ash-flow Fg A	5496305	554420	21U	Y	Y	410
KP91029	Aphyric Ash-flow Fg A	5496310	554420	21U	Y	Y	540
KP91030	Aphyric Ash-flow Fg A red sot	5496460	554375	21U	Y	Y	420
KP91031	A porph Ash-flow red spot	5496525	554325	21U	Y	Y	485
KP91032	Q-F-A Porphyry	5497280	555265	21U	Y	Y	380
KP91033	Aphyric Ash-flow Fg A red sot	5497595	555460	21U	Y	Y	370
KP91034	Q-F-A Porphyry	5497595	555460	21U	Y	N	320
KP91035	Q-F-A Porphyritic ash-flow	5498020	556180	21U	Y	Y	400
KP91036	Aphyric Ash-flow	5497745	556725	21U	Y	Y	n/a
KP91037	Aphyric Ash-flow (red)	5497100	556670	21U	Y	Y	n/a
KP91038	Q poor Porphyritic flow	5497110	556270	21U	Y	Y	n/a
KP91039	Q-F Porphyritic Ash-flow	5497140	555835	21U	Y	Y	n/a
KP91040	Q Syenite - Granite	5498200	555915	21U	Y	Y	n/a
KP91041	Q-F-A Porphyry	5498170	560835	21U	Y	Y	n/a
KP91042	A porph Flow red spot	5498295	560810	21U	Y	Y	n/a
KP91043	Aphyric Ash-flow	5498425	560800	21U	Y	N	n/a
KP91044	Q+F poor porphyritic ash-flow	5499195	560120	21U	Y	Y	n/a
KP91045	Fg Granite	5500555	560230	21U	Y	Y	n/a
KP91046	Fg Granite	5500555	560230	21U	Y	N	n/a
KP91047	Q-F poor A Porphyry	5500000	559830	21U	Y	N	n/a
KP91048	Q+F poor A porphyritic ash-flow	5499140	559810	21U	Y	Y	n/a
KP91049	Aphyric Ash-Flow Fg A red spot	5497910	560365	21U	Y	Y	n/a
KP91050	A porph Flow red spot	5497760	560200	21U	Y	N	n/a
KP91051	Mg Granite	5497805	560610	21U	Y	N	n/a
KP91052	Q-F-A Porphyry	5496850	559290	21U	Y	Y	n/a
KP91053	Aphyric Ash-flow breccia	5496820	559010	21U	Y	Y	n/a
KP91054	Aphyric Ash-flow breccia	5495930	558120	21U	Y	Y	n/a
KP91055	Q-F Porphyry	5496010	558050	21U	Y	N	n/a
KP91056	Q-F-A Porphyry						
KP91057	A porph Flow red spot						

Table A-6 Kings Point Field Sample Data

Field Samp No.	Rock Type	U.T.M. Coordinate N	U.T.M. Coordinate E	U.T.M. ZONE	Thin Section	Geo Chem	Total Counts
KP91058	F porph Ash-flow Fg A red sot						
KP91059	Aphyric Ash-flow (red)						
KP91060	Aphyric Ash-flow						
KP91061	Aphyric Ash-flow						
KP91062	A porph Ash-flow						
KP91063	Q-F-A Porphyritic Granite						
KP91064	Aphyric Ash-flow Fg A red sot						
KP91065	A porph Ash-flow red sot						
KP91066	Q-F-A Porphyritic Ash-flow red spot						
KP91067	Q-F-A Porphyry						
KP91068	Q-A Porphyritic Ash-flow red spot						
KP91069	Q-F-A Porphyritic Ash-flow red spot						
KP91070	Q-F-A Porphyry						
KP91071	Aphyric Ash-flow Fg A						
KP91072	Aphyric Ash-flow (green)						
KP91073	A porph Ash-flow red sot						
KP92001	Q-F-A Porphyry	5510060	563570	21U	Y	Y	250
KP92002	Q+F-poor-A Porphyry	5510100	563810	21U	Y	Y	400
KP92003	Q+F-poor-A Porphyry	5510270	564030	21U	Y	Y	430
KP92004	A porph Ash-flow red sot	5510360	564200	21U	Y	Y	430
KP92005	Aphyric Ash-flow Fg A red sot	5510060	565650	21U	Y	Y	510
KP92006	Q+F-poor-A Porphyry/Ash-flow	5509900	566100	21U	Y	Y	400
KP92007	Q+F-poor-A Ash-flow	5509690	566610	21U	Y	Y	440
KP92008	A porph Ash-flow red sot	5509600	565490	21U	Y	Y	470
KP92009	QFA intrusive?	5510650	565550	21U	Y	Y	240
KP92010	Q-F porphyritic ash-flow	5510620	566160	21U	Y	Y	370
KP92011	Aphyric ash-flow lapilli-tuff	5510460	566320	21U	Y	Y	330
KP92012	Ash-flow breccia	5510140	566680	21U	N	Y	400
KP92013	Q-F porphyritic ash-flow	5509140	567420	21U	Y	Y	400
KP92014	Q-F-A ash-flow	5509320	567080	21U	Y	Y	420
KP92015	A porph ash-flow red spot	5509080	566230	21U	Y	Y	410
KP92016	Q-F-A porphyry	5504630	567640	21U	Y	Y	280
KP92017	contact	5504670	567722	21U	Y	Y	n/a
KP92018	A porph ash-flow fg A	5504671	567720	21U	Y	Y	470
KP92019	Q-F-A porphyritic granite/syenite	5504710	567820	21U	Y	Y	260
KP92020	Q-F-A porphyritic ash-flow	5504480	567720	21U	Y	Y	350
KP92021	Q-F-A porphyry	5504310	567660	21U	Y	Y	275
KP92022	Aphyric Ash-flow	5504240	567720	21U	Y	Y	400
KP92023	Q-F-A porphyry	5503990	567670	21U	Y	Y	250
KP92024	Aphyric Ash-flow Fg A red spot	5504030	567800	21U	Y	Y	630
KP92025	Aphyric Ash-flow	5503880	567830	21U	Y	Y	660
KP92026	Breccia - F porph frags	5503840	567880	21U	Y	Y	420
KP92027	Aphyric ash-flow	5503790	567930	21U	Y	Y	580
KP92028	A-Q porph Ash-flow	5504250	567980	21U	Y	Y	420
KP92029	A porph Ash-flow Red spot	5504500	568000	21U	Y	Y	420
KP92030	Q-F-A porphyry	5504510	567990	21U	Y	Y	320

Table A-6 Kings Point Field Sample Data

Field Samp No.	Rock Type	U.T.M. Coordinate N	U.T.M. Coordinate E	U.T.M. ZONE	Thin Section	Geo Chem	Total Counts
KP92031	A porph Ash-flow/Q-F-A porphyry	5504520	567980	21U	Y	Y	450
KP92032	A porph Ash-flow	5504530	567970	21U	Y	Y	470
KP92033	A porph Ash-flow Red spot	5504540	567950	21U	Y	Y	600
KP92034	Aphyric Ash-flow Fg A Red spot	5504545	567930	21U	Y	Y	420
KP92035	Aphyric flow	5504680	568040	21U	Y	Y	n/a
KP92036	Q-F-A porphyry	5504790	567950	21U	Y	Y	n/a
KP92037	Aphyric Ash-flow Fg A Red spot	5510650	564140	21U	Y	Y	600
KP92038	Q-F-A porphyritic ash-flow red spots	5510590	564310	21U	Y	Y	370
KP92039	Q-F-A porphyry	5510190	564460	21U	Y	Y	390
KP92040	Aphyric Ash-flow	5509840	564490	21U	Y	Y	420
KP92041	A porph Ash flow	5509280	565180	21U	Y	Y	490
KP92042	Breccia	5508900	566480	21U	Y	Y	370
KP92043	Fluorite breccia	5508910	566490	21U	Y	Y	350
KP92044	Aphyric Ash flow	5508890	566410	21U	Y	Y	500
KP92045	A porph Ash-flow Red spot	5508720	566430	21U	Y	Y	480
KP92046	A-Q porph Ash-flow Red spot	5508610	566520	21U	Y	Y	420
KP92047	A porph Ash-flow Red spot	5508600	566420	21U	Y	Y	520
KP92048	A porph Ash-flow Red spot	5508560	566310	21U	Y	N	n/a
KP92049	Aphyric Ash-flow	5497500	551560	21U	Y	Y	400
KP92050	Aphyric Ash-flow	5496180	552300	21U	Y	Y	460
KP92051	Aphyric Ash-flow	5496110	552450	21U	Y	Y	370
KP92052	A porph Ash-flow	5495430	552250	21U	Y	Y	465
KP92053	Aphyric Ash-flow	5495860	552710	21U	Y	Y	450
KP92054	Contact	5498330	560860	21U	Y	N	n/a
KP92055	Q-F porphyry	5498320	560610	21U	Y	N	n/a

Table A-7 Mooring Cove Formation Field Data

Field Sample No.	Rock Type	U.T.M. Coordinate N	U.T.M. Coordinate E	U.T.M. ZONE	Thin Section	Geochem.	Total Counts
MC90001	Mafic Flow	5282940	660810	21T	Y	Y	120
MC90002	Sheared Tuff	5282855	660170	21T	Y	Y	265
MC90003	Felsic Ash-flow?	5282795	659605	21T	Y	Y	600
MC90004	Felsic Dyke	5283100	659185	21T	Y	Y	700
MC90005	Aphy. Ash-flow	5283045	658510	21T	Y	Y	360
MC90006	Quartz Vein	5283490	657825	21T	Y	Y	210
MC90007	Aphy. Ash-flow	5283490	657825	21T	Y	Y	310
MC90008	Q Ash-flow	5283300	657405	21T	Y	Y	340
MC90009	Mafic Flow	5283240	657300	21T	Y	Y	155
MC90010	Aphy. Ash-flow	5283140	656920	21T	Y	Y	360
MC90011	Felsic breccia	5282770	656410	21T	Y	Y	240
MC90012	Aphy. Ash-flow	5282095	656300	21T	Y	Y	350
MC90013	Aphy. Ash-flow	5281800	656005	21T	Y	Y	315
MC90014	Aphy. Ash-flow	5281400	655910	21T	Y	Y	315
MC90015	Aphy. Ash-flow	5280995	656465	21T	Y	Y	305
MC90016	Aphy. Ash-flow	5280900	656755	21T	Y	Y	310
MC90017	F Ash-flow	5280875	657060	21T	Y	Y	300
MC90018	Felsic breccia	5280735	657385	21T	Y	Y	330
MC92005	Mafic Flow	5283090	659270	21T	Y	Y	240
MC92006	Aphy. Ash flow CJ	5283400	657200	21T	Y	Y	330
MC92007	Aphy. Ash flow CJ	5283700	659150	21T	Y	Y	400
MC92008	Felsic breccia	5283650	659060	21T	Y	N	340
MC92009	Felsic Dyke	5283620	658990	21T	Y	Y	650
MC92010	Felsic Dyke	5283470	659080	21T	Y	Y	720
MC92011	Aphy. Ash-flow	5283274	659180	21T	Y	Y	500
MC92012	Aphy. Ash-flow	5283290	659130	21T	Y	Y	500
MC92013	Aphy. Ash-flow	5283350	658150	21T	Y	Y	350
MC92014	Aphy. Ash-flow	5283590	658154	21T	Y	Y	370
MC92015	Aphy. Ash-flow	5283920	658980	21T	Y	Y	380
MC92016	Aphy. Ash-flow CJ	5283520	658710	21T	Y	Y	350
MC92017	Aphy. Ash-flow CJ	5284300	657400	21T			320
MC92018	Aphy. Ash-flow CJ	5284740	657250	21T	Y	Y	340
MC92019	Aphy. Ash-flow	5283550	657680	21T	Y	Y	320
MC92020	Aphy. Ash-flow	5283430	657820	21T	Y	Y	350
MC92021	Aphy. Ash-flow	5283340	658300	21T	Y	Y	400
MC92022	Aphy. Ash-flow	5283290	658400	21T	Y	Y	660

Table A-8 Cross Hills Complex Field Data (Mooring Cove area)

Field Sample No.	Rock Type	U.T.M. Coordinate N	U.T.M. Coordinate E	U.T.M. ZONE	Thin Section	Geochem.	Total Counts
MC92001	Radio. P Gran	5284140	663700	21T	Y	Y	560
MC92002	Normal P Gran	5284100	663780	21T	Y	Y	410
MC92003	Radio. P Gran	5284234	663650	21T	Y	N	620
MC92004	Normal P Gran	5284330	664060	21T	Y	Y	415
MC90019	F-Mg Normal PG	5284420	664550	21T	Y	Y	440
MC90020	Normal P Gran	5284610	664940	21T	Y	Y	375
MC90021	Normal P Gran	5284860	665290	21T	Y	Y	440
MC90022	Normal P Gran	5284775	664600	21T	Y	Y	400
MC90023	Normal P Gran	5284665	663830	21T	Y	Y	370
MC90024	Aplite	5284620	663700	21T	Y	Y	375
MC90025	F-Mg Radio. PG	5284315	663630	21T	Y	Y	500
MC90026	Peg-aplite	5284210	663610	21T	Y	Y	1400
MC90027	Peg-aplite	5284210	663610	21T	Y	Y	1100
MC90028	Normal P Gran	5284040	663220	21T	Y	Y	485
MC90029	Aplite	5284100	662725	21T	Y	Y	385
MC90030	Aplite	5284025	662570	21T	Y	Y	880
MC90031	F-Mg Normal PG	5283820	662380	21T	Y	Y	470
MC90032	F-Mg Radio. PG	5283820	662380	21T	Y	Y	1020
MC90033	Radio. P Gran	5283435	661965	21T	Y	Y	660
MC90034	Radio. P Gran	5283800	662920	21T	Y	Y	660
MC90035	F-Mg Normal PG	5289860	668580	21T	Y	Y	350
MC90036	Aplite?	5290200	668460	21T	Y	Y	400
MC90037	Normal P Gran	5290155	667995	21T	Y	Y	355
MC90038	F-Mg Normal PG	5289960	667770	21T	Y	Y	400
MC90039	Normal P Gran	5289600	668135	21T	Y	Y	345
MC92023	F-Mg Radio. PG	5284000	663450	21T	Y	Y	520
MC92024	Radio. P Gran	5284270	663190	21T	Y	Y	520
MC92025	F-Mg Radio. PG	5284080	662860	21T	Y	Y	720
MC92026	Aplite	5284160	662830	21T	Y	Y	370
MC92027	F-Mg Radio. PG	5284050	662640	21T	Y	Y	500
MC92028	Radio. P Gran	5284030	662440	21T	Y	N	620
MC92029	F-Mg Normal PG	5283690	661730	21T	Y	Y	420
MC92030	Radio. P Gran	5283820	662800	21T	Y	Y	590

Table A-9 Grand Beach Complex Field Sample Data

Field Sample Number	Rock Type	U.T.M. Coordinate N	U.T.M. Coordinate E	U.T.M. ZONE	Thin Section	Geochem.	Total Counts
GB90001	QF Porph	5221395	611530	21T	Y	Y	310
GB90002	QF Porph (M)	5221140	611195	21T	Y	Y	340
GB90003	QF Porph (M)	5221040	610800	21T	Y	Y	375
GB90004	QF Porph (M)	5220795	610310	21T	Y	Y	500
GB90005	FA±Q Porph	5220695	610000	21T	Y	Y	370
GB90006	QF Porph (M)	5220595	609510	21T	Y	Y	370
GB90007	Q Porph	5220360	609225	21T	Y	Y	490
GB90008	Calcite Vein	5220100	608925	21T	Y	N	400
GB90009	QF Porph	5220055	608795	21T	Y	Y	430
GB90010	FA±Q Porph	5219855	608475	21T	Y	Y	340
GB90011	QF Porph (M)	5219465	608160	21T	Y	Y	430
GB90012	QF Ash Flow	5219310	607930	21T	Y	Y	430
GB90013	QF Ash Flow	5219185	607610	21T	Y	Y	410
GB90014	QF Ash Flow (M)	5219075	607350	21T	Y	Y	525
GB90015	QF Porph	5219020	607210	21T	Y	Y	545
GB90016	QF Ash Flow	5219020	607210	21T	Y	Y	550
GB90017	QF Porph	5218965	607045	21T	Y	Y	370
GB90018	QF Porph	5221425	613040	21T	Y	Y	n/a
GB90019	Red Tuff	5216915	606115	21T	Y	Y	425
GB90020	Debris Flow	5216915	606115	21T	Y	Y	360
GB90021	Debris Flow	5216250	606610	21T	Y	Y	450
GB90022	QF Ash Flow	5216315	606890	21T	Y	Y	380
GB90023	QF flow	5216315	606890	21T	Y	Y	680
GB90024	QF flow	5216275	607165	21T	Y	Y	480
GB90025	F Flow	5214050	608915	21T	Y	Y	210
GB90026	F Tuff	5214170	609495	21T	Y	Y	250
GB90027	QF Porph	5215295	609510	21T	Y	Y	280
GB90028	QF Ash Flow	5216795	609935	21T	Y	Y	330
GB90029	QF Ash Flow	5217055	609665	21T	Y	Y	350
GB90030	QF Porph	5217055	609665	21T	Y	Y	350
GB90031	QF Porph	5217755	609130	21T	Y	Y	360
GB90032	QF Ash Flow	5219055	614330	21T	Y	Y	370
GB90033	QF Ash Flow	5218240	614500	21T	Y	Y	320
GB90034	QF Ash Flow	5217810	614500	21T	Y	Y	370
GB90035	QF Ash Flow	5217455	613795	21T	Y	Y	330
GB90036	QF Porph	5218880	611600	21T	Y	Y	340
GB90037	QF Porph	5219190	611215	21T	Y	Y	400
GB90038	QF Porph	5220485	614195	21T	Y	Y	360
GB90039	QF Porph (M)	5218005	607100	21T	Y	Y	425
GB90040	QF Porph (M)	5217995	608320	21T	Y	N	400
GB90041	Mafic flow	5218375	608895	21T	Y	Y	190
GB90042	QF Ash Flow	5218520	608925	21T	Y	Y	375
GB90043	QF Ash Flow	5218910	609550	21T	Y	Y	370
GB90044	QF Porph	5219390	610295	21T	Y	Y	395
GB90045	QF Porph	5220000	612390	21T	Y	Y	420
GB90046	QF Porph (M)	5220110	613340	21T	Y	Y	420
GB90047	QF Ash Flow	5220140	613430	21T	Y	Y	400

Table A-9 Grand Beach Complex Field Sample Data

Field Sample Number	Rock Type	U.T.M. Coordinate N	U.T.M. Coordinate E	U.T.M. ZONE	Thin Section	Geochem.	Total Counts
GB90048	F Tuff	5220695	615995	21T	Y	N	270
GB90049	QF Ash Flow	5220700	615860	21T	Y	Y	385
GB90050	F±Q Porph	5220820	615895	21T	Y	Y	380
GB90051	QF Ash Flow	5220820	615895	21T	Y	Y	410
GB90052	QF Ash Flow (M)	5220830	615655	21T	Y	Y	405

Table A-10 St. Lawrence Granite Field Data

Field Sample No.	Rock Type	U.T.M. Coordinate N	U.T.M. Coordinate E	U.T.M. ZONE	Thin Section	Geochem.	Total Counts
SG90001	F Porph	5215390	624960	21T	Y	Y	230
SG90002	QF±A Porph	5214525	626100	21T	Y	Y	345
SG90003	F±Q Porph	5213900	626385	21T	Y	Y	275
SG90004	F±Q Porph	5213300	626190	21T	Y	Y	255
SG90005	QA Syenite	5213400	624950	21T	Y	Y	470
SG90006	QA Syenite	5212100	623795	21T	Y	Y	405
SG90007	QA Syenite	5212945	623005	21T	Y	Y	415
SG90008	FQ (poor) porph	5216310	624295	21T	Y	Y	400
SG90009	Aphyric Ash Flow	5218700	623555	21T	Y	Y	340
SG90010	FA±Q Porph	5224230	629325	21T	Y	Y	370
SG90011	Mg Gran	5202000	618065	21T	Y	Y	475
SG90012	Mg Gran	5202660	618180	21T	Y	Y	405
SG90013	Mg Gran	5203255	618100	21T	Y	Y	395
SG90014	QF Porph	5203690	615740	21T	Y	Y	500
SG90015	QF Porph	5203220	615190	21T	Y	Y	420
SG90016	QF Porph	5200500	617700	21T	Y	Y	530
SG90017	QF Porph	5202300	615810	21T	Y	Y	580
SG90018	QF Porph	5202280	616000	21T	Y	Y	800
SG90019	Gran Porph	5200950	611880	21T	Y	Y	535
SG90020	Gran Porph	5201890	612040	21T	Y	Y	440
SG90021	Gran Porph	5198215	618295	21T	Y	Y	525
SG90022	Gran Porph	5198195	619925	21T	Y	Y	430
SG90023	F Vein	5198195	619925	21T	Y	Y	380
SG90024	Gran Porph	5197870	620930	21T	Y	Y	480
SG90025	Gran Porph	5195245	621825	21T	Y	Y	n/a
SG90026	Mg Gran	5196495	623440	21T	Y	Y	500
SG90027	Mg Gran	5201320	624780	21T	Y	Y	610
SG90028	Mg Gran	5202340	624475	21T	Y	Y	410
SG90029	Gran Porph	5202735	624420	21T	Y	Y	440
SG90030	Aplite	5204695	623960	21T	Y	Y	470
SG90031	FQ (poor) porph	5205675	624055	21T	Y	Y	270
SG90032	Mg Gran	5205675	624055	21T	Y	Y	515
SG90033	Mg Gran	5205000	623720	21T	Y	Y	480
SG90034	Gran Porph	5204685	623295	21T	Y	Y	525
SG90035	Gran Porph	5203830	623150	21T	Y	Y	445
SG90036	Mg Gran	5201645	623130	21T	Y	Y	470
SG90037	Gran Porph	5201270	622975	21T	Y	Y	440
SG90038	Gran Porph	5200670	623035	21T	Y	Y	520
SG90039	Gran Porph	5199915	623225	21T	Y	Y	430
SG90040	Mg Gran	5199400	623490	21T	Y	Y	470
SG90041	Syenite Porph	5216215	625205	21T	Y	Y	240
SG90042	Syenite Porph	5217115	625305	21T	Y	Y	250
SG90043	A Syenite	5217245	625450	21T	Y	Y	230
SG90044	Syenite Porph	5217275	625715	21T	Y	Y	250
SG90045	QF Porph	5217865	624545	21T	Y	Y	305
SG90046	Mg Gran	5193095	623260	21T	Y	Y	860

Table A-10 St. Lawrence Granite Field Data

Field Sample No.	Rock Type	U.T.M. Coordinate N	U.T.M. Coordinate E	U.T.M. ZONE	Thin Section	Geochem.	Total Counts
SG90047	FQ (poor) porph	5193095	623260	21T	Y	Y	420
SG90048	Mg Gran	5192785	623000	21T	Y	Y	420
SG90049	F Vein	5192700	623395	21T	Y	Y	n/a
SG90050	F Vein	5192700	623395	21T	Y	Y	n/a
SG90051	Mg Gran	5192655	622890	21T	Y	Y	640
SG90052	F Vein	5192655	622890	21T	Y	Y	250
SG90053	Mg Gran	5193405	622810	21T	Y	Y	540
SG90054	Gran Porph	5193100	619905	21T	Y	Y	425
SG90055	F Vein	5193100	619905	21T	Y	Y	n/a
SG90056	Gran Porph	5193665	620470	21T	Y	Y	360
SG90057	F Vein	5193665	620470	21T	Y	Y	n/a
SG90058	F Vein	5193665	620470	21T	Y	N	n/a
SG90059	Gran Porph	5193395	620200	21T	Y	Y	540
SG90060	F Vein	5193660	619995	21T	Y	Y	250
SG90061	Gran Porph	5193660	619995	21T	Y	Y	460
SG90062	Gran Porph	5192830	620090	21T	Y	Y	420
SG90063	F Vein	5192830	620090	21T	Y	Y	n/a
SG90064	Gran Porph	5192700	620450	21T	Y	Y	470
SG90065	Mg Gran	5192310	621150	21T	Y	Y	580
SG90066	F Vein	5192310	621150	21T	Y	Y	n/a
SG90067	Mg Gran	5193055	622000	21T	Y	Y	720
SG90068	Gran Porph	5193065	621595	21T	Y	Y	570
SG90069	Mg Gran	5199895	622275	21T	Y	Y	370
SG90070	Gran Porph	5198295	622300	21T	Y	Y	370
SG90071	Mg Gran	5197685	623095	21T	Y	Y	520
SG90072	Mg Gran	5197875	624090	21T	Y	Y	505

Table A-11 Terranceville Area Field Sample Data

Field Sample No.	Rock Type	U.T.M. Coordinate N	U.T.M. Coordinate E	U.T.M. ZONE	Thin Section	Geochem.	Total Counts
TV92001	Aphy. Flow	5285000	667630	21T	Y	Y	300
TV92002	Aphy. Flow	5281800	667380	21T	Y	Y	280
TV92003	F Flow	5281300	667180	21T	Y	Y	300
TV92004	Aphryic Flow	5267500	665800	21T	Y	Y	380
TV92005	Aphryic Flow	5266800	665880	21T	Y	Y	380
TV92006	Aphryic Flow	5268800	666150	21T	Y	Y	380
TV92007	Aphryic Flow	5270000	666180	21T	Y	Y	400

Table A-12 Bull Arm Formation Field Sample Data

Field Sample No.	Rock Type	U.T.M. Coordinate N	U.T.M. Coordinate E	U.T.M. ZONE	Thin Section	Geo Chem.	Total Counts	Location
BA90001	Aphyric Felsic	5398295	280915	22U	Y	Y	210	1Traytown
BA90002	Aphyric Felsic	5395290	281610	22U	Y	Y	140	1Traytown
BA90003	Aphyric Felsic	5394545	281195	22U	Y	Y	260	1Traytown
BA90004	QF Porph Breccia	5396390	283560	22U	Y	Y	200	1Traytown
BA90005	QF Porph	5396320	283370	22U	Y	Y	168	1Traytown
BA90006	Peralkaline Granite	5394005	284410	22U	Y	Y	480	1Louil Hills PG
BA90007	Peralkaline Granite	5394005	284410	22U	Y	Y	750	1Louil Hills PG
BA90008	Peralkaline Granite	5394040	284565	22U	Y	Y	520	1Louil Hills PG
BA90009	Peralkaline Granite	5394050	284760	22U	Y	Y	500	1Louil Hills PG
BA90010	Peralkaline Granite	5393205	283300	22U	Y	Y	400	1Louil Hills PG
BA90011	Peralkaline Granite	5393240	283695	22U	Y	Y	n/a	1Louil Hills PG
BA90012	Peralkaline Granite	5392525	283100	22U	Y	N	n/a	1Louil Hills PG
BA90013	Peralkaline Granite	5392555	283265	22U	Y	Y	400	1Louil Hills PG
BA90014	Peralkaline Granite	5392695	283550	22U	Y	Y	380	1Louil Hills PG
BA90015	Red Sandstone	5363295	706600	22U	Y	Y	270	2Port Blandford
BA90016	Tuffaceous sandstone?	5362255	707000	22U	Y	Y	270	2Port Blandford
BA90017	Tuffaceous sandstone?	5362095	707550	22U	Y	Y	185	2Port Blandford
BA90018	Tuffaceous sandstone?	5361805	708300	22U	Y	Y	210	2Port Blandford
BA90019	Tuffaceous sandstone?	5358765	709275	22U	Y	Y	200	2Port Blandford
BA90020	Tuffaceous sandstone?	5358595	709910	22U	Y	Y	220	2Port Blandford
BA90021	Mafic flow (A)	5358495	711145	22U	Y	Y	95	2Port Blandford
BA90022	F Porph Mafic flow (A)	5358555	711520	22U	Y	Y	120	2Port Blandford
BA90023	Tuffaceous sandstone?	5359120	711995	22U	Y	Y	170	2Port Blandford
BA90024	Intermediate?	5363690	714520	22U	Y	Y	170	2Port Blandford
BA90025	Aphyric flow	5364640	716800	22U	Y	Y	380	2Port Blandford
BA90026	Intermediate?	5364640	716800	22U	Y	Y	180	2Port Blandford
BA90027	Aphyric Felsic tuff?	5364125	718570	22U	Y	Y	205	2Port Blandford
BA90028	QF Porph	5364300	719720	22U	Y	Y	280	2Port Blandford
BA90054	Aphyric flow	5356120	710355	22U	Y	Y	220	2Port Blandford
BA90055	Aphyric Felsic tuff?	5355800	710560	22U	Y	Y	250	2Port Blandford
BA90056	Aphyric flow	5354855	710050	22U	Y	Y	235	2Port Blandford
BA90057	Mafic flow (A)	5351295	709970	22U	Y	Y	65	2Port Blandford
BA90058	Pebble Conglomerate	5351295	710190	22U	Y	Y	170	2Port Blandford

Table A-12 Bull Arm Formation Field Sample Data

Field Sample No.	Rock Type	U.T.M. Coordinate N	U.T.M. Coordinate E	U.T.M. ZONE	Thin Section	Geo Chem.	Total Counts	Location
BA90029	Tuffaceous sandstone?	5365345	278805	22U	Y	Y	200	3Musgravetown
BA90030	Pebble Conglomerate	5365345	279390	22U	Y	Y	175	3Musgravetown
BA90031	Aphyric flow	5364930	280125	22U	Y	Y	200	3Musgravetown
BA90032	Pebble Conglomerate	5365280	280185	22U	Y	Y	170	3Musgravetown
BA90033	Pebble Conglomerate	5365295	280700	22U	Y	Y	280	3Musgravetown
BA90034	Mafic tuff?	5365240	281005	22U	Y	Y	235	3Musgravetown
BA90035	Pebble Conglomerate	5365030	281640	22U	Y	Y	175	3Musgravetown
BA90036	Aphyric flow	5365110	282500	22U	Y	Y	350	3Musgravetown
BA90037	Aphyric flow	5365070	283085	22U	Y	Y	170	3Musgravetown
BA90038	Pebble Conglomerate	5364105	284920	22U	Y	N	250	3Musgravetown
BA90039	F Porph ash-flow	5364105	284920	22U	Y	Y	n/a	3Musgravetown
BA90040	Pebble Conglomerate	5364295	285550	22U	Y	Y	240	3Musgravetown
BA90041	Mafic flow	5365610	283400	22U	Y	Y	70	3Musgravetown
BA90042	F Porph ash-flow	5367020	283410	22U	Y	Y	240	3Musgravetown
BA90043	Mafic flow	5367380	283500	22U	Y	Y	100	3Musgravetown
BA90044	Mafic tuff	5369510	283455	22U	Y	Y	205	3Musgravetown
BA90045	Intermediate tuff	5369300	283190	22U	Y	Y	150	3Musgravetown
BA90046	Aphyric flow	5369090	282935	22U	Y	Y	500	3Musgravetown
BA90047	Mafic flow	5368600	282235	22U	Y	Y	50	3Musgravetown
BA90048	Aphyric flow	5368485	281995	22U	Y	Y	350	3Musgravetown
BA90049	Aphyric tuff	5367575	280595	22U	Y	Y	720	3Musgravetown
BA90050	Aphyric ash-flow	5367445	280480	22U	Y	Y	310	3Musgravetown
BA90051	Aphyric ash-flow	5367100	280050	22U	Y	Y	505	3Musgravetown
BA90052	Aphyric ash-flow	5367050	279900	22U	Y	Y	360	3Musgravetown
BA90053	Aphyric ash-flow	5366685	279510	22U	Y	Y	340	3Musgravetown
BA92001	F Porph ash-flow	5366420	283000	22T	Y	Y	320	3Musgravetown
BA92002	F Porph ash-flow	5366420	282700	22T	Y	Y	300	3Musgravetown
BA92003	F Porph ash-flow	5366410	282090	22T	Y	Y	270	3Musgravetown
BA92004	Aphyric ash-flow	5366360	280440	22T	Y	Y	320	3Musgravetown
BA92005	Aphyric ash-flow	5366720	279660	22T	Y	Y	435	3Musgravetown
BA92006	Aphyric ash-flow	5367090	279980	22T	Y	Y	500	3Musgravetown
BA92007	F Porph ash-flow	5367380	280380	22T	Y	Y	300	3Musgravetown
BA92008	Breccia	5366860	281640	22T	Y	Y	340	3Musgravetown
BA92009	F Porph ash-flow	5366870	281840	22T	Y	Y	260	3Musgravetown
BA92010	F Porph ash-flow	5366890	282960	22T	Y	Y	300	3Musgravetown
BA90064	Aphyric ash-flow	5372910	314320	22U	Y	Y	410	4Plate Cove
BA90065	F Porph ash-flow	5371000	313600	22U	Y	Y	305	4Plate Cove
BA90066	Aphyric ash-flow	5370175	313080	22U	Y	Y	305	4Plate Cove
BA90067	QF Porph Ash-flow	5369460	312155	22U	Y	Y	270	4Plate Cove
BA90068	Aphyric ash-flow	5368070	311645	22U	Y	Y	270	4Plate Cove
BA90069	Mafic flow	5368070	311645	22U	Y	N	120	4Plate Cove
BA90070	F Porph ash-flow	5363300	311660	22U	Y	Y	290	4Plate Cove
BA90071	Aphy Felsic Ash-flow	5363165	310925	22U	Y	Y	315	4Plate Cove
BA90072	QF Porph ash-flow	5363130	310795	22U	Y	Y	320	4Plate Cove
BA90073	Aphyric ash-flow	5363270	309950	22U	Y	Y	220	4Plate Cove

Table A-12 Bull Arm Formation Field Sample Data

Field Sample No.	Rock Type	U.T.M. Coordinate N	U.T.M. Coordinate E	U.T.M. ZONE	Thin Section	Geo Chem.	Total Counts	Location
BA90077	F Porph ash-flow	5321895	280640	22U	Y	Y	380	5Clarenville - NWB
BA90078	F Porph ash-flow	5322280	280490	22U	Y	Y	320	5Clarenville - NWB
BA90079	F Porph ash-flow	5319650	279400	22U	Y	Y	240	5Clarenville - NWB
BA90080	F Porph ash-flow	5321145	279570	22U	Y	Y	220	5Clarenville - NWB
BA90081	QF Porph ash-flow	5321340	279700	22U	Y	Y	180	5Clarenville - NWB
BA90082	F Porph ash-flow	5323890	279910	22U	Y	Y	420	5Clarenville - NWB
BA90083	F Porph ash-flow	5323940	281055	22U	Y	Y	420	5Clarenville - NWB
BA90084	F Porph ash-flow	5323940	281055	22U	Y	Y	220	5Clarenville - NWB
BA90085	F Porph ash-flow	5338335	278695	22U	Y	Y	235	5Clarenville
BA90086	Aphyric Ash-flow	5339270	279055	22U	Y	Y	320	5Clarenville
BA90087	Aphyric Ash-flow	5341600	278540	22U	Y	Y	280	5Clarenville
BA90088	Aphyric Ash-flow	5344855	279000	22U	Y	Y	180	5Clarenville
BA90089	Aphyric Ash-flow	5346080	278665	22U	Y	Y	215	5Clarenville
BA90090	Aphyric Ash-flow	5345760	279045	22U	Y	Y	210	5Clarenville
BA90059	sandstone	5335030	300400	22U	Y	Y	160	5Clarenville-RI
BA90060	sandstone	5335000	301480	22U	Y	Y	205	5Clarenville-RI
BA90061	Greywacke	5335240	303210	22U	Y	N	150	5Clarenville-RI
BA90062	Aphyric Ash-flow	5334280	303975	22U	Y	Y	180	5Clarenville-RI
BA90063	Aphyric Ash-flow	5334370	303910	22U	Y	Y	205	5Clarenville-RI
BA90074	Aphyric intermediate	5320755	295520	22U	Y	Y	270	6Hodges Cove
BA90075	Aphyric intermediate	5320800	294980	22U	Y	Y	250	6Hodges Cove
BA90076	tuffaceous sandstone?	5320840	293895	22U	Y	Y	170	6Hodges Cove

Table A-12 Bull Arm Formation Field Sample Data

Field Sample No.	Rock Type	U.T.M. Coordinate N	U.T.M. Coordinate E	U.T.M. ZONE	Thin Section	Geo Chem.	Total Counts	Location
BA90091	Aphyric ash-flow breccia	5302315	284960	22T	Y	Y	360	7Sunnyside
BA90092	F-poor Porph ash-flow	5302460	284890	22T	Y	Y	390	7Sunnyside
BA90093	F Porph ash-flow	5302645	284805	22T	Y	Y	300	7Sunnyside
BA90094	Aphyric ash-flow	5302745	284795	22T	Y	N	300	7Sunnyside
BA90095	Aphyric ash-flow	5302800	284755	22T	Y	N	280	7Sunnyside
BA90096	Q-poor ash-flow	5302895	284730	22T	Y	Y	460	7Sunnyside
BA90097	QF Porph ash-flow	5303125	284645	22T	Y	Y	420	7Sunnyside
BA90098	Aphy ash-flow breccia	5303245	284500	22T	Y	Y	260	7Sunnyside
BA90099	QF Porph ash-flow	5303595	284415	22T	Y	Y	460	7Sunnyside
BA90100	Q±F Porph ash-flow	5303795	284380	22T	Y	Y	390	7Sunnyside
BA90101	Q±F Porph ash-flow	5304700	284950	22T	Y	Y	280	7Sunnyside
BA90102	Lapilli ash-flow tuff	5304640	285995	22T	Y	N	140	7Sunnyside
BA90103	Aphyric ash-flow	5304670	286195	22T	Y	Y	220	7Sunnyside
BA90104	QF Porph Ash-flow	5304720	286355	22T	Y	Y	240	7Sunnyside
BA90105	QF Porph Ash-flow	5305345	286235	22T	Y	Y	220	7Sunnyside
BA90106	Tuffaceous sandstone	5305885	286495	22T	Y	Y	140	7Sunnyside
BA90107	QF ash-flow breccia	5306665	286325	22T	Y	Y	345	7Sunnyside
BA90108	QF ash-flow breccia	5307430	286465	22T	Y	Y	210	7Sunnyside
BA90109	QF ash-flow breccia	5307580	286380	22T	Y	Y	375	7Sunnyside
BA90110	QF ash-flow breccia	5307840	286110	22T	Y	Y	220	7Sunnyside
BA90111	Aphyric ash-flow	5307730	285870	22T	Y	Y	185	7Sunnyside
BA90112	Q±F Porph ash-flow	5307555	285665	22T	Y	Y	270	7Sunnyside
BA90113	Q±F Porph ash-flow breccia	5307155	285480	22T	Y	Y	280	7Sunnyside
BA90114	Mafic flow	5306745	284940	22T	Y	N	70	7Sunnyside
BA90115	F Porph breccia	5306390	285220	22T	Y	Y	240	7Sunnyside
BA90116	[QF]poor ash-flow	5305765	285110	22T	Y	Y	340	7Sunnyside
BA90117	QF Porph ash-flow breccia	5305595	284540	22T	Y	Y	335	7Sunnyside
BA90118	Aphyric ash-flow breccia	5305960	284050	22T	Y	Y	215	7Sunnyside
BA90119	Aphyric ash-flow	5305120	284065	22T	Y	Y	235	7Sunnyside
BA90120	F Porphyry ash-flow	5304910	284400	22T	Y	Y	320	7Sunnyside
BA90121	F Porphyry ash-flow	5304925	284215	22T	Y	Y	460	7Sunnyside
BA90136	Pebble conglom	5289730	284310	22T	Y	Y	220	8Masters Head
BA90137	Aphyric ash-flow	5290065	284755	22T	Y	Y	200	8Masters Head
BA90138	F Porph ash-flow	5290100	285125	22T	Y	Y	370	8Masters Head
BA90139	F Porph ash-flow	5290020	285760	22T	Y	Y	285	8Masters Head
BA90140	F Porph ash-flow	5290310	286060	22T	Y	Y	305	8Masters Head
BA90141	F Porph ash-flow	5290615	286440	22T	Y	Y	285	8Masters Head
BA90142	F Porph lapilli ash-flow	5290890	285965	22T	Y	Y	315	8Masters Head
BA90143	F Porph ash-flow	5291300	285825	22T	Y	Y	325	8Masters Head
BA90144	Debris flow	5291490	285400	22T	Y	Y	225	8Masters Head
BA90145	Aphyric ash-flow	5291390	285100	22T	Y	Y	325	8Masters Head
BA90146	F Porph ash-flow	5291500	284730	22T	Y	Y	270	8Masters Head
BA90147	F Porph mafic flow	5291500	284530	22T	Y	N	85	8Masters Head

Table A-12

Bull Arm Formation Field Sample Data

Field Sample No.	Rock Type	U.T.M. Coordinate N	U.T.M. Coordinate E	U.T.M. ZONE	Thin Section	Geo Chem.	Total Counts	Location
BA90122	F Porph ash-flow lapilli	5283955	285080	22T	Y	Y	280	9Doe Hills
BA90123	F Porph ash-flow lapilli	5284020	284755	22T	Y	Y	265	9Doe Hills
BA90124	F Porph ash-flow	5284585	284695	22T	Y	Y	315	9Doe Hills
BA90125	F Porph ash-flow	5284685	284920	22T	Y	Y	265	9Doe Hills
BA90126	F Porph ash-flow lapilli	5284880	285225	22T	Y	Y	300	9Doe Hills
BA90127	F Porph ash-flow breccia	5284815	285500	22T	Y	Y	240	9Doe Hills
BA90128	F Porph breccia	5283940	285220	22T	Y	Y	280	9Doe Hills
BA90129	F Porph ash-flow	5281150	284400	22T	Y	Y	285	9Doe Hills
BA90130	F Porph breccia	5280330	284010	22T	Y	Y	240	9Doe Hills
BA90131	F Porph breccia	5279890	284315	22T	Y	Y	270	9Doe Hills
BA90132	F Porph breccia	5279700	283770	22T	Y	Y	205	9Doe Hills
BA90133	F Porph ash-flow breccia	5279300	283450	22T	Y	Y	180	9Doe Hills
BA90134	F Porph ash-flow breccia	5279210	283720	22T	Y	Y	200	9Doe Hills
BA90135	F Porph ash-flow lapilli	5279125	283935	22T	Y	Y	300	9Doe Hills
BA90148	Intermediate tuff	5285520	282400	22T	Y	Y	220	9Doe Hills
BA90149	Tuffaceous sediment	5285310	282710	22T	Y	Y	170	9Doe Hills
BA90150	Debris flow	5284520	282895	22T	Y	Y	240	9Doe Hills
BA90151	Pebble conglom	5283890	283550	22T	Y	Y	230	9Doe Hills
BA90152	Pebble conglom	5283855	283735	22T	Y	Y	230	9Doe Hills
BA90153	F Porph ash-flow	5283255	284235	22T	Y	Y	285	9Doe Hills
BA90154	F Porph lapilli ash-flow	5283200	284300	22T	Y	Y	275	9Doe Hills
BA90155	Aphyric ash-flow	5283070	284340	22T	Y	Y	340	9Doe Hills
BA90156	F Porph ash-flow	5283000	284420	22T	Y	Y	260	9Doe Hills
BA90157	Aphyric ash-flow	5282600	284560	22T	Y	Y	260	9Doe Hills
BA90158	F Porph ash-flow	5282485	284655	22T	Y	Y	310	9Doe Hills
BA90159	F Porph ash-flow	5282055	284600	22T	Y	Y	310	9Doe Hills
BA90160	F-poor ash-flow	5281865	284595	22T	Y	Y	370	9Doe Hills
BA90161	F Porph ash-flow breccia	5281360	284795	22T	Y	Y	370	9Doe Hills
BA90162	F Porph ash-flow lapilli	5281260	284800	22T	Y	N	370	9Doe Hills
BA90163	F Porph ash-flow lapilli	5281095	284815	22T	Y	Y	380	9Doe Hills
BA90164	F Porph ash flow	5280510	285610	22T	Y	Y	275	9Doe Hills
BA90165	Sandstone	5268220	281950	22T	Y	Y	170	9Doe Hills
BA90166	Sandstone	5268680	282200	22T	Y	Y	270	9Doe Hills
BA90167	Sandstone	5272700	287000	22T	Y	Y	150	9Doe Hills
BA90168	Intermediate lapilli tuff	5277300	290610	22T	Y	Y	270	9Doe Hills
BA90169	Aphy lapilli ash-flow	5280725	290210	22T	Y	Y	310	9Doe Hills
BA90170	F Porph lapilli ash-flow	5280900	290115	22T	Y	Y	230	9Doe Hills
BA90171	Intermediate tuff	5280930	289890	22T	Y	Y	285	9Doe Hills
BA90172	F Porph lapilli ash-flow	5284800	287920	22T	Y	Y	320	9Doe Hills
BA90173	F Porph ash-flow breccia	5284050	287690	22T	Y	Y	350	9Doe Hills
BA90174	F Porph ash-flow breccia	5284080	287895	22T	Y	Y	285	9Doe Hills
BA90175	F Porph ash-flow	5284100	288260	22T	Y	Y	415	9Doe Hills
BA90176	F Porph ash-flow	5283580	288470	22T	Y	Y	310	9Doe Hills
BA90177	F Porph ash-flow lapilli	5282330	289100	22T	Y	Y	210	9Doe Hills
BA90178	F Porph ash-flow lapilli	5279780	286505	22T	Y	Y	285	9Doe Hills
BA90179	Aphyric ash-flow	5279555	286465	22T	Y	Y	340	9Doe Hills
BA90180	QF Porph ash-flow breccia	5279450	286500	22T	Y	Y	360	9Doe Hills

Table A-12 Bull Arm Formation Field Sample Data

Field Sample No.	Rock Type	U.T.M. Coordinate N	U.T.M. Coordinate E	U.T.M. ZONE	Thin Section	Geo Chem.	Total Counts	Location
BA90181	QF Porph ash-flow breccia	5279360	286515	22T	Y	Y	600	9Doe Hills
BA90182	QF Porph ash-flow breccia	5279200	286570	22T	Y	Y	300	9Doe Hills
BA90183	QF Porph ash-flow breccia	5279130	286570	22T	Y	Y	320	9Doe Hills
BA90184	QF Porph ash-flow breccia	5279070	286575	22T	Y	Y	340	9Doe Hills
BA90185	QF Porph ash-flow	5279010	286575	22T	Y	Y	480	9Doe Hills
BA90186	Carbonate vein	5278950	286580	22T	Y	Y	200	9Doe Hills
BA90187	QF Porph ash-flow	5278895	286580	22T	Y	Y	300	9Doe Hills
BA90188	QF Porph ash-flow	5278715	286745	22T	Y	Y	440	9Doe Hills
BA90189	QF Porph ash-flow breccia	5278690	286770	22T	Y	Y	540	9Doe Hills
BA90190	QF Porph ash-flow breccia	5278660	286795	22T	Y	Y	525	9Doe Hills
BA90191	QF Porph ash-flow ±breccia	5278620	286820	22T	Y	Y	430	9Doe Hills
BA90192	QF Porph ash-flow ±breccia	5278590	286845	22T	Y	Y	530	9Doe Hills
BA90193	QF Porph ash-flow	5278550	286870	22T	Y	Y	520	9Doe Hills
BA90194	QF Porph ash-flow breccia	5278510	286895	22T	Y	Y	530	9Doe Hills
BA90195	QF Porph ash-flow breccia	5278470	286920	22T	Y	Y	390	9Doe Hills
BA90196	Intermediate tuff	5278430	286945	22T	Y	Y	420	9Doe Hills
BA90197	Aphy ash-flow breccia	5278390	286970	22T	Y	Y	320	9Doe Hills
BA90198	F Porph ash-flow breccia	5278350	286995	22T	Y	Y	270	9Doe Hills
BA90199	F Porph ash-flow breccia	5278310	287010	22T	Y	Y	420	9Doe Hills
BA90200	F Porph ash-flow breccia	5278180	287135	22T	Y	Y	220	9Doe Hills
BA90201	F Porph ash-flow	5278120	287275	22T	Y	Y	270	9Doe Hills
BA90202	Aphy ash-flow	5278145	287420	22T	Y	Y	420	9Doe Hills
BA90203	F Porph ash-flow	5278040	287500	22T	Y	Y	295	9Doe Hills
BA90204	F Porph ash-flow	5278000	287580	22T	Y	Y	365	9Doe Hills
BA90205	siltstone	5278000	287580	22T	Y	Y	320	9Doe Hills
BA90206	Mafic flow	5278000	287580	22T	Y	Y	140	9Doe Hills
BA90207	F Porph ash-flow breccia	5277820	287730	22T	Y	Y	210	9Doe Hills
BA90208	F Porph ash-flow breccia	5277690	287955	22T	Y	Y	320	9Doe Hills
BA90209	F Porph ash-flow breccia	5277580	288350	22T	Y	Y	275	9Doe Hills
BA90210	Mafic breccia??	5277710	288700	22T	Y	Y	210	9Doe Hills
BA90211	F Porph ash-flow breccia	5277780	289820	22T	Y	Y	280	9Doe Hills
BA90212	F Porph ash-flow breccia	5277780	289820	22T	Y	Y	320	9Doe Hills
BA90213	F Porph ash-flow	5277780	289820	22T	Y	Y	320	9Doe Hills
BA90214	siltstone	5277710	290415	22T	Y	Y	265	9Doe Hills
BA90215	siltstone	5276590	290800	22T	Y	Y	210	9Doe Hills

Table A-13 Flowers River Field Sample Data

Field Samp. No.	Rock Type	Unit/Caldera	U.T.M. Coordinate N	U.T.M. Coordinate E	U.T.M. Zone	Thin Section	Geo. Chem.	Total Counts
FR91001	F-Q ash-flow	2	6163780	612550	20U	Y	Y	300
FR91002	Altered F-Q ash-flow	3	6165495	614610	20U	Y	Y	310
FR91003		3	6166280	615095	20U	Y	Y	400
FR91004	F-Q ash-flow	3	6167595	615225	20U	Y	Y	325
FR91005	A Ignimbrite	2	6168010	615425	20U	Y	Y	570
FR91006			6168015	615530	20U	Y	N	n/a
FR91007	PG-Porph peralkaline granite	Micro G	6168035	615630	20U	Y	Y	490
FR91008	Altered F-Q ash-flow	3	6168010	615970	20U	Y	Y	285
FR91009			6168390	616935	20U	Y	N	n/a
FR91010	Q Porphyry	3	6165695	617695	20U	Y	Y	310
FR91011			6165695	617700	20U	Y	N	n/a
FR91012	Altered F-Q ash-flow	3	6162140	615480	20U	Y	Y	400
FR91013	Altered F-Q ash-flow	3	6162305	616040	20U	Y	Y	250
FR91014	Aphyric ash-flow	4	6162550	616095	20U	Y	Y	720
FR91015			6162400	616045	20U	Y	N	320
FR91016	Aphyric ash-flow breccia	4	6162585	616090	20U	Y	Y	1000
FR91017	Aphyric ash-flow	4	6162615	616075	20U	Y	Y	1120
FR91018	F-Q ash-flow	3	6162700	617060	20U	Y	Y	270
FR91019	Q-F ash-flow	4	6163000	617695	20U	Y	Y	570
FR91020			6162810	617600	20U	Y	N	520
FR91021	Q-F ash-flow	4	6162500	617405	20U	Y	Y	720
FR91022	Q-F ash-flow	4	6162505	617545	20U	Y	Y	680
FR91023	Altered F-Q ash-flow	5	6162205	617215	20U	Y	Y	540
FR91024	Altered F-Q ash-flow	4	6162045	617335	20U	Y	Y	320
FR91025			6161785	616690	20U	Y	N	320
FR91026	Altered F-Q ash-flow	3	6264495	613550	20U	Y	Y	370
FR91027	Q-A Ash-flow	2	6264805	613400	20U	Y	Y	520
FR91028	A ignimbritic flow (subalk)	2	6167975	615405	20U	Y	Y	n/a
FR91029	A ignimbritic flow (subalk)	2	6167995	615395	20U	Y	Y	520
FR91030			6168000	615370	20U	Y	N	200
FR91031			6167800	615095	20U	Y	N	500
FR91032	F-Q-A porphyry (peralk)	Peralk	6266900	613805	20U	Y	Y	300
FR91033			6167635	615500	20U	Y	N	320
FR91034	Altered F-Q ash-flow	3	6166315	615380	20U	Y	Y	280
FR91035	Altered F-Q ash-flow	3	6165490	614990	20U	Y	Y	660
FR91036	F-Q ash-flow	2	6164600	615910	20U	Y	Y	250
FR91037	A ignimbritic flow (subalk)	2	6164900	616950	20U	Y	Y	550
FR91038	A-aegirine porphyry (peralk)	Micro G	6164650	616800	20U	Y	Y	450
FR91039			6164655	617900	20U	Y	N	200?
FR91040	A ignimbritic porphyry	2	6165050	617150	20U	Y	Y	430
FR91041	A Porphyry	2	6165595	616815	20U	Y	Y	460
FR91042			6165590	616885	20U	Y	N	270
FR91043	F-Q-A ash-flow	3	6166550	617400	20U	Y	Y	330
FR91044	Altered F-Q ash-flow	3	6166005	617075	20U	Y	Y	250
FR91045	Aphyric Ash-flow	4	6165895	616700	20U	Y	Y	370
FR91046			6165205	616590	20U	Y	N	n/a
FR91047			6163960	612750	20U	Y	N	280

Table A-13 Flowers River Field Sample Data

Field Samp. No.	Rock Type	Unit/Caldera	U.T.M. Coordinate N	U.T.M. Coordinate E	U.T.M. Zone	Thin Section	Geo. Chem.	Total Counts
FR91048	Altered F-Q ash-flow	2	6164125	613090	20U	Y	Y	320
FR91049	Aphyric Ash-flow	4	6165350	613120	20U	Y	Y	310
FR91050	Aphyric Ash-flow	3	6165420	613040	20U	Y	Y	510
FR91051	PG - Porph Granite	Peralk	6165650	613000	20U	Y	N	450
FR91052			6166400	613310	20U	Y	Y	285
FR91053			6165280	612010	20U	Y	N	n/a
FR91054			6165380	612160	20U	Y	N	330
FR91055			6165290	612160	20U	Y	N	510
FR91056	Aphyric Ash-flow	4	6165405	612605	20U	Y	Y	210
FR91057	Aphyric Ash-flow	4	6165240	612855	20U	Y	Y	220
FR91058			6162610	616080	20U	Y	N	750
FR91059			6162580	616090	20U	Y	N	700
FR91060			6162500	616080	20U	Y	N	340
FR91061	Aphyric Ash-flow	4	6162501	616080	20U	Y	Y	560
FR91062			6162460	616065	20U	Y	N	355
FR91063			6162175	617225	20U	Y	N	n/a
FR91064			6163780	615770	20U	Y	N	225
FR91065	F-Q-A Ash-flow	2	6162020	611645	20U	Y	Y	225
FR91066	Subalkaline granite	Micro G	6158770	613395	20U	Y	Y	325
FR91067	F-Q porphyry (subalk)	Micro G	6159980	613660	20U	Y	Y	375
FR91068	F-Q Ash-flow	2	6160795	614870	20U	Y	Y	330
FR91069	F-Q Ash-flow	2	61661345	614400	20U	Y	Y	330
FR91070	F-Q Ash-flow	2	6161210	613025	20U	Y	Y	225
FR91071	Altered F-Q ash-flow	3	6165395	613905	20U	Y	Y	250
FR91072	Aphyric ash-flow	4	6165090	614355	20U	Y	Y	200
FR91073	Q Ash-flow	3	6164885	614285	20U	Y	Y	490
FR91074			6164845	614295	20U	Y	N	n/a
FR91075	Aphyric Ash-flow	4	6164775	614305	20U	Y	Y	1000
FR91076	Aphyric Ash-flow	4	6164710	614315	20U	Y	Y	760
FR91077	Q-F ash-flow	3	6164310	614710	20U	Y	Y	520
FR91078	Q ash-flow	3	6161910	615100	20U	Y	Y	200
FR91079	F-Q-A porphyry (subalk)	Micro G	6163995	617395	20U	Y	Y	400
FR91080	Aphyric Ash-flow	4	6164295	618205	20U	Y	Y	340
FR91081	Aphyric Ash-flow breccia	4	6164300	618185	20U	Y	Y	300
FR91082			6164075	617685	20U	Y	N	n/a
FR91083	F-Q Ash-flow	2	6164850	621655	20U	Y	Y	370
FR91084	F-Q-A ash-flow	3	6164565	622645	20U	Y	Y	420
FR91085	Aphyric ash-flow lapilli	5	6160900	619870	20U	Y	Y	520
FR91086	F ash-flow	5	6161910	619780	20U	Y	Y	340
FR91087	Q ash-flow	5	6162800	620050	20U	Y	Y	580
FR91088	Aphyric Ash-flow	4	6163395	620870	20U	Y	Y	260
FR91089	Q ash-flow	4	6163450	621320	20U	Y	Y	520
FR91090	F-Q ash-flow	3	6163115	622760	20U	Y	Y	310
FR91091	Altered F-Q ash-flow	3	6162785	622140	20U	Y	Y	340
FR91092	Q ash-flow	4	6162680	672005	20U	Y	Y	560
FR91093			6162655	622010	20U	Y	N	300
FR91094	Aphyric Ash-flow	4	6162655	621995	20U	Y	Y	510

Table A-13 Flowers River Field Sample Data

Field Samp. No.	Rock Type	Unit/Caldera	U.T.M. Coordinate N	U.T.M. Coordinate E	U.T.M. Zone	Thin Section	Geo. Chem.	Total Counts
FR91095	Aphyric ash-flow	4	6162822	621350	20U	Y	Y	285
FR91096	Altered F-Q ash-flow	4	6162795	621025	20U	Y	Y	1100
FR91097	Q-poor ash-flow	4	6161905	620610	20U	Y	Y	850
FR91098	Aphyric ash-flow	4	6161840	620590	20U	Y	Y	900
FR91099			6161500	620620	20U	Y	N	800
FR91100	Q ash-flow	4	6161020	620750	20U	Y	Y	580
FR91101	Q ash-flow	4	6160800	620105	20U	Y	Y	800
FR91102	Aphyric ash-flow	4	6160250	620260	20U	Y	Y	370
FR91103	Aphyric ash-flow	4	6160200	620250	20U	Y	Y	580
FR91104	Aphyric ash-flow	4	6160145	620225	20U	Y	Y	810
FR91105	Aphyric ash-flow (mafic sp	4	6160100	620230	20U	Y	Y	340
FR91106	Aphyric ash-flow lapilli	4	6159850	620220	20U	Y	Y	1200
FR91107	Q ash-flow lapilli	4	6159700	620200	20U	Y	Y	2050
FR91108	Aphyric ash-flow	4	6159505	620100	20U	Y	Y	230
FR91109	Q ash-flow lapilli	4	6159375	620035	20U	Y	Y	700
FR91110	Aphyric ash-flow	4	6158720	620000	20U	Y	Y	280
FR91111	Q ash-flow	4	6158390	620255	20U	Y	Y	1050
FR91112	F-Q ash-flow	5	6158175	620595	20U	Y	Y	440
FR91113	Q ash-flow	5	6157700	620915	20U	Y	Y	420
FR91114	Q ash-flow	4	6157690	620985	20U	Y	Y	1506
FR91115	Q ash-flow	4	6160145	620420	20U	Y	Y	900
FR91116	Altered F-Q ash-flow	3	6160645	621320	20U	Y	Y	600
FR91117	A ignimbritic flow	5	6161020	621190	20U	Y	Y	840
FR91118	Aphyric ash-flow breccia	3	6162590	623220	20U	Y	Y	310
FR91119			6162710	623395	20U	Y	N	520
FR91120			6162810	624020	20U	Y	N	n/a
FR91121	Altered F-Q ash-flow	3	6161655	623500	20U	Y	Y	300
FR91122	F-Q-A ash-flow	5	6161230	622300	20U	Y	Y	380
FR91123	Q ash-flow	5	6160500	621585	20U	Y	Y	520
FR91124	Q ash-flow	5	6160280	622190	20U	Y	Y	560
FR91125	Altered F-Q ash-flow	4	6159410	623495	20U	Y	Y	440
FR91126	Aphyric ash-flow	?	6159565	623650	20U	Y	Y	420
FR91127	F-Q-(A) ash-flow (peralk)	5	6159445	623295	20U	Y	Y	520
FR91128	F-Q-(A) ash-flow (subalk)	Micro G	6157160	623485	20U	Y	Y	330
FR91129	F-Q-(A) ash-flow (subalk)	Micro G	6157160	623487	20U	Y	Y	260
FR91130	F-Q ash-flow	2	6156760	623185	20U	Y	Y	340
FR91131			6156780	623210	20U	Y	N	260
FR91132			6156710	623205	20U	Y	N	n/a
FR91133	F-Q ash-flow	5	6156950	621310	20U	Y	Y	600
FR91134	Q-poor ash-flow	4	6156950	621205	20U	Y	Y	1750
FR91135	Altered F-Q ash-flow	3	6156910	621190	20U	Y	Y	750
FR91136	Altered F-Q ash-flow	5	6159260	620200	20U	Y	Y	1000
FR91137	F-Q ash-flow	4	6159105	619870	20U	Y	Y	540
FR91138	F-Q-A porphyry	Micro G	6155980	622895	20U	Y	Y	250
FR91139	Q ash-flow	2	6155800	622905	20U	Y	Y	400
FR91140	Q ash-flow	4	6157175	621170	20U	Y	Y	580
FR91141	(Q & F)-poor ash-flow	4	6157160	621125	20U	Y	Y	3000

Table A-13 Flowers River Field Sample Data

Field Samp. No.	Rock Type	Unit/Caldera	U.T.M. Coordinate N	U.T.M. Coordinate E	U.T.M. Zone	Thin Section	Geo. Chem.	Total Counts
FR91142	Q ash-flow	4	6157040	621190	20U	Y	Y	980
FR91143			6156770	621105	20U	Y	N	320
FR91144	Altered F-Q ash-flow	3	6156605	621070	20U	Y	Y	440
FR91145	Layered tuff?	4?	6155900	621195	20U	Y	Y	380
FR91146	Q ash-flow	4	6155850	621145	20U	Y	Y	780
FR91147			6155850	621150	20U	Y	N	n/a
FR91148	A ash-flow	4	6156595	622600	20U	Y	Y	750
FR91149	(Q & F)-poor ash-flow	4	6156605	622605	20U	Y	Y	950
FR91161	F-Q-A porphyry (subalk)	Micro G	6155695	623030	20U	Y	Y	340
FR91164	F-Q ash-flow	3	6155760	620995	20U	Y	Y	385
FR91165	(Q & F)-poor ash-flow	4	6159805	619600	20U	Y	Y	580
FR91166	Aphyric ash-flow	4	6157310	620415	20U	Y	Y	330
FR91167	Qp Ash-flow	3	6156110	620600	20U	Y	Y	320
FR91168	F-Q ash-flow	3	6155580	620600	20U	Y	Y	310
FR91169			6154850	620920	20U	Y	N	225
FR91170	F-Q-A porphyry (peralk)	Micro G	6154895	620270	20U	Y	Y	300
FR91171	Q vein	?	6157060	619935	20U	Y	Y	220
FR91172	F-Q ash-flow	3	6157300	619320	20U	Y	Y	310
FR91173	(Q & F)-poor ash-flow	4	6159045	619160	20U	Y	Y	620
FR91174	F-Q-A ash-flow	2	6159810	619095	20U	Y	Y	400
FR91175	F-Q-A porph	Micro G	6159495	618900	20U	Y	Y	330
FR91176	A-Q syenite (peralk)	Micro G	615905	618850	20U	Y	Y	440
FR91177	F-Q-(A) ash-flow	2	6159525	618795	20U	Y	Y	340
FR91178	(Q & F)-poor ash-flow	4	6159070	619870	20U	Y	Y	540
FR91179	Altered F-Q ash-flow	3	6156030	619100	20U	Y	Y	300
FR91180	F-Q-A ash-flow	2	6155110	619190	20U	Y	Y	300
FR91181	Altered F-Q ash-flow	2	6155110	619105	20U	Y	Y	310
FR91182	Q-A porphyry dyke (+/-)	FQ porph.	6155050	618700	20U	Y	Y	260
FR91183	Banded flow	1	6155150	618510	20U	Y	Y	300
FR91184	F-Q-A ash-flow	2	6158240	618405	20U	Y	Y	340
FR91185	(Q & F)-poor ash-flow	4	6159850	617845	20U	Y	Y	540
FR91186			6159450	617440	20U	Y	N	300
FR91187	altered F-Q ash-flow	2	6158330	617070	20U	Y	Y	280
FR91188	Altered F-Q ash-flow	2	6158130	616905	20U	Y	Y	240
FR91189	F-Q-A ash-flow	2	6158210	616700	20U	Y	Y	300
FR91190	Gabbro	gabbro	6157995	616615	20U	Y	Y	200
FR91191	Banded flow	1	6157940	616600	20U	Y	Y	340
FR91192	Banded flow	1	6156975	617255	20U	Y	Y	370
FR91193	PG-SubAlk	Sub Alk	6156620	617070	20U	Y	Y	380
FR91194	PG-SubAlk	Sub Alk	6156900	616490	20U	Y	Y	380
FR91195	F-Q-A ash-flow	2	6160020	617900	20U	Y	Y	360
FR91196	Q-F ash-flow	2	6159050	617410	20U	Y	Y	270
FR91197	F-Q ash-flow	2	6157620	617450	20U	Y	Y	260
FR91198			6155300	615800	20U	Y	N	160
FR91199	Banded flow	1	6155350	615845	20U	Y	Y	470
FR91200	Carbonate	1	6155445	615600	20U	Y	Y	140
FR91201			6155475	615620	20U	Y	N	n/a

Table A-13 Flowers River Field Sample Data

Field Samp. No.	Rock Type	Unit/Caldera	U.T.M. Coordinate N	U.T.M. Coordinate E	U.T.M. Zone	Thin Section	Geo. Chem.	Total Counts
FR91202	F-Q-A porphyry (subalk)	Micro G	6155430	615305	20U	Y	Y	370
FR91203	F-Q-A porphyry (subalk)	Micro G (2?)	6155980	615080	20U	Y	Y	280
FR91204			6156500	614455	20U	Y	N	n/a
FR91205	F-Q-(A) ash-flow	2	6158375	615730	20U	Y	Y	280
FR91206			6159810	617005	20U	Y	N	n/a
FR91207	Aphyric ash-flow	4	6160785	620955	20U	Y	Y	810
FR91208			6161010	621080	20U	Y	N	810
FR91209	A-(Q-poor) ash-flow	5	6161050	621020	20U	Y	Y	750
FR91210	F-Q-A ash-flow	5	6162100	621295	20U	Y	Y	440
FR91211	Q-F ash-flow breccia	4	6161080	622435	20U	Y	Y	1150
FR91212	F-Q-A ash-flow	5	6161095	622390	20U	Y	Y	580
FR91213	(Q & F)-poor ash-flow	4	6161030	622495	20U	Y	Y	2220
FR91214	Q-poor ash-flow	4	6161010	622570	20U	Y	Y	2000
FR91215	Aphyric ash-flow	4	6161080	622595	20U	Y	Y	480
FR91216	Q-poor ash-flow	3	6161070	622660	20U	Y	Y	480
FR91217	Q ash-flow	3	6161095	622920	20U	Y	Y	400
FR91218	Q ash-flow (zeol)	3	6160850	623000	20U	Y	Y	275
FR91219	Aphyric ash-flow	4	6160460	623340	20U	Y	Y	650
FR91220	Q ash-flow	4	6160460	623345	20U	Y	Y	370
FR91221	F-Q-A porphyry (peralk)	Micro G	6160390	621110	20U	Y	Y	500
FR91222			6160970	618420	20U	Y	N	250
FR91223	F-Q-A porphyry (peralk)	Micro G	6161890	618050	20U	Y	Y	500
FR91224	F-Q ash-flow	3	6162090	618140	20U	Y	Y	330
FR91225	F-Q ash-flow	3	6166550	620090	20U	Y	Y	310
FR91226	PG-Peralkaline granite	Micro G	6169950	623285	20U	Y	Y	380
FR91227			6169995	623285	20U	Y	N	n/a
FR91228	F-Q ash-flow	3	6167770	617600	20U	Y	Y	300
FR91229	F-Q-A ash-flow	3	6167580	616345	20U	Y	Y	310
FR91230	Porphyritic F granite (subalk)	Sub Alk	6165655	609205	20U	Y	Y	240
FR91231	PG-Peralkaline granite	Micro G	6161680	611150	20U	Y	Y	260
FR91232	Porphyritic F granite (subalk)	Micro G	6160800	610620	20U	Y	Y	250
FR91233	Porphyritic F granite (subalk)	Micro G	6160700	609660	20U	Y	Y	240
FR91234	PG-Peralkaline granite	Peralk	6161800	609045	20U	Y	Y	300
FR91235	Porphyritic F granite (subalk)	Micro G	6160770	608090	20U	Y	Y	260
FR91236	PG-Peralkaline granite	Peralk	6158395	612680	20U	Y	Y	500
FR91237			6156495	613700	20U	Y	N	285
FR91238			6154410	612540	20U	Y	Y	300
FR91239	PG-Peralkaline granite	Peralk	6152320	613285	20U	Y	Y	360
FR91240	PG-Peralkaline granite	Peralk	6154385	615000	20U	Y	Y	200
FR91241			6154135	615525	20U	Y	N	200
FR91242	PG-Porph. F granite (peralk)	Micro G	6154580	615910	20U	Y	Y	360
FR91243	Aplitic granite (subalk)	Micro G	6154810	616450	20U	Y	Y	940
FR91244	Granite (subalk)	Sub Alk	6153010	619085	20U	Y	Y	340
FR91245	F-Q ash-flow	3	6155640	621755	20U	Y	Y	500
FR91246	Q-F ash-flow	3	6155805	622270	20U	Y	Y	335
FR91247	PG-Peralkaline granite	Peralk	6154560	624850	20U	Y	Y	320
FR91248	Aphyric ash-flow	4	6158845	623005	20U	Y	Y	970

Table A-13 Flowers River Field Sample Data

Field Samp. No.	Rock Type	Unit/Caldera	U.T.M. Coordinate N	U.T.M. Coordinate E	U.T.M. Zone	Thin Section	Geo. Chem.	Total Counts
FR91249	Aphyric ash-flow breccia	4	6158840	623025	20U	Y	Y	880
FR91250			6158700	622540	20U	Y	N	340
FR91251	F-Q-(A) ash-flow	5	6158015	622420	20U	Y	Y	470
FR91252	Granite (subalk)	Sub Alk	6166090	624550	20U	Y	Y	220
FR91253			6160810	623950	20U	Y	N	n/a
FR91254	PG-Peralkaline granite	Micro G	6160710	624430	20U	Y	Y	340
FR91255			6159940	624050	20U	Y	Y	440
FR91256			6159380	622445	20U	Y	N	210
FR91257	Aphyric ash-flow	4	6159180	622750	20U	Y	Y	980
FR91258	F-Q-A porphyry (subalk)	Micro G	6159130	622800	20U	Y	Y	290
FR91259	PG-Porph. peralkaline granite	Peralk	6153495	617710	20U	Y	Y	270
FR91260	Gabbro	1	6153995	616950	20U	Y	Y	185
FR91261	Banded felsic	1	6153990	616945	20U	Y	Y	160
FR91262	Banded aplitic felsic	1	6153970	616930	20U	Y	Y	150
FR91263	Banded aplitic felsic	1	6153930	616910	20U	Y	Y	340
FR91264			6153880	616905	20U	Y	N	n/a
FR91265	PG-Aplitic Peralkaline granite	Micro G	6153850	616900	20U	Y	Y	n/a
FR91266	Qp ash-flow	4	6163630	614070	20U	Y	Y	560
FR91267	A ignimbritic flow	2	6164390	615990	20U	Y	Y	680
FR91268			6164410	616005	20U	Y	N	n/a
FR91269	Aphyric ash-flow	4	6165405	617280	20U	Y	Y	380
FR91270	F-Q-A ash-flow	3	6165295	617395	20U	Y	Y	310
FR91271			6165295	617420	20U	Y	N	500
FR91272	Aphyric ash-flow	4	6165350	617580	20U	Y	Y	370
FR91273	PG-Peralkaline granite	Peralk	6165880	617020	20U	Y	Y	260
FR91274	A syenite	Sub alk	6165890	616980	20U	Y	Y	340
FR91275	F-Q-(A) ash-flow	3	6165700	616230	20U	Y	Y	420
FR91276	F-Q-(A) ash-flow	3	6163750	613410	20U	Y	Y	320
FR91277	Qp ash-flow	4	6164010	613730	20U	Y	Y	800
FR91278	Altered F-Q ash-flow lapilli	4	6164080	613810	20U	Y	Y	400
FR91279	(Q & F)-poor ash-flow	4	6164180	613810	20U	Y	Y	1000
FR91280	F-Q-A porphyry (peralk)	Micro G	6164210	613810	20U	Y	Y	460
FR91281	A ignimbritic flow (peralk)	Amph Ign	6164220	613820	20U	Y	Y	480
FR91282			6164220	613825	20U	Y	N	n/a
FR91283	F-Q-A porphyry (peralk)	Micro G	6164225	613830	20U	Y	Y	380
FR91284	A ignimbritic flow (peralk)	Amph Ign	6164230	613835	20U	Y	Y	600
FR91285	A ignimbritic flow (peralk)	Amph Ign	6164240	613835	20U	Y	Y	600
FR91286	F-Q-A porphyry (peralk)	Micro G	6164260	613840	20U	Y	Y	n/a
FR91287			6164280	613850	20U	Y	N	n/a
FR91288	(Q & F)-poor ash-flow	4	6164460	613870	20U	Y	Y	560
FR91289			6164450	613865	20U	Y	Y	600
FR91290	Q-F-poor ash-flow	4	6164470	613880	20U	Y	Y	600
FR91291	F-Q ash-flow	4	6164490	613900	20U	Y	Y	600
FR91292	Aphyric ash-flow	4	6164660	613910	20U	Y	Y	580
FR91293	(Q & F)-poor ash-flow	4	6164580	614000	20U	Y	Y	600

Table A-13 Flowers River Field Sample Data

Field Samp. No.	Rock Type	Unit/Caldera	U.T.M. Coordinate N	U.T.M. Coordinate E	U.T.M. Zone	Thin Section	Geo. Chem.	Total Counts
FR92001	Monzonite	Sub alk	6158930	616820	20U	Y	Y	200
FR92002	Q flow	1	6157180	617140	20U	Y	Y	290
FR92003	Altered F-Q ash-flow	2	6157180	617220	20U	Y	Y	310
FR92004	Gabbro Dyke	Gab	6156990	617200	20U	Y	Y	275
FR92005	Q syenite	Peralk	6155330	617600	20U	Y	Y	345
FR92006	Sil flow	1	6155450	617850	20U	Y	Y	190
FR92007	Sil flow?	1	6155430	617830	20U	Y	Y	385
FR92008			6155190	617940	20U	Y	Y	n/a
FR92009	PG-peralkaline granite	Peralk	6154780	617520	20U	Y	Y	320
FR92010	Q-M porphyry	2	6154140	618090	20U	Y	Y	265
FR92011	PG-peralkaline granite	Micro G	6154280	618110	20U	Y	Y	400
FR92012	F Porphyry	2	6154340	617920	20U	Y	Y	500
FR92013	Sil flow	1	6154250	617790	20U	Y	Y	300
FR92014	Sil flow	1	6154245	617792	20U	Y	Y	270
FR92015			6154240	617790	20U	Y	Y	400
FR92016	Gabbro Dyke	Gabbro	6154235	617790	20U	Y	Y	170
FR92017	Sil flow	1	6154340	616920	20U	Y	Y	180
FR92018	F-Q-A ash-flow	3	6158570	618120	20U	Y	Y	380
FR92019	A ignimbritic flow (peralk)	Amph Ign	6161920	618080	20U	Y	Y	330
FR92020			6162160	618080	20U	Y	N	n/a
FR92021	F-Q ash-flow breccia	3	6162520	618810	20U	Y	Y	380
FR92022			6163340	620680	20U	Y	N	n/a
FR92023			6164040	621350	20U	Y	N	n/a
FR92024	F-Q ash-flow	5	6162160	620390	20U	Y	Y	580
FR92025			6161890	620620	20U	Y	N	n/a
FR92026	F-Q ash-flow	3	6165960	620410	20U	Y	Y	380
FR92027	F-Q ash-flow	3	6166670	620190	20U	Y	Y	520
FR92028	F-Q ash-flow	3	6166860	620050	20U	Y	Y	540
FR92029	F-Q ash-flow	3	6167220	620040	20U	Y	Y	300
FR92030	Aphyric ash-flow	4	6164650	622540	20U	Y	Y	660
FR92031	Sil flow	1	6164440	623230	20U	Y	Y	180
FR92032	Q ash-flow	4	6162590	621270	20U	Y	Y	1700
FR92033	altered F-Q ash-flow	2	6155020	618850	20U	Y	Y	300
FR92034	PG-Granite	Peralk	6154570	618750	20U	Y	Y	340
FR92035	PG-Granite	Micro G	6154000	618190	20U	Y	Y	560
FR92036	F-Q-A porphyry (peralk)	Micro G	6153930	617060	20U	Y	Y	380?
FR92037	PG-Peralkaline Breccia	Micro G	6153930	617065	20U	Y	Y	420
FR92038	PG-peralkaline granite	Micro G	6153925	617065	20U	Y	Y	360
FR92039	Sil flow	1	6154400	516650	20U	Y	Y	270
FR92040	Gabbro - very fine grained	Gabbro	6154300	617520	20U	Y	Y	320
FR92041	Altered F-Q ash-flow	3	6159750	619010	20U	Y	Y	n/a
FR92042	Altered F-Q ash-flow	3	6159740	619030	20U	Y	Y	440
FR92043	Altered F-Q ash-flow	3	6159730	619060	20U	Y	Y	435
FR92044	Altered F-Q ash-flow	3	6159720	619060	20U	Y	Y	380
FR92045	Altered F-Q ash-flow	3	6159710	619120	20U	Y	Y	420
FR92046	Altered F-Q ash-flow	3	6159700	619140	20U	Y	Y	440
FR92047	Altered F-Q ash-flow	3	6159670	619160	20U	Y	Y	380

Table A-13 Flowers River Field Sample Data

Field Samp. No.	Rock Type	Unit/Caldera	U.T.M. Coordinate N	U.T.M. Coordinate E	U.T.M. Zone	Thin Section	Geo. Chem.	Total Counts
FR92048	Altered F-Q ash-flow	3	6159680	619180	20U	Y	Y	440
FR92049	Altered F-Q ash-flow	3	6159670	619200	20U	Y	Y	440
FR92050	Monzonite	Sub alk	6155490	613890	20U	Y	Y	n/a
FR92051	Monzonite	Sub alk	6156990	612410	20U	Y	Y	n/a
FR92052	PG-peralkaline aplite	Micro G	6154660	621410	20U	Y	Y	n/a
FR92053	Monzonite	Sub alk	6163650	625190	20U	Y	Y	n/a
FR92054	Monzonite	Sub alk	6166260	622150	20U	Y	Y	n/a
FR92055	F Porphyry	Sub alk	6145270	592480	20U	Y	Y	230
FR92056	Syenite	Sub alk	6145680	592540	20U	Y	Y	320
FR92057	Q Monzonite	Sub alk	6146620	589450	20U	Y	Y	n/a
FR92058			6144880	572550	20U	Y	N	n/a
FR92059			6144890	572550	20U	Y	Y	n/a
FR92060	Gabbro	Gabbro	6144900	572550	20U	Y	Y	n/a
FR92061	Syenite	Sub alk	6164980	612220	20U	Y	Y	n/a
FR92062	Aphyric ash-flow	4	6164400	612940	20U	Y	Y	800
FR92063	Aphyric ash-flow	4	6164500	612980	20U	Y	Y	n/a
FR92064	F-A porphyry	Micro G	6155430	621740	20U	Y	Y	310
FR92065	PG-peralkaline granite	Peralk	6155610	622800	20U	Y	Y	340
FR92066	F-Porphyry	Micro G	6155620	622796	20U	Y	Y	320
FR92067	F-Porphyry	Micro G	6155630	622793	20U	Y	Y	320
FR92068	F-Porphyry	Micro G	6155640	622790	20U	Y	Y	360
FR92069	Q ash-flow	3	6155650	622788	20U	Y	Y	380
FR92070	F (Q) porphyry	Micro G	6155660	622786	20U	Y	Y	340
FR92071	F-Q-A porphyry	Micro G	6155670	622783	20U	Y	Y	400
FR92072	F-Q-A porphyry	Micro G	6155690	622780	20U	Y	Y	330
FR92073	F-Q ash flow	5	6156490	622680	20U	Y	Y	620
FR92074	Aphyric flow	1	6157080	623150	20U	Y	Y	400
FR92075	F-Q-A ash-flow	3?	6157410	623440	20U	Y	Y	480
FR92076	F-Q-A porphyry	Micro G	6157440	623340	20U	Y	Y	215
FR92077	F-Q ash-flow	3?	6157600	623510	20U	Y	Y	385
FR92078	A ignimbrite	2	6157670	623560	20U	Y	Y	670
FR92079			6157650	623450	20U	Y	N	n/a
FR92080	F-Q ash flow	5	6158520	621040	20U	Y	Y	620
FR92081	Aphyric ash-flow	4	6157900	620930	20U	Y	Y	2300
FR92082	(F+Q) poor ash-flow	4	6157900	620935	20U	Y	Y	980
FR92083	Aphyric ash-flow	4	6157700	620960	20U	Y	Y	1700
FR92084	Aphyric ash-flow	4	6157450	621010	20U	Y	Y	1750
FR92085	Aphyric ash-flow	4	6157270	621110	20U	Y	Y	1900
FR92086	F-Q ash flow	5	6156950	621740	20U	Y	Y	550
FR92087	A ignimbrite	5	6157630	622570	20U	Y	Y	930
FR92088	Aphyric ash-flow	5	6157310	622420	20U	Y	Y	1050
FR92089	Sil flow	1	6157890	623290	20U	Y	Y	230
FR92090	A ignimbrite	2	6158220	623260	20U	Y	Y	610
FR92091			6159530	622440	20U	Y	Y	420
FR92092	F-Q ash flow	5	6159360	621210	20U	Y	Y	630
FR92093	Aphyric ash-flow	4	6158690	622650	20U	Y	Y	940
FR92094	Aphyric ash-flow frag	4	6161000	622600	20U	Y	Y	1390

Table A-13 Flowers River Field Sample Data

Field Samp. No.	Rock Type	Unit/Caldera	U.T.M. Coordinate N	U.T.M. Coordinate E	U.T.M. Zone	Thin Section	Geo. Chem.	Total Counts
FR92095	Aphyric ash-flow frag	4	6161000	622601	20U	Y	Y	1280
FR92096	Aphyric ash-flow	4	6161000	622602	20U	Y	Y	1760
FR92097	Aphyric ash-flow	4	6161005	622600	20U	Y	Y	2800
FR92098	Q-F ash-flow	4	6161005	622595	20U	Y	Y	1000
FR92099	Ash-flow breccia	5	6161020	620110	20U	Y	Y	660
FR92100	Aphyric ash-flow breccia	5	6161000	620560	20U	Y	Y	790
FR92101	F-Q ash flow	5	6161630	620660	20U	Y	Y	400
FR92102	Aphyric ash-flow	5	6161630	620663	20U	Y	Y	870
FR92103	Aphyric ash-flow	5	6161630	620668	20U	Y	Y	1500
FR92104	Aphyric ash-flow	5	6161760	620640	20U	Y	Y	1100
FR92105	Aphyric ash-flow	5	6161760	620645	20U	Y	Y	1000
FR92106	Aphyric ash-flow breccia	5	6161980	620500	20U	Y	Y	580
FR92107	F-Q-A ash flow	5	6262080	620370	20U	Y	Y	460
FR92108	Aphyric ash-flow breccia	5	6161980	620505	20U	Y	Y	720
FR92109	A ignimbrite	5	6262190	620310	20U	Y	Y	580
FR92110	F-Q-A ash flow	5	6262230	620230	20U	Y	Y	400
FR92111			6262240	620170	20U	Y	N	370
FR92112	F-A ash-flow	5	6162000	620330	20U	Y	Y	590
FR92113	Altered F-Q ash-flow	3	6159760	619250	20U	Y	Y	480
FR92114	Altered F-Q ash-flow	3	6159650	619220	20U	Y	Y	360
FR92115	Altered F-Q ash-flow	3	6159600	619180	20U	Y	Y	450
FR92116	Altered F-Q ash-flow	3	6159550	619160	20U	Y	Y	320
FR92117	Altered F-Q ash-flow	3	6159780	619260	20U	Y	Y	420
FR92118	PG-F porphyritic peralk	Micro G	6155190	617560	20U	Y	Y	n/a
FR92119	PG-F porphyritic peralk	Sub alk	6161980	618100	20U	Y	Y	n/a
FR92120	Aphyric flow amygdular	1	6262190	618080	20U	Y	Y	n/a
FR92121	F-Q ash-flow	2	6262540	618770	20U	Y	Y	n/a
FR92122	F-Q ash-flow	3	6159520	618850	20U	Y	Y	n/a
FR92123	Altered F-Q ash-flow	3	6159500	618870	20U	Y	Y	n/a
FR92124	F-A porphyry	Micro G??	6159480	618880	20U	Y	Y	n/a
FR92125	Altered F-Q ash-flow	3	6159470	618900	20U	Y	Y	n/a
FR92126	F-Q-A porphyry	Micro G	6159450	618920	20U	Y	Y	n/a
FR92127	F-Q-A porphyry	Micro G	6159430	618940	20U	Y	Y	n/a
FR92128	Sil flow	1	6154245	617793	20U	Y	Y	n/a
FR92129	Gabbro	Gabbro	6154240	617791	20U	Y	Y	n/a
FR92130	F-Q porphyry	Micro G	6154235	617791	20U	Y	Y	n/a

Table B-1 Little Pond Brook Geochemical Analyses

Field No.	TS91045	TS91046	TS91047	TS91048	TS91049	TS91050	TS91051	TS91052	TS91053	TS91054A	TS91055	TS91057	TS91058
SiO2	73.55	78.50	77.10	76.10	75.95	76.25	75.00	75.55	77.10	76.73	77.55	70.15	71.85
TiO2	0.39	0.19	0.21	0.23	0.23	0.20	0.21	0.17	0.17	0.13	0.12	0.23	0.19
Al2O3	13.12	11.41	10.41	11.58	11.69	11.02	11.02	10.78	10.80	11.97	11.56	11.34	14.09
Fe2O3	2.09	1.40	3.48	2.57	2.20	1.63	2.78	1.28	1.89	1.66	1.32	1.41	1.63
FeO	0.53	0.31	0.13	0.48	0.63	1.16	0.45	1.02	0.67	0.19	0.18	0.70	0.49
MnO	0.07	0.02	0.04	0.05	0.07	0.06	0.06	0.02	0.04	0.02	0.03	0.11	0.02
MgO	0.13	0.07	0.10	0.04	0.05	0.07	0.05	0.09	0.14	0.09	0.08	0.09	0.02
CaO	0.15	0.01	0.01	0.03	0.04	0.13	0.01	0.14	0.26	0.01	0.21	3.35	0.45
Na2O	3.66	4.03	1.41	3.75	3.71	3.86	2.60	1.55	1.34	2.39	2.88	2.72	5.45
K2O	4.87	2.97	5.27	4.65	4.88	4.74	5.34	6.94	5.11	5.72	4.59	5.42	4.18
P2O5	0.05	0.01	0.01	0.01	0.02	0.01	0.01	0.01	0.01	0.01	0.01	0.01	0.01
F	0.05	0.03	0.03	0.01	0.02	0.05	0.01	0.08	0.03	0.02	0.05	0.02	0.01
H2O+	1.16	0.90	1.08	0.66	0.78	0.49	0.87	0.61	1.07	0.86	0.92	0.77	0.99
H2O-	0.37	0.26	0.23	0.22	0.34	0.32	0.26	0.20	0.28	0.26	0.22	0.16	0.20
CO2	0.13	0.12	0.11	0.10	0.12	0.11	0.17	0.49	0.23	0.07	0.14	2.59	0.46
S	0.03	0.03	0.03	0.04	0.03	0.03	0.04	0.05	0.04	0.04	0.04	0.01	0.04
Total	100.35	100.26	99.65	100.52	100.76	100.13	98.88	98.98	99.18	100.14	99.90	99.08	100.08
A.I.	0.86	0.86	0.77	0.97	0.97	1.04	0.91	0.93	0.72	0.84	0.84	0.91	0.96
Cu	7	5	2	4	4	4	12	10	15	7	8	7	6
Pb	7	0	0	17	15	24	1	6	18	7	5	7	1
Zn	86	42	42	111	123	162	91	78	150	103	76	27	45
Ni	4	5	5	0	1	0	0	0	0	0	0	1	0
Ga	25	27	32	34	33	29	27	24	25	23	20	21	21
Sc	4.5	1.5	0.3	0.6	0.9	0.3	0.3	0.4	0.3	0.9	0.8	1.6	0.4
Nb	28	42	44	44	41	45	41	48	49	36	36	42	60
Zr	462	615	826	783	722	960	854	904	958	384	356	740	1094
Y	59	102	122	111	95	123	102	110	122	66	101	88	133
Ce	160	7	131	204	213	243	104	217	165	83	147	198	172
U	6	8	5	5	4	6	5	9	3	4	3	6	16
Th	21	23	17	14	14	18	14	23	26	25	23	25	34
Sr	57	21	12	9	10	11	15	35	16	15	16	40	29
Rb	163	84	184	132	134	157	174	267	194	221	173	151	111
Ba	573	94	97	117	173	76	157	416	70	58	48	73	85

Table B-1

Field No.	TS91059	TS91060	TS91061A	TS91062R	TS91063A	TS91064A	TS91065	TS91066	TS91067	TS91068A	TS91069	TS91070	TS91071
SiO2	72.00	72.00	73.19	75.69	74.90	75.54	75.00	75.45	74.40	76.60	75.95	74.85	75.35
TiO2	0.37	0.37	0.39	0.24	0.24	0.25	0.25	0.22	0.22	0.21	0.22	0.26	0.27
Al2O3	13.63	13.09	13.21	11.45	11.30	11.49	11.65	11.09	11.18	11.04	11.04	11.53	11.88
Fe2O3	0.90	1.06	1.40	1.76	1.69	1.57	1.66	1.63	1.54	1.60	1.45	1.65	1.70
FeO	1.41	1.26	0.97	0.89	1.07	1.38	1.24	1.07	1.23	1.03	1.26	1.24	0.98
MnO	0.03	0.03	0.03	0.04	0.06	0.06	0.07	0.06	0.06	0.05	0.05	0.07	0.06
MgO	0.41	0.30	0.45	0.14	0.13	0.09	0.16	0.07	0.05	0.08	0.09	0.05	0.05
CaO	0.45	0.64	0.20	0.04	0.28	0.18	0.18	0.21	0.17	0.13	0.10	0.25	0.20
Na2O	4.02	3.79	3.39	2.52	3.58	4.05	3.95	3.62	3.92	3.81	3.60	3.87	3.92
K2O	5.21	5.52	5.91	6.00	5.36	4.83	4.92	5.14	4.75	4.65	4.96	4.97	5.13
P2O5	0.05	0.05	0.07	0.04	0.02	0.03	0.01	0.01	0.01	0.01	0.01	0.01	0.02
F	0.05	0.02	0.02	0.01	0.04	0.03	0.04	0.03	0.04	0.04	0.04	0.03	0.03
H2O+	1.01	0.77	0.91	1.08	0.78	0.86	0.74	0.59	0.85	0.83	1.06	1.33	1.20
H2O-	0.28	0.27	0.27	0.36	0.35	0.37	0.34	0.24	0.28	0.38	0.29	0.39	0.39
CO2	0.27	0.49	0.02	0.00	0.16	0.17	0.19	0.15	0.18	0.17	0.20	0.19	0.24
S	0.01	0.01	0.02	0.03	0.02	0.02	0.04	0.02	0.03	0.03	0.04	0.05	0.05
Total	100.10	99.67	100.44	100.29	99.96	100.90	100.44	99.60	98.91	100.63	100.36	100.74	101.47
A.I.	0.90	0.93	0.91	0.93	1.03	1.03	1.01	1.04	1.04	1.02	1.02	1.02	1.01
Cu	7	4	5	7	4	3	4	4	2	3	16	6	3
Pb	3	1	3	16	13	12	13	12	14	14	18	13	12
Zn	91	52	167	78	109	114	114	118	130	129	112	121	188
Ni	1	0	1	0	0	0	5	0	0	0	0	0	0
Ga	21	20	21	28	29	28	29	28	28	27	30	30	29
Sc	4	4.1	4	0.7	0.8	0.8	0.9	0.7	0.4	0.5	0.6	1	0.9
Nb	23	23	26	31	32	35	34	38	39	37	37	34	32
Zr	418	431	481	704	684	698	648	760	709	730	727	626	643
Y	53	55	50	96	82	69	72	73	93	79	90	74	73
Ce	118	131	129	236	223	164	200	133	173	121	201	179	187
U	6	6	6	4	4	3	4	5	5	5	5	4	4
Th	17	14	18	9	9	5	12	9	8	11	13	9	10
Sr	56	44	61	30	13	10	11	13	8	7	7	11	13
Rb	154	159	183	140	134	111	119	152	128	122	134	123	122
Ba	576	560	674	174	150	142	141	97	87	77	108	160	164

Table B-1

Field No.	TS91072	TS91073	TS91074	TS91075	TS91076A	TS91077	TS91078A	TS91079	TS91080	TS91081	TS91082	TS91083	TS91084
SiO2	76.60	74.80	75.85	78.60	78.41	76.80	77.07	79.70	74.55	72.35	73.30	73.75	72.75
TiO2	0.21	0.25	0.25	0.01	0.26	0.18	0.22	0.15	0.26	0.37	0.37	0.38	0.37
Al2O3	10.98	11.56	11.12	11.06	11.43	12.58	11.22	8.31	13.17	12.80	13.23	13.16	13.52
Fe2O3	1.74	1.50	1.63	1.12	1.10	0.90	2.11	3.49	1.38	1.21	1.13	1.23	2.45
FeO	0.94	1.27	0.22	0.08	0.34	0.33	0.20	0.79	0.34	1.29	1.13	1.02	0.16
MnO	0.05	0.07	0.03	0.01	0.02	0.02	0.04	0.04	0.01	0.05	0.05	0.03	0.04
MgO	0.13	0.24	0.05	0.01	0.04	0.02	0.10	0.07	0.11	0.42	0.49	0.32	0.12
CaO	0.14	0.20	0.01	1.48	0.01	0.01	0.04	0.01	0.03	0.72	0.27	0.31	0.11
Na2O	3.58	3.23	1.21	6.27	3.80	5.11	2.80	1.20	2.78	3.26	3.80	3.94	3.92
K2O	4.82	5.70	6.93	0.27	4.14	3.38	4.81	4.65	6.60	5.42	4.98	4.90	5.18
P2O5	0.01	0.01	0.01	0.00	0.03	0.01	0.02	0.01	0.02	0.05	0.05	0.05	0.05
F	0.03	0.03	0.02	0.03	0.00	0.01	0.05	0.03	0.04	0.05	0.05	0.04	0.04
H2O+	1.45	1.66	1.28	1.35	1.05	0.77	1.46	1.21	0.99	0.87	0.82	0.83	0.97
H2O-	0.33	0.40	0.31	0.39	0.28	0.20	0.25	0.26	0.16	0.25	0.23	0.27	0.30
CO2	0.19	0.20	0.13	0.08	0.06	0.10	0.14	0.17	0.07	0.53	0.11	0.16	0.09
S	0.04	0.05	0.10	0.07	0.05	0.07	0.06	0.09	0.02	0.02	0.04	0.06	0.03
Total	101.24	101.17	99.15	100.83	100.99	100.49	100.57	100.18	100.53	99.66	100.05	100.45	100.10
A.I.	1.01	0.99	0.85	0.96	0.94	0.96	0.87	0.84	0.89	0.88	0.88	0.90	0.89
Cu	2	3	3	7	10	3	5	6	2	5	5	10	5
Pb	16	12	0	0	0	0	16	12	0	1	9	0	4
Zn	119	99	60	26	46	36	26	112	12	64	64	176	79
Ni	0	0	0	0	0	0	7	0	0	1	1	1	1
Ga	212	29	30	28	23	27	24	27	18	20	21	19	22
Sc	0.4	1	0.8	0.7	0.7	0.6	1.7	0.8	2.3	3.9	3.8	3.7	3.8
Nb	37	29	31	34	32	20	38	31	22	23	23	23	23
Zr	769	562	700	745	754	487	790	810	290	429	465	478	402
Y	95	57	80	98	85	49	113	84	34	53	57	50	49
Ce	223	165	182	200	190	118	144	229	71	105	132	140	154
U	4	3	6	4	6	2	11	15	6	6	6	6	6
Th	9	7	14	16	13	8	23	9	23	13	18	17	18
Sr	12	19	19	13	16	13	20	18	24	32	52	45	43
Rb	129	136	223	183	105	95	162	166	224	158	152	148	163
Ba	91	229	295	182	114	74	149	163	556	604	594	557	573

Table B-1

Field No.	TS91085	TS91086	TS91087A	TS91088	TS91089	TS91091A	TS91092A	TS91093R	TS91094	TS91096A	TS91097	TS91098	TS91099
SiO2	73.45	72.10	73.02	78.00	75.45	75.70	75.66	75.32	74.90	75.26	67.90	75.25	74.85
TiO2	0.38	0.39	0.39	0.25	0.25	0.23	0.25	0.26	0.26	0.26	0.32	0.27	0.27
Al2O3	13.17	13.67	13.54	11.53	11.68	11.48	11.60	11.54	11.99	11.61	14.68	11.68	11.67
Fe2O3	1.38	1.09	1.41	0.82	2.64	2.85	2.72	1.80	1.72	1.61	1.20	2.57	1.85
FeO	0.94	1.25	0.97	0.13	0.27	0.18	0.35	0.91	1.05	1.18	1.12	0.33	1.18
MnO	0.06	0.07	0.07	0.01	0.08	0.07	0.10	0.07	0.06	0.07	0.05	0.08	0.07
MgO	0.31	0.51	0.58	0.06	0.03	0.02	0.06	0.16	0.12	0.11	0.84	0.07	0.12
CaO	0.13	0.27	0.19	0.01	0.03	0.01	0.06	0.32	0.36	0.27	0.13	0.19	0.30
Na2O	3.84	4.27	4.28	2.83	2.88	3.69	3.67	3.16	3.86	3.09	0.40	3.56	4.00
K2O	5.00	4.56	4.68	5.24	5.81	4.47	4.83	5.32	4.64	5.75	11.84	4.88	4.67
P2O5	0.05	0.06	0.06	0.01	0.01	0.01	0.02	0.04	0.02	0.03	0.04	0.02	0.02
F	0.02	0.03	0.03	0.02	0.01	0.00	0.01	0.01	0.03	0.03	0.02	0.04	0.03
H2O+	0.91	0.89	1.19	0.51	0.77	0.64	1.05	0.99	0.90	0.89	1.14	0.83	0.84
H2O-	0.30	0.20	0.28	0.21	0.32	0.19	0.29	0.33	0.27	0.33	0.28	0.31	0.35
CO2	0.17	0.17	0.08	0.07	0.12	0.07	0.04	0.24	0.31	0.00	0.03	0.22	0.06
S	0.05	0.04	0.02	0.05	0.06	0.02	0.00	0.00	0.01	0.00	0.04	0.01	0.02
Total	100.16	99.57	100.75	99.75	100.42	99.60	100.67	100.47	100.50	100.47	100.03	100.31	100.30
A.I.	0.89	0.87	0.89	0.90	0.94	0.95	0.97	0.95	0.95	0.97	0.92	0.95	1.00
Cu	3	4	5	4	4	3	4	4	4	5	7	4	5
Pb	4	55	16	0	12	0	7	17	9	13	11	9	13
Zn	100	71	64	13	109	56	13	139	115	124	104	98	96
Ni	1	2	1	0	0	0	1	0	0	0	3	0	3
Ga	20	21	20	24	26	28	29	28	29	28	19	28	29
Sc	4.1	3.8	4	0.7	0.8	0.5	0.7	0.9	0.9	0.8	3	0.7	0.8
Nb	24	23	23	28	28	31	34	27	29	31	23	32	35
Zr	441	473	452	677	587	709	667	550	591	598	362	684	664
Y	50	57	64	55	55	77	86	76	73	75	57	73	71
Ce	124	146	140	141	184	217	231	230	217	209	126	220	183
U	6	6	6	4	4	5	5	3	3	3	8	4	4
Th	21	20	20	16	10	13	12	9	9	10	34	7	9
Sr	50	50	42	13	20	7	14	28	39	24	88	15	18
Rb	152	121	122	142	146	109	115	131	121	145	468	116	113
Ba	621	585	567	177	228	78	147	197	203	156	698	141	146

Table B-1

Field No.	TS91100A	TS91101	TS91102	TS91103	TS91104	TS91105	TS91106	TS91107	TS91108	TS91109	TS91110	TS91111	TS91112
SiO2	64.31	74.50	76.95	74.70	75.75	75.85	74.65	76.05	75.05	74.40	75.95	76.10	74.75
TiO2	1.37	0.25	0.20	0.26	0.25	0.24	0.22	0.23	0.23	0.21	0.18	0.17	0.23
Al2O3	13.24	11.43	10.81	11.42	11.27	11.38	11.09	11.30	11.27	11.17	10.97	10.63	11.30
Fe2O3	2.25	1.88	1.74	1.82	1.87	3.17	1.66	2.36	1.60	1.08	1.72	1.49	1.56
FeO	4.61	1.35	0.97	1.30	1.18	0.18	1.16	0.50	1.17	1.73	1.17	1.32	1.58
MnO	0.14	0.09	0.05	0.09	0.06	0.09	0.07	0.06	0.06	0.07	0.06	0.06	0.08
MgO	1.46	0.16	0.08	0.17	0.04	0.04	0.09	0.05	0.12	0.04	0.02	0.01	0.04
CaO	2.11	0.39	0.19	0.20	0.21	0.02	0.18	0.06	0.17	0.18	0.13	0.10	0.28
Na2O	4.35	3.39	3.70	3.73	3.86	3.39	3.64	3.44	3.60	4.24	4.04	3.98	3.81
K2O	3.20	5.03	4.39	4.66	4.57	4.74	4.90	5.19	4.93	4.44	4.60	4.44	4.75
P2O5	0.43	0.02	0.01	0.02	0.02	0.02	0.01	0.01	0.01	0.01	0.01	0.01	0.02
F	0.08	0.03	0.05	0.03	0.03	0.01	0.04	0.02	0.02	0.05	0.04	0.04	0.03
H2O+	1.51	0.71	0.75	0.95	0.60	0.89	0.72	0.66	0.81	0.75	0.47	0.50	0.60
H2O-	0.27	0.16	0.19	0.27	0.36	0.33	0.34	0.33	0.40	0.25	0.26	0.22	0.20
CO2	0.13	0.26	0.05	0.04	0.09	0.07	0.05	0.02	0.06	0.03	0.08	0.02	0.04
S	0.06	0.02	0.00	0.01	0.00	0.05	0.05	0.07	0.08	0.05	0.04	0.07	0.06
Total	99.49	99.67	100.13	99.67	100.16	100.47	98.87	100.35	99.58	98.70	99.74	99.16	99.33
A.I.	0.80	0.96	1.00	0.98	1.00	0.94	1.02	1.00	1.00	1.05	1.06	1.07	1.01
Cu	5	7	5	7	4	4	4	5	3	8	3	3	12
Pb	8	13	16	11	13	8	16	13	10	18	19	20	16
Zn	113	126	134	91	121	94	127	116	97	134	104	169	114
Ni	1	2	1	1	0	0	0	0	0	1	0	0	0
Ga	24	28	29	27	29	28	29	25	26	29	31	31	28
Sc	13.1	0.8	0.4	0.9	0.9	0.9	0.6	0.5	0.6	0.4	0.1	0	0.6
Nb	16	35	48	32	34	30	37	39	31	43	51	52	37
Zr	402	656	981	590	650	661	641	825	564	728	1032	1089	752
Y	52	86	117	71	62	79	96	111	72	105	127	140	82
Ce	109	211	195	200	137	262	229	246	177	185	223	190	167
U	6	5	7	4	4	4	5	6	5	6	7	7	5
Th	10	13	22	10	12	10	14	17	9	17	20	21	13
Sr	106	19	9	15	11	17	18	11	12	5	4	3	9
Rb	101	140	145	118	121	124	139	153	133	145	168	170	141
Ba	335	136	59	157	146	144	114	112	131	87	39	23	122

Table B-1

Field No.	TS91113	TS91114A	TS91115	TS91116	TS91117	TS91118A	TS91120
SiO2	75.25	75.28	75.00	71.90	76.45	76.43	76.75
TiO2	0.26	0.25	0.25	0.39	0.21	0.22	0.17
Al2O3	10.99	11.45	11.73	13.78	11.35	10.73	11.05
Fe2O3	2.28	1.79	0.96	0.76	1.49	1.50	2.18
FeO	1.30	1.05	2.19	1.71	1.51	1.19	0.84
MnO	0.09	0.07	0.06	0.05	0.04	0.04	0.03
MgO	0.07	0.21	0.13	0.31	0.10	0.09	0.14
CaO	0.15	0.15	0.24	0.55	0.02	0.86	0.46
Na2O	3.24	3.75	3.20	4.62	2.80	3.10	2.28
K2O	4.83	4.87	5.00	4.60	4.71	3.91	4.89
P2O5	0.02	0.02	0.02	0.05	0.01	0.02	0.01
F	0.04	0.04	0.01	0.03	0.02	0.01	0.06
H2O+	0.71	1.28	1.07	0.98	1.07	0.55	0.91
H2O-	0.24	0.33	0.35	0.30	0.34	0.24	0.31
CO2	0.03	0.02	0.20	0.31	0.03	0.68	0.37
S	0.06	0.05	0.06	0.07	0.06	0.09	0.06
Total	99.56	100.59	100.47	100.41	100.21	99.64	100.51
A.I.	0.96	1.00	0.91	0.91	0.85	0.87	0.82
Cu	6	2	7	11	8	4	4
Pb	16	10	6	13	0	2	15
Zn	111	113	117	80	46	82	120
Ni	0	0	0	0	0	0	0
Ga	22	27	28	21	31	25	26
Sc	0.5	0.7	0.8	3.9	0.1	0.9	0.2
Nb	42	35	27	22	39	23	46
Zr	702	657	587	473	889	605	915
Y	88	97	62	56	129	85	115
Ce	97	241	183	138	307	183	224
U	4	5	4	6	5	2	6
Th	16	13	9	20	13	16	22
Sr	19	13	13	61	10	35	19
Rb	140	123	131	125	157	95	173
Ba	124	138	177	571	79	84	50

Table B-2 Gaff Topsail Geochemical Analyses

Field No.	TS91031	TS91032	TS91033	TS91034	TS91035	TS91036	TS91037	TS91042	TS91043	TS91123	TS91124	TS91125	TS91126A
SiO2	75.20	75.30	76.35	75.10	75.95	75.30	75.55	73.35	74.75	74.40	74.95	74.45	74.40
TiO2	0.19	0.20	0.22	0.22	0.23	0.25	0.24	0.37	0.20	0.25	0.24	0.27	0.35
Al2O3	11.63	11.54	10.90	11.71	11.45	11.74	11.87	12.06	12.00	12.34	12.24	12.51	12.04
Fe2O3	0.95	0.96	1.29	1.01	1.29	1.72	1.11	3.74	2.10	1.24	1.15	1.04	1.28
FeO	1.35	1.24	1.24	1.43	1.31	0.83	1.53	0.00	0.44	1.52	1.42	1.52	1.66
MnO	0.05	0.04	0.06	0.05	0.06	0.03	0.06	0.10	0.05	0.05	0.06	0.06	0.06
MgO	0.07	0.09	0.08	0.12	0.10	0.08	0.13	0.20	0.07	0.14	0.14	0.13	0.27
CaO	0.20	0.21	0.19	0.26	0.25	0.06	0.24	0.53	0.22	0.27	0.30	0.33	0.61
Na2O	4.22	4.21	3.99	4.33	4.14	3.99	4.22	4.31	4.41	4.49	4.48	4.44	4.26
K2O	4.37	4.42	4.33	4.63	4.37	4.49	4.59	4.53	4.71	4.67	4.53	4.63	4.26
P2O5	0.01	0.01	0.01	0.01	0.01	0.01	0.01	0.02	0.01	0.02	0.03	0.02	0.05
F	0.04	0.03	0.03	0.03	0.03	0.01	0.04	0.04	0.04	0.04	0.02	0.03	0.04
H2O+	0.46	0.51	0.46	0.50	0.38	0.51	0.39	0.58	0.38	0.54	0.50	0.71	0.42
H2O-	0.19	0.19	0.14	0.12	0.13	0.21	0.17	0.18	0.22	0.31	0.26	0.24	0.28
CO2	0.04	0.07	0.05	0.04	0.04	0.03	0.03	0.06	0.04	0.04	0.02	0.05	0.06
S	0.01	0.03	0.03	0.02	0.03	0.03	0.03	0.04	0.06	0.06	0.08	0.09	0.05
Total	98.98	99.05	99.37	99.58	99.77	99.29	100.21	100.11	99.70	100.38	100.42	100.52	100.05
A.I.	1.00	1.01	1.03	1.04	1.01	0.97	1.00	0.99	1.03	1.01	1.00	0.98	0.96
Cu	3	2	2	2	2	2	2	2	2	0	0	0	1
Pb	9	8	7	1	6	2	15	5	8	2	2	0	10
Zn	114	102	112	98	10	75	110	110	124	110	110	89	104
Ni	0	0	0	0	2	0	1	1	1	0	0	0	0
Ga	26	25	24	26	25	25	27	26	27	26	24	27	28
Sc	1.3	1.3	1.3	1.3	1.3	1.3	1.3	2.3	1.1	1.8	1.8	1.9	3.2
Nb	28	21	23	22	28	21	26	19	24	21	16	22	29
Zr	724	557	566	542	557	601	601	561	638	715	663	670	755
Y	96	41	62	49	60	47	48	30	65	49	56	51	79
Ce	103	64	159	118	83	115	118	225	156	137	204	120	92
U	5	3	3	3	4	3	4	1	4	4	3	3	3
Th	13	5	9	9	10	9	9	1	9	7	1	4	10
Sr	9	9	8	10	8	9	9	14	9	11	11	14	36
Rb	102	93	99	104	107	92	103	45	114	90	81	89	104
Ba	644	711	388	376	246	400	307	833	337	538	628	669	600

Table B-2

Field No.	TS91127	TS91129	TS91130	TS91131	TS91132	TS91134	TS91135	TS91136	TS91137	TS91138	TS91140	TS91141	TS91142
SiO2	73.55	77.30	73.85	75.25	73.35	75.40	75.90	75.30	74.90	75.65	75.65	75.30	73.95
TiO2	0.28	0.14	0.22	0.17	0.28	0.17	0.20	0.20	0.22	0.22	0.21	0.20	0.29
Al2O3	12.05	11.64	11.93	11.55	12.04	11.80	11.31	11.56	11.92	11.83	11.64	12.12	12.34
Fe2O3	1.13	1.62	1.40	1.07	1.55	1.54	1.44	1.16	1.44	1.05	0.82	0.81	1.07
FeO	1.49	0.29	1.33	1.32	1.82	1.04	1.30	1.34	1.42	1.38	1.61	1.49	1.68
MnO	0.05	0.03	0.08	0.05	0.08	0.04	0.06	0.05	0.06	0.06	0.06	0.05	0.06
MgO	0.23	0.04	0.06	0.05	0.17	0.06	0.08	0.06	0.06	0.10	0.06	0.15	0.26
CaO	0.56	0.11	0.36	0.33	0.36	0.08	0.25	0.28	0.26	0.33	0.38	0.30	0.59
Na2O	4.33	4.31	4.60	4.50	4.75	4.41	4.40	4.43	4.63	4.38	4.34	4.44	4.33
K2O	4.25	4.31	4.64	4.53	4.63	4.57	4.44	4.45	4.61	4.51	4.36	4.51	4.41
P2O5	0.04	0.01	0.01	0.01	0.02	0.01	0.01	0.02	0.02	0.02	0.01	0.02	0.06
F	0.04	0.00	0.05	0.06	0.11	0.05	0.06	0.06	0.06	0.07	0.06	0.04	0.04
H2O+	0.37	0.29	0.31	0.21	0.70	0.63	0.66	0.63	0.29	0.30	0.23	0.26	0.32
H2O-	0.17	0.33	0.38	0.23	0.31	0.24	0.20	0.19	0.20	0.18	0.29	0.24	0.24
CO2	0.05	0.00	0.01	0.03	0.00	0.01	0.00	0.02	0.00	0.00	0.03	0.04	0.06
S	0.10	0.12	0.06	0.09	0.02	0.02	0.06	0.07	0.02	0.06	0.01	0.01	0.01
Total	98.69	100.54	99.29	99.45	100.19	100.07	100.37	99.82	100.11	100.14	99.76	99.98	99.71
A.I.	0.97	1.01	1.06	1.07	1.07	1.03	1.06	1.05	1.06	1.02	1.02	1.01	0.96
Cu	0	1	8	2	0	0	9	8	9	10	7	5	7
Pb	12	13	5	10	15	14	24	5	16	11	10	9	15
Zn	98	59	131	129	172	134	160	132	142	125	110	108	93
Ni	0	0	0	0	0	0	0	0	0	0	0	1	0
Ga	28	28	29	29	31	30	29	29	30	28	27	28	28
Sc	2.8	0.4	1.3	1	1.8	1	1	1.2	1.3	1.5	1.4	1.9	2.9
Nb	28	23	27	25	25	24	37	24	24	23	19	18	26
Zr	626	165	683	745	765	761	1043	687	741	607	765	536	714
Y	83	37	87	102	81	64	122	51	64	60	74	66	63
Ce	128	37	228	193	283	79	219	132	227	185	181	157	125
U	4	3	5	5	4	5	6	3	4	4	3	3	4
Th	17	4	9	16	10	7	17	8	12	4	7	5	12
Sr	37	5	10	14	10	4	8	8	8	10	14	12	42
Rb	120	103	119	122	114	135	132	114	113	103	74	78	123
Ba	493	54	631	474	526	298	439	480	471	488	747	570	619

Table B-2

Field No.	TS91143	TS91144	TS91145	TS91146	TS91147	TS91039	TS91041	TS91128	TS91133	TS91030A	TS91038	TS91040	TS91139
SiO2	74.45	76.05	74.65	74.90	76.70	75.70	70.75	72.85	76.00	68.95	76.50	75.30	64.30
TiO2	0.26	0.18	0.24	0.22	0.21	0.25	0.68	0.30	0.14	0.47	0.08	0.11	0.60
Al2O3	12.17	11.66	11.89	12.01	11.13	11.97	12.43	13.35	11.49	13.67	11.63	12.27	16.16
Fe2O3	1.00	1.08	1.34	1.22	1.01	0.87	1.87	0.96	0.77	0.94	0.93	1.21	0.59
FeO	1.74	1.20	1.67	1.49	1.41	1.56	2.61	1.28	1.54	3.94	0.98	1.04	2.99
MnO	0.06	0.04	0.06	0.05	0.05	0.05	0.13	0.06	0.04	0.14	0.03	0.04	0.08
MgO	0.17	0.05	0.09	0.11	0.11	0.18	0.67	0.39	0.07	0.12	0.02	0.04	0.72
CaO	0.42	0.22	0.36	0.34	0.36	0.32	1.35	1.30	0.06	1.30	0.01	0.14	1.89
Na2O	4.45	4.35	4.54	4.53	4.20	3.82	4.69	4.02	4.41	4.73	4.49	4.46	5.91
K2O	4.42	4.48	4.60	4.64	4.17	4.96	3.83	4.00	4.39	4.87	4.06	4.82	5.89
P2O5	0.05	0.01	0.02	0.02	0.02	0.01	0.24	0.01	0.01	0.07	0.01	0.01	0.15
F	0.05	0.05	0.07	0.05	0.05	0.03	0.06	0.04	0.07	0.03	0.06	0.03	0.05
H2O+	0.32	0.36	0.34	0.23	0.20	0.48	0.49	0.87	0.69	0.45	0.27	0.39	0.21
H2O-	0.25	0.24	0.22	0.30	0.23	0.20	0.11	0.22	0.23	0.20	0.10	0.14	0.13
CO2	0.04	0.05	0.07	0.08	0.04	0.04	0.07	0.13	0.01	0.02	0.05	0.04	0.00
S	0.01	0.02	0.00	0.01	0.05	0.02	0.04	0.10	0.05	0.01	0.03	0.03	0.07
Total	99.86	100.04	100.16	100.20	99.94	100.46	100.02	99.88	99.97	99.88	99.25	100.07	99.74
A.I.	0.99	1.03	1.05	1.04	1.03	0.97	0.95	0.82	1.04	0.95	1.01	1.02	1.00
Cu	7	11	5	6	11	2	3	3	1	9	3	3	17
Pb	12	8	15	5	2	6	4	13	16	6	5	6	0
Zn	120	112	143	134	117	99	109	41	174	118	123	119	73
Ni	0	0	0	0	0	1	1	0	0	3	1	1	0
Ga	29	28	27	29	25	24	28	20	30	30	30	28	26
Sc	2.2	1	1.6	1.5	1.7	2	8.5	5.3	0.6	5.5	0.3	0.5	7.4
Nb	24	24	26	29	20	20	17	17	51	23	27	16	13
Zr	725	662	835	727	721	624	497	292	1011	367	321	334	810
Y	58	44	62	63	60	47	62	66	101	50	21	39	65
Ce	131	98	240	150	117	116	130	109	131	112	37	64	111
U	4	3	4	5	3	3	1	4	7	2	3	3	2
Th	9	8	9	13	9	10	0	14	22	2	13	9	0
Sr	22	9	10	9	11	18	67	128	4	58	1	6	90
Rb	112	106	120	131	97	102	61	145	175	65	174	153	53
Ba	543	479	509	493	416	422	535	702	144	675	21	143	2025

Table B-3 Sheffield Lake Geochemical Analyses

Field No.	TS91001D	TS91002R	TS91003	TS91004A	TS91005	TS91007	TS91008R	TS91009	TS91010	TS91012	TS91013	TS91014D
SiO2	75.75	74.60	75.35	76.43	74.70	75.65	74.25	75.95	74.00	74.35	75.90	75.80
TiO2	0.20	0.22	0.24	0.17	0.23	0.18	0.27	0.20	0.29	0.25	0.17	0.19
Al2O3	11.12	11.36	12.11	10.67	11.20	10.65	12.07	11.55	12.37	11.94	10.58	10.86
Fe2O3	2.98	1.96	1.70	2.31	2.30	2.04	1.42	1.42	1.62	1.86	2.19	1.68
FeO	0.39	1.22	0.88	1.00	1.13	1.76	1.57	1.07	1.38	1.36	1.38	1.18
MnO	0.04	0.04	0.05	0.04	0.06	0.06	0.07	0.05	0.10	0.07	0.05	0.05
MgO	0.07	0.10	0.10	0.08	0.12	0.06	0.15	0.10	0.24	0.08	0.04	0.06
CaO	0.07	0.18	0.10	0.13	0.18	0.10	0.21	0.17	0.21	0.30	0.10	0.21
Na2O	4.33	4.25	4.21	4.11	3.92	4.36	4.17	3.98	4.01	4.35	4.35	3.94
K2O	4.12	4.52	4.94	4.54	4.89	4.45	4.97	4.93	5.01	4.85	4.51	4.63
P2O5	0.01	0.03	0.01	0.02	0.01	0.01	0.03	0.01	0.02	0.01	0.01	0.01
F	0.01	0.04	0.03	0.04	0.05	0.06	0.03	0.04	0.04	0.04	0.06	0.04
H2O+	0.46	0.56	0.77	0.59	1.07	0.51	0.59	0.52	0.77	0.46	0.49	0.49
H2O-	0.42	0.38	0.41	0.34	0.40	0.29	0.34	0.31	0.34	0.32	0.32	0.30
CO2	0.17	0.07	0.11	0.11	0.25	0.01	0.00	0.00	0.04	0.00	0.01	0.10
S	0.07	0.04	0.04	0.06	0.07	0.07	0.08	0.07	0.07	0.07	0.07	0.03
Total	100.21	99.58	101.05	100.62	100.58	100.26	100.22	100.37	100.51	100.31	100.23	99.57
A.I.	1.04	1.05	1.01	1.09	1.05	1.13	1.01	1.03	0.97	1.04	1.14	1.06
Cu	4	6	5	8	12	9	6	6	10	5	9	5
Pb	17	6	30	33	62	15	9	26	6	16	14	29
Zn	111	116	89	201	200	228	104	136	133	135	211	148
Ni	1	1	1	1	1	2	1	1	1	0	2	3
Ga	31	30	30	33	30	31	27	29	29	28	33	35
Sc	0.4	0.6	0.9	0.1	0.4	0.1	1.4	0.6	1.3	1	0.1	0.9
Nb	51	39	33	52	66	67	29	33	25	33	66	45
Zr	1141	924	664	1251	1466	1642	538	745	466	710	1537	906
Y	125	113	73	148	175	168	65	90	63	93	178	80
Ce	160	214	183	232	337	276	152	196	208	187	223	169
U	7	6	4	9	10	12	4	5	3	5	11	7
Th	19	8	10	20	26	23	1	13	1	5	20	27
Sr	9	9	4	5	5	4	18	9	15	13	4	10
Rb	152	126	114	193	198	201	98	143	95	113	216	152
Ba	37	79	66	15	49	16	167	74	144	134	12	50

Table B-3

Field No.	TS91015	TS91016A	TS91017	TS91018	TS91019	TS91021	TS91022	TS91023	TS91024	TS91025	TS91026	TS91027
SiO2	74.50	74.84	74.70	74.05	73.85	75.55	74.40	76.05	75.40	73.70	75.75	74.35
TiO2	0.27	0.24	0.25	0.26	0.25	0.23	0.30	0.20	0.21	0.27	0.23	0.26
Al2O3	11.82	12.15	12.16	12.29	12.43	11.95	12.38	12.11	12.32	12.59	11.26	12.04
Fe2O3	1.10	1.41	1.72	1.43	1.68	2.21	2.13	1.86	0.42	1.50	3.06	1.90
FeO	1.78	1.21	0.87	1.55	1.18	0.27	0.60	0.36	1.75	1.13	0.50	1.08
MnO	0.08	0.07	0.06	0.07	0.05	0.06	0.06	0.03	0.06	0.09	0.04	0.07
MgO	0.37	0.26	0.26	0.09	0.06	0.09	0.12	0.06	0.12	0.66	0.01	0.25
CaO	0.30	0.12	0.08	0.33	0.18	0.20	0.09	0.09	0.45	0.09	0.52	0.09
Na2O	4.12	4.20	4.17	4.28	4.23	3.71	4.01	3.61	3.59	4.30	3.97	3.86
K2O	4.71	4.89	4.98	4.95	5.05	4.21	3.93	4.51	3.98	4.28	3.87	4.91
P2O5	0.03	0.02	0.01	0.01	0.02	0.03	0.06	0.03	0.03	0.02	0.01	0.01
F	0.04	0.03	0.02	0.03	0.03	0.02	0.01	0.01	0.02	0.02	0.00	0.03
H2O+	0.67	0.77	0.61	0.54	1.06	0.86	0.92	0.95	0.80	0.93	0.18	0.78
H2O-	0.37	0.39	0.28	0.32	0.25	0.22	0.22	0.17	0.30	0.38	0.25	0.38
CO2	0.01	0.01	0.03	0.03	0.17	0.27	0.15	0.17	0.34	0.05	0.42	0.14
S	0.05	0.06	0.07	0.06	0.03	0.02	0.02	0.03	0.01	0.00	0.00	0.01
Total	100.22	100.66	100.27	100.29	100.52	99.90	99.40	100.24	99.80	100.01	100.07	100.16
A.I.	1.00	1.00	1.01	1.01	1.00	0.89	0.88	0.89	0.83	0.93	0.95	0.97
Cu	8	8	4	4	5	4	4	4	5	7	15	7
Pb	16	7	2	6	3	1	0	16	0	6	3	14
Zn	121	124	109	87	96	44	53	31	86	116	24	96
Ni	4	1	1	1	1	1	2	0	1	0	4	1
Ga	26	29	30	28	30	18	18	18	20	31	24	30
Sc	1.6	1	1	1.2	1.2	7	7.5	5.7	5.6	1.2	1.8	1
Nb	27	25	26	25	26	11	10	10	9	27	21	31
Zr	532	457	466	434	466	386	382	400	383	511	533	562
Y	74	62	61	50	47	39	32	26	42	81	73	69
Ce	172	202	180	138	147	112	120	132	154	176	138	157
U	3	3	3	2	3	3	2	3	3	4	3	4
Th	3	7	5	5	4	9	8	12	9	8	10	7
Sr	25	13	12	17	14	48	65	34	35	11	8	9
Rb	94	89	84	75	100	81	79	91	78	81	101	102
Ba	126	135	135	165	164	829	1013	783	779	118	820	118

Table B-4 Cape St. John Volcanic Suite Geochemical Analyses

Field No.	CJ90001	CJ90003	CJ90004	CJ90005	CJ90008	CJ90010	CJ90012	CJ90015	CJ90017	CJ90019	CJ90020	CJ90021	CJ90024
SiO2	74.45	75.05	74.45	76.85	75.65	76	76.7	68.2	71.7	69.55	69.05	75.75	70.55
TiO2	0.21	0.23	0.23	0.14	0.28	0.21	0.1	0.32	0.26	0.37	0.33	0.27	0.34
Al2O3	12.03	12.55	12.76	11.56	12.41	11.97	11.95	15.51	14.16	13.72	14.27	10.94	13.46
Fe2O3	1.84	1.99	1.4	0.97	0.5	1.44	0.83	3.31	0.96	2.03	1.33	0.41	2.46
FeO	0.87	0.7	1.43	1.1	1.52	0.96	0.67	0.43	1.57	1.89	1.61	1.72	0.23
MnO	0.07	0.05	0.06	0.04	0.05	0.04	0.01	0.05	0.02	0.06	0.06	0.06	0.05
MgO	0.02	0.02	0.02	0.02	0.26	0.13	0.21	0.2	0.18	0.38	0.32	0.22	0.41
CaO	0.26	0.04	0.05	0.02	0.43	0.09	0.26	0.77	0.29	1.29	1.71	1.32	2.07
Na2O	5.03	4.68	4.9	3.53	3.6	3.6	1.22	4.89	3.64	2.19	3.7	2.58	2.32
K2O	3.97	4.07	4.29	4.67	4.53	4.37	6.17	3.6	4.78	5.81	4.52	4.42	5.15
P2O5	0.01	0.01	0.01	0.01	0.04	0.05	0.02	0.06	0.04	0.1	0.08	0.07	0.09
F	0.01	0.01	0.02	0.01	0.02	0.01	0.03	0.02	0.01	0.06	0.03	0.02	0.04
H2O+	0.27	0.25	0.35	0.26	0.68	0.66	1.21	1.34	1.69	1.26	1.16	0.56	2.05
H2O-	0.23	0.21	0.26	0.2	0.22	0.19	0.11	0.13	0.36	0.37	0.23	0.25	0.23
CO2	0.13	0.09	0.15	0.06	0.35	0.17	0.33	0.72	0.37	0.45	1.32	1.12	1.6
%S	0.00	0.00	0.00	0.00	0.00	0.00	0.00	0.00	0.41	0.00	0.00	0.00	0.00
Total	99.4	99.95	100.38	99.44	100.54	99.89	99.82	99.55	100.44	99.53	99.72	99.71	101.05
A.I.	1.04	0.96	1.00	0.94	0.87	0.89	0.73	0.77	0.79	0.72	0.77	0.83	0.70
Cu	3	1	1	12	12	269	14	2	11	11	12	10	2
Pb	13	14	16	98	42	14	29	11	33	18	17	12	18
Zn	144	86	108	89	69	24	124	72	76	68	51	40	52
Ni	3	1	5	8	5	4	6	3	1	4	2	4	3
Ga	27	28	29	25	20	19	29	21	27	20	17	10	19
Sc	1.2	1.3	1.4	0.6	2.3	3.3	1.2	9.4	7.5	7.7	7.8	6.3	7.1
Nb	37	35	40	35	21	25	33	28	25	22	23	19	20
Zr	576	692	624	637	362	529	305	624	603	349	355	279	359
Y	40	45	32	80	52	61	73	27	46	48	47	38	42
Ce	75	95	54	157	124	142	142	121	153	106	114	84	95
U	3	3	2	5	3	3	4	5	13	4	5	4	5
Th	14	18	21	25	25	15	29	17	17	20	20	17	14
Sr	8	7	5	24	43	40	50	72	40	162	105	101	134
Rb	105	105	110	120	115	105	200	110	150	195	140	105	105
Ba	412	684	600	140	343	739	204	600	1052	1065	772	742	863

Table B-4

Field No.	CJ90026	CJ90027	CJ90029	CJ90030	CJ90032	CJ90035	CJ90037	CJ90038	CJ90039	CJ90043A	CJ90044	CJ90046	CJ90048
SiO2	70.65	63.2	76.95	74.65	74.9	79.55	77.6	74.6	78.6	75.275	74.8	74.1	73.65
TiO2	0.49	0.61	0.11	0.19	0.15	0.1	0.14	0.14	0.11	0.165	0.18	0.29	0.31
Al2O3	12.71	13.28	12.32	12.83	13.56	10.55	11.32	11.95	11.17	12.33	12.02	12.64	12.41
Fe2O3	1.55	2.34	1.04	0.44	0.58	1.32	1.65	1.77	1.21	0.665	0.03	1.3	1.23
FeO	2.17	2.64	0.2	1.52	0.79	0.47	0.69	0.93	0.87	1.245	1.91	1.54	0.58
MnO	0.07	0.12	0.02	0.04	0.01	0.02	0.03	0.04	0.02	0.04	0.05	0.06	0.05
MgO	1.06	1.18	0.09	0.39	0.1	0.03	0.11	0.11	0.05	0.415	0.47	0.38	0.2
CaO	1.71	4.84	0.22	0.59	0.06	0.41	0.11	0.82	0.09	0.675	0.63	0.84	1.74
Na2O	2.85	1.99	2.78	3.25	4.13	3.67	3.24	4.22	4.06	2.665	2.92	3.02	3.2
K2O	3.8	3.85	6.39	5.19	5.44	3.52	5.03	3.43	2.96	5.18	5.19	4.9	4.44
P2O5	0.08	0.13	0.01	0.03	0.05	0.01	0.02	0.01	0.01	0.025	0.02	0.06	0.07
F	0.03	0.03	0.02	0.03	0.02	0.01	0.02	0.01	0.01	0.015	0.02	0.03	0.01
H2O+	1.43	1.86	0.07	0.73	0.33	0	0.04	0.19	0.54	0.76	0.46	0.4	0.34
H2O-	0.15	0.22	0.19	0.21	0.21	0.17	0.46	0.38	0.25	0.285	0.27	0.2	0.2
CO2	1.02	3.53	0.12	0.21	0.12	0.38	0.13	0.7	0.09	0.1	0.49	0.19	0.92
%S	0.00	0.00	0.00	0.00	0.00	0.00	0.00	0.00	0.00	0	0.00	0.00	0.00
Total	99.77	99.82	100.53	100.3	100.45	100.21	100.59	99.3	100.04	99.84	99.46	99.95	99.35
A.I.	0.69	0.56	0.93	0.85	0.94	0.93	0.95	0.89	0.88	0.81	0.87	0.81	0.81
Cu	3	7	1	3	5	12	11		5	5	8	6	4
Pb	14	7	6	10	5	26	10		13	9	8	9	16
Zn	79	120	23	74	23	34	85		44	69	67	109	29
Ni	11	6	1	9	1	3	1		3	17	15	5	6
Ga	17	22	15	18	17	14	22		18	18	19	19	17
Sc	11.7	12.2	2.7	7.7	4.4	1	0.5		0.8	6.1	6.1	8	8.8
Nb	13	14	23	20	17	28	40		31	18	16	13	15
Zr	412	388	171	257	198	285	648	645	316	254	238	334	351
Y	37	34	57	59	24	58	79		62	56	51	39	42
Ce	168	178	94	200	87	127	150		109	165	170	205	182
U	2	2	5	4	4	4	2	4	4	2	3	2	3
Th	13	14	17	18	18	17	18		17	18	15	17	15
Sr	122	171	54	81	50	109	38		74	44	69	104	129
Rb	75	80	215	110	145	90	145	85	70	133	115	100	65
Ba	1581	1743	480	831	810	148	102		149	719	914	1769	1823

Table B-4

Field No.	CJ90050	CJ90052	CJ90054	CJ90056	CJ90058	CJ90060	CJ90063A	CJ90065R	CJ90067	CJ90069R	CJ90071	CJ90073R
SiO2	76.7	74.9	75	75.65	70.75	72.75	77.75	80.23	75.4	77.01	73.1	75.19
TiO2	0.09	0.19	0.13	0.21	0.6	0.24	0.255	0.08	0.11	0.09	0.28	0.15
Al2O3	11.87	12.08	11.96	11.99	12.45	11.98	10.79	10.19	12.29	11.93	12.73	12.8
Fe2O3	1.53	1.58	0.8	1.6	2.13	1.71	1.985	1.21	0.16	0.53	2.09	0.31
FeO	0	0.94	1.32	0.97	1.97	0.98	0	0	1.54	0.78	1.16	1.13
MnO	0.02	0.04	0.04	0.05	0.07	0.06	0.01	0.01	0.06	0.02	0.06	0.03
MgO	0.17	0.33	0.28	0.81	0.6	0.26	0.195	0.25	0.15	0.07	0.27	0.11
CaO	0.49	0.96	0.63	0.69	2.38	1.36	0.1	0.12	0.45	0.77	0.59	0.45
Na2O	3.35	3.49	3.14	2.71	3.57	2.68	2.64	2.66	2.59	4.07	3.16	3.56
K2O	4.41	4.59	4.82	4.43	3.47	4.81	4.385	3.81	5.74	3.32	4.96	4.89
P2O5	0.01	0.03	0.01	0.03	0.14	0.05	0.025	0	0.03	0	0.05	0.01
F	0.04	0.02	0.02	0.02	0.02	0.01	0.025	0.01	0.02	0.04	0.04	0.04
H2O+	0.23	0.35	0.3	0.69	0.5	1.01	0.985	0.76	0.81	0.56	0.96	0.63
H2O-	0.16	0.17	0.18	0.45	0.38	0.19	0.235	0.3	0.24	0.12	0.12	0.15
CO2	0	0.51	0.08	0	1.04	0.85	0.115	0.08	0.3	0.49	0.2	0.04
%S	0.00	0.00	0.00	0.00	0.00	0.00	0.435	0.00	0.00	0.09	0.03	0.00
Total	99.07	100.18	98.71	100.3	100.07	98.94	99.93	99.72	99.89	99.9	99.8	99.49
A.I.	0.87	0.89	0.87	0.77	0.77	0.80	0.84	0.83	0.85	0.86	0.83	0.87
Cu	12	4	7	7	9	8	5	4	4	9	4	5
Pb	37	1	22	9	6	6	21	8	9	9	7	12
Zn	36	45	59	74	43	42	24	28	50	40	63	39
Ni	6	6	8	25	8	3	1	1	5	6	1	3
Ga	20	16	19	18	19	15	13	10	19	24	17	18
Sc	7.7	6	6.1	6.6	10.6	8.3	5.8	2.1	2.6	2.3	8.6	4.5
Nb	31	13	19	15	14	14	20	20	33	25	26	25
Zr	112	238	187	297	353	323	322	132	165	150	461	233
Y	78	52	61	40	45	37	17	34	62	53	45	52
Ce	49	181	141	183	170	190	23	79	103	94	102	99
U	6	3	4	2	3	2	5	4	5	4	4	5
Th	22	13	20	13	8	10	14	15	14	18	13	20
Sr	30	52	51	65	158	82	49	38	31	32	72	35
Rb	170	95	120	100	70	100	133	115	190	100	160	165
Ba	90	702	545	970	1362	1621	621	111	296	306	865	561

Table B-5 Micmac Lake Geochemical Data

Field No.	ML90003	ML90004	ML90005	ML90006
SiO2	74.25	76.60	76.45	76.80
TiO2	0.19	0.18	0.17	0.18
Al2O3	13.04	10.87	10.78	10.69
Fe2O3	0.42	2.39	2.43	3.10
FeO	0.89	0.19	1.27	0.67
MnO	0.05	0.06	0.05	0.01
MgO	0.34	0.43	0.18	0.24
CaO	0.70	1.53	0.41	0.01
Na2O	3.82	1.50	3.86	2.37
K2O	4.10	3.04	4.18	5.17
P2O5	0.04	0.01	0.01	0.01
F	0.02	0.05	0.07	0.05
H2O+	0.64	1.33	0.15	0.78
H2O-	0.11	0.27	0.33	0.38
CO2	0.50	1.16	0.37	0.52
S	0.00	0.00	0.00	0.00
Total	99.11	99.61	100.71	100.98
A.I.	0.82	0.53	1.01	0.89
Cu	12	13	12	5
Pb	10	10	25	20
Zn	50	89	219	51
Ni	8	1	2	1
Sc	4.1	2.4	0.1	0.1
Ga	17	21	34	34
Nb	13	25	59	68
Zr	91	610	1419	1602
Y	23	68	158	117
Ce	54	162	247	179
U	5	3	9	7
Th	13	16	16	8
Sr	93	61	15	19
Rb	115	75	166	195
Ba	1025	665	27	90

Table B-6 Kings Point Complex Geochemical Data

Field No.	KP90002	KP90003	KP90004	KP90006	KP90007	KP90008	KP90009	KP90012	KP90013	KP90014R	KP90015R	KP90016
SiO2	73.90	73.65	75.10	76.45	74.90	72.75	71.90	74.30	75.00	76.90	74.93	74.70
TiO2	0.17	0.27	0.18	0.16	0.33	0.49	0.34	0.24	0.22	0.14	0.23	0.29
Al2O3	12.79	12.30	11.71	12.34	12.96	12.27	12.77	13.09	13.06	11.02	11.64	13.09
Fe2O3	0.91	1.47	0.92	0.19	0.51	2.40	0.62	0.06	0.65	1.65	1.60	0.84
FeO	0.99	1.45	1.38	1.25	0.82	1.96	2.90	1.38	0.85	1.05	1.30	0.79
MnO	0.04	0.07	0.04	0.03	0.03	0.10	0.09	0.03	0.03	0.03	0.05	0.03
MgO	0.34	0.05	0.06	0.20	0.35	0.40	0.05	0.27	0.21	0.18	0.05	0.25
CaO	0.31	0.35	0.27	0.51	0.86	0.83	0.68	0.57	0.35	0.32	0.31	0.43
Na2O	3.75	4.35	4.36	3.83	4.01	4.55	4.65	3.93	3.91	3.40	4.04	3.92
K2O	4.76	4.98	4.47	4.36	3.90	3.26	5.10	4.67	4.91	4.31	4.76	4.97
P2O5	0.05	0.05	0.04	0.06	0.11	0.15	0.07	0.06	0.03	0.02	0.04	0.05
F		0.02	0.03	0.01	0.02	0.03	0.02	0.02	0.01	0.19	0.02	0.02
H2O+		0.75	0.64	0.55	0.91	0.63	0.46	0.51	0.78	0.29	0.80	0.73
H2O-		0.21	0.16	0.34	0.34	0.29	0.54	0.57	0.51	0.34	0.45	0.41
CO2		0.06	0.04	0.02	0.11	0.05	0.06	0.06	0.10	0.07	0.13	0.11
S		0.01	0.00	0.01	0.00	0.01	0.01	0.00	0.00	0.00	0.00	0.00
Total		100.04	99.40	100.31	100.16	100.17	100.26	99.76	100.62	99.91	100.36	100.63
A.I.	0.88	1.02	1.03	0.89	0.83	0.90	1.03	0.88	0.90	0.93	1.01	0.90
Cu		3	3	3	6	3	6	2	3	4	4	3
Pb		16	4	11	1	2	9	10	13	31	16	7
Zn		96	113	11	27	48	91	20	27	50	99	28
Ni		1	1	1	1	1	1	1	1	0	1	1
Sc		1.6	1.1	1.9	3.3	13.2	1.9	3	2.2	0.6	0.9	3.1
Ga		26	23	12	9	20	26	17	20	29	29	19
Nb		32	18	8	6	22	24	11	10	23	29	10
Zr		492	448	107	154	530	414	201	202	930	504	247
Y		61	62	14	14	77	44	27	24	89	40	32
Ce		130	132	63	63	131	113	69	58	190	132	79
U		3	3	4	2	5	2	5	6	12	4	4
Th		8	13	18	14	13	7	23	23	31	9	17
Sr		19	9	59	122	61	20	65	65	46	9	60
Rb		75	90	115	95	70	75	175	155	330	95	160
Ba		177	612	624	834	990	225	488	421	23	114	453

Table B-6

Field No.	KP90017	KP90018	KP90020	KP90022	KP90024A	KP90025	KP90027	KP90028R	KP90030	KP90032A	KP90033
SiO2	72.70	75.35	82.25	67.85	76.98	69.30	79.40	68.84	75.50	66.78	67.45
TiO2	0.36	0.21	0.19	0.83	0.17	0.51	0.12	0.63	0.21	0.95	0.87
Al2O3	13.45	12.90	8.71	13.80	11.22	13.16	10.19	13.26	11.68	13.23	12.99
Fe2O3	0.76	0.45	1.12	1.72	1.92	1.48	0.52	3.17	1.97	2.08	2.76
FeO	1.23	0.77	0.00	2.19	0.94	3.28	1.83	1.63	0.89	3.74	2.98
MnO	0.04	0.02	0.03	0.11	0.02	0.17	0.01	0.11	0.03	0.15	0.13
MgO	0.49	0.24	0.48	1.09	0.02	0.38	0.07	0.54	0.39	1.04	0.86
CaO	0.97	0.24	0.54	2.30	0.43	1.07	0.05	0.85	0.11	1.88	1.70
Na2O	4.19	3.99	3.05	4.18	4.10	5.20	4.96	4.28	3.10	4.71	4.78
K2O	4.35	4.65	2.02	3.48	3.63	3.70	1.65	4.48	5.41	3.76	3.94
P2O5	0.08	0.04	0.09	0.26	0.04	0.10	0.02	0.14	0.03	0.29	0.25
F	0.07	0.01	0.02	0.06	0.01	0.03	0.00	0.03	0.01	0.05	0.05
H2O+	0.79	0.55	0.66	0.72	0.10	1.01	0.08	1.00	0.52	1.04	0.80
H2O-	0.27	0.27	0.43	0.45	0.26	0.33	0.13	0.53	0.30	0.56	0.29
CO2	0.24	0.12	0.14	0.10	0.11	0.43	0.11	0.11	0.10	0.12	0.10
S	0.00	0.00	0.00	0.00	0.00	0.00	0.00	0.00	0.00	0.00	0.00
Total	99.99	99.81	99.73	99.14	99.92	100.15	99.14	99.60	100.25	100.36	99.95
A.I.	0.86	0.90	0.83	0.77	0.95	0.95	0.98	0.90	0.94	0.89	0.93
Cu	24	3	11	4	5	6	6	6	9	10	6
Pb	19	0	8	14	0	0	23	0	0	10	10
Zn	45	42	33	74	40	116	44	107	123	136	137
Ni	5	1	4	6	1	4	5	1	5	5	2
Sc	4.3	2.4	2.1	10.8	0.4	5.1	0.4	6.3	0.6	9.5	8.6
Ga	17	17	9	21	28	31	23	29	32	31	28
Nb	10	10	4	11	34	28	37	23	31	24	28
Zr	215	195	98	309	973	378	721	328	614	518	569
Y	30	26	12	49	110	54	86	51	74	66	74
Ce	76	56	42	93	206	133	13	121	185	125	136
U	5	7	4	5	9	2	12	3	4	4	4
Th	21	26	12	17	25	8	22	4	10	7	7
Sr	82	48	74	202	48	77	21	95	12	132	99
Rb	140	160	60	115	95	55	30	75	105	75	85
Ba	488	380	525	634	282	530	71	436	314	495	371

Table B-6

Field No.	KP90034	KP90035R	KP90036R	KP90037R	KP90039	KP90040	KP90041	KP90042	KP90043	KP90044	KP90045
SiO2	66.30	76.75	66.68	66.10	75.40	66.45	66.80	44.00	66.55	72.50	75.95
TiO2	0.87	0.19	0.85	0.91	0.18	0.88	0.86	2.70	0.90	0.48	0.18
Al2O3	12.92	10.41	12.68	12.83	10.72	13.00	12.83	16.67	13.16	11.85	10.46
Fe2O3	2.86	2.85	3.10	2.86	1.76	2.81	2.44	3.85	2.54	2.25	2.50
FeO	2.65	1.11	2.45	2.75	1.60	3.01	3.14	8.91	3.19	2.01	1.55
MnO	0.11	0.03	0.12	0.12	0.05	0.13	0.12	0.20	0.13	0.09	0.06
MgO	0.76	0.07	0.78	0.80	0.03	0.99	1.09	6.44	0.96	0.47	0.02
CaO	2.28	0.09	2.07	2.20	0.43	1.87	1.75	9.07	1.99	0.78	0.23
Na2O	4.66	3.12	4.76	4.81	3.33	4.60	4.76	2.87	4.77	4.44	4.22
K2O	3.62	3.90	3.59	3.54	4.55	4.87	3.87	0.95	3.73	4.06	4.54
P2O5	0.24	0.01	0.24	0.28	0.04	0.27	0.23	0.53	0.26	0.11	0.03
F	0.15	0.01	0.12	0.10	0.05	0.14	0.07	0.12	0.07	0.05	0.02
H2O+	0.86	0.67	0.77	1.03	0.46	0.88	1.13	3.21	1.23	0.86	0.38
H2O-	0.54	0.48	0.28	0.58	0.51	0.55	0.49	0.66	0.44	0.51	0.32
CO2	1.36	0.05	1.26	0.81	0.66	0.04	0.51	0.02	0.56	0.05	0.01
S	0.00	0.00	0.00	0.01	0.00	0.00	0.00	0.15	0.01	0.01	0.01
Total	100.18	99.74	99.76	99.72	99.77	100.49	100.09	100.35	100.49	100.52	100.48
A.I.	0.90	0.90	0.92	0.92	0.97	0.99	0.94	0.34	0.90	0.99	1.13
Cu	10	8	8	7	9	11	8	45	9	7	5
Pb	10	3	12	0	4	11	1	0	10	22	26
Zn	127	118	127	116	172	117	124	164	133	120	216
Ni	2	6	9	5	1	5	0	116	4	0	0
Sc	8.3	0.1	8.2	8.9	0.2	8.7	8.7	31.5	9.4	3.8	0.1
Ga	29	35	29	29	35	28	30	26	31	27	30
Nb	23	71	24	24	57	26	26	1	28	42	69
Zr	541	1569	544	503	1288	530	538	178	532	834	1546
Y	55	182	61	65	147	66	73	31	71	93	157
Ce	131	329	133	118	246	127	132	44	130	184	279
U	4	11	4	3	8	3	4	0	3	6	11
Th	9	31	7	8	25	8	10	0	9	14	29
Sr	97	9	114	114	15	153	112	336	113	46	22
Rb	75	150	85	60	160	105	85	35	70	100	180
Ba	348	47	432	372	51	454	451	290	547	186	33

Table B-6

Field No.	KP90046	KP90047	KP90048	KP90049	KP90051	KP90052	KP90054	KP90055A	KP90057	KP90058	KP90059
SiO2	74.95	66.50	76.85	77.40	75.05	77.10	77.20	80.33	59.80	78.20	77.15
TiO2	0.22	0.89	0.19	0.16	0.36	0.15	0.14	0.17	0.89	0.11	0.15
Al2O3	11.42	13.00	10.85	11.00	11.06	11.31	10.69	8.81	16.55	10.83	11.24
Fe2O3	1.55	4.62	2.01	1.43	1.36	1.87	0.90	1.44	1.86	2.23	1.88
FeO	1.19	1.33	0.51	1.29	2.31	0.55	1.08	0.00	3.51	0.00	0.37
MnO	0.06	0.10	0.04	0.05	0.06	0.01	0.03	0.01	0.10	0.04	0.02
MgO	0.05	0.96	0.79	0.05	0.49	0.02	0.18	0.01	2.48	0.21	0.15
CaO	0.30	1.74	0.04	0.11	0.49	0.03	0.06	0.03	4.07	0.04	0.04
Na2O	3.97	3.90	3.07	3.97	4.58	3.25	0.95	0.24	4.65	3.75	1.54
K2O	4.68	4.65	4.51	4.34	2.14	5.18	7.04	7.48	2.41	3.28	5.99
P2O5	0.05	0.25	0.05	0.02	0.12	0.02	0.05	0.02	0.30	0.01	0.01
F	0.04	0.05	0.01	0.01	0.06	0.00	0.01	0.00	0.04	0.01	0.03
H2O+	0.42	1.03	0.52	0.14	0.78	0.31	0.99	0.76	2.07	0.73	1.35
H2O-	0.24	0.58	0.48	0.44	0.52	0.38	0.41	0.25	0.23	0.22	0.29
CO2	0.10	0.83	0.00	0.02	0.18	0.05	0.05	0.04	0.93	0.07	0.29
S	0.00	0.00	0.00	0.02	0.13	0.00	0.00	0.39	0.01	0.26	0.02
Total	99.24	100.43	99.92	100.45	99.69	100.23	99.78	99.94	99.90	99.99	100.52
A.I.	1.02	0.88	0.92	1.02	0.89	0.97	0.86	0.96	0.62	0.90	0.80
Cu	3	4	3	7	9	8	3	5	28	24	5
Pb	14	5	0	24	8	28	20	20	0	7	16
Zn	131	108	136	140	120	80	78	35	73	49	101
Ni	0	0	2	0	2	0	1	0	12	10	0
Sc	0.6	8.5	1.1	0.4	3.8	0.5	0.9	1.5	13.9	0.6	1
Ga	28	28	24	27	28	29	20	15	20	23	26
Nb	35	28	28	40	35	40	30	22	7	34	32
Zr	642	576	612	1072	890	835	537	467	170	621	567
Y	82	68	70	152	118	98	88	52	22	83	88
Ce	191	125	130	193	137	154	105	53	77	107	152
U	4	4	5	6	6	9	8	4	2	11	2
Th	12	9	18	22	17	26	21	12	3	31	16
Sr	14	89	30	10	172	11	48	22	485	22	42
Rb	100	105	120	155	50	215	205	258	40	105	160
Ba	94	407	206	252	388	28	502	805	1034	142	457

Table B-6

Field No.	KP90060	KP90061	KP90063	KP90064	KP90065	KP90066	KP90068	KP90069	KP90070	KP90071	KP90072	KP90073
SiO2	76.25	78.20	67.15	72.05	75.55	73.55	75.55	77.10	76.85	75.50	74.45	68.30
TiO2	0.13	0.13	0.90	0.30	0.18	0.28	0.24	0.10	0.07	0.21	0.23	0.80
Al2O3	11.49	10.79	13.17	12.40	10.61	12.27	10.90	11.67	11.76	11.27	11.54	13.04
Fe2O3	0.71	1.59	3.06	2.05	1.75	1.59	1.59	0.92	1.33	1.68	1.23	2.81
FeO	1.39	0.58	2.76	1.66	1.65	1.71	1.65	0.93	0.46	1.12	1.51	2.67
MnO	0.02	0.02	0.14	0.09	0.06	0.07	0.08	0.03	0.01	0.07	0.06	0.14
MgO	0.02	0.04	0.77	0.10	0.05	0.10	0.07	0.35	0.03	0.05	0.04	0.73
CaO	0.04	0.01	2.01	0.37	0.13	0.35	0.23	0.24	0.03	0.16	0.15	1.35
Na2O	3.36	4.61	4.55	4.28	3.95	4.32	3.48	2.57	4.35	3.90	3.97	4.54
K2O	4.63	2.50	3.63	4.97	4.29	4.89	4.03	5.05	3.72	4.59	4.67	4.09
P2O5	0.01	0.01	0.24	0.04	0.01	0.03	0.02	0.01	0.01	0.01	0.01	0.21
F	0.02	0.08	0.05	0.03	0.05	0.03	0.02	0.02	0.01	0.01	0.01	0.06
H2O+	0.57	0.37	1.00	0.65	0.46	0.78	0.49	0.51	0.30	0.42	0.43	0.81
H2O-	0.24	0.26	0.41	0.56	0.26	0.42	0.34	0.26	0.20	0.29	0.26	0.34
CO2	0.22	0.24	0.60	0.13	0.10	0.09	0.09	0.06	0.07	0.10	0.10	0.26
S	0.16	0.01	0.02	0.01	0.00	0.02	0.01	0.00	0.01	0.00	0.02	0.03
Total	99.26	99.44	100.46	99.69	99.10	100.50	98.79	99.82	99.21	99.38	98.68	100.18
A.I.	0.92	0.95	0.87	1.00	1.05	1.01	0.93	0.83	0.95	1.01	1.00	0.91
Cu	7	5	9	7	6	4	4	7	4	4	7	8
Pb	0	0	10	4	19	3	8	18	0	16	7	15
Zn	13	13	175	96	189	103	114	62	11	98	86	124
Ni	1	3	3	0	0	1	0	5	2	1	0	1
Sc	3.9	0.5	9.7	2.2	0.2	1.5	1.1	7.9	0.3	0.9	1.1	8.5
Ga	19	23	30	31	34	28	29	21	27	29	27	31
Nb	21	29	26	28	59	28	32	27	45	31	28	27
Zr	459	688	531	431	1260	471	659	139	549	610	481	524
Y	50	76	76	51	101	57	52	52	108	57	49	70
Ce	99	98	132	136	243	138	173	76	73	182	141	145
U	6	6	3	3	8	3	4	4	13	4	3	3
Th	14	20	8	8	23	9	12	14	42	13	9	12
Sr	12	19	137	25	10	19	13	78	9	14	14	102
Rb	115	50	65	70	150	70	90	185	185	95	80	75
Ba	586	84	411	312	55	203	107	346	42	131	122	685

Table B-6

Field No.	KP90074	KP90076	KP90077	KP90079R	KP90080A	KP90081	KP90082	KP90083	KP90084	KP90085	KP90086
SiO2	78.00	75.85	67.35	67.48	66.85	66.00	73.20	65.65	75.90	75.50	73.50
TiO2	0.15	0.17	0.85	0.87	0.92	0.97	0.27	1.13	0.23	0.22	0.27
Al2O3	10.80	10.24	13.35	12.96	12.96	13.01	12.13	13.46	11.00	11.40	12.89
Fe2O3	0.05	2.27	4.15	3.15	2.52	1.87	2.42	5.66	2.31	1.90	0.81
FeO	1.60	1.13	0.28	2.46	3.39	4.00	0.97	0.67	0.93	1.20	0.80
MnO	0.03	0.04	0.09	0.11	0.13	0.14	0.07	0.11	0.02	0.03	0.03
MgO	0.04	0.07	0.71	0.86	0.94	1.15	0.08	1.58	0.04	0.06	0.31
CaO	0.19	0.56	1.95	1.70	2.03	1.93	0.33	1.12	0.26	0.19	0.60
Na2O	4.17	3.34	5.28	4.50	4.60	4.04	3.68	4.67	3.66	3.90	3.95
K2O	2.93	3.74	3.49	3.86	3.96	4.45	5.29	3.56	4.25	4.28	4.73
P2O5	0.01	0.02	0.21	0.23	0.26	0.28	0.01	0.28	0.01	0.01	0.01
F	0.01	0.00	0.04	0.06	0.07	0.05	0.01	0.06	0.00	0.01	0.02
H2O+	1.07	0.98	0.95	1.31	0.73	1.06	0.40	0.98	0.47	0.36	0.67
H2O-	0.30	0.26	0.31	0.24	0.31	0.28	0.14	0.42	0.28	0.35	0.36
CO2	0.24	0.54	1.33	0.02	0.03	0.31	0.13	0.14	0.21	0.05	0.06
S	0.00	0.00	0.00	0.00	0.02	0.00	0.00	0.00	0.00	0.00	0.00
Total	99.59	99.21	100.34	99.80	99.66	99.54	99.13	99.49	99.57	99.46	99.01
A.I.	0.93	0.93	0.93	0.89	0.91	0.88	0.97	0.86	0.97	0.97	0.90
Cu	7	9	2	7	10	10	6	7	8	13	10
Pb	0	12	0	6	7	3	4	7	9	5	6
Zn	52	97	99	86	110	119	105	157	37	89	27
Ni	4	1	2	0	3	0	1	1	5	5	8
Sc	0.9	0.1	8.1	8.9	9.5	9.6	1.2	11.7	0.7	0.7	3.8
Ga	25	31	33	31	27	27	32	30	27	32	18
Nb	28	66	29	27	25	21	29	23	42	41	12
Zr	712	1541	581	537	544	439	486	481	768	752	193
Y	78	196	60	69	75	60	68	64	96	99	30
Ce	166	284	129	129	140	118	170	124	215	226	73
U	7	11	4	4	4	3	3	3	5	5	5
Th	18	27	8	9	8	7	9	5	16	16	22
Sr	10	10	86	123	149	163	30	126	17	14	103
Rb	75	125	70	75	80	90	70	70	105	100	170
Ba	54	33	318	366	447	534	219	354	129	103	534

Table B-6

Field No.	KP90087	KP90089R	KP90091	KP90092	KP90093	KP90094	KP90095	KP90097	KP90098	KP90100A	KP90101
SiO2	73.60	69.66	77.10	75.80	74.95	65.95	72.15	72.55	67.30	72.35	66.20
TiO2	0.33	0.71	0.20	0.23	0.23	0.97	0.32	0.29	0.88	0.50	0.86
Al2O3	13.35	12.56	10.91	11.52	11.83	12.97	13.12	12.18	13.01	11.79	12.60
Fe2O3	0.79	3.27	2.17	1.77	1.66	3.55	2.80	2.58	2.85	1.92	2.33
FeO	1.07	1.90	0.61	1.11	1.03	2.79	0.81	0.84	2.85	1.83	2.98
MnO	0.04	0.13	0.04	0.07	0.06	0.15	0.05	0.07	0.11	0.07	0.09
MgO	0.45	0.76	0.08	0.06	0.09	0.97	0.17	0.70	0.11	0.55	1.17
CaO	0.89	2.02	0.13	0.28	0.13	2.12	0.26	0.52	1.74	0.90	2.50
Na2O	4.00	3.62	2.91	3.97	3.91	4.11	4.07	3.21	4.69	4.06	4.30
K2O	4.48	4.12	5.12	4.85	4.52	3.88	5.17	5.42	3.79	3.97	3.26
P2O5	0.06	0.22	0.01	0.01	0.01	0.26	0.01	0.01	0.22	0.11	0.22
F	0.03	0.06	0.00	0.02	0.01	0.10	0.01	0.01	0.06	0.06	0.05
H2O+	1.04	0.57	0.40	0.52	0.63	1.80	0.53	0.71	0.95	0.61	1.23
H2O-	0.37	0.26	0.18	0.22	0.28	0.24	0.24	0.48	0.46	0.28	0.34
CO2	0.06	0.04	0.02	0.05	0.06	0.00	0.04	0.35	0.08	0.20	1.31
S	0.00	0.00	0.00	0.00	0.00	0.02	0.01	0.02	0.02	0.01	0.00
Total	100.56	99.90	99.88	100.48	99.40	99.88	99.76	99.94	99.12	99.18	99.44
A.I.	0.86	0.83	0.95	1.02	0.96	0.84	0.94	0.92	0.91	0.93	0.84
Cu	9	3	3	4	8	8	7	3	8	5	26
Pb	14	10	7	7	14	9	2	0	6	56	20
Zn	30	94	83	108	88	147	76	139	99	96	138
Ni	8	9	5	3	6	6	8	6	6	8	4
Sc	4	14.3	2.3	0.7	0.8	10.3	2.2	1.8	9	5	9
Ga	20	25	22	30	30	33	28	28	27	23	27
Nb	13	20	28	35	32	28	27	25	28	56	24
Zr	236	456	596	589	534	550	462	376	548	982	494
Y	30	69	77	77	71	74	66	53	75	110	70
Ce	74	124	128	201	180	127	163	113	139	224	132
U	5	5	3	4	4	3	3	2	3	11	3
Th	23	10	16	12	13	8	9	7	12	35	10
Sr	104	156	26	19	14	143	30	28	122	55	85
Rb	145	100	145	85	80	75	75	95	75	80	65
Ba	540	1143	677	118	220	436	258	343	358	260	293

Table B-6

Field No.	KP90107R	KP90108	KP90109	KP90110	KP90112	KP90113	KP90115	KP90116	KP90117	KP90119	KP90120A
SiO2	75.49	77.05	85.20	76.40	79.35	77.60	77.75	74.40	74.50	75.90	75.39
TiO2	0.11	0.12	0.08	0.13	0.11	0.19	0.08	0.22	0.27	0.20	0.18
Al2O3	11.90	11.46	6.60	11.80	10.59	10.89	11.75	11.67	11.91	10.95	10.56
Fe2O3	1.11	1.38	0.73	1.40	1.28	0.43	0.56	1.72	2.11	1.27	1.70
FeO	1.11	0.78	0.58	0.53	0.37	1.85	0.90	1.32	0.48	1.48	2.15
MnO	0.02	0.03	0.02	0.03	0.02	0.05	0.03	0.05	0.05	0.05	0.06
MgO	0.04	0.08	0.09	0.09	0.02	0.40	0.41	0.03	0.11	0.02	0.07
CaO	0.17	0.08	0.02	0.07	0.04	0.18	0.26	0.17	0.38	0.18	0.16
Na2O	3.70	4.16	0.72	3.34	4.51	3.07	2.38	4.24	3.41	4.04	4.35
K2O	4.53	3.61	4.00	4.44	2.37	3.80	4.92	4.55	5.17	4.49	4.44
P2O5	0.00	0.01	0.01	0.01	0.01	0.02	0.01	0.01	0.03	0.01	0.01
F	0.04	0.01	0.01	0.01	0.00	0.01	0.03	0.01	0.01	0.03	0.08
H2O+	0.35	0.26	0.65	0.54	0.05	0.80	0.76	0.37	0.42	0.58	0.42
H2O-	0.16	0.15	0.19	0.13	0.25	0.30	0.24	0.31	0.27	0.13	0.13
CO2	0.04	0.04	0.34	0.04	0.03	0.24	0.04	0.09	0.25	0.05	0.03
S	0.03	0.00	0.03	0.00	0.00	0.03	0.00	0.01	0.00	0.02	0.01
Total	98.81	99.22	99.27	98.96	99.00	99.86	100.12	99.17	99.37	99.40	99.71
A.I.	0.92	0.94	0.84	0.87	0.94	0.84	0.79	1.02	0.94	1.05	1.13
Cu	7	6	5	3	1	3	9	6	4	4	7
Pb	42	0	45	7	0	0	14	11	46	7	30
Zn	119	50	54	45	34	70	54	103	58	127	264
Ni	4	7	5	4	3	8	16	6	5	9	4
Sc	0.5	2.6	2.7	3.8	3.2	3.5	7.5	0.7	2.9	0.5	0.2
Ga	27	19	14	23	22	20	23	28	24	32	34
Nb	37	17	16	20	16	21	24	29	24	40	72
Zr	601	362	241	368	335	419	122	544	517	790	1577
Y	165	47	25	64	51	48	49	61	62	62	212
Ce	189	92	50	117	87	65	55	148	127	153	288
U	12	4	48	4	6	4	3	3	4	4	12
Th	42	14	12	20	17	14	14	10	13	16	29
Sr	14	31	29	20	18	63	50	9	21	5	5
Rb	260	80	120	140	55	95	180	85	115	115	210
Ba	21	511	499	643	223	630	198	101	227	48	9

Table B-6

Field No.	KP90121R	KP90122	KP90123	KP90124	KP90125	KP90126	KP90127	KP90128	KP90130	KP90131	KP90132
SiO2	76.33	77.10	76.45	73.95	75.40	75.55	75.90	75.50	68.55	68.30	44.40
TiO2	0.17	0.18	0.16	0.17	0.18	0.23	0.20	0.24	0.83	0.80	2.40
Al2O3	11.14	11.15	11.43	10.40	10.47	11.55	11.49	11.88	13.04	13.21	16.24
Fe2O3	3.58	0.86	2.00	2.71	2.22	1.06	1.92	2.08	5.82	5.20	3.21
FeO	0.00	2.15	0.90	0.76	1.79	1.85	0.84	0.93	0.00	0.00	7.76
MnO	0.02	0.04	0.03	0.12	0.06	0.06	0.02	0.04	0.14	0.10	0.22
MgO	0.02	0.05	0.09	0.46	0.03	0.04	0.18	0.39	0.98	0.76	7.15
CaO	0.15	0.11	0.31	1.96	0.15	0.18	0.07	0.11	1.24	1.63	9.04
Na2O	4.03	3.66	3.47	2.85	4.33	3.87	3.64	3.59	4.02	4.62	2.06
K2O	3.77	4.09	4.85	4.86	4.46	4.57	4.57	4.21	4.49	3.79	1.29
P2O5	0.03	0.01	0.01	0.01	0.01	0.02	0.02	0.01	0.22	0.21	0.34
F	0.00	0.03	0.07	0.03	0.05	0.01	0.03	0.01	0.06	0.04	0.03
H2O+	0.47	0.56	0.48	0.46	0.35	0.63	0.42	0.67	0.70	0.77	4.41
H2O-	0.13	0.16	0.21	0.19	0.16	0.26	0.24	0.17	0.30	0.24	0.23
CO2	0.08	0.00	0.07	1.44	0.01	0.04	0.04	0.02	0.08	0.76	1.35
S	0.00	0.15	0.02	0.00	0.00	0.00	0.01	0.01	0.00	0.01	0.06
Total	99.92	100.30	100.55	100.37	99.67	99.92	99.59	99.86	100.47	100.44	100.19
A.I.	0.96	0.94	0.96	0.96	1.14	0.98	0.95	0.88	0.88	0.89	0.29
Cu	4	7	5	4	9	7	7	9	8	2	49
Pb	7	11	20	17	26	4	2	4	7	7	0
Zn	387	204	188	195	222	80	63	91	129	96	95
Ni	4	4	2	5	8	1	1	9	5	7	85
Sc	0.3	0.4	0.8	0.2	0.2	0.9	0.7	0.9	7.7	7.4	27.8
Ga	32	32	26	30	33	29	27	28	27	27	31
Nb	49	45	29	54	63	27	34	24	23	24	11
Zr	1089	1125	910	1333	1481	553	680	529	606	593	165
Y	148	136	100	156	169	54	72	54	62	66	24
Ce	232	224	216	231	254	139	144	162	124	127	35
U	6	11	10	9	11	3	5	4	3	4	0
Th	66	21	23	27	29	9	14	9	9	12	0
Sr	18	14	33	22	6	11	13	27	135	91	407
Rb	125	150	185	185	200	85	105	65	110	75	30
Ba	33	29	52	34	14	108	89	140	347	330	162

Table B-6

Field No.	KP90133	KP90135	KP90136	KP90138A	KP90139R	KP90140	KP90142	KP90143	KP90144	KP90146R	KP90147R
SiO2	71.05	75.20	74.00	76.28	75.09	76.90	75.90	75.50	76.35	75.62	66.47
TiO2	0.46	0.25	0.28	0.21	0.23	0.19	0.22	0.22	0.23	0.23	0.91
Al2O3	12.46	11.82	12.26	11.67	11.38	10.69	11.60	11.81	11.71	11.96	13.41
Fe2O3	4.46	1.29	1.91	1.73	1.35	2.10	2.26	3.02	2.85	1.45	3.78
FeO	0.00	1.45	1.43	1.03	1.68	1.10	0.70	0.00	0.00	1.03	2.11
MnO	0.07	0.07	0.06	0.06	0.04	0.01	0.03	0.02	0.01	0.04	0.13
MgO	0.40	0.11	0.14	0.02	0.25	0.01	0.10	0.07	0.03	0.08	0.79
CaO	1.15	0.56	0.77	0.24	0.48	0.01	0.21	0.48	0.19	0.18	2.04
Na2O	4.17	3.76	4.00	3.92	2.73	3.57	3.72	4.33	3.70	3.58	4.48
K2O	4.34	4.36	4.27	4.52	5.73	4.27	4.68	3.64	4.30	5.05	3.85
P2O5	0.08	0.02	0.02	0.01	0.03	0.01	0.01	0.01	0.01	0.01	0.24
F	0.02	0.02	0.01	0.01	0.03	0.00	0.01	0.00	0.01	0.01	0.04
H2O+	0.58	0.51	0.57	0.32	0.53	0.51	0.54	0.68	0.62	0.77	1.40
H2O-	0.28	0.14	0.15	0.12	0.34	0.15	0.23	0.15	0.13	0.23	0.37
CO2	0.67	0.36	0.63	0.23	0.18	0.08	0.09	0.46	0.13	0.07	0.11
S	0.02	0.01	0.00	0.00	0.03	0.00	0.00	0.00	0.00	0.00	0.00
Total	100.21	99.93	100.50	100.34	100.10	99.60	100.30	100.40	100.27	100.31	100.14
A.I.	0.93	0.92	0.91	0.97	0.94	0.98	0.96	0.94	0.92	0.95	0.86
Cu	8	7	37	15	18	10	23	3	5	3	5
Pb	0	22	0	10	14	37	0	0	0	1	10
Zn	61	141	51	93	72	160	80	18	26	50	114
Ni	7	4	6	3	4	4	2	5	4	3	7
Sc	4.1	1.2	1.3	0.7	1.1	0.1	0.7	0.7	0.7	0.8	8.5
Ga	28	32	35	29	26	35	30	29	23	25	25
Nb	32	28	33	22	35	63	29	26	28	31	24
Zr	632	482	682	592	797	1549	579	515	585	611	474
Y	74	67	82	39	95	104	87	55	72	63	57
Ce	181	181	184	169	190	193	223	176	139	152	126
U	4	3	5	4	6	10	4	3	4	4	3
Th	12	11	14	9	14	30	10	8	8	8	5
Sr	60	22	28	11	89	11	19	17	29	25	151
Rb	55	65	80	88	135	155	85	55	85	100	55
Ba	317	200	193	84	153	17	117	250	174	177	411

Table B-6

Field No.	KP90148	KP90150R	KP90151	KP90153	KP90154	KP90155R	KP90159R	KP90160R	KP90161	KP90162A	KP90163A
SiO2	74.05	75.54	75.50	75.95	75.55	76.02	75.52	76.02	76.05	75.48	75.98
TiO2	0.29	0.23	0.20	0.21	0.22	0.23	0.17	0.18	0.18	0.22	0.18
Al2O3	11.90	11.92	12.94	11.14	11.79	11.75	10.47	10.62	12.43	12.66	10.56
Fe2O3	1.25	2.11	0.34	2.12	2.28	1.27	1.36	0.13	1.60	1.49	1.89
FeO	1.61	0.59	1.04	1.37	0.68	1.26	1.98	3.19	0.00	0.00	2.98
MnO	0.07	0.05	0.02	0.05	0.04	0.03	0.06	0.04	0.02	0.03	0.07
MgO	0.18	0.08	0.13	0.05	0.06	0.10	0.19	0.06	0.07	0.16	0.05
CaO	0.47	0.20	0.29	0.06	0.05	0.05	0.85	0.72	0.74	0.70	0.28
Na2O	3.73	3.99	3.85	3.82	3.92	3.69	2.99	2.93	3.73	4.06	3.72
K2O	4.72	4.45	5.29	4.51	4.70	4.36	4.50	3.73	4.75	3.70	3.65
P2O5	0.04	0.03	0.02	0.01	0.01	0.02	0.02	0.01	0.01	0.03	0.01
F	0.03	0.02	0.03	0.02	0.01	0.00	0.01	0.04	0.11	0.02	0.01
H2O+	0.75	0.75	0.56	0.66	0.60	0.95	0.79	0.98	0.75	0.81	0.62
H2O-	0.24	0.20	0.34	0.29	0.21	0.19	0.34	0.15	0.17	0.30	0.15
CO2	0.07	0.09	0.08	0.12	0.08	0.11	0.76	0.61	0.42	0.52	0.29
S	0.01	0.00	0.00	0.01	0.00	0.04	0.00	0.01	0.02	0.30	0.42
Total	99.41	100.24	100.63	100.39	100.20	100.08	100.00	99.41	101.05	100.45	100.84
A.I.	0.94	0.95	0.93	1.00	0.98	0.92	0.93	0.83	0.91	0.84	0.95
Cu	7	3	5	11	12	12	13	13	15	16	24
Pb	23	10	18	20	20	37	22	6	0	13	0
Zn	57	112	17	116	93	183	208	111	14	20	198
Ni	3	2	2	2	6	4	1	1	6	5	4
Sc	2.6	0.7	2	0.5	0.7	0.5	0.1	0.1	1.8	3.1	0.1
Ga	23	24	18	27	27	27	27	31	19	16	29
Nb	25	28	11	37	29	30	50	56	11	10	53
Zr	543	538	199	877	608	711	1365	1330	166	179	1294
Y	45	66	30	95	66	76	150	148	26	27	154
Ce	115	186	73	203	155	202	243	248	84	77	246
U	4	4	7	6	4	5	10	6	7	8	8
Th	12	7	22	12	10	11	24	27	20	21	26
Sr	40	21	39	11	13	11	22	11	24	49	14
Rb	100	75	175	105	90	105	165	130	125	108	115
Ba	295	120	359	66	108	87	47	20	292	435	30

Table B-6

Field No.	KP90164A	KP90165	KP90167A	KP90169	KP90170	KP90171	KP90172	KP90173	KP90174	KP91001	KP91003
SiO2	73.63	76.70	76.92	76.70	76.15	76.60	76.45	76.95	76.85	73.65	75.90
TiO2	0.30	0.18	0.19	0.17	0.18	0.18	0.21	0.19	0.20	0.25	0.19
Al2O3	12.57	10.74	10.73	10.71	10.74	10.69	11.09	10.98	11.38	12.23	10.75
Fe2O3	1.53	2.43	2.37	1.71	2.73	1.94	1.36	0.51	0.99	3.01	1.74
FeO	1.84	0.99	1.10	1.88	1.15	1.38	1.91	2.66	1.68	0.37	1.91
MnO	0.06	0.01	0.07	0.06	0.05	0.03	0.11	0.04	0.04	0.04	0.06
MgO	0.13	0.03	0.05	0.04	0.01	0.02	0.05	0.05	0.07	0.43	0.09
CaO	0.50	0.08	0.18	0.24	0.01	0.04	0.26	0.10	0.28	0.38	0.10
Na2O	3.91	3.45	2.96	4.11	3.56	4.12	4.21	3.34	3.43	3.69	4.19
K2O	5.08	4.35	5.26	4.19	4.40	4.49	3.18	4.78	4.80	5.02	4.53
P2O5	0.03	0.01	0.01	0.01	0.01	0.01	0.02	0.01	0.01	0.02	0.01
F	0.01	0.04	0.01	0.04	0.01	0.02	0.01	0.00	0.01	0.02	0.04
H2O+	0.64	0.62	0.32	0.45	0.61	0.45	0.70	0.39	0.55	0.46	0.24
H2O-	0.17	0.40	0.39	0.38	0.33	0.32	0.16	0.29	0.27	0.26	0.24
CO2	0.37	0.08	0.50	0.13	0.12	0.04	0.21	0.09	0.24	0.39	0.15
S	0.04	0.02	0.00	0.00	0.01	0.00	0.00	0.00	0.00	0.00	0.00
Total	100.79	100.13	101.04	100.82	100.07	100.33	99.93	100.38	100.80	100.22	100.14
A.I.	0.95	0.97	0.98	1.05	0.99	1.09	0.93	0.97	0.95	0.94	1.10
Cu	50	22	14	15	18	19	19	28	20	9	25
Pb	18	52	8	28	28	31	4	28	8	11	36
Zn	101	179	189	249	188	206	125	214	198	138	231
Ni	2	3	5	6	2	5	8	9	2	2	3
Sc	1.9	0	0.1	0.1	0.1	0.3	0.7	0.4	0.5	1.2	0.2
Ga	28	31	32	34	33	33	27	31	32	29	34
Nb	26	58	54	61	51	55	22	45	36	27	62
Zr	476	1357	1397	1563	1255	1314	482	1045	862	511	1534
Y	59	152	156	183	128	138	60	131	100	66	164
Ce	153	268	267	272	189	160	171	269	227	167	251
U	3	8	9	12	10	12	5	7	6	3	10
Th	7	14	22	29	24	28	8	25	21	8	23
Sr	60	6	17	19	4	5	21	17	10	15	3
Rb	85	170	205	160	170	170	65	135	115	120	219
Ba	274	16	24	19	18	20	90	70	63	143	9

Table B-6

Field No.	KP91004	KP91005A	KP91007	KP91008	KP91009	KP91010	KP91011	KP91012	KP91016	KP91017R	KP91020
SiO2	76.00	75.35	76.00	75.70	76.20	76.50	75.00	75.85	76.00	76.18	76.30
TiO2	0.19	0.19	0.18	0.19	0.18	0.19	0.18	0.19	0.20	0.18	0.19
Al2O3	10.76	10.42	10.67	10.59	10.59	11.05	10.56	10.59	11.16	10.50	11.16
Fe2O3	1.06	1.77	2.21	1.76	3.14	0.96	1.02	2.01	1.78	1.16	1.00
FeO	2.33	2.35	1.54	1.97	0.82	1.53	2.75	1.86	0.71	2.44	1.82
MnO	0.06	0.06	0.05	0.05	0.05	0.04	0.05	0.06	0.04	0.09	0.05
MgO	0.15	0.06	0.08	0.05	0.03	0.02	0.03	0.02	0.08	0.09	0.03
CaO	0.12	0.19	0.15	0.15	0.10	0.45	0.17	0.10	0.98	0.17	0.18
Na2O	4.15	4.22	4.30	4.38	4.37	3.90	4.36	4.28	3.87	4.19	4.14
K2O	4.42	4.36	4.45	4.48	4.06	4.39	4.46	4.37	4.02	3.58	4.72
P2O5	0.01	0.01	0.01	0.01	0.01	0.01	0.01	0.01	0.01	0.00	0.01
F	0.03	0.04	0.04	0.04	0.02	0.03	0.04	0.04	0.00	0.01	0.02
H2O+	0.37	0.23	0.15	0.10	0.26	0.37	0.29	0.39	0.46	0.63	0.39
H2O-	0.22	0.18	0.21	0.16	0.18	0.15	0.13	0.16	0.15	0.37	0.30
CO2	0.19	0.16	0.15	0.16	0.14	0.30	0.05	0.01	0.65	0.05	0.09
S	0.01	0.01	0.01	0.01	0.01	0.00	0.01	0.02	0.01	0.02	0.01
Total	100.07	99.58	100.20	99.80	100.16	99.89	99.11	99.96	100.12	99.67	100.41
A.I.	1.08	1.12	1.11	1.14	1.09	1.01	1.14	1.11	0.96	1.03	1.07
Cu	19	21	18	26	11	13	44	20	18	27	16
Pb	45	42	29	40	6	14	34	24	49	38	9
Zn	246	252	215	234	163	122	206	216	79	227	113
Ni	2	3	2	5	2	2	6	2	2	5	2
Sc	0.2	0.1	0.2	0.7	0.7	0.5	0.2	0.3	0.5	0.2	0.7
Ga	33	33	33	33	33	30	34	34	29	34	28
Nb	63	63	61	63	62	38	65	64	39	64	35
Zr	1607	1587	1582	1600	1584	863	1504	1587	914	1552	784
Y	186	178	166	178	165	105	151	128	101	169	59
Ce	286	265	245	272	227	225	232	200	221	237	131
U	12	12	10	11	11	6	10	9	6	11	5
Th	30	25	30	29	27	17	25	25	13	23	10
Sr	5	4	6	4	6	24	5	4	18	13	5
Rb	200	208	206	211	172	132	212	207	117	135	126
Ba	14	9	10	12	25	43	11	10	69	29	42

Table B-6

Field No.	KP91021R	KP91022	KP91023	KP91024	KP91025	KP91026	KP91027	KP91028	KP91029	KP91030	KP91031
SiO2	75.42	74.80	75.50	74.70	75.30	77.65	76.05	75.30	75.15	75.35	73.90
TiO2	0.18	0.17	0.18	0.18	0.17	0.17	0.18	0.19	0.17	0.17	0.17
Al2O3	10.53	10.61	10.53	10.56	10.64	10.55	10.89	10.65	10.52	10.52	10.49
Fe2O3	2.15	1.69	0.57	2.11	2.06	1.65	1.89	2.84	1.72	1.90	1.56
FeO	1.77	2.06	3.05	1.69	1.58	1.44	1.49	0.79	2.18	1.72	2.88
MnO	0.06	0.06	0.05	0.05	0.05	0.05	0.07	0.06	0.06	0.05	0.06
MgO	0.13	0.01	0.06	0.04	0.06	0.32	0.04	0.04	0.01	0.04	0.08
CaO	0.13	0.24	0.09	0.15	0.08	0.20	0.32	0.22	0.17	0.12	0.17
Na2O	4.39	4.46	4.40	4.45	4.37	2.05	4.35	4.50	4.57	4.32	4.32
K2O	4.48	4.52	4.57	4.52	4.51	4.58	4.31	4.34	4.54	4.53	4.41
P2O5	0.01	0.01	0.01	0.01	0.01	0.02	0.01	0.01	0.01	0.01	0.01
F	0.05	0.06	0.04	0.05	0.06	0.02	0.11	0.00	0.06	0.06	0.07
H2O+	0.44	0.39	0.46	0.43	0.37	0.97	0.46	0.21	0.26	0.27	0.21
H2O-	0.27	0.16	0.18	0.13	0.18	0.18	0.17	0.13	0.15	0.14	0.22
CO2	0.08	0.07	0.06	0.05	0.04	0.02	0.06	0.03	0.03	0.09	0.04
S	0.02	0.01	0.01	0.02	0.02	0.01	0.02	0.02	0.01	0.01	0.03
Total	100.10	99.32	99.76	99.14	99.50	99.88	100.42	99.33	99.61	99.30	98.62
A.I.	1.15	1.15	1.16	1.16	1.13	0.79	1.09	1.14	1.18	1.14	1.13
Cu	21	20	22	16	20	14	32	12	22	24	20
Pb	32	37	30	42	36	5	22	26	36	16	26
Zn	255	235	241	250	230	123	222	179	239	214	228
Ni	2	2	2	2	1	6	1	3	4	5	4
Sc	0.8	0.2	0.2	0.2	0.1	0.8	0.3	0.3	0.2	0.2	0
Ga	33	34	34	34	33	26	31	31	32	33	34
Nb	64	55	70	65	66	42	49	53	62	60	61
Zr	1589	1535	1608	1585	1587	1296	1242	1256	1596	1611	1459
Y	181	145	176	182	184	207	136	133	180	129	149
Ce	263	220	159	261	255	234	258	246	270	230	258
U	11	10	10	10	11	9	6	6	11	10	10
Th	26	25	33	27	27	34	13	19	25	22	20
Sr	3	7	4	4	3	37	13	28	9	10	10
Rb	215	209	217	215	216	198	168	164	215	217	202
Ba	7	11	8	11	6	139	30	34	8	10	9

Table B-6

Field No.	KP91032	KP91033	KP91035	KP91036	KP91037	KP91038R	KP91039	KP91040	KP91041	KP91042	KP91043
SiO2	76.45	75.00	76.50	76.70	77.45	76.21	78.65	74.75	73.50	75.30	76.65
TiO2	0.18	0.17	0.07	0.13	0.13	0.20	0.16	0.23	0.23	0.18	0.14
Al2O3	10.91	10.52	12.21	11.02	11.23	11.02	10.36	12.69	11.78	10.54	12.05
Fe2O3	0.88	1.79	1.49	2.15	1.11	3.25	1.12	0.78	0.99	2.19	0.75
FeO	2.14	2.01	0.00	0.00	0.73	0.00	2.06	1.04	1.87	1.59	1.04
MnO	0.05	0.05	0.02	0.05	0.02	0.08	0.04	0.04	0.06	0.05	0.02
MgO	0.04	0.02	0.30	0.24	0.03	0.18	0.15	0.14	0.02	0.01	0.04
CaO	0.12	0.06	0.50	0.31	0.13	0.27	0.01	0.26	0.28	0.05	0.27
Na2O	4.16	4.44	2.11	1.92	2.99	2.96	0.05	3.89	4.33	4.45	4.33
K2O	4.56	4.49	4.99	5.15	5.13	4.00	4.88	4.88	4.89	4.51	3.66
P2O5	0.01	0.01	0.01	0.01	0.01	0.01	0.01	0.03	0.01	0.01	0.01
F	0.05	0.06	0.10	0.03	0.01	0.12	0.03	0.01	0.03	0.06	0.02
H2O+	0.39	0.47	0.89	0.95	0.42	1.04	1.78	0.68	0.26	0.21	0.33
H2O-	0.20	0.19	0.15	0.16	0.15	0.19	0.21	0.28	0.20	0.16	0.26
CO2	0.09	0.13	0.39	0.19	0.06	0.04	0.04	0.06	0.13	0.03	0.18
S	0.03	0.03	0.03	0.29	0.05	0.47	0.02	0.02	0.08	0.05	0.05
Total	100.26	99.44	99.76	99.30	99.65	100.04	99.57	99.78	98.66	99.39	99.80
A.I.	1.08	1.16	0.73	0.79	0.93	0.83	0.52	0.92	1.05	1.16	0.92
Cu	15	20	13	17	10	21	57	19	111	5	8
Pb	22	13	3	41	7	0	30	12	11	11	0
Zn	183	225	41	59	45	73	84	57	102	223	32
Ni	1	1	13	1	1	2	2	2	1	0	2
Sc	0.3	0.1	7.6	3.6	2.7	2.6	0.5	2.6	0.7	0.2	3.3
Ga	31	34	22	22	16	24	26	22	28	33	20
Nb	46	70	26	17	19	26	35	22	30	56	19
Zr	1056	1545	124	385	375	663	1095	349	601	1541	434
Y	108	160	43	63	68	82	139	52	34	96	54
Ce	194	193	64	214	124	206	153	106	78	154	150
U	6	6	4	6	6	4	8	7	4	9	9
Th	12	22	14	10	12	12	13	16	5	22	13
Sr	6	2	47	38	45	25	17	42	7	2	11
Rb	153	210	219	177	147	118	188	162	101	199	97
Ba	22	7	130	652	582	443	222	320	95	9	471

Table B-6

Field No.	KP91044	KP91045	KP91048R	KP91049D	KP91052	KP91053	KP91054R	KP91056	KP91057	KP91058	KP91059
SiO2	70.30	73.70	77.56	75.70	75.35	78.05	76.93	75.45	75.85	75.80	78.25
TiO2	0.58	0.23	0.19	0.18	0.22	0.21	0.12	0.21	0.17	0.18	0.17
Al2O3	12.22	13.05	11.00	10.60	12.33	11.23	11.08	11.70	10.59	10.51	9.71
Fe2O3	2.97	0.87	1.57	1.54	0.73	1.93	1.73	1.50	2.60	1.83	3.04
FeO	1.75	0.66	1.05	2.11	1.39	0.40	0.00	1.37	1.15	1.83	0.59
MnO	0.11	0.03	0.03	0.05	0.03	0.04	0.01	0.06	0.05	0.05	0.02
MgO	0.57	0.18	0.02	0.02	0.07	0.09	0.06	0.05	0.10	0.04	0.02
CaO	1.28	0.47	0.09	0.04	0.65	0.11	0.10	0.29	0.07	0.10	0.24
Na2O	4.48	3.77	3.65	4.25	2.78	1.44	1.05	4.16	4.25	4.33	3.58
K2O	3.90	5.11	4.13	4.62	5.28	5.43	6.99	4.79	4.50	4.44	2.40
P2O5	0.20	0.03	0.01	0.01	0.02	0.02	0.03	0.01	0.01	0.01	0.01
F	0.07	0.01	0.00	0.06	0.01	0.01	0.01	0.02	0.02	0.02	0.01
H2O+	0.31	0.46	0.25	0.19	0.33	0.66	0.40	0.51	0.34	0.36	0.26
H2O-	0.25	0.26	0.21	0.16	0.17	0.16	0.23	0.31	0.21	0.22	0.26
CO2	0.04	0.02	0.10	0.04	0.05	0.03	0.07	0.07	0.06	0.13	0.26
S	0.05	0.06	0.06	0.07	0.06	0.07	0.61	0.01	0.00	0.01	0.03
Total	99.08	98.91	99.92	99.64	99.47	99.88	99.43	100.51	99.97	99.86	98.85
A.I.	0.95	0.90	0.95	1.13	0.83	0.73	0.84	1.03	1.12	1.13	0.87
Cu	5	4	20	11	4	4	7	7	3	12	3
Pb	13	8	8	20	7	12	32	13	29	20	13
Zn	89	29	54	217	62	47	103	90	234	208	22
Ni	1	1	6	2	1	0	1	0	0	1	0
Sc	10.8	2.5	1.8	0.2	5.5	6.1	3.2	0.7	0.1	0.1	0.2
Ga	24	18	23	33	18	17	16	28	34	33	30
Nb	22	12	22	64	11	10	19	30	67	68	57
Zr	549	203	582	1544	407	365	341	590	1539	1564	1365
Y	75	31	55	176	44	28	55	65	165	159	156
Ce	124	78	149	187	148	122	92	185	218	188	236
U	4	6	6	10	3	4	7	4	11	11	9
Th	5	23	9	18	8	5	13	1	18	16	17
Sr	65	47	5	2	52	33	63	13	4	2	12
Rb	109	196	108	220	110	117	182	94	198	202	100
Ba	798	387	164	12	893	820	697	99	15	12	20

Table B-6

Field No.	KP91061	KP91063	KP91066	KP91067	KP91068	KP91069	KP91070	KP91071	KP91072	KP92001	KP92002	KP92003
SiO2	76.00	75.60	75.50	75.40	75.40	76.00	71.80	74.80	75.55	75.58	75.77	76.98
TiO2	0.18	0.20	0.18	0.20	0.16	0.18	0.31	0.18	0.17	0.22	0.18	0.17
Al2O3	10.59	11.38	10.46	11.18	10.47	10.58	12.96	10.57	10.62	11.82	10.54	10.61
Fe2O3	2.42	0.84	1.81	1.31	1.94	1.55	1.91	1.44	2.41	2.29	1.91	2.61
FeO	1.12	1.88	1.82	1.50	1.49	1.61	1.65	2.32	0.93	0.57	1.24	0.88
MnO	0.05	0.05	0.05	0.05	0.06	0.05	0.07	0.06	0.04	0.06	0.03	0.04
MgO	0.02	0.04	0.04	0.03	0.02	0.02	0.03	0.01	0.01	0.03	0.04	0.03
CaO	0.08	0.18	0.10	0.20	0.16	0.07	0.23	0.13	0.20	0.03	0.15	0.11
Na2O	4.21	4.03	3.96	4.06	4.05	4.09	4.18	4.60	4.26	3.67	3.62	3.64
K2O	4.29	4.63	4.49	4.51	4.41	4.51	5.41	4.55	4.42	4.78	3.97	4.29
P2O5	0.01	0.01	0.01	0.01	0.01	0.01	0.03	0.01	0.01	0.01	0.02	0.01
F	0.01	0.01	0.05	0.03	0.05	0.05	0.04	0.09	0.08	0.00	0.00	0.01
H2O+	0.24	0.43	0.37	0.39	0.34	0.25	0.67	0.25	0.32	0.66	0.47	0.44
H2O-	0.24	0.22	0.17	0.20	0.15	0.17	0.23	0.13	0.17			
CO2	0.03	0.02	0.03	0.05	0.12	0.04	0.03	0.03	0.19	0.11	0.18	0.08
S	0.00	0.02	0.00	0.01	0.00	0.01	0.02	0.00	0.02	0.03	0.01	0.02
Total	99.49	99.54	99.04	99.13	98.83	99.19	99.56	99.17	99.40	99.86	98.13	99.92
A.I.	1.09	1.02	1.09	1.03	1.09	1.10	0.98	1.18	1.11	0.95	0.97	1.00
Cu	9	7	7	5	7	7	7	10	7	7	13	7
Pb	27	12	7	11	30	8	4	40	40	3	33	7
Zn	207	123	234	118	239	187	116	249	224	101	207	170
Ni	0	0	1	0	0	0	1	0	0	2	1	1
Sc	0.1	0.5	0.1	0.5	0.1	0.2	2	0	0.1	0.7	0.3	0.2
Ga	35	31	34	31	35	32	31	35	35	29	30	33
Nb	67	32	65	39	65	55	22	72	65	29	60	60
Zr	1549	650	1502	868	1514	1194	511	1583	1551	527	1201	1246
Y	147	63	99	57	165	85	45	216	157	58	155	132
Ce	238	148	176	131	247	123	163	319	265	173	246	228
U	11	4	9	5	10	6	4	11	10	4	9	8
Th	21	5	10	4	18	7	0	30	20	13	30	30
Sr	4	8	7	7	11	3	19	6	8	7	11	16
Rb	205	106	209	120	193	182	118	220	195	95	133	153
Ba	15	70	12	62	12	23	283	9	20	99	38	24

Table B-6

Field No.	KP92004	KP92005	KP92006	KP92007	KP92008	KP92009	KP92010	KP92011A	KP92013	KP92014	KP92015
SiO2	76.85	76.13	74.89	76.16	76.31	71.19	78.27	78.21	75.85	76.28	75.87
TiO2	0.18	0.17	0.18	0.18	0.18	0.44	0.07	0.09	0.18	0.19	0.17
Al2O3	10.64	10.39	10.68	10.88	10.77	14.29	11.86	12.83	10.91	10.95	10.37
Fe2O3	3.41	2.09	2.50	2.48	2.71	0.89	0.83	0.87	1.90	1.49	2.77
FeO	0.43	1.30	1.11	1.12	1.06	1.73	0.24	0.27	0.96	1.72	1.23
MnO	0.04	0.07	0.05	0.03	0.05	0.04	0.01	0.01	0.03	0.04	0.04
MgO	0.07	0.04	0.08	0.10	0.07	0.91	0.14	0.29	0.05	0.12	0.21
CaO	0.13	0.29	0.41	0.15	0.23	1.98	0.27	0.26	0.37	0.19	0.91
Na2O	3.85	3.74	2.99	3.22	3.64	3.53	4.25	1.85	3.15	3.32	3.78
K2O	3.70	3.48	4.82	4.50	3.90	3.38	3.33	3.26	4.60	4.44	3.28
P2O5	0.01	0.01	0.00	0.00	0.00	0.14	0.01	0.01	0.01	0.00	0.00
F	0.02	0.01	0.04	0.01	0.01	0.04	0.01	0.03	0.01	0.00	0.01
H2O+	0.4	0.25	0.6	0.5	0.46	1.26	0.62	1.36	0.38	0.58	0.51
H2O-											
CO2	0.14	0.83	0.31	0.2	0.3	0.11	0.25	0.21	0.34	0.2	0.73
S	0.01	0.00	0.00	0.00	0.00	0.1	0.04	0.01	0	0	0
Total	99.88	98.80	98.66	99.53	99.69	100.03	100.20	99.53	98.74	99.52	99.88
A.I.	0.97	0.95	0.95	0.93	0.95	0.66	0.89	0.51	0.93	0.94	0.94
Cu	10	7	6	21	9	23	3	48.5	8	10	4
Pb	29	9	56	93	46	30	8	0	33	35	0
Zn	157	220	285	214	293	31	32	16	136	244	123
Ni	1	0	2	1	0	15	0	0	1	1	1
Sc	0.1	0.1	0.1	0.1	0.1	4	8.7	9.9	0.2	0.1	0.2
Ga	33	33	30	30	32	19	17	21	31	31	32
Nb	70	71	63	63	72	9	30	32	64	64	68
Zr	1531	1519	1387	1348	1576	140	113	126	1278	1359	1439
Y	168	182	164	152	168	12	40	72	176	166	166
Ce	250	270	266	236	250	45	60	58	278	268	254
U	10	10	8	6	11	1	5	9	9	8	10
Th	36	35	28	19	39	9	22	24	30	22	32
Sr	14	16	12	8	8	420	39	30	10	10	16
Rb	125	136	190	174	152	90	122	99	165	163	94
Ba	54	22	20	30	22	564	69	100	28	17	47

Table B-6

Field No.	KP92016	KP92018	KP92019	KP92020	KP92021	KP92022	KP92023	KP92024	KP92025	KP92026	KP92027	KP92028
SiO2	74.44	75.65	74.19	74.61	73.38	78.22	73.24	75.54	75.15	78.06	77.36	76.51
TiO2	0.23	0.17	0.25	0.24	0.28	0.13	0.28	0.18	0.18	0.14	0.14	0.13
Al2O3	11.77	10.71	12.25	11.62	12.25	10.39	12.38	10.79	10.70	11.09	11.30	11.23
Fe2O3	1.64	1.99	1.01	1.84	2.27	1.91	1.96	2.39	2.57	1.53	2.44	2.47
FeO	1.31	1.50	1.18	0.96	1.67	0.48	1.32	1.03	1.05	0.72	0.45	0.27
MnO	0.05	0.05	0.02	0.06	0.06	0.01	0.07	0.06	0.04	0.02	0.01	0.01
MgO	0.06	0.02	0.14	0.17	0.18	0.07	0.07	0.05	0.20	0.08	0.05	0.04
CaO	0.23	0.14	0.24	0.22	0.37	0.01	0.30	0.17	0.55	0.12	0.04	0.06
Na2O	4.33	4.32	4.07	3.78	4.12	2.61	4.31	4.17	3.63	5.82	4.10	3.74
K2O	4.88	4.63	4.56	4.65	4.25	4.50	5.05	4.45	3.97	1.01	3.31	4.49
P2O5	0.01	0.01	0.03	0.01	0.03	0.00	0.02	0.01	0.00	0.01	0.00	0.01
F	0.04	0.06	0.01	0.02	0.00	0.01	0.03	0.05	0.01	0.00	0.01	0.00
H2O+	0.39	0.32	0.43	0.6	0.62	0.62	0.65	0.33	0.55	0.5	0.53	0.38
H2O-												
CO2	0.08	0.11	0.09	0.11	0.25	0.08	0.11	0.13	0.41	0.16	0.14	0.1
S	0	0	0	0	0.01	0.01	0.02	0	0.01	0.04	0.03	0.01
Total	99.46	99.68	98.47	98.89	99.74	99.05	99.81	99.35	99.02	99.30	99.91	99.45
A.I.	1.05	1.13	0.95	0.97	0.93	0.88	1.01	1.08	0.96	0.96	0.91	0.98
Cu	6	11	10	9	9	8	7	9	12	6	8	9
Pb	13	29	7	14	20	11	11	34	32	26	7	7
Zn	130	216	73	130	159	37	126	241	244	154	21	38
Ni	1	1	1	3	1	0	3	0	1	0	3	0
Sc	0.7	0.2	1.8	0.9	1.8	0.6	1.2	0.2	0.1	0.6	0.5	0.4
Ga	30	35	27	30	29	25	31	34	35	25	25	28
Nb	37	61	28	33	29	35	33	66	71	35	36	41
Zr	669	1347	363	598	538	800	550	1481	1560	802	835	958
Y	75	107	63	85	72	90	74	163	182	103	66	120
Ce	172	209	140	204	190	130	185	252	261	166	86	160
U	4	8	4	3	3	7	3	9	11	9	7	9
Th	14	28	14	15	12	27	13	33	34	28	30	33
Sr	8	5	27	20	21	9	19	11	9	17	12	14
Rb	112	191	108	104	80	165	90	173	138	23	99	161
Ba	80	20	202	117	163	75	176	35	69	61	108	133

Table B-6

Field No.	KP92029	KP92030	KP92031	KP92032	KP92033	KP92034	KP92037	KP92039	KP92040A	KP92041	KP92043	KP92044
SiO2	76.33	74.90	74.67	76.46	75.69	75.31	76.35	75.95	75.82	75.38	46.37	75.70
TiO2	0.18	0.22	0.18	0.18	0.18	0.18	0.18	0.20	0.20	0.18	0.57	0.18
Al2O3	10.18	11.78	10.88	10.90	10.70	10.35	10.36	10.77	13.50	10.42	8.08	10.51
Fe2O3	2.62	1.64	1.76	2.52	2.23	2.27	2.94	2.72	0.35	2.48	2.66	3.04
FeO	1.07	1.17	1.86	1.10	1.37	1.45	0.81	0.76	1.01	1.43	0.47	0.47
MnO	0.05	0.06	0.06	0.05	0.05	0.05	0.03	0.03	0.01	0.06	0.09	0.03
MgO	0.03	0.05	0.03	0.05	0.03	0.05	0.09	0.07	0.24	0.03	1.48	0.09
CaO	0.12	0.11	0.16	0.10	0.13	0.16	0.15	0.07	0.01	0.06	21.50	0.25
Na2O	4.01	3.95	4.49	4.22	4.38	3.92	3.83	3.38	1.08	3.84	1.21	2.96
K2O	4.57	5.15	4.55	4.48	4.40	4.15	3.29	4.39	5.12	4.40	3.97	5.16
P2O5	0.01	0.01	0.01	0.00	0.01	0.01	0.01	0.00	0.03	0.01	0.10	0.01
F	0.06	0.02	0.06	0.03	0.04	0.04	0.00	0.00	0.07	0.03	0.44	0.01
H2O+	0.58	0.68	0.5	0.54	0.49	0.54	0.43	0.63	1.38	0.54	0.49	0.39
H2O-												
CO2	0.23	0.12	0.13	0.13	0.21	0.17	0.19	0.12	0.13	0.12	9.38	0.28
S	0.04	0.02	0.02	0.01	0.01	0.01	0.04	0.02	0.20	0	0.01	0.02
Total	100.08	99.88	99.36	100.77	99.92	98.66	98.70	99.11	99.11	98.98	96.82	99.10
A.I.	1.13	1.02	1.13	1.08	1.12	1.06	0.95	0.96	0.54	1.06	0.78	0.99
Cu	3	7	9	14	28	11	14	8	7	10	19	16
Pb	0	14	30	22	31	31	14	0	41	37	13	31
Zn	186	123	218	205	222	235	340	170	26	267	111	234
Ni	1	0	3	1	0	3	0	0	0	2	31	0
Sc	0.3	0.7	0.2	0.2	0.1	0.1	< 0.1	0.2	3	0.1	7.6	< 0.1
Ga	34	32	34	35	35	35	34	33	23	36	18	34
Nb	66	33	54	63	64	72	75	63	11	72	14	75
Zr	1515	611	1022	1342	1353	1573	1587	1274	213	1562	429	1578
Y	132	108	138	118	122	154	194	151	21	201	43	188
Ce	164	261	218	200	220	251	283	249	69	290	87	260
U	9	3	7	9	9	10	14	8	6	10	4	11
Th	25	13	25	28	30	33	35	29	25	35	11	34
Sr	6	11	6	5	5	7	13	15	18	8	465	27
Rb	168	120	167	171	187	189	115	147	227	198	130	174
Ba	25	120	32	30	24	25	45	50	411	13	527	42

Table B-6

Field No.	KP92045	KP92046	KP92047	KP92049	KP92050	KP92051	KP92052	KP92053	KP92055
SiO2	76.13	74.89	75.52	75.37	75.71	75.67	75.63	75.65	76.65
TiO2	0.17	0.18	0.19	0.18	0.18	0.19	0.16	0.19	0.23
Al2O3	10.74	10.59	10.64	10.62	10.65	10.72	10.88	10.64	11.55
Fe2O3	2.87	3.25	2.71	2.44	3.17	2.05	1.95	2.70	2.18
FeO	0.35	0.69	1.09	1.04	0.28	1.43	0.91	0.67	0.83
MnO	0.03	0.04	0.06	0.04	0.06	0.06	0.04	0.05	0.02
MgO	0.07	0.06	0.06	0.02	0.03	0.02	0.01	0.11	0.09
CaO	0.16	0.37	0.42	0.27	0.12	0.33	0.23	0.42	0.15
Na2O	3.83	3.60	3.54	4.44	4.96	3.74	4.21	3.90	3.88
K2O	3.83	4.23	4.24	4.31	4.24	4.90	4.48	4.73	4.19
P2O5	0.01	0.01	0.00	0.01	0.01	0.01	0.00	0.01	0.01
F	0.01	0.01	0.02	0.07	0.02	0.06	0.03	0.06	0.01
H2O+	0.42	0.41	0.58	0.33	0.25	0.23	0.34	0.18	0.29
H2O-									
CO2	0.25	0.42	0.44	0.22	0.16	0.07	0.09	0.07	0.07
S	0.01	0.01	0.01	0.01	0.02	0.01	0.02	0.00	0.01
Total	98.88	98.76	99.52	99.37	99.86	99.49	98.98	99.38	100.16
A.I.	0.97	0.99	0.98	1.13	1.20	1.07	1.08	1.08	0.95
Cu	8	13	12	22	9	7	7	10	8
Pb	1	23	41	32	13	23	22	11	3
Zn	115	192	251	248	211	209	206	149	79
Ni	1	0	1	0	2	0	0	0	2
Sc	0.1	0.1	0.1	0.1	0.3	0.3	0.2	0.2	0.9
Ga	36	35	36	35	37	35	35	34	32
Nb	69	69	77	73	64	62	57	60	42
Zr	1481	1510	1581	1572	1237	1256	1188	1268	776
Y	163	166	167	176	128	142	136	157	94
Ce	216	252	257	268	186	239	193	224	212
U	10	9	10	11	9	4	7	10	5
Th	43	36	31	35	29	26	29	43	23
Sr	9	9	9	6	7	26	11	27	13
Rb	132	161	159	181	159	193	176	183	132
Ba	50	25	23	23	18	29	19	39	126

Table B-7 Mooring Cove Geochemical Data

Field No.	MC90001D	MC90003	MC90004	MC90008	MC90010	MC90012	MC90014	MC90016	MC90018	MC92005	MC92006
SiO2	54.65	67.00	75.85	78.10	74.55	75.25	74.65	74.75	74.60	72.99	75.77
TiO2	0.92	0.28	0.14	0.18	0.27	0.28	0.28	0.31	0.25	0.28	0.19
Al2O3	17.66	16.27	11.59	10.75	11.45	11.49	11.48	11.73	11.40	11.62	11.45
Fe2O3	4.80	2.45	2.29	2.17	2.99	3.19	2.86	4.16	2.66	1.46	2.67
FeO	5.08	2.51	2.28	0.80	0.65	0.78	1.01	0.00	0.92	1.93	0.15
MnO	0.29	0.07	0.06	0.06	0.07	0.08	0.12	0.08	0.14	0.12	0.03
MgO	3.92	0.63	0.04	0.14	0.03	0.07	0.09	0.06	0.07	0.40	0.08
CaO	3.70	0.19	0.01	0.29	0.51	0.23	0.18	0.13	0.42	1.89	0.01
Na2O	3.43	4.55	5.22	2.21	3.01	4.12	3.41	4.40	4.28	3.51	3.01
K2O	2.06	4.53	1.81	4.88	5.54	4.32	5.07	3.91	4.54	2.17	5.24
P2O5	0.25	0.04	0.01	0.01	0.01	0.02	0.02	0.01	0.02	0.05	0.01
F	0.08	0.18	0.02	0.02	0.01	0.01	0.01	0.01	0.01	0.03	0.01
H2O+	3.24	1.59	0.87	0.51	0.11	0.12	0.21	0.28	0.12	1.24	0.38
H2O-	0.28	0.26	0.24	0.14	0.12	0.16	0.22	0.28	0.15		
CO2	0.06	0.07	0.08	0.17	0.26	0.05	0.05	0.07	0.05	0.05	0.04
S	0.02	0.10	0.07	0.00	0.00	0.00	0.00	0.00	0.00	1.41	0.04
Total	100.44	100.72	100.58	100.43	99.58	100.17	99.66	100.18	99.63	99.15	99.08
A.I.	0.45	0.76	0.91	0.83	0.96	1.00	0.97	0.98	1.05	0.70	0.93
Cu	7	13	21	14	16	12	20	14	10	13	6
Pb	3	6	17	25	11	15	17	9	3	12	10
Zn	228	340	288	116	134	114	125	131	204	128	114
Ni	4	7	4	1	5	3	6	6	4	4	0
Sc	17.4	2.2	0	0.1	2	1.6	1.7	1.9	0.4	2.6	0.1
Ga	24	51	38	29	19	28	27	33	32	33	34
Nb	6	394	442	41	28	33	33	32	36	48	51
Zr	153	1801	2938	938	809	759	766	719	881	937	1013
Y	28	159	296	120	88	144	116	102	168	118	142
Ce	41	473	881	200	187	198	170	185	288	269	121
U	1	11	18	3	4	3	4	4	4	3	3
Th	0	57	79	19	17	17	16	16	17	21	20
Sr	230	73	21	42	16	4	10	5	17	318	22
Rb	90	150	35	105	170	125	140	110	120	87	182
Ba	342	204	19	67	125	53	201	157	46	90	38

Table B-7

Field No.	MC92009	MC92009D	MC92010	MC92011	MC92012	MC92013	MC92014	MC92015	MC92016	MC92017	MC92018
SiO2	75.22	74.32	75.66	65.60	66.23	83.54	75.76	75.57	78.80	75.78	76.19
TiO2	0.14	0.14	0.18	0.26	0.25	0.18	0.20	0.27	0.19	0.19	0.18
Al2O3	11.68	11.61	11.65	16.63	16.71	10.39	12.23	12.06	11.28	11.10	11.35
Fe2O3	3.19	3.01	2.49	1.96	1.83	0.26	3.01	1.51	1.57	2.64	2.46
FeO	1.02	1.17	1.25	2.60	2.72	0.66	0.69	0.75	0.55	0.29	0.64
MnO	0.04	0.05	0.10	0.13	0.11	0.00	0.03	0.04	0.01	0.06	0.02
MgO	0.03	0.03	0.16	0.21	0.10	0.00	0.05	0.10	0.03	0.10	0.02
CaO	0.01	0.01	0.18	0.09	0.03	0.00	0.01	0.05	0.00	0.06	0.08
Na2O	4.98	4.82	5.26	6.20	6.36	0.09	2.08	1.65	0.05	2.61	4.36
K2O	2.49	2.50	1.50	4.72	4.76	2.84	4.81	5.71	4.92	5.59	3.56
P2O5	0.01	0.01	0.01	0.02	0.02	0.01	0.01	0.02	0.00	0.01	0.01
F	0.01	0.01	0.08	0.02	0.01	0.02	0.01	0.01	0.01	0.00	0.00
H2O+	0.67	0.67	0.68	0.89	0.73	1.56	1.06	1.07	1.61	0.38	0.22
H2O-											
CO2	0.03	0.03	0.04	0.04	0.01	0.01	< 0.01	0.03	0.03	0.03	0.03
S	0.06	0.06	0.05	0.11	0.1	0	0.03	0.06	0.04	0.03	0.01
Total	99.58	98.44	99.29	99.48	99.97	99.56	99.97	98.90	99.09	98.87	99.13
A.I.	0.93	0.92	0.88	0.92	0.93	0.31	0.71	0.74	0.48	0.93	0.97
Cu	11	11	7	11	7	7	6	11	9	8	9
Pb	14	14	5	2	0	0	15	94	0	18	21
Zn	173	173	158	223	75	12	202	66	45	96	37
Ni	0	0	5	4	5	1	1	1	0	5	0
Sc	0	0	0.3	1.6	1.2	0.1	< 0.1	3.4	0.1	0.1	< 0.1
Ga	42	42	42	46	43	29	35	19	34	31	34
Nb	582	582	403	233	191	53	55	18	54	50	50
Zr	3055	3055	2483	1414	1588	950	1037	242	1007	969	915
Y	251	251	247	156	113	112	140	33	171	143	172
Ce	348	348	517	724	596	65	150	105	96	191	278
U	14	14	15	7	5	4	4	4	6	3	4
Th	77	77	63	42	33	23	20	26	22	20	20
Sr	18	18	24	39	16	6	23	57	16	8	12
Rb	57	57	52	106	131	78	166	215	187	-5	107
Ba	25	25	27	33	22	15	30	420	36	57	38

Table B-7

Field No.	MC92019	MC92020	MC92021	MC92021D	MC92022
SiO2	79.28	82.35	76.40	75.92	84.62
TiO2	0.19	0.17	0.24	0.25	0.47
Al2O3	10.90	8.58	15.04	15.29	10.45
Fe2O3	2.75	1.12	0.03	0.12	0.01
FeO	0.51	0.00	0.08	0.00	0.23
MnO	0.01	0.01	0.00	0.00	0.00
MgO	0.01	0.02	0.00	0.00	0.02
CaO	0.00	0.00	0.00	0.00	0.03
Na2O	0.10	0.09	0.14	0.14	0.06
K2O	3.24	5.58	4.22	4.27	0.27
P2O5	0.01	0.00	0.02	0.00	0.06
F	0.02	0.01	0.03	0.04	0.02
H2O+	1.59	0.89	2.02	2.02	2.03
H2O-					
CO2	0.04	0.03	0.05	0.05	0.04
S	0.01	0.47	0.06	0.06	0.03
Total	98.66	99.32	98.33	98.16	98.34
A.I.	0.34	0.72	0.32	0.32	0.04
Cu	5	9	4	4	7
Pb	0	10	5	5	79
Zn	32	26	6	6	12
Ni	1	0	0	0	0
Sc	0.1	0.1	0	0	3.7
Ga	37	13	40	40	42
Nb	56	58	74	74	97
Zr	1004	918	1324	1324	1856
Y	139	113	69	69	120
Ce	109	71	103	103	266
U	4	6	6	6	8
Th	21	18	29	29	40
Sr	4	34	6	6	28
Rb	105	146	111	111	10
Ba	12	53	12	12	18

Table B-8 Cross Hills Complex Geochemical Data

Field No.	MC90019A	MC90020	MC90021	MC90022	MC90023	MC90024	MC90025	MC90026	MC90027	MC90028	MC90029
SiO2	77.33	77.05	76.10	77.50	78.05	75.15	76.45	79.35	78.55	77.35	75.55
TiO2	0.12	0.11	0.20	0.14	0.12	0.22	0.14	0.26	0.37	0.14	0.22
Al2O3	10.99	11.34	12.61	11.13	11.37	12.68	11.26	7.85	7.43	11.26	12.57
Fe2O3	2.52	2.10	1.33	1.51	1.82	0.48	2.91	5.14	5.37	2.10	1.14
FeO	0.29	0.30	0.37	0.80	0.40	1.07	0.19	0.25	0.63	0.32	0.69
MnO	0.03	0.04	0.03	0.05	0.03	0.04	0.07	0.07	0.12	0.03	0.03
MgO	0.02	0.04	0.15	0.06	0.03	0.18	0.05	0.16	0.28	0.03	0.18
CaO	0.05	0.01	0.17	0.14	0.06	0.39	0.02	0.01	0.01	0.01	0.37
Na2O	3.70	3.50	3.69	3.60	3.78	4.39	3.72	1.38	0.86	3.81	3.68
K2O	4.38	4.67	5.39	4.50	4.63	4.24	4.37	3.61	3.05	4.17	5.03
P2O5	0.01	0.01	0.01	0.01	0.01	0.02	0.01	0.01	0.01	0.01	0.02
F	0.00	0.00	0.01	0.01	0.01	0.01	0.00	0.01	0.01	0.00	0.02
H2O+	0.29	0.52	0.52	0.35	0.24	0.31	0.24	1.12	1.44	0.41	0.34
H2O-	0.18	0.23	0.20	0.23	0.20	0.24	0.23	0.34	0.43	0.21	0.12
CO2	0.09	0.07	0.09	0.08	0.07	0.07	0.06	0.45	0.24	0.04	0.03
S	0.02	0.00	0.01	0.00	0.00	0.00	0.00	0.01	0.00	0.00	0.00
Total	99.97	99.99	100.88	100.11	100.82	99.49	99.72	100.02	98.80	99.89	99.99
A.I.	0.98	0.95	0.94	0.97	0.99	0.93	0.96	0.79	0.63	0.96	0.91
Cu	15	19	9	29	30	15	19	30	58	20	10
Pb	6	5	9	27	12	18	1	21	24	5	12
Zn	38	57	75	137	103	70	86	125	176	50	52
Ni	1	1	1	1	1	2	0	0	1	0	2
Sc	0.2	0.3	1.5	0.6	0.3	2	0.2	0	0	0.3	1.9
Ga	29	28	21	28	29	23	31	27	25	31	22
Nb	72	59	30	46	50	29	83	339	467	72	28
Zr	852	667	245	512	580	252	913	4430	8490	792	252
Y	152	135	51	72	86	89	182	613	1030	127	77
Ce	167	110	106	123	115	157	160	409	842	129	110
U	8	6	3	5	5	4	8	38	58	8	4
Th	29	22	18	21	16	22	33	127	183	29	18
Sr	10	11	31	12	8	37	14	10	14	8	36
Rb	176	173	181	179	209	141	205	214	186	206	182
Ba	57	79	243	123	74	253	40	89	135	67	272

Table B-8

Field No.	MC90031	MC90032	MC90033	MC90034	MC90035	MC90036	MC90037	MC90038	MC90039	MC92001	MC92002
SiO2	77.65	76.00	75.75	76.90	77.10	76.00	74.60	77.55	77.95	76.95	77.03
TiO2	0.12	0.15	0.14	0.13	0.16	0.20	0.19	0.13	0.13	0.16	0.14
Al2O3	10.75	10.60	10.61	10.89	11.81	12.19	12.02	11.02	11.21	10.61	10.99
Fe2O3	1.47	2.69	4.85	2.92	1.30	1.37	2.06	1.69	1.89	2.33	2.74
FeO	1.23	1.21	0.39	0.28	0.30	0.56	0.19	0.67	0.37	0.57	0.22
MnO	0.05	0.05	0.04	0.03	0.02	0.05	0.03	0.09	0.02	0.07	0.03
MgO	0.05	0.03	0.01	0.04	0.05	0.16	0.14	0.02	0.04	0.05	0.11
CaO	0.10	0.18	0.06	0.02	0.02	0.10	0.09	0.02	0.01	0.09	0.10
Na2O	3.35	3.36	3.44	3.40	3.75	3.71	3.75	3.64	3.70	4.24	4.06
K2O	4.38	4.09	4.27	4.51	4.89	5.06	5.04	4.56	4.50	3.91	4.07
P2O5	0.01	0.01	0.01	0.01	0.01	0.03	0.02	0.01	0.01	0.00	0.00
F	0.00	0.00	0.00	0.00	0.00	0.01	0.01	0.01	0.01	0.01	0.00
H2O+	0.31	0.35	0.25	0.36	0.29	0.39	0.47	0.26	0.32	0.33	0.37
H2O-	0.12	0.14	0.10	0.22	0.13	0.25	0.26	0.28	0.30		
CO2	0.05	0.07	0.05	0.04	0.05	0.11	0.10	0.07	0.07	0.1	0.09
S	0.01	0.00	0.00	0.00	0.01	0.01	0.00	0.00	0.00	0.00	0.00
Total	99.65	98.93	99.97	99.75	99.89	100.20	98.97	100.02	100.53	99.42	99.95
A.I.	0.95	0.94	0.97	0.96	0.97	0.95	0.97	0.99	0.98	1.06	1.01
Cu	11	11	8	11	6	6	4	14	10	12	9
Pb	9	17	20	5	4	7	5	14	23	28	17
Zn	108	102	94	115	37	69	50	145	89	426	199
Ni	2	0	1	0	1	2	1	1	1	0	0
Sc	0.4	0.2	0.1	0.2	1	1.6	1.2	0.4	0.4	0.2	0.2
Ga	26	33	32	28	25	25	27	29	30	36	36
Nb	77	217	92	82	36	31	34	53	50	141	80
Zr	733	2668	1376	1094	293	400	563	602	603	1196	815
Y	113	446	226	172	39	67	73	95	84	170	115
Ce	118	343	225	98	108	152	152	123	72	196	156
U	7	24	10	7	3	4	4	4	4	10	6
Th	26	90	36	31	20	14	13	18	13	63	32
Sr	16	17	6	8	22	24	16	4	17	5	6
Rb	178	180	227	212	171	153	157	188	173	204	199
Ba	62	44	45	67	143	223	217	77	49	43	42

Table B-8

Field No.	MC92004	MC92023	MC92024	MC92025	MC92027	MC92029	MC92030
SiO2	76.28	77.15	76.50	63.19	76.06	78.41	74.19
TiO2	0.14	0.13	0.13	0.20	0.13	0.13	0.16
Al2O3	10.82	11.05	10.89	17.93	11.04	9.99	11.82
Fe2O3	3.09	2.72	2.24	3.68	2.12	2.48	3.16
FeO	0.13	0.17	0.34	0.34	0.61	0.18	0.19
MnO	0.03	0.04	0.17	0.09	0.15	0.05	0.08
MgO	0.03	0.03	0.03	0.07	0.03	0.05	0.08
CaO	0.02	0.03	0.02	0.28	0.17	0.22	0.09
Na2O	3.63	3.68	3.70	5.99	3.52	3.92	4.42
K2O	4.29	4.40	4.31	6.69	4.60	2.94	3.73
P2O5	0.00	0.01	0.01	0.04	0.00	0.00	0.00
F	0.00	0.00	0.02	0.01	0.10	0.00	0.00
H2O+	0.22	0.45	0.35	0.48	0.35	0.3	0.44
H2O-							
CO2	0.00	0.04	0.06	0.06	0.09	0.06	0.05
S	0.03	0.01	0.03	0.01	0.03	0.02	0.00
Total	98.68	99.90	98.77	99.05	98.97	98.73	98.41
A.I.	0.98	0.98	0.99	0.95	0.98	0.96	0.96
Cu	13	9	19	9	12	15	28
Pb	21	20	44	24	16	29	7
Zn	177	100	525	475	265	155	258
Ni	0	0	5	0	0	0	0
Sc	0.2	0.2	0.3	0.4	0.3	0.1	0.1
Ga	35	35	32	49	34	29	36
Nb	75	90	82	130	99	80	120
Zr	1032	1050	799	1309	922	1056	1513
Y	145	228	79	352	92	142	313
Ce	139	172	125	255	146	195	278
U	6	7	5	11	6	5	11
Th	31	42	35	60	41	36	55
Sr	8	10	13	27	15	16	11
Rb	230	216	240	284	260	129	148
Ba	43	40	59	92	67	64	64

Table B-9 Grand Beach Complex Geochemical Analyses

Field No.	GB90001	GB90002	GB90004	GB90005	GB90006	GB90007	GB90009R	GB90011	GB90012	GB90014	GB90015	GB90016
SiO2	77.45	77.80	77.15	69.90	77.15	77.60	76.72	77.15	76.45	71.85	77.25	76.95
TiO2	0.10	0.08	0.10	0.23	0.09	0.09	0.09	0.09	0.11	0.38	0.06	0.05
Al2O3	11.98	11.89	11.88	14.33	11.91	11.76	11.87	12.04	11.99	12.68	12.30	12.24
Fe2O3	1.27	0.60	0.57	0.72	0.34	0.03	1.07	0.59	0.76	1.33	0.05	0.23
FeO	0.59	0.80	0.95	1.45	0.98	1.23	0.45	0.71	0.81	1.87	0.66	1.27
MnO	0.02	0.03	0.03	0.05	0.03	0.03	0.02	0.03	0.03	0.06	0.02	0.04
MgO	0.37	0.15	0.22	0.41	0.20	0.13	0.17	0.18	0.30	1.37	0.12	0.14
CaO	0.10	0.22	0.28	0.28	0.25	0.19	0.17	0.21	0.41	0.78	0.17	0.40
Na2O	2.93	3.53	3.70	2.31	3.45	3.06	3.08	3.93	3.76	3.76	4.10	4.93
K2O	3.97	4.28	4.54	8.34	4.70	5.10	5.05	4.37	4.57	4.20	4.57	2.84
P2O5	0.01	0.02	0.01	0.03	0.01	0.01	0.01	0.01	0.01	0.08	0.01	0.01
F	0.03	0.06	0.04	0.01	0.05	0.01	0.01	0.02	0.08	0.17	0.01	0.13
H2O+	1.29	0.75	0.78	1.39	0.82	0.85	0.79	0.61	0.64	1.25	0.49	0.65
H2O-	0.42	0.18	0.31	0.28	0.21	0.29	0.28	0.23	0.21	0.27	0.25	0.21
CO2	0.05	0.11	0.08	0.05	0.13	0.11	0.05	0.02	0.09	0.09	0.01	0.01
S	0.00	0.05	0.01	0.05	0.04	0.01	0.00	0.00	0.00	0.01	0.00	0.08
Total	100.58	100.55	100.65	99.83	100.36	100.50	99.83	100.19	100.22	100.15	100.07	100.18
A.I.	0.76	0.88	0.93	0.89	0.90	0.90	0.89	0.93	0.93	0.85	0.95	0.91
Cu	3	3	9	12	5	19	4	7	10	6	8	7
Pb	4	4	9	11	1	130	6	1	1	2	1	393
Zn	42	45	38	48	47	52	36	43	40	89	22	63
Ni	5	1	2	5	7	7	5	6	1	14	1	5
Ga	19	22	21	27	20	17	19	18	18	20	20	27
Sc	1.6	1.8	2.1	3.5	1.8	1.8	1.8	1.8	2.4	6.8	2.1	2
Nb	46	47	49	45	47	44	42	44	50	67	98	129
Zr	151	138	140	348	137	137	155	131	139	151	149	152
Y	50	89	72	69	66	65	43	69	89	84	105	126
Ce	93	143	94	161	109	94	63	101	108	68	72	102
U	2	5	6	6	5	7	3	5	5	6	11	16
Th	22	24	24	25	21	29	29	29	29	35	46	49
Sr	37	59	60	88	41	33	32	28	27	73	20	25
Rb	175	185	205	270	195	200	220	105	205	265	290	175
Ba	72	74	76	414	97	87	74	58	60	112	59	45

Table B-9

Field No.	GB90017	GB90018R	GB90019A	GB90022A	GB90023	GB90024	GB90027R	GB90028	GB90030	GB90031	GB90032
SiO2	78.00	76.68	61.26	81.43	77.90	78.45	75.63	75.60	74.95	76.35	73.70
TiO2	0.09	0.09	0.69	0.06	0.05	0.05	0.13	0.14	0.13	0.11	0.20
Al2O3	11.88	12.17	17.91	9.99	11.95	11.75	12.44	12.67	12.56	12.40	12.78
Fe2O3	0.86	0.37	6.32	0.69	0.96	0.75	0.60	0.21	1.68	0.43	2.22
FeO	0.53	0.91	0.38	0.37	0.00	0.45	0.97	1.48	0.62	1.00	0.50
MnO	0.02	0.02	0.05	0.02	0.04	0.03	0.03	0.03	0.02	0.03	0.04
MgO	0.12	0.21	2.27	0.33	0.22	0.20	0.23	0.19	0.29	0.14	0.24
CaO	0.18	0.19	0.98	0.19	0.17	0.43	0.22	0.14	0.20	0.15	0.12
Na2O	3.68	3.44	1.08	3.98	3.37	1.55	3.41	3.56	3.27	3.46	3.13
K2O	4.38	4.78	5.62	1.71	4.44	4.51	4.67	4.95	4.76	4.88	4.71
P2O5	0.01	0.00	0.15	0.03	0.01	0.01	0.01	0.01	0.01	0.02	0.04
F	0.00	0.04	0.08	0.02	0.01	0.10	0.01	0.01	0.01	0.02	0.01
H2O+	0.53	0.73	4.31	0.85	0.93	1.53	0.85	0.75	0.98	0.61	0.81
H2O-	0.25	0.44	1.05	0.28	0.27	0.33	0.28	0.15	0.39	0.23	0.31
CO2	0.00	0.01	0.05	0.07	0.07	0.20	0.08	0.07	0.07	0.07	0.07
S	0.03	0.01	0.06	0.03	0.00	0.00	0.00	0.00	0.00	0.00	0.00
Total	100.56	100.09	102.26	100.02	100.39	100.34	99.55	99.96	99.94	99.90	98.88
A.I.	0.91	0.89	0.44	0.84	0.87	0.63	0.86	0.88	0.84	0.88	0.80
Cu	6	21	21	7	24	5	5	5	6	6	4
Pb	27	1	8	5	171	17	6	2	13	3	13
Zn	25	33	67	30	46	46	49	42	59	45	46
Ni	5	1	27	2	1	1	5	2	4	3	1
Ga	21	24	30	12	20	21	23	23	22	21	19
Sc	1.7	1.7	15.3	2	2.1	2.2	2.1	2.3	2.1	1.9	2.9
Nb	42	46	29	22	35	34	36	38	42	39	33
Zr	145	149	148	89	102	109	176	199	184	179	265
Y	39	67	62	29	60	90	44	37	29	70	22
Ce	81	117	54	20	55	97	122	102	40	131	50
U	3	5	4	4	8	3	3	4	2	5	2
Th	27	25	27	26	35	35	21	24	22	24	22
Sr	26	53	135	53	41	49	48	46	29	37	43
Rb	145	180	360	70	210	285	180	155	170	170	150
Ba	93	79	302	44	107	68	136	165	135	117	224

Table B-9

Field No.	GB90033	GB90034	GB90035	GB90036R	GB90037	GB90038A	GB90039R	GB90040	GB90042	GB90043A	GB90044
SiO2	74.85	74.20	74.20	76.38	77.05	76.18	76.98	76.15	76.80	76.78	77.25
TiO2	0.15	0.17	0.18	0.10	0.09	0.12	0.11	0.11	0.10	0.10	0.10
Al2O3	12.71	12.94	12.95	11.86	12.13	12.60	11.72	12.37	12.13	12.20	12.06
Fe2O3	0.99	0.97	0.59	0.65	0.93	0.80	1.03	0.39	0.25	0.40	0.38
FeO	0.69	0.80	1.26	0.92	0.63	0.72	0.85	0.94	1.21	1.14	0.77
MnO	0.03	0.05	0.04	0.04	0.02	0.03	0.02	0.03	0.02	0.03	0.02
MgO	0.30	0.29	0.30	0.21	0.15	0.14	0.21	0.19	0.18	0.17	0.16
CaO	0.22	0.25	0.20	0.21	0.14	0.24	0.20	0.14	0.17	0.21	0.17
Na2O	3.38	3.85	3.78	3.19	3.29	3.70	3.35	3.63	3.84	3.57	3.02
K2O	5.19	4.99	5.13	4.64	4.82	5.00	4.42	4.77	4.39	4.78	5.10
P2O5	0.02	0.05	0.05	0.00	0.06	0.02	0.01	0.03	0.03	0.03	0.04
F	0.01	0.01	0.00	0.02	0.01	0.01	0.01	0.01	0.01	0.01	0.02
H2O+	0.72	0.71	0.70	0.73	0.68	0.43	0.79	0.53	0.62	0.66	0.86
H2O-	0.23	0.28	0.28	0.31	0.33	0.47	0.38	0.25	0.29	0.30	0.35
CO2	0.10	0.07	0.08	0.08	0.04	0.06	0.03	0.08	0.09	0.05	0.03
S	0.00	0.00	0.00	0.00	0.00	0.00	0.00	0.00	0.00	0.00	0.00
Total	99.59	99.63	99.74	99.34	100.37	100.51	100.11	99.62	100.13	100.40	100.33
A.I.	0.88	0.91	0.91	0.87	0.88	0.91	0.88	0.90	0.91	0.90	0.87
Cu	3	50	8	3	4	3	5	4	7	6	26
Pb	8	1	6	1	17	4	9	1	4	8	4
Zn	53	46	35	34	27	65	35	40	43	37	29
Ni	2	1	2	4	3	1	2	1	1	1	1
Ga	22	20	20	19	19	21	20	20	19	20	19
Sc	2.4	2.6	2.7	1.8	1.7	1.9	1.6	2.1	1.9	1.9	1.8
Nb	35	34	33	41	42	38	42	43	48	42	43
Zr	212	241	259	171	174	202	169	176	184	180	170
Y	50	36	39	58	52	47	29	39	72	86	62
Ce	143	88	81	128	92	112	27	99	119	122	100
U	3	4	3	6	3	3	5	4	4	4	4
Th	25	24	21	22	25	25	24	22	25	24	22
Sr	50	56	61	28	40	39	22	38	25	33	38
Rb	160	140	135	195	185	155	155	175	160	170	225
Ba	227	260	211	84	84	119	95	110	80	107	93

Table B-9

Field No.	GB90045	GB90047	GB90049	GB90050A	GB90051
SiO2	75.95	77.00	74.90	71.45	70.55
TiO2	0.09	0.09	0.19	0.38	0.23
Al2O3	12.04	11.90	12.88	13.80	13.70
Fe2O3	0.54	1.00	0.83	1.09	3.69
FeO	0.73	0.60	0.87	1.45	0.51
MnO	0.02	0.02	0.03	0.06	0.03
MgO	0.16	0.14	0.42	1.01	0.62
CaO	0.31	0.19	0.28	0.44	0.21
Na2O	3.68	3.07	3.73	3.85	3.38
K2O	4.69	5.25	4.61	4.34	5.22
P2O5	0.03	0.05	0.07	0.11	0.07
F	0.06	0.01	0.02	0.03	0.03
H2O+	0.56	0.69	0.98	1.27	1.27
H2O-	0.23	0.55	0.39	0.43	0.35
CO2	0.04	0.05	0.06	0.15	0.05
S	0.00	0.00	0.00	0.01	0.00
Total	99.13	100.61	100.26	99.85	99.91
A.I.	0.92	0.90	0.86	0.80	0.82
Cu	4	4	6	5	5
Pb	2	5	4	2	10
Zn	44	30	51	63	49
Ni	1	3	1	3	3
Ga	21	18	17	17	17
Sc	1.7	1.6	3.6	6.1	4.3
Nb	47	42	37	30	36
Zr	177	154	178	207	193
Y	74	54	47	48	54
Ce	119	90	126	98	99
U	5	3	4	5	3
Th	29	22	21	18	20
Sr	57	35	53	77	54
Rb	190	225	135	120	150
Ba	82	75	215	278	259

Table B-10 St. Lawrence Granite Geochemical Data

Field No.	SG90002	SG90004	SG90005	SG90007	SG90008	SG90009	SG90010	SG90011	SG90012	SG90013	SG90014	SG90016D
SiO2	74.65	65.35	76.55	75.40	69.50	74.55	75.75	77.15	75.90	77.15	77.35	77.05
TiO2	0.27	0.58	0.18	0.18	0.48	0.27	0.23	0.13	0.18	0.17	0.07	0.07
Al2O3	11.02	13.67	11.25	11.26	13.16	10.39	10.73	11.74	12.14	11.67	11.28	11.66
Fe2O3	1.57	2.23	2.03	3.01	2.95	3.69	1.76	1.35	1.18	0.74	1.15	1.05
FeO	2.25	4.43	0.58	0.32	1.40	0.00	1.81	0.25	0.38	0.56	0.39	0.59
MnO	0.14	0.24	0.04	0.03	0.13	0.05	0.13	0.02	0.02	0.03	0.01	0.01
MgO	0.23	0.24	0.05	0.03	0.43	0.10	0.09	0.04	0.02	0.13	0.03	0.01
CaO	0.27	1.48	0.09	0.03	0.37	1.04	0.32	0.27	0.16	0.31	0.07	0.21
Na2O	3.96	4.59	3.80	3.16	4.06	2.23	3.35	3.57	3.22	3.32	2.99	4.22
K2O	4.84	4.97	5.01	5.57	5.41	4.89	5.32	4.82	5.30	4.96	4.64	3.88
P2O5	0.02	0.12	0.01	0.01	0.09	0.02	0.01	0.01	0.02	0.02	0.01	0.01
F	0.05	0.02	0.02	0.00	0.02	0.02	0.06	0.09	0.01	0.07	0.06	0.11
H2O+	0.50	0.58	0.35	0.19	0.64	0.80	0.27	0.13	0.36	0.37	0.66	0.18
H2O-	0.29	0.34	0.19	0.15	0.21	0.25	0.20	0.16	0.20	0.19	0.25	0.19
CO2	0.08	0.12	0.07	0.10	0.05	0.74	0.14	0.06	0.03	0.09	0.08	0.06
S	0.00	0.00	0.00	0.00	0.00	0.83	0.00	0.00	0.00	0.04	0.01	0.00
Total	100.14	98.96	100.22	99.44	98.90	99.87	100.17	99.79	99.12	99.82	99.05	99.30
A.I.	1.07	0.95	1.04	1.00	0.95	0.86	1.05	0.94	0.91	0.93	0.88	0.96
Cu	17	13	9	16	14	67	12	12	21	11	33	20
Pb	22	4	23	17	3	10	25	20	20	20	57	14
Zn	194	98	112	56	142	60	204	30	63	41	51	17
Ni	4	1	2	7	1	4	6	2	1	3	2	1
Sc	1	8.5	0.5	0.5	6.1	2.1	0.2	1.4	1.9	1.7	0.3	0.2
Ga	32	29	30	32	32	19	27	19	20	17	23	27
Nb	56	32	82	71	44	55	60	49	35	28	82	82
Zr	751	421	811	758	556	747	834	154	183	178	260	299
Y	99	47	63	101	73	93	106	59	27	49	78	117
Ce	243	107	103	166	168	221	239	126	110	128	88	128
U	6	2	8	5	4	6	5	6	3	6	8	8
Th	20	8	36	28	17	22	25	46	39	35	40	32
Sr	8	48	5	7	20	50	13	14	24	27	7	16
Rb	175	85	250	280	150	175	250	305	295	255	335	243
Ba	78	779	104	86	473	763	105	64	136	136	40	58

Table B-10

Field No.	SG90018	SG90019	SG90020A	SG90021	SG90023	SG90024	SG90026R	SG90027	SG90028	SG90029	SG90030R	SG90032
SiO2	81.50	78.00	78.75	75.70	6.45	77.05	77.36	75.90	76.90	77.80	76.12	74.75
TiO2	0.07	0.08	0.07	0.17	0.01	0.15	0.14	0.12	0.12	0.11	0.14	0.19
Al2O3	11.02	11.97	11.76	11.40	0.28	11.34	11.82	10.97	11.39	11.24	12.80	11.23
Fe2O3	0.22	0.99	0.82	2.74	0.21	1.39	0.59	2.18	0.99	1.90	0.08	2.10
FeO	0.66	0.47	0.23	1.09	0.00	0.49	0.29	0.15	0.99	0.24	1.08	0.76
MnO	0.02	0.01	0.01	0.03	0.01	0.03	0.01	0.02	0.06	0.02	0.03	0.06
MgO	0.08	0.03	0.01	0.02	0.02	0.04	0.04	0.05	0.02	0.02	0.16	0.07
CaO	0.05	0.02	0.02	0.04	67.20	0.08	0.04	0.20	0.18	0.01	0.09	0.16
Na2O	0.16	2.95	4.02	3.68	0.01	3.39	3.45	3.35	3.84	3.53	1.38	4.02
K2O	3.94	4.73	4.36	4.45	0.07	4.79	5.09	4.65	4.88	4.58	5.68	4.73
P2O5	0.01	0.01	0.01	0.01	0.01	0.01	0.01	0.01	0.01	0.01	0.01	0.01
F	0.05	0.02	0.03	0.01	17.30	0.04	0.01	0.08	0.15	0.01	0.04	0.09
H2O+	1.59	0.85	0.42	0.40		0.04	0.44	0.78	0.36	0.52	1.26	0.63
H2O-	0.35	0.30	0.30	0.20	0.19	0.24	0.23	0.37	0.30	0.23	0.26	0.19
CO2	0.07	0.06	0.06	0.05		0.07	0.18	0.14	0.16	0.20	0.13	0.14
S	0.02	0.00	0.00	0.00		0.00	0.00	0.01	0.00	0.00	0.27	0.00
Total	99.81	100.49	100.85	99.99		99.15	99.70	98.98	100.35	100.42	99.52	99.13
A.I.	0.41	0.83	0.96	0.95	0.33	0.95	0.95	0.96	1.02	0.96	0.66	1.04
Cu	26	28	14	19	9	12	17	13	13	14	17	20
Pb	10	27	23	41	29	21	34	55	23	48	40	35
Zn	73	50	48	46	20	52	34	115	151	100	187	197
Ni	8	2	26	2	1	2	2	7	3	1	9	3
Sc	0.3	0.5	0.2	0.4	0.1	0.4	0.7	0.1	0.2	0.2	2.2	0.5
Ga	34	28	30	32	4	28	30	33	25	27	20	28
Nb	95	126	106	87	1	61	67	137	66	78	43	78
Zr	332	353	355	568	1	447	492	832	472	532	170	856
Y	95	58	27	87	83	138	64	117	79	115	45	123
Ce	79	42	60	117	10	163	182	208	141	161	121	191
U	9	12	11	9	2	6	9	14	6	7	8	9
Th	44	55	42	36	0	23	31	60	21	25	27	22
Sr	14	6	3	14	365	5	6	6	5	4	17	6
Rb	345	360	310	195	10	245	265	328	270	240	295	235
Ba	1247	62	24	133	4	53	73	59	35	54	254	52

Table B-10

Field No.	SG90033R	SG90034R	SG90035	SG90036	SG90038	SG90039R	SG90040	SG90042R	SG90044	SG90045	SG90046	SG90047
SiO2	76.81	76.88	76.85	76.75	76.55	77.87	76.65	62.23	62.35	71.35	76.85	79.00
TiO2	0.15	0.12	0.14	0.12	0.13	0.11	0.12	1.09	1.09	0.51	0.12	0.10
Al2O3	11.07	10.97	11.17	10.99	11.30	11.03	11.42	14.31	14.53	12.75	11.20	11.12
Fe2O3	1.56	1.29	1.57	2.35	2.08	1.44	2.35	3.50	3.58	2.94	1.77	0.58
FeO	0.96	0.76	0.47	0.15	0.25	0.14	0.14	3.89	3.87	1.59	0.21	0.24
MnO	0.07	0.05	0.03	0.01	0.03	0.01	0.01	0.40	0.41	0.11	0.01	0.01
MgO	0.08	0.02	0.05	0.01	0.06	0.02	0.01	1.62	1.65	0.05	0.01	0.02
CaO	0.24	0.15	0.08	0.10	0.04	0.06	0.22	1.40	1.40	0.66	0.23	0.02
Na2O	3.87	3.75	3.06	3.23	3.27	3.31	3.27	4.31	4.42	3.57	3.69	3.35
K2O	4.58	4.65	5.43	4.91	4.86	4.52	4.73	4.52	4.75	5.30	4.41	4.76
P2O5	0.01	0.00	0.01	0.01	0.01	0.01	0.01	0.37	0.36	0.12	0.01	0.01
F	0.12	0.09	0.04	0.06	0.02	0.02	0.12	0.07	0.07	0.02	0.15	0.04
H2O+	0.55	0.39	0.66	0.34	0.57	0.67	0.39	1.90	1.90	0.86	0.47	0.26
H2O-	0.15	0.18	0.23	0.19	0.13	0.31	0.34	0.40	0.40	0.35	0.15	0.15
CO2	0.14	0.14	0.14	0.12	0.14	0.01	0.00	0.04	0.04	0.38	0.02	0.00
S	0.01	0.00	0.02	0.01	0.01	0.07	0.01	0.03	0.03	0.02	0.01	0.00
Total	100.36	99.45	99.95	99.35	99.45	99.60	99.79	100.08	100.85	100.58	99.31	99.66
A.I.	1.02	1.02	0.98	0.97	0.94	0.94	0.92	0.84	0.85	0.91	0.97	0.96
Cu	14	29	17	26	18	19	14	19	11	37	15	11
Pb	45	56	53	72	18	42	65	57	45	10	40	14
Zn	195	155	110	28	71	21	25	321	240	96	51	26
Ni	2	2	7	3	1	43	1	5	6	9	48	4
Sc	0.2	0.2	0.2	0.1	0.1	0.2	0.2	12.1	13.8	6	0.2	0.4
Ga	26	27	26	28	33	29	31	29	30	30	32	31
Nb	90	85	88	87	89	83	101	33	32	47	258	106
Zr	551	534	660	567	592	507	626	423	413	603	1317	500
Y	149	110	130	128	162	110	136	55	53	79	133	45
Ce	199	146	164	170	190	155	171	136	129	179	207	59
U	10	9	10	11	7	6	8	3	3	5	27	7
Th	30	22	31	23	29	26	27	0	0	0	82	25
Sr	6	5	6	5	4	4	4	116	210	31	7	3
Rb	245	250	310	270	280	270	280	110	135	180	365	335
Ba	48	39	56	37	36	48	33	833	1052	434	42	43

Table B-10

Field No.	SG90048	SG90049	SG90050	SG90051	SG90052	SG90053A	SG90054	SG90055	SG90056	SG90057	SG90059	SG90060
SiO2	78.50	4.60	0.35	75.80	25.65	77.55	80.50	36.40	76.65	92.20	76.30	2.30
TiO2	0.10	0.01	0.01	0.10	0.02	0.12	0.13	0.01	0.13	0.01	0.15	0.01
Al2O3	11.41	0.27	0.03	9.69	2.06	11.46	9.94	0.50	11.20	0.31	11.52	0.02
Fe2O3	1.38	0.05	0.03	0.83	0.24	1.12	0.99	0.19	1.09	0.32	1.22	0.04
FeO	0.30	0.00	0.00	0.20	0.22	0.23	0.36	0.00	0.87	0.00	1.01	0.00
MnO	0.01	0.01	0.01	0.02	0.01	0.01	0.01	0.01	0.01	0.01	0.05	0.01
MgO	0.02	0.01	0.01	0.02	0.01	0.01	0.02	0.01	0.01	0.01	0.02	0.01
CaO	0.02	68.26	71.43	4.03	49.70	0.07	0.08	44.67	0.67	5.08	0.18	70.16
Na2O	3.36	0.05	0.05	1.92	0.06	3.47	2.02	0.01	3.20	0.01	3.52	0.01
K2O	4.80	0.10	0.01	4.52	1.07	4.73	4.86	0.05	4.89	0.06	4.80	0.02
P2O5	0.01	0.01	0.01	0.01	0.01	0.01	0.01	0.01	0.01	0.01	0.01	0.01
F	0.03	14.00	13.30	1.55	21.20	0.04	0.05	22.40	0.38	0.30	0.10	11.70
H2O+	0.30					0.44	0.90				0.59	
H2O-	0.25	0.19	0.16	0.22	0.15	0.31	0.34	0.20	0.25	0.12	0.19	0.11
CO2	0.07					0.09	0.08				0.05	
S	0.02					0.04	0.04				0.03	
Total	100.58					99.67	100.33				99.74	
A.I.	0.94	0.71	3.10	0.83	0.61	0.94	0.86	0.14	0.94	0.26	0.95	1.90
Cu	14	23	12	23	90	11	11	17	37	13	18	13
Pb	17	595	4	106	361	19	37	35	49	39	22	127
Zn	30	13	7	36	2131	19	70	12	52	12	69	7
Ni	3	4	2	4	13	7	2	3	6	2	6	6
Sc	0.5	0	0	0.1	0.2	0.6	0.4	0.1	0.4	0.1	0.5	0
Ga	32	1	1	27	7	32	24	4	27	4	28	3
Nb	110	2	0	112	22	113	56	4	60	4	127	1
Zr	567	9	7	480	144	563	636	30	473	16	816	2
Y	69	747	582	141	282	73	72	295	97	100	140	612
Ce	158	20	20	129	46	141	148	24	142	13	217	21
U	8	1	0	9	2	9	5	0	6	0	13	0
Th	30	3	3	43	14	44	27	10	18	8	47	12
Sr	5	57	43	10	18	4	6	26	14	7	10	49
Rb	310	0	0	305	55	305	265	5	240	0	225	0
Ba	75	3	4	52	16	55	74	427	76	16	108	3

Table B-10

Field No.	SG90061	SG90062	SG90063	SG90064	SG90065	SG90066	SG90067	SG90068	SG90069R	SG90070	SG90071	SG90072
SiO2	78.15	77.95	3.80	76.10	77.50	1.75	75.30	75.20	76.30	77.15	80.10	76.40
TiO2	0.13	0.14	0.01	0.14	0.12	0.01	0.15	0.13	0.14	0.12	0.11	0.12
Al2O3	10.99	11.08	0.27	11.49	11.12	0.04	11.67	11.24	11.39	10.88	9.06	11.26
Fe2O3	1.31	1.74	0.01	1.87	1.21	0.06	1.52	1.44	1.81	1.82	1.80	0.33
FeO	0.38	0.29	0.06	0.37	0.17	0.00	0.38	0.25	0.34	0.53	0.48	0.35
MnO	0.01	0.01	0.01	0.01	0.03	0.01	0.04	0.04	0.08	0.01	0.02	0.01
MgO	0.01	0.01	0.01	0.01	0.01	0.01	0.04	0.01	0.08	0.01	0.01	0.01
CaO	0.05	0.06	67.80	1.13	0.32	68.99	0.84	1.09	0.06	0.09	0.24	1.69
Na2O	2.44	3.29	0.06	3.86	3.40	0.05	3.51	3.53	3.24	3.11	2.11	3.68
K2O	5.69	4.87	0.16	4.58	4.76	0.02	5.14	4.92	5.25	4.93	4.86	4.65
P2O5	0.01	0.01	0.01	0.01	0.01	0.01	0.01	0.01	0.02	0.01	0.01	0.01
F	0.02	0.04	15.00	0.55	0.17	11.70	0.18	0.26	0.01	0.05	0.13	0.88
H2O+	0.58	0.44			0.46		0.61		0.56	0.39	0.47	
H2O-	0.24	0.20	0.15	0.15	0.30	0.24	0.26	0.16	0.21	0.20	0.15	0.15
CO2	0.05	0.04			0.05		0.50		0.03	0.04	0.02	
S	0.03	0.03			0.06		0.06		0.06	0.06	0.02	
Total	100.09	100.20			99.69		100.21		99.57	99.40	99.59	
A.I.	0.93	0.96	1.01	0.98	0.97	2.60	0.97	0.99	0.97	0.96	0.96	0.98
Cu	16	17	13	19	28	9	23	22	15	15	25	23
Pb	68	13	6	12	65	14	11	13	40	90	26	115
Zn	40	40	12	19	84	8	79	29	159	21	34	81
Ni	2	2	83	1	3	1	1	7	4	2	4	1
Sc	0.4	0.4	0.1	0.4	0.3	0	0.6	0.3	0.4	0.2	0.1	0.2
Ga	24	25	4	26	31	2	28	29	29	26	22	30
Nb	52	60	2	88	95	1	84	89	73	76	89	92
Zr	453	488	11	675	489	2	521	846	568	529	529	521
Y	79	73	595	134	127	706	135	158	139	102	95	88
Ce	194	168	20	208	152	22	166	170	175	168	151	154
U	4	6	0	6	9	0	7	6	6	6	9	9
Th	25	16	9	27	31	0	23	29	20	20	20	33
Sr	7	6	30	14	8	42	12	8	6	5	11	6
Rb	290	235	10	240	285	0	265	295	250	260	285	280
Ba	88	58	11	94	74	3	75	63	66	42	57	38

Table B-11 Terranceville Area Geochemical Data

Field No.	TV92001	TV92002	TV92003	TV92004	TV92005	TV92006	TV92007
SiO2	69.91	63.29	74.73	76.42	70.84	76.17	72.46
TiO2	0.42	1.05	0.18	0.20	0.21	0.19	0.19
Al2O3	14.70	14.21	11.84	10.41	11.93	11.47	13.08
Fe2O3	2.27	6.19	2.44	2.55	2.72	2.41	2.86
FeO	0.75	1.55	0.28	0.34	0.69	0.39	0.06
MnO	0.08	0.17	0.04	0.06	0.11	0.07	0.06
MgO	1.33	1.85	0.25	0.04	0.07	0.03	0.06
CaO	1.66	2.86	0.09	0.42	2.29	0.03	0.22
Na2O	1.95	2.23	3.89	1.79	4.01	4.16	3.90
K2O	3.72	3.69	4.09	6.88	4.34	4.02	5.69
P2O5	0.06	0.15	0.02	0.00	0.00	0.01	0.04
F	0.05	0.06	0.01	0.01	0.01	0.00	0.01
H2O+	2.13	2.17	0.53	0.43	0.51	0.23	0.29
H2O-							
CO2	0.1	0.11	0.06	0.43	1.8	0.17	0.17
S	0.09	0.13	0.04	0.07	0.04	0	0.02
Total	99.13	99.58	98.45	99.98	99.53	99.35	99.09
A.I.	0.49	0.54	0.91	1.00	0.95	0.98	0.96
Cu	13	11	12	7	6	12	7
Pb	10	3	5	12	0	12	16
Zn	90	131	83	151	143	120	111
Ni	1	9	0	1	0	4	2
Sc	6.1	21.2	2.2	< 0.1	< 0.1	< 0.1	0.1
Ga	25	21	23	25	37	39	45
Nb	18	5	30	50	46	49	59
Zr	423	175	535	992	1082	1008	1168
Y	53	29	81	116	97	130	148
Ce	122	56	164	206	261	222	259
U	4	2	3	2	4	3	4
Th	23	2	15	17	21	17	22
Sr	179	247	32	30	39	3	16
Rb	197	163	76	194	121	119	171
Ba	534	516	671	47	31	23	59

Table B-12 Bull Arm Formation Geochemical Data

Field No.	BA90001	BA90005A	BA90006	BA90007	BA90008	BA90010R	BA90011A	BA90013	BA90014R	BA90016	BA90019
SiO2	73.80	76.98	76.25	75.45	76.75	74.38	77.03	75.65	76.40	63.55	76.30
TiO2	0.16	0.18	0.14	0.15	0.10	0.18	0.09	0.11	0.10	0.98	0.64
Al2O3	12.74	11.01	11.86	12.07	11.53	12.51	11.65	12.14	12.01	16.66	11.24
Fe2O3	1.58	0.33	1.01	1.14	0.70	1.16	0.44	1.00	0.61	6.13	2.91
FeO	1.11	1.04	0.79	0.72	1.02	0.97	1.32	0.48	0.87	0.64	0.56
MnO	0.07	0.03	0.02	0.01	0.02	0.03	0.03	0.01	0.03	0.10	0.11
MgO	0.43	0.34	0.08	0.06	0.02	0.14	0.02	0.04	0.05	2.12	1.35
CaO	1.88	2.21	0.17	0.27	0.19	0.43	0.26	0.06	0.27	1.77	0.84
Na2O	4.36	4.23	4.19	4.37	4.48	4.33	3.92	4.23	3.91	2.61	1.92
K2O	2.05	2.00	4.53	4.51	4.06	4.45	4.50	4.61	4.67	1.74	1.20
P2O5	0.02	0.04	0.01	0.03	0.01	0.03	0.01	0.02	0.00	0.06	0.01
F	0.04	0.01	0.11	0.14	0.13	0.10	0.11	0.02	0.11	0.02	0.01
H2O+	0.94	0.67	0.43	0.58	0.17	0.44	0.24	0.28	0.18	2.67	2.00
H2O-	0.29	0.40	0.38	0.56	0.30	0.30	0.18	0.22	0.43	0.47	0.45
CO2	0.05	1.04	0.08	0.09	0.01	0.05	0.10	0.01	0.08	0.27	0.01
S	0.02	0.01	0.00	0.00	0.00	0.00	0.00	0.00	0.00	0.01	0.01
Total	99.54	100.48	100.05	100.15	99.49	99.50	99.87	98.88	99.71	99.80	99.56
A.I.	0.74	0.83	0.99	1.00	1.02	0.95	0.97	0.98	0.96	0.37	0.40
Cu	5	3	6	5	3	12	11	4	4	1	16
Pb	13	3	11	15	9	18	18	9	6	14	4
Zn	68	14	36	86	122	86	69	37	68	77	74
Ni	4	6	3	4	2	5	6	2	3	23	24
Ga	27	12	30	33	34	27	27	25	25	20	13
Sc	1.8	3.3	1.1	1.2	0.4	2.3	0.4	0.6	0.7	14	9.8
Nb	53	6	56	80	97	47	58	46	44	10	10
Zr	565	113	420	453	499	388	252	297	266	472	213
Y	123	16	60	61	118	86	81	51	76	31	26
Ce	180	41	100	133	102	98	100	112	103	91	59
U	3	2	5	5	8	4	7	4	6	4	2
Th	13	9	21	48	35	21	22	20	21	25	6
Sr	217	148	9	13	7	32	5	11	11	203	107
Rb	40	23	165	190	205	150	155	120	140	60	40
Ba	387	493	128	107	23	243	21	91	83	419	282

Table B-12

Field No.	BA90022	BA90025	BA90028	BA90031A	BA90036	BA90037	BA90041	BA90042	BA90043	BA90045	BA90046	BA90047
SiO2	47.95	62.50	69.05	66.05	71.35	56.60	47.85	66.80	43.95	60.20	73.90	42.35
TiO2	0.96	0.63	0.47	1.39	0.56	1.48	2.80	0.49	1.99	0.92	0.26	2.28
Al2O3	15.80	19.82	13.16	12.89	12.25	15.85	18.08	12.46	15.47	17.00	7.85	13.18
Fe2O3	8.74	2.06	3.89	4.82	5.10	4.43	0.95	6.26	6.01	3.14	4.45	3.94
FeO	1.64	0.72	0.00	1.48	0.64	6.24	8.62	0.55	5.88	4.09	4.68	7.62
MnO	0.15	0.06	0.09	0.18	0.11	0.16	0.19	0.12	0.49	0.14	0.25	0.30
MgO	7.18	1.05	1.39	1.02	0.08	2.61	4.73	0.12	5.22	2.82	0.13	4.33
CaO	8.66	2.13	1.33	2.56	0.08	1.90	6.59	3.20	8.68	1.78	2.10	9.65
Na2O	3.85	2.63	1.81	3.97	2.39	5.06	3.59	5.37	3.03	3.09	2.79	3.23
K2O	1.06	4.59	5.74	1.51	5.72	0.93	0.24	1.03	0.22	2.68	0.14	0.20
P2O5	0.26	0.11	0.12	0.15	0.03	0.41	0.57	0.03	0.35	0.17	0.01	0.43
F	0.03	0.05	0.03	0.03	0.02	0.04	0.10	0.02	0.03	0.03	0.01	0.03
H2O+	2.48	2.61	1.66	1.71	0.81	2.74	3.98	0.40	3.36	3.33	1.25	3.40
H2O-	0.26	0.17	0.20	0.39	0.32	0.50	0.59	0.15	0.30	0.39	0.14	0.34
CO2	0.06	0.14	0.42	1.09	0.11	0.04	0.75	2.44	4.16	0.00	1.03	7.72
S	0.00	0.01	0.91	0.01	0.00	0.00	0.00	0.00	0.00	0.00	0.00	0.00
Total	99.08	99.28	100.27	99.22	99.57	98.99	99.63	99.44	99.14	99.78	98.99	99.00
A.I.	0.47	0.47	0.70	0.63	0.83	0.59	0.34	0.80	0.34	0.47	0.60	0.42
Cu	53	34	30	53.5	7	66	86	239	32	49	10	67
Pb	8	7	5	10	14	1	1	25	5	9	25	3
Zn	78	54	57	102	185	115	133	74	104	101	381	114
Ni	104	5	11	19.5	3	5	72	5	64	23	3	55
Ga	19	26	14	18	43	26	28	27	25	23	38	22
Sc	40.5	16.3	9.5	14.6	0.2	31.7	33.9	0.7	30.6	22.2	0.3	28.7
Nb	0	20	5	12	122	5	12	130	10	7	284	9
Zr	62	364	159	343	674	162	172	560	146	181	2521	147
Y	21	77	17	31	89	32	31	57	27	29	248	26
Ce	33	146	51	70	171	63	51	138	47	57	589	41
U	0	20	2	2	5	38	0	3	0	2	11	0
Th	1	18	11	7	15	7	1	14	1	10	38	1
Sr	322	228	152	175	73	152	507	235	370	228	224	266
Rb	25	130	140	58	130	20	5	25	10	60	0	0
Ba	614	938	566	448	110	288	108	172	140	535	30	74

Table B-12

Field No.	BA90048	BA90049	BA90050	BA90051	BA90052R	BA90053	BA90054	BA90056	BA90057	BA90064	BA90066	BA90067A
SiO2	74.40	82.20	73.95	73.90	75.82	72.95	74.45	72.30	41.60	75.70	72.85	74.85
TiO2	0.32	0.26	0.22	0.48	0.46	0.47	0.27	0.28	2.17	0.21	0.30	0.23
Al2O3	8.06	5.82	13.75	13.62	11.60	10.45	13.45	14.28	13.89	10.76	10.59	10.81
Fe2O3	9.17	4.72	1.39	0.76	0.61	7.03	1.94	1.40	16.50	3.13	4.49	3.10
FeO	0.00	0.00	0.72	0.81	2.64	0.47	0.21	0.74	0.00	0.21	0.19	0.61
MnO	0.18	0.03	0.07	0.01	0.06	0.03	0.04	0.26	0.23	0.09	0.07	0.06
MgO	0.39	0.39	0.39	0.03	0.04	0.03	0.38	0.30	5.17	0.09	0.03	0.02
CaO	1.26	0.04	0.96	0.02	0.05	0.01	0.40	1.01	12.74	0.29	0.95	1.05
Na2O	0.24	0.07	5.92	3.14	2.05	1.19	5.39	4.62	2.85	1.95	2.36	4.15
K2O	1.36	1.21	0.86	4.70	3.68	4.70	1.56	3.49	0.03	6.42	5.59	3.20
P2O5	0.01	0.02	0.04	0.03	0.03	0.02	0.04	0.08	0.27	0.04	0.05	0.03
F	0.05	0.03	0.01	0.02	0.02	0.01	0.02	0.01	0.03	0.01	0.01	0.01
H2O+	2.30	2.06	0.88	1.45	1.66	1.62	1.31	1.25	3.62	0.40	0.34	0.39
H2O-	0.21	0.45	0.37	0.31	0.30	0.39	0.21	0.22	0.28	0.31	0.15	0.17
CO2	0.75	0.22	0.75	0.09	0.18	0.56	0.04	0.15	1.10	0.04	0.73	0.58
S	0.65	2.08	0.00	0.00	0.00	0.28	0.01	0.04	0.06	0.07	0.03	0.05
Total	99.35	99.60	100.28	99.37	99.19	100.21	99.72	100.43	100.54	99.72	98.73	99.28
A.I.	0.23	0.24	0.78	0.75	0.63	0.67	0.78	0.80	0.34	0.94	0.94	0.95
Cu	6	11	7	12	8	5	13	8	17	7	6	5
Pb	22	63	2	3	11	14	3	11	6	23	16	18
Zn	338	320	47	208	310	240	35	30	102	45	59	26
Ni	5	4	4	2	5	1	2	4	63	5	2	2
Ga	41	30	19	37	34	45	16	16	33	31	26	26
Sc	0.1	0.1	2.8	0.5	0.1	0.1	4.1	3.9	38.9	0.6	0.8	1.2
Nb	220	426	28	142	126	173	18	20	7	36	38	33
Zr	1577	3892	321	981	755	1019	255	285	144	746	696	770
Y	186	347	37	118	116	79	29	31	33	110	63	87
Ce	427	470	82	177	425	253	80	94	37	166	161	163
U	7	16	5	18	7	2	2	2	0	3	2	3
Th	27	56	18	29	20	20	13	13	1	20	14	15
Sr	41	18	165	39	18	21	86	151	72	39	20	63
Rb	40	45	20	135	100	150	55	85	0	180	130	65
Ba	325	192	166	50	40	25	416	965	21	289	94	271

Table B-12

Field No.	BA90068	BA90070	BA90071	BA90072	BA90073	BA90075	BA90077	BA90081	BA90082	BA90083	BA90085	BA90086
SiO2	72.05	75.90	77.95	75.05	74.65	66.65	67.50	60.75	67.15	75.90	64.85	71.65
TiO2	0.45	0.22	0.26	0.31	0.29	0.66	0.70	1.07	0.58	0.12	0.74	0.23
Al2O3	12.89	10.64	8.14	10.08	12.54	15.08	14.61	16.14	15.05	12.18	15.44	15.17
Fe2O3	2.28	2.91	3.38	3.64	1.82	3.80	3.41	6.28	2.76	0.09	4.34	1.64
FeO	0.81	0.79	0.98	1.20	0.78	1.01	0.79	1.17	1.29	0.86	1.09	0.50
MnO	0.05	0.03	0.07	0.06	0.06	0.11	0.06	0.14	0.08	0.02	0.15	0.03
MgO	0.36	0.25	0.38	0.24	0.71	1.85	0.38	1.80	0.28	0.10	1.31	0.16
CaO	0.48	0.25	0.46	0.31	0.55	1.29	1.31	1.85	1.40	1.02	2.06	0.09
Na2O	4.01	2.74	2.30	3.55	4.10	4.13	3.84	5.39	4.82	3.61	4.85	5.17
K2O	4.71	4.95	3.59	3.43	1.89	3.04	5.52	3.07	4.74	4.18	3.12	4.45
P2O5	0.11	0.04	0.01	0.02	0.06	0.09	0.18	0.38	0.13	0.02	0.20	0.05
F	0.02	0.01	0.00	0.01	0.03	0.03	0.03	0.03	0.02	0.01	0.04	0.01
H2O+	0.67	0.64	0.38	0.37	1.73	2.46	1.09	1.82	0.80	0.65	1.41	0.44
H2O-	0.17	0.25	0.16	0.13	0.36	0.35	0.29	0.39	0.29	0.18	0.21	0.21
CO2	0.03	0.29	0.66	0.34	0.02	0.04	0.50	0.06	0.03	0.70	0.00	0.02
S	0.05	0.06	0.05	0.03	0.02	0.08	0.07	0.06	0.06	0.00	0.00	0.00
Total	99.14	99.97	98.77	98.77	99.61	100.67	100.28	100.40	99.48	99.64	99.81	99.82
A.I.	0.91	0.93	0.94	0.95	0.70	0.67	0.84	0.76	0.87	0.86	0.74	0.88
Cu	6	6	16	6	14	12	27	54	7	6	47	9
Pb	7	9	19	17	2	10	6	9	6	5	5	9
Zn	105	101	63	92	57	102	59	96	44	12	97	38
Ni	2	2	2	4	5	16	1	13	1	2	3	3
Ga	16	26	28	31	12	23	19	21	20	12	21	19
Sc	13.7	0.6	0.8	0.8	8	13.1	9.4	17.6	8	1.6	15.3	6.2
Nb	21	35	26	38	13	15	17	11	16	7	8	17
Zr	401	792	539	733	136	329	428	289	438	111	265	356
Y	51	110	66	82	29	46	42	46	44	12	47	39
Ce	89	225	141	185	55	71	102	89	110	51	79	97
U	3	3	2	2	3	2	6	4	5	4	3	6
Th	10	20	13	14	10	8	18	8	15	21	10	21
Sr	51	21	25	26	155	282	168	311	242	68	220	49
Rb	55	135	90	85	60	95	155	60	100	100	80	135
Ba	768	74	83	76	342	488	1409	970	1407	837	968	453

Table B-12

Field No.	BA90089	BA90091	BA90092	BA90096	BA90097R	BA90098R	BA90099R	BA90100	BA90101R	BA90103	BA90105
SiO2	62.25	66.10	73.70	68.00	77.28	73.10	75.81	77.85	76.57	72.10	79.20
TiO2	0.88	0.41	0.23	0.11	0.09	0.20	0.09	0.09	0.09	0.39	0.09
Al2O3	14.75	15.96	11.97	14.95	11.50	13.07	11.72	11.15	11.40	13.78	10.80
Fe2O3	5.07	3.81	2.83	2.09	0.85	1.95	1.67	1.17	1.60	2.59	1.18
FeO	1.07	0.71	0.51	0.67	0.99	0.58	0.26	0.25	0.11	0.37	0.50
MnO	0.13	0.09	0.09	0.05	0.01	0.07	0.02	0.02	0.05	0.08	0.05
MgO	0.84	1.72	0.10	0.13	0.01	0.81	0.02	0.01	0.06	0.10	0.01
CaO	3.82	0.44	0.09	0.06	0.07	2.29	0.17	0.04	0.23	0.37	0.46
Na2O	2.21	3.20	2.51	0.78	3.43	1.46	2.32	1.68	2.23	5.59	4.50
K2O	3.64	5.32	6.33	11.68	5.03	4.46	6.80	7.15	6.53	3.38	2.73
P2O5	0.18	0.06	0.05	0.02	0.01	0.02	0.01	0.02	0.01	0.06	0.06
F	0.04	0.08	0.01	0.00	0.00	0.08	0.01	0.00	0.00	0.02	0.01
H2O+	1.86	2.08	1.19	0.60	0.28	1.66	0.31	0.32	0.25	0.19	0.24
H2O-	0.23	0.32	0.23	0.26	0.32	0.37	0.32	0.29	0.31	0.25	0.17
CO2	2.59	0.03	0.25	0.04	0.02	0.04	0.11	0.01	0.07	0.06	0.14
S	0.00	0.00	0.00	0.00	0.00	0.00	0.00	0.00	0.00	0.00	0.00
Total	99.56	100.33	100.09	99.44	99.90	100.17	99.63	100.05	99.51	99.33	100.14
A.I.	0.51	0.69	0.92	0.93	0.96	0.55	0.95	0.94	0.94	0.93	0.96
Cu	11	6	4	23	5	15	3	2	1	3	5
Pb	10	8	14	22	1	18	13	8	12	10	12
Zn	109	145	204	195	20	141	41	29	235	82	58
Ni	1	14	1	3	4	7	4	3	3	3	6
Ga	20	28	14	26	18	27	22	19	16	17	17
Sc	15.3	15.7	18.6	11	5.5	9.6	6.2	4.1	6.8	19.1	5.4
Nb	6	20	19	29	20	21	24	23	23	17	21
Zr	204	512	701	462	342	396	351	336	347	596	342
Y	36	96	77	159	69	119	54	42	126	91	103
Ce	34	128	156	156	105	124	119	97	115	181	102
U	2	2	3	6	4	4	3	3	3	2	3
Th	6	14	10	22	14	17	15	20	14	8	14
Sr	141	102	38	30	20	169	27	28	39	68	29
Rb	95	268	130	315	130	240	175	180	160	65	40
Ba	832	717	3176	1277	421	887	703	749	1379	2228	267

Table B-12

Field No.	BA90107	BA90109	BA90110	BA90112	BA90113	BA90116	BA90118A	BA90120	BA90121	BA90123R	BA90124	BA90126
SiO2	76.25	77.20	72.10	67.20	78.95	77.65	66.39	76.40	77.45	64.87	71.30	68.30
TiO2	0.10	0.10	0.22	0.50	0.16	0.09	0.79	0.10	0.10	0.69	0.51	0.53
Al2O3	11.67	11.18	13.28	14.87	10.09	10.99	15.92	11.26	10.99	15.42	14.29	15.25
Fe2O3	1.30	1.76	2.46	4.12	1.36	0.81	4.98	0.73	1.06	3.61	2.55	1.77
FeO	0.54	0.26	0.30	0.88	0.70	0.75	0.00	1.15	0.66	1.09	0.41	1.42
MnO	0.08	0.05	0.15	0.43	0.04	0.02	0.09	0.04	0.03	0.17	0.06	0.13
MgO	0.02	0.04	0.51	0.74	0.17	0.02	1.83	0.22	0.55	1.71	0.10	0.81
CaO	0.26	0.06	2.17	0.52	0.28	0.06	1.09	0.15	0.07	3.61	0.88	1.61
Na2O	1.12	1.59	3.17	4.18	2.71	1.03	3.58	1.87	1.75	2.09	5.02	4.83
K2O	8.31	7.32	3.78	5.68	4.69	8.08	2.49	6.83	6.60	3.30	4.24	3.72
P2O5	0.02	0.03	0.03	0.12	0.03	0.03	0.08	0.03	0.02	0.28	0.13	0.15
F	0.00	0.00	0.03	0.01	0.02	0.00	0.03	0.01	0.01	0.06	0.02	0.05
H2O+	0.81	0.56	1.23	0.86	0.42	0.92	2.78	0.65	0.99	2.72	0.46	1.17
H2O-	0.19	0.17	0.17	0.17	0.14	0.14	0.14	0.12	0.13	0.18	0.14	0.17
CO2	0.13	0.09	0.08	0.08	0.07	0.25	0.16	0.16	0.11	0.08	0.03	0.05
S	0.00	0.00	0.00	0.00	0.03	0.03	0.61	0.08	0.05	0.03	0.06	0.05
Total	100.80	100.41	99.68	100.36	99.86	100.87	100.95	99.80	100.57	99.91	100.20	100.01
A.I.	0.93	0.94	0.70	0.88	0.94	0.95	0.54	0.93	0.91	0.45	0.90	0.78
Cu	5	3	7	3	5	7	16	4	8	22	2	6
Pb	49	22	23	17	20	21	12	15	19	16	19	17
Zn	72	66	154	124	83	57	107	153	192	89	43	71
Ni	5	6	7	3	5	5	12	5	8	6	6	7
Ga	16	15	26	22	15	16	19	20	23	20	12	16
Sc	5.6	10.6	11.8	36.8	9	5.1	14.7	6.5	6.5	15.7	10.2	10.8
Nb	23	21	23	17	19	24	10	25	24	6	8	7
Zr	366	407	408	785	366	314	212	361	355	169	159	164
Y	105	87	120	75	87	71	29	62	56	37	29	29
Ce	117	120	126	152	106	87	55	118	104	79	78	82
U	4	2	3	2	2	4	2	4	4	4	4	3
Th	18	15	15	8	13	14	8	14	13	12	14	14
Sr	56	30	184	124	41	28	137	35	29	237	159	185
Rb	175	135	90	115	80	215	70	175	160	118	105	110
Ba	719	1020	808	4933	741	1046	570	945	1251	1294	1885	1636

Table B-12

Field No.	BA90129	BA90132	BA90135	BA90139	BA90141	BA90143	BA90145	BA90146R	BA90153	BA90155	BA90158	BA90160
SiO2	80.10	62.90	64.40	81.15	70.70	77.10	76.40	69.33	66.80	67.35	67.80	74.60
TiO2	0.21	0.75	0.75	0.30	0.35	0.24	0.24	0.34	0.66	0.66	0.32	0.27
Al2O3	11.28	15.76	16.42	10.23	15.69	12.99	12.94	15.98	14.33	14.34	17.57	13.70
Fe2O3	1.03	4.06	3.94	0.62	1.69	0.35	0.72	1.86	2.65	4.16	2.16	1.27
FeO	0.31	2.21	0.84	0.70	0.15	0.84	0.70	0.00	2.66	0.31	0.28	0.19
MnO	0.13	0.17	0.18	0.07	0.02	0.06	0.04	0.12	0.18	0.08	0.17	0.17
MgO	0.22	1.71	0.87	0.17	0.05	0.21	0.25	0.51	1.30	1.21	0.45	0.40
CaO	1.71	5.10	4.00	0.07	0.36	0.09	0.09	5.45	3.84	1.58	3.23	1.53
Na2O	0.75	2.27	2.04	1.94	5.51	4.04	3.33	0.48	1.94	0.72	1.58	1.76
K2O	3.26	2.02	3.24	2.92	5.26	3.61	4.72	3.04	2.14	5.34	4.51	3.82
P2O5	0.03	0.29	0.23	0.04	0.03	0.04	0.02	0.02	0.26	0.29	0.03	0.02
F	0.02	0.04	0.05	0.00	0.01	0.01	0.02	0.01	0.04	0.06	0.02	0.02
H2O+	1.62	2.14	2.03	0.78	0.21	0.47	0.43	1.83	2.64	2.96	2.04	1.54
H2O-	0.20	0.20	0.24	0.25	0.21	0.34	0.26	0.18	0.20	0.27	0.28	0.17
CO2	0.18	0.02	0.05	0.04	0.00	0.00	0.00	0.00	0.05	0.91	0.09	0.14
S	0.08	0.01	0.05	0.03	0.00	0.00	0.00	0.05	0.07	0.00	0.00	0.00
Total	101.13	99.65	99.33	99.31	100.24	100.39	100.16	99.20	99.76	100.24	100.53	99.60
A.I.	0.42	0.38	0.42	0.62	0.94	0.81	0.82	0.26	0.38	0.49	0.43	0.51
Cu	3	24	6	8	1	6	7	4	29	5	28	4
Pb	20	23	20	2	4	23	16	15	23	5	48	23
Zn	75	95	97	25	21	38	87	76	104	40	126	83
Ni	3	9	2	3	3	3	7	4	6	1	1	1
Ga	13	18	20	12	10	15	20	16	19	19	31	19
Sc	7.3	20.2	16.6	8.1	8.4	7.9	7.3	8.6	17.7	17.5	10.1	8.9
Nb	8	5	8	9	8	9	9	9	6	4	12	11
Zr	180	133	196	229	261	199	200	267	177	146	255	227
Y	42	27	33	29	39	28	33	37	34	31	59	49
Ce	96	72	94	36	58	77	99	94	82	112	135	114
U	3	3	4	4	3	4	4	2	4	3	5	4
Th	18	8	20	17	14	14	14	20	13	15	20	18
Sr	102	665	719	55	84	87	53	441	272	38	280	162
Rb	100	50	95	95	95	95	155	90	50	175	165	160
Ba	691	1144	1684	1939	1967	1844	1506	1161	1750	1183	1418	1217

Table B-12

Field No.	BA90163	BA90164	BA90170	BA90171	BA90173	BA90175A	BA90179	BA90181	BA90183	BA90185	BA90188R	BA90189
SiO2	65.65	69.90	71.05	57.80	65.30	67.16	82.85	75.90	77.55	75.45	71.80	71.15
TiO2	0.56	0.43	0.52	0.83	0.77	0.48	0.08	0.11	0.09	0.13	0.10	0.10
Al2O3	15.18	15.31	14.13	18.74	15.47	15.28	8.22	11.70	11.75	12.72	14.63	14.86
Fe2O3	3.35	1.84	3.09	1.19	3.62	1.89	0.29	0.80	1.44	0.05	1.31	1.26
FeO	0.63	0.61	0.36	4.72	0.79	1.81	0.67	0.86	0.73	0.39	0.87	0.67
MnO	0.21	0.13	0.04	0.16	0.12	0.10	0.01	0.07	0.04	0.05	0.05	0.07
MgO	1.61	0.81	0.09	1.73	1.11	1.35	0.12	0.22	0.12	0.09	0.17	0.08
CaO	1.11	3.35	0.84	3.02	2.38	2.35	0.01	0.15	0.16	0.52	0.44	1.53
Na2O	2.60	3.15	7.05	2.21	2.66	2.21	0.10	0.89	4.46	3.63	4.94	3.61
K2O	7.24	2.38	1.58	4.17	5.60	5.74	6.11	8.71	3.81	5.63	4.23	5.71
P2O5	0.13	0.06	0.16	0.67	0.13	0.11	0.02	0.03	0.02	0.08	0.00	0.02
F	0.04	0.02	0.03	0.08	0.04	0.04	0.01	0.00	0.00	0.01	0.01	0.00
H2O+	1.23	1.68	0.14	3.31	1.44	1.48	0.35	0.29	0.08	0.11	0.59	0.43
H2O-	0.16	0.43	0.29	0.18	0.15	0.49	0.31	0.22	0.20	0.21	0.28	0.23
CO2	0.17	0.01	0.17	0.98	0.02	0.01	0.00	0.01	0.02	0.12	0.00	0.00
S	0.00	0.00	0.00	0.00	0.02	0.00	0.00	0.00	0.00	0.00	0.00	0.00
Total	99.87	100.11	99.54	99.79	99.62	100.48	99.15	99.96	100.47	99.19	99.42	99.72
A.I.	0.80	0.51	0.94	0.43	0.67	0.64	0.82	0.93	0.98	0.95	0.87	0.82
Cu	3	15	5	54	12	41	47	5	8	117	25	37
Pb	24	9	5	43	22	19	4	27	10	185	30	33
Zn	113	87	29	180	90	112	19	101	72	215	65	69
Ni	3	9	5	25	5	4	1	2	1	2	4	1
Ga	23	20	18	27	22	22	15	17	22	23	28	30
Sc	12.5	13.8	12.6	20.7	13.5	15	3.1	4.7	4.8	7	4.9	5.5
Nb	11	15	14	14	7	11	15	19	21	33	22	18
Zr	222	261	272	242	169	215	182	255	317	459	334	334
Y	39	59	61	41	32	61	53	78	40	811	92	94
Ce	95	112	93	79	98	99	63	90	65	366	151	116
U	2	2	2	3	4	4	4	10	4	11	5	3
Th	13	13	10	11	13	17	13	22	22	36	20	28
Sr	171	927	114	93	229	636	27	31	28	62	107	281
Rb	75	35	35	140	190	170	185	225	85	135	130	140
Ba	2422	1297	827	1154	1750	2534	1122	1484	491	890	973	1222

Table B-12

Field No.	BA90190	BA90192R	BA90194R	BA90199R	BA90208	BA90209	BA90212A	BA92001	BA92002	BA92003	BA92004A
SiO2	73.85	75.03	69.62	57.88	68.10	69.75	71.45	69.21	72.36	70.39	75.36
TiO2	0.12	0.10	0.15	0.94	0.57	0.63	0.47	0.54	0.47	0.50	0.48
Al2O3	12.59	11.95	15.60	16.36	14.97	13.67	14.13	14.44	10.77	11.79	12.84
Fe2O3	0.07	1.00	2.36	5.02	3.11	3.93	2.09	5.90	7.69	7.03	1.21
FeO	1.51	0.95	0.28	2.65	1.19	0.61	0.43	0.16	0.44	0.80	0.49
MnO	0.08	0.06	0.07	0.19	0.13	0.06	0.10	0.13	0.08	0.09	0.02
MgO	0.10	0.10	0.14	2.57	1.13	0.18	0.91	0.10	0.06	0.03	0.03
CaO	1.31	0.16	3.36	4.04	0.79	0.89	0.99	0.13	0.03	0.00	0.02
Na2O	1.09	2.21	2.80	4.71	5.42	5.79	2.73	4.53	1.36	3.46	3.07
K2O	7.81	6.93	4.09	2.83	3.99	2.99	4.48	3.53	5.09	4.88	4.45
P2O5	0.03	0.00	0.00	0.39	0.11	0.14	0.04	0.03	0.04	0.01	0.02
F	0.00	0.00	0.01	0.05	0.03	0.03	0.03	0.04	0.02	0.00	0.02
H2O+	0.34	0.49	1.44	2.12	0.83	0.32	1.46	0.96	0.95	0.58	1.12
H2O-	0.34	0.22	0.26	0.28	0.33	0.25	0.32				
CO2	0.00	0.12	0.06	0.07	0.14	0.28	0.24	0.01	0.02	0.00	0.00
S	0.00	0.01	0.00	0.00	0.00	0.00	0.00	0.12	0.09	0.08	0.08
Total	99.24	99.33	100.24	100.09	100.84	99.52	99.84	99.83	99.47	99.63	99.16
A.I.	0.81	0.93	0.58	0.66	0.88	0.93	0.66	0.78	0.72	0.93	0.77
Cu	22	34	19	66	5	10	10.5	6	10	8	11
Pb	25	35	58	17	9	10	12	3	15	4	4
Zn	40	86	56	119	92	72	70.5	166	240	93	162
Ni	1	5	1	11	9	8	3	1	< 1	< 1	4
Ga	28	18	49	21	22	17	19	45	39	40	44.5
Sc	5.7	4.8	7.4	18.5	16.6	16.7	10.4	2.1	< 0.1	< 0.1	0
Nb	24	25	33	11	11	13	14.5	145	163	116	149
Zr	292	332	548	196	298	319	259.5	920	719	793	801.5
Y	103	96	131	29	54	61	52	122	61	86	95.5
Ce	94	116	167	119	93	96	103.5	217	278	196	244
U	6	5	7	4	2	3	3	10	2	5	8
Th	29	28	35	28	14	17	15	20	15	16	17.5
Sr	302	50	244	744	136	97	260.5	113	42	19	29.5
Rb	205	165	125	60	95	60	180	102	108	105	125
Ba	2014	1553	943	1017	1428	882	1526	156	140	49	30

Table B-12

Field No.	BA92005	BA92006	BA92007	BA92008	BA92009	BA92010
SiO2	72.16	69.46	73.81	73.29	72.43	57.77
TiO2	0.58	0.48	0.23	0.57	0.49	0.82
Al2O3	9.97	12.19	14.22	10.36	10.49	17.72
Fe2O3	8.24	0.73	1.35	7.65	7.04	12.10
FeO	0.20	5.02	0.37	0.16	0.61	0.53
MnO	0.20	0.16	0.06	0.11	0.10	0.12
MgO	0.04	0.02	0.30	0.01	0.05	0.19
CaO	0.02	0.02	1.13	0.01	0.07	0.02
Na2O	1.41	2.02	6.39	2.70	3.95	5.65
K2O	5.43	5.78	0.91	4.95	3.11	3.19
P2O5	0.02	0.02	0.02	0.02	0.01	0.08
F	0.01	0.01	0.01	0.01	0.01	0.06
H2O+	0.9	1.05	1.05	0.6	0.69	1.62
H2O-						
CO2	0.02	0.09	0.02	0.00	0.02	0.00
S	0.14	2.48	0.76	0.08	0.13	0.09
Total	99.34	99.53	100.63	100.52	99.20	99.96
A.I.	0.82	0.79	0.81	0.95	0.94	0.72
Cu	8	8	8	17	14	8
Pb	12	< 1	< 1	15	10	29
Zn	487	267	38	162	182	462
Ni	< 1	1	< 1	2	< 1	< 1
Ga	48	52	21	39	52	79
Sc	< 0.1	0.1	2.8	1.8	< 0.1	0.2
Nb	200	161	31	158	153	186
Zr	1083	781	334	930	902	1054
Y	148	70	38	95	87	91
Ce	376	214	86	249	145	559
U	8	8	5	5	4	3
Th	21	15	18	16	19	12
Sr	35	14	194	29	16	102
Rb	142	134	20	127	78	113
Ba	30	28	152	52	19	67

Table B-13-1 Flowers River Cauldron Complex Geochemical Data

Field No.	FR91001	FR91002	FR91003	FR91004A	FR91005	FR91007	FR91008	FR91010R	FR91012	FR91013	FR91014	FR91016
SiO2	73.50	79.20	79.50	74.73	73.50	71.80	77.30	75.51	77.85	82.90	80.50	80.35
TiO2	0.50	0.33	0.29	0.32	0.30	0.34	0.23	0.32	0.39	0.38	0.17	0.25
Al2O3	11.58	9.86	11.47	11.53	9.76	11.80	10.33	12.03	12.37	13.58	8.35	10.42
Fe2O3	0.35	0.95	0.33	1.33	5.95	2.38	3.61	1.43	0.60	0.75	0.66	0.42
FeO	4.11	3.87	2.39	1.66	0.00	2.23	0.71	2.86	2.37	0.25	5.53	2.23
MnO	0.06	0.06	0.05	0.06	0.07	0.09	0.02	0.04	0.03	0.01	0.07	0.02
MgO	0.20	0.11	0.09	0.27	0.01	0.03	0.27	0.24	0.12	0.01	0.02	0.02
CaO	1.02	0.03	0.03	0.48	0.36	0.81	0.02	0.07	0.01	0.03	0.01	0.01
Na2O	2.33	0.02	0.05	3.48	2.99	4.43	0.06	0.04	0.02	0.23	0.06	0.08
K2O	4.73	2.54	3.46	4.52	4.46	4.52	5.22	3.83	3.53	0.58	1.69	2.92
P2O5	0.08	0.07	0.03	0.03	0.01	0.02	0.01	0.05	0.05	0.01	0.01	0.01
F	0.10	0.04	0.03	0.03	0.25	0.14	0.03	0.04	0.04	0.02	0.04	0.05
H2O+	1.03	2.15	2.03	0.54	0.24	0.43	1.39	2.18	1.95	1.15	2.13	1.87
H2O-	0.15	0.31	0.30	0.19	0.21	0.23	0.26	0.22	0.20	0.23	0.16	0.24
CO2	0.30	0.03	0.04	0.19	0.31	0.38	0.07	0.04	0.01	0.02	0.06	0.08
S	0.01	0.02	0.05	0.03	0.03	0.03	0.01	0.17	0.01	0.04	0.26	0.32
Total	100.05	99.59	100.14	99.35	98.45	99.66	99.54	99.08	99.55	100.19	99.72	99.29
A.I.	0.77	0.28	0.33	0.92	1.00	1.03	0.56	0.35	0.31	0.07	0.23	0.32
Cu	26	21	39	10	25	17	21	20	17	13	68	31
Pb	19	71	8	222	27	33	10	6	17	14	17	20
Zn	108	99	64	281	453	232	84	43	39	19	71	94
Ni	2	2	2	2	6	2	2	2	1	0	1	0
Sc	6.6	2.2	1.3	1.7	0.0	0.4	0.4	1.6	2.1	1.3	0.0	0.0
Ga	24	33	30	27	51	48	25	36	32	27	49	54
Nb	20	45	58	57	291	114	38	48	67	72	258	429
Zr	568	669	860	804	3574	1469	846	773	938	1378	3819	5838
Y	50	69	76	90	333	120	79	89	92	94	361	640
Ce	199	268	193	356	624	562	179	505	358	317	811	1237
U	1	2	3	3	9	3	2	2	4	3	13	19
Th	0	0	8	11	35	5	0	7	14	21	49	116
Sr	94	10	4	27	7	13	14	4	7	4	4	5
Rb	164	149	197	160	365	168	217	228	176	29	217	429
Ba	1559	95	96	257	24	168	329	92	179	59	33	30

Table B-13-1

Field No.	FR91017A	FR91018A	FR91019	FR91021	FR91022	FR91023	FR91024A	FR91026	FR91027	FR91028	FR91029	FR91032
SiO2	74.30	75.26	76.35	77.40	77.15	79.80	81.60	76.00	78.85	74.45	74.80	69.35
TiO2	0.32	0.41	0.39	0.38	0.38	0.37	0.24	0.29	0.35	0.30	0.29	0.43
Al2O3	11.95	11.41	8.99	8.39	9.11	8.12	8.48	11.68	7.47	9.70	9.81	12.99
Fe2O3	5.89	0.54	1.62	2.25	1.40	1.32	0.89	1.10	1.42	3.85	5.58	1.84
FeO	1.02	3.32	5.08	3.65	3.74	3.39	2.48	3.79	6.66	2.37	0.40	3.83
MnO	0.03	0.06	0.07	0.07	0.04	0.05	0.04	0.03	0.05	0.10	0.08	0.13
MgO	0.08	0.37	0.05	0.12	0.07	0.07	0.08	0.08	0.09	0.02	0.01	0.02
CaO	0.02	0.24	0.02	0.01	0.01	0.01	0.01	0.01	0.01	0.24	0.01	1.07
Na2O	0.14	1.90	0.08	0.10	0.08	0.05	0.06	0.04	0.02	2.91	3.02	4.96
K2O	3.28	5.07	5.33	5.54	5.69	5.11	4.42	4.38	1.14	4.23	4.36	4.87
P2O5	0.01	0.06	0.01	0.01	0.01	0.01	0.02	0.01	0.01	0.01	0.01	0.04
F	0.08	0.02	0.02	0.02	0.01	0.01	0.01	0.07	0.02	0.15	0.03	0.10
H2O+	2.19	1.23	1.47	1.05	1.20	1.12	1.17	2.09	2.30	0.27	0.54	0.39
H2O-	0.33	0.25	0.27	0.28	0.28	0.25	0.22	0.34	0.25	0.21	0.19	0.24
CO2	0.06	0.05	0.04	0.07	0.08	0.08	0.07	0.09	0.10	1.18	0.17	0.15
S	0.09	0.07	0.04	0.10	0.08	0.01	0.02	0.01	0.01	0.03	0.02	0.02
Total	99.76	100.22	99.83	99.44	99.33	99.77	99.79	100.01	98.75	100.02	99.32	100.43
A.I.	0.32	0.75	0.66	0.73	0.69	0.69	0.57	0.41	0.17	0.97	0.99	1.03
Cu	11	15	24	28	31	17	6	4	18	6	8	5
Pb	8	35	109	119	77	96	23	6	38	15	12	30
Zn	79	130	427	802	519	200	136	54	69	398	373	214
Ni	0	3	1	0	1	1	1	1	1	1	2	0
Sc	0.2	2.6	0.0	0.0	0.0	0.0	1.1	0.7	0.0	0.0	0.0	1.3
Ga	32	27	39	30	36	26	21	34	46	49	49	46
Nb	473	54	208	203	204	186	51	82	184	288	278	115
Zr	7085	825	4429	4382	4205	4055	730	1253	3736	3771	3604	1662
Y	692	83	345	392	331	333	73	104	228	371	320	137
Ce	593	338	988	988	925	826	242	315	403	728	461	860
U	25	3	10	12	9	10	4	4	10	10	8	4
Th	116	5	57	57	60	57	8	4	35	42	43	5
Sr	5	29	10	11	7	10	14	6	2	5	3	15
Rb	313	240	433	420	444	332	252	313	86	384	407	171
Ba	40	288	46	41	34	40	118	114	27	19	13	181

Table B-13-1

Field No.	FR91034	FR91035	FR91036	FR91037	FR91038	FR91040	FR91041	FR91043R	FR91044	FR91045	FR91048	FR91049
SiO2	76.95	75.15	69.70	73.75	73.35	73.30	75.00	76.10	80.50	75.15	79.15	78.40
TiO2	0.34	0.38	0.44	0.29	0.31	0.32	0.30	0.30	0.52	0.35	0.31	0.47
Al2O3	11.54	9.15	13.49	9.82	9.52	10.44	9.86	11.74	9.90	12.23	11.09	12.00
Fe2O3	0.95	1.53	0.78	3.68	4.41	2.73	4.21	2.86	0.17	0.28	1.13	0.03
FeO	2.45	6.78	4.13	1.94	1.61	3.07	1.59	0.00	3.27	4.02	2.52	3.01
MnO	0.04	0.08	0.03	0.09	0.08	0.11	0.03	0.01	0.02	0.02	0.04	0.03
MgO	0.10	0.08	0.14	0.01	0.07	0.04	0.01	0.07	0.18	0.03	0.16	0.07
CaO	0.03	0.01	0.85	0.34	0.08	0.27	0.29	0.37	0.05	0.10	0.02	0.01
Na2O	0.11	0.03	3.01	4.51	4.43	4.33	3.28	2.87	0.09	0.17	0.07	0.07
K2O	5.22	3.34	5.25	4.30	4.32	4.41	4.14	4.19	2.81	4.60	3.10	3.19
P2O5	0.04	0.01	0.08	0.01	0.01	0.02	0.01	0.03	0.08	0.01	0.01	0.03
F	0.07	0.03	0.09	0.28	0.12	0.22	0.41	0.30	0.12	0.88	0.07	0.05
H2O+	1.39	1.87	1.17	0.12	0.28	0.39	0.07	0.85	1.75	1.05	2.18	2.51
H2O-	0.16	0.21	0.27	0.17	0.22	0.20	0.20	0.20	0.23	0.16	0.18	0.17
CO2	0.13	0.10	0.48	0.10	0.14	0.19	0.13	0.17	0.15	0.08	0.06	0.10
S	0.01	0.04	0.03	0.01	0.00	0.00	0.00	0.05	0.04	0.08	0.07	0.10
Total	99.53	98.79	99.94	99.42	98.95	100.04	99.53	100.10	99.88	99.21	100.16	100.24
A.I.	0.51	0.40	0.79	1.23	1.26	1.14	1.00	0.79	0.32	0.43	0.31	0.30
Cu	6	31	3	9	9	6	24	9	9	49	5	13
Pb	15	139	9	87	53	66	149	33	4	11	18	24
Zn	81	658	83	508	382	299	344	54	30	32	135	348
Ni	1	2	0	1	1	1	0	1	3	1	1	1
Sc	1.6	0.5	3.7	0.0	0.0	0.6	0.0	1.4	3.4	0.4	0.7	2.0
Ga	33	47	32	49	48	47	49	25	26	36	38	38
Nb	55	214	64	287	317	240	290	54	45	88	51	74
Zr	866	4535	1135	3550	3781	2986	3645	846	732	1831	937	1289
Y	80	420	84	339	283	189	328	70	63	139	85	101
Ce	307	650	373	701	612	568	659	339	278	478	210	435
U	3	14	3	10	10	8	10	3	3	4	4	3
Th	10	48	0	36	33	31	38	13	5	12	9	8
Sr	16	6	45	7	4	7	7	21	8	13	5	4
Rb	282	284	333	407	351	337	389	254	203	766	183	209
Ba	225	55	842	20	11	71	21	170	135	30	108	71

Table B-13-1

Field No.	FR91050	FR91052D	FR91056	FR91057	FR91061	FR91065	FR91066	FR91067	FR91068	FR91069R	FR91070	FR91071
SiO2	76.30	69.70	81.75	69.30	84.15	71.85	72.45	73.15	77.25	76.13	71.35	83.50
TiO2	0.33	0.39	0.36	0.79	0.19	0.56	0.36	0.43	0.31	0.42	0.59	0.34
Al2O3	8.93	12.43	8.48	19.46	8.04	11.87	11.88	11.46	10.05	10.75	11.28	8.15
Fe2O3	1.86	1.25	0.55	0.24	1.22	0.79	2.38	2.07	0.75	0.48	0.96	0.11
FeO	7.31	3.71	3.10	1.18	1.07	3.74	1.58	2.48	2.62	3.16	4.49	2.73
MnO	0.07	0.11	0.03	0.02	0.01	0.06	0.06	0.05	0.06	0.06	0.09	0.03
MgO	0.23	0.04	0.12	0.01	0.02	0.27	0.16	0.09	0.19	0.31	0.24	0.11
CaO	0.01	0.90	0.01	0.01	0.01	0.85	0.31	0.13	0.01	0.11	2.03	0.04
Na2O	0.03	4.85	0.05	0.17	0.12	2.63	3.15	2.24	0.07	0.08	0.15	0.02
K2O	1.43	4.70	2.25	5.23	2.29	4.64	5.07	5.39	5.73	5.54	5.77	2.25
P2O5	0.02	0.04	0.03	0.04	0.01	0.09	0.03	0.03	0.03	0.08	0.11	0.05
F	0.03	0.13	0.05	0.07	0.06	0.19	0.01	0.01	0.02	0.02	0.07	0.06
H2O+	3.00	0.76	1.85	2.90	1.64	1.57	1.04	1.54	1.51	1.67	1.65	1.80
H2O-	0.23	0.26	0.23	0.22	0.23	0.22	0.30	0.31	0.17	0.14	0.15	0.33
CO2	0.06	0.09	0.05	0.05	0.21	0.05	0.12	0.14	0.08	0.06	0.39	0.03
S	0.07	0.05	0.06	0.08	0.08	0.07	0.09	0.06	0.08	0.03	0.02	0.03
Total	99.91	99.41	98.97	99.77	99.35	99.45	98.99	99.58	98.93	99.04	99.34	99.58
A.I.	0.18	1.05	0.30	0.31	0.33	0.79	0.90	0.83	0.63	0.57	0.58	0.30
Cu	17	4	11	4	65	9	3	4	9	9	16	5
Pb	86	23	136	6	11	23	13	6	21	50	54	2
Zn	222	231	144	39	20	124	102	138	121	117	131	37
Ni	1	0	2	1	1	1	1	0	1	2	1	1
Sc	0.1	2.0	2.2	3.6	0.1	7.2	2.5	1.1	1.5	2.8	8.5	2.2
Ga	39	45	40	62	43	21	32	34	22	26	28	20
Nb	191	116	65	117	270	20	62	71	54	50	20	48
Zr	3825	1548	1052	2259	3806	567	1192	1497	768	798	576	759
Y	275	137	86	166	338	58	110	82	82	76	62	68
Ce	341	695	323	493	476	208	436	397	282	306	204	234
U	7	3	4	5	11	1	4	4	3	3	1	2
Th	38	2	9	29	66	0	7	8	12	7	0	10
Sr	3	18	4	7	5	99	32	18	20	24	142	6
Rb	90	182	146	423	261	144	216	233	272	289	225	122
Ba	84	221	128	75	43	1585	426	130	596	306	2081	124

Table B-13-1

Field No.	FR91072	FR91073A	FR91075	FR91076	FR91077	FR91078	FR91079	FR91080	FR91081R	FR91083R	FR91084A
SiO2	80.90	75.13	75.25	75.65	75.10	80.80	74.70	82.20	85.86	78.02	75.09
TiO2	0.32	0.45	0.22	0.23	0.30	0.26	0.42	0.34	0.25	0.34	0.28
Al2O3	8.72	15.40	10.13	9.85	10.60	10.45	11.70	10.01	7.66	11.22	11.02
Fe2O3	0.49	1.04	1.12	1.15	0.28	0.89	0.21	0.58	1.48	0.83	0.14
FeO	4.90	0.22	5.06	5.05	6.00	1.35	4.05	1.57	0.00	2.24	2.98
MnO	0.02	0.01	0.07	0.08	0.03	0.01	0.07	0.03	0.01	0.04	0.06
MgO	0.02	0.02	0.04	0.02	0.08	0.10	0.09	0.03	0.03	0.19	0.08
CaO	0.01	0.01	0.12	0.16	0.06	0.01	0.06	0.01	0.02	0.08	0.19
Na2O	0.03	0.22	0.02	0.05	0.06	0.01	0.14	0.05	0.07	0.10	2.10
K2O	1.61	3.52	4.58	4.43	3.18	3.11	6.33	2.71	2.29	5.47	5.27
P2O5	0.01	0.03	0.01	0.01	0.01	0.04	0.03	0.01	0.02	0.04	0.02
F	0.03	0.06	0.12	0.12	0.06	0.02	0.01	0.06	0.03	0.02	0.01
H2O+	2.19	2.68	1.78	1.65	2.15	1.97	1.06	1.43	0.99	1.35	0.73
H2O-	0.34	0.34	0.24	0.22	0.26	0.27	0.22	0.17	0.11	0.18	0.22
CO2	0.03	0.14	0.13	0.09	0.12	0.11	0.10	0.08	0.12	0.09	0.19
S	0.03	0.08	0.00	0.07	0.50	0.00	0.00	0.05	0.26	0.00	0.00
Total	99.65	99.32	98.89	98.83	98.79	99.40	99.19	99.33	99.20	100.21	98.35
A.I.	0.21	0.27	0.49	0.50	0.33	0.32	0.61	0.30	0.34	0.54	0.83
Cu	9	3	8	10	30	6	4	4	4	5	5
Pb	17	25	156	169	379	39	27	12	14	24	47
Zn	92	12	453	516	567	34	112	64	17	98	171
Ni	1	0	0	0	2	1	1	1	0	1	1
Sc	0.4	1.3	0.0	0.0	0.0	1.2	1.7	0.5	0.3	1.8	0.3
Ga	40	51	47	43	43	27	33	41	36	27	27
Nb	84	99	338	350	151	48	69	90	73	52	50
Zr	1689	1678	4912	5185	2409	743	1325	1980	1506	760	941
Y	119	127	492	499	226	71	100	141	111	69	102
Ce	192	317	1081	1006	754	273	425	204	174	236	360
U	3	4	15	14	9	2	4	4	4	3	3
Th	5	25	79	82	18	9	8	23	20	10	10
Sr	3	7	7	9	4	3	16	4	3	15	21
Rb	153	404	542	542	304	181	330	257	206	254	209
Ba	25	58	29	23	19	57	252	44	36	280	160

Table B-13-1

Field No.	FR91085	FR91086	FR91087	FR91088	FR91089	FR91090A	FR91091	FR91092	FR91094	FR91095	FR91096	FR91097
SiO2	77.70	70.60	82.80	74.80	79.40	74.32	78.75	81.05	85.20	82.65	80.45	70.12
TiO2	0.17	0.36	0.42	0.51	0.33	0.30	0.29	0.35	0.29	0.44	0.21	0.35
Al2O3	9.63	13.55	12.82	14.91	8.95	11.52	10.76	9.16	6.71	10.39	9.13	15.08
Fe2O3	1.23	4.57	0.79	0.81	1.07	0.59	0.85	1.04	0.84	0.87	1.00	3.72
FeO	2.44	0.39	0.00	1.22	3.42	2.69	2.06	1.99	2.39	0.54	3.76	3.37
MnO	0.06	0.02	0.01	0.01	0.04	0.04	0.03	0.04	0.04	0.01	0.03	0.03
MgO	0.04	0.04	0.01	0.02	0.09	0.15	0.08	0.05	0.03	0.02	0.03	0.04
CaO	0.18	0.03	0.01	0.01	0.01	0.09	0.01	0.01	0.01	0.01	0.01	0.01
Na2O	3.17	4.05	0.06	0.06	0.02	2.37	0.03	0.02	0.01	0.03	0.03	1.07
K2O	2.66	4.72	0.08	4.06	2.96	5.21	4.12	2.48	1.76	3.26	2.28	1.75
P2O5	0.01	0.02	0.01	0.03	0.01	0.02	0.02	0.01	0.01	0.03	0.01	0.01
F	0.11	0.06	0.01	0.03	0.03	0.01	0.11	0.06	0.08	0.04	0.04	0.09
H2O+	0.71	0.37	1.10	2.33	1.95	0.80	1.42	1.64	1.64	1.51	1.90	2.57
H2O-	0.26	0.28	0.25	0.24	0.23	0.24	0.17	0.29	0.29	0.20	0.32	0.31
CO2	0.09	0.12	0.08	0.09	0.11	0.11	0.11	0.20	0.25	0.04	0.10	0.06
S	0.00	0.01	0.00	0.03	0.02	0.03	0.03	0.10	0.02	0.00	0.00	0.00
Total	98.46	99.19	98.45	99.16	98.64	98.46	98.84	98.49	99.57	100.04	99.30	98.58
A.I.	0.84	0.87	0.01	0.30	0.36	0.83	0.42	0.30	0.29	0.34	0.28	0.24
Cu	5	7	10	3	6	3	5	7	10	6	5	6
Pb	11	28	5	20	100	9	31	197	23	3	57	210
Zn	141	89	19	19	189	68	114	780	207	33	232	249
Ni	1	1	1	0	0	0	0	0	0	0	0	0
Sc	0.0	0.9	1.0	1.3	0.3	1.5	1.3	0.2	0.2	2.2	0.0	0.1
Ga	40	38	39	42	32	28	27	28	31	31	44	56
Nb	325	96	305	90	182	50	48	203	180	56	278	365
Zr	2100	1438	3987	1990	3910	829	829	4203	3728	1174	4880	4702
Y	373	106	456	122	364	79	78	397	208	83	422	584
Ce	410	472	328	399	676	375	356	740	873	334	994	452
U	12	3	13	3	10	3	3	12	8	2	12	14
Th	44	4	91	21	59	10	9	66	57	18	84	94
Sr	4	11	1	7	10	19	13	7	3	4	3	6
Rb	215	198	5	220	171	192	272	169	156	142	241	220
Ba	9	105	20	125	105	232	197	247	49	88	35	27

Table B-13-1

Field No.	FR91098	FR91100	FR91101	FR91102A	FR91103	FR91104	FR91105	FR91106	FR91107A	FR91108	FR91109
SiO2	73.05	73.15	75.50	77.87	81.40	44.60	79.40	76.70	79.75	79.50	75.75
TiO2	0.23	0.25	0.25	0.38	0.39	1.16	0.38	0.45	0.25	0.45	0.39
Al2O3	10.27	10.86	10.43	11.11	9.96	31.75	10.46	13.51	7.17	11.59	10.69
Fe2O3	6.13	1.77	0.36	0.52	0.66	4.03	0.96	1.24	0.64	0.74	7.01
FeO	0.54	3.80	4.83	3.14	1.24	3.63	2.04	0.42	5.24	1.31	0.06
MnO	0.09	0.04	0.08	0.03	0.02	0.07	0.03	0.01	0.08	0.02	0.04
MgO	0.03	0.12	0.04	0.05	0.03	0.09	0.03	0.04	0.05	0.02	0.06
CaO	0.29	0.36	0.12	0.01	0.01	0.01	0.01	0.01	0.01	0.01	0.06
Na2O	2.51	3.42	2.17	0.12	0.07	0.13	0.05	0.03	0.03	0.01	0.02
K2O	4.57	3.52	5.11	2.86	2.76	8.79	2.88	4.05	1.52	3.31	2.79
P2O5	0.01	0.01	0.01	0.01	0.02	0.05	0.03	0.02	0.04	0.02	0.01
F	0.13	0.18	0.09	0.03	0.03	0.05	0.03	0.05	0.06	0.05	0.04
H2O+	0.36	0.93	0.78	2.00	1.68	5.10	1.86	1.88	1.98	1.92	1.99
H2O-	0.21	0.32	0.18	0.18	0.23	0.44	0.28	0.25	0.24	0.22	0.13
CO2	0.18	0.10	0.08	0.07	0.10	0.12	0.07	0.09	0.14	0.05	0.09
S	0.00	0.02	0.10	0.00	0.03	0.00	0.03	0.03	0.17	0.02	0.00
Total	98.60	98.85	100.13	98.36	98.63	100.02	98.54	98.78	97.37	99.24	99.13
A.I.	0.88	0.87	0.87	0.30	0.31	0.31	0.31	0.33	0.24	0.31	0.29
Cu	7	25	12	8	15	2	14	61	18	6	9
Pb	133	116	44	9	14	63	25	41	350	12	119
Zn	459	184	257	56	39	198	54	35	432	22	459
Ni	0	2	1	1	0	0	0	0	0	0	1
Sc	0.0	0.0	0.0	0.6	1.4	3.1	0.7	0.7	0.0	2.2	0.3
Ga	43	43	42	37	37	98	37	52	44	45	53
Nb	405	218	262	77	58	222	74	128	616	64	206
Zr	5300	2806	3478	1693	1253	4539	1595	2500	10519	1209	4250
Y	587	379	425	93	101	392	137	256	910	85	439
Ce	1062	689	536	414	921	1225	473	563	2278	305	898
U	14	8	10	2	3	12	3	7	36	2	11
Th	107	48	64	13	14	29	9	40	211	9	57
Sr	11	9	10	3	2	10	3	7	5	5	8
Rb	707	234	481	177	185	468	145	484	171	126	210
Ba	32	21	19	44	43	157	90	79	27	33	26

Table B-13-1

Field No.	FR91110	FR91111	FR91112A	FR91113	FR91114	FR91115	FR91116	FR91117	FR91118	FR91121	FR91122	FR91123
SiO2	72.15	75.60	75.70	78.35	79.95	80.60	74.35	73.10	65.90	79.15	76.95	74.90
TiO2	0.48	0.21	0.30	0.32	0.36	0.21	0.36	0.23	1.48	0.30	0.29	0.37
Al2O3	12.38	9.32	10.76	11.40	6.76	8.76	10.29	9.77	13.37	11.46	10.61	10.67
Fe2O3	4.13	1.75	2.88	0.65	0.91	0.14	2.46	3.49	0.49	0.58	0.55	2.84
FeO	1.55	4.67	0.51	0.88	5.78	4.15	3.38	2.86	7.32	2.00	3.14	4.86
MnO	0.02	0.04	0.01	0.01	0.07	0.05	0.05	0.05	0.20	0.01	0.03	0.05
MgO	0.04	0.05	0.03	0.05	0.04	0.04	0.16	0.07	0.86	0.10	0.06	0.03
CaO	0.04	0.02	0.06	0.03	0.01	0.01	0.02	0.20	1.05	0.02	0.06	0.01
Na2O	1.52	0.94	2.21	0.13	0.02	0.07	0.51	3.04	3.73	0.08	1.97	0.06
K2O	5.34	4.77	5.53	5.62	1.18	2.26	5.08	4.54	3.11	3.99	4.90	2.24
P2O5	0.03	0.01	0.02	0.01	0.02	0.01	0.01	0.01	0.52	0.03	0.01	0.01
F	0.02	0.02	0.01	0.02	0.04	0.04	0.03	0.19	0.04	0.04	0.02	0.06
H2O+	1.08	1.25	0.43	1.34	2.12	1.96	1.95	0.65	1.65	1.80	1.03	2.36
H2O-	0.21	0.20	0.10	0.17	0.15	0.20	0.46	0.29	0.23	0.23	0.27	0.26
CO2	0.05	0.08	0.09	0.12	0.16	0.08	0.16	0.12	0.05	0.07	0.10	0.06
S	0.01	0.02	0.00	0.14	0.01	0.01	0.00	0.00	0.00	0.02	0.08	0.00
Total	99.05	98.95	98.62	99.24	97.58	98.59	99.27	98.61	100.00	99.88	100.07	98.78
A.I.	0.67	0.72	0.89	0.55	0.19	0.29	0.62	1.01	0.71	0.39	0.81	0.24
Cu	9	12	4	8	136	18	20	8	4	8	5	8
Pb	22	174	58	21	133	82	29	147	14	9	7	33
Zn	223	683	50	15	924	238	257	527	270	42	52	119
Ni	0	0	0	2	1	0	0	2	10	3	1	2
Sc	2.1	0.0	0.3	0.5	0.0	0.0	0.1	0.0	10.0	1.1	0.3	0.1
Ga	41	40	36	37	46	41	39	42	32	32	34	39
Nb	65	357	124	137	647	259	203	329	45	65	114	191
Zr	1359	6195	2158	2030	9382	4226	2976	4502	709	838	1918	3101
Y	93	552	169	197	1039	404	263	462	71	93	165	295
Ce	451	1180	354	154	2151	940	724	808	320	343	493	636
U	3	15	6	3	32	12	10	15	2	4	4	9
Th	1	113	29	36	202	77	40	94	0	23	30	39
Sr	10	14	11	12	5	4	6	6	36	7	11	2
Rb	187	637	327	343	135	250	430	558	185	188	344	209
Ba	113	32	50	70	27	16	52	19	295	130	57	19

Table B-13-1

Field No.	FR91124	FR91125A	FR91126	FR91127	FR91128	FR91129	FR91130	FR91133A	FR91134A	FR91135	FR91136
SiO2	76.35	76.73	63.45	73.60	56.60	60.50	75.00	74.43	75.55	76.45	74.95
TiO2	0.34	0.30	0.62	0.29	1.60	1.22	0.31	0.35	0.40	0.36	0.22
Al2O3	10.06	10.83	18.42	10.63	13.34	13.30	11.22	10.36	8.60	11.41	10.07
Fe2O3	0.80	0.88	1.51	2.55	1.84	2.12	0.04	4.93	1.53	5.33	2.63
FeO	5.03	5.09	7.42	2.71	9.92	7.55	3.71	1.09	5.58	0.00	4.54
MnO	0.06	0.07	0.12	0.06	0.24	0.21	0.09	0.04	0.10	0.04	0.06
MgO	0.02	0.04	0.13	0.02	1.60	0.99	0.06	0.04	0.03	0.03	0.10
CaO	0.07	0.01	0.07	0.14	3.76	3.29	0.02	0.02	0.01	0.01	0.01
Na2O	0.14	0.05	0.07	3.70	4.81	5.10	1.33	0.59	0.01	0.01	0.04
K2O	3.98	3.13	4.28	4.56	3.51	3.77	5.70	5.96	2.01	2.67	3.51
P2O5	0.01	0.01	0.02	0.01	0.95	0.63	0.02	0.01	0.02	0.02	0.01
F	0.05	0.04	0.10	0.07	0.15	0.17	0.01	0.04	0.04	0.10	0.05
H2O+	1.40	2.01	2.57	0.50	1.28	0.96	1.29	0.79	2.47	2.51	2.09
H2O-	0.19	0.23	0.17	0.13	0.26	0.32	0.23	0.15	0.24	0.26	0.21
CO2	0.07	0.08	0.06	0.12	0.03	0.11	0.03	0.18	0.27	0.17	0.19
S	0.07	0.01	0.04	0.04	0.07	0.05	0.29	0.01	0.02	0.24	0.02
Total	98.64	99.48	99.05	99.13	99.96	100.29	99.35	98.95	96.88	99.61	98.70
A.I.	0.45	0.32	0.26	1.04	0.88	0.94	0.74	0.72	0.25	0.25	0.38
Cu	9	9	9	20	22	25	12	32	29	19	23
Pb	140	42	70	65	21	25	51	88	134	166	62
Zn	444	168	341	312	214	264	199	352	606	322	450
Ni	1	2	1	1	2	1	2	1	0	1	2
Sc	0.0	0.1	0.7	0.2	21.6	16.8	0.4	0.0	0.0	0.0	0.0
Ga	37	39	61	39	40	41	34	36	48	48	50
Nb	205	183	142	164	82	100	109	194	766	262	313
Zr	3073	2958	2826	2585	1410	1501	1576	2985	11569	4769	4723
Y	303	269	168	249	119	132	111	285	1161	402	453
Ce	790	653	922	688	487	533	468	788	2237	860	1143
U	8	9	7	6	3	3	3	8	42	11	18
Th	47	45	18	35	0	0	22	43	247	68	95
Sr	6	3	9	7	150	120	10	10	4	4	7
Rb	367	254	263	277	116	117	272	427	295	381	495
Ba	45	22	226	37	1158	929	93	42	29	38	26

Table B-13-1

Field No.	FR91137	FR91138	FR91139	FR91140	FR91141A	FR91142	FR91144	FR91145	FR91146	FR91148	FR91149	FR91161
SiO2	79.70	53.15	78.80	82.60	50.82	78.10	79.10	69.15	83.65	75.10	76.35	60.00
TiO2	0.35	1.80	0.24	0.29	0.83	0.49	0.31	0.61	0.50	0.29	0.41	0.84
Al2O3	9.25	13.94	11.76	8.20	17.25	15.69	11.25	15.52	10.73	9.96	8.96	14.72
Fe2O3	0.93	2.31	0.34	3.58	4.87	0.72	0.73	1.04	0.16	4.83	1.46	2.67
FeO	4.12	10.71	2.04	0.00	12.34	0.00	2.95	8.83	0.33	1.09	6.96	6.89
MnO	0.04	0.27	0.03	0.03	0.44	0.01	0.05	0.09	0.01	0.06	0.09	0.26
MgO	0.02	1.69	0.05	0.03	0.12	0.01	0.04	0.05	0.01	0.02	0.05	0.64
CaO	0.01	4.93	0.02	0.01	0.00	0.02	0.01	0.01	0.34	0.11	0.05	2.53
Na2O	0.01	4.55	0.05	0.06	0.15	0.12	0.01	0.03	0.05	3.82	0.07	4.93
K2O	2.34	3.44	3.45	2.45	2.80	1.75	2.82	1.45	1.76	4.23	2.39	4.66
P2O5	0.01	1.07	0.02	0.01	0.04	0.01	0.01	0.05	0.01	0.01	0.01	0.22
F	0.02	0.13	0.03	0.03	0.08	0.04	0.03	0.02	0.04	0.09	0.04	0.11
H2O+	2.14	0.75	1.85	1.30	4.38	1.88	2.00	3.12	1.99	0.26	1.78	1.60
H2O-	0.16	0.16	0.19	0.16	0.40	0.26	0.23	0.22	0.24	0.22	0.20	0.32
CO2	0.15	0.17	0.15	0.14	0.34	0.11	0.20	0.15	0.19	0.18	0.15	0.33
S	0.00	0.08	0.01	0.00	0.30	0.22	0.02	0.03	0.03	0.02	0.03	0.04
Total	99.25	99.15	99.03	98.89	95.17	99.43	99.76	100.37	100.04	100.29	99.00	100.76
A.I.	0.28	0.80	0.32	0.34	0.19	0.13	0.27	0.10	0.19	1.09	0.30	0.89
Cu	23	22	14	15	37	27	19	11	15	12	26	12
Pb	110	17	7	71	537	18	20	36	26	37	125	17
Zn	196	221	88	180	2809	14	165	148	17	327	644	223
Ni	1	1	1	2	1	1	1	1	1	2	2	2
Sc	0.4	26.8	0.5	0.1	0.0	0.3	0.2	1.8	0.4	0.0	0.0	17.0
Ga	48	37	40	31	92	51	37	62	42	53	46	40
Nb	201	66	45	164	1414	349	129	100	196	297	328	78
Zr	3903	1314	868	2522	21104	6977	2179	2123	4144	3804	6622	2148
Y	317	106	85	236	1888	446	189	147	234	333	499	120
Ce	499	456	252	531	2518	410	566	575	296	693	1416	643
U	8	2	2	8	65	17	7	4	13	10	16	3
Th	57	0	17	42	403	109	34	5	74	47	86	0
Sr	4	194	5	3	10	4	2	5	15	4	7	129
Rb	172	85	196	232	568	249	188	103	114	336	262	119
Ba	32	1419	131	30	68	39	27	107	111	17	64	1675

Table B-13-1

Field No.	FR91164	FR91165	FR91166	FR91167	FR91168	FR91170A	FR91171	FR91172	FR91173	FR91174	FR91175	FR91176
SiO2	81.15	78.50	81.95	77.55	76.80	70.83	92.75	74.15	78.30	77.25	69.50	72.70
TiO2	0.36	0.38	0.32	0.33	0.29	0.38	0.07	0.30	0.38	0.36	0.39	0.28
Al2O3	12.40	9.73	9.45	8.47	11.81	12.18	3.88	11.44	9.83	11.14	12.38	10.72
Fe2O3	0.20	3.04	1.38	1.87	3.75	2.57	1.05	3.26	1.41	1.17	1.71	1.78
FeO	0.42	2.22	1.62	6.17	0.35	2.36	0.00	1.21	3.34	1.09	3.42	2.84
MnO	0.01	0.04	0.03	0.10	0.02	0.10	0.01	0.05	0.03	0.04	0.12	0.08
MgO	0.01	0.09	0.02	0.14	0.12	0.10	0.06	0.16	0.08	0.06	0.05	0.01
CaO	0.01	0.01	0.01	0.01	0.01	0.57	0.01	0.01	0.01	0.06	0.87	0.34
Na2O	0.05	0.04	0.01	0.01	0.01	4.53	0.01	0.11	0.04	1.93	4.93	4.60
K2O	3.02	3.02	2.67	1.42	5.65	4.80	1.12	7.09	3.15	5.17	4.76	4.52
P2O5	0.03	0.01	0.02	0.01	0.01	0.04	0.01	0.02	0.01	0.03	0.05	0.01
F	0.03	0.04	0.03	0.02	0.02	0.08	0.02	0.01	0.03	0.01	0.17	0.18
H2O+	1.99	2.23	2.11	2.91	1.88	1.09	0.96	1.71	2.12	0.91	1.08	0.52
H2O-	0.21	0.19	0.15	0.43	0.39	0.43	0.32	0.31	0.22	0.21	0.20	0.17
CO2	0.19	0.09	0.05	0.11	0.04	0.03	0.03	0.04	0.02	0.03	0.07	0.01
S	0.00	0.07	0.03	0.04	0.01	0.01	0.01	0.03	0.04	0.03	0.03	0.01
Total	100.08	99.70	99.85	99.59	101.16	100.05	100.31	99.90	99.01	99.49	99.73	98.77
A.I.	0.27	0.34	0.31	0.18	0.52	1.04	0.32	0.69	0.35	0.79	1.07	1.16
Cu	13	18	11	9	14	7	21	15	26	12	16	10
Pb	21	20	8	24	15	30	15	25	84	37	49	46
Zn	16	317	91	346	94	233	39	266	406	142	225	341
Ni	1	1	0	0	0	1	1	1	2	2	1	0
Sc	1.6	0.5	0.6	0.1	0.6	2.0	0.4	1.6	0.4	1.8	1.9	0.0
Ga	30	50	35	33	32	45	10	26	38	29	49	48
Nb	65	187	80	139	49	114	13	59	196	54	144	165
Zr	866	3755	1434	2673	844	1549	199	794	4001	780	1699	1934
Y	86	166	122	248	90	130	20	83	2	82	145	120
Ce	328	895	333	330	207	604	83	282	589	325	772	390
U	4	5	6	3	1	4	1	3	7	3	4	5
Th	27	55	17	25	9	10	0	12	2484	16	13	16
Sr	8	4	4	2	13	21	4	21	4	23	19	5
Rb	187	293	177	79	240	178	65	335	220	234	188	266
Ba	85	79	47	69	475	222	35	230	50	228	212	21

Table B-13-1

Field No.	FR91177	FR91178	FR91179	FR91180	FR91181	FR91182	FR91183R	FR91184	FR91185	FR91187R	FR91188A
SiO2	73.90	75.05	75.55	70.50	74.55	72.75	62.58	73.65	76.75	74.22	73.05
TiO2	0.44	0.40	0.28	0.52	0.47	0.28	0.53	0.35	0.38	0.55	0.58
Al2O3	12.06	9.40	12.22	12.36	13.33	12.72	14.85	12.10	9.80	12.30	11.40
Fe2O3	0.23	1.32	1.45	0.88	0.69	1.54	0.69	1.09	0.68	0.21	2.11
FeO	2.65	4.87	2.54	4.10	3.30	1.74	3.80	2.92	5.10	4.87	4.10
MnO	0.04	0.07	0.06	0.06	0.05	0.07	0.06	0.05	0.07	0.08	0.10
MgO	0.07	0.07	0.23	0.25	0.25	0.28	3.97	0.13	0.08	0.32	0.31
CaO	0.12	0.01	0.01	2.07	0.33	0.50	3.60	0.05	0.24	0.42	1.16
Na2O	3.06	0.10	0.03	0.91	0.12	4.57	0.77	2.84	0.17	0.08	0.19
K2O	5.16	5.38	5.40	6.67	3.88	4.69	7.25	4.78	4.62	3.69	4.38
P2O5	0.04	0.01	0.02	0.09	0.09	0.05	0.15	0.04	0.02	0.11	0.11
F	0.02	0.02	0.04	0.10	0.04	0.07	0.11	0.00	0.06	0.10	0.06
H2O+	1.02	1.49	2.34	1.40	2.37	0.66	2.04	1.35	1.43	2.44	2.03
H2O-	0.20	0.18	0.39	0.38	0.29	0.38	0.29	0.33	0.20	0.20	0.19
CO2	0.05	0.04	0.01	0.20	0.01	0.03	0.18	0.07	0.09	0.05	0.05
S	0.06	0.03	0.00	0.02	0.02	0.01	0.03	0.04	0.06	0.03	0.02
Total	99.12	98.44	100.57	100.51	99.79	100.34	100.89	99.79	99.75	99.67	99.83
A.I.	0.88	0.64	0.48	0.71	0.33	0.99	0.61	0.81	0.54	0.34	0.44
Cu	26	17	27	16	14	8	21	8	19	16	12
Pb	37	126	18	34	0	11	0	8	52	8	14
Zn	158	639	164	86	68	181	37	124	229	120	141
Ni	2	2	1	2	1	1	30	15	93	2	3
Sc	2.3	0.0	1.5	7.0	6.0	1.8	13.1	2.0	0.1	9.0	8.8
Ga	32	39	34	29	28	44	22	32	37	30	29
Nb	60	209	51	21	17	45	13	50	145	17	19
Zr	840	4615	779	592	552	841	205	870	3044	539	530
Y	90	377	74	79	51	64	36	83	242	59	67
Ce	423	851	290	226	221	159	93	347	727	210	211
U	4	9	3	2	2	1	4	3	5	2	2
Th	16	64	8	0	1	0	0	12	39	5	0
Sr	29	10	18	102	19	20	177	19	17	23	87
Rb	176	481	250	202	166	147	239	173	308	187	197
Ba	218	43	287	2574	529	180	776	248	83	603	2032

Table B-13-1

Field No.	FR91189	FR91190R	FR91191	FR91192R	FR91193A	FR91194	FR91195	FR91196	FR91197	FR91199	FR91200
SiO2	72.70	47.27	62.80	67.70	67.06	68.50	75.85	71.55	69.75	62.50	3.95
TiO2	0.55	2.11	0.58	0.25	0.51	0.43	0.36	0.54	0.61	0.40	0.01
Al2O3	11.74	15.86	15.68	11.50	13.69	13.30	11.37	12.85	12.46	17.06	0.22
Fe2O3	0.99	0.64	0.40	0.21	2.25	2.04	0.51	1.37	1.36	0.11	0.12
FeO	2.62	12.34	2.04	3.10	3.33	3.08	3.42	3.51	4.30	1.36	0.00
MnO	0.04	0.19	0.04	0.10	0.12	0.10	0.04	0.09	0.08	0.02	0.06
MgO	0.35	5.50	3.13	4.00	0.25	0.11	0.07	0.21	0.30	2.37	0.35
CaO	1.58	8.35	3.53	4.61	1.38	1.11	0.06	0.98	1.58	1.41	55.09
Na2O	1.47	3.10	5.09	2.41	4.27	4.28	0.17	2.09	1.96	2.62	0.01
K2O	6.18	1.47	6.57	4.94	5.41	5.25	6.21	5.36	4.92	10.73	0.02
P2O5	0.09	0.32	0.07	0.06	0.07	0.05	0.02	0.12	0.11	0.06	0.01
F	0.23	0.06	0.12	0.07	0.28	0.17	0.02	0.02	0.04	0.13	0.01
H2O+	0.92	2.82	0.66	0.90	1.33	1.07	1.46	1.19	1.59	0.56	0.16
H2O-	0.15	0.17	0.14	0.17	0.32	0.33	0.22	0.18	0.23	0.14	0.13
CO2	0.68	0.09	0.07	0.09	0.16	0.23	0.06	0.07	0.09	0.07	36.80
S	0.01	0.01	0.01	0.01	0.02	0.03	0.01	0.02	0.01	0.02	0.03
Total	100.30	100.30	100.93	100.12	100.42	100.08	99.85	100.15	99.39	99.56	96.97
A.I.	0.78	0.42	0.99	0.81	0.94	0.96	0.62	0.72	0.69	0.93	0.17
Cu	11	46	15	13	9	30	11	19	13	23	4
Pb	16	6	11	4	26	65	30	22	19	8	4
Zn	39	148	32	17	87	249	241	116	132	14	89
Ni	3	66	22	10	2	1	2	2	3	10	1
Sc	6.2	27.7	13.9	7.9	3.8	2.7	0.7	8.3	8.3	9.3	0.2
Ga	20	29	20	17	41	42	34	21	28	16	2
Nb	16	3	13	12	103	126	72	16	20	22	1
Zr	612	182	235	205	1483	1413	1260	530	630	238	3
Y	56	31	57	38	116	184	117	44	3	22	3
Ce	186	53	83	116	763	769	442	197	218	57	9
U	2	0	4	6	4	4	3	2	1	4	0
Th	5	0	8	14	16	23	10	1	0	20	0
Sr	171	257	137	133	47	42	25	122	148	162	107
Rb	236	91	246	145	220	264	275	154	138	471	5
Ba	1811	441	622	783	438	341	199	1718	1795	604	41

Table B-13-1

Field No.	FR91202	FR91203	FR91205	FR91207	FR91209	FR91210A	FR91211	FR91212A	FR91213	FR91214	FR91215R
SiO2	73.05	69.40	62.80	76.35	73.85	76.05	77.55	75.80	77.50	76.90	76.57
TiO2	0.39	0.62	1.13	0.23	0.24	0.28	0.25	0.29	0.29	0.31	0.41
Al2O3	11.15	12.36	14.38	9.27	10.04	10.65	8.91	10.76	9.04	7.55	12.55
Fe2O3	2.98	1.70	0.96	3.51	3.28	1.84	6.62	2.32	4.58	8.25	3.17
FeO	1.98	4.46	6.78	2.06	2.65	2.44	0.00	1.73	0.00	0.00	0.63
MnO	0.08	0.08	0.13	0.05	0.05	0.05	0.04	0.04	0.03	0.03	0.03
MgO	0.07	0.21	0.85	0.05	0.03	0.04	0.10	0.05	0.04	0.04	0.03
CaO	0.67	2.22	1.10	0.32	0.10	0.06	0.04	0.06	0.01	0.01	0.00
Na2O	3.69	3.28	1.49	0.25	4.39	1.65	0.08	0.85	0.08	0.05	0.16
K2O	4.50	4.16	7.08	4.55	3.90	5.09	3.46	5.87	5.72	2.52	3.68
P2O5	0.02	0.12	0.36	0.01	0.01	0.01	0.01	0.04	0.03	0.01	0.04
F	0.01	0.08	0.07	0.31	0.21	0.04	0.06	0.01	0.04	0.07	0.03
H2O+	0.54	1.10	2.14	1.20	0.53	1.01	1.60	1.10	0.97	1.43	1.92
H2O-	0.17	0.29	0.27	0.22	0.17	0.18	0.17	0.24	0.19	0.12	0.11
CO2	0.09	0.02	0.49	0.08	0.03	0.03	0.06	0.08	0.07	0.18	0.03
S	0.01	0.04	0.02	0.03	0.03	0.05	0.02	0.03	0.04	0.05	0.03
Total	99.40	100.14	100.05	98.49	99.51	99.46	98.97	99.24	98.62	97.52	99.39
A.I.	0.98	0.80	0.70	0.58	1.14	0.77	0.44	0.72	0.70	0.37	0.34
Cu	14	15	15	12	24	19	28	13	20	22	18
Pb	30	19	31	42	186	51	228	57	100	65	52
Zn	210	135	222	249	515	203	506	199	183	195	70
Ni	1	3	5	1	2	1	1	1	1	1	2
Sc	1.2	9.2	11.8	0.0	0.0	0.2	0.0	0.3	0.0	0.0	0.5
Ga	35	28	42	40	42	36	49	34	36	44	43
Nb	79	21	35	324	327	109	521	126	375	646	112
Zr	1578	625	737	4151	4286	1700	8094	1968	6293	11162	2158
Y	115	69	62	533	546	161	792	176	553	1024	240
Ce	492	222	250	929	558	440	1542	501	1178	1876	566
U	4	2	2	15	15	4	24	4	23	38	4
Th	9	0	0	86	82	21	164	26	118	222	20
Sr	18	149	41	15	6	11	11	12	15	11	11
Rb	191	122	339	701	468	290	721	403	938	528	343
Ba	129	1552	751	54	19	63	32	67	62	41	96

Table B-13-1

Field No.	FR91216	FR91217	FR91218	FR91219	FR91220	FR91221	FR91223	FR91224	FR91225	FR91226	FR91228	FR91229
SiO2	76.95	71.50	86.30	79.80	83.40	73.35	73.85	76.45	76.00	75.00	75.15	74.55
TiO2	0.36	0.45	0.26	0.21	0.01	0.29	0.29	0.38	0.32	0.28	0.32	0.32
Al2O3	10.39	17.28	10.14	8.88	10.52	9.69	10.32	12.28	11.89	10.93	11.60	11.88
Fe2O3	0.79	0.65	0.70	0.86		1.75	2.52	2.54	0.78	1.14	1.98	1.26
FeO	4.48	3.08	0.00	4.22	0.01	3.80	2.17	0.00	1.62	2.03	1.19	1.93
MnO	0.09	0.01	0.01	0.05	0.02	0.11	0.09	0.04	0.02	0.05	0.02	0.05
MgO	0.05	0.01	0.01	0.02	0.01	0.23	0.08	0.04	0.19	0.03	0.08	0.25
CaO	0.28	0.04	0.06	0.27	0.29	0.31	0.33	0.07	0.07	0.26	0.13	0.23
Na2O	0.05	0.22	0.11	0.17	2.53	3.64	3.94	2.51	2.19	3.82	3.04	3.46
K2O	3.09	3.17	0.63	1.68	0.27	4.43	4.51	4.33	5.41	4.85	4.95	4.15
P2O5	0.02	0.08	0.02	0.01	0.00	0.01	0.01	0.02	0.03	0.01	0.03	0.02
F	0.16	0.04	0.02	0.20	0.07	0.19	0.16	0.05	0.02	0.09	0.02	0.03
H2O+	2.19	2.83	1.56	2.19	1.41	0.77	0.72	1.06	1.41	0.74	1.10	1.61
H2O-	0.13	0.33	0.32	0.30	0.20	0.28	0.27	0.18	0.30	0.22	0.25	0.36
CO2	0.06	0.02	0.04	0.10	0.04	0.11	0.05	0.02	0.05	0.11	0.13	0.10
S	0.05	0.06	0.05	0.06	0.03	0.03	0.03	0.04	0.01	0.02	0.03	0.05
Total	99.14	99.77	100.23	99.02	98.81	98.99	99.34	100.01	100.31	99.58	100.02	100.25
A.I.	0.33	0.22	0.09	0.24	0.42	1.11	1.10	0.72	0.80	1.06	0.89	0.86
Cu	14	15	11	27	22	13	9	29	19	10	20	26
Pb	23	47	0	14	0	51	60	21	17	17	7	15
Zn	300	68	15	136	15	461	314	220	74	136	39	377
Ni	2	1	1	2	1	2	1	2	2	0	2	2
Sc	0.3	1.8	1.4	0.0	1.4	0.0	0.0	1.0	1.4	1.2	1.6	1.4
Ga	36	54	23	42	27	52	50	36	30	31	28	31
Nb	118	89	45	312	45	234	259	89	52	74	56	57
Zr	2409	1326	747	4259	797	3049	2579	1505	865	1018	836	887
Y	176	128	50	442	58	313	299	117	78	59	72	108
Ce	620	730	139	894	262	620	687	516	429	271	302	404
U	6	9	8	18	5	7	8	3	3	2	3	3
Th	22	25	18	85	20	31	38	17	14	9	10	13
Sr	7	17	8	9	8	6	6	13	18	6	23	26
Rb	204	161	33	181	235	336	267	162	216	199	178	130
Ba	72	195	45	45	111	16	27	109	203	61	236	208

Table B-13-1

Field No.	FR91230A	FR91231	FR91232A	FR91233	FR91234	FR91235	FR91236	FR91239	FR91240A	FR91242	FR91243
SiO2	74.65	75.90	73.11	76.45	75.45	72.85	74.75	73.55	72.59	73.00	75.85
TiO2	0.28	0.31	0.37	0.36	0.30	0.38	0.30	0.36	0.40	0.43	0.29
Al2O3	11.42	10.74	12.06	11.24	11.10	11.80	10.65	11.01	12.48	11.43	8.98
Fe2O3	1.06	2.37	1.21	0.91	1.67	1.58	2.24	2.42	1.72	3.67	4.35
FeO	1.65	1.75	2.57	1.56	1.76	1.92	1.46	1.64	2.01	1.09	2.07
MnO	0.04	0.05	0.07	0.04	0.05	0.05	0.04	0.05	0.06	0.06	0.10
MgO	0.09	0.03	0.10	0.03	0.03	0.09	0.07	0.02	0.08	0.14	0.04
CaO	0.39	0.15	0.60	0.22	0.13	0.44	0.32	0.37	0.57	0.50	0.29
Na2O	3.61	3.33	4.00	3.61	3.73	4.09	2.26	3.99	4.21	3.90	2.47
K2O	4.84	4.35	4.95	4.57	4.75	4.84	5.43	4.63	5.19	4.71	3.64
P2O5	0.02	0.01	0.05	0.01	0.01	0.03	0.01	0.01	0.04	0.03	0.01
F	0.08	0.02	0.05	0.02	0.05	0.02	0.01	0.02	0.06	0.02	0.01
H2O+	0.74	1.11	0.92	0.47	0.61	0.58	0.87	0.57	1.07	1.07	0.32
H2O-	0.35	0.34	0.26	0.30	0.26	0.36	0.34	0.21	0.49	0.41	0.21
CO2	0.07	0.12	0.10	0.09	0.12	0.12	0.27	0.10	0.10	0.10	0.08
S	0.04	0.02	0.01	0.06	0.04	0.06	0.04	0.06	0.06	0.06	0.02
Total	99.30	100.60	100.40	99.94	100.06	99.21	99.06	99.01	101.10	100.62	98.73
A.I.	0.98	0.95	0.99	0.97	1.02	1.01	0.90	1.05	1.00	1.01	0.89
Cu	6	5	4	3	24	7	14	4	4	9	8
Pb	20	25	22	10	25	22	17	15	25	33	148
Zn	96	203	99	70	143	104	105	96	127	169	552
Ni	1	1	1	0	1	1	0	0	0	1	0
Sc	1.7	0.8	2.9	0.9	1.2	2.5	0.3	0.3	2.6	1.7	0.1
Ga	28	34	32	31	32	30	32	35	32	36	37
Nb	57	85	52	55	87	58	116	60	74	83	289
Zr	633	1315	931	414	1195	835	2029	610	1295	1488	5599
Y	58	108	59	28	84	45	175	51	65	99	432
Ce	328	302	384	325	258	238	529	311	251	322	838
U	3	4	2	2	3	2	6	2	2	3	18
Th	12	8	7	7	12	4	34	9	5	17	92
Sr	17	10	24	8	5	17	16	7	21	14	26
Rb	169	210	130	141	206	149	227	182	176	206	294
Ba	204	56	325	111	69	234	72	48	302	181	84

Table B-13-1

Field No.	FR91244	FR91245	FR91246	FR91247A	FR91248	FR91249	FR91251	FR91252	FR91254	FR91257	FR91258A	FR91259
SiO2	76.00	75.85	75.85	75.12	72.85	82.60	75.50	72.80	72.40	76.88	76.83	74.80
TiO2	0.36	0.28	0.26	0.34	0.25	0.30	0.36	0.32	0.31	0.24	0.39	0.33
Al2O3	10.41	10.07	10.88	11.30	10.66	9.19	10.20	12.15	12.78	10.55	10.39	11.41
Fe2O3	1.48	1.72	2.63	1.19	3.31	0.53	4.10	1.23	1.64	1.07	0.65	1.04
FeO	1.85	3.04	1.71	1.79	3.15	1.08	1.16	1.55	1.76	2.66	2.76	2.36
MnO	0.05	0.06	0.04	0.05	0.06	0.03	0.02	0.05	0.02	0.04	0.06	0.06
MgO	0.05	0.06	0.15	0.07	0.06	0.02	0.02	0.05	0.06	0.07	0.24	0.07
CaO	0.24	0.01	0.03	0.36	0.15	0.01	0.03	0.27	0.53	0.06	0.91	0.48
Na2O	2.90	0.11	1.21	3.72	3.06	0.07	2.55	4.07	3.31	1.91	1.51	3.86
K2O	3.95	5.81	4.86	4.84	4.29	2.82	4.60	4.98	5.35	4.83	4.83	4.79
P2O5	0.01	0.01	0.01	0.02	0.01	0.01	0.01	0.01	0.02	0.01	0.06	0.03
F	0.07	0.01	0.01	0.08	0.04	0.10	0.02	0.04	0.21	0.02	0.11	0.07
H2O+	0.47	1.45	1.96	0.62	0.95	1.76	0.58	0.79	1.59	1.02	1.11	0.53
H2O-	0.30	0.30	0.35	0.29	0.17	0.27	0.22	0.30	0.37	0.22	0.27	0.30
CO2	0.07	0.08	0.10	0.07	0.13	0.07	0.05	0.08	0.13	0.13	0.05	0.13
S	0.04	0.13	0.02	0.03	0.14	0.21	0.04	0.04	0.03	0.05	0.05	0.03
Total	98.25	98.99	100.07	99.85	99.28	99.07	99.46	98.73	100.51	99.76	100.17	100.29
A.I.	0.87	0.64	0.67	1.00	0.91	0.34	0.90	0.99	0.88	0.79	0.74	1.01
Cu	3	22	103	2	18	9	19	5	4	4	29	5
Pb	22	199	18	26	68	21	85	9	1	183	27	15
Zn	95	842	106	106	454	628	209	86	46	171	113	119
Ni	0	0	1	0	0	0	0	0	0	0	2	2
Sc	1.7	0.2	0.3	1.8	0.0	0.0	0.1	1.0	0.9	0.0	2.4	2.5
Ga	29	35	34	29	47	40	39	36	44	43	25	31
Nb	66	123	95	69	365	361	176	49	116	382	48	65
Zr	712	2055	1443	844	4937	5118	2683	543	967	4999	749	904
Y	46	183	131	51	525	537	258	58	89	501	76	69
Ce	371	455	329	342	689	1067	530	357	573	1130	309	450
U	2	8	3	2	12	20	8	1	5	17	3	2
Th	12	30	18	14	92	94	36	5	22	104	13	10
Sr	12	10	9	8	12	7	9	14	12	13	87	16
Rb	170	337	218	174	389	420	317	141	265	531	166	156
Ba	139	82	81	108	18	24	34	140	138	26	334	237

Table B-13-2 Flowers River Cauldron Complex Geochemical Data

Field No.	FR91260R	FR91261	FR91262	FR91263	FR91265	FR91266	FR91267	FR91269	FR91270	FR91272	FR91273A	FR91274R
SiO2	49.42	65.85	89.35	81.55	75.55	78.7	74	76.7	68	78.6	74.65	65.71
TiO2	1.9	0.51	0.14	0.33	0.23	0.29	0.3	0.35	0.44	0.34	0.25	0.38
Al2O3	15.41	16.62	4.67	7.64	10.92	6.68	9.79	11	13.24	10.28	10.98	15.84
Fe2O3	3.27	0.16	0.07	0.66	2.69	0.99	4.51	0.92	3.42	1.41	2.80	2.45
FeO	7.71	0.68	0.58	1.41	1.07	7.91	1.21	3.53	3.23	1.32	1.06	2.15
MnO	0.16	0.02	0.01	0.02	0.04	0.08	0.09	0.04	0.11	0.04	0.06	0.12
MgO	5.99	2.64	1.06	0.93	0.03	0.1	0.02	0.06	0.15	0.03	0.11	0.05
CaO	7.42	2.51	0.46	0.09	0.17	0.01	0.1	0.01	0.27	0.01	0.16	0.51
Na2O	4.1	9.85	2.39	0.17	4.17	0.02	4.7	0.08	1.98	0.21	3.57	5.7
K2O	2.02	0.37	0.37	5.47	3.82	0.82	4.38	4.84	7.94	6.13	4.95	5.55
P2O5	0.32	0.07	0.05	0.01	0.01	0.01	0.01	0.01	0.04	0.01	0.01	0.03
F	0.18	0.21	0.29	0.04	0.05	0.03	0.12	0.02	0.12	0.03	0.07	0.06
H2O+	2.13	0.63	0.62	1.08	0.36	2.55	0.36	1.61	1.03	0.87	0.61	0.79
H2O-	0.32	0.27	0.22	0.26	0.25	0.2	0.17	0.2	0.19	0.17	0.27	0.29
CO2	0.1	0.15	0.09	0.06	0.09	0.09	0	0.06	0.08	0.06	0.11	0.1
S	0.03	0.05	0.04	0.03	0.05	0.09	0.02	0.06	0.05	0.05	0.03	0.01
Total	100.47	100.59	100.41	99.75	99.5	98.57	99.78	99.49	100.29	99.56	99.65	99.75
A.I.	0.58	1.00	0.93	0.81	1.01	0.14	1.27	0.49	0.89	0.68	1.02	0.97
Cu	22	8	5	6	12	32	8	12	11	17	7	12
Pb	22	0	1	24	55	216	68	0	762	15	6	20
Zn	95	41	30	84	156	1733	298	125	175	38	83	160
Ni	77	7	5	6	0	2	0	1	0	0	2	0
Sc	26.2	10.1	2.0	2.6	0.3	0.0	0.0	0.4	2.3	0.4	0.6	0.0
Ga	27	23	8	17	35	46	50	38	37	25	33	58
Nb	4	14	4	33	96	153	330	110	79	81	33	110
Zr	157	309	200	1467	1091	3905	3753	2102	1546	1566	451	867
Y	31	27	7	120	127	529	129	146	96	100	44	139
Ce	54	50	26	397	345	1867	427	295	497	602	257	834
U	1	1	0	6	5	13	10	3	3	2	1	3
Th	0	5	3	30	26	57	108	22	4	21	4	10
Sr	368	83	15	21	8	3	4	7	20	6	8	11
Rb	147	17	41	255	230	55	387	301	314	367	164	159
Ba	718	136	16	458	47	25	17	83	200	72	46	76

Table B-13-2

Field No.	FR91275	FR91276	FR91277	FR91278	FR91279	FR91280	FR91281	FR91283	FR91284	FR91285	FR91286	FR91288
SiO2	71.3	73.9	77.35	80.1	75.1	72.85	73.75	72.05	73.4	73.6	71.95	77.45
TiO2	0.32	0.32	0.34	0.28	0.33	0.3	0.29	0.33	0.29	0.29	0.33	0.3
Al2O3	12.68	12.36	8.88	10.81	9.04	11.52	9.93	11.93	9.81	9.75	11.3	10.41
Fe2O3	0.33	1.11	1.29	1.17	1.34	3.05	3.58	3.41	3.89	3.19	3.2	0.56
FeO	4.29	2.09	5.16	2.11	6.45	1.06	2.12	1.22	2.53	2.63	1.66	3.62
MnO	0.05	0.03	0.07	0.04	0.06	0.04	0.07	0.06	0.08	0.08	0.09	0.03
MgO	0.1	0.16	0.09	0.12	0.23	0.41	0.07	0.03	0.03	0.11	0.01	0.03
CaO	0.52	0.02	0.01	0.01	0.01	0.48	0.04	0.17	0.04	0.23	0.32	0.03
Na2O	3.34	0.64	0.05	0.04	0.09	3.83	3.76	4.73	3.93	4.09	4.83	0.16
K2O	4.98	7.03	4.41	3.14	4.14	5.05	4.59	4.91	4.56	4.44	4.66	4.06
P2O5	0.01	0.01	0.01	0.01	0.01	0.01	0.01	0.01	0.01	0.01	0.02	0.01
F	0.14	0.02	0.01	0.04	0.03	0.25	0.12	0.08	0.09	0.17	0.14	0.08
H2O+	0.95	1.39	1.27	1.83	1.77	0.94	0.61	0.63	0.39	0.23	0.21	1.55
H2O-	0.17	0.18	0.11	0.14	0.13	0.39	0.34	0.32	0.27	0.26	0.26	0.23
CO2	0.08	0.1	0.06	0.04	0.1	0.09	0.06	0.08	0.06	0.06	0.16	0.06
S	0.12	0	0.01	0.03	0.06	0.04	0.03	0.02	0.02	0.03	0.02	0.05
Total	99.38	99.36	99.12	99.91	98.89	100.31	99.36	99.98	99.4	99.17	99.17	98.63
A.I.	0.86	0.70	0.55	0.32	0.51	1.02	1.12	1.10	1.16	1.18	1.15	0.45
Cu	21	15	23	21	10	19	17	13	20	19	15	14
Pb	15	32	129	19	54	41	73	41	50	80	50	7
Zn	71	170	463	125	523	370	426	237	410	432	177	61
Ni	0	2	2	7	1	1	1	1	5	3	1	1
Sc	0.8	0.6	0.0	0.6	0.0	0.2	0.0	0.2	0.0	0.0	0.0	0.2
Ga	37	24	34	44	43	49	52	49	53	53	48	39
Nb	96	41	205	42	205	187	316	155	310	307	184	185
Zr	1184	947	4578	974	4576	2105	3657	1645	3565	3643	2861	2609
Y	122	122	502	90	411	170	418	120	385	390	144	237
Ce	428	502	922	284	1258	579	739	630	783	734	822	528
U	4	4	9	2	11	6	10	4	10	10	7	8
Th	16	21	91	18	87	23	51	23	56	56	30	48
Sr	19	29	14	5	14	10	6	8	6	7	8	6
Rb	226	304	235	205	223	230	414	201	402	391	261	471
Ba	101	220	57	100	60	39	13	76	11	12	42	21

Table B-13-2

Field No.	FR91290	FR91291	FR91292	FR91293	FR92001	FR92002	FR92003	FR92004	FR92005	FR92006	FR92007	FR92009
SiO2	74.2	73.8	80.3	73.5	54	71.6	70.32	58.57	67.23	90.75	64.49	73.57
TiO2	0.29	0.27	0.3	0.29	2.13	0.37	0.59	0.82	0.5	0.3	0.19	0.33
Al2O3	10.8	10.53	9.86	10.03	14.54	12.25	13	17.26	13.79	3.87	16.18	11.24
Fe2O3	0.95	0.72	0.54	3.52	1.69	0.47	1.18	0.64	2.29	0.1	0.33	3.32
FeO	4.1	4.08	3.08	2.74	9.53	1.74	3.94	6.53	2.78	0.22	0.5	0.43
MnO	0.02	0.05	0.05	0.05	0.21	0.04	0.05	0.09	0.13	0.01	0.02	0.05
MgO	0.01	0.16	0.01	0.05	2.54	1.77	0.45	1.4	0.22	0.56	0.96	0.16
CaO	0.39	0.54	0.07	0.31	4.84	2.15	2.72	2.54	1.01	0.68	3.38	0.28
Na2O	2.24	2.32	0.06	2.2	4.34	3.82	1.84	2.68	4.33	0.2	0.4	3.81
K2O	5.01	4.51	2.92	5.93	3.69	3.26	3.37	6.83	5.47	1.23	12.9	5.12
P2O5	0.01	0.01	0.01	0.01	0.93	0.11	0.1	0.12	0.06	0.08	0.08	0.02
F	0.21	0.22	0.06	0.17	0.1	0.1	0.05	0.09	0.13	0.41	0.95	0.01
H2O+	0.7	1.24	1.64	0.26	1.57	1.4	1.43	1.5	1.01	0.72	0.55	0.71
H2O-	0.19	0.21	0.3	0.16								
CO2	0.08	0.07	0.19	0.15	0.13	0.72	0.23	0.15	0.12	0.07	0.09	0.07
S	0.28	0.1	0.08	0	0.05	0.00	0.02	0.00	0.00	0.00	0.00	0.00
Total	99.48	98.83	99.47	99.37	100.29	99.8	99.29	99.22	99.07	99.2	101.02	99.12
A.I.	0.84	0.83	0.33	1.00	0.77	0.80	0.51	0.68	0.95	0.43	0.90	1.05
Cu	17	30	14	23	29	6	6	10	14	5	10	10
Pb	16	81	13	174	24	0	7	11	72	0	18	54
Zn	82	502	156	403	181	40	48	109	201	13	29	132
Ni	1	1	1	2	21	15	2	2	0	1	1	5
Sc	0.2	0.0	0.0	0.0	14.3	7.2	8.1	11.0	3.6	1.2	2.4	0.6
Ga	40	40	40	38	39	16	29	34	46	6	13	36
Nb	182	168	222	204	55	11	23	32	120	2	4	108
Zr	2788	2593	3455	3267	1122	292	646	932	1458	563	186	1289
Y	267	253	320	327	90	30	75	96	157	17	14	116
Ce	546	571	701	637	605	89	249	278	853	80	60	395
U	8	8	12	12	2	3	2	2	3	2	1	4
Th	46	44	64	52	11	15	18	22	31	11	10	36
Sr	16	8	5	7	186	98	179	228	47	7	153	15
Rb	516	255	302	566	101	63	125	248	209	108	551	190
Ba	21	21	13	20	685	693	1281	3449	496	73	1269	119

Table B-13-2

Field No.	FR92010	FR92011	FR92012	FR92013	FR92014	FR92016	FR92017	FR92018	FR92019	FR92021	FR92024	FR92026
SiO2	76.25	73.44	56.29	81.27	66.85	47.29	88.26	75.74	73.45	73.67	72.53	76.06
TiO2	0.52	0.28	0.64	0.17	0.34	1.54	0.11	0.35	0.25	0.22	0.27	0.29
Al2O3	11.04	11.54	18.9	8.4	11.5	18.65	4.41	12.26	9.96	12.37	11.87	11.21
Fe2O3	1.02	1.66	2.5	0.39	0.37	2.08	0.09	2.91	3.26	3.16	3.03	1.42
FeO	3.15	1.34	3.53	0.99	2.72	9.46	0.68	0.73	2.24	0.22	1.25	1.6
MnO	0.05	0.05	0.09	0.01	0.07	0.15	0.01	0.03	0.07	0.02	0.02	0.04
MgO	0.26	0.04	0.66	0.85	2.66	6.24	0.52	0.09	0.13	0.04	0.11	0.2
CaO	0.13	0.6	3.41	0.18	6.51	8.24	0.67	0.15	0.3	0.03	0.41	0.14
Na2O	0.12	3.41	0.45	0.32	3.09	2.73	0.2	2.45	4.09	3.73	3.22	2.95
K2O	4.02	5.18	11.5	6.11	5.05	1.3	2.99	3.57	4.45	4.49	5.16	4.69
P2O5	0.1	0.01	0.12	0.06	0.07	0.25	0.04	0.02	0	0	0.01	0.03
F	0.07	0.22	0.46	0.06	0.33	0.11	0.11	0.02	0.19	0.06	0.2	0.01
H2O+	1.89	1.04	1.74	0.96	0.71	1.98	0.55	1.12	0.49	0.66	0.88	0.98
H2O-												
CO2	0.08	0.25	0.09	0.09	0.11	0.11	0.21	0.11	0.09	0.08	0.08	0.11
S	0.02	0.01	0.04	0.01	0.03	0.04	0.03	0.05	0.03	0.02	0.02	0.03
Total	98.72	99.07	100.42	99.87	100.41	100.17	98.88	99.6	99	98.77	99.06	99.76
A.I.	0.41	0.97	0.70	0.85	0.92	0.32	0.81	0.64	1.16	0.89	0.92	0.89
Cu	7	7	23	11	12	46	6	7	10	4	8	13
Pb	6	138	43	25	0	0	7	29	17	36	29	26
Zn	94	367	81	53	39	131	8	75	380	87	181	121
Ni	6	0	0	6	10	91	4	0	0	0	2	0
Sc	8.9	1.3	8.7	4.2	8.6	21.5	2.1	0.7	< 0.1	0.2	0.6	1.4
Ga	24	36	33	7	11	22	2	32	56	42	41	31
Nb	17	161	23	9	9	0	2	60	165	180	123	56
Zr	534	1268	802	112	165	124	168	1115	2164	1030	1415	830
Y	38	191	78	37	40	25	14	113	163	151	122	85
Ce	208	743	310	57	54	43	47	244	360	199	458	316
U	2	5	2	3	2	0	0	3	5	4	5	3
Th	18	43	23	13	11	1	5	28	28	31	31	23
Sr	26	16	196	68	81	374	45	19	5	6	14	23
Rb	178	270	420	187	164	63	92	164	277	263	266	140
Ba	934	165	971	373	365	393	458	183	17	40	82	204

Table B-13-2

Field No.	FR92027	FR92028	FR92029	FR92030	FR92031D	FR92032	FR92033	FR92034	FR92035	FR92036	FR92037	FR92038
SiO2	75.49	75.14	75.61	76.6	89.66	79.5	71.24	66.4	74.4	72.83	74.6	74.8
TiO2	0.3	0.29	0.32	0.36	0.09	0.32	0.56	0.54	0.32	0.36	0.26	0.32
Al2O3	11.25	11.63	11.36	9.4	5.31	10.05	12.22	13.49	9.72	10.4	10.8	11.25
Fe2O3	0.72	0.91	1.03	1.08	0.11	2.38	0.77	2.28	2.86	3.48	1.64	1.58
FeO	2.62	2.02	2.48	4.45	0.2	2.41	4.39	3.5	2.23	2.25	1.72	1.84
MnO	0.06	0.04	0.04	0.06	0.01	0.04	0.07	0.13	0.07	0.12	0.05	0.06
MgO	0.2	0.16	0.16	0.13	0.24	0.09	0.25	0.28	0.07	0.02	0.02	0.06
CaO	0.29	0.14	0.07	0.03	0.19	0	2.49	1.28	0.39	0.34	0.07	0.34
Na2O	2.07	2.93	2.34	0.06	2.79	0.07	0.43	4.57	3.04	4.36	3.81	4.02
K2O	5.16	4.6	5.04	4.16	0.13	3.07	5.17	5.14	4.28	4.06	4.75	4.65
P2O5	0.03	0.03	0.03	0.01	0.05	0.02	0.09	0.08	0	0.01	0	0.02
F	0.01	0.01	0.01	0.03	0.06	0.08	0.03	0.16	0.01	0.24	0.07	0.05
H2O+	1.14	0.99	1.09	1.59	0.48	1.92	1.65	0.86	0.4	0.47	0.6	0.67
H2O-												
CO2	0.25	0.11	0.09	0.11	0.08	0.14	0.1	0.09	0.11	0.07	0.07	0.12
S	0.03	0.04	0.03	0.02	0.00	0.02	0.02	0.02	0.00	0.00	0.00	0.00
Total	99.62	99.04	99.7	98.09	99.4	100.11	99.48	98.82	97.9	99.01	98.46	99.78
A.I.	0.80	0.84	0.82	0.49	0.89	0.34	0.52	0.97	0.99	1.11	1.06	1.04
Cu	8	5	4	10	6	22	7	9	16	6	8	12
Pb	20	29	17	171	0	153	33	26	70	53	41	32
Zn	75	129	102	438	10	217	241	200	349	410	191	155
Ni	0	0	0	3	2	0	1	4	0	0	0	3
Sc	1.6	1.5	1.9	0.2	1.3	< 0.1	7.6	4.2	0.6	0.1	0.7	2.0
Ga	34	30	32	42	4	49	30	42	40	51	34	32
Nb	58	58	57	174	3	736	24	131	216	226	125	96
Zr	801	843	781	3132	84	11320	596	1451	2715	2554	1037	967
Y	89	91	92	197	5	1070	68	173	330	196	59	83
Ce	371	359	358	837	13	2059	251	959	699	452	253	380
U	3	3	3	6	1	28	2	4	10	6	3	2
Th	24	24	24	67	6	251	17	32	74	39	24	24
Sr	23	22	20	14	18	6	111	52	25	6	5	11
Rb	199	154	189	259	9	400	169	201	239	242	266	167
Ba	233	217	233	60	18	50	2467	428	108	26	51	185

Table B-13-2

Field No.	FR92039	FR92040	FR92041	FR92042	FR92043	FR92044	FR92045	FR92046	FR92047	FR92048	FR92049	FR92050
SiO2	91.11	57.85	79.62	77.03	78.22	77.04	77.13	78.53	78.09	79.28	76.68	55.45
TiO2	0.16	0.51	0.28	0.29	0.38	0.29	0.32	0.39	0.33	0.29	0.28	1.93
Al2O3	3.29	17.27	10.69	11	11.56	11.01	11.26	10.68	11.16	10.9	11.73	14.61
Fe2O3	0.49	1.27	0.83	0.89	0.05	3.29	0.67	1.18	0.98	0.7	1.22	3.82
FeO	0.51	2.9	2.04	2.27	2.49	0	1.8	1.47	1.77	1.3	2.08	7.18
MnO	0.01	0.05	0.04	0.04	0.05	0.05	0.04	0.03	0.03	0.04	0.04	0.19
MgO	0.12	3.8	0.05	0.06	0.07	0.06	0.06	0.09	0.07	0.03	0.06	1.96
CaO	0.17	1.57	0.02	0.08	0.05	0.11	0.02	0	0.03	0.03	0.06	4.49
Na2O	0.31	2.18	0.09	1.18	0.12	1.76	1.47	0.11	0.12	1.22	0.73	4.7
K2O	2.39	10	3.4	4.43	4.51	4.99	4.92	4.71	4.92	4.68	5.59	3.57
P2O5	0.02	0.2	0.03	0.03	0.04	0.02	0.03	0.04	0.03	0.02	0.03	0.8
F	0.05	0.45	0.04	0.02	0.03	0.02	0.01	0.02	0.03	0.02	0.03	0.11
H2O+	0.44	0.91	1.61	1.33	1.61	1	1.13	1.44	1.51	1.1	1.31	1.02
H2O-												
CO2	0.08	0.05	0.07	0.08	0.07	0.12	0.07	0.05	0.11	0.07	0.08	0.02
S	0.00	0.00	0.02	0.02	0.01	0.01	0.01	0.01	0.02	0.02	0.01	0.01
Total	99.15	99.01	98.83	98.75	99.26	99.77	98.94	98.75	99.2	99.7	99.93	99.86
A.I.	0.94	0.83	0.36	0.61	0.44	0.75	0.69	0.49	0.49	0.65	0.62	0.79
Cu	10	18	7	7	7	121	11	7	7	7	6	27
Pb	13	5	15	25	29	43	35	18	26	28	36	17
Zn	13	17	119	84	126	87	107	134	147	59	112	185
Ni	3	31	1	1	1	2	4	0	1	0	1	16
Sc	1.8	15.5	1.5	1.6	2.1	1.4	1.8	2.6	1.9	1.4	1.4	14.3
Ga	5	20	39	31	37	27	35	38	34	31	30	41
Nb	7	13	59	63	59	55	60	55	58	54	58	61
Zr	113	101	783	801	834	810	779	755	854	771	798	1171
Y	15	28	84	94	89	96	86	82	89	72	86	94
Ce	31	80	307	323	375	363	297	338	343	277	290	580
U	1	4	3	3	3	3	4	4	3	3	3	1
Th	4	17	23	25	22	25	25	21	23	21	25	10
Sr	16	222	5	17	14	26	21	15	14	19	21	150
Rb	99	493	182	195	200	201	224	244	235	185	251	82
Ba	526	1317	41	217	212	266	261	320	200	262	263	655

Table B-13-2

Field No.	FR92051	FR92052	FR92053	FR92054	FR92055	FR92056	FR92057	FR92060	FR92061	FR92062	FR92063	FR92064
SiO2	62.89	75.21	50.3	60.29	58.04	66.68	68.28	51.76	58.55	88.96	76.24	72.71
TiO2	0.42	0.28	2.69	1.08	1.03	0.45	0.4	1.55	1.06	0.3	0.34	0.35
Al2O3	16.8	9.08	14.81	16.02	13.68	14.46	13.82	15.02	16.38	5.77	9.01	11.88
Fe2O3	4.18	3.82	1.78	2.21	3.52	1.18	2	1.1	2.77	0.53	1.29	1.88
FeO	0.92	1.87	11.55	5.23	8.88	3.14	2.3	9.49	5.41	0.14	5.44	2.01
MnO	0.16	0.08	0.23	0.15	0.25	0.07	0.08	0.17	0.19	0.01	0.09	0.07
MgO	0.34	0.11	3.07	0.83	0.19	0.28	0.31	4.7	0.82	0.05	0.14	0.05
CaO	0.64	0.53	5.69	3.52	3.68	1.45	1.22	7.39	3.82	0	0.11	0.4
Na2O	4.93	3.39	4.65	5.27	4.72	4.75	4.57	2.47	5.42	0.11	0.17	4.36
K2O	6.72	3.61	2.21	3.93	4.79	5.23	5.26	1.04	3.64	1.97	4.41	4.93
P2O5	0.07	0.01	1.31	0.38	0.24	0.07	0.06	0.25	0.41	0.01	0.02	0.03
F	0.04	0.01	0.09	0.08	0.02	0.07	0.06	0.04	0.07	0.02	0.02	0.06
H2O+	1.51	0.56	0.84	1.03	0.89	0.67	0.61	2.21	1.04	1.03	1.48	0.69
H2O-												
CO2	0.16	0.06	0.05	0.06	0.04	0.04	0.05	1.62	0.1	0.08	0.05	0.08
S	0.00	0.00	0.13	0.01	0.03	0.00	0.00	0.11	0.06	0.03	0.05	0.02
Total	99.78	98.62	99.4	100.09	100	98.54	99.02	98.92	99.74	99.01	98.86	99.52
A.I.	0.92	1.04	0.68	0.81	0.95	0.93	0.96	0.35	0.78	0.40	0.56	1.05
Cu	8	8	36	15	23	9	5	19	15	22	18	6
Pb	13	78	6	14	7	15	13	2	13	57	144	25
Zn	141	407	178	150	192	102	119	116	150	96	485	155
Ni	1	3	27	4	0	1	0	16	6	0	3	0
Sc	1.1	0.2	18.9	8.9	19.7	4.0	2.9	26.5	9.2	0.2	< 0.1	1.4
Ga	46	40	35	38	30	30	32	27	41	27	46	44
Nb	43	254	41	61	31	34	36	3	41	205	204	98
Zr	1437	4454	932	1644	658	1027	830	143	1329	3815	4299	1244
Y	97	364	75	88	58	62	73	28	74	326	423	86
Ce	1262	819	486	498	207	207	322	61	454	263	1545	500
U	2	13	1	2	0	2	2	0	0	10	11	2
Th	19	90	4	13	2	12	15	4	8	85	89	19
Sr	81	23	215	173	37	86	54	303	190	6	18	12
Rb	131	247	33	101	55	114	127	21	77	191	300	179
Ba	324	87	796	760	1040	1210	695	449	888	23	74	149

Table B-13-2

Field No.	FR92065D	FR92066	FR92067	FR92068	FR92069	FR92070	FR92071	FR92072	FR92073	FR92074	FR92075	FR92076
SiO2	73.55	51.68	64.58	64.7	82.21	58.86	73.39	61.58	75.99	59.72	74.39	54.14
TiO2	0.37	2.31	0.91	1.02	0.24	0.88	0.33	0.8	0.35	0.46	0.27	1.87
Al2O3	11.55	14.58	12.78	12.93	9.05	14.9	10.99	14.18	9.73	14.55	10.44	13.98
Fe2O3	1.5	0.00	2.62	1.85	1.56	3.07	2.13	3.04	3.99	0.00	2.7	0.00
FeO	2.13	12.91	5.64	5.29	1.38	6.62	1.95	5.87	0.77	4.69	1.93	13.05
MnO	0.06	0.24	0.19	0.14	0.03	0.24	0.08	0.22	0.04	0.07	0.07	0.28
MgO	0.1	2.65	0.63	1.06	0.12	0.39	0.05	0.33	0.06	3.75	0.04	1.78
CaO	0.63	5.42	2.43	2.24	0	3.43	0.34	2.64	0.04	4.13	0.29	5.06
Na2O	4.04	4.71	4.35	4.45	0.06	5.02	4.21	4.88	1.68	4.54	3.93	4.53
K2O	4.92	2.75	4.24	4.17	2.74	4.49	4.63	4.6	4.73	5.69	4.79	3.28
P2O5	0.04	1.39	0.39	0.41	0.02	0.24	0.02	0.2	0.07	0.72	0.01	1.08
F	0.05	0.15	0.15	0.13	0.02	0.08	0.15	0.09	0.02	0.18	0.16	0.13
H2O+	0.56	1.12	0.74	1	1.58	1.05	0.63	1.14	0.85	0.98	0.39	0.56
H2O-												
CO2	0.07	0.12	0.04	0.04	0.05	0.07	0.09	0.1	0.09	0.38	0.08	0.07
S	0.00	0.14	0.03	0.02	0.00	0.00	0.00	0.01	0.00	0.00	0.00	0.06
Total	99.57	100.03	99.72	99.45	99.06	99.34	98.99	99.68	98.41	99.86	99.49	99.81
A.I.	1.04	0.74	0.92	0.92	0.34	0.88	1.09	0.92	0.81	0.94	1.12	0.79
Cu	7	30	11	15	8	17	12	18	17	7	12	26
Pb	12	7	23	21	7	13	65	10	119	0	10	11
Zn	131	192	251	203	140	198	326	229	281	34	211	220
Ni	0	16	2	9	3	0	0	0	0	35	1	0
Sc	2.8	21.4	11.1	7.8	0.4	20.9	< 0.1	16.5	< 0.1	13.0	0.3	30.9
Ga	33	36	43	39	32	50	52	40	49	20	44	38
Nb	66	50	127	94	47	78	194	85	285	12	149	66
Zr	886	1038	1583	1168	717	2023	1787	2003	5044	158	2096	1241
Y	59	93	154	125	69	117	146	119	345	51	204	111
Ce	318	482	608	523	135	644	486	638	1258	91	554	474
U	2	2	3	3	2	2	4	3	9	2	4	2
Th	15	11	22	18	20	14	35	17	85	40	40	13
Sr	21	222	82	86	6	158	6	126	14	131	7	220
Rb	136	66	141	137	150	96	189	110	442	170	273	76
Ba	271	1050	755	488	175	2206	43	1731	44	453	48	1734

Table B-13-2

Field No.	FR92077	FR92078	FR92080	FR92081	FR92082	FR92083	FR92084	FR92085	FR92086	FR92087	FR92088	FR92089D
SiO2	74.06	72.44	75.13	66.99	75.56	73.49	76.11	73.92	74.77	73.04	73.11	88.43
TiO2	0.3	0.29	0.35	0.49	0.41	0.38	0.33	0.39	0.33	0.21	0.21	0.1
Al2O3	10.76	9.78	10.35	8.46	9.38	7.94	7.36	9.09	9.93	9.03	9.06	4.41
Fe2O3	3.21	2.58	2.66	17.93	0.09	2.67	2.85	2.19	4.46	5.1	6.83	0.13
FeO	1.29	2.95	1.86	0	8.21	7.9	6.63	5.45	0.36	2.4	0.14	0.73
MnO	0.06	0.08	0.04	0.14	0.06	0.07	0.06	0.09	0.02	0.1	0.1	0.02
MgO	0.11	0.19	0.04	0.08	0.04	0.11	0.11	0.26	0.02	0.01	0.06	0.19
CaO	0.18	0.44	0.04	0	0.04	0	0	0	0.03	0.09	0.05	0.42
Na2O	4.06	4.44	2.33	0.03	0.05	0.02	0.02	0	2.48	3.59	3.65	0.67
K2O	4.81	4.45	5.19	0.84	1.86	2.28	1.41	2.23	5.26	4.14	4.46	2.24
P2O5	0.01	0.01	0	0.09	0.01	0.02	0.02	0.01	0	0.01	0.01	0.01
F	0.03	0.23	0.02	0.03	0.05	0.04	0.05	0.05	0.01	0.11	0.03	0.15
H2O+	0.46	0.54	0.66	2.89	2.32	2.12	2.11	2.44	0.61	0.51	0.53	0.56
H2O-												
CO2	0.08	0.09	0.1	0.09	0.12	0.18	0.16	0.2	0.1	0.1	0.17	0.19
S	0.00	0.00	0.00	0.67	0.44	0.15	0.25	0.02	0.00	0.02	0.03	0.02
Total	99.42	98.51	98.77	98.73	98.64	97.37	97.47	96.34	98.38	98.46	98.44	98.27
A.I.	1.10	1.24	0.91	0.11	0.22	0.31	0.21	0.27	0.98	1.15	1.20	0.80
Cu	12	11	13	36	17	20	31	22	13	12	11	8
Pb	24	84	10	204	168	322	331	439	92	191	101	0
Zn	238	501	78	177	935	1004	998	848	170	410	455	12
Ni	3	0	0	0	0	0	0	2	0	0	3	3
Sc	0.6	< 0.1	< 0.1	< 0.1	< 0.1	< 0.1	< 0.1	< 0.1	0.1	< 0.1	< 0.1	1.3
Ga	40	56	43	54	53	46	35	53	37	47	50	7
Nb	143	340	206	1000	370	745	655	775	190	469	458	65
Zr	1951	3365	2802	12081	6749	9228	8990	9846	2558	5753	5551	750
Y	170	417	303	1372	363	1102	958	1195	268	632	678	61
Ce	509	764	876	1947	1419	2491	2458	3359	743	1358	1692	91
U	5	10	11	40	10	27	29	33	6	18	18	2
Th	37	63	60	327	110	233	209	261	55	135	138	17
Sr	9	15	9	4	3	8	5	4	12	8	13	13
Rb	254	384	373	110	268	353	202	207	349	597	581	89
Ba	64	21	40	43	37	62	34	50	42	29	70	223

Table B-13-2

Field No.	FR92090	FR92092	FR92093	FR92094	FR92095	FR92096	FR92097R	FR92098	FR92099	FR92100	FR92101	FR92102
SiO2	72.76	73.84	85.7	81.03	83.41	75.14	70.59	76.02	77.28	75.98	69.65	73.03
TiO2	0.29	0.34	0.35	0.47	0.36	0.35	0.37	0.2	0.18	0.19	0.32	0.23
Al2O3	9.67	10.07	11.15	6.24	4.65	11.81	11.52	9.51	11.1	10.97	13.84	10.04
Fe2O3	3.98	2.18	0.5	7.51	7.3	4.82	7.7	5.09	0.85	2.14	1.55	6.83
FeO	1.71	3.8	0	0.19	0.19	0.26	0.23	1.14	2.71	1.81	2.89	0.43
MnO	0.09	0.08	0.01	0.01	0.02	0.02	0.05	0.03	0.04	0.03	0.03	0.03
MgO	0	0.03	0	0.03	0.01	0.07	0.12	0.04	0	0.07	0.05	0
CaO	0.48	0.27	0	0	0	0	0	0.03	0.06	0.22	0.05	0.11
Na2O	4.41	2.35	0.06	0.02	0.01	0.05	0.06	0.13	1.62	2.82	2.61	3.5
K2O	4.35	4.6	0.03	1.5	0.68	3.4	3.89	4.58	4.37	4.11	6.71	3.62
P2O5	0	0	0.01	0.03	0.02	0.02	0.01	0.01	0	0	0.01	0
F	0.33	0.11	0.02	0.02	0.02	0.06	0.12	0.03	0.06	0.14	0.03	0.09
H2O+	0.51	0.77	0.47	1.47	1.28	1.9	1.64	1.02	1.02	0.96	1.02	0.37
H2O-												
CO2	0.13	0.11	0.13	0.09	0.09	0.15	0.21	0.13	0.11	0.14	0.13	0.15
S	0.03	0.06	0.01	0.05	0.04	0.03	0.03	0.03	0.05	0.02	0.02	0.00
Total	98.74	98.61	98.44	98.66	98.08	98.08	96.54	97.99	99.45	99.6	98.91	98.43
A.I.	1.24	0.88	0.01	0.27	0.16	0.32	0.37	0.54	0.67	0.83	0.83	0.96
Cu	9	9	19	9	11	13	26	13	8	16	7	12
Pb	69	93	15	29	19	3	198	143	44	32	13	54
Zn	425	550	17	73	47	163	340	367	244	241	213	153
Ni	0	0	4	0	0	0	0	0	3	2	1	1
Sc	< 0.1	< 0.1	0.5	1.6	0.3	< 0.1	< 0.1	< 0.1	< 0.1	0.1	0.8	< 0.1
Ga	53	42	46	26	17	60	86	41	47	40	39	47
Nb	304	206	494	162	235	673	977	336	400	355	114	496
Zr	3489	2758	5060	1252	2075	10002	13532	4456	1880	1994	1536	4509
Y	332	281	601	106	148	687	1528	486	367	359	135	590
Ce	600	684	395	426	340	1743	2509	911	415	475	393	1899
U	8	9	18	3	6	20	46	13	12	11	4	12
Th	57	56	139	23	37	236	327	112	64	59	27	138
Sr	9	10	2	5	4	8	14	13	7	8	13	10
Rb	354	327	-5	139	56	452	861	719	540	375	277	399
Ba	21	38	18	100	57	44	53	52	10	40	109	57

Table B-13-2

Field No.	FR92103	FR92104	FR92105	FR92106	FR92107	FR92108	FR92109	FR92110	FR92112	FR92113	FR92114	FR92115
SiO2	72.16	73.65	73.44	74.7	75.26	74.84	74.12	75.4	75.07	78.12	78.12	73.96
TiO2	0.24	0.26	0.26	0.17	0.18	0.19	0.17	0.18	0.17	0.4	0.33	0.33
Al2O3	10.58	10.35	10.67	11.4	11.24	10.82	11.33	11.28	11.08	10.57	10.82	12.7
Fe2O3	5.64	4.36	5.24	1.91	1.11	1.97	2.21	2.32	1.85	0.97	1.09	0.83
FeO	0.71	1.11	0.32	1.38	1.96	2.13	2.14	1.41	1.73	2.6	1.78	2.56
MnO	0.04	0.02	0.04	0.06	0.05	0.06	0.06	0.03	0.04	0.04	0.03	0.03
MgO	0.05	0.04	0.04	0	0	0	0	0	0	0.06	0.04	0.04
CaO	0.05	0.37	0.21	0.25	0.18	0.45	0.03	0.16	0.06	0.02	0.02	0.03
Na2O	2.72	3.16	3.61	3.71	4.18	3.71	4.52	3.92	4.42	0.53	0.67	1.54
K2O	5.39	3.99	4.21	4.52	4.6	4.32	4.22	4.81	4.44	3.68	4.64	5.41
P2O5	0.01	0	0	0	0	0	0	0	0	0.01	0.02	0.03
F	0.06	0.22	0.11	0.18	0.17	0.47	0.14	0.11	0.13	0.02	0.02	0.03
H2O+	0.33	0.65	0.4	0.4	0.36	0.35	0.38	0.35	0.36	1.48	1.17	1.24
H2O-												
CO2	0.13	0.14	0.19	0.12	0.08	0.08	0.09	0.1	0.1	0.09	0.09	0.11
S	0.01	0.02	0.03	0.04	0.00	0.00	0.00	0.00	0.00	0.02	0.01	0.03
Total	98.12	98.34	98.77	98.84	99.37	99.39	99.41	100.07	99.45	98.61	98.85	98.87
A.I.	0.97	0.92	0.98	0.96	1.05	1.00	1.06	1.03	1.09	0.46	0.57	0.66
Cu	10	9	13	12	8	12	10	10	11	9	10	8
Pb	136	15	209	172	82	86	117	46	68	17	23	25
Zn	539	244	359	606	374	514	542	263	528	158	72	80
Ni	1	1	0	0	1	2	2	1	1	1	1	4
Sc	< 0.1	< 0.1	0.1	< 0.1	< 0.1	< 0.1	< 0.1	< 0.1	< 0.1	2.4	2.1	2.1
Ga	43	41	41	43	42	46	51	43	49	39	39	36
Nb	511	379	347	370	252	371	430	210	408	68	59	60
Zr	4776	3966	3906	2108	1412	2257	2232	1150	2149	934	821	822
Y	732	620	530	537	179	387	198	140	152	102	87	96
Ce	1050	647	534	429	333	440	344	171	346	355	311	381
U	23	18	14	11	1	12	12	4	11	4	3	4
Th	138	118	114	65	40	65	61	38	56	25	24	25
Sr	11	8	9	7	5	37	6	4	5	9	17	24
Rb	730	366	473	441	335	504	469	327	463	191	224	228
Ba	47	43	33	24	9	25	11	16	7	150	270	302

Table B-13-2

Field No.	FR92116	FR92117	FR92118	FR92119	FR92120	FR92121	FR92122	FR92123	FR92124R	FR92125	FR92126	FR92127
SiO2	75.94	75.24	69.41	69.33	72.89	71.66	75.07	76.06	72.35	75.68	72.85	72.57
TiO2	0.31	0.32	0.37	0.43	0.52	0.51	0.29	0.27	0.28	0.3	0.34	0.31
Al2O3	11.4	11.48	12.47	12.81	11.42	12.32	11.61	11.53	9.49	11.04	11.84	11.08
Fe2O3	0.94	2.7	1.68	2.35	0.93	0.36	0.34	0.88	1.05	1.06	2.17	2.74
FeO	2.19	0.72	3.2	2.7	3.6	4.31	2.63	2.15	5.61	1.96	2.41	1.82
MnO	0.04	0.02	0.14	0.12	0.08	0.05	0.06	0.04	0.15	0.05	0.1	0.09
MgO	0.05	0.09	0.08	0.11	0.26	0.1	0.11	0.11	0.09	0.16	0.05	0.03
CaO	0.05	0.03	1.03	0.93	1.29	0.65	0.13	0.02	0.19	0.02	0.52	0.08
Na2O	0.92	1.63	3.99	3.98	0.33	0.75	2.5	0.19	2.71	0.31	4.67	4.41
K2O	5.34	5.5	4.7	4.84	5.93	6.01	4.6	5.98	0.76	7.23	4.79	4.73
P2O5	0.03	0.02	0.04	0.04	0.1	0.08	0.02	0.02	0.03	0.03	0.02	0.01
F	0.02	0.01	0.31	0.14	0.17	0.02	0.02	0.03	0.05	0.02	0.15	0.08
H2O+	1	0.72	0.57	0.83	0.83	1.12	0.84	1.26	1.64	0.87	0.49	0.46
H2O-												
CO2	0.11	0.09	0.12	0.1	0.11	0.12	0.11	0.07	0.22	0.07	0.09	0.12
S	0.01	0.00	0.01	0.00	0.00	0.01	0.03	0.03	0.17	0.03	0.05	0.01
Total	98.35	98.57	98.12	98.71	98.46	98.07	98.36	98.64	94.79	98.83	100.54	98.54
A.I.	0.64	0.75	0.93	0.92	0.61	0.63	0.78	0.59	0.56	0.75	.09	1.12
Cu	10	10	23	8	19	15	10	9	30	10	8	10
Pb	29	32	269	33	19	17	23	51	466	48	36	62
Zn	60	97	619	167	113	77	118	216	955	77	208	385
Ni	0	2	1	1	2	1	3	1	0	2	3	0
Sc	1.8	1.8	2.8	2.3	8.6	7.4	1.6	1.1	< 0.1	1.7	0.8	< 0.1
Ga	34	31	46	43	24	23	30	29	45	26	49	53
Nb	63	68	273	122	16	22	57	75	992	63	147	253
Zr	819	870	1599	1468	479	512	785	895	14192	834	1448	2255
Y	86	97	509	161	56	66	81	109	1847	88	158	281
Ce	346	303	721	792	199	238	370	389	3563	340	642	647
U	3	4	9	4	2	1	3	4	43	3	4	6
Th	28	28	39	31	17	16	25	32	299	24	27	39
Sr	22	26	40	48	75	89	22	23	36	20	13	5
Rb	236	237	338	220	223	168	173	352	43	358	181	251
Ba	291	263	441	339	1864	2326	217	256	37	309	100	24

Table B-13-2

Field No.	FR92128	FR92129	FR92130
SiO2	64.94	46.97	76.22
TiO2	0.31	2.21	0.34
Al2O3	10.73	16.12	10
Fe2O3	0.3	2.62	0.96
FeO	2.93	11.29	4.04
MnO	0.07	0.22	0.08
MgO	2.92	5.99	0.06
CaO	7.93	6.3	0.21
Na2O	2.54	3.25	0.21
K2O	5.47	1.75	5.59
P2O5	0.07	0.35	0
F	0.84	0.2	0.03
H2O+	0.37	2.13	1.16
H2O-			
CO2	0.17	0.08	0.09
S	0.03	0.03	0.02
Total	99.62	99.51	99.01
A.I.	0.94	0.45	0.64
Cu	15	42	12
Pb	0	14	16
Zn	40	151	293
Ni	12	71	0
Sc	8.5	28.2	0.1
Ga	14	30	31
Nb	9	3	197
Zr	163	174	2815
Y	42	34	289
Ce	66	61	737
U	2	0	7
Th	12	2	57
Sr	81	319	27
Rb	178	102	307
Ba	364	477	74

Table C1 Little Pond Brook Average and Unique Geochemical Data

	F Porph. Ash-flow		FQA(1)		FQA (2)		QF Porph		QF-poor	QF-poor (2)		Aphryic	Aphryic
	Ave(13)	Range	Ave (5)	Range	Ave(24)	Range	Ave(17)	Range	Ave(2)	Ave(7)	Range	Breccia	Ash-flow
SiO2	72.92	71.9 - 74.55	76.26	75.95 - 76.95	75.21	74.4 - 76.6	76.44	74.9 - 78.6	77.14	76.11	70.15 - 79.7	71.85	67.90
TiO2	0.37	0.26 - 0.39	0.20	0.17 - 0.23	0.24	0.21 - 0.27	0.22	0.01 - 0.26	0.13	0.19	0.15 - 0.23	0.19	0.32
Al2O3	13.31	12.8 - 13.78	10.95	10.63 - 11.3	11.35	10.98 - 11.88	11.43	10.41 - 12.58	11.77	10.69	8.31 - 11.35	14.09	14.68
Fe2O3	1.35	0.76 - 2.45	1.79	1.49 - 2.36	1.77	1.08 - 3.17	1.94	0.82 - 3.48	1.49	1.98	1.28 - 3.49	1.63	1.20
FeO	1.00	0.16 - 1.71	1.02	0.5 - 1.32	1.14	0.18 - 1.73	0.47	0.08 - 1.19	0.19	0.82	0.2 - 1.51	0.49	1.12
MnO	0.05	0.01 - 0.07	0.06	0.05 - 0.06	0.07	0.05 - 0.09	0.05	0.01 - 0.10	0.03	0.05	0.02 - 0.11	0.02	0.05
MgO	0.34	0.11 - 0.58	0.05	0.01 - 0.08	0.10	0.04 - 0.24	0.06	0.01 - 0.16	0.09	0.10	0.07 - 0.14	0.02	0.84
CaO	0.31	0.03 - 0.72	0.12	0.06 - 0.19	0.20	0.02 - 0.39	0.19	0.01 - 1.48	0.11	0.61	0.01 - 3.35	0.45	0.13
Na2O	3.81	2.78 - 4.62	3.80	3.44 - 4.04	3.68	3.09 - 4.24	3.39	1.21 - 6.27	2.63	2.10	1.2 - 2.8	5.45	0.40
K2O	5.19	4.56 - 6.6	4.67	4.39 - 5.19	4.93	4.44 - 5.75	4.59	0.27 - 6.93	5.15	5.22	4.65 - 6.94	4.18	11.84
P2O5	0.05	0.02 - 0.07	0.01	0.01 - 0.01	0.02	0.01 - 0.03	0.02	0 - 0.04	0.01	0.01	0.01 - 0.02	0.01	0.04
F	0.04	0.02 - 0.05	0.04	0.02 - 0.05	0.03	0.01 - 0.05	0.02	0 - 0.03	0.04	0.04	0.02 - 0.08	0.01	0.02
H2O+	0.95	0.77 - 1.19	0.57	0.47 - 0.75	0.91	0.59 - 1.66	0.90	0.51 - 1.35	0.89	1.01	0.61 - 1.46	0.99	1.14
H2O-	0.27	0.16 - 0.37	0.26	0.19 - 0.33	0.32	0.16 - 0.4	0.28	0.19 - 0.39	0.24	0.26	0.16 - 0.34	0.20	0.28
CO2	0.20	0.02 - 0.53	0.06	0.02 - 0.11	0.13	0 - 0.26	0.15	0 - 0.68	0.10	0.57	0.03 - 2.59	0.46	0.03
S	0.03	0.01 - 0.07	0.04	0 - 0.07	0.04	0 - 0.08	0.04	0 - 0.1	0.04	0.05	0.01 - 0.09	0.04	0.04
A.I.	0.89	0.86 - 0.91	1.03	1.00 - 1.07	1.00	0.94 - 1.05	0.92	0.85 - 0.97	0.84	0.85	0.72 - 0.93	0.957	0.918
Cu	6	2 - 11	4	3 - 5	5	2 - 16	5	2 - 12	7	8	4 - 15	6	7
Pb	9	0 - 55	18	13 - 24	13	8 - 18	6	0 - 17	6	11	0 - 18	1	11
Zn	85	12 - 176	137	104 - 169	117	91 - 188	70	13 - 139	90	80	26 - 150	45	104
Ni	1	0 - 4	0	0 - 1	1	0 - 5	1	0 - 5	0	1	0 - 7	0	3
Ga	21	18 - 25	29	25 - 31	36	22 - 212	28	23 - 34	21	25	21 - 31	21	19
Sc	3.8	2.3 - 4.5	0.3	0 - 0.5	0.7	0.4 - 1	0.7	0.3 - 1.5	0.9	0.7	0.1 - 1.7	0.4	3
Nb	24	22 - 28	47	39 - 52	35	29 - 43	33	20 - 44	36	42	31 - 49	60	23
Zr	438	290 - 481	977	825 - 1089	671	562 - 769	681	487 - 854	370	858	740 - 958	1094	362
Y	53	34 - 64	124	111 - 140	80	57 - 105	85	49 - 122	84	109	84 - 129	133	57
Ce	130	71 - 160	219	190 - 246	187	97 - 262	176	7 - 236	115	212	144 - 307	172	126
U	6	6 - 6	7	6 - 7	4	3 - 6	4	2 - 8	4	8	3 - 15	16	8
Th	18	13 - 23	20	17 - 22	11	5 - 17	13	8 - 23	24	20	9 - 26	34	34
Sr	47	24 - 61	8	3 - 11	13	5 - 24	18	6.5 - 39	16	23	10 - 40	29	88
Rb	156	121 - 224	159	145 - 170	129	111 - 152	136	84 - 223	197	181	151 - 267	111	468
Ba	585	556 - 674	62	23 - 112	133	77 - 229	152	74 - 295	53	143	50 - 416	85	698

Table C-2 Gaff Topsail Average and Unique Geochemical Data

	TS91129	A Gran Porph TS91133	Fg Incl. TS91139	A Gran Porph Ave(3)	Range	Fg A Gran Ave(2)	A Gran. (1) Ave(28)	Range	A Gran. (2) Ave(2)
SiO2	77.30	76.00	64.30	70.85	68.95 - 72.85	75.90	74.98	73.35 - 76.7	75.28
TiO2	0.14	0.14	0.60	0.48	0.3 - 0.68	0.10	0.23	0.17 - 0.37	0.22
Al2O3	11.64	11.49	16.16	13.15	12.43 - 13.67	11.95	11.85	10.9 - 12.51	11.60
Fe2O3	1.62	0.77	0.59	1.26	0.94 - 1.87	1.07	1.29	0.81 - 3.74	1.39
FeO	0.29	1.54	2.99	2.61	1.28 - 3.94	1.01	1.33	0 - 1.82	1.49
MnO	0.03	0.04	0.08	0.11	0.06 - 0.14	0.04	0.06	0.03 - 0.1	0.06
MgO	0.04	0.07	0.72	0.39	0.12 - 0.67	0.03	0.12	0.05 - 0.27	0.09
CaO	0.11	0.06	1.89	1.32	1.30 - 1.35	0.08	0.32	0.06 - 0.61	0.31
Na2O	4.31	4.41	5.91	4.48	4.02 - 4.73	4.48	4.36	3.99 - 4.75	4.47
K2O	4.31	4.39	5.89	4.23	3.83 - 4.87	4.44	4.49	4.17 - 4.71	4.52
P2O5	0.01	0.01	0.15	0.11	0.01 - 0.24	0.01	0.02	0.01 - 0.06	0.02
F	0.00	0.07	0.05	0.04	0.03 - 0.06	0.05	0.05	0.01 - 0.11	0.07
H2O+	0.29	0.69	0.21	0.60	0.45 - 0.87	0.33	0.42	0.2 - 0.71	0.50
H2O-	0.33	0.23	0.13	0.18	0.11 - 0.22	0.12	0.23	0.12 - 0.38	0.21
CO2	0.00	0.01	0.00	0.07	0.02 - 0.13	0.05	0.04	0 - 0.08	0.04
S	0.12	0.05	0.07	0.05	0.01 - 0.1	0.03	0.04	0.01 - 0.1	0.03
A.I.	1.01	1.04	1.00	0.91	0.82 - 0.96	1.02	1.02	0.96 - 1.07	1.06
Cu	1	1	17	5	3 – 9	3	4	0 - 11	7
Pb	13	16	0	8	4 - 13	6	8	0 - 16	20
Zn	59	174	73	89	41 - 118	121	112	10 - 172	152
Ni	0	0	0	1	0 - 3	1	0	0 - 2	0
Ga	28	30	26	26	20 - 30	29	27	24 - 31	28
Sc	0.4	0.6	7.4	6.4	5.3 - 8.5	0	1.6	1 - 3.2	1.3
Nb	23	51	13	19	17 - 23	22	24	16 - 29	32
Zr	165	1011	810	385	292 - 497	328	665	536 - 765	939
Y	37	101	65	59	50 - 66	30	63	30 - 102	92
Ce	37	131	111	117	109 - 130	51	147	64 - 283	230
U	3	7	2	2	1 - 4	3	4	1 - 5	5
Th	4	22	0	5	0 - 14	11	9	1 - 17	13
Sr	5	4	90	84	58 - 128	4	13	4 - 42	9
Rb	103	175	53	90	61 - 145	164	103	45 - 135	126
Ba	54	144	2025	637	535 - 702	82	514	246 - 833	474

Table C-3 Sheffield Lake Average and Unique Geochemical Data

	A Porph Ash-flow		Aphyric	FQA Ash-flow (1)		FQA Ash-flow (2)		FQ±A Ash-flow	
	Ave(3)	Range	Ash-flow	Ave(3)	Range	Ave(3)	Range	Ave(14)	Range
SiO2	75.99	75.65 - 76.43	75.75	75.03	74.6 - 75.8	75.22	74.35 - 75.95	74.67	73.7 - 76.05
TiO2	0.17	0.17 - 0.18	0.20	0.21	0.19 - 0.23	0.23	0.2 - 0.25	0.25	0.2 - 0.3
Al2O3	10.63	10.58 - 10.67	11.12	11.14	10.86 - 11.36	11.87	11.55 - 12.11	12.14	11.26 - 12.59
Fe2O3	2.18	2.04 - 2.31	2.98	1.98	1.68 - 2.3	1.66	1.42 - 1.86	1.68	0.42 - 3.06
FeO	1.38	1 - 1.76	0.39	1.18	1.13 - 1.22	1.10	0.88 - 1.36	1.09	0.27 - 1.78
MnO	0.05	0.04 - 0.06	0.04	0.05	0.04 - 0.06	0.06	0.05 - 0.07	0.07	0.03 - 0.1
MgO	0.06	0.04 - 0.08	0.07	0.09	0.06 - 0.12	0.09	0.08 - 0.1	0.20	0.01 - 0.66
CaO	0.11	0.1 - 0.13	0.07	0.19	0.18 - 0.21	0.19	0.1 - 0.3	0.21	0.08 - 0.52
Na2O	4.27	4.11 - 4.36	4.33	4.04	3.92 - 4.25	4.18	3.98 - 4.35	4.02	3.59 - 4.3
K2O	4.50	4.45 - 4.54	4.12	4.68	4.52 - 4.89	4.91	4.85 - 4.94	4.59	3.87 - 5.05
P2O5	0.01	0.01 - 0.02	0.01	0.02	0.01 - 0.03	0.01	0.01 - 0.01	0.02	0.01 - 0.06
F	0.05	0.04 - 0.06	0.01	0.04	0.04 - 0.05	0.04	0.03 - 0.04	0.02	0 - 0.04
H2O	0.53	0.49 - 0.59	0.46	0.71	0.49 - 1.07	0.58	0.46 - 0.77	0.75	0.18 - 1.06
H2O-	0.32	0.29 - 0.34	0.42	0.36	0.3 - 0.4	0.35	0.31 - 0.41	0.30	0.17 - 0.39
CO2	0.04	0.01 - 0.11	0.17	0.14	0.07 - 0.25	0.04	0 - 0.11	0.13	0 - 0.42
S	0.07	0.06 - 0.07	0.07	0.05	0.03 - 0.07	0.06	0.04 - 0.07	0.04	0 - 0.08
A.I.	1.12	1.09-1.14	1.04	1.05	1.05 - 1.06	1.03	1.01 - 1.04	0.95	0.83 - 1.01
Cu	9	8 - 9	4	8	4.5 - 12	5	5 - 6	7	4 - 15
Pb	21	14 - 33	17	32	6 - 62	24	16 - 30	6	0 - 16
Zn	213	201 - 228	111	155	116 - 200	120	89 - 136	87	24 - 133
Ni	2	1 - 2	1	2	1 - 3	1	0 - 1	1	0 - 4
Ga	32	31 - 33	31	32	30 - 35	29	28 - 30	26	18 - 31
Sc	0.1	0.1 - 0.1	0.4	0.6	0.4 - 0.9	0.8	0.6 - 1	2.8	1 - 7.5
Nb	62	52 - 67	51	50	39 - 66	33	33 - 33	22	9 - 31
Zr	1477	1251 - 1642	1141	1099	906 - 1466	706	664 - 745	465	382 - 562
Y	165	148 - 178	125	123	80 - 175	85	73 - 93	56	26 - 81
Ce	244	223 - 276	160	240	169 - 337	189	183 - 196	156	112 - 208
U	11	9 - 12	7	8	6 - 10	5	4 - 5	3	2 - 4
Th	21	20 - 23	19	20	8 - 27	9	5 - 13	6	1 - 12
Sr	4	4 - 5	9	8	5 – 10	9	4 - 13	23	8 - 65
Rb	203	193 - 216	152	159	126 - 198	123	113 - 143	89	75 - 102
Ba	14	12 - 16	37	59	49 - 79	91	66 - 134	393	118 - 1013

Table C-4 Cape St. John Area Average and Unique Geochemical Data

	Low-Zr Aphyric Ash-flow Ave(11)	Range	Cape Brule QF Porph Ave(12)	Range	CJ90008 Fg Gran	CJ90027 QF Porph	CJ90012 QF Porph	CJ90039 Q Flow	CJ90035 QF-Poor	CJ90024 QF-Poor
SiO2	74.99	69.05 - 80.23	74.07	70.65 - 76.7	75.65	63.2	76.7	78.6	79.55	70.55
TiO2	0.20	0.08 - 0.37	0.26	0.09 - 0.6	0.28	0.61	0.1	0.11	0.1	0.34
Al2O3	12.32	10.19 - 14.27	12.27	11.87 - 12.83	12.41	13.28	11.95	11.17	10.55	13.46
Fe2O3	1.06	0.16 - 2.09	1.21	0.03 - 2.13	0.5	2.34	0.83	1.21	1.32	2.46
FeO	0.98	0 - 1.89	1.26	0.00 - 2.17	1.52	2.64	0.67	0.87	0.47	0.23
MnO	0.04	0.01 - 0.06	0.05	0.02 - 0.07	0.05	0.12	0.01	0.02	0.02	0.05
MgO	0.20	0.07 - 0.38	0.45	0.17 - 1.06	0.26	1.18	0.21	0.05	0.03	0.41
CaO	0.64	0.06 - 1.71	1.06	0.49 - 2.38	0.43	4.84	0.26	0.09	0.41	2.07
Na2O	3.10	2.19 - 4.13	3.07	2.67 - 3.57	3.6	1.99	1.22	4.06	3.67	2.32
K2O	4.88	3.32 - 6.39	4.60	3.47 - 5.19	4.53	3.85	6.17	2.96	3.52	5.15
P2O5	0.04	0 - 0.1	0.05	0.01 - 0.14	0.04	0.13	0.02	0.01	0.01	0.09
F	0.03	0.01 - 0.06	0.02	0.01 - 0.04	0.02	0.03	0.03	0.01	0.01	0.04
H2O+	0.74	0.07 - 1.26	0.60	0.23 - 1.43	0.68	1.86	1.21	0.54	0	2.05
H2O-	0.22	0.12 - 0.37	0.24	0.15 - 0.45	0.22	0.22	0.11	0.25	0.17	0.23
CO2	0.40	0.04 - 1.32	0.45	0.00 - 1.04	0.35	3.53	0.33	0.09	0.38	1.6
S	0.05	0 - 0.44	0.00	0 - 0	0.00	0.00	0.00	0.00	0.00	0.00
A.I.	0.84	0.72 - 0.94	0.82	0.69 - 0.89	0.87	0.56	0.73	0.88	0.93	0.70
Cu	6	1 - 12	6	3 - 12	12	7	14	5	12	2
Pb	11	5 - 21	12	1 - 37	42	7	29	13	26	18
Zn	41	23 - 68	61	29 - 109	69	120	124	44	34	52
Ni	3	1 - 6	10	3 - 25	5	6	6	3	3	3
Ga	16	10 - 24	18	15 - 20	20	22	29	18	14	19
Sc	5.0	2.1 - 8.6	7.8	6 - 11.7	2.3	12.2	1.2	0.8	1	7.1
Nb	23	17 - 33	17	13 - 31	21	14	33	31	28	20
Zr	256	132 - 461	280	112 - 412	362	388	305	316	285	359
Y	43	17 - 62	50	37 - 78	52	34	73	62	58	42
Ce	90	23 - 114	167	49 - 205	124	178	142	109	127	95
U	4	4 - 5	3	2 - 6	3	2	4	4	4	5
Th	17	13 - 20	15	8 - 22	25	14	29	17	17	14
Sr	66	31 - 162	82	30 - 158	43	171	50	74	109	134
Rb	151	100 - 215	104	65 - 170	115	80	200	70	90	105
Ba	603	111 - 1065	1077	90 - 1823	343	1743	204	149	148	863

Table C-4

	High Al Aphyric Ave(2)	CJ90005 QF Porph	High Zr Aphyic Ash-flow Ave(3)	Range	Seal Is. Bight P Granite Ave(3)	Range
SiO2	69.95	76.85	76.07	74.6 - 77.6	74.65	74.45 - 75.05
TiO2	0.29	0.14	0.16	0.14 - 0.21	0.22	0.21 - 0.23
Al2O3	14.84	11.56	11.75	11.32 - 11.97	12.45	12.03 - 12.76
Fe2O3	2.14	0.97	1.62	1.44 - 1.77	1.74	1.4 - 1.99
FeO	1.00	1.1	0.86	0.69 - 0.96	1.00	0.7 - 1.43
MnO	0.04	0.04	0.04	0.03 - 0.04	0.06	0.05 - 0.07
MgO	0.19	0.02	0.12	0.11 - 0.13	0.02	0.02 - 0.02
CaO	0.53	0.02	0.34	0.09 - 0.82	0.12	0.04 - 0.26
Na2O	4.27	3.53	3.69	3.24 - 4.22	4.87	4.68 - 5.03
K2O	4.19	4.67	4.28	3.43 - 5.03	4.11	3.97 - 4.29
P2O5	0.05	0.01	0.03	0.01 - 0.05	0.01	0.01 - 0.01
F	0.02	0.01	0.01	0.01 - 0.02	0.01	0.01 - 0.02
H2O+	1.52	0.26	0.30	0.04 - 0.66	0.29	0.25 - 0.35
H2O-	0.25	0.2	0.34	0.19 - 0.46	0.23	0.21 - 0.26
CO2	0.55	0.06	0.33	0.13 - 0.7	0.12	0.09 - 0.15
S	0.21	0.00	0.00	0 - 0	0.00	0 - 0
A.I.	0.78	0.94	0.91	0.89 - 0.95	1.00	0.96 - 1.04
Cu	7	12	11	11 - 11	2	1 - 3
Pb	22	98	12	10 - 14	14	13 - 16
Zn	74	89	55	24 - 85	113	86 - 144
Ni	2	8	3	1 - 4	3	1 - 5
Ga	24	25	21	19 - 22	28	27 - 29
Sc	8.5	0.6	1.9	0.5 - 3.3	1.3	1.2 - 1.4
Nb	27	35	33	25 - 40	37	35 - 40
Zr	614	637	607	529 - 648	631	576 - 692
Y	37	80	70	61 - 79	39	32 - 45
Ce	137	157	146	142 - 150	75	54 - 95
U	9	5	3	2 - 4	3	2 - 3
Th	17	25	17	15 - 18	18	14 - 21
Sr	56	24	39	38 - 40	7	5 - 8
Rb	130	120	112	85 - 145	107	105 - 110
Ba	826	140	421	102 - 739	565	412 - 684

Table C-6 Kings Point Complex Unique and Average Geochemical Data

	A porph Ash-flow (6AAf)		A porph Ash-flow Red spot		A porph Flow red spot		Aphyric Ash-flow (U6A)		Aphyric Ash-flow Fg A RS	
	Ave (4)	Range	Ave (13)	Range (6AAf)	Ave (10)	Range (6AAf)	Ave (11)	Range	Ave (11)	Range (6A)
SiO2	75.72	75.38 - 76.46	75.61	73.9 - 76.85	75.67	74.8 - 76.7	76.05	75.15 - 78.25	75.52	74.8 - 76.35
TiO2	0.18	0.16 - 0.18	0.18	0.17 - 0.19	0.18	0.17 - 0.19	0.18	0.17 - 0.19	0.18	0.17 - 0.19
Al2O3	10.68	10.42 - 10.9	10.57	10.18 - 10.77	10.61	10.47 - 10.76	10.50	9.71 - 10.72	10.56	10.35 - 10.89
Fe2O3	2.28	1.95 - 2.52	2.31	1.02 - 3.41	1.75	0.57 - 2.6	2.52	1.65 - 3.17	2.07	1.44 - 2.94
FeO	1.30	0.91 - 1.77	1.49	0.35 - 2.88	1.98	1.15 - 3.05	0.92	0.28 - 1.44	1.56	0.79 - 2.32
MnO	0.05	0.04 - 0.06	0.05	0.03 - 0.06	0.06	0.05 - 0.06	0.04	0.02 - 0.06	0.06	0.03 - 0.07
MgO	0.06	0.01 - 0.13	0.07	0.03 - 0.21	0.06	0.01 - 0.15	0.08	0.01 - 0.32	0.04	0.01 - 0.09
CaO	0.13	0.06 - 0.23	0.23	0.08 - 0.91	0.13	0.05 - 0.24	0.29	0.08 - 0.56	0.17	0.04 - 0.32
Na2O	4.17	3.84 - 4.39	4.08	3.54 - 4.45	4.30	4.11 - 4.46	3.73	2.05 - 4.96	4.24	3.74 - 4.6
K2O	4.46	4.4 - 4.48	4.20	3.28 - 4.57	4.45	4.19 - 4.57	4.25	2.4 - 5.16	4.25	3.29 - 4.62
P2O5	0.01	0 - 0.01	0.01	0 - 0.01	0.01	0.01	0.01	0 - 0.02	0.01	0.01 - 0.01
F	0.04	0.03 - 0.05	0.04	0.01 - 0.07	0.05	0.02 - 0.08	0.03	0 - 0.08	0.05	0 - 0.11
H2O+	0.44	0.44 - 0.44	0.28	0.15 - 0.43	0.36	0.21 - 0.46	0.55	0.24 - 0.98	0.30	0.19 - 0.47
H2O-	0.27	0.27 - 0.27	0.17	0.13 - 0.22	0.20	0.13 - 0.38	0.22	0.17 - 0.26	0.15	0.13 - 0.19
CO2	0.08	0.08 - 0.08	0.08	0.04 - 0.16	0.07	0.01 - 0.19	0.21	0.02 - 0.54	0.06	0.03 - 0.13
S	0.02	0.02 - 0.02	0.02	0.005 - 0.03	0.01	0 - 0.05	0.01	0 - 0.03	0.02	0 - 0.07
A.I.	1.09		1.07		1.12		1.02		1.10	
Cu	13	7 - 21	16	3 - 44	15	3 - 25	11	3 - 22	16	7 - 32
Pb	28	22 - 37	27	0 - 46	30	11 - 45	22	5 - 40	24	9 - 40
Zn	233	205 - 267	210	115 - 293	236	216 - 264	179	22 - 248	235	179 - 340
Ni	1	0 - 2	2	0 - 6	3	0 - 8	1	0 - 6	1	0 - 5
Sc	0.3	0.1 - 0.8	0.1	0 - 0.3	0.2	0.1 - 0.3	0.2	< 0.1 - 0.8	0.1	< 0.1 - 0.3
Ga	35	33 - 36	34	32 - 36	34	33 - 34	33	26 - 37	33	31 - 35
Nb	64	57 - 72	67	61 - 77	63	55 - 72	64	42 - 75	65	49 - 75
Zr	1420	1188 - 1589	1522	1353 - 1587	1557	1481 - 1608	1434	1237 - 1578	1503	1242 - 1611
Y	159	118 - 201	161	122 - 184	162	96 - 212	167	128 - 207	166	129 - 216
Ce	237	193 - 290	241	164 - 265	230	154 - 288	245	186 - 284	251	187 - 319
U	9	7 - 11	10	9 - 12	11	9 - 12	10	4 - 11	9	6 - 14
Th	30	26 - 35	30	20 - 43	26	18 - 33	29	17 - 43	26	13 - 35
Sr	7	3 - 11	8	3 - 16	6	2 - 19	16	4 - 37	11	2 - 28
Rb	190	171 - 215	175	94 - 216	202	160 - 219	168	100 - 205	184	115 - 220
Ba	17	7 - 30	23	6 - 54	12	8 - 19	41	15 - 139	22	7 - 45

Table C-6

	Aphyric flow (red?)		QF Ash flow/porph		Aphyric Ash-flow (Red)		Aphyric flow breccia		F porphyritic syenite	
	Ave (6)	Range (U6A)	Ave (9)	Range (U6P)	Ave(6)	Range (U7A)	Ave(7)	Range (U7A)	Ave(23)	Range (U3)
SiO2	76.43	75.7 - 77.1	76.29	74.89 - 78.65	76.94	75.85 - 78.05	76.83	69.66 - 82.25	66.91	65.65 - 68.55
TiO2	0.17	0.14 - 0.19	0.18	0.16 - 0.19	0.16	0.12 - 0.21	0.24	0.11 - 0.71	0.89	0.8 - 1.13
Al2O3	10.73	10.41 - 11.31	10.63	10.36 - 10.91	11.68	11.02 - 13.44	11.24	8.71 - 12.66	13.07	12.6 - 13.8
Fe2O3	2.30	1.65 - 3.14	2.05	1.12 - 2.61	1.35	0.45 - 2.15	1.48	0.43 - 3.27	3.24	1.72 - 5.82
FeO	1.18	0.55 - 1.97	1.44	0.88 - 2.98	0.52	0 - 1.04	0.78	0 - 1.9	2.36	0 - 4
MnO	0.04	0.01 - 0.06	0.04	0.01 - 0.07	0.03	0.01 - 0.05	0.05	0.02 - 0.13	0.12	0.09 - 0.15
MgO	0.06	0.02 - 0.18	0.06	0.01 - 0.15	0.12	0.03 - 0.24	0.28	0.02 - 0.76	0.91	0.11 - 1.58
CaO	0.15	0.03 - 0.32	0.18	0.01 - 0.41	0.16	0.02 - 0.31	0.52	0.04 - 2.02	1.88	1.12 - 2.5
Na2O	3.79	3.12 - 4.38	3.11	0.05 - 4.05	2.13	1.05 - 4.33	3.69	3.05 - 4.51	4.54	3.9 - 5.28
K2O	4.41	3.9 - 5.18	4.38	3.65 - 4.88	5.24	3.66 - 6.99	3.44	2.02 - 4.44	3.88	3.26 - 4.87
P2O5	0.02	0.01 - 0.03	0.01	0 - 0.02	0.02	0.01 - 0.03	0.06	0.01 - 0.22	0.25	0.21 - 0.29
F	0.05	0 - 0.19	0.02	0 - 0.05	0.03	0.01 - 0.07	0.02	0 - 0.06	0.07	0.04 - 0.15
H2O+	0.34	0.1 - 0.67	0.81	0.34 - 1.78	0.55	0.33 - 0.95	0.53	0.05 - 0.81	1.01	0.7 - 1.8
H2O-	0.31	0.16 - 0.48	0.17	0.15 - 0.21	0.19	0.15 - 0.26	0.26	0.13 - 0.43	0.39	0.24 - 0.58
CO2	0.08	0.01 - 0.16	0.13	0.04 - 0.29	0.11	0.03 - 0.19	0.15	0.03 - 0.52	0.47	0 - 1.36
S	0.01	0 - 0.01	0.11	0 - 0.42	0.21	0.05 - 0.61	0.05	0 - 0.3	0.01	0 - 0.03
A.I.	1.03		0.93		0.79		0.87		0.89	
Cu	10	4 - 26	17	6 - 57	9	4 - 17	6	1 - 16	8	2 - 26
Pb	22	3 - 40	35	0 - 93	22	0 - 41	5	0 - 13	8	0 - 20
Zn	144	50 - 234	188	84 - 285	52	26 - 103	49	20 - 94	121	74 - 175
Ni	2	0 - 6	2	0 - 4	1	0 - 2	6	3 - 9	4	0 - 9
Sc	0.5	0.1 - 0.7	0.2	0.1 - 0.5	3.7	2.7 - 6.1	4.7	2.1 - 14.3	9.0	7.4 - 11.7
Ga	32	29 - 35	31	26 - 35	19	16 - 23	19	9 - 25	29	21 - 33
Nb	55	23 - 71	58	35 - 65	16	10 - 19	15	4 - 21	25	11 - 29
Zr	1344	835 - 1600	1324	1095 - 1549	352	213 - 434	317	98 - 456	524	309 - 606
Y	145	89 - 182	149	104 - 176	48	21 - 68	45	12 - 69	66	49 - 76
Ce	242	154 - 329	233	153 - 278	129	69 - 214	86	42 - 124	128	93 - 145
U	11	9 - 12	8	6 - 10	6	4 - 9	5	4 - 8	4	3 - 5
Th	29	26 - 31	25	13 - 30	13	5 - 25	15	10 - 21	9	5 - 17
Sr	16	4 - 46	12	8 - 17	35	11 - 63	59	18 - 156	123	85 - 202
Rb	210	150 - 330	163	115 - 193	158	97 - 227	91	55 - 140	80	55 - 115
Ba	28	12 - 47	47	12 - 222	606	411 - 820	587	223 - 1143	426	293 - 685

Table C-6

	Q Syenite - Granite		Fg-Mg granite		Pheno poor porph		QF±A Porph Granite		QF Porph (1)	
	Ave (5)	Range (U4)	Ave (13)	Range (U4)	Ave (5)	Range (U7P)	Ave (15)	Range (U7P)	Ave (29)	Range (U7P)
SiO2	73.90	71.05 - 75.1	74.83	72.7 - 77.1	77.37	75.5 - 79.4	75.61	74.19 - 76.85	74.91	69.3 - 80.33
TiO2	0.27	0.18 - 0.46	0.24	0.1 - 0.36	0.17	0.11 - 0.21	0.21	0.07 - 0.27	0.24	0.11 - 0.51
Al2O3	12.15	11.64 - 12.69	12.86	11.67 - 13.45	10.94	10.19 - 11.68	11.50	10.9 - 12.25	11.75	8.81 - 13.16
Fe2O3	2.15	0.78 - 4.46	0.68	0.06 - 1.6	1.91	0.52 - 3.25	1.54	0.84 - 2.31	1.74	0.62 - 3.02
FeO	0.82	0 - 1.38	0.89	0 - 1.38	0.75	0 - 1.83	1.24	0.46 - 1.91	1.13	0 - 3.28
MnO	0.05	0.04 - 0.07	0.03	0.02 - 0.04	0.04	0.01 - 0.08	0.05	0.01 - 0.11	0.05	0.01 - 0.17
MgO	0.22	0.05 - 0.43	0.27	0.07 - 0.49	0.17	0.02 - 0.39	0.09	0.02 - 0.39	0.14	0.01 - 0.79
CaO	0.47	0.26 - 1.15	0.55	0.24 - 0.97	0.11	0.04 - 0.27	0.17	0.03 - 0.38	0.29	0.03 - 1.07
Na2O	4.03	3.69 - 4.36	3.82	2.57 - 4.19	3.68	2.96 - 4.96	3.89	3.41 - 4.35	3.58	0.24 - 5.2
K2O	4.69	4.34 - 5.02	4.71	3.9 - 5.29	3.69	1.65 - 5.41	4.38	3.18 - 5.17	4.93	3.64 - 7.48
P2O5	0.04	0.02 - 0.08	0.04	0.01 - 0.11	0.02	0.01 - 0.03	0.02	0.01 - 0.03	0.03	0 - 0.1
F	0.02	0.01 - 0.03	0.03	0.01 - 0.11	0.03	0 - 0.12	0.01	0 - 0.03	0.02	0 - 0.04
H2O+	0.63	0.46 - 0.8	0.68	0.46 - 1.04	0.52	0.08 - 1.04	0.53	0.3 - 0.95	0.63	0.32 - 1.35
H2O-	0.29	0.16 - 0.45	0.34	0.17 - 0.57	0.21	0.13 - 0.3	0.23	0.13 - 0.34	0.27	0.12 - 0.56
CO2	0.26	0.04 - 0.67	0.11	0.02 - 0.42	0.08	0.04 - 0.11	0.10	0.02 - 0.25	0.15	0 - 0.46
S	0.01	0 - 0.02	0.01	0 - 0.06	0.16	0 - 0.47	0.01	0 - 0.04	0.03	0 - 0.39
A.I.	0.96		0.89		0.92		0.97		0.96	
Cu	9	3 - 19	7	2 - 24	16	6 - 24	9	4 - 19	7	3 - 50
Pb	9	0 - 16	10	0 - 19	8	0 - 23	12	0 - 46	10	0 - 42
Zn	94	57 - 138	29	11 - 62	69	44 - 123	93	11 - 183	89	13 - 141
Ni	3	1 - 7	3	1 - 8	6	2 - 10	4	0 - 9	3	0 - 8
Sc	2.0	0.9 - 4.1	3.2	1.8 - 7.9	1.2	0.4 - 2.6	0.9	0.3 - 2.9	1.5	0.5 - 5.1
Ga	26	22 - 29	17	9 - 21	25	23 - 32	28	24 - 32	27	15 - 32
Nb	26	18 - 32	12	6 - 27	30	22 - 37	32	22 - 45	28	21 - 37
Zr	489	349 - 632	189	107 - 247	640	582 - 721	612	363 - 790	522	376 - 642
Y	59	40 - 74	28	14 - 52	76	55 - 86	67	52 - 108	67	39 - 165
Ce	144	106 - 181	71	56 - 84	132	13 - 206	152	73 - 215	150	53 - 223
U	4	3 - 7	5	2 - 7	7	4 - 12	5	3 - 13	4	2 - 12
Th	12	8 - 16	20	14 - 26	17	9 - 31	13	5 - 42	12	7 - 42
Sr	27	9 - 60	69	24 - 122	17	5 - 25	14	5 - 27	26	11 - 77
Rb	104	55 - 162	154	95 - 196	93	30 - 118	103	65 - 185	104	55 - 260
Ba	301	114 - 612	473	292 - 834	227	71 - 443	106	42 - 227	272	21 - 805

Table C-6

	QF Porph (2)		QF Porph (3)		QFA Porphyry		QFA Porph (2)		QF A-F	
	Ave(11)	Range (U7P?)	Ave (11)	Range (U6P)	Ave (10)	Range (U7P)	Ave (9)	Range (U6P)	Ave (4)	Range (U5)
SiO2	76.33	74 - 78.2	76.39	75.4 - 77.4	74.23	71.8 - 75.58	76.09	75.4 - 76.6	77.63	76.5 - 78.27
TiO2	0.21	0.13 - 0.36	0.18	0.16 - 0.19	0.24	0.21 - 0.31	0.19	0.18 - 0.2	0.08	0.07 - 0.09
Al2O3	11.29	10.79 - 12.26	10.82	10.47 - 11.15	12.04	11.62 - 12.96	10.81	10.46 - 11.18	12.16	11.75 - 12.83
Fe2O3	1.62	0.05 - 2.18	1.62	0.13 - 3.58	1.68	0.73 - 2.29	1.71	0.88 - 2.73	0.94	0.56 - 1.49
FeO	1.23	0.58 - 2.31	1.66	0 - 3.19	1.33	0.57 - 1.87	1.51	0.76 - 2.14	0.35	0 - 0.9
MnO	0.04	0.02 - 0.06	0.04	0.01 - 0.07	0.06	0.03 - 0.07	0.04	0.03 - 0.05	0.02	0.01 - 0.03
MgO	0.11	0.02 - 0.49	0.06	0.02 - 0.19	0.07	0.02 - 0.18	0.04	0.01 - 0.12	0.29	0.14 - 0.41
CaO	0.35	0.01 - 0.98	0.29	0.08 - 0.85	0.27	0.03 - 0.65	0.14	0.01 - 0.45	0.33	0.26 - 0.5
Na2O	3.98	3.43 - 4.61	3.46	2.93 - 4.03	3.96	2.78 - 4.33	3.84	3.32 - 4.16	2.65	1.85 - 4.25
K2O	3.83	2.14 - 4.85	4.37	3.73 - 5.26	4.91	4.25 - 5.41	4.46	4.39 - 4.56	4.12	3.25 - 4.99
P2O5	0.02	0.01 - 0.12	0.02	0.01 - 0.04	0.02	0.01 - 0.03	0.01	0 - 0.01	0.01	0 - 0.01
F	0.03	0 - 0.08	0.02	0 - 0.05	0.02	0 - 0.04	0.03	0 - 0.05	0.04	0.01 - 0.1
H2O+	0.54	0.10 - 1.07	0.52	0.14 - 0.98	0.44	0.26 - 0.67	0.40	0.25 - 0.61	0.83	0.76 - 0.89
H2O-	0.28	0.15 - 0.52	0.31	0.13 - 0.51	0.23	0.17 - 0.31	0.22	0.15 - 0.33	0.20	0.15 - 0.24
CO2	0.25	0.05 - 0.65	0.29	0 - 0.76	0.07	0.03 - 0.13	0.10	0.03 - 0.3	0.22	0.04 - 0.39
S	0.02	0 - 0.13	0.02	0 - 0.15	0.04	0.01 - 0.08	0.01	0 - 0.03	0.02	0 - 0.03
A.I.	0.95		0.96		0.98		1.03	1.03	0.73	
Cu	13	5 - 37	12	4 - 28	17	4 - 111	11	5 - 19	18	3 - 48.5
Pb	10	0 - 49	18	4 - 52	11	3 - 20	17	0 - 35	6	0 - 14
Zn	93	13 - 198	199	111 - 387	114	62 - 159	184	118 - 244	36	16 - 54
Ni	3	1 - 6	3	0 - 9	1	-1 - 3	1	0 - 5	7	0 - 16
Sc	1.0	0.4 - 3.8	0.2	0 - 0.4	1.5	0.7 - 5.5	0.3	0.1 - 0.5	8.4	7.5 - 9.9
Ga	29	23 - 35	31	27 - 35	29	18 - 32	32	30 - 34	21	17 - 23
Nb	35	28 - 42	51	40 - 59	29	11 - 37	53	38 - 65	28	24 - 32
Zr	821	682 - 973	1233	1045 - 1397	560	407 - 669	1187	863 - 1502	121	113 - 126
Y	96	76 - 118	142	101 - 156	66	34 - 108	115	57 - 166	51	40 - 72
Ce	191	98 - 227	243	193 - 269	176	78 - 261	191	123 - 268	59	55 - 64
U	6	5 - 10	8	6 - 11	4	3 - 4	8	5 - 12	5	3 - 9
Th	18	12 - 25	27	14 - 66	9	0 - 15	17	4 - 29	19	14 - 24
Sr	34	10 - 172	14	6 - 22	18	7 - 52	9	3 - 24	42	30 - 50
Rb	100	50 - 185	155	125 - 205	102	80 - 120	161	120 - 209	155	99 - 219
Ba	135	52 - 388	60	16 - 252	213	80 - 893	30	12 - 62	124	69 - 198

Table C-6

	F porph	QF-poor Ash Flow	Porph A-F (U6P) Ave (8)	Range	A A-F/Porph (U6AAf) Ave (5)	Range
SiO2	72.75	70.30	75.60	72.35 - 78.22	75.29	73.95 - 76.18
TiO2	0.49	0.58	0.24	0.13 - 0.5	0.18	0.17 - 0.18
Al2O3	12.27	12.22	11.24	10.39 - 11.85	10.54	10.4 - 10.71
Fe2O3	2.40	2.97	1.95	1.35 - 2.47	2.19	1.16 - 3.25
FeO	1.96	1.75	1.16	0.27 - 2.01	1.44	0.69 - 2.44
MnO	0.10	0.11	0.04	0.01 - 0.09	0.07	0.04 - 0.12
MgO	0.40	0.57	0.19	0.03 - 0.55	0.13	0.02 - 0.46
CaO	0.83	1.28	0.32	0.01 - 0.90	0.55	0.1 - 1.96
Na2O	4.55	4.48	4.00	2.61 - 5.82	3.86	2.85 - 4.33
K2O	3.26	3.90	3.95	1.01 - 5.73	4.35	3.58 - 4.86
P2O5	0.15	0.20	0.03	0 - 0.11	0.01	0 - 0.01
F	0.03	0.07	0.03	0 - 0.06	0.03	0.01 - 0.06
H2O+	0.63	0.31	0.67	0.53 - 0.86	0.48	0.36 - 0.63
H2O-	0.29	0.25	0.38	0.28 - 0.51	0.26	0.19 - 0.37
CO2	0.05	0.04	0.14	0.05 - 0.2	0.54	0.05 - 1.44
S	0.01	0.05	0.02	0.01 - 0.03	0.01	0 - 0.02
A.I.	0.90	0.95	0.97		1.05	
Cu	3	5	9	5 - 18	13	4 - 27
Pb	2	13	22	7 - 56	25	17 - 38
Zn	48	89	95	21 - 218	208	192 - 227
Ni	1	1	2	-1 - 8	2	-1 - 5
Sc	13.2	10.8	1.5	0.2 - 5	0.2	0.1 - 0.2
Ga	20	24	27	23 - 34	33	30 - 35
Nb	22	22	42	35 - 56	63	54 - 69
Zr	530	549	879	797 - 1022	1461	1333 - 1564
Y	77	75	102	66 - 138	151	107 - 169
Ce	131	124	170	86 - 224	223	188 - 252
U	5	4	8	6 - 11	10	8 - 11
Th	13	5	26	14 - 35	26	16 - 36
Sr	61	65	31	6 - 89	10	2 - 22
Rb	70	109	116	23 - 167	175	135 - 202
Ba	990	798	126	32 - 260	24	12 - 34

Table C-6

	F-poor Porph	Mafic dyke	Fluorite Breccia	Q porph	QF porph Granite	QFA intr?	Peg-aplite Vein
SiO2	44.00	44.40	46.37	59.80	68.84	71.19	85.20
TiO2	2.70	2.40	0.57	0.89	0.63	0.44	0.08
Al2O3	16.67	16.24	8.08	16.55	13.26	14.29	6.60
Fe2O3	3.85	3.21	2.66	1.86	3.17	0.89	0.73
FeO	8.91	7.76	0.47	3.51	1.63	1.73	0.58
MnO	0.20	0.22	0.09	0.10	0.11	0.04	0.02
MgO	6.44	7.15	1.48	2.48	0.54	0.91	0.09
CaO	9.07	9.04	21.50	4.07	0.85	1.98	0.02
Na2O	2.87	2.06	1.21	4.65	4.28	3.53	0.72
K2O	0.95	1.29	3.97	2.41	4.48	3.38	4.00
P2O5	0.53	0.34	0.10	0.30	0.14	0.14	0.01
F	0.12	0.03	0.44	0.04	0.03	0.04	0.01
H2O+	3.21	4.41		2.07	1.00		0.65
H2O-	0.66	0.23		0.23	0.53		0.19
CO2	0.02	1.35		0.93	0.11		0.34
S	0.15	0.06		0.01	0.00		0.03
A.I.	0.34	0.29	0.78	0.62	0.90	0.66	0.84
Cu	45	49	19	28	6	23	5
Pb	0	0	13	0	0	30	45
Zn	164	95	111	73	107	31	54
Ni	116	85	31	12	1	15	5
Sc	31.5	27.8	7.6	13.9	6.3	4	2.7
Ga	26	31	18	20	29	19	14
Nb	1	11	14	7	23	9	16
Zr	178	165	429	170	328	140	241
Y	31	24	43	22	51	12	25
Ce	44	35	87	77	121	45	50
U	0	0	4	2	3	1	48
Th	0	0	11	3	4	9	12
Sr	336	407	465	485	95	420	29
Rb	35	30	130	40	75	90	120
Ba	290	162	527	1034	436	564	499

Table C-7 Mooring Cove Formation Average & Unique Geochemical Data

Field No.	Aphyric Ash-flow Ave (16)	Range	Trachyte Ave (3)	Felsic Dyke Ave (3)	Aphyric Ash Flow	Aphyric Ash Flow - NP	Aphyric Flow	Q Ash Flow	Mafic Flow
SiO2	77.06	74.55 - 83.54	66.28	75.28	84.62	75.57	72.99	78.10	54.65
TiO2	0.22	0.17 - 0.31	0.26	0.15	0.47	0.27	0.28	0.18	0.92
Al2O3	11.63	8.58 - 15.29	16.54	11.62	10.45	12.06	11.62	10.75	17.66
Fe2O3	2.11	0.03 - 4.16	2.08	2.60	0.01	1.51	1.46	2.17	4.80
FeO	0.50	0 - 1.12	2.61	1.57	0.23	0.75	1.93	0.80	5.08
MnO	0.05	0 - 0.14	0.10	0.07	0.00	0.04	0.12	0.06	0.29
MgO	0.04	0 - 0.1	0.31	0.08	0.02	0.10	0.40	0.14	3.92
CaO	0.10	0 - 0.51	0.10	0.07	0.03	0.05	1.89	0.29	3.70
Na2O	2.00	0.04 - 4.4	5.70	5.10	0.06	1.65	3.51	2.21	3.43
K2O	4.53	2.84 - 5.59	4.67	1.94	0.27	5.71	2.17	4.88	2.06
P2O5	0.01	0 - 0.02	0.03	0.01	0.06	0.02	0.05	0.01	0.25
F	0.01	0 - 0.04	0.07	0.04	0.02	0.01	0.03	0.02	0.08
H2O+	0.17	0.11 - 0.28	1.59	0.87	2.03	1.07	1.24	0.51	3.24
H2O-	0.19	0.12 - 0.28	0.26	0.24				0.14	0.28
CO2	0.10	0.05 - 0.26	0.07	0.08	0.04	0.03	1.41	0.17	0.06
S	0.00	0 - 0	0.10	0.07	0.03	0.06	0.05	0.00	0.02
A.I.	0.70		0.87	0.90	0.04	0.74	0.70	0.83	0.45
Cu	9	4 - 20	10	13	7	11	13	14	7
Pb	10	0 - 21	2	12	79	94	12	25	3
Zn	85	6 - 204	213	206	12	66	128	116	228
Ni	2	0 - 6	5	3	0	1	4	1	4
Sc	0.5	< 0.1 - 2	2	0.1	3.7	3.4	2.6	0.1	17.4
Ga	31	13 - 40	47	41	42	19	33	29	24
Nb	49	28 - 74	273	476	97	18	48	41	6
Zr	958	719 - 1324	1601	2825	1856	242	937	938	153
Y	125	69 - 172	143	265	120	33	118	120	28
Ce	152	65 - 288	598	582	266	105	269	200	41
U	4	3 - 6	8	16	8	4	3	3	1
Th	20	16 - 29	44	73	40	26	21	19	0
Sr	13	4 - 34	43	21	28	57	318	42	230
Rb	128	< 5 - 195	129	48	10	215	87	105	90
Ba	59	12 - 201	86	24	18	420	90	67	342

Table C-8 Cross Hills Complex Average and Unique Geochemical Data

Field No.	Aplite Ave(3)	Range	Fg Normal granite Ave(3)	Range	MC90035 Fg Normal	MC92029 Fg Normal	Mg Normal Granite Ave(8)	Range
SiO2	75.57	75.15 - 76	77.51	77.33 - 77.65	77.10	78.41	76.95	74.6 - 78.05
TiO2	0.21	0.2 - 0.22	0.12	0.12 - 0.13	0.16	0.13	0.15	0.11 - 0.2
Al2O3	12.48	12.19 - 12.68	10.92	10.75 - 11.02	11.81	9.99	11.49	10.99 - 12.61
Fe2O3	1.00	0.48 - 1.37	1.89	1.47 - 2.52	1.30	2.48	1.94	1.33 - 2.74
FeO	0.77	0.56 - 1.07	0.73	0.29 - 1.23	0.30	0.18	0.37	0.19 - 0.8
MnO	0.04	0.03 - 0.05	0.06	0.03 - 0.09	0.02	0.05	0.03	0.02 - 0.05
MgO	0.17	0.16 - 0.18	0.03	0.02 - 0.05	0.05	0.05	0.08	0.03 - 0.15
CaO	0.29	0.1 - 0.39	0.06	0.02 - 0.1	0.02	0.22	0.07	0.01 - 0.17
Na2O	3.93	3.68 - 4.39	3.56	3.35 - 3.70	3.75	3.92	3.74	3.5 - 4.06
K2O	4.78	4.24 - 5.06	4.44	4.375 - 4.56	4.89	2.94	4.62	4.07 - 5.39
P2O5	0.02	0.02 - 0.03	0.01	0.01 - 0.01	0.01	0.00	0.01	0 - 0.02
F	0.01	0.01 - 0.02	0.00	0 - 0.01	0.00	0.00	0.01	0 - 0.01
H2O+	0.35	0.31 - 0.39	0.29	0.26 - 0.31	0.29		0.40	0.24 - 0.52
H2O-	0.20	0.12 - 0.25	0.19	0.12 - 0.28	0.13		0.23	0.2 - 0.3
CO2	0.07	0.03 - 0.11	0.07	0.05 - 0.085	0.05		0.07	0.04 - 0.1
S	0.00	0 - 0.01	0.01	0 - 0.015	0.01		0.00	0 - 0.01
A.I.	0.93	0.91 - 0.95	0.98	0.95 - 0.99	0.97	0.96	0.97	0.94 - 1.01
Cu	10	6 - 15	13	11 - 15	6	15	16	4 - 30
Pb	12	7 - 18	10	6 - 14	4	29	13	5 - 27
Zn	64	52 - 70	97	38 - 145	37	155	95	50 - 199
Ni	2	2 - 2	1	1 - 2	1	0	1	0
Sc	1.8	1.6 - 2	0.3	0.2 - 0.4	1	0.1	0.6	0.2 - 1.5
Ga	23	22 - 25	28	26 - 29	25	29	29	21 - 36
Nb	29	28 - 31	67	53 - 77	36	80	53	30 - 80
Zr	301	252 - 400	729	602 - 852	293	1056	597	245 - 815
Y	78	67 - 89	120	95 - 152	39	142	93	51 - 135
Ce	140	110 - 157	136	118 - 167	108	195	120	72 - 156
U	4	4 - 4	6	4 - 8	3	5	5	3 - 8
Th	18	14 - 22	24	18 - 29	20	36	21	13 - 32
Sr	32	24 - 37	10	4 - 16	22	16	14	6 - 31
Rb	159	141 - 182	181	176 - 188	171	129	185	157 - 209
Ba	249	223 - 272	65	57 - 77	143	64	112	42 - 243

Table C-8

Field No.	Fg Radioactive granite Ave(4)	Range	MC92025 Fg Radio.	Mg Radioactive granite Ave(6)	Range	Pegmatite-aplite	
SiO2	76.42	76 - 77.15	63.19	76.10	74.19 - 76.95	79.35	78.55
TiO2	0.14	0.13 - 0.15	0.20	0.14	0.13 - 0.16	0.26	0.37
Al2O3	10.99	10.6 - 11.26	17.93	10.94	10.61 - 11.82	7.85	7.43
Fe2O3	2.61	2.12 - 2.91	3.68	3.10	2.24 - 4.85	5.14	5.37
FeO	0.55	0.17 - 1.21	0.34	0.32	0.13 - 0.57	0.25	0.63
MnO	0.08	0.04 - 0.15	0.09	0.07	0.03 - 0.17	0.07	0.12
MgO	0.04	0.03 - 0.05	0.07	0.04	0.01 - 0.08	0.16	0.28
CaO	0.10	0.02 - 0.18	0.28	0.05	0.02 - 0.09	0.01	0.01
Na2O	3.57	3.36 - 3.72	5.99	3.81	3.4 - 4.42	1.38	0.86
K2O	4.37	4.09 - 4.6	6.69	4.17	3.73 - 4.51	3.61	3.05
P2O5	0.01	0 - 0.01	0.04	0.01	0 - 0.01	0.01	0.01
F	0.03	0 - 0.1	0.01	0.01	0 - 0.02	0.01	0.01
H2O+	0.30	0.24 - 0.35		0.31	0.25 - 0.36	1.12	1.44
H2O-	0.19	0.14 - 0.23		0.16	0.1 - 0.22	0.34	0.43
CO2	0.07	0.06 - 0.07		0.05	0.04 - 0.05	0.45	0.24
S	0.00	0 - 0		0.00	0 - 0	0.01	0.00
A.I.	0.96	0.94 - 0.98	0.95	0.99	0.96 - 1.06	0.79	0.63
Cu	13	9 - 19	9	15	8 - 28	30	58
Pb	14	1 - 20	24	21	5 - 44	21	24
Zn	138	86 - 265	475	266	94 - 525	125	176
Ni	0	0.00	0	1	0 - 5	0	1
Sc	0.2	0.2 - 0.3	0.4	0.2	0.1 - 0.3	0	0
Ga	33	31 - 35	49	33	28 - 36	27	25
Nb	122	83 - 217	130	99	75 - 141	339	467
Zr	1388	913 - 2668	1309	1168	799 - 1513	4430	8490
Y	237	92 - 446	352	184	79 - 313	613	1030
Ce	205	146 - 343	255	177	98 - 278	409	842
U	11	6 - 24	11	8	5 - 11	38	58
Th	52	33 - 90	60	42	31 - 63	127	183
Sr	14	10 - 17	27	9	5 - 13	10	14
Rb	215	180 - 260	284	210	148 - 240	214	186
Ba	48	40 - 67	92	54	43 - 67	89	135

Table C-9 Grand Beach Complex Average and Unique Geochemical Data

Field No.	Low silica QF Porph Ave (4)	Range	Q Porph	QF Ash Flow Ave (12)	Range	QF Porph Ave (15)	Range	QF Porph (M) Ave (6)	Range	Red Tuff
SiO2	70.94	69.9 - 71.85	77.60	76.07	73.7 - 81.43	76.81	74.95 - 78.45	77.06	76.15 - 77.8	61.26
TiO2	0.31	0.23 - 0.38	0.09	0.13	0.05 - 0.2	0.09	0.05 - 0.13	0.10	0.08 - 0.11	0.69
Al2O3	13.63	12.68 - 14.33	11.76	12.28	9.99 - 12.95	12.13	11.75 - 12.60	11.97	11.72 - 12.37	17.91
Fe2O3	1.71	0.72 - 3.69	0.03	0.76	0.21 - 2.22	0.76	0.05 - 1.68	0.59	0.34 - 1.03	6.32
FeO	1.32	0.51 - 1.87	1.23	0.92	0.37 - 1.48	0.66	0 - 1	0.87	0.71 - 0.98	0.38
MnO	0.05	0.03 - 0.06	0.03	0.03	0.02 - 0.05	0.03	0.02 - 0.04	0.03	0.02 - 0.03	0.05
MgO	0.85	0.41 - 1.37	0.13	0.25	0.14 - 0.42	0.19	0.12 - 0.37	0.19	0.15 - 0.22	2.27
CaO	0.43	0.21 - 0.78	0.19	0.23	0.12 - 0.41	0.20	0.1 - 0.43	0.22	0.14 - 0.28	0.98
Na2O	3.32	2.31 - 3.85	3.06	3.71	3.07 - 4.93	3.28	1.55 - 4.1	3.60	3.35 - 3.93	1.08
K2O	5.53	4.2 - 8.34	5.10	4.43	1.71 - 5.25	4.68	3.97 - 5.1	4.51	4.28 - 4.77	5.62
P2O5	0.07	0.03 - 0.11	0.01	0.03	0.01 - 0.07	0.02	0 - 0.06	0.02	0.01 - 0.03	0.15
F	0.06	0.01 - 0.17	0.01	0.03	0 - 0.13	0.02	0 - 0.1	0.03	0.01 - 0.06	0.08
H2O+	1.30	1.25 - 1.39	0.85	0.73	0.62 - 0.98	0.80	0.43 - 1.53	0.71	0.53 - 0.82	4.31
H2O-	0.33	0.27 - 0.43	0.29	0.29	0.15 - 0.55	0.32	0.23 - 0.47	0.26	0.18 - 0.38	1.05
CO2	0.08	0.05 - 0.15	0.11	0.07	0.01 - 0.1	0.06	0 - 0.2	0.08	0.02 - 0.13	0.05
S	0.02	0 - 0.05	0.01	0.01	0 - 0.08	0.00	0 - 0.03	0.02	0 - 0.05	0.06
A.I.	0.84		0.90	0.89		0.86		0.90		0.44
Cu	7	5 - 12	19	10	3 - 50	9	3 - 26	6	3 - 9	21
Pb	6	2 - 11	130	38	1 - 393	18	1 - 171	4	1 - 9	8
Zn	62	48 - 89	52	43	30 - 63	40	22 - 65	41	35 - 47	67
Ni	6	3 - 14	7	2	1 - 5	3	1 - 5	3	1 - 7	27
Ga	20	17 - 27	17	20	12 - 27	21	19 - 24	20	18 - 22	30
Sc	5.2	3.5 - 6.8	1.8	2.4	1.6 - 3.6	1.9	1.6 - 2.2	1.9	1.6 - 2.1	15.3
Nb	45	30 - 67	44	45	22 - 129	45	34 - 98	45	42 - 49	29
Zr	225	151 - 348	137	188	89 - 265	160	102 - 202	149	131 - 176	148
Y	64	48 - 84	65	57	22 - 126	59	29 - 105	61	29 - 89	62
Ce	107	68 - 161	94	96	20 - 143	95	40 - 131	96	27 - 143	54
U	5	3 - 6	7	5	2 - 16	4	2 - 11	5	4 - 6	4
Th	25	18 - 35	29	26	21 - 49	27	21 - 46	24	21 - 29	27
Sr	73	54 - 88	33	42	25 - 61	38	20 - 57	41	22 - 60	135
Rb	201	120 - 270	200	157	70 - 225	198	145 - 290	170	105 - 205	360
Ba	266	112 - 414	87	143	44 - 260	93	59 - 136	85	58 - 110	302

Table C-10 St. Lawrence Granite Geochemical Data

Field No.	Aplite SG90030R	F-vein Ave(5)	F-vein Range	L Zr G Porph Ave(2)	Low Zr Mg Granite Ave(3)	Low Zr Mg Granite Range	QF Porph Ave(2)	QF Porph SG90018	FQ-poor Porph SG90008	F±Q Porph SG90004	Sy porph Ave(2)
SiO2	76.12	2.56	0.35 - 4.6	78.37	76.73	75.9 - 77.15	77.20	81.50	69.50	65.35	62.29
TiO2	0.14	0.01	0.01 - 0.01	0.08	0.16	0.13 - 0.18	0.07	0.07	0.48	0.58	1.09
Al2O3	12.80	0.13	0.02 - 0.27	11.87	11.85	11.67 - 12.14	11.47	11.02	13.16	13.67	14.42
Fe2O3	0.08	0.04	0.01 - 0.06	0.90	1.09	0.74 - 1.35	1.10	0.22	2.95	2.23	3.54
FeO	1.08	0.01	0 - 0.06	0.35	0.40	0.25 - 0.56	0.49	0.66	1.40	4.43	3.88
MnO	0.03	0.01	0.01 - 0.01	0.01	0.02	0.02 - 0.03	0.01	0.02	0.13	0.24	0.41
MgO	0.16	0.01	0.01 - 0.01	0.02	0.06	0.02 - 0.13	0.02	0.08	0.43	0.24	1.64
CaO	0.09	69.33	67.8 - 71.43	0.02	0.25	0.16 - 0.31	0.14	0.05	0.37	1.48	1.40
Na2O	1.38	0.04	0.01 - 0.06	3.49	3.37	3.22 - 3.57	3.61	0.16	4.06	4.59	4.37
K2O	5.68	0.06	0.01 - 0.16	4.55	5.03	4.82 - 5.3	4.26	3.94	5.41	4.97	4.64
P2O5	0.01	0.01	0.01 - 0.01	0.01	0.02	0.01 - 0.02	0.01	0.01	0.09	0.12	0.37
F	0.04	13.14	11.7 - 15	0.03	0.06	0.01 - 0.09	0.09	0.05	0.02	0.02	0.07
H2O+	1.26			0.64	0.29	0.13 - 0.37	0.42	1.59	0.64	0.58	1.90
H2O-	0.26	0.17	0.11 - 0.24	0.30	0.18	0.16 - 0.2	0.22	0.35	0.21	0.34	0.40
CO2	0.13			0.06	0.06	0.03 - 0.09	0.07	0.07	0.05	0.12	0.04
S	0.27			0.00	0.01	0 - 0.04	0.01	0.02	0.00	0.00	0.03
A.I.	0.66			0.90	0.93	0.91 - 0.94	0.92	0.41	0.95	0.95	0.85
Cu	17	14	9 - 23	21	15	11 - 21	27	26	14	13	15
Pb	40	149	4 - 595	25	20	20 - 20	36	10	3	4	51
Zn	187	9	7 - 13	49	45	30 - 63	34	73	142	98	281
Ni	9	19	1 - 83	14	2	1 - 3	2	8	1	1	6
Sc	2.2	0.0	0 - 0.1	0.4	1.7	1.4 - 1.9	0.3	0.3	6.1	8.5	13.0
Ga	20	2	1 - 4	29	19	17 - 20	25	34	32	29	30
Nb	43	1	0 - 2	116	37	28 - 49	82	95	44	32	33
Zr	170	6	2 - 11	354	172	154 - 183	280	332	556	421	418
Y	45	648	582 - 747	43	45	27 - 59	98	95	73	47	54
Ce	121	21	20 - 22	51	121	110 - 128	108	79	168	107	133
U	8	0	0 - 1	12	5	3 - 6	8	9	4	2	3
Th	27	5	0 - 12	49	40	35 - 46	36	44	17	8	0
Sr	17	44	30 - 57	5	22	14 - 27	12	14	20	48	163
Rb	295	2	0 - 10	335	285	255 - 305	289	345	150	85	123
Ba	254	5	3 - 11	43	112	64 - 136	49	1247	473	779	943

Table C-10

Field No.	Aphyric A-f SG90009	AQ porph sy Ave (2)	QF Porph SG90045	QF±A Porph SG90002	Q-poor Porph Ave(3)	Q-poor Porph Range	Porphyritic Granite Ave(15)	Porphyritic Granite Range	Mg Granite Ave (13)	Mg Granite Range	Zr Mg Gran Ave(2)
SiO2	74.55	75.98	71.35	74.65	76.50	74.75 - 79	77.11	75.2 - 80.5	77.07	75.3 - 80.1	76.38
TiO2	0.27	0.18	0.51	0.27	0.17	0.1 - 0.23	0.13	0.11 - 0.17	0.12	0.1 - 0.15	0.12
Al2O3	10.39	11.26	12.75	11.02	11.03	10.73 - 11.23	11.12	9.94 - 11.52	11.06	9.06 - 11.82	11.09
Fe2O3	3.69	2.52	2.94	1.57	1.48	0.58 - 2.1	1.59	0.99 - 2.74	1.37	0.33 - 2.35	1.98
FeO	0.00	0.45	1.59	2.25	0.94	0.24 - 1.81	0.50	0.14 - 1.09	0.38	0.14 - 0.99	0.18
MnO	0.05	0.04	0.11	0.14	0.07	0.01 - 0.13	0.02	0.01 - 0.05	0.03	0.01 - 0.08	0.02
MgO	0.10	0.04	0.05	0.23	0.06	0.02 - 0.09	0.02	0.01 - 0.06	0.03	0.01 - 0.08	0.03
CaO	1.04	0.06	0.66	0.27	0.17	0.02 - 0.32	0.25	0.01 - 1.13	0.62	0.02 - 4.03	0.22
Na2O	2.23	3.48	3.57	3.96	3.57	3.35 - 4.02	3.26	2.02 - 3.86	3.26	1.92 - 3.87	3.52
K2O	4.89	5.29	5.30	4.84	4.94	4.73 - 5.32	4.85	4.45 - 5.69	4.84	4.52 - 5.245	4.53
P2O5	0.02	0.01	0.12	0.02	0.01	0.01 - 0.01	0.01	0 - 0.01	0.01	0.01 - 0.015	0.01
F	0.02	0.01	0.02	0.05	0.06	0.04 - 0.09	0.11	0.01 - 0.55	0.27	0.01 - 1.55	0.12
H2O+	0.80	0.27	0.86	0.50	0.39	0.26 - 0.63	0.51	0.04 - 0.9	0.45	0.3 - 0.61	0.63
H2O-	0.25	0.17	0.35	0.29	0.18	0.15 - 0.2	0.22	0.13 - 0.34	0.24	0.15 - 0.34	0.26
CO2	0.74	0.09	0.38	0.08	0.09	0 - 0.14	0.08	0.01 - 0.2	0.12	0 - 0.5	0.08
S	0.83	0.00	0.02	0.00	0.00	0 - 0	0.02	0 - 0.07	0.03	0 - 0.06	0.01
A.I.	0.86	1.02	0.91	1.07	1.02	0.96 - 1.05	0.95	0.86 - 1.02	0.96	0.83 - 1.02	0.96
Cu	67	13	37	17	14	11 - 20	19	11 - 37	19	11 - 28	14
Pb	10	20	10	22	25	14 - 35	39	12 - 90	49	11 - 115	48
Zn	60	84	96	194	142	26 - 204	60	19 - 155	73	19 - 195	83
Ni	4	5	9	4	4	3 - 6	6	1 - 43	3	1 - 7	28
Sc	2.1	0.5	6	1	0.4	0.2 - 0.5	0.3	0.1 - 0.5	0.3	0.1 - 0.7	0.2
Ga	19	31	30	32	29	27 - 31	27	24 - 33	29	22 - 32	33
Nb	55	77	47	56	81	60 - 106	79	52 - 127	91	66 - 113	198
Zr	747	785	603	751	730	500 - 856	584	447 - 846	534	472 - 626	1075
Y	93	82	79	99	91	45 - 123	114	72 - 162	109	64 - 149	125
Ce	221	135	179	243	163	59 - 239	167	117 - 217	161	129 - 199	208
U	6	7	5	6	7	5 - 9	7	4 - 13	8	6 - 11	21
Th	22	32	0	20	24	22 - 25	27	16 - 47	29	20 - 44	71
Sr	50	6	31	8	7	3 - 13	7	4 - 14	7	4 - 12	7
Rb	175	265	180	175	273	235 - 335	256	195 - 310	278	245 - 310	347
Ba	763	95	434	78	67	43 - 105	68	36 - 133	55	33 - 75	51

Table C-12-1 Traytown Average and Unique Geochemical Data

	Per Granite (North)		Per Granite (South)		Aphyric	QF Porph
	Ave (3)	Range	Ave (4)	Range		
SiO2	76.15	75.45 - 76.75	75.87	74.38 - 77.03	73.80	76.98
TiO2	0.13	0.1 - 0.15	0.12	0.09 - 0.18	0.16	0.18
Al2O3	11.82	11.53 - 12.07	12.08	11.65 - 12.51	12.74	11.01
Fe2O3	0.95	0.7 - 1.14	0.80	0.44 - 1.16	1.58	0.33
FeO	0.84	0.72 - 1.02	0.91	0.48 - 1.32	1.11	1.04
MnO	0.02	0.01 - 0.02	0.02	0.01 - 0.03	0.07	0.03
MgO	0.05	0.02 - 0.08	0.06	0.02 - 0.14	0.43	0.34
CaO	0.21	0.17 - 0.27	0.26	0.06 - 0.43	1.88	2.21
Na2O	4.35	4.19 - 4.48	4.10	3.91 - 4.33	4.36	4.23
K2O	4.37	4.06 - 4.53	4.56	4.45 - 4.67	2.05	2.00
P2O5	0.02	0.01 - 0.03	0.01	0 - 0.03	0.02	0.04
F	0.13	0.11 - 0.14	0.09	0.02 - 0.11	0.04	0.01
H2O+	0.39	0.17 - 0.58	0.29	0.18 - 0.44	0.94	0.67
H2O-	0.41	0.3 - 0.56	0.28	0.18 - 0.43	0.29	0.40
CO2	0.06	0.01 - 0.09	0.06	0.01 - 0.1	0.05	1.04
S	0.00	0 - 0	0.00	0.00	0.02	0.01
A.I.	1.00	0.99 - 1.02	0.97	0.95 - 0.98	0.74	0.83
Cu	5	3 - 6	8	4 - 12	5	3
Pb	12	9 - 15	13	6 - 18	13	3
Zn	81	36 - 122	65	37 - 86	68	14
Ni	3	2 - 4	4	2 - 6	4	6
Ga	32	30 - 34	26	25 - 27	27	12
Sc	0.9	0.4 - 1.2	1.0	0.4 - 2.3	1.8	3.3
Nb	78	56 - 97	49	44 - 58	53	6
Zr	457	420 - 499	301	252 - 388	565	113
Y	80	60 - 118	74	51 - 86	123	16
Ce	112	100 - 133	103	98 - 112	180	41
U	6	5 - 8	5	4 - 7	3	2
Th	35	21 - 48	21	20 - 22	13	9
Sr	10	7 - 13	15	5 - 32	217	148
Rb	187	165 - 205	141	120 - 155	40	23
Ba	86	23 - 128	110	21 - 243	387	493

Table C-12-2 Port Blandford Average and Unique Geochemical Data

	Aphyric Flow	Aphyric Flow	Aphyric Flow	F Porph Mafic Flow	Mafic flow Flow	QF Porph	Tuffaceous Sandstone	Tuffaceous Sandstone
SiO2	62.50	74.45	72.30	47.95	41.60	69.05	63.55	76.30
TiO2	0.63	0.27	0.28	0.96	2.17	0.47	0.98	0.64
Al2O3	19.82	13.45	14.28	15.80	13.89	13.16	16.66	11.24
Fe2O3	2.06	1.94	1.40	8.74	16.50	3.89	6.13	2.91
FeO	0.72	0.21	0.74	1.64	0.00	0.00	0.64	0.56
MnO	0.06	0.04	0.26	0.15	0.23	0.09	0.10	0.11
MgO	1.05	0.38	0.30	7.18	5.17	1.39	2.12	1.35
CaO	2.13	0.40	1.01	8.66	12.74	1.33	1.77	0.84
Na2O	2.63	5.39	4.62	3.85	2.85	1.81	2.61	1.92
K2O	4.59	1.56	3.49	1.06	0.03	5.74	1.74	1.20
P2O5	0.11	0.04	0.08	0.26	0.27	0.12	0.06	0.01
F	0.05	0.02	0.01	0.03	0.03	0.03	0.02	0.01
H2O+	2.61	1.31	1.25	2.48	3.62	1.66	2.67	2.00
H2O-	0.17	0.21	0.22	0.26	0.28	0.20	0.47	0.45
CO2	0.14	0.04	0.15	0.06	1.10	0.42	0.27	0.01
S	0.01	0.01	0.04	0.00	0.06	0.91	0.01	0.01
A.I.	0.47	0.78	0.80	0.47	0.34	0.70	0.37	0.40
Cu	34	13	8	53	17	30	1	16
Pb	7	3	11	8	6	5	14	4
Zn	54	35	30	78	102	57	77	74
Ni	5	2	4	104	63	11	23	24
Ga	26	16	16	19	33	14	20	13
Sc	16.3	4.1	3.9	40.5	38.9	9.5	14	9.8
Nb	20	18	20	0	7	5	10	10
Zr	364	255	285	62	144	159	472	213
Y	77	29	31	21	33	17	31	26
Ce	146	80	94	33	37	51	91	59
U	20	2	2	0	0	2	4	2
Th	18	13	13	1	1	11	25	6
Sr	228	86	151	322	72	152	203	107
Rb	130	55	85	25	0	140	60	40
Ba	938	416	965	614	21	566	419	282

Table C-12-3 Musgravetown Unique & Average Geochemical Data

	Aphyric Ash-flow Ave (8)	Aphyric Ash-flow Range	Aphyric Flow	Aphyric Flow	Aphyric Ash-flow	F Porph	F Porph	F Porph	F Porph Ave (3)
SiO2	73.04	69.46 - 75.82	73.90	74.40	82.20	66.80	69.21	57.77	71.73
TiO2	0.51	0.46 - 0.58	0.26	0.32	0.26	0.49	0.54	0.82	0.49
Al2O3	11.66	9.97 - 13.62	7.85	8.06	5.82	12.46	14.44	17.72	11.02
Fe2O3	3.92	0.61 - 8.24	4.45	9.17	4.72	6.26	5.90	12.10	7.25
FeO	1.30	0.16 - 5.02	4.68	0.00	0.00	0.55	0.16	0.53	0.62
MnO	0.09	0.01 - 0.2	0.25	0.18	0.03	0.12	0.13	0.12	0.09
MgO	0.03	0.01 - 0.08	0.13	0.39	0.39	0.12	0.10	0.19	0.05
CaO	0.03	0.01 - 0.08	2.10	1.26	0.04	3.20	0.13	0.02	0.03
Na2O	2.25	1.19 - 3.14	2.79	0.24	0.07	5.37	4.53	5.65	2.92
K2O	4.93	3.68 - 5.78	0.14	1.36	1.21	1.03	3.53	3.19	4.36
P2O5	0.02	0.02 - 0.03	0.01	0.01	0.02	0.03	0.03	0.08	0.02
F	0.02	0.01 - 0.02	0.01	0.05	0.03	0.02	0.04	0.06	0.01
H2O+	1.39	0.81 - 1.66	1.25	2.30	2.06	0.40	0.96	1.62	
H2O-	0.33	0.3 - 0.39	0.14	0.21	0.45	0.15			
CO2	0.24	0.09 - 0.56	1.03	0.75	0.22	2.44	0.12	0.09	
S	0.07	0 - 0.28	0.00	0.65	2.08	0.00	0.01	0.00	
A.I.	0.78	0.63 - 0.95	0.60	0.23	0.24	0.80	0.78	0.72	0.86
Cu	10	5 - 17	10	6	11	239	6	8	11
Pb	9	0 - 15	25	22	63	25	3	29	10
Zn	253	162 - 487	381	338	320	74	166	462	172
Ni	2	0 - 5	3	5	4	5	1	0	0
Ga	43	34 - 52	38	41	30	27	45	79	44
Sc	0.3	< 0.1 - 1.8	0.3	0.1	0.1	0.7	2.1	0.2	< 0.1
Nb	154	122 - 200	284	220	426	130	145	186	144
Zr	878	674 - 1083	2521	1577	3892	560	920	1054	805
Y	101	70 - 148	248	186	347	57	122	91	78
Ce	264	171 - 425	589	427	470	138	217	559	206
U	8	2 - 18	11	7	16	3	10	3	4
Th	19	15 - 29	38	27	56	14	20	12	17
Sr	32	14 - 73	224	41	18	235	113	102	26
Rb	130	100 - 150	0	40	45	25	102	113	97
Ba	46	25 - 110	30	325	192	172	156	67	69

Table C-12-3

	Aphyric Flow	F Porph	Aphyric Ash-flow	Aphyric Flow	Inter. Tuff	Mafic Flow Ave (3)	Range
SiO2	73.95	73.81	56.60	66.05	60.20	44.72	42.35 - 47.85
TiO2	0.22	0.23	1.48	1.39	0.92	2.36	1.99 - 2.8
Al2O3	13.75	14.22	15.85	12.89	17.00	15.58	13.18 - 18.08
Fe2O3	1.39	1.35	4.43	4.82	3.14	3.63	0.95 - 6.01
FeO	0.72	0.37	6.24	1.48	4.09	7.37	5.88 - 8.62
MnO	0.07	0.06	0.16	0.18	0.14	0.33	0.19 - 0.49
MgO	0.39	0.30	2.61	1.02	2.82	4.76	4.33 - 5.22
CaO	0.96	1.13	1.90	2.56	1.78	8.31	6.59 - 9.65
Na2O	5.92	6.39	5.06	3.97	3.09	3.28	3.03 - 3.59
K2O	0.86	0.91	0.93	1.51	2.68	0.22	0.2 - 0.24
P2O5	0.04	0.02	0.41	0.15	0.17	0.45	0.35 - 0.57
F	0.01	0.01	0.04	0.03	0.03	0.05	0.03 - 0.1
H2O+	0.88	1.05	2.74	1.71	3.33	3.58	3.36 - 3.98
H2O-	0.37		0.50	0.39	0.39	0.41	0.3 - 0.59
CO2	0.75	0.76	0.04	1.09	0.00	4.21	0.75 - 7.72
S	0.00	0.02	0.00	0.01	0.00	0.00	0.00
A.I.	0.78	0.81	0.59	0.63	0.47	0.36	0.34 - 0.42
Cu	7	8	66	53.5	49	62	32 - 86
Pb	2	0	1	10	9	3	1 - 5
Zn	47	38	115	102	101	117	104 - 133
Ni	4	0	5	19.5	23	64	55 - 72
Ga	19	21	26	18	23	25	22 - 28
Sc	2.8	2.8	31.7	14.6	22.2	31.1	28.7 - 33.9
Nb	28	31	5	12	7	10	9 - 12
Zr	321	334	162	343	181	155	146 - 172
Y	37	38	32	31	29	28	26 - 31
Ce	82	86	63	70	57	46	41 - 51
U	5	5	38	2	2	0	0
Th	18	18	7	7	10	1	1
Sr	165	194	152	175	228	381	266 - 507
Rb	20	20	20	58	60	5	0 - 10
Ba	166	152	288	448	535	107	74 - 140

Table C-12-4 Plate Cove Unique & Average Geochemical Data

	Aphyric Flow	Aphyric Ash-flow Ave (4)	Range	QF Porph Ash-Flow Ave (3)	Range
SiO2	74.65	74.64	72.05 - 77.95	75.27	74.85 - 75.9
TiO2	0.29	0.31	0.21 - 0.45	0.25	0.22 - 0.31
Al2O3	12.54	10.60	8.14 - 12.89	10.51	10.08 - 10.81
Fe2O3	1.82	3.32	2.28 - 4.49	3.22	2.91 - 3.64
FeO	0.78	0.55	0.19 - 0.98	0.87	0.61 - 1.2
MnO	0.06	0.07	0.05 - 0.09	0.05	0.03 - 0.06
MgO	0.71	0.22	0.03 - 0.38	0.17	0.02 - 0.25
CaO	0.55	0.55	0.29 - 0.95	0.54	0.25 - 1.05
Na2O	4.10	2.66	1.95 - 4.01	3.48	2.74 - 4.15
K2O	1.89	5.08	3.59 - 6.42	3.86	3.20 - 4.95
P2O5	0.06	0.05	0.01 - 0.11	0.03	0.02 - 0.04
F	0.03	0.01	0 - 0.02	0.01	0.01 - 0.01
H2O+	1.73	0.45	0.34 - 0.67	0.47	0.37 - 0.64
H2O-	0.36	0.20	0.15 - 0.31	0.18	0.13 - 0.25
CO2	0.02	0.37	0.03 - 0.73	0.40	0.29 - 0.58
S	0.02	0.05	0.03 - 0.07	0.05	0.03 - 0.06
A.I.	0.70	0.93	0.91 - 0.94	0.94	0.93 - 0.95
Cu	14	9	6 - 16	6	5 - 6
Pb	2	16	7 - 23	15	9 – 18
Zn	57	68	45 - 105	73	26 - 101
Ni	5	3	2 - 5	3	2 - 4
Ga	12	25	16 - 31	28	26 - 31
Sc	8	4.0	0.6 - 13.7	0.9	0.6 - 1.2
Nb	13	30	21 - 38	35	33 - 38
Zr	136	596	401 - 746	765	733 - 792
Y	29	73	51 - 110	93	82 - 110
Ce	55	139	89 - 166	191	163 - 225
U	3	3	2 - 3	3	2 - 3
Th	10	14	10 - 20	16	14 - 20
Sr	155	34	20 - 51	37	21 - 63
Rb	60	114	55 - 180	95	65 - 135
Ba	342	309	83 - 768	140	74 - 271

Table C-12-5/6 Clarenville and Hodges Cove Unique Average Geochemical Data

	Clarenville					Hodges Cove	
	Aphyric Ash-flow	F Porph. Flow	F Porphyritic Flow Ave (4)	Range		Aphyric
SiO2	71.65	75.90	64.50	60.75 - 67.5		66.65
TiO2	0.23	0.12	0.79	0.58 - 1.07		0.66
Al2O3	15.17	12.18	15.20	14.61 - 16.14		15.08
Fe2O3	1.64	0.09	4.37	2.76 - 6.28		3.80
FeO	0.50	0.86	1.08	0.79 - 1.29		1.01
MnO	0.03	0.02	0.11	0.06 - 0.15		0.11
MgO	0.16	0.10	0.92	0.28 - 1.8		1.85
CaO	0.09	1.02	2.09	1.31 - 3.82		1.29
Na2O	5.17	3.61	4.22	2.21 - 5.39		4.13
K2O	4.45	4.18	4.02	3.07 - 5.52		3.04
P2O5	0.05	0.02	0.21	0.13 - 0.38		0.09
F	0.01	0.01	0.03	0.02 - 0.04		0.03
H2O+	0.44	0.65	1.40	0.8 - 1.86		2.46
H2O-	0.21	0.18	0.28	0.21 - 0.39		0.35
CO2	0.02	0.70	0.64	0 - 2.59		0.04
S	0.00	0.00	0.04	0 - 0.07		0.08
A.I.	0.88	0.86	0.74	0.51 - 0.87		0.67
Cu	9	6	29	7 - 54		12
Pb	9	5	7	5 - 10		10
Zn	38	12	81	44 - 109		102
Ni	3	2	4	1 - 13		16
Ga	19	12	20	19 - 21		23
Sc	6.2	1.6	13.1	8 - 17.6		13.1
Nb	17	7	12	6 - 17		15
Zr	356	111	325	204 - 438		329
Y	39	12	43	36 - 47		46
Ce	97	51	83	34 - 110		71
U	6	4	4	2 - 6		2
Th	21	21	11	6 - 18		8
Sr	49	68	216	141 - 311		282
Rb	135	100	98	60 - 155		95
Ba	453	837	1117	832 - 1409		488

Table C-12-7 Sunnyside Unique & Average Geochemical Data

Field No.	Aphyric Ash-flow	Aphyric Ash-flow	Aphyric Ash-flow	Intermediate? Ave (3)	Range	Aphyric Ash-flow Ave (7)	Range	Q/QF Porph Ash-flow Ave (6)	Range
SiO2	72.10	73.10	68.00	66.56	66.1 - 67.2	76.58	73.7 - 78.95	76.73	72.1 - 79.2
TiO2	0.39	0.20	0.11	0.57	0.41 - 0.79	0.12	0.09 - 0.23	0.12	0.09 - 0.22
Al2O3	13.78	13.07	14.95	15.58	14.87 - 15.96	11.31	10.09 - 11.97	11.47	10.8 - 13.28
Fe2O3	2.59	1.95	2.09	4.30	3.81 - 4.98	1.36	0.73 - 2.83	1.54	1.06 - 2.46
FeO	0.37	0.58	0.67	0.53	0 - 0.88	0.70	0.26 - 1.15	0.35	0.11 - 0.66
MnO	0.08	0.07	0.05	0.20	0.09 - 0.43	0.04	0.01 - 0.09	0.06	0.02 - 0.15
MgO	0.10	0.81	0.13	1.43	0.74 - 1.83	0.08	0.01 - 0.22	0.20	0.01 - 0.55
CaO	0.37	2.29	0.06	0.68	0.44 - 1.09	0.15	0.06 - 0.28	0.51	0.04 - 2.17
Na2O	5.59	1.46	0.78	3.65	3.2 - 4.18	2.14	1.03 - 3.43	2.49	1.59 - 4.5
K2O	3.38	4.46	11.68	4.50	2.49 - 5.68	6.58	4.69 - 8.31	5.69	2.73 - 7.32
P2O5	0.06	0.02	0.02	0.09	0.06 - 0.12	0.03	0.01 - 0.05	0.03	0.01 - 0.06
F	0.02	0.08	0.00	0.04	0.01 - 0.08	0.01	0 - 0.02	0.01	0 - 0.03
H2O+	0.19	1.66	0.60	1.91	0.86 - 2.78	0.65	0.28 - 1.19	0.60	0.24 - 1.23
H2O-	0.25	0.37	0.26	0.21	0.14 - 0.32	0.21	0.12 - 0.32	0.21	0.13 - 0.31
CO2	0.06	0.04	0.04	0.09	0.03 - 0.16	0.14	0.02 - 0.25	0.08	0.01 - 0.14
S	0.00	0.00	0.00	0.20	0 - 0.61	0.02	0 - 0.08	0.01	0 - 0.05
A.I.	0.93	0.55	0.93	0.73		0.94		0.89	
Cu	3	15	23	8	3 - 16	5	3 - 7	4	1 - 8
Pb	10	18	22	12	8 - 17	19	1 - 49	16	8 - 23
Zn	82	141	195	125	107 - 145	90	20 - 204	122	29 - 235
Ni	3	7	3	10	3 - 14	4	1 - 5	6	3 - 8
Ga	17	27	26	23	19 - 28	17	14 - 22	19	15 - 26
Sc	19.1	9.6	11	22.4	14.7 - 36.8	8.1	5.1 - 18.6	7.5	4.1 - 11.8
Nb	17	21	29	16	10 - 20	22	19 - 25	23	21 - 24
Zr	596	396	462	503	212 - 785	400	314 - 701	366	336 - 408
Y	91	119	159	67	29 - 96	75	54 - 105	89	42 - 126
Ce	181	124	156	112	55 - 152	115	87 - 156	111	97 - 126
U	2	4	6	2	2 - 2	3	2 - 4	3	2 - 4
Th	8	17	22	10	8–14	14	10 - 18	15	13 - 20
Sr	68	169	30	121	102 - 137	35	20 - 56	57	28 - 184
Rb	65	240	315	151	70 - 268	154	80 - 215	128	40 - 180
Ba	2228	887	1277	2073	570 - 4933	1107	421 - 3176	912	267 - 1379

Table C-12-8 Masters Head Unique Geochemical Data

	F Porph Ash-flow	Aphyric Flow	F Porph Ash-flow	F Porph Ash-flow	F Porph Ash-flow
SiO2	81.15	76.40	77.10	70.70	69.33
TiO2	0.30	0.24	0.24	0.35	0.34
Al2O3	10.23	12.94	12.99	15.69	15.98
Fe2O3	0.62	0.72	0.35	1.69	1.86
FeO	0.70	0.70	0.84	0.15	0.00
MnO	0.07	0.04	0.06	0.02	0.12
MgO	0.17	0.25	0.21	0.05	0.51
CaO	0.07	0.09	0.09	0.36	0.48
Na2O	1.94	3.33	4.04	5.51	5.45
K2O	2.92	4.72	3.61	5.26	3.04
P2O5	0.04	0.02	0.04	0.03	0.02
F	0.00	0.02	0.01	0.01	0.01
H2O+	0.78	0.43	0.47	0.21	1.83
H2O-	0.25	0.26	0.34	0.21	0.18
CO2	0.04	0.00	0.00	0.00	0.00
S	0.03	0.00	0.00	0.00	0.05
A.I.	0.62	0.82	0.81	0.94	0.77
Cu	8	7	6	1	4
Pb	2	16	23	4	15
Zn	25	87	38	21	76
Ni	3	7	3	3	4
Ga	12	20	15	10	16
Sc	8.1	7.3	7.9	8.4	8.6
Nb	9	9	9	8	9
Zr	229	200	199	261	267
Y	29	33	28	39	37
Ce	36	99	77	58	94
U	4	4	4	3	2
Th	17	14	14	14	20
Sr	55	53	87	84	441
Rb	95	155	95	95	90
Ba	1939	1506	1844	1967	1161

Table C-12-9

Field No.	FP Ash-flow (Si-Na) Ave(3)	Range	FP Ash-flow (high K) Ave(4)	Range	FP Ash-flow (low Si) Ave(3)	Range	F porph Ash-flow Ave(6)	Range	F Porph	Aphryic	F Porph	F Porph
SiO2	70.70	69.75 - 71.3	66.36	65.3 - 67.35	64.06	62.9 - 64.87	68.73	66.8 - 71.45	57.88	57.80	74.60	80.10
TiO2	0.55	0.51 - 0.63	0.62	0.48 - 0.77	0.73	0.69 - 0.75	0.50	0.32 - 0.66	0.94	0.83	0.27	0.21
Al2O3	14.03	13.67 - 14.29	15.07	14.34 - 15.47	15.87	15.42 - 16.42	15.26	14.13 - 17.57	16.36	18.74	13.70	11.28
Fe2O3	3.19	2.55 - 3.93	3.25	1.89 - 4.16	3.87	3.61 - 4.06	2.27	1.77 - 3.11	5.02	1.19	1.27	1.03
FeO	0.46	0.36 - 0.61	0.88	0.31 - 1.81	1.38	0.84 - 2.21	1.10	0.28 - 2.66	2.65	4.72	0.19	0.31
MnO	0.05	0.04 - 0.06	0.13	0.08 - 0.21	0.17	0.17 - 0.18	0.14	0.10 - 0.18	0.19	0.16	0.17	0.13
MgO	0.12	0.09 - 0.18	1.32	1.11 - 1.61	1.43	0.87 - 1.71	0.90	0.45 - 1.3	2.57	1.73	0.40	0.22
CaO	0.87	0.84 - 0.89	1.86	1.11 - 2.38	4.24	3.61 - 5.1	2.30	0.79 - 3.84	4.04	3.02	1.53	1.71
Na2O	5.95	5.02 - 7.05	2.05	0.72 - 2.66	2.13	2.04 - 2.27	3.27	1.58 - 5.42	4.71	2.21	1.76	0.75
K2O	2.94	1.58 - 4.24	5.98	5.34 - 7.24	2.85	2.02 - 3.3	3.54	2.14 - 4.51	2.83	4.17	3.82	3.26
P2O5	0.14	0.13 - 0.16	0.17	0.11 - 0.29	0.27	0.23 - 0.29	0.11	0.03 - 0.26	0.39	0.67	0.02	0.03
F	0.03	0.02 - 0.03	0.05	0.04 - 0.06	0.05	0.04 - 0.06	0.03	0.02 - 0.05	0.05	0.08	0.02	0.02
H2O+	0.31	0.14 - 0.46	1.78	1.23 - 2.96	2.30	2.03 - 2.72	1.64	0.83 - 2.64	2.12	3.31	1.54	1.62
H2O-	0.23	0.14 - 0.29	0.27	0.15 - 0.49	0.21	0.18 - 0.24	0.29	0.17 - 0.43	0.28	0.18	0.17	0.20
CO2	0.16	0.03 - 0.28	0.28	0.01 - 0.91	0.05	0.02 - 0.08	0.10	0.01 - 0.24	0.07	0.98	0.14	0.18
S	0.02	0 - 0.06	0.01	0 - 0.02	0.03	0.01 - 0.05	0.02	0 - 0.07	0.00	0.00	0.00	0.08
A.I.	0.92	0.90 - 0.94	0.65	0.49 - 0.80	0.42	0.38 - 0.45	0.61	0.38 - 0.88	0.66	0.43	0.51	0.42
Cu	6	2 - 10	15	3 - 41	17	6 - 24	16	5 - 29	66	54	4	3
Pb	11	5 - 19	18	5 - 24	20	16 - 23	20	9 - 48	17	43	23	20
Zn	48	29 - 72	89	40 - 113	94	89 - 97	92	71 - 126	119	180	83	75
Ni	6	5 - 8	3	1 - 5	6	2 - 9	6	1 - 9	11	25	1	3
Ga	16	12 - 18	22	19 - 23	19	18 - 20	21	16 - 31	21	27	19	13
Sc	13.2	10.2 - 16.7	14.6	12.5 - 17.5	17.5	15.7 - 20.2	13.2	10.1 - 17.7	18.5	20.7	8.9	7.3
Nb	12	8 - 14	8	4 - 11	6	5 - 8	11	6 - 15	11	14	11	8
Zr	250	159 - 319	188	146 - 222	166	133 - 196	236	164 - 298	196	242	227	180
Y	50	29 - 61	41	31 - 61	32	27 - 37	48	29 - 59	29	41	49	42
Ce	89	78 - 96	101	95 - 112	82	72 - 94	101	82 - 135	119	79	114	96
U	3	2 - 4	3	2 - 4	4	3 - 4	3	2 - 5	4	3	4	3
Th	14	10 - 17	15	13 - 17	13	8 - 20	15	13 - 20	28	11	18	18
Sr	123	97 - 159	269	38 - 636	540	237 - 719	343	136 - 927	744	93	162	102
Rb	67	35 - 105	153	75 - 190	88	50 - 118	106	35 - 180	60	140	160	100
Ba	1198	827 - 1885	1972	1183 - 2534	1374	1144 - 1684	1509	1297 - 1750	1017	1154	1217	691

Table C-12-9 Doe Hills Unique and Average Geochemical Data

Field No.	Aphyric Porph	QFP Ash-flow	QFP Ash-flow	QFP Ash-flow	QF Porph Af (high Al) Ave(3)	Range	QFP - low Al - Ave(2)
SiO2	82.85	77.55	75.45	73.85	70.86	69.62 - 71.8	75.47
TiO2	0.08	0.09	0.13	0.12	0.12	0.1 - 0.15	0.11
Al2O3	8.22	11.75	12.72	12.59	15.03	14.63 - 15.6	11.83
Fe2O3	0.29	1.44	0.05	0.07	1.64	1.26 - 2.36	0.90
FeO	0.67	0.73	0.39	1.51	0.61	0.28 - 0.87	0.91
MnO	0.01	0.04	0.05	0.08	0.06	0.05 - 0.07	0.07
MgO	0.12	0.12	0.09	0.10	0.13	0.08 - 0.17	0.16
CaO	0.01	0.16	0.52	1.31	1.78	0.44 - 3.36	0.16
Na2O	0.10	4.46	3.63	1.09	3.78	2.8 - 4.94	1.55
K2O	6.11	3.81	5.63	7.81	4.68	4.09 - 5.71	7.82
P2O5	0.02	0.02	0.08	0.03	0.01	0 - 0.02	0.02
F	0.01	0.00	0.01	0.00	0.01	0 - 0.01	0.00
H2O+	0.35	0.08	0.11	0.34	0.82	0.43 - 1.44	0.39
H2O-	0.31	0.20	0.21	0.34	0.26	0.23 - 0.28	0.22
CO2	0.00	0.02	0.12	0.00	0.02	0 - 0.06	0.07
S	0.00	0.00	0.00	0.00	0.00	0 - 0	0.01
A.I.	0.82	0.98	0.95	0.81	0.75	0.58 - 0.87	0.93
Cu	47	8	117	22	27	19 - 37	20
Pb	4	10	185	25	40	30 - 58	31
Zn	19	72	215	40	63	56 - 69	94
Ni	1	1	2	1	2	1 - 4	4
Ga	15	22	23	28	36	28 - 49	18
Sc	3.1	4.8	7	5.7	5.9	4.9 - 7.4	4.8
Nb	15	21	33	24	24	18 - 33	22
Zr	182	317	459	292	405	334 - 548	294
Y	53	40	811	103	106	92 - 131	87
Ce	63	65	366	94	145	116 - 167	103
U	4	4	11	6	5	3 - 7	8
Th	13	22	36	29	28	20 - 35	25
Sr	27	28	62	302	211	107 - 281	41
Rb	185	85	135	205	132	125 - 140	195
Ba	1122	491	890	2014	1046	943 - 1222	1519

Table C-13-1 Flowers River Geochemical Average Data and Unique samples (A Ignimbrites, Aphryic Ash-flows & Unit 1

	A Ash-flow tuff		Aphyric ash-flow (Al-rich)		Banded-Aphy. flows (U-1)		FR92002	FR92120	Silicified Flow (Unit 1)	
	Ave(18)	Range	Ave (3)	Range	Ave (10)	Range	Q flow	Aphyric	Ave (7)	Range
SiO2	73.75	72.44 - 75.1	67.30	63.45 - 69.3	63.37	56.29 - 67.7	71.6	72.89	88.40	81.27 - 91.11
TiO2	0.27	0.17 - 0.32	0.67	0.61 - 0.79	0.42	0.19 - 0.64	0.37	0.52	0.15	0.09 - 0.3
Al2O3	9.90	9.03 - 11.33	17.80	15.52 - 19.46	14.76	10.73 - 18.9	12.25	11.42	4.91	3.29 - 8.4
Fe2O3	3.88	2.21 - 5.95	0.93	0.24 - 1.51	1.03	0.11 - 5.21	0.47	0.93	0.20	0.07 - 0.49
FeO	1.99	0 - 3.07	5.81	1.18 - 8.83	2.07	0 - 3.8	1.74	3.6	0.56	0.2 - 0.99
MnO	0.08	0.03 - 0.11	0.08	0.02 - 0.12	0.06	0.02 - 0.1	0.04	0.08	0.01	0.01 - 0.02
MgO	0.04	0 - 0.19	0.06	0.01 - 0.13	2.71	0.66 - 4	1.77	0.26	0.51	0.12 - 1.06
CaO	0.20	0.01 - 0.48	0.03	0.01 - 0.07	4.10	1.41 - 7.93	2.15	1.29	0.40	0.17 - 0.68
Na2O	3.88	2.91 - 4.7	0.09	0.03 - 0.17	3.18	0.4 - 9.85	3.82	0.33	0.98	0.2 - 2.79
K2O	4.34	3.9 - 4.59	3.65	1.45 - 5.23	7.05	0.37 - 12.9	3.26	5.93	2.21	0.13 - 6.11
P2O5	0.01	0 - 0.02	0.04	0.02 - 0.05	0.15	0.06 - 0.72	0.11	0.1	0.04	0.01 - 0.08
F	0.19	0.03 - 0.41	0.06	0.02 - 0.1	0.34	0.07 - 0.95	0.1	0.17	0.16	0.05 - 0.41
H2O+	0.36	0.07 - 0.65	2.86	2.57 - 3.12	0.96	0.56 - 2.04	1.4	0.83	0.62	0.62 - 0.62
H2O-	0.22	0.17 - 0.34	0.20	0.17 - 0.22	0.20	0.14 - 0.29			0.22	0.22 - 0.22
CO2	0.20	0 - 1.18	0.09	0.05 - 0.15	0.11	0.07 - 0.18	0.72	0.11	0.09	0.09 - 0.09
S	0.02	0 - 0.03	0.05	0.03 - 0.08	0.02	0.01 - 0.05	0	0	0.04	0.04 - 0.04
A.I.	1.12	0.96 - 1.27	0.22	0.10 - 0.31	0.87	0.61 - 1.00	0.80	0.61	0.81	0.43 - 0.94
Cu	13	6 - 25	8	4 - 11	15	7 - 23	6	19	7	5 - 11
Pb	82	12 - 191	37	6 - 70	8	0 - 43	0	19	6	0 - 25
Zn	420	298 - 542	176	39 - 341	36	14 - 81	40	113	20	8 - 53
Ni	1	0 - 6	1	1	14	0 - 35	15	2	3	1 - 6
Sc	0.0	< 0.1 - 0.6	2.0	0.7 - 3.6	9.6	2.4 - 13.9	7.2	8.6	2.0	1.2 - 4.2
Ga	50	42 - 56	62	61 - 62	19	11 - 33	16	24	6	2 - 8
Nb	311	165 - 469	120	100 - 142	13	4 - 23	11	16	13	2 - 65
Zr	3630	2164 - 5753	2403	2123 - 2826	267	158 - 802	292	479	284	84 - 750
Y	349	129 - 632	160	147 - 168	41	14 - 78	30	56	22	5 – 61
Ce	662	344 - 1358	663	493 - 922	98	50 - 310	89	199	49	12.5 - 91
U	10	5 - 18	5	4 - 7	3	1 - 6	3	2	1	0 - 3
Th	59	28 - 135	17	5 - 29	14	0 - 40	15	17	8	3 - 17
Sr	7	3 - 15	7	5 - 9	133	81 - 196	98	75	26	7 - 68
Rb	407	277 - 597	263	103 - 423	260	17 - 551	63	223	89	9 - 187
Ba	21	11 - 71	136	75 - 226	634	136 - 1269	693	1864	241	16 - 526

Table C-13-1

	FR91200 Carbonate	Aphyric ash flow (U 4-1) Ave (26)	Range	Aphyric Flow (U 4-2) Ave(24)	Range	Aphyric Flow Min. (U 4) Ave(5)	Range	FR92081 Aphyric A-F	FR91104 Aphyric A-F
SiO2	3.95	78.56	72.15 - 85.86	77.77	72.16 - 88.96	73.85	70.59 - 76.11	66.99	44.60
TiO2	0.01	0.34	0.17 - 0.51	0.26	0.17 - 0.36	0.36	0.33 - 0.39	0.49	1.16
Al2O3	0.22	10.48	4.65 - 14.91	9.55	5.77 - 11.945	9.54	7.36 - 11.81	8.46	31.75
Fe2O3	0.12	1.74	0.03 - 7.51	2.56	0.42 - 6.83	4.05	2.19 - 7.7	17.93	4.03
FeO	0.00	1.84	0 - 4.9	2.47	0 - 7.31	4.09	0.23 - 7.9	0	3.63
MnO	0.06	0.03	0.01 - 0.06	0.05	0.01 - 0.1	0.06	0.02 - 0.09	0.14	0.07
MgO	0.35	0.03	0 - 0.12	0.05	0 - 0.23	0.13	0.07 - 0.26	0.08	0.09
CaO	55.09	0.06	0 - 0.45	0.10	0 - 0.37	0.00	0 - 0	0	0.01
Na2O	0.01	0.79	0.01 - 3.71	1.07	0.01 - 3.65	0.03	0 - 0.06	0.03	0.13
K2O	0.02	3.41	0.68 - 6.13	3.34	0.03 - 5.39	2.64	1.41 - 3.89	0.84	8.79
P2O5	0.01	0.02	0 - 0.04	0.01	0 - 0.02	0.02	0.01 - 0.02	0.09	0.05
F	0.01	0.10	0.02 - 0.88	0.09	0.02 - 0.31	0.06	0.04 - 0.12	0.03	0.05
H2O+	0.16	1.66	0.71 - 2.51	1.67	0.36 - 3			2.89	5.10
H2O-	0.13	0.20	0.11 - 0.34	0.24	0.16 - 0.33				0.44
CO2	36.80	0.07	0.03 - 0.12	0.12	0.06 - 0.25			0.09	0.12
S	0.03	0.05	0 - 0.26	0.10	0 - 0.32			0.67	0.00
A.I.	0.17	0.46	0.16 - 1.00	0.55	0.01 - 1.20	0.3	0.21 - 0.37	0.11	0.31
Cu	4	14	3 - 61	18	4 - 68	22	13 - 31	36	2
Pb	4	33	0 - 172	78	8 - 209	259	3 - 439	204	63
Zn	89	139	17 - 606	279	17 - 628	671	163 - 1004	177	198
Ni	1	1	0 - 3	1	0 - 4	0	0 - 2	0	0
Sc	0.2	0.8	< 0.1 - 2.2	0.0	< 0.1 - 0.5	< 0.1	< 0.1	< 0.1	3.1
Ga	2	38	17 - 52	42	27 - 54	56	35 - 86	54	98
Nb	1	156	56 - 400	339	174 - 511	765	655 - 977	1000	222
Zr	3	1734	1052 - 2500	4560	3132 - 7085	10320	8990 - 13532	12081	4539
Y	3	189	83 - 537	485	197 - 732	1094	687 - 1528	1372	392
Ce	9	418	174 - 921	906	263 - 1899	2512	1743 - 3359	1947	1225
U	0	5	2 - 12	15	6 - 25	31	20 - 46	40	12
Th	0	27	1 - 65	94	38 - 139	253	209 - 327	327	29
Sr	107	7	2 - 37	9	2 - 18	8	4 - 14	4	10
Rb	5	279	56 - 766	378	-5 - 730	415	202 - 861	110	468
Ba	41	60	9 - 128	40	13 - 84	49	34 - 62	43	157

Table C-13-2

	Monzonite Ave(7)	Range	Gabbro Ave (5)	Range	FR92040 Banded Flow	FR92004 Banded Flow	FR91038 A Porph	FR91176 A-Q Per Sy	FR91274R A Syenite	FR91263 Banded Felsic
SiO2	57.07	50.3 - 62.89	48.54	46.97 - 51.76	57.85	58.57	73.35	72.70	65.71	81.55
TiO2	1.48	0.42 - 2.69	1.86	1.54 - 2.21	0.51	0.82	0.31	0.28	0.38	0.33
Al2O3	15.26	13.68 - 16.8	16.21	15.02 - 18.65	17.27	17.26	9.52	10.72	15.84	7.64
Fe2O3	2.85	1.69 - 4.18	1.94	0.64 - 3.27	1.27	0.64	4.41	1.78	2.45	0.66
FeO	6.96	0.92 - 11.55	10.06	7.71 - 12.34	2.9	6.53	1.61	2.84	2.15	1.41
MnO	0.20	0.15 - 0.25	0.18	0.15 - 0.22	0.05	0.09	0.08	0.08	0.12	0.02
MgO	1.39	0.19 - 3.07	5.68	4.7 - 6.24	3.8	1.4	0.07	0.01	0.05	0.93
CaO	3.81	0.64 - 5.69	7.54	6.3 - 8.35	1.57	2.54	0.08	0.34	0.51	0.09
Na2O	4.86	4.34 - 5.42	3.13	2.47 - 4.1	2.18	2.68	4.43	4.60	5.7	0.17
K2O	4.08	2.21 - 6.72	1.52	1.04 - 2.02	10	6.83	4.32	4.52	5.55	5.47
P2O5	0.59	0.07 - 1.31	0.30	0.25 - 0.35	0.2	0.12	0.01	0.01	0.03	0.01
F	0.07	0.02 - 0.11	0.12	0.04 - 0.2	0.45	0.09	0.12	0.18	0.06	0.04
H2O+			2.48	2.13 - 2.82			0.28	0.52	0.79	1.08
H2O-			0.25	0.17 - 0.32			0.22	0.17	0.29	0.26
CO2			0.10	0.09 - 0.1			0.14	0.01	0.1	0.06
S			0.02	0.01 - 0.03			0.00	0.01	0.01	0.03
A.I.	0.81	0.68 - 0.95	0.42	0.32 - 0.58	0.83	0.68	1.26	1.16	0.97	0.81
Cu	22	8 - 36	35	19 - 46	18	10	9	10	12	6
Pb	13	6 - 24	9	0 - 22	5	11	53	46	20	24
Zn	168	141 - 192	128	95 - 151	17	109	382	341	160	84
Ni	11	0 - 27	64	16 - 91	31	2	1	0	0	6
Sc	12.3	1.1 - 19.7	26.0	21.5 - 28.2	15.5	11.0	0.0	0.0	0.0	2.6
Ga	39	30 - 46	27	22 - 30	20	34	48	48	58	17
Nb	48	31 - 61	2	0 - 4	13	32	317	165	110	33
Zr	1185	658 - 1644	156	124 - 182	101	932	3781	1934	867	1467
Y	82	58 - 97	30	25 - 34	28	96	283	120	139	120
Ce	585	207 - 1262	54	43 - 61	80	278	612	390	834	397
U	1	0 - 2	0	0 - 1	4	2	10	5	3	6
Th	10	2 - 19	1	0 - 4	17	22	33	16	10	30
Sr	147	37 - 215	324	257 - 374	222	228	4	5	11	21
Rb	83	33 - 131	85	21 - 147	493	248	351	266	159	255
Ba	735	324 - 1040	496	393 - 718	1317	3449	11	21	76	458

Table C-13-2

	FR91233	FR91258A	FR91203	Peralaline Granite		Subalkaline granite		Subalkaline granite?	
	Porph. F GRan.	FQA Porph	FQA Porph	Ave(9)	Range	Ave (7)	Range	Ave (5)	Range
SiO2	76.45	76.83	69.40	73.21	69.35 - 75.45	67.64	66.4 - 69.33	74.33	72.8 - 76
TiO2	0.36	0.39	0.62	0.35	0.3 - 0.43	0.47	0.4 - 0.54	0.31	0.25 - 0.36
Al2O3	11.24	10.39	12.36	11.68	10.65 - 12.99	13.62	12.81 - 14.46	11.19	10.41 - 12.15
Fe2O3	0.91	0.65	1.70	1.75	1.04 - 3.32	2.06	1.18 - 2.35	1.80	1.06 - 2.8
FeO	1.56	2.76	4.46	2.16	0.43 - 3.83	2.98	2.3 - 3.5	1.55	1.06 - 1.85
MnO	0.04	0.06	0.08	0.07	0.04 - 0.13	0.11	0.07 - 0.13	0.05	0.04 - 0.06
MgO	0.03	0.24	0.21	0.07	0.02 - 0.16	0.22	0.11 - 0.31	0.06	0.02 - 0.11
CaO	0.22	0.91	2.22	0.53	0.13 - 1.07	1.20	0.93 - 1.45	0.29	0.16 - 0.39
Na2O	3.61	1.51	3.28	3.94	2.26 - 4.96	4.39	3.98 - 4.75	3.63	2.9 - 4.07
K2O	4.57	4.83	4.16	4.96	4.7 - 5.43	5.23	4.84 - 5.47	4.67	3.95 - 4.98
P2O5	0.01	0.06	0.12	0.03	0.01 - 0.04	0.06	0.04 - 0.08	0.01	0.01 - 0.02
F	0.02	0.11	0.08	0.06	0.01 - 0.13	0.14	0.06 - 0.28	0.06	0.02 - 0.08
H2O+	0.47	1.11	1.10	0.69	0.39 - 1.07	1.20	1.07 - 1.33	0.64	0.47 - 0.79
H2O-	0.30	0.27	0.29	0.31	0.24 - 0.49	0.33	0.32 - 0.33	0.28	0.21 - 0.35
CO2	0.09	0.05	0.02	0.13	0.07 - 0.27	0.20	0.16 - 0.23	0.09	0.07 - 0.11
S	0.06	0.05	0.04	0.04	0.02 - 0.06	0.03	0.02 - 0.03	0.04	0.03 - 0.06
A.I.	0.97	0.74	0.80	1.01	0.90 - 1.05	0.95	0.92 - 0.97	0.98	.87 - 1.05
Cu	3	29	15	8	2 - 24	12	5 - 30	5	32938.00
Pb	10	27	19	25	12 – 54	36	13 - 72	14	33045.00
Zn	70	113	135	145	105 - 231	161	87 - 249	91	83 - 96
Ni	0	2	3	1	0 - 5	1	0 - 4	0	0 - 2
Sc	0.9	2.4	9.2	1.7	0.3 - 2.8	3.4	2.3 - 4.2	1.1	0.3 - 1.7
Ga	31	25	28	35	29 - 46	39	30 - 46	32	28 - 36
Nb	55	48	21	91	65 - 116	96	34 - 131	53	33 - 66
Zr	414	749	625	1295	844 - 2029	1304	830 - 1483	590	451 - 712
Y	28	76	69	99	51 - 175	132	62 - 184	51	44 - 58
Ce	325	309	222	455	251 - 860	666	207 - 959	325	257 - 371
U	2	3	2	3	2 - 6	3	2 - 4	2	1 – 3
Th	7	13	0	15	2 - 36	23	12 - 32	8	4 - 12
Sr	8	87	149	15	5 - 21	54	42 - 86	12	33070.00
Rb	141	166	122	180	136 - 227	194	114 - 264	165	141 - 182
Ba	111	334	1552	175	69 - 302	564	339 - 1210	115	46 - 204

Table C-13-2 Flowers River Geochemical Averages and Unique Samples (Intrusive Rocks)

	FR91182	FR91066	FR91171	Syenite Micro Granite		Peralkaline Micro Granite		FR92124R	High Per Micro Granite	
	Q-A porph.	Micro G	Q vein	Ave(10)	Range	Ave (19)	Range	FA Porph Min.	Ave (10)	Range
SiO2	72.75	72.45	92.75	58.58	51.68 - 64.7	73.09	69.41 - 75.9	72.35	73.71	71.95 - 76.22
TiO2	0.28	0.36	0.07	1.33	0.8 - 2.31	0.35	0.23 - 0.43	0.28	0.31	0.28 - 0.36
Al2O3	12.72	11.88	3.88	13.87	12.78 - 14.9	11.64	10.74 - 12.78	9.49	10.42	8.98 - 11.93
Fe2O3	1.54	2.38	1.05	4.84	1.84 - 14.5	1.94	0.21 - 3.67	1.05	2.86	0.96 - 4.35
FeO	1.74	1.58	0.00	5.85	0 - 10.71	2.17	1.07 - 4.05	5.61	2.18	1.06 - 4.04
MnO	0.07	0.06	0.01	0.23	0.14 - 0.28	0.07	0.02 - 0.14	0.15	0.08	0.04 - 0.12
MgO	0.28	0.16	0.06	1.18	0.33 - 2.65	0.06	0.02 - 0.14	0.09	0.10	0.01 - 0.41
CaO	0.50	0.31	0.01	3.57	2.24 - 5.42	0.46	0.06 - 1.03	0.19	0.32	0.08 - 0.53
Na2O	4.57	3.15	0.01	4.73	4.35 - 5.1	3.73	0.14 - 4.93	2.71	3.59	0.21 - 4.83
K2O	4.69	5.07	1.12	3.89	2.75 - 4.66	4.85	3.82 - 6.33	0.76	4.51	3.61 - 5.59
P2O5	0.05	0.03	0.01	0.66	0.2 - 1.39	0.02	0 - 0.05	0.03	0.01	0 - 0.02
F	0.07	0.01	0.02	0.13	0.08 - 0.17	0.09	0.01 - 0.31	0.05	0.11	0.01 - 0.25
H2O+	0.66	1.04	0.96	1.15	0.75 - 1.6	0.93	0.36 - 1.59		0.60	0.21 - 0.94
H2O-	0.38	0.30	0.32	0.27	0.16 - 0.32	0.29	0.17 - 0.43		0.29	0.21 - 0.39
CO2	0.03	0.12	0.03	0.16	0.03 - 0.33	0.12	0.03 - 0.38		0.10	0.05 - 0.16
S	0.01	0.09	0.01	0.06	0.04 - 0.08	0.03	0 - 0.06		0.03	0.02 - 0.04
A.I.	0.99	0.90	0.32	0.87	0.74 - 0.94	0.98	0.61 - 1.19	0.56	1.03	0.64 - 1.15
Cu	8	3	21	20	11 - 30	9	4 - 23	30	12	6 - 19
Pb	11	13	15	17	7 - 25	47	1 - 269	466	61	16 - 148
Zn	181	102	39	222	192 - 264	198	46 - 619	955	357	177 - 552
Ni	1	1	1	3	0 - 16	1	0 - 3	0	0	0 - 3
Sc	1.8	2.5	0.4	19.1	7.8 - 30.9	1.5	0.3 - 2.9	< 0.1	0.1	< 0.1 - 0.6
Ga	44	32	10	40	36 - 50	38	30 - 49	45	46	31 - 53
Nb	45	62	13	83	50 - 127	108	52 - 273	992	221	155 - 289
Zr	841	1192	199	1543	1038 - 2148	1280	835 - 1699	14192	2868	1645 - 5599
Y	64	110	20	120	93 - 154	124	45 - 509	1847	257	120 - 432
Ce	159	436	83	549	456 - 644	470	238 - 772	3563	668	452 - 838
U	1	4	1	3	2 - 3	4	2 - 9	43	8	4 - 18
Th	0	7	0	10	0 - 22	17	4 - 43	299	48	23 - 92
Sr	20	32	4	149	82 - 222	15	5 - 40	36	13	5 - 27
Rb	147	216	65	106	66 - 141	215	130 - 338	43	255	189 - 336
Ba	180	426	35	1315	488 - 2206	171	47 - 441	37	54	16 - 108

Table C-13-3 Flowers River Geochemical Averages and Unique Samples - FQA Porphyritic Ash Flows

	FR91141A (Q-F)-p A-F	FR91097 Q-poor A-F	FR91134A Q-poor A-F	FR91214 Q-poor A-F	(Q+F) poor ash flow Ave (16)	Range	FQ Ash-flow (Unit 2 Alt) Ave (6)	Range	FQ Ash-flow (Unit 3 alt) Ave (30)	Range
SiO2	50.82	70.12	75.55	76.90	76.73	73.5 - 78.85	73.27	70.32 - 76.25	78.11	73.96 - 83.5
TiO2	0.83	0.35	0.40	0.31	0.35	0.29 - 0.41	0.55	0.47 - 0.59	0.32	0.23 - 0.52
Al2O3	17.25	15.08	8.60	7.55	9.27	6.68 - 10.8	12.22	11.04 - 13.33	11.06	8.15 - 13.58
Fe2O3	4.87	3.72	1.53	8.25	1.58	0.09 - 4.58	1.00	0.21 - 2.11	1.09	0.05 - 3.61
FeO	12.34	3.37	5.58	0.00	4.87	0 - 8.21	3.96	3.15 - 4.87	2.08	0 - 3.87
MnO	0.44	0.03	0.10	0.03	0.06	0.02 - 0.1	0.07	0.05 - 0.10	0.04	0.01 - 0.06
MgO	0.12	0.04	0.03	0.04	0.08	0.01 - 0.23	0.31	0.25 - 0.45	0.10	0.01 - 0.27
CaO	0.00	0.01	0.01	0.01	0.09	0.01 - 0.39	1.21	0.13 - 2.72	0.03	0 - 0.11
Na2O	0.15	1.07	0.01	0.05	0.34	0.01 - 2.24	0.46	0.08 - 1.84	0.45	0.02 - 1.76
K2O	2.80	1.75	2.01	2.52	3.51	0.82 - 5.93	4.09	3.37 - 5.17	4.35	0.58 - 7.23
P2O5	0.04	0.01	0.02	0.01	0.01	0.01 - 0.03	0.10	0.09 - 0.11	0.03	0.01 - 0.08
F	0.08	0.09	0.04	0.07	0.06	0.01 - 0.21	0.06	0.03 - 0.1	0.04	0.01 - 0.12
H2O+	4.38	2.57	2.47	1.43	1.70	0.26 - 2.91	2.28	2.03 - 2.44	1.74	1.15 - 2.34
H2O-	0.40	0.31	0.24	0.12	0.20	0.11 - 0.43	0.23	0.19 - 0.29	0.24	0.14 - 0.39
CO2	0.34	0.06	0.27	0.18	0.08	0.02 - 0.15	0.04	0.01 - 0.05	0.06	0.01 - 0.15
S	0.30	0.00	0.02	0.05	0.06	0 - 0.28	0.02	0.02 - 0.03	0.02	0 - 0.07
A.I.	0.19	0.24	0.25	0.37	0.45	0.14 - 1.00	0.42	0.33 - 0.52	0.49	0.07 - 0.75
Cu	37	6	29	22	19	9 - 32	10	6 - 16	14	4 - 121
Pb	537	210	134	65	85	7 - 216	11	0 - 33	25	2 - 71
Zn	2809	249	606	195	458	61 - 1733	119	48 - 241	96	19 - 216
Ni	1	0	0	1	7	0 - 93	2	1 - 6	1	0 - 7
Sc	0.0	0.1	0.0	0.0	0.1	< 0.1 - 0.5	8.1	6 - 9	1.6	0.4 - 3.4
Ga	92	56	48	44	41	33 - 53	28	24 - 30	32	20 - 44
Nb	1414	365	766	646	212	118 - 375	20	17 - 24	58	38 - 82
Zr	21104	4702	11569	11162	4101	2409 - 6749	566	530 - 646	857	669 - 1378
Y	1888	584	1161	1024	342	166 - 553	60	38 - 75	86	63 - 109
Ce	2518	452	2237	1876	887	330 - 1867	225	208 - 251	311	179 - 389
U	65	14	42	38	10	3 - 23	2	2	3	2 - 4
Th	403	94	247	222	62	22 - 118	10	0 - 18	18	0 - 32
Sr	10	6	4	11	8	2 - 17	74	19 - 178.5	14	4 - 26
Rb	568	220	295	528	325	55 - 938	170	125 - 197	219	29 - 358
Ba	68	27	29	41	49	20 - 83	1308	529 - 2467	203	41 - 329

Table C-13-3

	FQ Ash-flow (Unit 4/5 alt)		FR91118	FQ ash-flow (Unit 5)		FR92012	FQ ash-flow (Unit 2)		FQ ash-flow (Unit 3)	
	Ave (8)	Range	Ash-flow breccia	Ave (5)	Range	F Porph.	Ave (9)	Range	Ave (28)	Range
SiO2	77.12	74.35 - 80.45	65.90	73.52	69.7 - 76.45	56.29	72.23	69.75 - 77.25	75.05	68 - 81.15
TiO2	0.31	0.21 - 0.38	1.48	0.37	0.31 - 0.44	0.64	0.52	0.31 - 0.61	0.33	0.22 - 0.44
Al2O3	10.03	8.12 - 11.41	13.37	12.38	11.22 - 13.55	18.9	11.83	10.05 - 12.85	11.81	10.75 - 13.84
Fe2O3	1.98	0.73 - 5.33	0.49	1.69	0.04 - 4.57	2.5	0.87	0.35 - 1.37	1.35	0.14 - 3.75
FeO	3.74	0 - 6.78	7.32	2.33	0 - 4.13	3.53	3.76	2.62 - 4.49	2.02	0 - 4.29
MnO	0.05	0.03 - 0.08	0.20	0.04	0.02 - 0.09	0.09	0.07	0.04 - 0.09	0.04	0.01 - 0.11
MgO	0.07	0.03 - 0.16	0.86	0.07	0.04 - 0.14	0.66	0.23	0.1 - 0.35	0.14	0.01 - 0.37
CaO	0.01	0.01 - 0.02	1.05	0.21	0.02 - 0.85	3.41	1.20	0.01 - 2.07	0.15	0.01 - 0.52
Na2O	0.09	0.01 - 0.51	3.73	2.21	0.17 - 4.05	0.45	1.37	0.07 - 2.63	2.04	0.01 - 3.73
K2O	3.49	2.28 - 5.11	3.11	5.24	4.33 - 6.21	11.5	5.56	4.64 - 6.67	5.10	3.02 - 7.94
P2O5	0.01	0.01 - 0.02	0.52	0.03	0.02 - 0.08	0.12	0.09	0.03 - 0.12	0.03	0 - 0.08
F	0.04	0.01 - 0.1	0.04	0.05	0.01 - 0.09	0.46	0.09	0.02 - 0.23	0.04	0 - 0.3
H2O+	1.93	1.12 - 2.51	1.65	1.07	0.37 - 1.46	1.74	1.36	0.92 - 1.65	1.28	0.54 - 2.03
H2O-	0.27	0.21 - 0.46	0.23	0.24	0.18 - 0.28		0.20	0.15 - 0.38	0.24	0.14 - 0.39
CO2	0.14	0.08 - 0.2	0.05	0.14	0.02 - 0.48	0.09	0.23	0.05 - 0.68	0.09	0.03 - 0.19
S	0.04	0 - 0.24	0.00	0.08	0.01 - 0.29	0.04	0.03	0.01 - 0.08	0.03	0 - 0.12
A.I.	0.40	0.25 - 0.69	0.71	0.75	0.62 - 0.87	0.70	0.70	0.58 - 0.79	0.75	0.27 - 0.92
Cu	18	5 - 31	4	12	3 - 29	23	15	9 - 26	13	3 - 39
Pb	76	20 - 166	14	28	9 - 51	43	25	16 - 54	58	7 - 762
Zn	307	165 - 658	270	166	83 - 241	81	104	39 - 132	129	16 - 377
Ni	1	0 - 2	10	1	0 - 2	-1	2	1 - 3	1	0 - 15
Sc	0.1	0 - 0.5	10.0	1.3	0.4 - 3.7	8.7	6.8	1.5 - 8.5	1.5	0.2 - 2.8
Ga	41	26 - 50	32	35	32 - 38	33	24	20 - 29	31	24 - 42
Nb	221	129 - 313	45	86	64 - 109	23	23	16 - 54	64	41 - 180
Zr	3884	2179 - 4880	709	1383	1135 - 1576	802	595	512 - 768	916	760 - 1546
Y	344	189 - 453	71	107	84 - 117	78	56	3 - 82	93	69 - 151
Ce	802	566 - 1143	320	454	373 - 516	310	218	186 - 282	342	193 - 502
U	11	7 - 18	2	3	3 - 3	2	2	1 - 3	3	1 - 4
Th	59	34 - 95	0	11	0 - 22	23	4	0 - 16	16	4 - 31
Sr	5	2 - 10	36	21	10 - 45	196	110	20 - 171	20	4 - 29
Rb	326	188 - 495	185	248	162 - 333	420	189	138 - 272	217	130 - 335
Ba	37	22 - 55	295	270	93 - 842	971	1783	596 - 2574	210	40 - 475

Table C-13-3

	FQ ash-flow (Unit 5)		FR91205	Q ash-flow (Unit 3?)		Q Ash-flow	Q ash-flow (min)		Q ash-flow (Unit 4)	
	Ave (27)	Range	FQ(A) A-F	Ave (6)	Range	Ave(2)	Ave(3)	Range	Ave(14)	Range
SiO2	75.53	72.53 - 79.7	62.80	81.17	75.51 - 86.3	73.31	79.73	79.5 - 79.95	78.41	73.15 - 83.65
TiO2	0.29	0.17 - 0.39	1.13	0.22	0.01 - 0.32	0.45	0.31	0.25 - 0.36	0.34	0.21 - 0.5
Al2O3	10.26	8.39 - 11.87	14.38	10.66	9.05 - 12.03	16.34	7.99	6.76 - 10.05	10.55	8.2 - 15.69
Fe2O3	2.59	0.28 - 6.62	0.96	0.98	0.34 - 1.56	0.85	1.31	0.64 - 2.38	1.62	0.14 - 7.01
FeO	2.29	0 - 6	6.78	1.27	0 - 2.86	1.65	4.48	2.41 - 5.78	2.43	0 - 5.03
MnO	0.04	0.01 - 0.08	0.13	0.02	0.01 - 0.04	0.01	0.06	0.04 - 0.08	0.04	0.01 - 0.08
MgO	0.06	0 - 0.16	0.85	0.09	0.01 - 0.24	0.02	0.06	0.04 - 0.09	0.04	0.01 - 0.12
CaO	0.11	0.01 - 0.54	1.10	0.08	0 - 0.29	0.03	0.01	0 - 0.01	0.08	0.01 - 0.36
Na2O	1.86	0.01 - 4.42	1.49	0.47	0.01 - 2.53	0.22	0.04	0.02 - 0.07	0.52	0.02 - 3.42
K2O	4.82	2.34 - 5.96	7.08	2.34	0.27 - 3.83	3.34	1.92	1.18 - 3.07	2.98	0.08 - 5.62
P2O5	0.01	0 - 0.07	0.36	0.03	0 - 0.05	0.06	0.03	0.02 - 0.04	0.01	0.01 - 0.01
F	0.06	0.01 - 0.22	0.07	0.03	0.02 - 0.07	0.05	0.06	0.04 - 0.08	0.05	0.01 - 0.18
H2O+	1.23	0.43 - 2.15	2.14	1.79	1.41 - 2.18	2.76	2.05	1.98 - 2.12	1.56	0.78 - 2.36
H2O-	0.22	0.1 - 0.35	0.27	0.24	0.19 - 0.32	0.34	0.20	0.15 - 0.24	0.22	0.13 - 0.32
CO2	0.09	0.03 - 0.18	0.49	0.08	0.04 - 0.15	0.08	0.15	0.14 - 0.16	0.11	0.06 - 0.2
S	0.08	0 - 0.5	0.02	0.05	0 - 0.17	0.07	0.09	0.01 - 0.17	0.05	0 - 0.22
A.I.	0.80	0.28 - 1.12	0.70	0.31	0.09 - 0.42	0.24	0.26	0.19-.34	0.40	0.01 - 0.87
Cu	21	4 - 103	15	14	6 - 22	9	59	18 - 136	13	6 - 27
Pb	91	7 - 379	31	10	0 - 39	36	212	133 - 350	82	5 - 197
Zn	336	50 - 842	222	56	15 - 140	40	524	217 - 924	257	14 - 780
Ni	1	0 - 3	5	2	1 - 3	1	0	0	1	0 - 2
Sc	0.1	< 0.1 - 0.6	11.8	1.1	0.4 - 1.6	1.6	0	0	0.2	0 - 1
Ga	40	30 - 49	42	31	23 - 40	53	46	44 - 49	40	28 - 53
Nb	200	95 - 521	35	46	45 - 48	94	666	616 - 736	231	137 - 357
Zr	2863	1150 - 8094	737	774	717 - 868	1502	10407	9382 - 11320	3922	2030 - 6977
Y	262	122 - 792	62	70	50 - 89	127	1006	910 - 1070	366	197 - 552
Ce	655	171 - 1542	250	261	135 - 505	523	2163	2059 - 2278	629	154 - 1180
U	8	1 - 24	2	4	2 - 8	7	32	28 - 36	11	3 - 17
Th	49	18 - 164	0	15	7 - 20	25	221	202 - 251	66	36 - 113
Sr	9	4 - 14	41	6	3 - 8	12	5	5 - 6	8	1 - 15
Rb	364	172 - 721	339	171	33 - 235	283	235	135 - 400	262	5 - 637
Ba	44	7 - 82	751	102	45 - 175	126	35	27 - 50	57	16 - 247